ÉCLAIRE Third Periodic Report, Author List

Coordinating lead authors

Mark A. Sutton, Clare M. Howard, Eiko Nemitz, Almut Arneth, Dave Simpson, Gina Mills, Wim de Vries, Wilfried Winiwarter, Markus Amann,

Lead authors

Rocio Alonso, Christof Ammann, William J. Bealey, Victoria Bermejo, Albert Bleeker, Alessandro Cescatti, Frank Dentener, Lisa Emberson, Chris Evans, Chris Flechard,

Edwin Haas, Jean-Paul Hettelingh, Mike Holland, Thomas Mentel, Elena Paoletti, Maximilian Posch, Gert Jan Reinds, Mark R. Theobald,

Contributing authors

Kristian Albert, Carsten Ambelas Skjøth, Helle Vibeke Andersen, Kirsti Ashworth, Stefan Åström, Niramson Azouz, Seraina Bassin, Agnieszka Becher, Claus Beier, Victoria Bermejo, Alan Briolat, Malin Broberg, Patrick Bueker, Juergen Burkhardt, Klaus Butterbach-Bahl, Héctor Calvete, Marco Carozzi, Pierre Cellier, Federico Centoni, Maria Chiesa, Stanislaw Cieslik, Lieven Clarisse, Pierre Coheur, Mhairi Coyle, Celine Decuq, Chiara Di Marco, Eugenio Diaz-Pines, Vesna Djuricic, Ruth Doherty, Ulli Dragosits, Jean-Louis, Drouet, Vedrana Dzaja Grgicin, Florian Egger, Susana Elvira, Magnuz Engardt, Sophia Etzold, Richard Falk, Silvano Fares, Yannick Fauvel, Angelo Finco, Dominique Flura, David Fowler, Martina Franz, Arnoud Frumau, Ivano Fumagalli, Laurens Ganzeveld, Héctor García Gómez, Rainer Gasche, Camilla Geels, Sophie Genermont, Giacomo Gerosa, Ignacio González Fernández, Iratxe, González-Aparicio, Christine Gritsch, Carsten Gruening, Daniel Hagberg, Pleijel Hakan, Helmut Haller, Harry Harmens, Berit Hasler, Didier Hauglustaine, Felicity Hayes, Carlijn Hendriks, Ole Hertel, Chris Heyes, Kevin Hicks, Lena Höglund-Isaksson, László Horváth, Rasmus Houborg, Johanna Joensuu, Laurence Jones, Per Erik Karlsson, Zbigniew Klimont, Alexander Komarov, Koen Kramer, Eric Lamaud, Ben Langford, Juliette Lathiere, David Leaver, Adrian Leip, Emeline Lequy, Maria Lindblad, Benjamin Loubet, Francesco Loretto, Rob Maas, Riccardo Marzuoli, Raia Silvia Massad, Olivier Maury, Sergiy Medinets, Lina Mercado, Palmira Messina, Mirco Migliavacca, Teis Mikkelsen, Saúl Molina Herrera, Robert Monga, Andrea Moring, Silvana Munzi, Doan Nainggolan, Yasmine Ngadi, Jérôme Ogée, Stefan Olin, Rebecca Oliver, Riinu Ots, Susan, Owen, Shyam Pariyar, Olga Pokorska, Elise Potier, Irina Priputina, Isaura Rabago, Pekka Rantala, Dave Reay, Stefan Reis, Janne Rinne, Elin Roberts, Emma Robinson, Edwin Rowe, Taina Ruuskanen, Javier Sanz, Alberto Sanz-Cobena, Katarzyna Sawicka, Martijn Schaap, Simon Schallart, Wolfgang Schöpp, Katarina Sharps, Lucy Sheppard, Jadranka Škevin Sovic, Ute Skiba, Ben Smith, Alexandra Tiefenbacher, Sam Tomlinson, Juha-Pekka Tuovinen, Marsailidh Twigg, Fernando Valino, Antonio Vallejo, Martin Van Damme, Netty Van Dijk, Violeta Velikova, Nico Vellinga, Sonja Vidic, Massimo Vieno, Polina Voylokov, Maria Raffaella Vuolo, Tamas Weidinger, Roy Wichink Kruit, Veronika Wolff, Roy Woolley, Cheng Wu, Sonke Zaehle, Sophie Zechmeister - Boltenstern, Pablo Zuazo and Elena Zubkova.

1 December 2015

2. Core of the report for the period: Project objectives, work progress and achievements, project management

2.1 Project objectives for the period

The ÉCLAIRE worked to improve the understanding of the interactions and feedbacks in the coupled biosphere-chemistry-climate system and develop novel approaches to quantifying ecosystem effects and threats together with improved tools for upscaling to Europe and extrapolating to future climates. The integration of these issues focused on the following **Specific Objectives** (for Work Package numbers see Figure 0.1):

S1. To develop improved process-based emissions parameterization of NH_3, NO and VOCs from natural and agricultural ecosystems in response to climate and pollutant deposition for incorporation into atmospheric Chemistry-Transport Models (CTMs), based on existing and new flux measurements in the field and laboratory, applying these to develop spatially resolved emission scenarios in response to climate, CO_2 and air pollutant change [WPs 1, 2, 3, 6].

S2. To determine the chief processes in atmospheric chemistry that respond to climate and air pollution change and the consequences for ozone and aerosol production and atmospheric lifetimes, in the context of the global O_3 background [WPs 5, 7 & through collaboration with PEGASOS FP7 project].

S3. To develop improved multi-layer dry deposition / bi-directional exchange parameterisations for O_3, NO_x, NH_3, VOCs and aerosols, taking into account near-surface chemical interactions and the role of local/regional spatial interactions, based on existing and new flux measurements and high resolution models and to estimate European patterns of air concentrations and deposition under climate change [WPs 1, 2, 4, 7, 8].

S4. To integrate the results of meta-analyses of existing datasets with the results of targeted experiments for contrasting European climates and ecosystems, thereby assessing the climate-dependence of thresholds for land ecosystem responses to air pollution, including the roles of ozone, N-deposition and interactions with VOCs, nitrogen form (wet/dry deposition) and aerosol [WPs 9, 10, 11, 12].

S5. To develop improved process-based parameterizations in dynamic global vegetation models (DGVMs) and soil vegetation models (DSVMs) to assess the combined interacting impacts of air quality, climate change and nutrient availability on plant productivity, carbon sequestration and plant species diversity and their uncertainties [WP13; WP14; WP15, WP17].

S6. To develop novel thresholds and dose-response relationships for air pollutants (especially for O_3 and N) under climate change, integrated into process-based models verified by experimental studies at site scales and mapped at the European scale, quantifying the effect of climate change scenarios [WPs 12, 13, 14, 15, 16].

S7. To assess the extent to which climate change alters the transport distance and spatial structure of air pollution impacts on land ecosystems considering local, regional, continental and global interactions, focusing on nitrogen and ozone effects [WPs 5, 6, 7, 8, 9].

S8. To apply the novel metrics to quantify multi-stress response of vegetation and soils, including effects on carbon storage and biodiversity to improve the overall risk assessments of pollution-climate effects on ecosystems at the European scale as the basis for development of mitigation options [WPs 12, 13, 14, 15, 16, 19, 20].

S9. To quantify the overall economic impacts of air pollution effects on land ecosystems and soils, including the valuation of ecosystem and other services, and the extent to which climate change contributes by altering emissions versus ecosystem vulnerability [WPs 3, 4, 6, 7, 12, 14, 15, 16, 18].

S10. To reassess the current recommendations regarding air pollution emission abatement policies, considering the interactions between ecosystem and other effects under conditions of climate change and to perform cost-benefit analysis of policy options under different scenarios [WPs 18, 19, 20].

These Specific Objectives are the culmination of work under several components and a variety of activities (see Figure 0.1). As this is the final periodic report of the project, all deliverables have now been completed and uploaded.
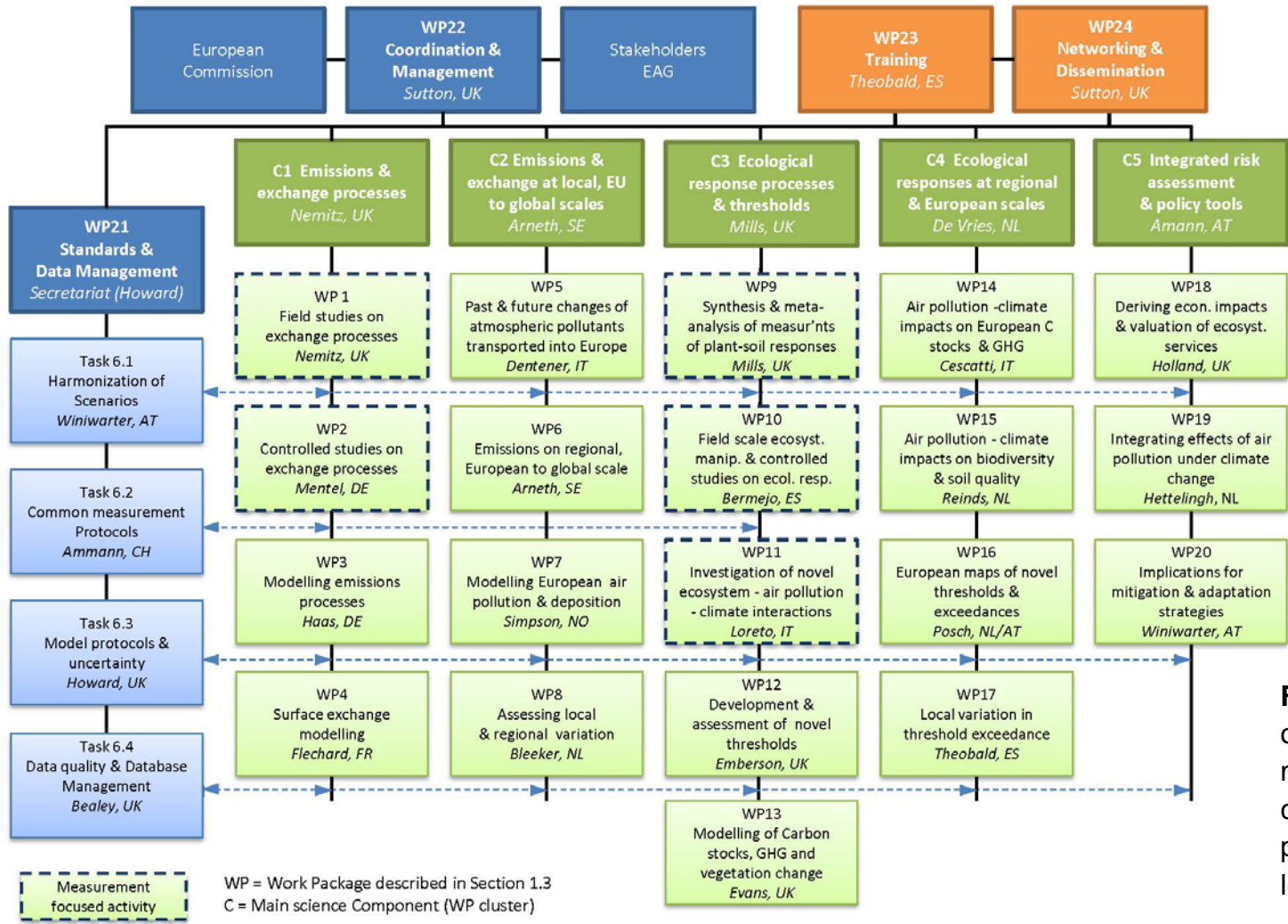
ÉCLAIRE Third Periodic Report: November 2015

2.2 Work progress and achievements during the period

Tables 0.2 and 0.3 provide an overview of person months by beneficiary and work package, 'budgeted' and 'actual'. Table 0.2 provides information for this period, and Table 0.3 for the whole project. Please note that the 'budgeted' figure is an indicative one only; it is derived by multiplying person months by the length of the first period, over the total length of the project (i.e. budgeted person months = total person months x 18/48).

Table 0.2: Person months by work package, for the third period of the project. Budgeted months are in italics on a grey background. Actual person months spent on the project are non-italic on a white background.

Beneficiary no. & short-name	WP1		WP2		WP3		WP4		WP5		WP6		WP7		WP8		WP9		WP10		WP11		WP12		WP13		WP14		WP15		WP16		WP17		WP18		WP19		WP20		WP21		WP22		WP23		WP24		Total	
1 - NERC	*6.0*	3.9	*0.3*	0.1	*0.5*	0.2	*1.0*	0.5			*0.4*	1.8			*1.8*	1.8	*1.8*	0.4	*3.5*	7.2	*4.8*	9.8	*1.5*	0.8	*3.0*	4.2	*13.5*	6.0	*1.8*	0.0			*1.3*	1.3	*0.2*	0.7	*0.2*	0.7	*0.8*	0.4	*3.3*	5.3	*13.0*	4.1	*0.3*	0.0	*0.3*	2.3	*58.8*	51.3
2 - ULUND											*0.1*	0.0													*0.0*	1.0																							*0.1*	1.0
3 - DTU																	*0.5*		*6.5*	2.4			*0.5*																						*0.1*	0.4			*7.6*	2.8
4 - ALTERRA											*0.5*	0.0					*0.5*	0.0							*1.5*	0.1	*2.3*	1.6	*1.8*	1.1	*1.3*	1.2	*1.0*	1.4	*0.5*	0.9			*0.2*	0.2	*0.8*	0.6				0.0	*0.1*	0.2	*10.3*	7.4
5 - IIASA																											*0.3*	0.1					*0.3*	0.1			*0.8*	0.9	*1.8*	1.9	*4.5*	2.7	*0.8*	0.9			*0.1*	0.0	*8.4*	6.6
6 - met.no							*0.3*	1.5	*0.3*	0.1			*4.3*	7.6			*0.3*	0.3																	*0.8*	0.2					*0.8*	0.3							*6.5*	10.0
7 - Juelich	*0.3*	1.0	*2.8*	3.2											*0.8*	3.1																																	*3.8*	7.2
8 - ECN	*2.5*	1.2															*1.8*	1.3																					*0.8*	0.1									*5.0*	2.6
9 - CNR	*0.5*		*4.5*																		*6.0*	3.0																											*11.0*	3.0
10 - KIT	*0.3*	0.0	*0.3*	0.0	*3.0*	0.0			*1.0*	0.0	*2.4*	2.7	*2.3*				*0.5*	0.0							*3.0*	11.3	*2.5*	18.0											*2.0*						*1.3*				*18.4*	32.0
11 - JRC	*3.0*	1.0							*1.8*	1.0			*1.0*														*2.0*	5.7											*1.0*										*8.8*	7.7
12 - SEI-Y,UoY							*1.5*	1.9									*0.8*		*2.8*	5.3			*2.8*	5.3	*2.3*	0.7									*0.5*	0.2					*0.1*								*7.8*	8.1
13 - INRA	*12.3*	8.6			*2.8*	0.3	*6.8*	4.8							*5.3*	1.7																														0.0			*27.0*	15.4
14 - RIVM																									*0.2*	0.2			*0.8*	0.8	*0.8*	0.8	*1.3*	1.3			*0.8*	0.8	*1.0*	1.0	*0.2*	0.4							*5.1*	4.9
15 - EDEA-ART	*9.0*	8.0																	*0.5*	0.5																					*0.3*	0.0							*9.8*	8.5
16 - UGOT							*0.8*	0.8									*0.8*	0.8					*1.5*	1.5																									*3.0*	3.0
17 - ERTI - FRI	*7.5*	7.5																																																*7.5*	7.5
18 - FMI	*1.3*						*1.8*	3.5																																										*3.0*	3.5
19 - UHEL	*3.3*																																																	*3.3*	0.0
20 - UNICATT	*5.5*	2.5																	*9.0*	8.0																														*14.5*	10.5
21 - ONU	*4.5*	5.0																													*0.5*																			*5.0*	5.0
22 - BOKU			*6.0*	6.0																			*1.8*	1.8																					*0.1*	0.1			*7.8*	7.8
23 - UPM	*1.5*	0.2			*1.0*	0.2											*0.8*	1.3																	*2.0*	2.8									*0.5*	0.0			*5.8*	4.4
24 - CIEMAT																			*5.5*	4.0																													*5.5*	4.0
25 - CNRS									*4.0*	10.5	*1.3*	0.6	*2.0*	0.9																																			*7.3*	12.0
26 - SMHI													*1.3*	1.1																											*0.3*	0.3							*1.5*	1.4
27 - DHMZ							*4.0*	7.9																																										*4.0*	7.9
28 - UEDIN											*0.8*	14.9																													*0.3*	0.3	*6.0*	8.4	*0.3*	0.3			*7.4*	23.9
29 - UBO																					*6.0*	0.2																												*6.0*	0.2
30 - WSL																					*1.3*	2.0																												*1.3*	2.0
31 - IVL																					*0.5*	0.7			*0.3*	0.0													*0.5*	0.4									*1.2*	1.0
32 - MPG																											*3.0*	0.5																							*3.0*	0.5
33 - IPBPSS																											*6.0*	6.0			*6.0*	6.0																	*12.0*	12.0
34 - EMRC																																									*2.0*	3.6									*2.0*	3.6
35 - AU											*1.0*	1.0					*0.4*	0.2																							*0.8*	4.2									*2.1*	5.4
36 - WU							*1.5*	0.2					*0.5*																																					*2.0*	0.2
37 - ULB	*0.3*	0.0															*1.0*	0.0																																*1.3*	0.0
38 - BAS - IFRG			*3.3*	2.0																																														*3.3*	2.0
39 - TNO													*1.0*	0.6																																				*1.0*	0.6
Total	*57.6*	39.0	*17.0*	11.3	*7.3*	0.6	*17.5*	21.0	*7.0*	11.6	*6.4*	21.0	*13.0*	13.3	*11.6*	6.5	*5.9*	3.9	*25.0*	22.1	*18.5*	14.7	*6.7*	7.7	*10.0*	17.3	*30.3*	38.6	*4.3*	1.9	*10.0*	8.8	*4.3*	5.4	*5.5*	10.7	*4.2*	4.9	*6.4*	3.7	*8.6*	7.4	*19.0*	12.5	*1.2*	0.4	*1.8*	2.8	*298.8*	287.0

Table 0.3: Person months by work package, for the whole project. Budgeted months are in italics on a grey background. Actual person months spent on the project are non-italic on a white background.

Beneficiary number and short-name	WP 1		WP 2		WP 3		WP 4		WP 5		WP 6		WP 7		WP 8		WP 9		WP 10		WP 11		WP 12		WP 13		WP 14		WP 15		WP 16		WP 17		WP 18		WP 19		WP 20		WP 21		WP 22		WP 23		WP 24		Total	
1 - NERC	*24.0*	34.6	*1.0*	1.7	*2.0*	2.1	*4.0*	5.4			*1.5*	3.8			*7.0*	2.9	*7.0*	12.0	*14.0*	18.7	*19.0*	32.0	*6.0*	3.1	*12.0*	14.3	*54.0*	38.9	*7.0*	6.3			*5.0*	4.7	*0.8*	1.6	*0.8*	1.1	*3.0*	2.3	*13.0*	31.5	*52.0*	34.1	*1.0*	0.0	*1.0*	5.3	*235.1*	256.2
2 - ULUND											*0.5*															1.0																							*0.5*	1.0
3 - DTU																	*2.0*	0.0	*26.0*	33.1			*2.0*	0.0																					*0.5*	0.4			*30.5*	33.5
4 - ALTERRA							*2.0*	3.0									*1.9*	2.4							*6.0*	5.8	*9.0*	11.7	*7.0*	6.0	*5.0*	5.1	*4.0*	4.0			*2.0*	2.7	*0.9*	0.4	*3.0*	3.1			*0.3*	0.3			*41.1*	44.4
5 - IIASA																											*1.0*	1.0			*1.0*	1.0			*3.0*	3.0	*7.0*	7.0	*18.0*	18.0	*3.0*	3.0			*0.5*	0.5			*33.5*	33.5
6 - met.no							*1.0*	6.4	*1.0*	2.4			*17.0*	16.9	*1.0*	1.4															*3.0*	1.1					*3.0*	1.2											*26.0*	29.5
7 - Juelich	*1.0*	5.1	*11.0*	34.3									*3.0*	9.4																																				*15.0*	48.9
8 - ECN	*10.0*	12.1													*7.0*	4.8																									*3.0*	0.3							*20.0*	17.2
9 - CNR	*2.0*	4.0	*18.0*	28.0																	*24.0*	9.0																											*44.0*	41.0
10 - KIT	*1.0*	1.4	*1.0*	1.5	*12.0*	10.5			*4.0*	2.0	*9.5*	12.2	*9.0*	4.5	*2.0*	2.0									*12.0*	19.8	*10.0*	23.0													*8.0*	0.0					*5.0*	0.0	*73.5*	76.9
11 - JRC	*12.0*	1.4							*7.0*	2.6					*4.0*	0.3											*8.0*	18.7													*4.0*	0.2							*35.0*	23.3
12 - SEI-Y,UoY							*6.0*	12.9									*3.0*	3.4									*11.0*	20.9	*9.0*	0.9									*2.0*	0.2							*0.2*	0.0	*31.2*	38.3
13 - INRA	*49.0*	61.1			*11.0*	6.8	*27.0*	40.9											*21.0*	25.1																											*0.0*	1.4	*108.0*	135.3
14 - RIVM																									*0.9*	0.7	*0.9*	0.6	*3.0*	5.3	*3.0*	3.0	*5.0*	7.1			*3.0*	1.9	*4.0*	3.9	*0.9*	1.4							*20.6*	23.7
15 -FDEA-ART	*36.0*	37.0															*2.0*	3.0																							*1.0*	1.5							*39.0*	41.5
16 - UGOT							*3.0*	2.7									*3.0*	3.2					*6.0*	5.6		0.0																							*12.0*	11.4
17 - ERTI - FRI	*30.0*	37.5																																																*30.0*	37.5
18 - FMI	*5.0*	0.0					*7.0*	12.0																																										*12.0*	12.0
19 - UHEL	*13.0*	11.0																																																*13.0*	11.0
20 - UNICATT	*22.0*	22.0																			*36.0*	33.3																											*58.0*	55.3
21 - ONU	*18.0*	20.5																													*2.0*	0.0																	*20.0*	20.5
22 - BOKU			*24.0*	37.6																			*7.0*	1.8																					*0.2*	0.1			*31.2*	39.4
23 - UPM	*6.0*	5.4					*4.0*	4.5									*3.0*	5.6															*8.0*	7.0											*2.0*	2.6			*23.0*	25.1
24 - CIEMAT																					*22.0*	23.3																											*22.0*	23.3
25 - CNRS									*16.0*	13.8	*5.0*	13.4	*8.0*	12.5																																			*29.0*	39.7
26 - SMHI													*5.0*	5.6																											*1.0*	1.3							*6.0*	6.9
27 - DHMZ							*16.0*	22.3																																										*16.0*	22.3
28 - UEDIN											*3.0*	35.9																			*0.0*	7.0									*1.3*	0.6	*24.0*	22.8	*1.3*	0.6			*29.6*	66.9
29 - UBO								8.1													*24.0*	25.3																											*24.0*	33.4
30 - WSL																	*5.0*	7.2																															*5.0*	7.2
31 - IVL																	*1.8*	1.8					*1.0*	1.0		0.0													*2.0*	1.9									*4.8*	4.7
32 - MPG																											*12.0*	9.5																					*12.0*	9.5
33 - IPBPSS																											*24.0*	24.0			*24.0*	26.0															*48.0*	50.0
34 - EMRC																																			*8.0*	8.5													*8.0*	8.5
35 - AU											*4.0*	3.2			*1.5*	1.6																			*3.0*	4.3													*8.5*	9.1
36 - WU							*6.0*	5.9							*2.0*	1.5																																	*8.0*	7.4
37 - ULB	*1.2*	1.0													*4.0*	3.7																																	*5.2*	4.7
38 - BAS - IFRG					*13.0*	13.0																																											*13.0*	13.0
39 - TNO															*4.0*	5.0																																	*4.0*	5.0
Total	*230.2*	254.2	*68.0*	116.1	*29.0*	23.9	*70.0*	116.6	*28.0*	20.9	*25.5*	71.5	*52.0*	55.8	*46.5*	47.0	*23.7*	29.9	*100.0*	111.5	*74.0*	68.0	*26.9*	31.3	*39.9*	42.3	*121.0*	132.0	*17.0*	15.2	*40.0*	47.2	*17.0*	15.6	*21.8*	21.3	*16.8*	15.9	*25.8*	22.4	*34.3*	41.1	*76.0*	56.9	*4.7*	4.7	*7.3*	6.5	*1,195.3*	*1,367.9*

ÉCLAIRE Third Periodic Report: November 2015

Figure 0.1: Schematic of ÉCLAIRE highlighting main science components, work packages and task leaders.

ÉCLAIRE Third Periodic Report: November 2015

2.1.1 Component 1: Emissions and Exchange Processes

Lead contractor: NERC

Component objectives

The specific objectives stated in the DoW that rely directly on Component 1 are:

S1. To develop improved process-based emissions parameterization of NH_3, NO and VOCs from natural and agricultural ecosystems in response to climate and pollutant deposition for incorporation into atmospheric Chemistry-Transport Models (CTMs), based on existing and new flux measurements in the field and laboratory, applying these to develop spatially resolved emission scenarios in response to climate, CO_2 and air pollutant change [WPs 1, 2, 3].

S3. To develop improved multi-layer dry deposition / bi-directional exchange parameterisations for O_3, NO_x, NH_3, VOCs and aerosols, taking into account near-surface chemical interactions and the role of local/regional spatial interactions, based on existing and new flux measurements and high resolution models and to estimate European patterns of air concentrations and deposition under climate change [WPs 1, 2, 4].

S9. To quantify the overall economic impacts of air pollution effects on land ecosystems and soils, including the valuation of ecosystem and other services, and the extent to which climate change contributes by altering emissions *versus* ecosystem vulnerability [WPs 2, 3, 4].

Progress and Key Results

Component 1 of ÉCLAIRE has been successful and met all objectives, deliverables and milestones. As would be expected, during the third reporting period WPs 1 and 2 focussed primarily on the final analysis and publication of measurements made during previous reporting periods, whilst the bulk of the activity in Component 1 was in WPs 3 and 4 which were now in the position to make full use of new data and modelling exercises to develop new parameterisations and work with related upscaling WPs in Component 2 (i.e. with WPs 6 and 7) in feeding upscaling the effects.

The wealth of measurements of WP 1 and 2 were fed through to the modelling and impact assessment to various degrees, as already planned in the Description of Work. The field studies included development of instrumentation and new analysis procedures and the full analysis of the associated measurements necessarily continued until the end of the project. Similarly, some of the controlled environment experiments were addressing novel responses and interactions and have highlighted areas where future research will be

necessary until the measurement database is sufficiently comprehensive that generalised parameterisations can be derived. It is anticipated that where the ÉCLAIRE process measurements could not be used to underpin the upscaling work, the next generation will be able to continue to exploit the well documented and archived ÉCLAIRE database, similar to the process by which ÉCLAIRE has been able to use data from former (EU) projects, including the FP6 NitroEurope IP, which could not be utilised fully for upscaling in those projects.

WP 1: Field studies on exchange processes

With 2013 having been the central year of measurements across the flux network, during this final reporting period (RP3), work focussed on the analysis of the results. This has happened both at the individual sites and across the network.

At the site level, selected highlights from RP3 include:

a) New VOC measurements at the Auchencorth site confirmed significant isoprene emissions from moorland and enabled emission factors to be derived with which the effect of climate change on moorland emissions can be assessed.
b) Aerosol fluxes were processed for Auchencorth, Speuld and Bosco Fontana and these formed the basis for a new empirical parameterisation of aerosol deposition velocities, accounting for the dissociation of NH_4NO_3 during the deposition process.
c) The first-ever field soil NO fluxes in Ukraine have resulted in a detailed picture of how NO exchange depends on combinations of drivers (soil NH_4^+, soil NO_3^-, soil temperature and soil water content), in support of the LandscapeDNDC development (cf. WP4 below).

Several cross-site analysis were conducted:

a) A statistical analysis was conducted in an attempt to identify the instantaneous effect of O_3 on net ecosystem exchange (NEE) of CO_2 at the ÉCLAIRE forest sites. The main driver of NEE is solar radiation, followed by temperature in the coniferous forests of N Europe (Netherlands & Finland), Leaf Area Index (LAI) at the deciduous site in N Italy and water availability at the S. European evergreen broadleaf site (S. Italy). Instantaneous O_3 had a significant negative effect only at the S. Italian site (all year) and the Dutch site in summer, where O_3 episodes are largest. Ozone averaged over the previous 24-hours, however, had a statistically significant negative effect at all sites.
b) The O_3 flux, canopy conductance as well as split into stomatal and non-stomatal pathways were compared with the predictions from a global chemistry and transport model. The stomatal dose predicted by the model significantly exceeds the stomatal dose derived from the field measurements. This suggests that there is further need in verifying the model predictions against fluxes of CO_2 and H_2O, also indicates that

ÉCLAIRE Third Periodic Report: November 2015

conventional methods of deriving stomatal conductance from field measurements may result in underestimates. Whilst ÉCLAIRE has highlighted an important issue here, investigations will need to carry on.

c) The VOC emission factors originating from the ÉCLAIRE work have been compiled, with particular emphasis of isoprene emissions from oak species. ÉCLAIRE has almost doubled the availability of measurements in this area.

d) Soil flux measurements of NO at suitable ÉCLAIRE sites have been used to further develop and/or assess the LandscapeDNDC model (cf. WP 4 below).

In addition, the analysis of the data from the ÉCLAIRE integrated campaign at Bosco Fontana, Po Valley, Italy, was finalised and four papers were written on the chemical interactions that could only be addressed by bringing together a large number of institutes. Two papers on the exchange of volatile organic compounds with the mixed hornbeam-oak forest, the comparison of measurement approaches and the interactions of VOCs with chemistry have been submitted to *Atmos. Chem. Phys*. Two other manuscripts are being tidied up for publication, dealing (a) with the N dry deposition budget of the site and the interaction of N compounds in the gas and aerosol phase and (b) the partitioning of the total ozone flux both in terms of height and exchange pathway (deposition through stomata, to soil, cuticles and chemical destruction).

WP 2: Controlled studies on exchange processes

Much of the work planned for WP 2 had been completed prior to this reporting period. The three areas in which further progress has been made are:

a) Gas exchange with soil monoliths and litter samples at BOKU had previously focussed on the exchanges of NO, N_2O, CH_4 and CO_2, and were extended by a measurement of NH_3. These show how litter emission of NH_3 are controlled by C: N ratio as well as water content and how they interact with emissions of NO.

b) ÉCLAIRE conducted some of the first controlled gas exchange measurements of isoprene oxidation products (iox) with plants under realistic concentrations. The measurements show that, in unstressed plants, constitutive emissions of these oxidation products are negligible and that compensation points are very small, thereby allowing iox deposition. Removal of these compounds from the air by deposition is very effective and there is no indication of saturation at ambient concentrations. This is consistent with some (but not all) of the field evidence which can only derive iox deposition rates indirectly. The results are being fed into parameterisations used in chemistry and transport models.

c) New measurements at the Juelich coupled plant-smog chamber system focussed on the effect of drought and recovery from drought on monoterpene emissions, distinguishing between constitutive *de-novo*, constitutive pool and stress induced emissions with a ^{13}C labelling technique. In addition, some of the measurements

previously reported on the measurements of the net effects of plants on ozone, once uptake and emission of ozone precursors are taken into account, were redone after a VOC interference of the commercial O_3 analyser was identified.

WP 3: Modelling emissions processes

There has been major activity in this WP during this reporting period.

An emission meta-model of NH_3 from fertiliser application has been further refined with focus on the temporal emission dynamics, by parameterising a Michaelis-Menten relationship against 1044 runs with the Volt'Air emission process model. The refined meta-model was then run for an example European grid cell to demonstrate its applicability in the context of a regional chemistry and transport model.

A sensitivity study was conducted to assess the response of emissions of NO and NH_3 with climate change (MS13). For this purpose simple meteorological scenario time-series were constructed by modifying the measurements made at the agricultural ÉCLAIRE flux site at Grignon, France (temperature +2, +4, +6°C; rainfall -20%, +20%). The Volt'Air process model revealed that temperature had the largest effect, suggesting an increase in the TAN fraction emitted as NH_4^+ by 12 (+2°C scenario) to 30% (+6 °C scenario). An increase in rainfall induced only a small reduction in TAN emission.

A further focus was work to improve the model framework of NH_3 exchange with vegetation. For this an existing generalised bidirectional exchange model was evaluated and improved further. The performance of the model was assessed against a number of measurement datasets (from NitroEurope, ÉCLAIRE and beyond) that were not used for the development of the original parameterisation (D3.2). In addition, the existing model had major limitations in predicting the NH_3 emission potential of fertilised vegetation and agricultural soils which was not linked to soil types and could result in emissions that are not mass constrained (i.e. potentially more could be emitted than was applied as fertiliser). To improve this part of the model, the CERES-EGC agro-ecosystem model was run to provide an offline map of emission potentials at 0.25° x 0.25° which can be used for European-scale chemistry and transport modelling. This model was run with a pH soil database, the agricultural management information extracted from the GHG-Europe project database as well as meteorological scenario data (RCP5.5 and RCP8.5) from the HadGEM2-ES climate model. The average temperature-normalised emission potential from soils showed only small seasonality, with the most extreme values occurring in Feb to July. The foliar temperature-normalised emission potentials peaked in the winter months, but the absolute dynamic range was rather small and is likely to be over-compensated by the direct temperature effect on emissions, which will still lead to the highest emission potential during the warmest months. In addition to agricultural intensification, soil pH is the prime controller of soil emission potentials spatially, resulting in particularly high emission potentials in E Spain, Italy, Bulgaria and Romania, although pH data for the latter two countries is less certain. Larger future soil emission potentials

are calculated with the RCP8.5 data than for RCP5.5, especially for N Europe, as it results in a different soil water content in the top soil layer. For the foliar compensation point the opposite was observed, except for southern Spain, which can be explained by increased growth (and thus N dilution) in all but water limited regions under the RCP8.5 scenario. A metamodel was fitted to the detailed CERES-EGC results for incorporation into CTMs.

Work has been finalised on the development of a new soil biogeochemical module for LandscapeDNDC, capable of simulating combined soil emissions of NO and N_2O from mineral soils (forests, arable and grassland). Bayesian calibrations against measurement data were used to narrow down the parameter distributions of the 15 most important process parameters. Model performance was assessed against 23 datasets each covering up to 15 years of measurements. Overall model performance was better for forests than for agricultural systems. The importance of chemo-nitrification results in a non-linear decrease in mean NO emission with increasing soil pH, whilst the emission is significantly positively correlated with atmospheric N deposition. The applicability of LandscapeDNDC at the regional scale was demonstrated at high spatial resolution for the German state of Saxony.

LandscapeDNDC was used to establish the climate sensitivity of NO fluxes using an analogous approach to the work on NH_3 emissions described above and the results were reported in the report that supports MS13. NO emissions were found to increase by about 4% per 1 K increase in average temperature and decrease slightly (< 1% change for a 10% change in precipitation) with increasing precipitation at the Grignon site. Similar responses, but of different magnitude, were found for forest sites. Changes in agricultural management (including those in response to climate change) are likely to dwarf direct climate impacts.

WP 4: Surface exchange modelling

As with WP3, much progress in this work package was achieved during this final reporting period. Early in the project it was realised that a true step change in biosphere / atmosphere exchange modelling required the development of a coupled exchange – transport – chemistry model that can be linked to a CTM and that is scalable to assess simplified modelling approaches against a state-of-the-art version of the model that embodies the current process understanding. ÉCLAIRE therefore took on an additional task that was not originally planned, to develop the ESX (ÉCLAIRE Ecosystem Surface eXchange) model. This has also been used as a focus to inform further developments on synthesising existing and new datasets into this ESX modelling system. This significantly increased the ambition compared with the original work programme and it eventually emerged that the ESX development was progressing too slowly to rely entirely on this concept. Thus, although ÉCLAIRE has made a significant start with the development of the ESX system, it will require further work beyond the duration of the project and in the

final year of ÉCLAIRE alternative schemes have been updated and developed, effectively returning to the original DoW for project delivery, albeit with some delay. In the longer, term however, this strategy has allowed ÉCLAIRE to develop a much more coherent foundation for future work, especially within the Convention on Long-range Transboundary Air Pollution (LRTAP).

For this Work Package the updated NH_3 exchange model described in WP3 above was developed further into a modelling system to simulate bi-directional ammonia exchange not only with agricultural but also semi-natural vegetation, incorporating the emission potential simulated offline with a meta-model trained on the CERES-EGC crop model and the VOLT'Air NH_3 volatilisation model (D4.1).

A mechanistic model (DEWS) that simulates the chemical processes on the leaf surfaces and thus predicts the equilibrium vapour concentration above the leaf cuticle was translated into FORTRAN earlier in the project and has now been updated to incorporate the AIOMFAC thermodynamic model which takes over when leaf water layers dry out so much that they become highly concentrated, non-ideal solutions and can be treated in analogy to aqueous aerosol.

Based on aerosol flux measurements at Speuld, Bosco Fontana (Po Valley, Italy) and Auchencorth (Scotland, UK) an empirical parameterisation was developed that corrects dry deposition velocities of volatile aerosol (NH_4NO_3) for the effect of dissociation during the deposition process. This has been tested at the European scale, causing a 30% reduction in fine nitrate concentrations at the surface at the annual average across Europe.

To improve the dry deposition parameterisation of ozone, three surface/atmosphere exchange models (DO3SE, SURFATM and MUSCIA) were developed further and tested against flux data from ÉCLAIRE and previous EU and national projects. Each model was examined with a different focus: DO3SE on stomatal exchange and link with photosynthesis; SURFATM on ground surface deposition, and MUSICA on O_3 deposition to wet leaf cuticles. New parameterisations have thus emerged: (i) a new stomatal uptake module (DO3SE_C) now includes a photosynthesis-based description of stomatal conductance in which the maximum carboxylation rate can be coupled to stomatal O_3 dose and N supply to simulate the effects of these two pollutants on plant growth and further O_3 uptake; (ii) a parameterisation has emerged that links O_3 deposition to bare soil to surface relative humidity; and (iii) a wet cuticular deposition module has been developed based on O_3 reaction rates in water films in relation to plant senescence.

In parallel, work has however continued on the ESX model, too. A multi-layer bi-directional exchange scheme has been introduced into the model, also incorporating the DO3SE_C model, and tested against big-leaf approaches and measurements, with emphasis on HNO_3 and O_3. One of the purposes of ESX is to assess which level of model simplification provides the best balance between being accurate and sufficiently

numerically efficient for incorporation into CTMs. The sensitivity of ESX calculations to the number of vertical layers has been tested in some detail. For O_3 the use of a single layer to describe the canopy, for example, was found to result in an error of <10% for stomatal conductance and <5% for the stomatal sink, demonstrating that the subgrid parameterisations implemented into ESX work well. Even with a single layer, ESX differs greatly from traditional exchange schemes in that it can simulate canopy storage. The effect of chemistry has been tested for simplified cases such as O_3-NO and VOC-NO_3 interactions. Comparison of ESX results with O_3 flux data from the ÉCLAIRE flux site at Hyytiala have demonstrated how the inclusion of a shrub layer (in addition to the tree canopy) improves model performance.

Progress towards the milestones and deliverables, use of resources and deviations from DoW

All outstanding milestones were met and deliverables submitted. In Component 1 this included:

D1.6. Finalisation of four papers on the ÉCLAIRE Bosco Fontana Integrated Experiment. Two are currently under review online for *Atmos. Chem. Phys.* and complete drafts of two further manuscripts were submitted within D1.6; these are being tidied up for submission to *Biogeosciences* and *Atmos. Chem. Phys.* The measurements have supported further papers beyond these four.

D2.5. This deliverable was altered into another paper during the previous RP, but a draft of the originally planned manuscript about the impacts of drought stress on BVOC emissions from conifers is now also at an advanced state of preparation.

D2.6. Advances in the parameterisation of VOC emission from plants made by ÉCLAIRE have been summarised as D2.6, focussing on (a) the response of monoterpene emissions to soil water stress, (b) isoprene emission factors from oak species and (c) the controls of gas-exchange of iox species with vegetation.

MS12 was achieved and a summary document is available that reports the application of Volt'air, CERES-EGC, the improved ÉCLAIRE bi-directional NH_3 exchange scheme and LandscapeDNDC to selected datasets from field sites of ÉCLAIRE, NitroEurope IP and other projects.

MS13 was achieved and provided a sensitivity analysis of climate change (temperature & precipitation) on emissions of NH_3 and NO from agricultural land. This MS also covers **MS22** in the DoW.

D3.2. This deliverable was submitted, describing the ÉCLAIRE improvements to an existing bi-directional exchange parameterisation, including (a) model performance assessment, (b) improvement of the non-stomatal (cuticular) uptake resistance and (c)

prediction of emission potentials through development of a meta-model trained to data produced by the CERES-EGC crop model.

D3.3. A deliverable was completed that describes the development of the LandscapeDNDC model outlined above.

D4.1, submitted during this RP3, describes the improved NH_3 biosphere / atmosphere exchange scheme for use in CTMs, including the meta-models of emission potentials from fertilised land, the improved DEWS model and the new empirical parameterisation for NH_4NO_3 aerosol under the influence of evaporation,

D4.2. A deliverable was submitted that describes the improvements ÉCLAIRE has made to the O_3 deposition models DO3SE, SURFATM and MUSICA.

D4.3. This deliverable describes the development of the DO3SE-C model and the coupling of stomatal conductance to leaf N and stomatal O_3 dose.

D4.4. A deliverable has been submitted reporting the improvements to the MLC-CHEM scheme as well as the ESX developments to date.

ÉCLAIRE Third Periodic Report: November 2015

Work Package 1: Field studies on exchange processes

Lead contractor: NERC
Contributors: JRC, FDEA-ART, FRI, ECN, UHEL, FMI, ECN, INRA(G), UNICATT, ONU, CNR, Juelich, KIT, ERTI-FRI, UPM, ULB

Work package objectives

The aim of the WP was to make field flux measurements across the ÉCLAIRE flux network and during campaigns, to provide targeted high-quality data to derive mechanistic parameterisations of biosphere/atmosphere exchange in response to environmental drivers, utilising the natural climate variability at and between sites. The specific objectives were:

1. To obtain 15 months of high temporal resolution flux data of key trace compounds (O_3, NO, CO_2, H_2O) across a 9-site European flux network for the study of fluxes in relation to climatic drivers, using changing meteorological conditions at the sites as a proxy for climate.
2. To study the exchange of additional compounds (NH_3, NO_x, VOCs) through synchronised intensive measurement periods across the 9-site flux network, in relation to meteorological drivers, and to provide a test database for the evaluation of European chemical transport models.
3. To quantify the effect of aerosols on gross primary productivity through modulating in-canopy light levels for three forest ecosystems.
4. To quantify the importance of in-canopy chemical transformations on the deposition mechanism and effective emission of biogenic compounds into the atmosphere, through an integrated intensive measurement campaign above/within a polluted forest.
5. To make targeted measurements of NH_3 exchange with Mediterranean semi-natural vegetation during distinct growth phases (active vs. dormant).

Progress and Results

Task 1.1: Long-term flux measurements across a 9-site European flux network.

As already alluded to in the first two periodic reports, there were a few changes to the network compared with the DoW:

- The Swiss site Oensingen was replaced by a similar Swiss grassland (Posieux) in response to changes of national funding.
- The Italian arable site was replaced by a forest site at Bosco Fontana to make full use of the investment ÉCLAIRE made by establishing a new tower for the integrated experiment (c.f. D1.5).

ÉCLAIRE Third Periodic Report: November 2015

- A further associate site (Italian forest site at Castelporziano) has delivered data to the database at no cost to the project.

The original plan was to start measurements in August 2012 and continue for 12 to 15 months. Due to delays with the setups, partly associated with the deployment of instruments for Task 1.4 in the Po Valley in July 2012, some sites started later (cf Table 1.1) and it was therefore decided that all sites should continue to run for the entire calendar year of 2013, with some sites reporting data beyond this period.

Table 1.1: Overview of the measurement approaches for O_3 and NO at the ÉCLAIRE flux network sites.

Ecosystem	Site	Period of O_3 flux measure-ments	Type of fast O_3 analyser	NO_x flux approach
Forest	Hyytiala (FI)	01/08/2012	LOZ-3 / Sextant	$NO/NO_2/O_3$ gradient
Forest	Speuld (NL)		Sextant	$NO/NO_2/O_3$ gradient; auto-chamber (1)
Forest	Bosco Fontana (IT)	13/07/2012	COFA	$NO/NO_2/O_3$ gradient
Forest	Ispra Forest (IT)	30/07/2012	NOAA	$NO/NO_2/O_3$ gradient
Forest	Castelporziano (IT)*	26/01/2012 – present	NOAA	
Grassland	Bugac (HU)	01/08/2012	Enviscope	Auto-chamber (2), manual chamber (2), $NO/NO_2/O_3$ gradient
Grassland	Auchencorth Moss (UK)	12/11/2012 – present	ROFI	Auto-chamber (4 + 1) + $NO/NO_2/O_3$ gradient
Grassland	Posieux (CH)	01/08/2012	Enviscope	NO/Nr eddy-covariance
Arable	Grignon (FR)	07/08/2012	Sextant	NO/NO_2 eddy-covariance
Arable	Potrodolinskoye (UE)	13/09/2012	ROFI	Auto-chamber (4+1)

The ÉCLAIRE flux network provided the first synchronised multi-site database of ozone fluxes measured with a harmonised eddy-covariance approach (Figure 1.1). In collaboration with COST Action ES0804 (ABBA), a harmonised data processing approach was developed to maximise inter-site comparability. First time-series of the measurements were presented in the 2nd periodic report.

In ÉCLAIRE's final reporting period the flux measurements were analysed both at a site basis and in meta-analyses to quantify the fraction of the O_3 flux that enters the stomata where it can cause damage to the plant and to understand the processes controlling the stomatal and non-stomatal ozone flux. Figure 1.1 shows the time-series of the O_3 flux at

17

an example site (Castelporziano) in relation to meteorological parameters (VPD & solar radiation) and as a function of day-of-year and hour-of-day.

As discussed in more detail by Fares et al. (2015), the total ozone flux was apportioned into the stomatal component as well as the components that are deposited to soil and leaf cuticles (Figure 1.2), demonstrating that the stomatal flux accounted for <50% of the total flux overall.

In addition, a similar analysis has been conducted in a harmonised approach for the site network, taking into account one further non-ÉCLAIRE site (Lochristi, Belgium). The analyses confirm a significant contribution of non-stomatal uptake to the total ozone flux.

Using these data, a statistical analysis was performed in an attempt to identify the effect of O_3 exposure to net ecosystem exchange (NEE) in the field data from the forest sites, in a multi-step process:

a) Seasonality was removed from the NEE time series using singular spectrum analysis;
b) Artificial Neural Network analysis was used to develop the non-linear relationships between NEE and a range of drivers, including ozone concentrations and stomatal conductance (their product reflecting the stomatal ozone dose);
c) A weight approach (Olden et al., 2004) was applied to assess the importance of each driver in determining NEE; Fig. 1.4 shows the results of this process.
d) The nature of the responses to each driver were assessed using the partial derivative method of Dimopoulus et al. (1995).
e) Finally, in a sensitivity analysis ambient O_3 concentration was reduced by 10, 20 and 30%, to identify whether the Neural Network predicts significantly different NEE under these modified conditions. This analysis was conducted for the entire period as well as by season.
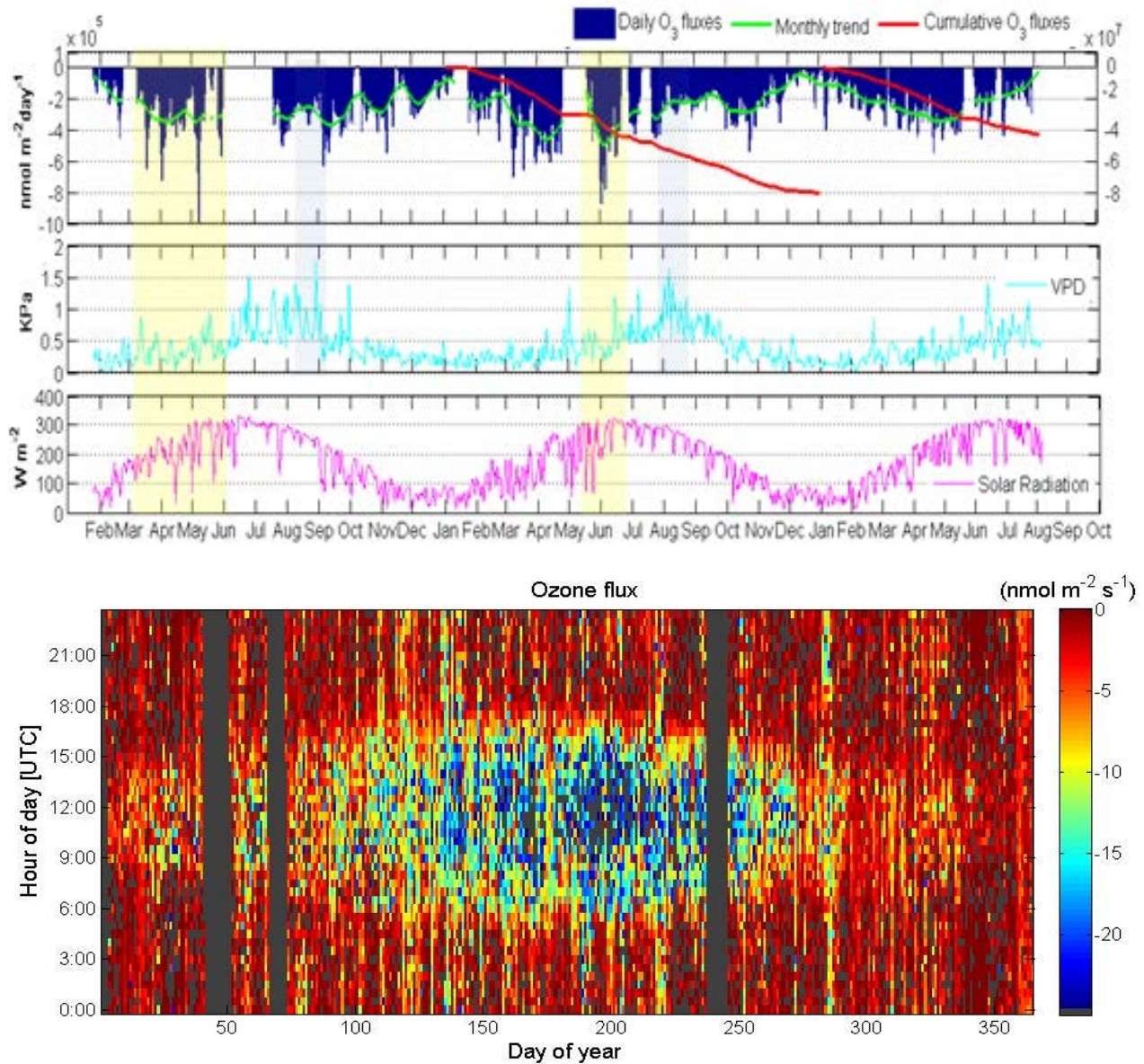
Figure 1.1. Ozone flux at Castelporizano in relation to (a) meteorological drivers and (b) time-of-day and day-of-year.
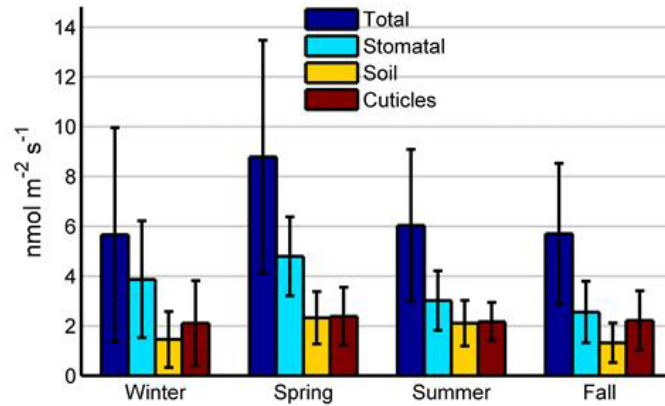
Figure 1.2. Seasonal division of the total measured ozone flux at Castelporziano into stomatal and non-stomatal components (Fares et al., 2015).
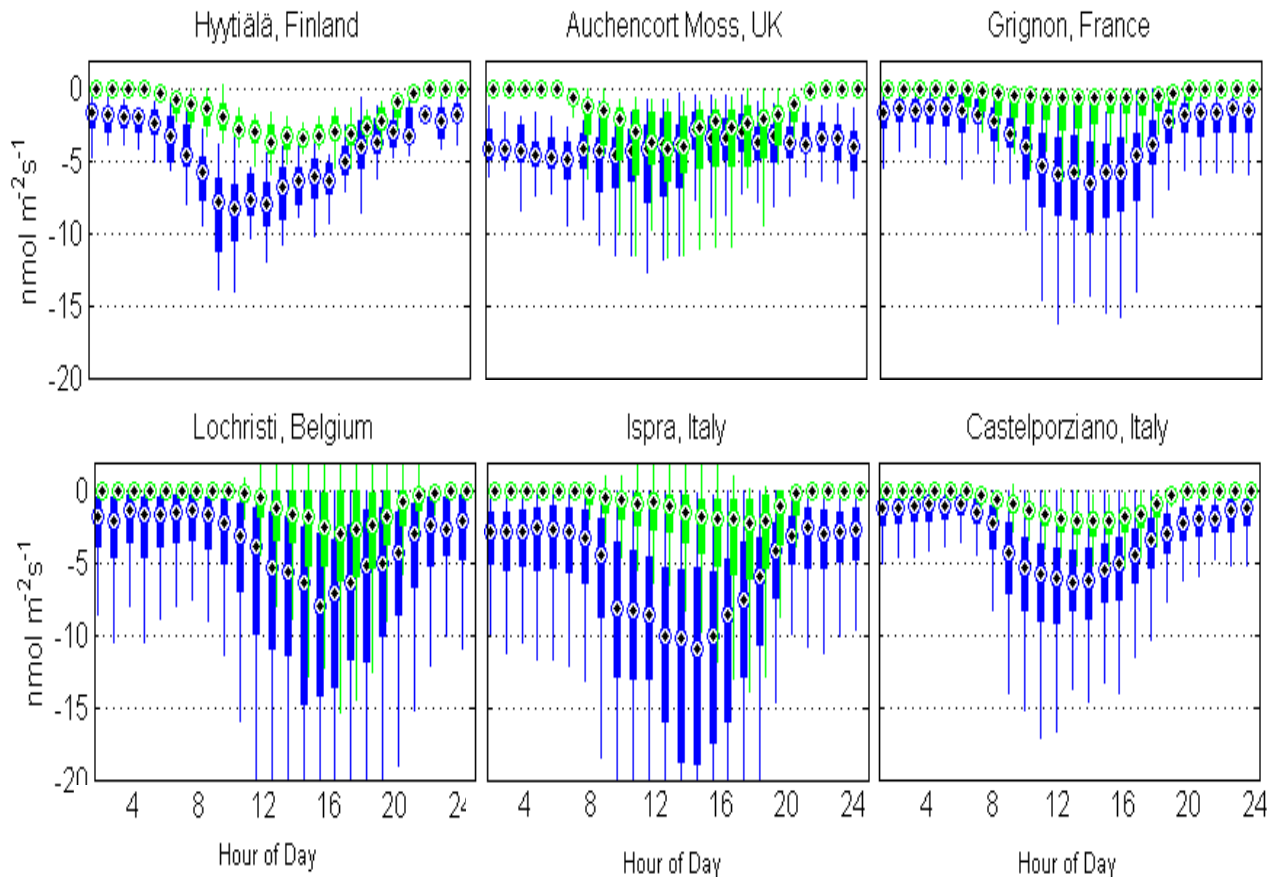
Figure 1.3. Attribution of the O_3 flux across the network. Shown is the stomatal flux estimated from the stomatal conductance derived from latent heat flux measurements (green) in comparison to the total flux (blue).
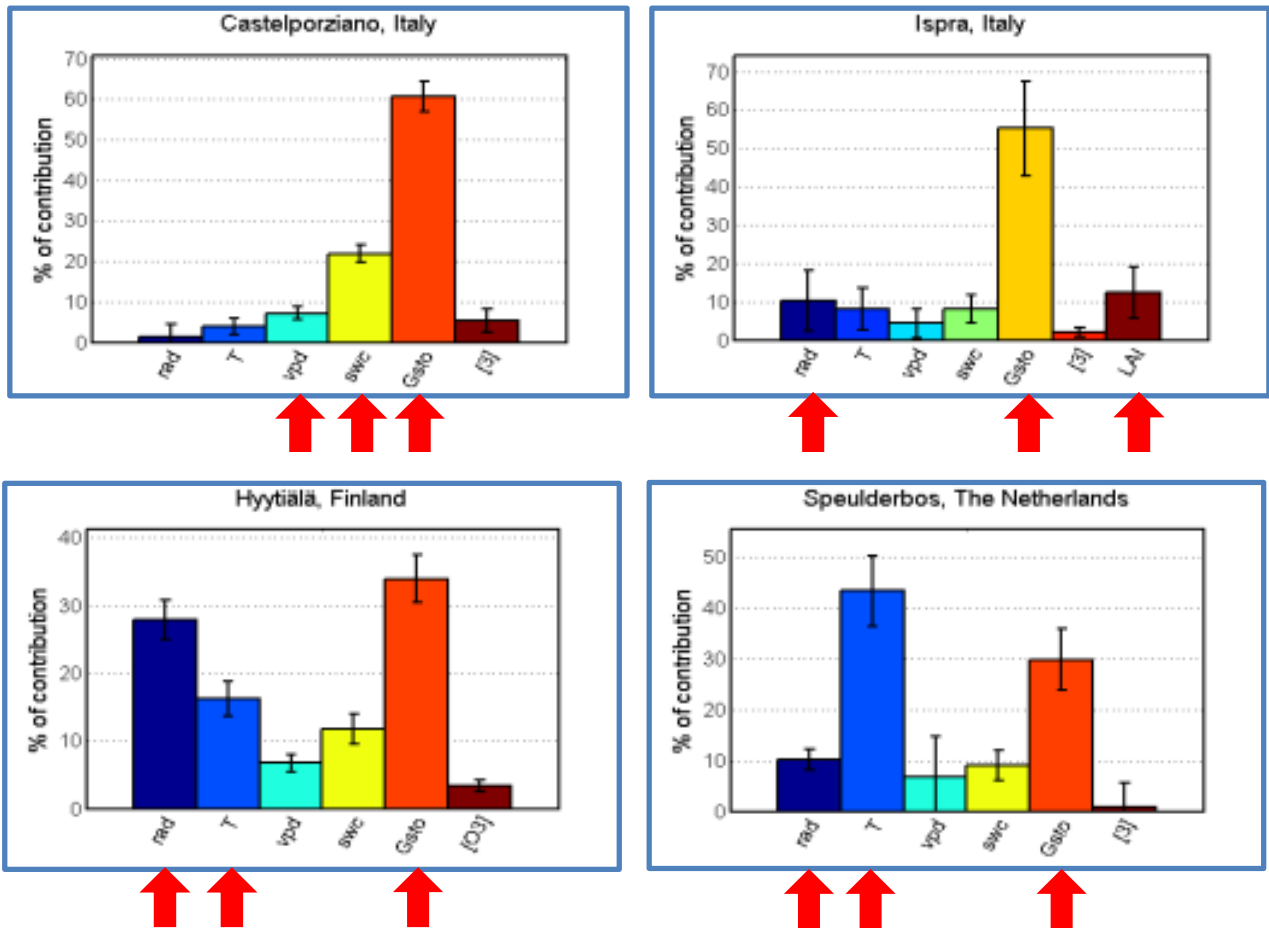
Figure 1.4: Attribution of the variability in normalised NEE to a range of drivers across the ÉCLAIRE forest flux sites (rad: solar radiation; T: ambient temperature; vpd: vapour pressure deficit; swc: soil water content; Gsto: stomatal conductance; [O₃]: ambient ozone concentration; LAI: leaf area index). The arrows indicate the main three drivers for each site.

Although the diurnal cycle was removed from the NEE time-series, stomatal conductance was found to be the strongest predictor of NEE overall. At the more northern European coniferous forests (Hyytiala & Speulderbos), temperature and radiation are the other important predictors. At the deciduous site in northern Italy (Ispra), NEE is strongly coupled to LAI, whilst at the southern Italian evergreen broadleaf forest (Castelporziano) water stress is important, reflected in vapour pressure deficit and soil moisture content (Figure 1.4). A statistically significant impact of ozone concentration on NEE could only be identified for Castelporziano. For a 10% O_3 reduction a significant increase in NEE was found for spring and the entire period, whilst for a 30% reduction NEE increased in all seasons. At Speulderbos a positive instantaneous effect of O_3 reduction was only

21

identified for the summer season, consistent with the much lower O_3 peaks at this site, which are limited to this season. Interestingly, the analysis revealed a negative effect of O_3 reduction on NEE at Hyytiala for changes exceeding 20% for almost all seasons. At this site O_3 is relatively low and a negative effect may therefore be difficult to identify. However, the apparent benefit for O_3 on NEE is probably not causal but reflects the influence of a further co-varying variable not explicitly used in the analysis.

The analysis was repeated using the ozone concentration averaged over the previous 24 hours rather than instantaneous O_3 concentration and at this point a statistically significant negative effect could be observed at all ÉCLAIRE forest sites.

The ozone flux measurements were also used to assess the prediction of ozone deposition by a global-scale chemistry and transport model. The UK Chemistry and Aerosol (UKCA) community model, a global chemistry and transport model that includes the Unified Model of the UK MetOffice, was run for the year 2013, nudged against reanalysed meteorology. Modelled and measured ozone were compared across the ÉCLAIRE site network in terms of concentration, flux, deposition velocity and allocation into stomatal and non-stomatal components. There are obvious reasons why model predictions of a global scale model may deviate from the measurements, including (a) the limitation in resolution and representation of topography, (b) the generalised description of an ecosystem type compared with actual site-specific characteristics, (c) simplified implementation of dry deposition schemes etc. Some of these can be eliminated by focussing the comparison on the canopy conductance, which eliminates the effect of some of the meteorological parameters that may not be captured correctly. The analysis indicates that although total canopy conductance agrees well at most sites, the model predicts a significantly different attribution of the ozone flux into stomatal and non-stomatal components, estimating a larger stomatal ozone dose than derived from the field data. This highlights the need to assess systematically the dry deposition scheme of the UKCA model with measurements of CO_2 exchange and water vapour fluxes. However, it does raise the question whether the approach used to estimate stomatal conductance, although commonly used in the literature, may underestimate the stomatal pathway. ÉCLAIRE has triggered this debate which will need to carry on beyond the lifetime of this project.

The other key flux measured at all sites is that of NO_x, measured either using chambers, the aerodynamic gradient approach or eddy-covariance. Figure 1.5 shows, as an example, the results from the chamber flux measurements at the Ukrainian crop site, the first if their kind in this country.
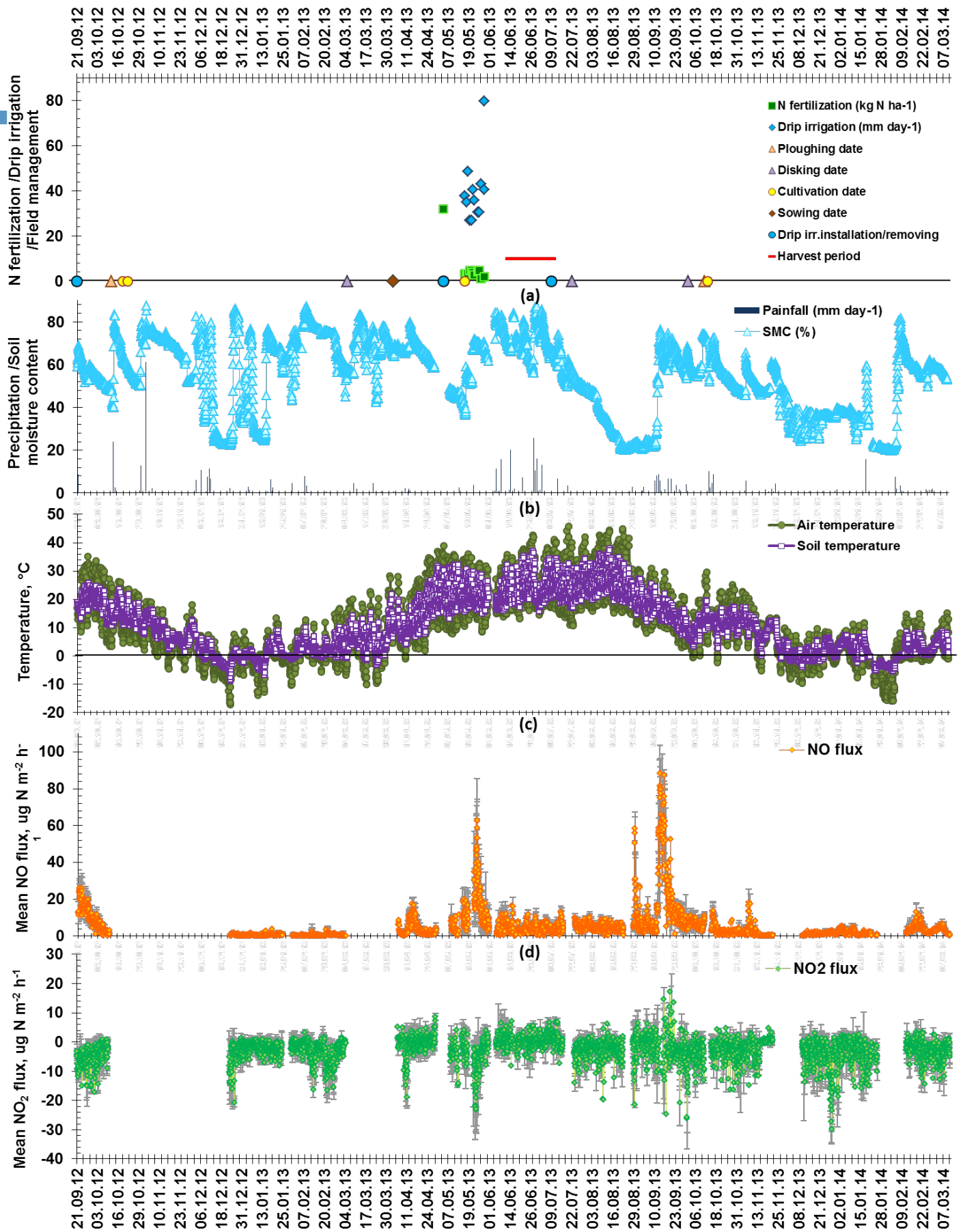
Figure 1.5: Fluxes of NO (d) and NO_2 (e) in relation to the timing of field operations and fertigation events (a), as well as temporal variability of soil moisture content (SMC) and rainfall (b), soil (5 cm soil depth) and air temperature (c) over the entire study period at Petrodolinskoe site (PTR_UA) in Southern Ukraine.

Figure 1.6 shows detailed pictures of the response of NO fluxes to a combination of drivers. Understanding of these responses contributed to the refinement of the LandscapeDNDC model, which was also assessed with the ÉCLAIRE measurements at suitable sites (i.e. non-organic soils) in WP4.
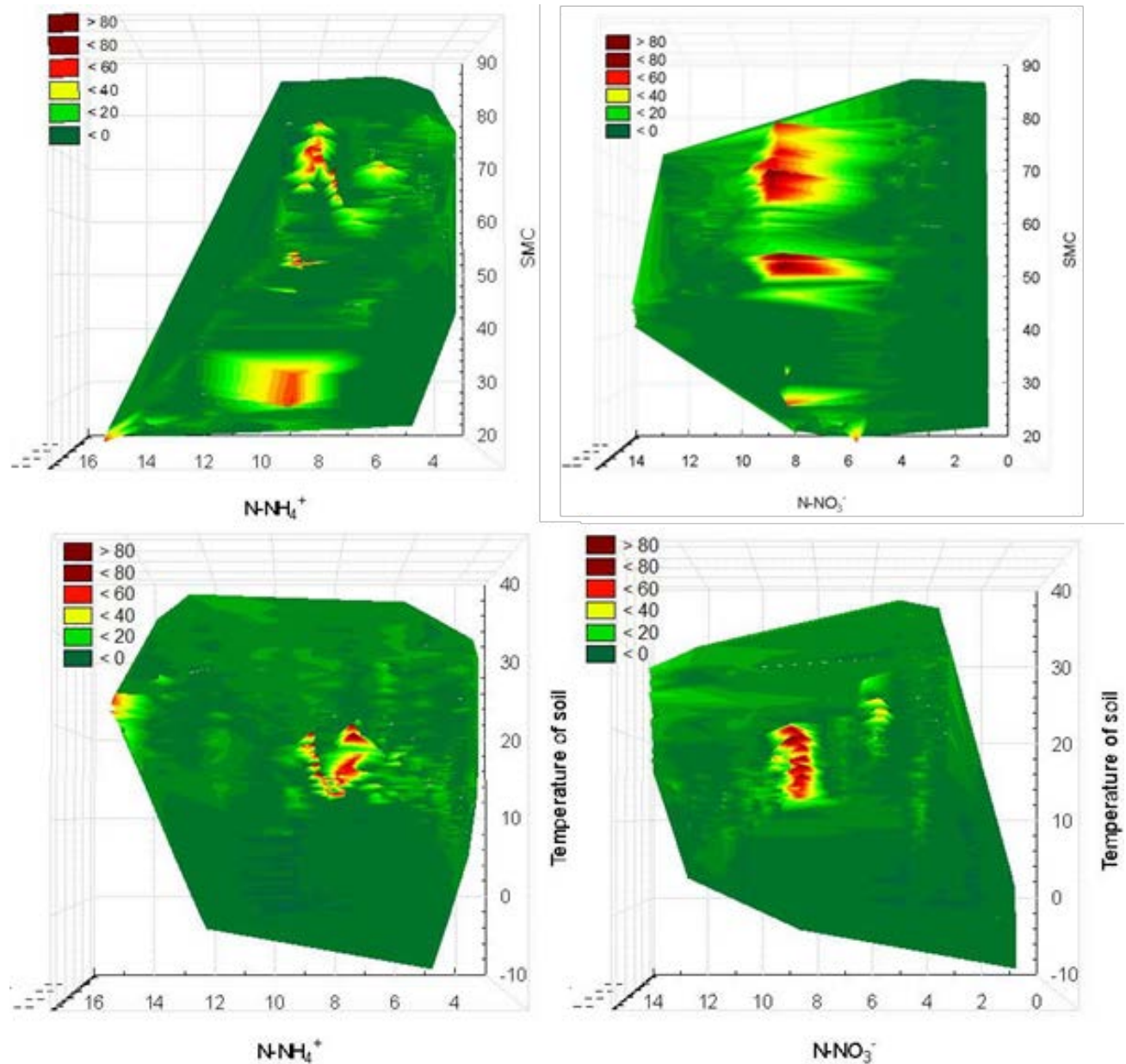
Figure 1.6: Dependence of the NO flux on driver combinations, combining soil concentrations of NH_4^+ and NO_3^- with soil moisture content (top panels) and soil temperature (lower panels).

Task 1.2: Intensive measurement periods across the flux network

Additional campaign-based measurements were implemented across the site network. Already at the ÉCLAIRE kick-off meeting, it was decided to change the original idea to make the campaign based measurements at the same times at all sites (see first report), so we could target key periods (which differ between ecosystems and with climate). This also allowed us to to make fuller use of the available instrumentation. Because this activity depended on the availability of further state-of-the-art instrumentation from national funding sources, the measurement programme had to be modified as the availability of instruments changed. For example, it turned out to be impossible to implement some of the measurements anticipated, while other opportunities became available. Due to import restrictions for further instrumentation to the Ukraine following the outbreak of the Crimean crisis in Feb 2014 the plan to make NH_3 flux measurements at this site had to be dropped, due to transport restrictions, allowing us to focus further on the instrumentation already deployed at the field site.

Flux measurements of volatile organic compounds were realised at Auchencorth, Ispra, Hyytiala, Castelporziano and, as part of Task 1.4, at Bosco Fontana, while historic measurements made under the FP6 NitroEurope IP were re-analysed and published for Speuld. ÉCLAIRE also contributed to VOC flux measurements at a French forest site (Kalogridis et al., 2014). Additional concentration measurements were made at Grignon. Ammonia fluxes were measured at Grignon, Posieux, Speuld, Bosco Fontana (Task 1.4) and also, in collaboration with other projects, at an agricultural site near Rutigliano, Italy, and recent existing data were analysed for Auchencorth.

Figure 1.7 exemplifies the isoprene fluxes measured above the mixed oak forest at Ispra. Midday fluxes averaged 25 nmol m^{-2} s^{-1} and daily maximum fluxes increased exponentially with temperatures. The rest of the variability is primarily explained by the light levels. These measurements were analysed systematically, with the emphasis to derive isoprene emission factors for European oak forests. Although oaks are estimated to account for 60% of the European isoprene emissions, emission estimates from the three dominant species are based on only seven (leaf-level) measurements (Keenan et al., 2009). ÉCLAIRE has contributed another five (canopy-scale) measurements to this database, almost doubling the data availability. Whilst canopy-scale flux measurements are directly representative of the actual emission from the forest, leaf-level measurements need to be scaled up using VOC emission models. The ÉCLAIRE analysis (Deliverable 2.4) has demonstrated that care needs to be taken when leaf level emission factors are derived from canopy scale flux measurements as these are highly dependent on the algorithm used (Figure 1.8).

Table 1.2. Overview of the campaign-based flux measurements across the ÉCLAIRE flux network

Eco-system	Site	VOCs	NH$_3$	NO$_y$	Aerosol
Forest	Hyytiala (FI)	Various (PTR-MS)			Total number
	Speuld (NL)	Analysis of NitroEurope measurements	Wet chemistry (GRAHAM gradient)		
	Bosco Fontana (IT)*	Various (PTR-MS; PTR-ToF-MS)	Wet chemistry (GRAEGOR gradient)	HNO$_3$, HONO (GRAEGOR gradient)	Water-soluble (GRAEGOR) and non-refractory (AMS EC)
	Ispra Forest (IT)	Various (PTRMS, PTR-ToF-MS); isoprene (FIS)			
	Castelporziano Forest#	Various (PTR-MS)			
Grassland	Bugac (HU)		Impossible due to power limitations		
	Auchencorth Moss (UK)§	Various (PTR-MS)	Unsuccessful; re-analysis of existing measurements	NO$_2$ EC (LIF)	non-refractory aerosol components (AMS EC)
	Posieux (CH)		By total N analyser EC	NO/NO$_2$/NO$_y$ EC	
Arable	Grignon (FR)		Wet chemistry (ROSAA gradient)	Analysis of HONO gradient measurements (LOPAP)	
	Potrodolinskoye (UE)		Impossible due to import restrictions following Crimean crisis.	Detailed spatial survey of soil emissions	

* Realised as part of the integrated campaign; # associated site; measurements not funded by ÉCLAIRE; § Final intensive measurements still ongoing.
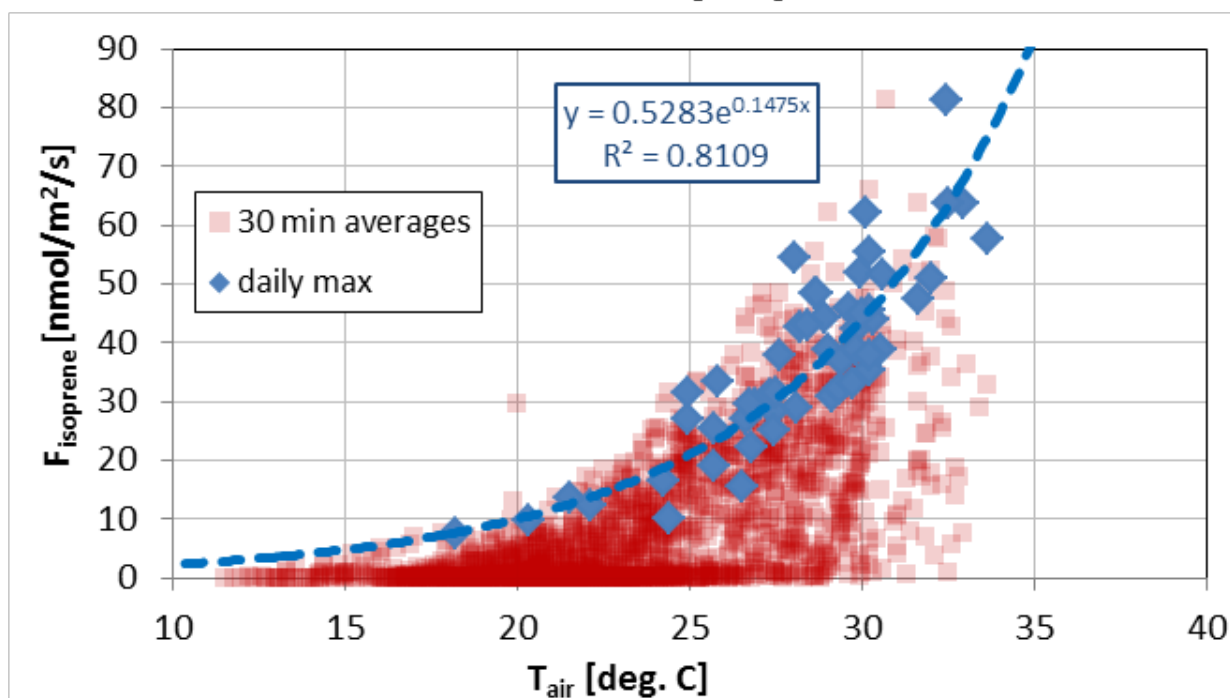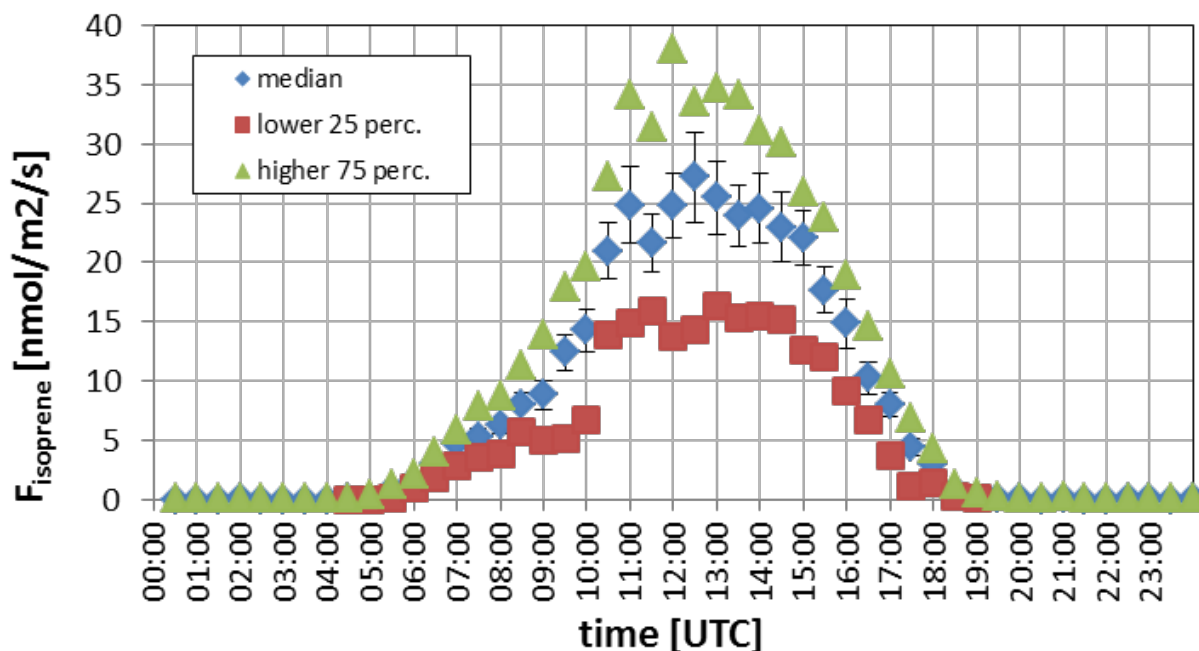
Figure 1.7. Results of the isoprene flux measurements at Ispra with the Fast Isoprene Sensor (FIS), showing (top) the average diurnal cycle of the flux and (bottom) the 30-minute and daily maximum fluxes as a function of air temperature.
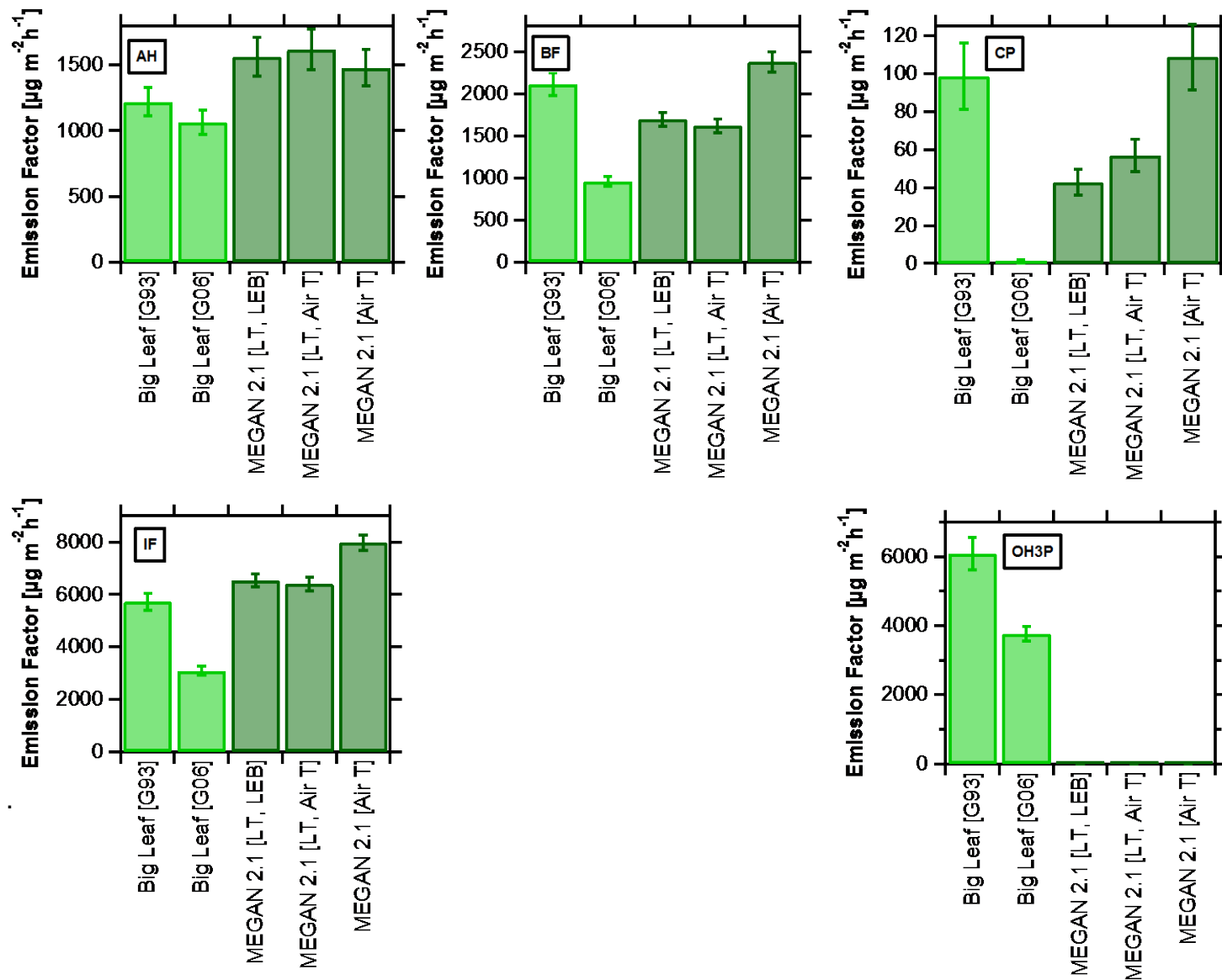
Figure 1.8. Isoprene emission factors for mixed oak forests derived from five datasets, covering Alice Holt (mixed *Q. robur / Q. petraea*, UK), Bosco Fontana (mixed hornbeam, *Q. rubra, Q. robur* forest, Italy), Castelporziano (mixed *P. pinea, Q. ilex* and *Q. suber*; Italy), Ispra Forest (*Q. robur* with *A. glutinosa* and *P. alba*; Italy) and Haut Provence (*Q. pubescence* with *A. monspessulanum*; France). The five bars showing the emission factors backed out of the data using five different emission algorithms, covering big leaf (light green) and multi-layer (dark green) approaches based on canopy environment models.

Fluxes of isoprene were also re-measured at the moorland of Auchencorth (Figure 1.9). Here surprisingly large fluxes had been detected during measurements in 2013, which only covered three days due to instrument problems. The new measurements support the original findings and provide a much more extensive and robust dataset to derive emission factors. LAI adjusted basal emission factors were found to be only a third smaller than those of an English oak forest. At present, due to the typically low Scottish temperatures significant emissions are limited to a relatively small number of days. However, with climate change, northern peatlands could become a significant source of isoprene. Work is continuing beyond ÉCLAIRE to identify the plant species that dominate this isoprene emission, which will also allow to assess whether climate change would change their prevalence.
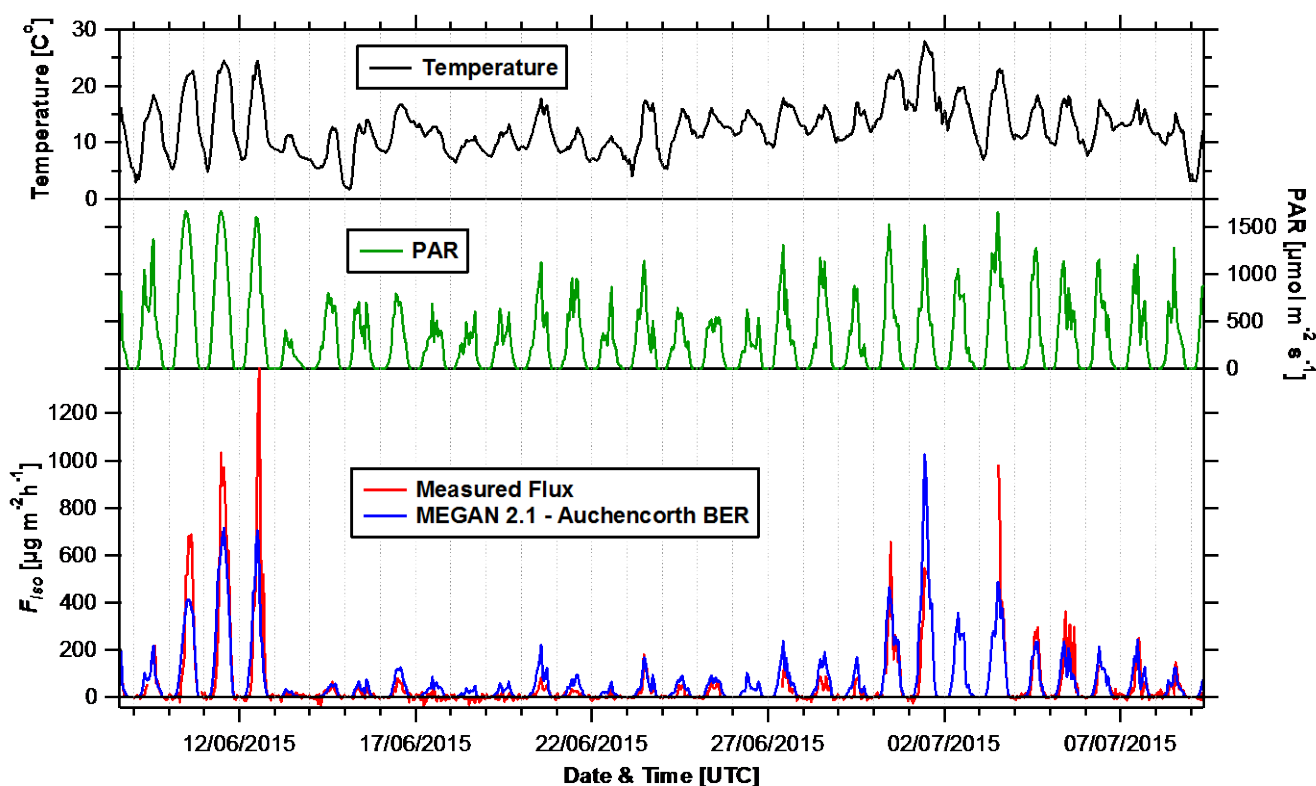
Figure 1.9: Measured (red) and modelled (blue) isoprene flux at Auchencorth in relation to the main drivers, temperature and photosynthetically active radiation (PAR).

Additional, campaign-based, measurements of further NO_y components at Posieux (total reactive nitrogen), Auchencorth (eddy-covariance flux measurements of NO_2 in collaboration with the University of D'Aquila and with support of Trans-National Access (TNA) funding from ACTRIS) and Grignon (HONO fluxes in collaboration with Univ. Wuppertal) (see Table 1.2 for an overview). An eddy-covariance system for aerosol chemical fluxes based on an Aerodyne aerosol mass spectrometer was used to measure fluxes of aerosol chemical components were measured at Auchencorth and Bosco

Fontana (within Task 1.4 below), whilst existing data were also reanalysed for Speuld. Figure 1.10 shows the averaged diurnal cycles in the deposition velocity of nitrate and sulphate aerosol to the Auchencorth moorland vegetation and similar measurements have been evaluated for Speuld and Bosco Fontana, showing significantly higher deposition rates for nitrate than sulphate. These measurements formed the basis for the development of an empirical correction for aerosol dry deposition velocities of nitrate and ammonium accounting for the evaporation of NH_4NO_3 during the deposition process in WP4.

In addition, ÉCLAIRE has contributed to the refinement of the analysis concepts and routines of organic aerosol fluxes. The organic mass spectral data from Aerosol Mass Spectrometers (AMS) are commonly analysed by positive matrix factorisation to derive concentrations of organic aerosol types reflecting different sources. Commonly organic aerosol fractions are hydrocarbon-like organic aerosol (HOA), low and semi-volatile oxidised organic aerosol (LV-OOA / SV-OOA) and biomass burning organic aerosol (BBOA). This approach has now been extended to the analysis of flux data, so that fluxes of these different organic aerosol components can be inferred. Figure 1.10 shows the average diurnal cycles of the concentrations, fluxes and deposition velocities of three organic aerosol components that could be identified at the ÉCLAIRE Speuld site. These include LV-OOA and SV-OOA and a component that has the mass spectral signature of secondary organic aerosol that has been freshly formed from biogenic VOCs (F-OA). The analysis shows that although the organic aerosol mass is dominated by SV-OOA, its flux is dominated by LV-OOA. In addition, whilst F-OA contributes 18% to the concentration it only contributes only 2% to the flux which is reflected in a lower deposition velocity than found for the other compounds. A possible explanation is that some of the F-OA deposition is masked by F-OA formation below the measurement height resulting in a reduced net flux being measured.
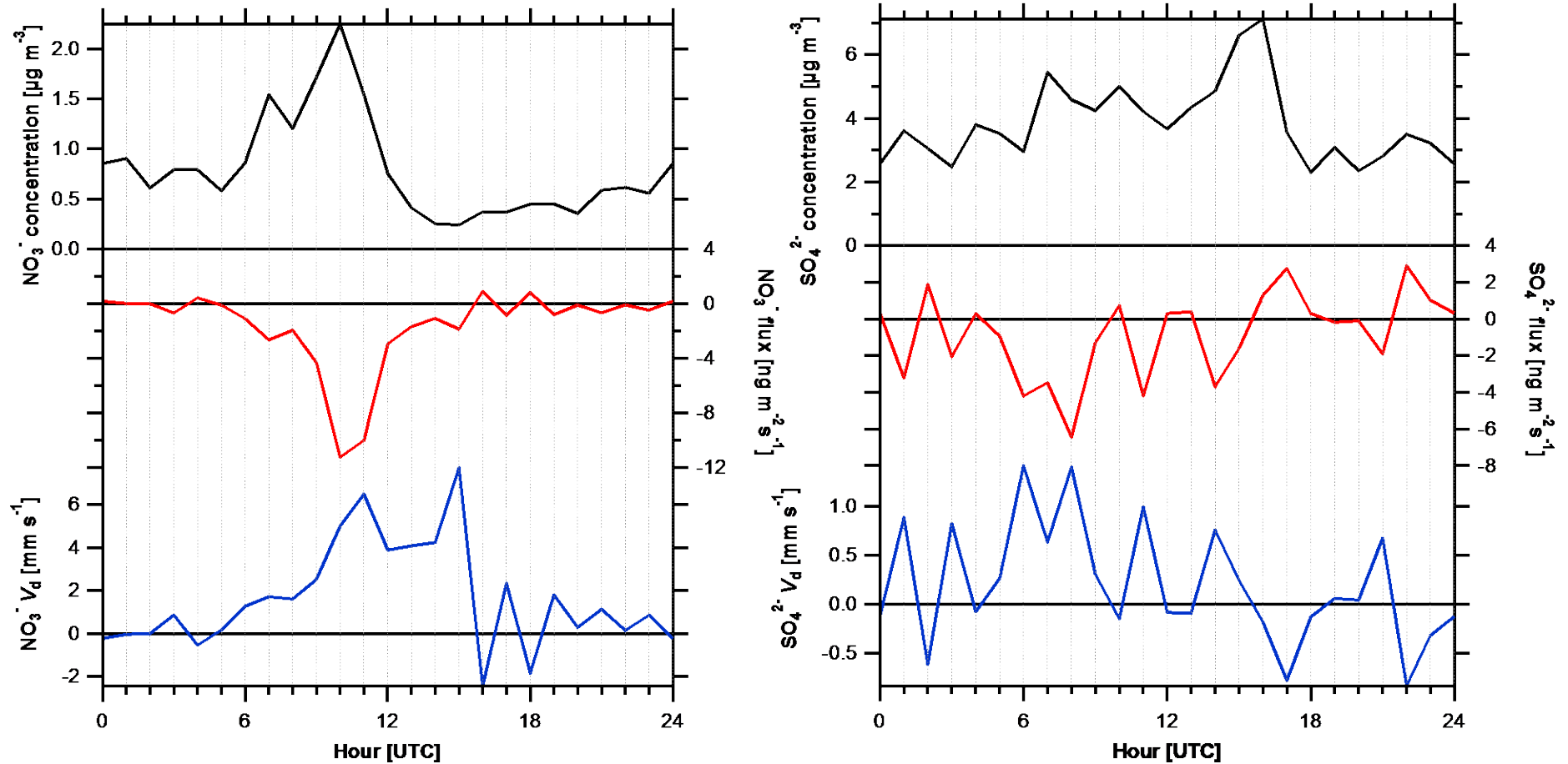
Figure 1.10: Average diurnal cycle of the dry deposition velocity of (a) nitrate and (b) sulfate aerosol at Auchencorth Moss.

ÉCLAIRE Third Periodic Report: November 2015
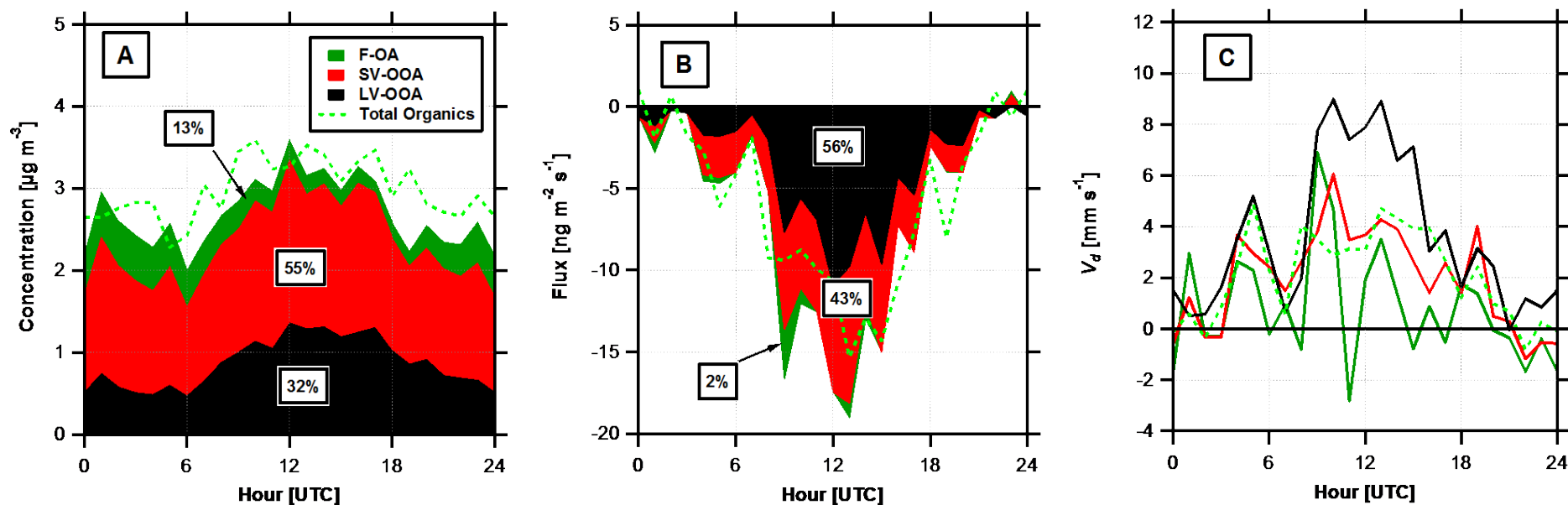
Figure 1.11. Results of the organic aerosol flux measurements above Speuld forest applying positive matrix factorisation in the analysis to the organic mass spectra of the eddy-covariance measurements with an aerosol mass spectrometer. The panels show the average diurnal cycles of the contributions of three different organic aerosol fractions (semi-volatile and low-volatility oxidised organic aerosol as well as a fresh organic aerosol factor likely originating from oxidisation of locally emitted biogenic VOCs) in terms of (A) concentrations, (B) fluxes and (C) their deposition velocities (V_d).

Task 1.3: Assessment of the effect of aerosol on gross primary productivity

Dedicated measurements in support of this task were made at all 9 network sites. This included direct (PAR_{dir}), diffuse (PAR_{diff}) and reflected (PAR_{refl}) Photosynthetically Active Radiation recorded at 1 minute resolution, as well as transmitted PAR at the forest floor at the forests at Ispra and Speuld. To analyse the data, measured CO_2 flux (NEE) was attributed into photosynthesis (gross primary productivity, GPP) and respiration (R) using the EUROFLUX online tool of Reichstein et al.

The light use efficiency (i.e. Gross Primary Productivity, GPP vs total incident PAR) clearly increases as the diffuse fraction increases at all forest sites, as illustrated for Hyytiala in Figure 1.12. This still holds if GPP is plotted against absorbed PAR (Ispra & Speuld) and the PAR balance at the top of the canopy (PARtot – PARrefl; Bosco Fontana & Hyytiala).
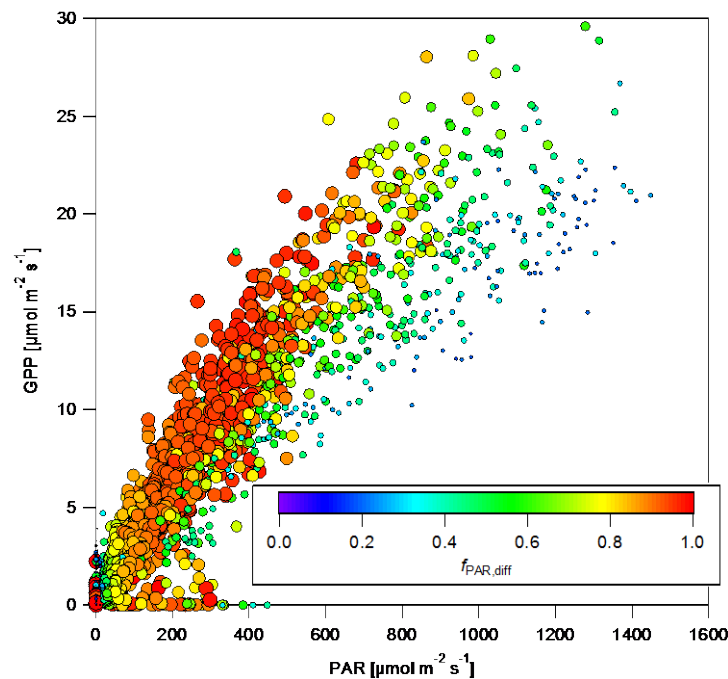
Figure 1.12. Dependency of gross primary productivity (GPP) on total photosynthetically active radiation (*PAR*) at Hyytiala, coloured by the fraction of diffuse PAR.

Typically, the dependence of photosynthesis on PAR can be described through a non-rectangular hyperbolic equation which relates GPP (*P*) to PAR (*Q*) via three parameters: the convexity of photosynthesis (θ), a response slope (α) and the light-saturated photosynthesis (A_{max}). This can be expanded to fit explicitly the light response curves to direct and diffuse *PAR* (Q_{dir} and Q_{diff}, respectively):

33

$$P = \frac{1}{2\theta}\left(\alpha Q + A_{max} - \sqrt{\left(\alpha Q + A_{max}\right)^2 - 4\alpha\theta Q A_{max}} \right)$$

$$Q = Q_{diff} + Q_{dir}$$

$$A_{max} = \left(A_{max}^{diff} Q_{diff} + A_{max}^{dir} Q_{dir}\right)/Q + c1 \; VPD$$

$$\alpha = \left(\alpha^{diff} Q_{diff} + \alpha^{dir} Q_{dir}\right)/Q + c2 \; T$$

This equation can be fitted to a relationship of GPP = fn(Q_{dir}, Q_{diff}, *VPD*, *T*) to fit the parameters α_{dir} and α_{diff} and $A_{max,diff}$ and $A_{max,dir}$, separately. For forest sites, this derives values of $A_{max,dir}$ that are typically about 50% larger than $A_{max,diff}$, demonstrating the effect. An increase in Amax and light-use efficiency does not automatically mean that an increase if $f_{PARdiff}$ automatically increases GPP, because it may be associated with an attenuation in total PAR. Indeed, Figure 1.13 indicates that $f_{PARdiff}$ is high when PAR is significantly below its maximum value. Ignoring dusk and dawn (purple and dark blue colours), high values of $f_{PAR,diff}$ are always associated with values of significantly reduced total PAR.
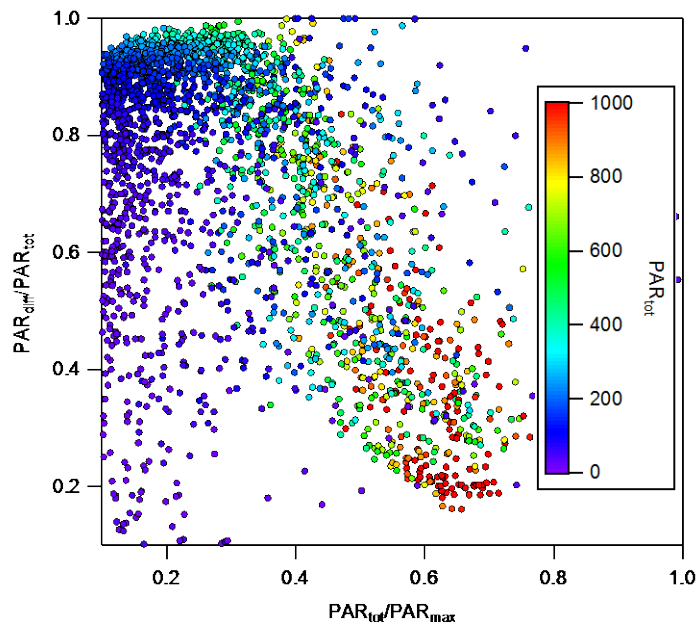
Figure 1.13. Relationship between the diffuse PAR fraction and the decrease in total PAR compared with clear-sky conditions (PAR$_{max}$).

Whilst this analysis does not isolate the effect of aerosol from the much larger effect of clouds, it is clear that at the European sites the increase in photosynthesis associated with an increase in PAR$_{diff}$ is unlikely to be larger than the effect in reducing light-levels overall.

ÉCLAIRE Third Periodic Report: November 2015

Task 1.4: Intensive measurement campaign

The activities during the intensive measurement campaign at Bosco Fontana (BF), near Mantova, Po Valley, Italy, in June 2012 were reported in the ÉCLAIRE report covering the first reporting period, with a list of measurements and preliminary results presented in the second periodic report. During Reporting Period 3, the analysis has continued and resulted in the drafting of four publications (Deliverable 1.6). Here we are presenting some highlights which go beyond what has been presented in the first two reports.

The Bosco Fontana campaign saw one of the first applications of the new-generation Proton Transfer Reaction – Time of Flight – Mass Specrometer (PTR-ToF-MS) for eddy covariant flux measurements of Volatile Organic Compounds (VOCs) , alongside a more conventional quadrupole-based PTR-MS. The newer instrument has the advantage that it measures a much larger number of compounds and does not require the target compounds to be preselected prior to the measurement. Through a systematic analysis the ÉCLAIRE team identified the number of compounds for which statistically significant fluxes could be derived, based on a range of criteria (Figure 1.14 and Schallhart et al., 2015). Overall, the chemical complexity at this site was much smaller than that found in a previous study (Park et al., 2013).

In addition to the two canopy flux measurements (PTR-MS and PTR-ToF-MS), ÉCLAIRE performed leaf-level measurements of VOC emissions from different tree species found at Bosco Fontana, the results of which were compared via the means of an emission model. The tree species mix at Bosco Fontana is not homogeneous but varies spatially. As a result it is expected that VOC fluxes differ with wind direction and position of the flux footprint. Based on previous remote sensing work which established a digital database of the spatial pattern of the various tree species, a detailed modelling exercise was performed to predict for each half-hour, the canopy flux that should have been measured based on the tree species composition in the footprint at the time. Figure 1.15 shows how, for an example day, a change in wind direction (black line) results in a change in the tree species that dominated the fluxes of isoprene (upper panel) and total monoterpenes (lower panel). It also shows the comparison of the total modelled flux (sum of stacked bars) with the measured canopy flux (black outline bars). It was found that accounting for the change in tree species composition with footprint improved the correlation between measured and modelled flux from $R^2 = 0.65$ to $R^2 = 0.75$, compared with a reference run based on a constant emission factor averaged for the site (Acton et al., 2015). However, the use of the measured leaf-level emission factors in the modelling exercise resulted in a systematic underestimation of the measured flux, whilst the use of literature values resulted in reasonable agreement.
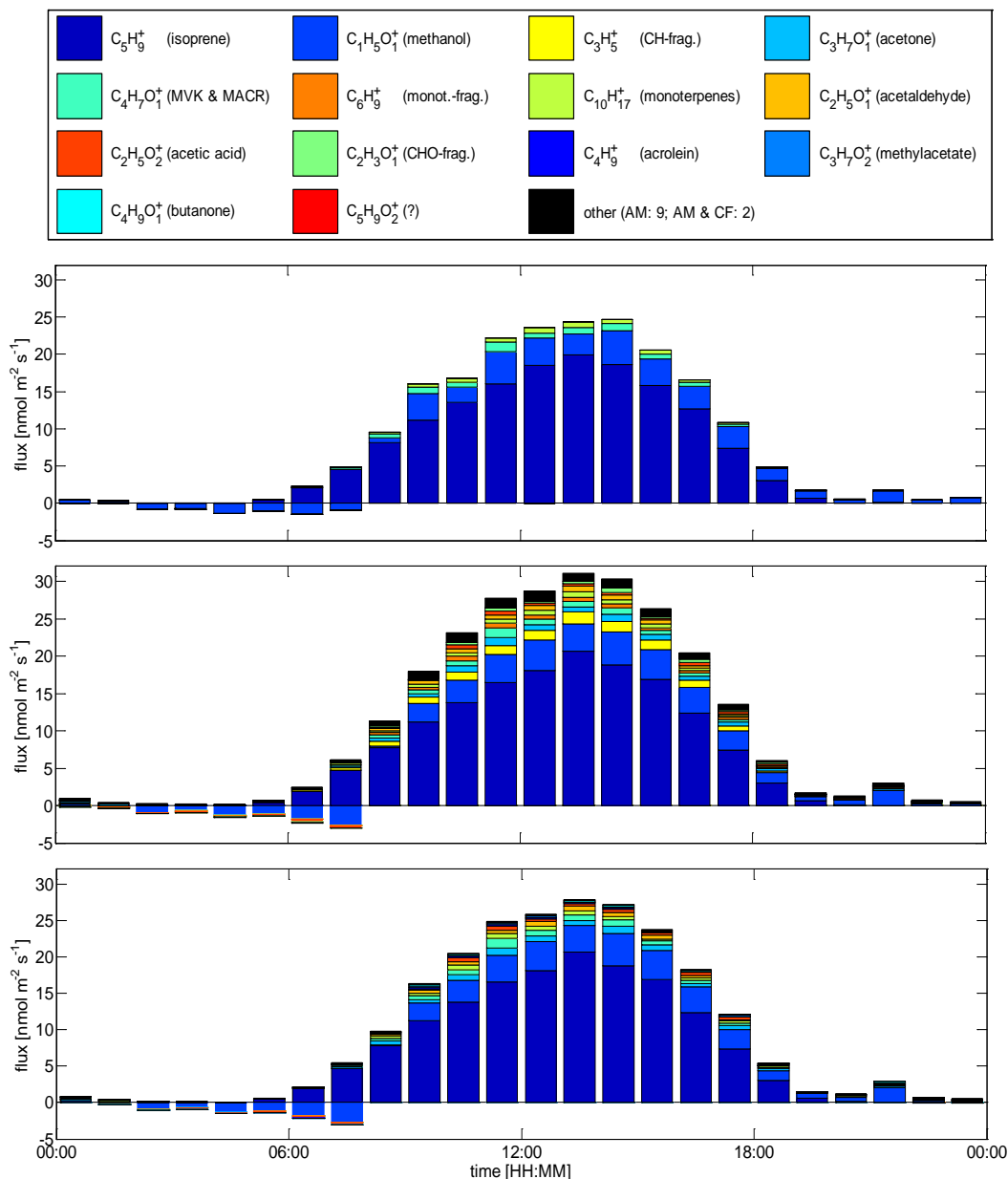
Figure 1.14: Average diurnal cycle of the VOC compounds resolved with the PTR-ToF-MS system at Bosco Fontana, comparing different methods for determining which fluxes are above the limit of detection: the classical method (top panel), the automated method (mid) and the automated method with compound filter (bottom panel). In each panel the ten most abundant flux compounds are shown, the remaining compounds are summed up and plotted as 'other'. For the automated method (AM) there were nine compounds summed up, for the automated method with compound filter (AM &CF) there were two. See Schallhart et al. (2015) for further detail.

Although an effort was made to make the leaf-level measurements from branches bordering on clearings and thus typically exposed to sunlight, it is possible that the accessible lower-hanging branches were characterised by lower emission factors than the branches at the top of the trees that dominate the canopy exchange.
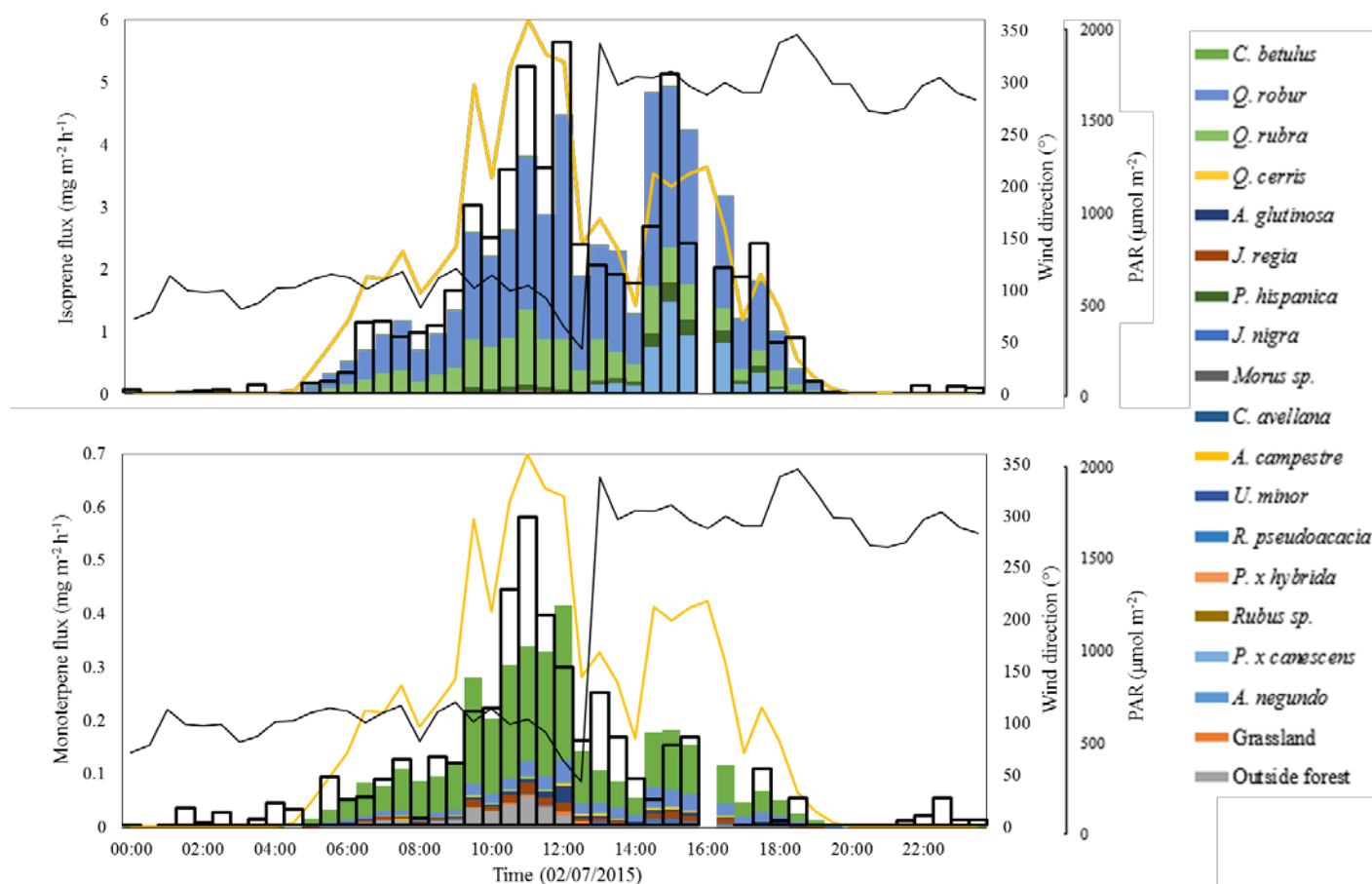
Figure 1.15: Comparison of bottom-up estimate (stacked coloured bars) of emissions of isoprene (upper panel) and total monoterpenes (lower panel) with canopy level measurements (black outline bars) at Bosco Fontana. The bottom-up estimate was calculated using a VOC emission algorithm driven by photosynthetically active radiation (PAR, yellow line) and temperature (not shown), weighted by the emission factors of the tree species within the flux footprint at the time of the canopy-scale measurement. This changed with wind direction (black line).

In addition to the VOC measurements, the gradient data from the GRAEGOR gradient analyser for reactive gases and water-soluble aerosol components has been fully analysed; the results of the nitrogen compounds at Bosco Fontana are shown in Figure 1.16, where the aerosol nitrate flux is also compared with an independent measurements

using the Aerosol Mass Spectrometer eddy-covariance system mentioned above. Because the bottom analyser was operated very close to the canopy a correction had to be developed to the aerodynamic gradient approach for measuring within the surface roughness layer.

For nitric acid, which is typically expected to deposit efficiently with a near-zero canopy resistance, the fluxes measured by eddy covariance were compared with the results from an inferential deposition model as well as fluxes obtained with the modified Bowen ratio approach, assuming that sources and sinks were identical for HNO_3 and sensible heat.

Good agreement between the three approaches to measure HNO_3 fluxes provides confidence in the resulting measurements (cf. Deliverable 1.6). The results show that, during this summer measurement period, the dry deposition flux of reactive N compounds was dominated by ammonia (NH_3), but that other N compounds made a significant contribution. Although there were systematic discrepancies between the concentrations and fluxes measured by GRAEGOR gradient and AMS eddy-covariance, likely related to differences in the size-cut off of the two instruments, nitrate deposition velocities agreed closely. Typically, physical processes limit deposition velocities of particles to < 10 mm s^{-1} above vegetation, whilst the average measured V_d of nitrate (and ammonium) peaks at 40 mm s^{-1} during the middle of the day. This observation also made at other sites (e.g. Speuld) is explained by dissociation of aerosol NH_4NO_3 intro HNO_3 and NH_3 gas during the deposition process as the aerosol approaches the canopy where gas-phase concentrations are depleted (supporting evaporation) and air temperatures are elevated. It is interesting that the apparent deposition velocity of the aerosol compounds approaches that measured for HNO_3. Although the generation of HNO_3 from NH_4NO_3 evaporation near the canopy may serve to reduce the deposition gradient of HNO_3 and thus the values for HNO_3 may be underestimates of the true deposition process, this comparison nevertheless shows for the first time that the effective sink for the aerosol species is controlled primarily by transport mechanisms to the ground and that additional kinetic limitations of NH_4NO_3 evaporation are of secondary importance.
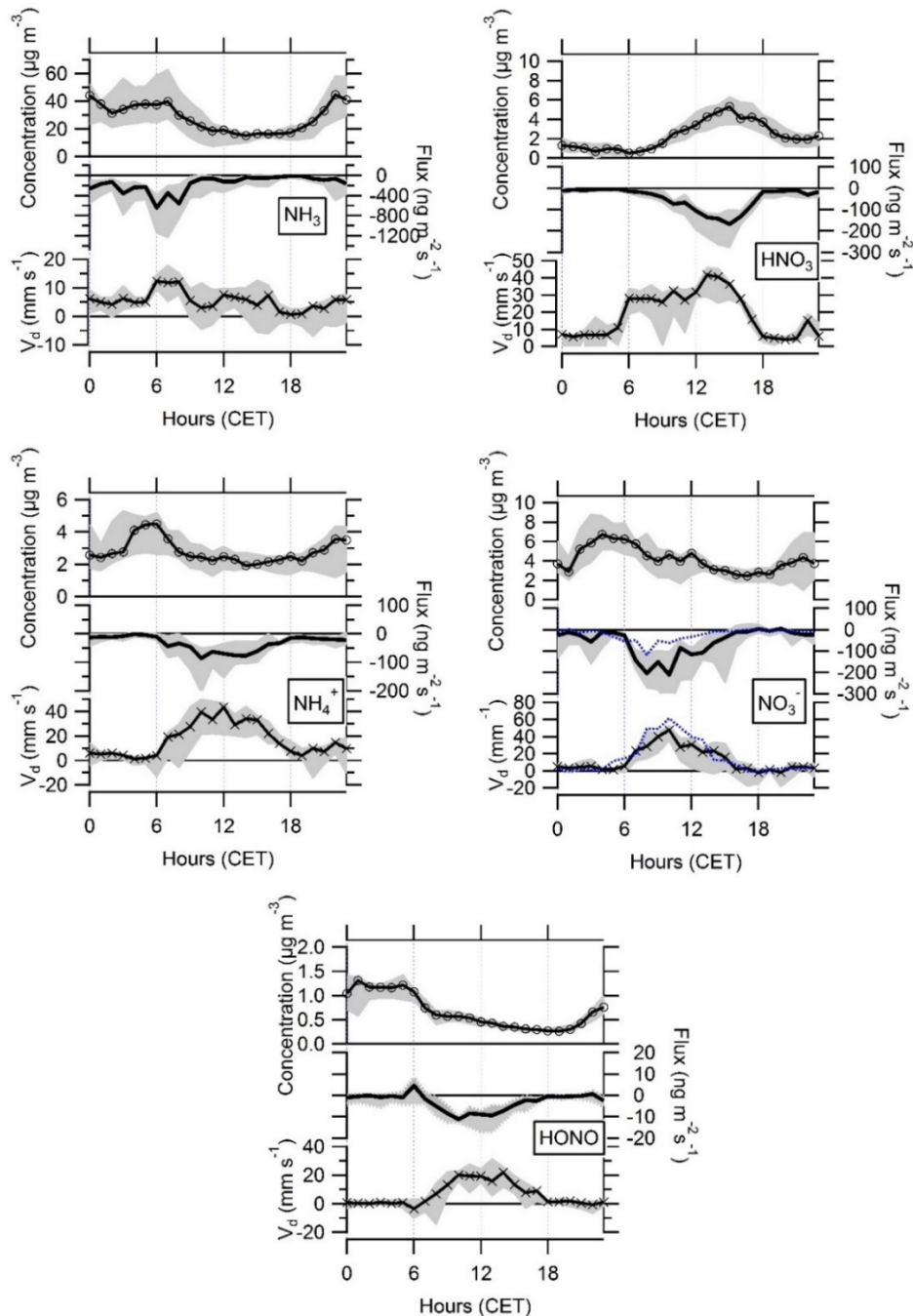
Figure 1.16: Averaged diurnal cycles of concentrations, fluxes and deposition velocities (*V*d) of water soluble nitrogen compounds as measured with a wet-chemistry gradient monitor (GRAEGOR; black lines) and an aerosol mass spectrometer eddy-covariance system (blue dotted lines) shown here for NO3- only) as deployed during the ÉCLAIRE Bosco Fontana Experiment. Shaded areas indicate the inter-quartile ranges.

Similarly, analysis of the ozone flux data has continued and resulted in the production of a manuscript for submission to *Biogeosciences* (Deliverable 1.6). The attribution of the total ozone flux into stomatal uptake, reaction with soil NO emission and deposition to cuticles / soils was presented in the previous report. Now the multi-height measurements of O_3 concentrations and fluxes have been fully evaluated. Figure 1.17 shows the averaged diurnal cycle of the ozone concentrations measured at five heights on the tower (8 - 41 m) as well as part of the chamber setup at an in-canopy location (0.15 m). Concentration differences were surprisingly small between the heights on the tower, but significantly reduced directly above the forest floor. It is possible that at the tower location vertical transport was more efficient than at other places within the canopy. There was a marked increase in concentration gradients in the afternoon at around 15:00 hrs, which could be seen throughout the canopy. This coincided with the sensible heatflux at 24 m changing from being directed upwards to downwards (on average), i.e. by this time the top of the canopy has heated sufficiently that the in-canopy inversion grows to this height. At the same time the vertical transport shows an increased occurrence of ramp structures representative of convective transport through the canopy.

The measurements of fluxes at various levels within the canopy allows the height of the exchange to be determined. The analysis presented in Figure 1.18 reveals that on average about 29% of the flux are taken up by the canopy located above 16 m. In the paper, the analysis of the attribution by height is combined with the attribution by pathway to derive an unusually comprehensive picture of the ozone exchange with the canopy at Bosco Fontana.

Task 1.5: Targeted measurements of NH₃ exchange with Mediterranean vegetation

These measurements were fully reported in the previous reporting period. No further activity has happened during Reporting Period 3.
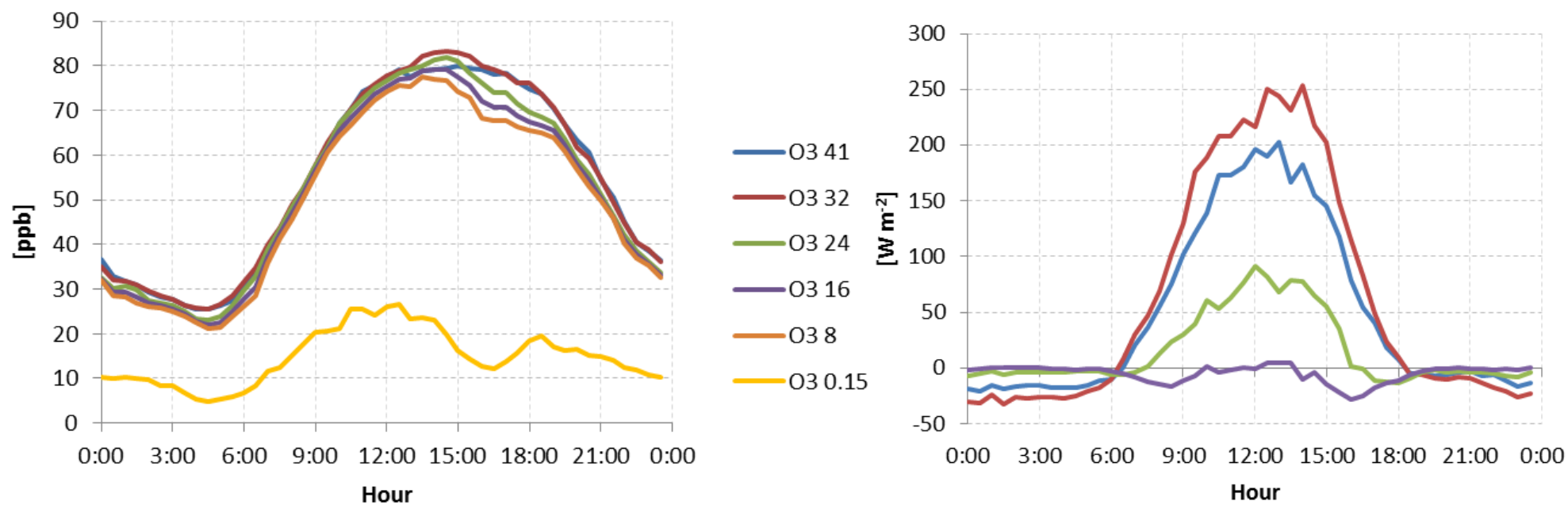
Figure 1.17: Compilation of the average diurnal cycle in (left) ozone concentration and (right) sensible heat flux at the various measurement heights during the ÉCLAIRE Intensive Measurement Campaign at Bosco Fontana.
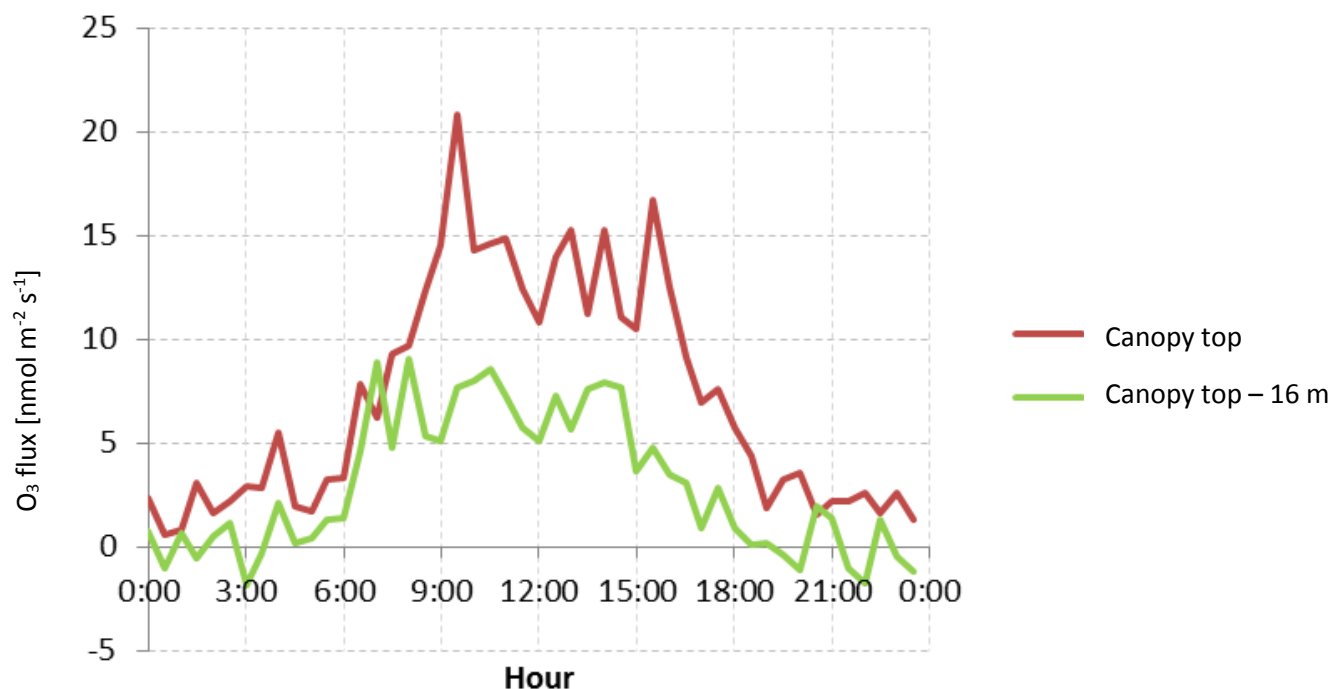
Figure 1.18: Vertical attribution of the flux through flux profile measurements at Bosco Fontana. Of the total canopy flux (red) about 29% is taken up by the canopy located above 16 m (green).

Progress towards the milestones and deliverables

All deliverables and milestones had been reported / reached in the previous reporting period, except for D1.6.

D1.6: Four publications on integrated campaign (Month 30)

Two papers have been published and two manuscripts are being tidied up for publication. Complete drafts have now been submitted as Deliverable 1.6.

1. **Canopy-scale flux measurements and bottom-up emission estimates of volatile organic compounds from a mixed oak and hornbeam forest in northern Italy**; Acton, W. J. F., Schallhart, S., Langford, B., Valach, A., Rantala, P., Fares, S., Carriero, G., Tillmann, R., Tomlinson, S. J., Dragosits, U., Gianelle, D., Hewitt, C. N., and Nemitz, E., *Atmos. Chem. Phys. Discuss.*, 15, 29213-29264, doi:10.5194/acpd-15-29213-2015, 2015.

ÉCLAIRE Third Periodic Report: November 2015

2. **Characterization of total ecosystem scale biogenic VOC exchange at a Mediterranean oak-hornbeam forest**; Schallhart, S., Rantala, P., Nemitz, E., Mogensen, D., Tillmann, R., Mentel, T. F., Rinne, J., and Ruuskanen, T. M., *Atmos. Chem. Phys. Discuss.*, 15, 27627-27673, doi:10.5194/acpd-15-27627-2015, 2015.
3. **Controls of reactive nitrogen fluxes and gas-aerosol interactions above a semi-natural forest in the Po Valley, Italy**. Twigg, M.M.; Di Marco, C.F.; Langford, B.; Loubet, B.; Gerosa, G.; Finco, A.; Sutton, M.A.; Nemitz, E.; *Atmos. Chem. Phys. Discuss.* [in preparation]
4. **Measurements of ozone flux at four levels above and within a mixed deciduous forest in northern Italy - importance of canopy storage and interactions with nitric oxide.** Finco, A., Coyle, M.; Marzuoli, R.; Chiesa, M.; Loubet, B.; Diaz-Pines, E.; Gasche, R.; Ammann, C.; Sutton, M.A.; Nemitz, E., Gerosa, G.; *Biogeosciences Discuss.* [in preparation]

Use of resources and deviations from DoW

Overall, the use of resources was as anticipated in the DoW, the number of man months spent was 39. Notable diversions include:

- *UNICATT*. As described in the first two reports, a decision was made for UNICATT to benefit from the newly established site as Bosco Fontana to make the network measurements of Tasks 1.1 & 1.2 than the originally envisaged crop site. This change has allowed the Bosco Fontana campaign measurements to be interpreted within the annual context and make best use of the major investment associated with installing a new forest tower to host the integrated measurement campaign. UNICATT received €50k of the unallocated budget during Reporting Period 1 to help with the increased costs of installing the new tower at Bosco Fontana.
- As already described in the first two reports *FRI* had to enter an agreement with SZIU (Szent István University) to obtain access to their CO_2 fluxes made under the EU FP7 Project 'Animal Change'), which allows all ÉCLAIRE partners to use these data, but they will not be uploaded to the ÉCLAIRE database. Operation of a 2nd CO_2 flux system was neither sensible nor affordable within the ÉCLAIRE budget, which assumes that CO_2 fluxes at the sites of the ÉCLAIRE flux network are supported by national contributions. The original plan to operate an AMANDA wet denuder system at Bugac had to be abandoned due to two reasons:
  - The Kiskunság National Park (landowner) did not allow the use of a power generator.
  - Due to the lack of permanent staff, the frequent demand of visiting AMANDA would have not been possible.
- As noted above, the original idea was to operate an AMANDA NH_3 gradient system to measure fluxes at the Ukrainian arable site at Potrodolinskoye and ONU received instrument training at NERC. Unfortunately, at the end this measurement could not be

realised for two reasons: first, the site was hit by a powerful hurricane on 31 May 2013, which destroyed the farm power supply. The replacement supply was not sufficient to maintain the NH_3 analyser. Second, the political situation in Ukraine following the Crimean conflict made it impossible to import / export equipment on a temporary basis.

- At Grignon the plan for the intensive measurement campaigns was revised: measurements of NO_2 were planned to be performed with a luminol analyser that was ordered in 2011 but was never delivered. To overcome this problem, a fast chemiluminescent analyser was loaned by MPI Mainz, from August to November 2012. The NO_2 flux was then measured by eddy-covariance. New analysers were then purchased. The end result is that the NO/NO_2 flux time series is not continuous for the entire period. On the other hand, HONO flux measurements were made and analysed in collaboration with the University of Wuppertal.
- At Auchencorth, despite considerable effort the GRAEGOR instrument to measure aerosol and reactive gas gradients did not work after return from Bosco Fontana. Instead, aerosol fluxes were measured with the eddy-covariance method using an Aerosol Mass Spectrometer and historical NH_3 fluxes were reanalysed. In addition to the DoW, NO_2 eddy-covariance flux measurements by eddy-covariance using laser induced fluorescence were realised at Auchencorth in collaboration with the University of D'Aquila.

Publications

Papers:

Acton, W.J.F.; Schallhart, S.; Langford, B.; Valach, A.; Rantala, P.; Fares, S.; Carriero, G.; Tillmann, R.; Tomlinson, S.J.; Dragosits, U.; Gianelle, D.; Hewitt, C.N.; Nemitz, E. (2015) Canopy-scale flux measurements and bottom-up emission estiamtes of volatile organic compounds from a mixed oak and hornbeam forest in norther Italy. *Atmospheric Chemistry and Physics Discussions* [accepted].

Fares, S.; Savi, F.; Muller, J.; Matteucci, G.; Paoletti, E. (2014) Simultaneous measurements of above and below canopy ozone fluxes help partitioning ozone deposition between its various sinks in a Mediterranean Oak Forest. *Agric. Forest Met.* 198-199, 181-191

Langford B, Acton W, Ammann C, Valach A, Nemitz E. (2015). Eddy-covariance data with low signal-to-noise ratio: time-lag determination, uncertainties and limit of detection. *Atmospheric Measurement Techniques* 8(10): 4197-4213

McKenzie, R. M., Özel, M. Z., Cape, J. N., Drewer, J., Dinsmore, K. J., Nemitz, E., Hamilton, J. F., Sutton, M. A., Gallagher, M. W., and Skiba, U.: The import and export of organic nitrogen species at a Scottish ombrotrophic peatland, Biogeosciences Discuss., 12, 515-554, doi:10.5194/bgd-12-515-2015, 2015.

Medinets S. (2014) The Black Sea Nitrogen Budget Revision in Accordance with Recent Atmospheric Deposition Study. Turkish Journal of Fisheries and Aquatic Sciences, 14, 1-13. doi: 10.4194/1303-2712-v14_4_18.

Medinets S., Skiba U., Rennenberg H., Butterbach-Bahl K. (2015) A review of soil NO transformation: associated processes and possible physiological significance on organisms. *Soil Biology and Biochemistry*, 80, 92-117. doi:10.1016/j.soilbio.2014.09.025. Medinets S.V. (2014) Results of atmospheric chemical investigations of greenhouse gases N_2O & CH_4. ONU Herald, 22, 79-91 (in Russian).

Medinets S.V., Morozov V.M., Boyko V.M., Kotogura S.S., Mileva A.P., Gruzova I.L. (2015) Assessment and constituents of fluvial sink of N and P compounds into the Dniester estuary. Scientific Notes of Ternopil National V. Gnatyuk Pedagogic University. Special issue *Hydroecology*, 64, 439-443 (in Ukrainian).

Medinets S.V., Skiba U.M., Medinets V.I., Bilanchin Ya.M., Pitsyk V.Z., Goshurenko L.M., Kotogura S.S. (2014) Changes in soil carbon and nitrogen dynamics during a three year crop rotation on a chernozem soil in the Ukraine. ONU Herald, 21, 28-37.

Rantala, P., Aalto, J., Taipale, R., Ruuskanen, T. M., and Rinne, J.: Annual cycle of volatile organic compound exchange between a boreal pine forest and the atmosphere, Biogeosciences, 12, 5753-5770, doi:10.5194/bg-12-5753-2015, 2015.

Schallhart S, Rantala P, Nemitz E, Mogensen D, Tillmann R, Mentel TF, Rinne J, Ruuskanen TM. (2015). Characterization of total ecosystem scale biogenic VOC exchange at a Mediterranean oak-hornbeam forest. *Atmospheric Chemistry and Physics Discussions* 15(19): 27627-27673

Skog, K.; Baltensperger, Urs; Collett, Jeffrey; Crippa, Monica; Decesari, S.; Hodas, Natasha; Kaltsonoudis, Christos; Laaksonen, Ari; Lim, Yong Bin; McNeill, V. Faye; Nemitz, Eiko; Poluzzi, Vanes; Prevot, Andre; Sullivan, Amy; Twigg, M.; Turpin, Barbara; Wolf, Robert; Keutsch, F. (2015) Gas-phase Acid Formation from Aqueous Aerosol Processing of Glyoxal during PEGASOS. *Environ. Sci. Technol.* [under review]

Sullivan, A.P., N. Hodas, B.J. Turpin, K Skog, F.N. Keutsch, S. Gilardoni, M. Paglione, M. Rinaldi, S. Decesari, M.C. Facchini, L. Poulain, H. Herrmann, A. Wiedensohler, E. Nemitz, M.M. Twigg, and J.L. Collett, Jr. (2015) Evidence for Ambient Dark Aqueous SOA Formation in the Po Valley, Italy. *Atmos. Chem. Phys. Discuss.* [under review]

Presentations

Acton, W., Simon Schallhart, Ben Langford, Amy Valach, Pekka Rantala, Silvano Fares, Giulia Carriero, Thomas Mentel, Sam Tomlinson, Ulrike Dragosits, Nicholas Hewitt, and Eiko Nemitz (2015) Comparison of three methods to derive canopy-scale flux measurements above a mixed oak and hornbeam forest in Northern Italy. *Geophysical Research Abstracts* **17**, EGU2015-11017, 2015

Medinets S., Gasche R., Skiba U., Butterbach-Bahl K., Medinets V. (2014) Flux measurements of NO_x in arable soil under dripping fertilization condition: Poster session of the ÉCLAIRE 4th Project Meeting and Open Science Conference "Integrating impacts of air pollution and climate change on ecosystems" (September, 29th – October, 3rd 2014, Budapest, Hungary). Budapest, 2014, S1_9.

Medinets S., Kotogura S., Gruzova I., Mileva A., Medinets V. (2014) Rate of atmospheric bulk N deposition in natural and agricultural areas in the Southern Ukraine: Poster session of the ÉCLAIRE 4th Project Meeting and Open Science Conference "Integrating impacts of air pollution and climate change on ecosystems" (September, 29th – October, 3rd 2014, Budapest, Hungary). Budapest, S1_12.

Medinets S., Gasche R., Skiba U., Schindlbacher A., Kiese R, Butterbach-Bahl K. (2015) Cool time period (below 5 °C) NO emission from soil and its significance to annual budget. Submitted to poster session of the ÉCLAIRE Final Project Meeting and 5th General Assembly (September 1-4, 2015, Edinburgh, UK). Edinburgh.

Medinets S., Gasche R., Skiba U., Schindlbacher A., Kiese R, Butterbach-Bahl K. (2015) Relationships between soil NO, N_2O and CO_2 Emission under cold condition. Submitted to poster session of the ÉCLAIRE Final Project Meeting and 5th General Assembly (September 1-4, 2015, Edinburgh, UK). Edinburgh.

Medinets S., Gasche R., Skiba U., Schindlbacher A., Kiese R, Butterbach-Bahl K. (2015) Preliminary results of gradient measurements of NO concentration in soil pore. Submitted to poster session of the ÉCLAIRE Final Project Meeting and 5th General Assembly (September 1-4, 2015, Edinburgh, UK). Edinburgh.

Medinets S., Gasche R., Skiba U., Butterbach-Bahl K., Medinets V. (2015) NO flux dependence on inorganic N availability and abiotic factors variations *in-situ* in the Black soil. Submitted to poster session of the ÉCLAIRE Final Project Meeting and 5th General Assembly (September 1-4, 2015, Edinburgh, UK). Edinburgh.

References not covered by the above

Dimopoulos, Y., Bourret, P., and Lek, S.: Use of some sensitivity criteria for choosing networks with good generalization ability, Neural Process Lett **2**, 1-4, 1995.

Olden, J.D., Joy, M.K., Russell G Death, An accurate comparison of methods for quantifying variable importance in artificial neural networks using simulated data, Ecological Modelling **178**(3–4), 389-397, 2004.

Work package 2 – Controlled studies on exchange processes

Lead contractor: Juelich
Contributors: Juelich, NERC, KIT, CNR, BOKU, BAS-IFRG

Work package objectives

The aim of this work package is the study and quantification of key emission mechanisms to provide targeted data that can be used to derive parameterisations of the emission processes in WP1.3.

1. To obtain response curves of soil and litter emissions to meteorological drivers (temperature, moisture) for CO_2, CH_4, O_3, N_2O, NO, NO_2 and NH_3 across a wide range of soils.
2. To provide data on NO emissions after rewetting events as a basis to improve the mechanistic understanding and predictive capability, through novel laboratory experiments.
3. To quantify VOC emission responses under combined environmental change scenarios and develop a process understanding of the controls.
4. To investigate the effect of stresses (drought, heat) on BVOC emissions and the impact on O_3 deposition and formation.
5. To quantify deposition rates of VOCs and their controls.

Progress and Results

Task 2.1 Controlled emission measurements of CO_2, CH_4, N_2O, NO and NH_3 using *monoliths and litter from the ÉCLAIRE flux network (BOKU, NERC(EDI)*

Whilst the work programme for CO_2, CH_4 and NO_x had been mostly completed during the previous two Reporting Periods (RPs), during this period additional litter incubation experiments were conducted at BOKU University with the new instrumental setup for measuring NH_3 emissions at part per trillion (ppt) level. It was shown that litter with C:N of 44 from a polluted site emitted twice as much NH_3 than litter with C:N of 66 from a clean air region. Moist litter emitted more NH_3 compared with dry litter. NH_3 emissions peaked during rewetting events after drought. This peak occurred after maximum NO emissions and before the start of microbial respiration i.e. CO_2 emissions. This is the first experiment showing temporal evolutions and environmental drivers of the full set of nitrogen gas emissions from the forest litter layer (Figure 1.19, Haller and Zechmeister-Boltenstern, in prep.).
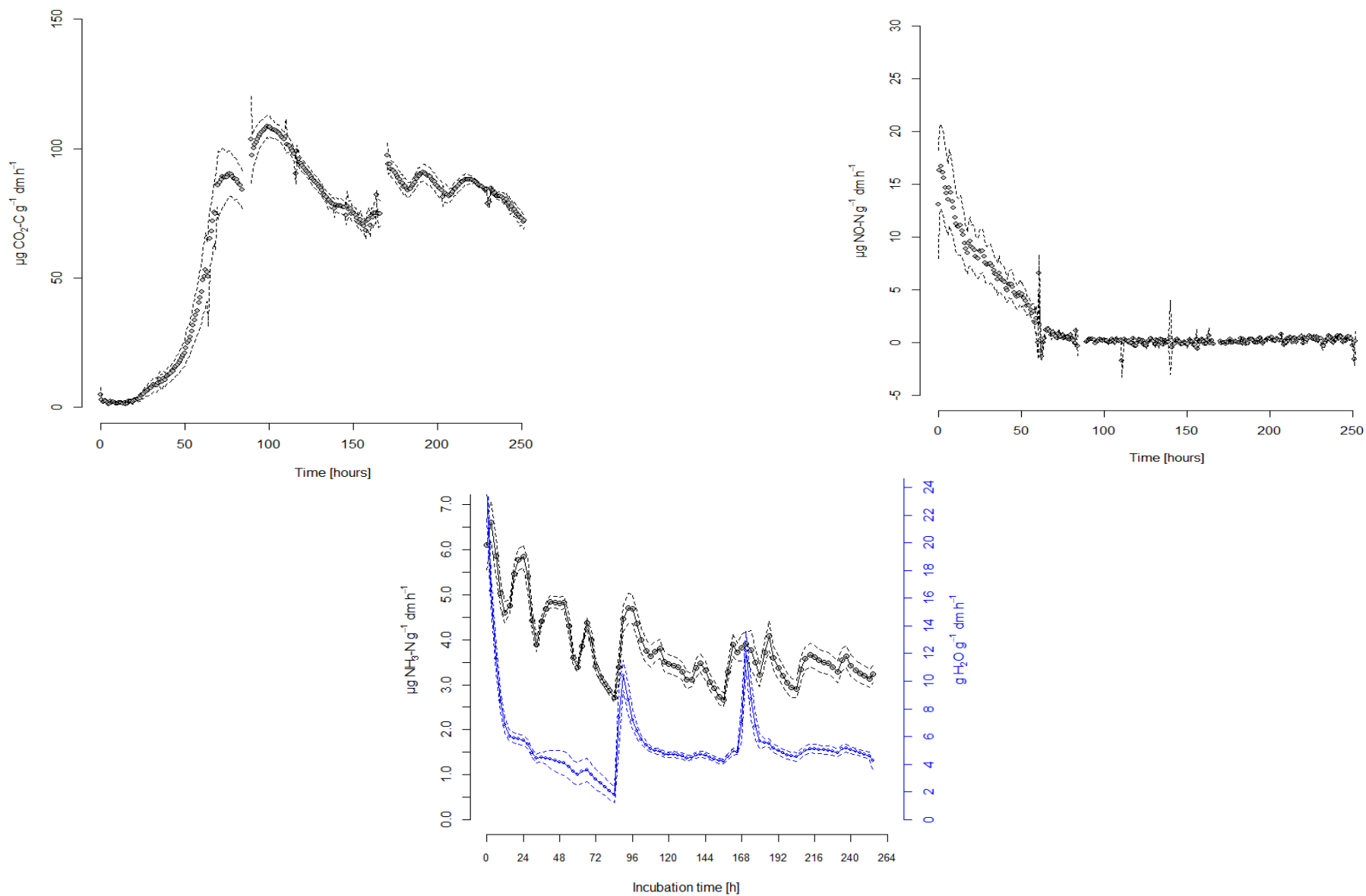
Figure 1.19: NH_3, NO and CO_2 emissions as well as water vapour emissions of beech leaf litter (SW) with the initial moisture level of 60 w/w%. During incubation three drought phases were simulated (~80 h) with subsequent rewetting events of an equivalent of 750 ml m^{-2} of deionized water. Water peaks after about 80h and 160h indicate the rewetting events. Dashed lines represent standard errors.

Task 2.2: Quantifying the effect of re-wetting on NO emissions (KIT).

No actions in the reporting period as the work had been completed before.

Task 2.3: Quantifying BVOCs exchanges in field experiments and in response to combined environmental change and pollution scenarios (CNR, BAS-IFRG)

Methyl vinyl ketone (MVK) and methacrolein (MAC) are key oxidation products (iox) of isoprene, the most abundant volatile organic compound (VOC) emitted by vascular plants in the atmosphere. Increasing attention has been dedicated to iox, as they are involved in the photochemical cycles ultimately leading to ozone (O_3) and particle formation. However, little is known about the capacity of plants to exchange iox under low and realistic ambient concentrations of iox. We hypothesized that a foliar uptake of iox exists even under realistic concentrations of iox. We tested the capacity of iox exchange in trees constitutively emitting isoprene (*Populus nigra*) or monoterpenes (*Quercus ilex*), or that do not emit isoprenoids (*Paulownia imperialis*). Laboratory experiments were carried out at the leaf level using enclosures under controlled environmental factors and manipulating isoprene and reactive oxygen species (ROS) production by using the isoprene specific inhibitor fosmidomycin, acute O_3 exposure (300 ppbv for 4 h), and dark conditions. We also tested whether stress conditions inducing accumulation of ROS significantly enhance iox formation in the leaf, and their emission.

Our results show a negligible level of constitutive iox emission in unstressed plants, and in plants treated with high O_3 (Figure 1.20). The uptake of iox increased linearly with exposure to increasing concentrations of ambient iox (from 0 to 6 ppbv of a 1:1 = MVK/MAC mixture) in all the investigated species, indicating iox fast removal by dry deposition with a low compensation point in unstressed and stressed conditions. We conclude that plant capacity to take up iox by dry deposition should be included in global models that integrate estimates of iox formation, emission, and photochemical reactions in the atmosphere.
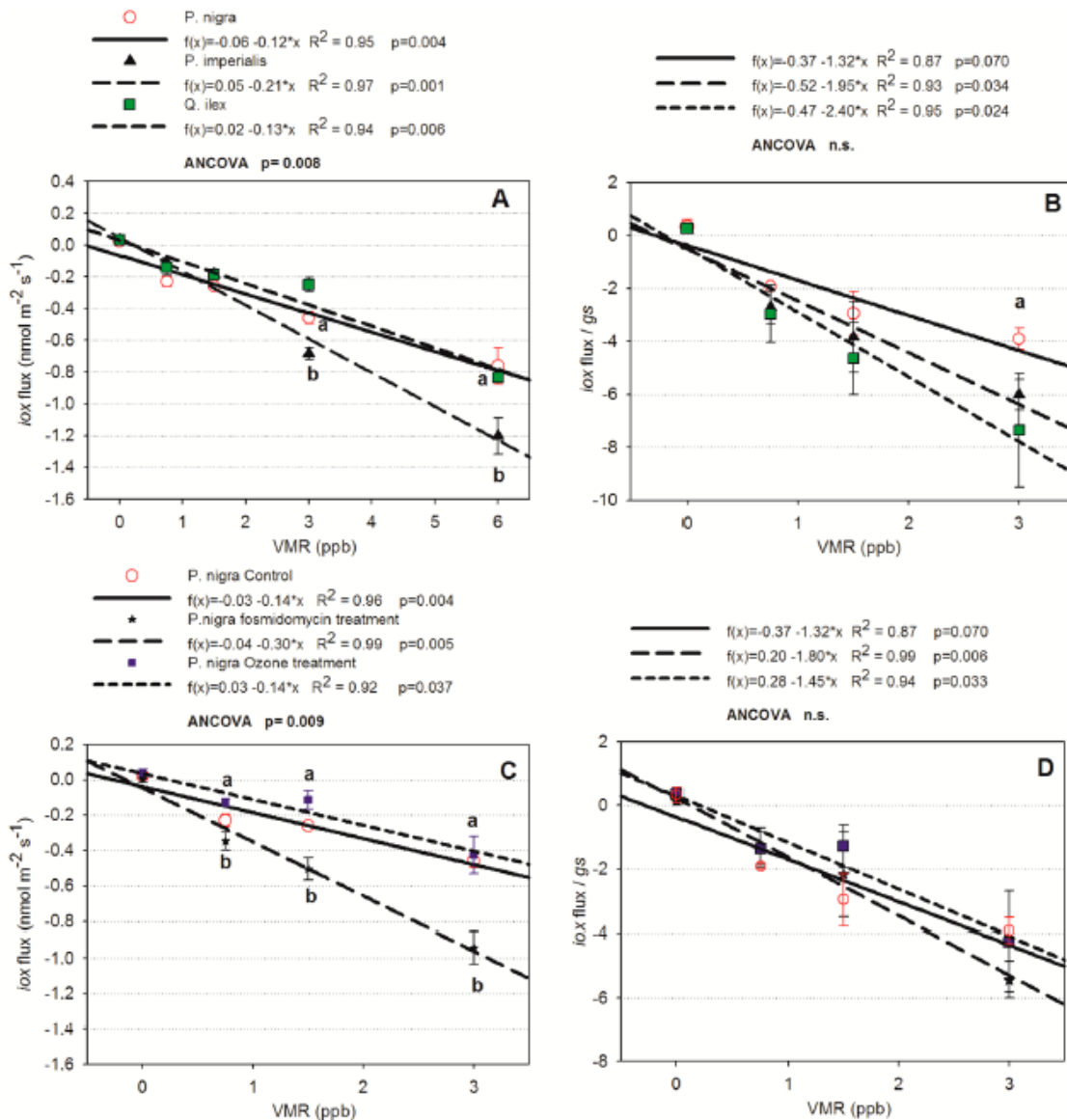
Figure 1.20: (A) Flux of MVK+MAC (iox) at increasing iox concentration fumigated in the leaf enclosure for *Paulownia imperialis*, *Quercus ilex*, and *Populus nigra* under control conditions; (B) the same relationships shown in (A) but using data normalized for corresponding values of stomatal conductance (gs). (C) iox flux for control, fosmidomycin, and ozone-treated poplar leaves. (D) Normalization for corresponding values of gs. Different letters show significant differences at the same iox concentration (average ± SE, n = 7, Holm−Sidak method, $p < 0.05$). Levels of significance, p, are shown for linear regressions and analysis of covariance (ANCOVA), that were used for testing whether iox fluxes were correlated to air concentrations and whether the regression slopes are different from each other, respectively.

Task 2.4 Coupling between climate change induced stresses on vegetation, BVOC emissions, O_3 and NO_x uptake, and O_3 forming potential (Juelich).

Our remaining two focuses for RP3 (Oct. 2014 – Oct. 2015) were 1) the impacts of drought stress on the emissions from conifers; 2) the investigation of the reliability of commercial O_3 measurement devices.

Impacts of drought on emissions from Norway spruce and Scots pine

Experiments:

Both constitutive emissions (including *de-novo* and pool emissions) and stress-induced emissions from Norway spruce and Scots pine were measured under well-watered and drought-stressed conditions as well as during the recovery period. The determination of *de-novo* and pool emissions was conducted by ^{13}C-labelling experiments.

Results:

BVOCs emitted by Norway spruce and Scots pine can be classified into three groups according to their different emission mechanisms: constitutive *de-novo*, constitutive pool and stress induced emissions. BVOC emissions from these groups showed different behaviour under drought stress: constitutive *de-novo* emissions decreased under severe drought stress when plants' transpiration and photolysis were restricted; stress induced emissions decreased also when the stress became severe; constitutive pool emissions were not substantially affected by drought even when the transpiration reduced to a very low level. However, during the recovery period, huge pluses of the pool emissions were found in some cases directly after the irrigation.

O_3 measurement:

During the measurements regarding O_3 formation from plant emissions we used commercial O_3 detectors based on UV light absorption at $\lambda = 254$ nm. During several measurements it was observed that strong interferences from so far unidentified oxidation products in a BVOC + NO_x mixture led to false data. We therefore now repeat some measurements regarding O_3 formation from BVOC oxidation using a chemiluminescence device that was adapted to measure O_3, alongside the commercial analytic devices.

Progress towards the milestones and deliverables

The milestones were achieved. All deliverables were delivered, either in their original form or compensated by extra work.

D2.5: This deliverable was modified and changed into a different paper when submitted during the previous Reporting Period. However, the originally planned manuscript about the impacts of drought stress on BVOC emissions from conifers is now also at an advanced state of preparation.

D2.6: A deliverable was submitted that summarises the improvements in the understanding of VOCs and their parameterisation as achieved during ÉCLAIRE. In addition to the work reported here it covers a summary of the parameteisations of isoprene emissions from oak (cf Figure 1.8 and associated text). ÉCLAIRE results on VOC exchange are also described in a PhD thesis (Emissions of Biogenic Volatile Organic Compounds and Ozone Balance under Future Climate Conditions, Cheng Wu, RWTH Aachen). A manuscript on that item will be submitted when the comparison between UV photometric O_3 analyzer and non-UV type analyzers are done and the resulting uncertainties in the ozone determinations are reduced.

Publications:

Fares, S., Paoletti, E., Loreto F., Brilli F.: 2015, Uptake of methyl vinyl ketone and methacrolein in trees with different isoprenoid emission under realistic ambient concentrations. *Environmental Science and Technology* **49**: 7735-7742.

Gritsch, C., M. Zimmermann, and S. Zechmeister-Boltenstern (2015) Interdependencies between temperature and moisture sensitivities of CO_2 emissions in European land ecosystems. *Biogeosciences Discuss.* [in press].

Gritsch, C., F. Egger, F. Zehetner and S. Zechmeister-Boltenstern (2015) The effect of temperature and moisture on trace gas emissions from deciduous and coniferous leaf litter. *Journal of Geophysical Research*, submitted.

Wu, Cheng, PhD thesis, (2015): Emissions of biogenic volatile organic compounds and ozone balance under future climate conditions.

Use of resources and deviations from DoW

A total of 11 person months were spent during this period, however overall Juelich, used more months than originally budgeted for solving the O_3 interference in order to measure the holistic ozone balance as promised in the DOW.

Work package 3 – Modelling emission processes

Lead contractor: KIT
Contributors: NERC, ULUND, UBM, KIT

Work package objectives

The aim of this work package is to provide improved parameterisations of biogenic and agricultural emissions to the modellers that include a robust response to climatic conditions that are predicted to change in the future. The individual objectives are:

1. To improve the climate response characteristics of NH_3 emission models for agricultural sources and vegetation,

2. To improve the climate response characteristics of soil NO emission models,

3. To improve European BVOC emission models and their response to meteorological drivers and stresses

Progress and Results

Task 3.1 Improve agricultural NH₃ emission modules in relation to meteorological drivers

Two main tasks have been carried out during the reporting period: sensitivity analyses of the Volt'Air model and the development of an hourly emission meta-model.

Sensitivity analyses of Volt'Air have been carried out for the model inputs that have the largest influence on emission estimates: fertiliser pH, application rate and application method. This has been done for three organic fertilisers (cow slurry, pig slurry and farmyard manure) and three synthetic fertilisers (urea, urea ammonium nitrate, ammonium nitrate) using the 1044 Volt'Air simulations that were used to develop the meta-models (see D3.1). A total of 85608 simulations were carried out (82 sensitivity scenarios × 1044 simulations). The results of these analyses allow us to estimate the uncertainty in the Volt'Air emission estimates (and, by extension, those of the meta-models) due to uncertainty in model inputs. Figure 1.21 shows an example of the sensitivity of Volt'Air emission estimates to cattle slurry pH, which highlights the increase of volatilisation with pH as well as the variability in the model sensitivity.

Volt'Air simulations, 522 loc. April. Bovine Slurry Emissions

blue = emissions after 1 day; red = emissions after 30 days
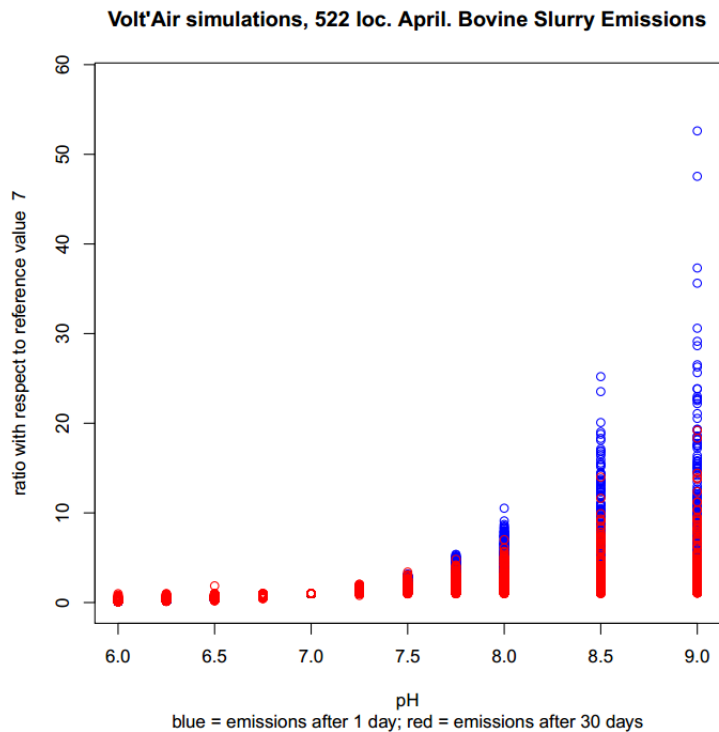
Figure 1.21. Ratio of TAN volatilized after 1 (blue) and 30 (red) days for a given cattle slurry pH to that volatilized for a pH of 7 (the reference value) for all 1044 simulations.

The meta-models described in D8.1 only provide estimates of total NH_3 emission following the application of fertilisers and the duration of the emission. If these emission estimates were to be used in a chemical transport model (CTM) the emission rate would have to be assumed to be constant. This is not realistic and would most likely lead to an overestimate of night-time emissions and an underestimate of daytime emissions. In order to improve on this, a procedure to estimate hourly variations in emissions from the meta-model estimates has been developed. This procedure makes use of the fact that the majority of the normalised cumulative emission curves of the 1044 Volt'Air simulations follow a similar curve (Figure 1.22). This curve can be approximated by a Michaelis-Menten type equation:

$$Proportion\ of\ Emissions = P_{max} \frac{Time\ to\ 95\%\ emissions}{Time\ to\ 95\%\ emissions + K_{95}/19}$$

where P_{max} and K_{95} are constants. A least squares fit to the median values in Figure 1.22 gives values of 1.03 and 2.38 for P_{max} and K_{95}, respectively.

55
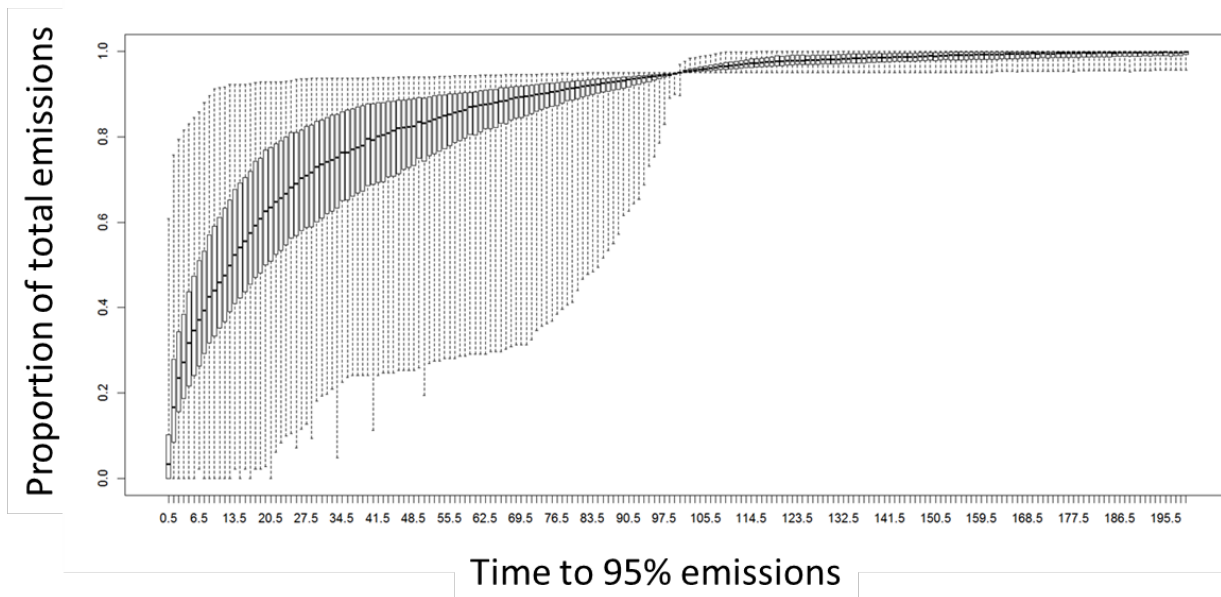
Figure 1: Box plot showing the proportion of total emissions emitted plotted against the % of time to "Time to 95% emissions" for all 1044 Volt'Air simulations. Note that all simulations pass through the point 100, 0.95 since, by definition, at "Time to 95% emissions", 95% of the 30 day emissions have been emitted.

Differentiating this relationship gives the hourly emission estimates for the Michaelis-Menten approximation. The residuals of these hourly emission estimates with respect to those of the Volt'Air simulations were then modelled using a multiple linear regression model with the hourly meteorological variables as the regressors. This relationship was then applied to the meta-model predictions in order to produce a realistic hourly emission curve from the constant value estimated from the meta-model (see example in Fig. 1.23).

In order to test how this hourly model could be applied to the emissions within a CTM grid cell, the following scenario was used:

- Cow slurry application at midday in spring
- Location: 15 km N of Aarhus, Denmark
- Meteorology: 2008 data from EMEP MSC-W model for corresponding grid cell
- Application probability: normally distributed, mean: day 105, standard deviation: 5 days
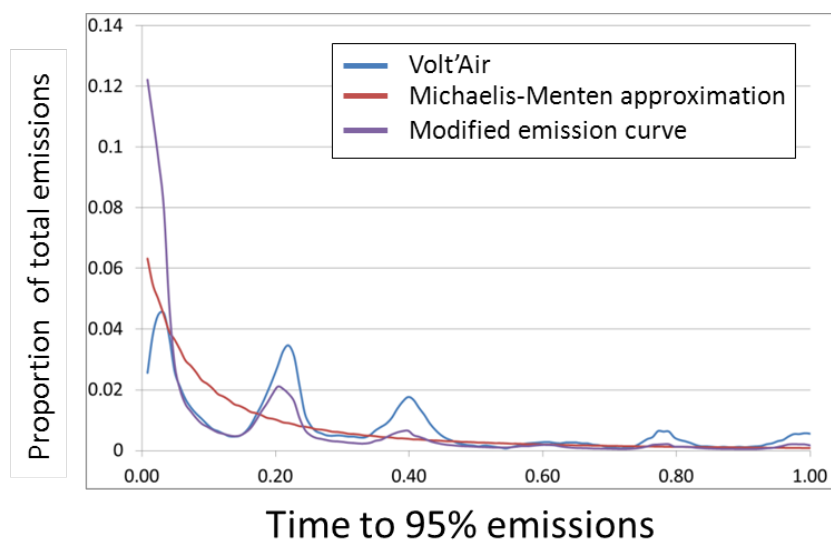
Figure 1.23. Percentage of the 30 day emissions emitted per hour plotted against the proportion of "Time to 95% emissions" (i.e. a value of one corresponds to the time when 95% of the emissions have been emitted) for the original Volt'Air simulation (blue line), the theoretical Michaelis-Menten emission (red line) and the corrected emission (purple line).

Figure 1.24 shows the total emission using the Michaelis-Menten emission equation, the total emission predicted by the hourly meta-model and the probability of application for the period: Julian day 90-120. The "saw-tooth" appearance of the Michaelis-Menten emission equation is due to the application always occurring at midday and the hourly emission profile not depending on the hourly meteorology. Note that the emissions peak two days after the most probable application date as a result of emissions from consecutive application days adding together. The emission curve modified to take into account the hourly meteorological conditions has a more irregular appearance, as a result of changing meteorological conditions. For example, the largest emissions relative to those predicted by the Michaelis-Menten approximation occur during days 108-114, which was a dry and sunny period. After that, emissions are estimated to drop substantially between days 114 and 115 due to rain on day 115.

Volt'Air and the emission meta-model have also been used to study the sensitivity of the models to climate change conditions (Milestone 13). Volt'Air was used to simulate the emissions for the ÉCLAIRE core site at Grignon, France for various simple climate scenarios (temperature increases of 2, 4, 6°C and rainfall changes of -20% to +20%) for three fertiliser types. The meta-model simulations were used to generalise these results by using all of the 1024 scenarios used to develop the meta-model. The results from the Grignon site showed that the change in climate did not significantly affect the NH₃ emissions, but this was because the dataset was too small to detect any differences. By

generalising the results using the meta-model, it was found that NH₃ emissions were mostly temperature dependent, with increases of 12 to 30% (% TAN) with increasing temperature (2-6°C increase). The response to changing rainfall was smaller with a small decrease (a few %) with increasing rainfall (20% rainfall increase).
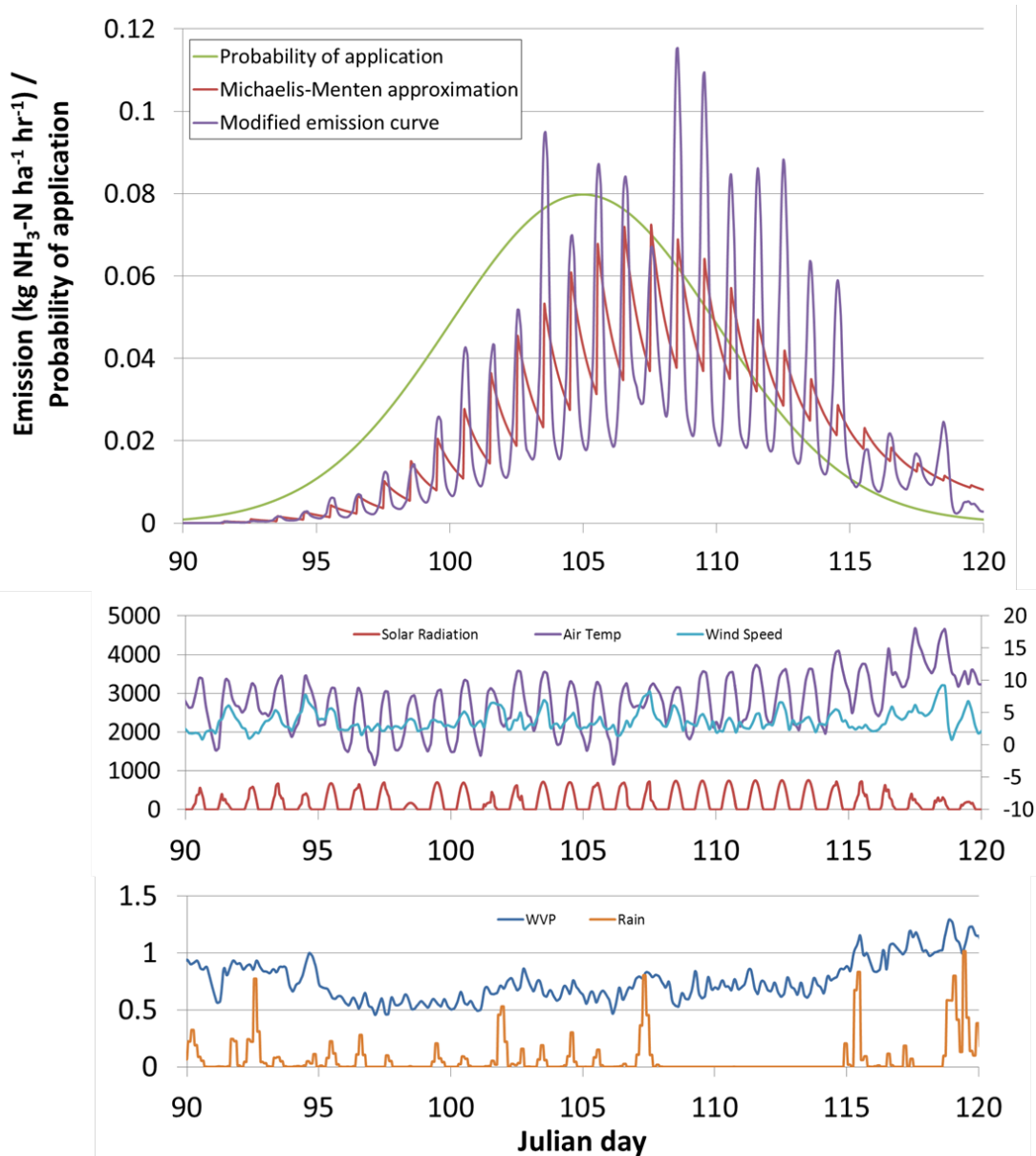
Figure 2: a) Probability of cow slurry application, total emission predicted using the Michaelis-Menten emission equation and the emission estimate modified by the meteorological conditions, plotted against Julian day; b) Solar radiation (W m^{-2}), air temperature (°C) and wind speed (m s^{-1}) and c) Water vapour pressure (kPa) and rainfall (mm) for the same period.

Task 3.2 Background bi-directional NH₃ exchange with soil/vegetation module

The objective of this task was to improve parameterisations and models of surface/atmosphere bi-directional NH_3 exchange with soil and vegetation for background conditions, i.e. for semi-natural ecosystems and for agro-ecosystems outside fertilisation events. The strategy to fulfil these requirements was to evaluate and refine an existing state-of-the-art parameterisation for bi-directional NH_3 exchange, the Massad-Nemitz-Sutton parameterisation scheme ("MNS-2010" hereafter; Massad et al., 2010). The stomatal emission potential (Γ_s) of semi-natural and agricultural vegetation was refined either by adjusting to existing datasets and the data generated within ÉCLAIRE for crops, grassland and forest, or by using crop modelling (CERES-EGC). CERES-EGC was also used to derive parameterisations of the soil emission potential (Γ_g) for background conditions (outside fertilisation events) for croplands across Europe. A meta-modelling approach was developed with the aim of deriving simplified empirical relationships between Γ_g and management and environmental variables, which could then be implemented at low computational cost within chemical transport models (CTMs). A sensitivity analysis indicated that lowering Γ_s values by a significant fraction would not significantly address the under-deposition issue in the model, but instead non-stomatal resistance to NH_3 deposition (R_w) was generally over-estimated and that its parameterisation should be revised. The proposed revision of the MNS-2010 consisted in dividing by 3 the minimum non-stomatal resistance and its response to temperature. This resulted in a significant improvement in model results and predictive capability when tested against ÉCLAIRE datasets. Soil and stomatal emission potential (Γ_g and Γ_s) were obtained from runs of the CERES-EGC crop model for the whole of Europe on a daily time step and with a 0.25°×0.25° grid resolution for three periods: a historical period (1950-2010) and two future periods with two different scenarios RCP4.5 (2010-2100) and RCP8.5 (2010 – 2100). The soil data were extracted from the European soil database (Panagos et al., 2012) and were aggregated on the 0.25°×0.25° grid. Management data were extracted from the open access GHG-Europe project database and were initially provided by M. Wattenbach. The data contains the crop sequences from 1976 to 2010 on a 1 km x 1 km grid which were aggregated in the 0.25°×0.25° grid. Meteorological data were derived from the HadGEM2-ES climate model for two scenarios as described above (RCP 4.5 and RCP 8.5). The Γ_g (Γ_s) simulated with CERES-EGC for background conditions vary between 50 and 6000 (20 and 250) and lie within reported values in literature. The simulated stomatal emissions potentials were almost homogeneously distributed in Europe while soil emissions potentials are larger in alkaline soils. Maps of monthly Γ_g and Γ_s were produced on the 0.25°×0.25° grid. A meta-model of yearly averaged Γ_g was fitted to the simulated values which were shown to respond predominantly and positively to soil pH and fertilization rates and slightly but negatively to temperature and precipitation. Overall, an updated parameterisation of the MNS-2010 is proposed and a new methodology for deriving Γ_g and Γ_s is evaluated.

Meta-modelling of crop emission potentials using CERES-EGC

Objectives

Within the main objectives of WP3 and WP4: developing updated parameterisation and models for simulating NH_3 emissions and improving the description of surface-atmosphere exchange processes for atmospheric pollutants under variable climatic conditions, one of the major challenges was deriving a new set of parameterization for background NH_3 emissions. NH_3 exchange with the vegetation outside fertilization periods is bi-directional and highly depends on the plant canopy and soil characteristics as well as the climate and air NH_3 concentrations (Flechard et al., 2013; Fowler et al., 2009; Massad et al., 2008; Sutton et al., 1995). A logical step towards a better integration of Soil-vegetation NH_3 exchange and atmospheric pollutant transport is coupling an ecosystem model and a chemistry and transport model (CTM). This type of online coupling is very challenging due to the complexity of both model types and variety of parameterisations. We propose here a methodology for offline coupling of NH_3 background exchange. The methodology is based on the two layer bi-directional NH_3 exchange model of Nemitz et al. (2001) and spatial modeling outputs with the CERES-EGC model, where we produce monthly and yearly maps of Γ_g and Γ_s at the European scale. These maps will either be directly used as input variables to the bi-directional NH_3 emissions scheme within a CTM or as a database to construct a meta-model, namely an equation function of the CTM variables, which can be directly incorporated in the CTM.

Methodology for deriving monthly maps of Γ_g and Γ_s

The emission potentials Γ_g and Γ_s simulations are obtained from runs of the CERES-EGC model for the whole of Europe on a daily time step and with a 0.25° x 0.25° grid resolution for three periods: a historical period (1950-2010) and two future periods with two different scenarios RCP4.5 (2010-2100) and RCP8.5 (2010 – 2100).

CERES-EGC model

CERES-EGC is an agro-ecosystem type model which is a version of the CERES family of models (Jones and Kiniry, 1986) adapted to simulate the environmental impacts of crops by Gabrielle et al. (2006). The model is based on several modules each for a different type of crop, but all share the same subroutines for water dynamics, and soil carbon and nitrogen dynamics. At the moment, CERES-EGC simulates the development and growth of several types of agricultural crops namely: maize, wheat, barley, rape, sorghum, sunflower, pea, sugar-beet, soya, and an intercrop (based on the rape crop). The soil organic matter decomposition is based on the NCSOIL model (Gabrielle et al., 2002a; Molina et al., 1983). CERES-EGC runs at a daily time step and for one type of crop at a time. The originality of the model lies in the coupling of a widely used and validated crop growth model (Gabrielle et al., 2002b; Langensiepen et al., 2008; Rezzoug

et al., 2008; Xiong et al., 2007) to several environmental impact modules linked to the Nitrogen cycle such as N_2O, NO and NH_3 emissions.

Upscaling method

Simulations by CERES-EGC are up-scaled by linking the model to a GIS database. The GIS database used for the model entry data is detailed below. The model runs independently for each grid cell and for consecutive 150 years of simulations.

Soil database. The soil data were extracted from the European soil database (Panagos et al., 2012) and were aggregated on the 0.25° x 0.25° grid. Several soil parameters necessary to run the CERES-EGC model were derived from pedotransfer functions (Ritchie, 1972). Figure 1.25 below shows the European map of the soil top layer pH values as used by the model simulations and further Γ_g calculations.

Management data. Data were extracted from the open access GHG-Europe project database and were initially provided by M. Wattenbach. The data contains the crop sequences from 1976 to 2010, the total yearly amount of nitrogen and the repartition in organic and mineral nitrogen on a 1 km x 1 km grid. The data were aggregated on a 0.25° x 0.25° grid by selecting the two major rotations from the pixels lying within this grid cell. Those two rotations represented on average 70% of the grid cell. Additional data such as dates of application of N fertilizer and sowing of crops were calculated from simple algorithms based on minimal and maximal temperature requirements, precipitation conditions as well as selected date intervals for each crop based on standard European management practice. Figure 1.26 below illustrates the total nitrogen fertilization used for 2005 as an input variable for the CERES-EGC simulation.
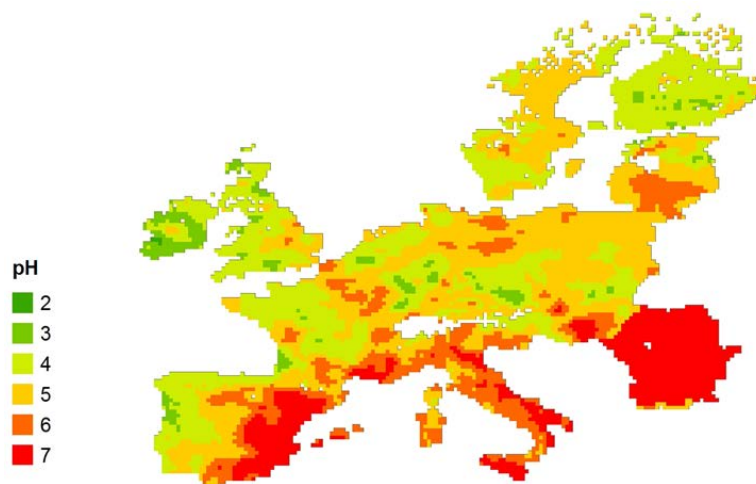
Figure 1.25: Soil pH values for the soil top layer used for model simulations and Γ_g calculations.
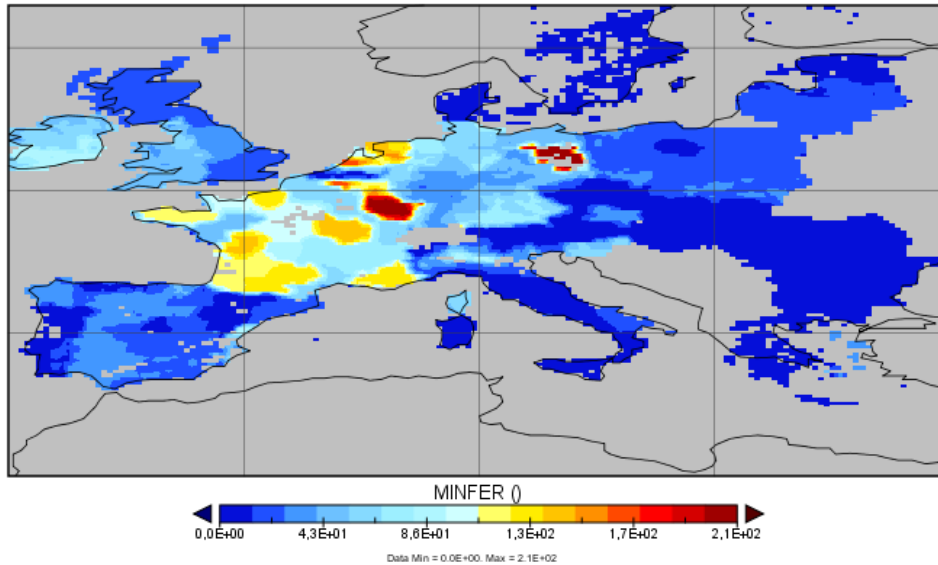
Figure 1.26: Total mineral fertilization application map in kg ha^{-1} as used as input for model test simulations.

Climate data. Meteorological data are derived from the HadGEM2-ES climate model for two scenarios as described above (RCP 4.5 and RCP 8.5). The variables needed to run the EGC-model on a daily time step are: maximum and minimum daily temperatures (°C), Cumulated daily precipitation (mm), average daily Short wave radiation (W m^{-2}), and average daily wind speed (m s^{-1}).

Emission potential calculations

Soil emission potential. Γ_g is defined as the soil ammonia emission potential and can be calculated using the equation below:

$$\Gamma_g = \frac{[NH_4^+]_{soil}}{[H^+]_{soil}}$$

Where [NH$_4^+$]$_{soil}$ is the top layer soil ammonium concentration in mol L^{-1} as simulated by the CERES-EGC model and [H$^+$]$_{soil}$ is derived from the soil pH map for the top layer. Note that the CERES-EGC outputs are given in gram NH$_4^+$-N per hectare. We therefore use the simulated soil water content of the soil top layer and the Soil bulk density to transform the NH$_4^+$ concentration into mol L^{-1}. [see note[1]]

---

[1]
$$[NH_4^+]_{soil} = \frac{NH4_{1}\left(\frac{kg}{ha}\right)}{M_{mol\,N}\left(\frac{g}{mol}\right) \times 10^{-3} \times \frac{SWC_{1(\%vol)}}{100} \times \frac{depth_{1(cm)}}{100} \times 10^{3}\left(\frac{L}{m^3}\right) \times 10^{4}\left(\frac{m^2}{ha}\right)}$$

ÉCLAIRE Third Periodic Report: November 2015

Stomatal emission potential. Otherwise called Γ_s is the stomatal emission potential which can be calculated from the equation below:

$$\Gamma_s = \frac{[NH_4^+]_{apo}}{[H^+]_{apo}}$$

where $[NH_4^+]_{apo}$ and $[H^+]_{apo}$ are the apoplastic NH_4^+ concentrations and apoplastic pH respectively. These two variables are not simulated explicitly by the CERES-EGC model; however, the model simulated NH_4^+ concentrations in g g^{-1} dry weight which we use as a proxy to estimate total plant NH_4^+ content and use the equation below from Massad et al. (2010) to estimate Γ_s:

$$\Gamma_s = 19.3 \times e^{0.0506 \times [NH_4^+]_{bulk}}$$

where $NH_4^+{}_{bulk}$ is the total plant ammonium concentration in µg NH_4^+ g^{-1} tissue fresh weight. We assume that the ratio of fresh weight to dry weight of the leaves is equal to 10.

Methodology for developing the meta-modeling concept of background Γ_g in Europe

The simulations of CERES-EGC Γ_g were used to retrieve a meta-model of Γ_g. Such a meta-model is useful as it is a simple representation of a complex model which can be included in a chemical transport model. The objective here is to develop a model of the Γ_g which is representative of the background conditions, away from any fertilization events, as the Γ_g following fertilization was developed based on the Volt'air model dedicated to such conditions, while the processes in CERES-EGC are not well adapted to reproduce these conditions. However, since CERES-EGC simulations include fertilization events, we used despiked yearly averaged Γ_g to evaluate the background Γ_g meta-model as detailed below.

The methodology used for finding the Γ_g meta-model was similar as the one used in D3.1 and D4.1. Monthly means of (Γ_g^{CERES}) were retrieved from the CERES-EGC computations in each 0.25°×0.25° grid cell in Europe, together with the drivers of the model (soil and meteorological data and nitrogen fertilization rates) for the year 2005. Extreme values of Γ_g were filtered out by a regressive despiking algorithm. All data were then averaged over the entire year. Then a multiple linear regression was performed between the logarithm of Γ_g^{CERES} and the other variables in the dataset, to find $\Gamma_g^{meta-model}(bgd)$ which satisfies:

$$ln\left(\Gamma_g^{meta-model}(bgd)\right) = \left[a_0 + \sum_{1:m} a_i x_i(site, period)\right]$$

where $a_0 \cdots a_m$ are the model coefficients and $x_1 \cdots x_m$ are the yearly averaged soil, meteorological and fertilisation variables which are by nature dependent on the sites and

periods. The linear regression retrieves the $a_0 \cdots a_m$ coefficients that minimize the mean square error of the logarithms using the linear model (*lm*) function in *R*:

$$MSE = \frac{1}{N} \sum_{European\ pixels} \left[ln\left(\Gamma_g^{meta-model}\right) - ln\left(\Gamma_g^{CERES}\right) \right]^2$$

The best model performance was retrieved with a stepwise algorithm that maximises the Akaïke *An Information Criterion* (AIC = $-2ln(L) - 2(N_P + 1)$), where *L* is the likelihood and N_P the number of parameters of the model.

Results of the CERES-EGC modeling of NH$_3$ emission potentials

We present here results for Γ_g and Γ_s calculations based on spatial CERES-EGC outputs for the year 2005 and for the year 2050 based on two different climate scenarios RCP4.5 and RCP8.5.

Annual dynamics of NH$_3$ emission potentials

Figure 1.27 illustrates the box plot for the yearly dynamics of all pixels of the European domain for Γ_g. The simulated values for Γ_g for background conditions vary between 50 and 6000 and lie within reported values in literature (Flechard et al., 2013; Massad et al., 2010). The yearly dynamics of the means and medians are however very small but could be explained by the bias of looking at monthly means of Γ_g. Peak Γ_g values are usually very temporary and only last a few days as given for example in Massad et al. (2010) with an exponential decrease and a decaying time of 2.8 days.
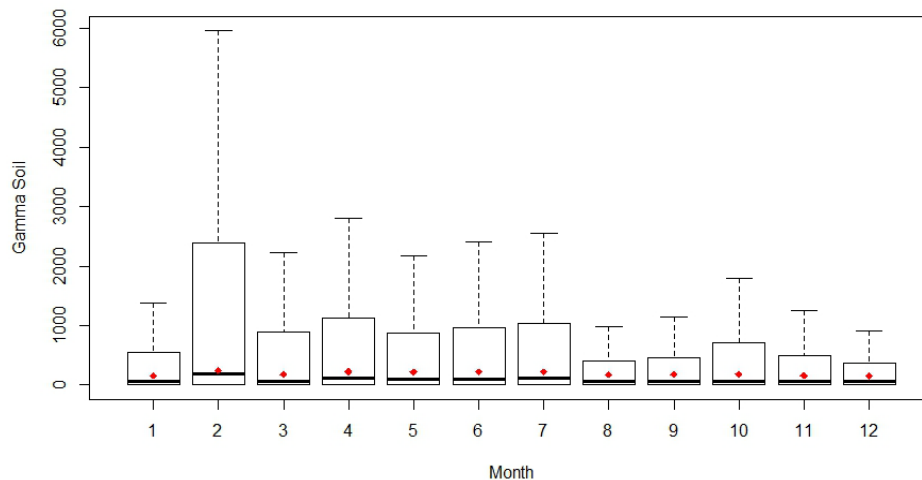
Figure 1.27: Box plot of yearly dynamics of Γ_g for the year 2005. Red dots represent means.

A similar pattern is noted also for Γ_s values as illustrated in Figure 1.28 below where monthly means and medians present little variability. Simulated Γ_s vary between 20 and 250 and are also in line with expected values as noted in the literature. We notice, however, a different distribution where maximum values are in the cold months and minimal values in warm months. This could be an artefact of the calculation we used since simulated NH_4^+ concentrations are normalized by the total biomass of the plant and months 11, 12, 1, 2 and 3 shows the lowest monthly biomass values.
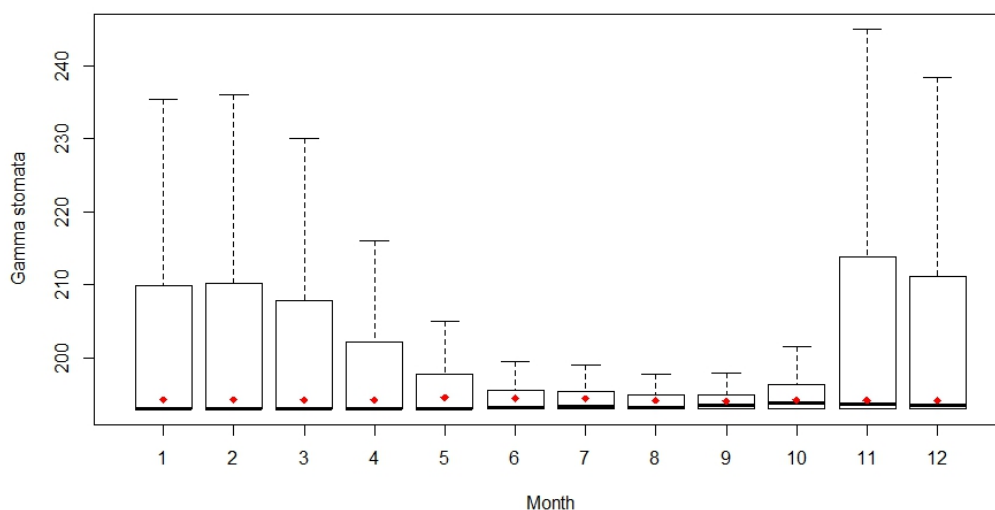
Figure 1.28: Box plot of yearly dynamics of Γ_s for the year 2005. Red dots represent means.

Spatial variability of Γ_g and Γ_s

The spatial variability of Γ_g values is tightly correlated to that of the soil pH values as illustrated in Figure 1.29 for the year 2005 with low values in acidic soils and high values in alkaline soils.
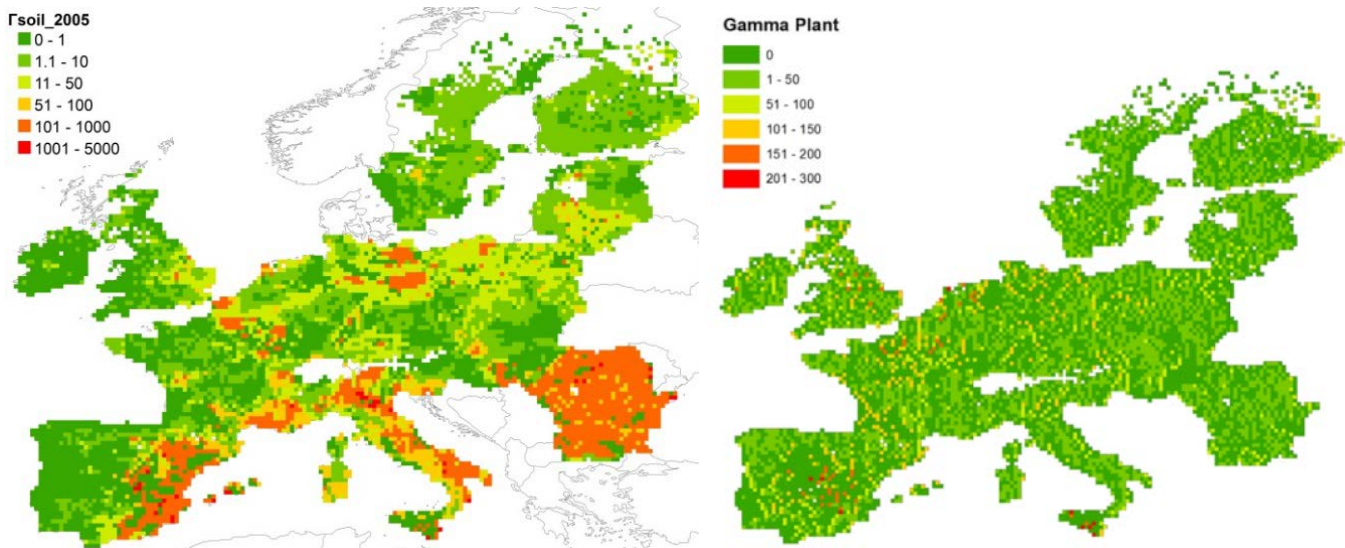
Figure 1.29: Spatial distribution of yearly average Γ_g and Γ_s values for 2005. Note that the two scales are different. The large Γ_g values in Bulgaria and Romania are due to default soil pH set to 7.

Concerning Γ_s, we notice a homogenous distribution on the entire domain (Figure 15) with some hot spots in France and Spain but with generally weak values. This is explained by the fact that plant NH_4^+ concentrations as modeled by CERES are a result of soil available NH_4^+ and plant demand which is a result of plant growth and therefore availability of Nitrogen and are therefore not very variable. An improvement of this modeling exercise would be to better parameterize plant roots absorption of NH_4^+ after the fertilization events when the absorption of the plant is peaking (Husted et al., 1996; Massad et al., 2009).

Effect of climate change on of NH3 emission potentials

Figure 1.30 illustrates the difference between yearly averages for 2050 between the two climatic scenarios RCP8.5 and RCP5.5 for Γ_g and Γ_s respectively. We notice an increase in Γ_g values with RCP8.5 scenario, especially for northern regions. This can partly be explained by the effect on soil water content in the soil top layer that affects the calculation of Γ_g. Concerning Γ_s, we notice a decrease for the RCP8.5 scenario as compared to the RCP4.5 scenario except for the south of Spain. This could be explained by an increase

in plant growth and therefore an increase in plant N uptake except where plants are water stressed and therefore growth is limited.
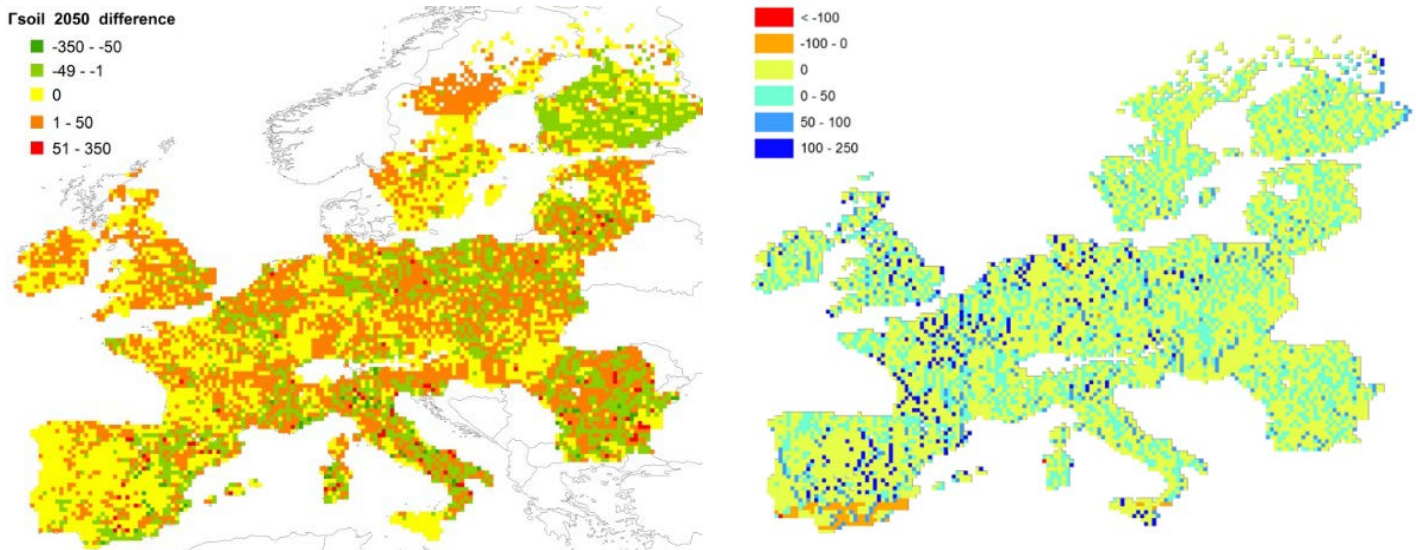
Figure 1.30: Difference in yearly Γ_g and Γ_s plant averaged for 2050 between two climatic scenarios RCP8.5 and RCP4.5. Note the different scales.

Results of the meta-modelling concept of background Γ_g in Europe

These results show the first attempt to retrieve the background Γ_g meta-model for European conditions.

Meta-model parameters and performance

Two meta-models were tested, one with the most available meteorological and soil variables (Model 1) and the second with only soil pH and annual fertilization (Model 2; Table 1.3). The meta-modelling approach was quite successful as shown by the quite high efficiency values (Table 1.4), although the RRMSE > 1 indicate that the Γ_g is correctly represented by the meta-model within roughly 60%. Nevertheless, bearing in mind the considerable range of Γ_g values, from below 10^{-1} to more than 10^3, it is clear that the meta-models reproduce the order of magnitude of Γ_g in Europe correctly as shown by Figure 1.31.

The parameters of the meta-model of Γ_g (Table 1.3) show that, as expected, Γ_g is responding positively to soil pH and nitrogen fertilisation. It is also positively correlated with minimum daily temperature, while it is negatively correlated with precipitation (which leads to more dilution of the soil ammonium in soil water) and maximum temperature. Overall the response to temperature is negative because the coefficient of maximum daily temperature is larger than that of the minimum temperature. Hence the response of the mean temperature will be negative.

The main drivers of Γ_g are however fertilization and soil pH, as shown by the overall good performance of the Model 2, which only uses these two variables. The corresponding simplified model gives the yearly averaged background Γ_g in the form:

Table 1.3: Coefficient values of the meta-models 1 and 2 of $ln\left(\Gamma_g^{meta-model}\right)$. The meteorological and soil variables are yearly averages.

Coefficient	Model 1		Model 2	
	Estimate	Std. Error	Estimate	Std. Error
a_0	-9.78	0.086	-10.3	0.06
Minimum daily temperature (°C)	0.028	0.0004	-	-
Maximum daily temperature (°C)	-0.059	0.008	-	-
Daily precipitation (mm)	-0.004	0.008	-	-
In(annual Fertilisation in kg N ha^{-1})	0.39	0.007	0.37	0.007
Soil pH	2.22	0.010	2.16	0.01

Table 1.4: Quality of fit of the meta-models 1 and 2 of background Γ_g for Europe. Model 1 incorporates all variables while Model 2 only uses fertilisation rate and soil pH. RMSE = Root Mean Square Error, RRMSE = Relative Root Mean Square Error, MAE = Mean Average Error, RMAE = Relative Mean Average Error, EF = Efficiency

	Model 1	Model 2
RMSE	135	134
RRMSE	1.61	1.60
MAE	44	44
RMAE	0.52	0.53
Bias	4.9	4.8
EF	0.56	0.56
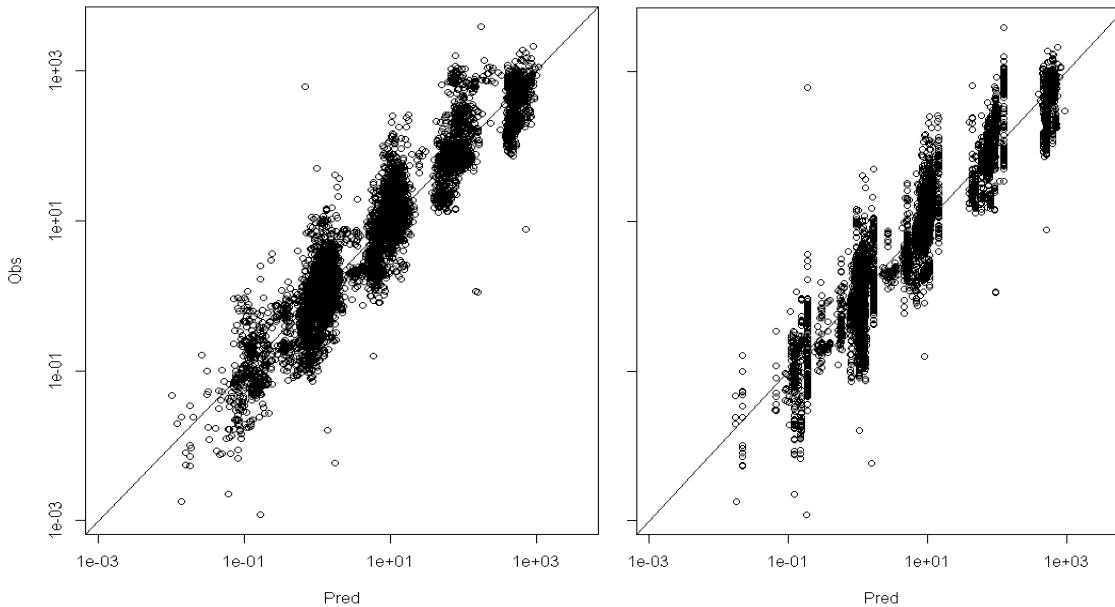
Figure 1.31. Observed (CERES-EGC) versus predicted (meta-model) yearly averaged Γ_g in Europe. Left: Model 1. Right: Model 2.

$$\Gamma_g^{bgd} \sim \alpha \times N_{applied}{}^{0.37} \times e^{2.16pH_{soil}}$$

where $N_{applied}$ is in kg N ha^{-1}. This equation however does not show any response to temperature, which means that in first order, Γ_g will not respond to climate change. The response to temperature and precipitation would however be of the following form:

$$\Gamma_g^{bgd} \sim \alpha \times e^{-0.03T} \times e^{-0.004P}$$

These equations have to be taken with caution as they have to be validated prior to being used. It is nevertheless demonstrated how new parameterisation in the MNS 2010 approach can be deduced from CERES-EGC modelling at European scale (see Table in Appendix 1 of Deliverable 3.2 where Γ_g is unknown).

Results:

This work, reported in Deliverable 3.2, has provided improved parameterisations for background bi-directional NH_3 exchange with soil and vegetation, based on extensive testing and calibration and/or meta-modelling using state-of-the-art models:

- the Massad-Nemitz-Sutton (2010) parameterisation for semi-natural and background agricultural vegetation, for stomatal exchange and non-stomatal uptake;
- the CERES-EGC crop model for meta-modelling of the background soil emission potential;

- A proof of concept for developing a meta-model of soil emission potential based on yearly averages.

The MNS parameterisation was found to provide realistic NH_3 exchange estimates over a range of semi-natural and agricultural sites in background conditions, with minimal adjustments required for some parameters. More field-scale testing using a wider range of flux datasets, as well as regional-scale testing within chemical transport models could further refine the model's calibration, but the scheme already shows good potential for a generalised implementation in CTMs. Some areas could be further improved, such as the characterisation of ground-layer emissions from decomposing leaf litter, even in unfertilised ecosystems.

We proved the concept of using the CERES-EGC modeling approach for retrieving soil and plant ammonia emission potentials. Preliminary results are satisfactory in the sense that values are consistent with values reported in the literature. We present a first analysis based on monthly averages which needs to be refined with respect to temporal variability as it would be more conclusive to look at daily values. These maps can be used as input variables to chemistry and transport models to simulate the effect of different climate change scenarios or land use change scenarios.

We showed that the approach of developing a meta-model of the soil emission potential was suitable and could lead to simple formulation of this potential in background conditions in Europe. Further developments should include monthly variations of the soil emission potential and species specific analysis.

Task 3.3: Soil NO emission model: Soil NO emission model (improved parameterization with regard to responses to changes in environmental conditions)

The aim of this work package was to provide improved process descriptions and parameterizations of biotic and abiotic (agricultural management) driven soil NO emissions that include a robust response to climatic conditions that are predicted to change in the future. The objective was to improve the climate response characteristics of soil NO emissions within the LandscapeDNDC model.

The final deliverable D3.3 (which was delivered within this reporting period) is an improvement of the process description of the biogeochemical ecosystem model LandscapeDNDC. This has been achieved by developing a new soil biogeochemical module for LandscapeDNDC. The progress of the deliverable will be evaluated by validation of simulation studies of combined soil N_2O and NO emissions from managed ecosystems (forest, arable and grassland). This included an assessment of the uncertainty of the model when predicting soil NO and N_2O emissions.

Collection of data for site scale model validation

Within the Éclaire project, NO field observations have been conducted at nine sites across Europe, but because LandscapeDNDC does not currently treat organic soils and due to some gaps in the database of the ÉCLAIRE database when this work commenced, only three datasets were used for the model development. To maximise representativeness of the model, we have therefore further increased the data foundation for the validation to other sources such as e.g. the European fluxes database cluster (http://gaia.agraria.unitus.it/), NitroEurope IP and from the NOFRETETE project.

Forest ecosystems

The new soil module was applied for simulation of soil NO and N_2O emissions at 12 different forest stands including the dominating tree species across Europe (*Picea abies, Fagus sylvatica, Picea sitchensis, Betula pendula, Pseudotsuga menziesii and Quercus robur*). Stands area are within a large latitudinal range representing Temperate and Mediterranean climatic conditions. Mean annual temperature varied between 6.8 and 12.2 ºC while annual precipitation ranged from 730 to 1500 mm. Similarly stand age was different in every single case. The youngest forest stand (31 years) corresponded to Glencourse-UK while the oldest forest was for the Austrian beech stand at Schottenwald (145 years). Atmospheric N deposition varied from 6.5 - 47 kg N ha-1 yr^{-1}. Humus type was moder except mull at beech forest of Hoeglwald, spruce forest at Achenkirchen and at the oak forest at Matrafuered. Data for model initialization regarding vegetation and soil properties was obtained from publications (Kesik *et al.*, 2005), from the European fluxes database cluster (http://gaia.agraria.unitus.it/), IP NitroEurope and ÉCLAIRE databases and from the NORFRETETE project. Daily climate data for model driving as well as daily NO and N_2O flux measurements were obtained from the same aforementioned sources.

Arable and grassland ecosystems

For the model validation six arable and four grassland sites have been selected due to observation data availability. All studied systems are under intensive cultivation practices using synthetic fertilizers, farm yard manure and slurries as main N inputs (except at Bugac-Hungary and at the grassland site at Virginia-USA). The studied sites are located in the Central and Mediterranean part of Europe and at the north part of the American Continent. Model input data and measurements were provided by the IP NitroEurope and ÉCLAIRE databases as well as from previous work (Butterbach-Bahl *et al.*, 2009). The evaluation sites present different management regimes including the main commodity crops (maize, wheat, barley, rape seeds, etc). For details on management practices we refer to (Laville *et al.*, 2005; Venterea *et al.*, 2005; Ammann *et al.*, 2009; Butterbach-Bahl *et al.*, 2009; Loubet *et al.*, 2011).

Model Parameterization

To improve the processes describing the soil carbon and nitrogen cycle a calibration of the process parameters was performed in order to optimize the prediction accuracy of the model. First a parameter sensitivity analysis for the new soil biogeochemistry module has been performed in order to identify the most sensitive parameters describing soil borne NO and N_2O emissions. In the next step parameter calibrations for different ecosystems including the available field observations of NO and N_2O emissions have been performed using a Bayesian Model Calibration method (BC) (Van Oijen *et al.*, 2005; Rahn *et al.*, 2012). The parameters addressed within the calibration are summarized in Table 1.5.

Table 1.5: The 15 most sensitive process parameters with respect to soil NO and N_2O emissions used for the calibration and Bayesian parameter uncertainty quantification

Symbol	Description	Units
CO_2_PROD_DECOMP	Factor of CO_2 production during decomposition	
F_DENIT_N_2O	Factor that regulates how much of the denitrified N goes to N_2 (directly)	
MUEMAX_C_DENIT	Microbial use efficiency for C consumption during de-nitrification	kg C d^{-1}
KF_NIT_N_2O	Factor reaction rate for N_2O reductase	
KMM_N_DENIT	Michaelis-Menten constant for N during denitrification	Kg N m^{-3}
AMAX	Maximal specific microbial death/reutilization rate	kg C d^{-1}
KR_HU_AORG	Humification rate for heterotrophic microbial biomass	kg C d^{-1}
F_DENIT_NO	Factor of NO production during denitrification	
KMM_C_DENIT	Michaelis-Menten constant for C use during de-nitrification	Kg C m^{-3}
MUEMAX_C_NIT	Microbial use efficiency for C consumption during nitrification	kg C d^{-1}
KR_HU_HUM_1	Rate of Humification of humus pool one	kg C d^{-1}
KR_DC_HUM_1	Rate of decomposition of humus pool one	kg C d^{-1}
KF_REDUCTION_ANVF	Reduction factor of the anaerobic volume fraction	
BIOSYNTH_EFF	Biosynthesis efficiency factor	
KR_DC_HUM_0	Rate of decomposition of humus pool cero	kg C d^{-1}

The BC method has been proved to be a powerful approach to obtain very good optimized parameters sets for process-based models. Figure 1.32 illustrates the Metropolis

algorithm for the Bayesian model calibration of the LandscapeDNDC soil biogeochemistry.

Performing four different Bayesian calibrations in parallel (Markov chains) for these parameter sets and using the convergence criteria of (Gelman and Rubin, 1992) a calibrated joint parameter distribution will be generated (Figure 1.33). This joint parameter distribution represents the posterior parameter distribution of the calibration, from where we sampled optimum sets for uncertainty quantification.

Results:

Model calibration

The Bayesian calibration resulted in a joint parameter distribution for the 15 most sensitive parameters (Figure 1.33). Model calibration was carried out for different sites using daily NO and N_2O measurement. Table 1.6 summarizes and Figure 1.33 illustrates the distribution of each parameter after the calibration.

The posterior parameter values were assigned uniform probability within their given ranges. The uncertainty of the prior parameter values (pre calibration model default values given with minimum and maximum values) were minimized considerably during the BC (e.g. see KF_NIT_N2O in Figure 1.33) while some parameters (like KR_HU_AORG, see Figure 1.33) did not reduce their uncertainty significantly. This parameter corresponds to the humification constant from heterotrophic microbes and it suggests that all values ranging from 0.001 to 0.15 present a similar probability. For this kind of parameter, uncertainty is not reduced by the BC method. Values exceeding 0.14 are less likely than the others.

Measured vs. simulated daily NO and N_2O emissions at the site scale

The evaluation of the model performance to predict daily NO emissions were done based on commonly used model fitting indicators (Engeland *et al.*, 2010; Kiese *et al.*, 2011; Ritter and Muñoz-Carpena, 2013) such as the coeffcient of determination (r^2), model efficiency (ME) and normalized root mean square prediction error (RMPPE$_n$). (Bouwman *et al.*, 2010) mentioned that r^2 values from model validation studies on daily time resolution are rarely reported for N_2O because model performance might be low and for validation of NO emissions model performance is in general even less precise. In our study the r^2 values indicate a fundamental good performance of the new calibrated process based module in LandscapeDNDC across the three different ecosystems.

The best posterior parameter values obtained from the BC was applied for the arable, grassland and forest ecosystem simulations. Modelled soil NO and N_2O emissions were compared against high and low temporal resolution field data from semi-natural (forest) and cultivated lands (arable and grasslands) across Europe. This validation embraces also a model evaluation including short and long term data series which range from

scattered point measurements up to continuous 15 years measurement campaigns. Table 1.7 summarizes the performance of the model to represent biogenic NO emissions.
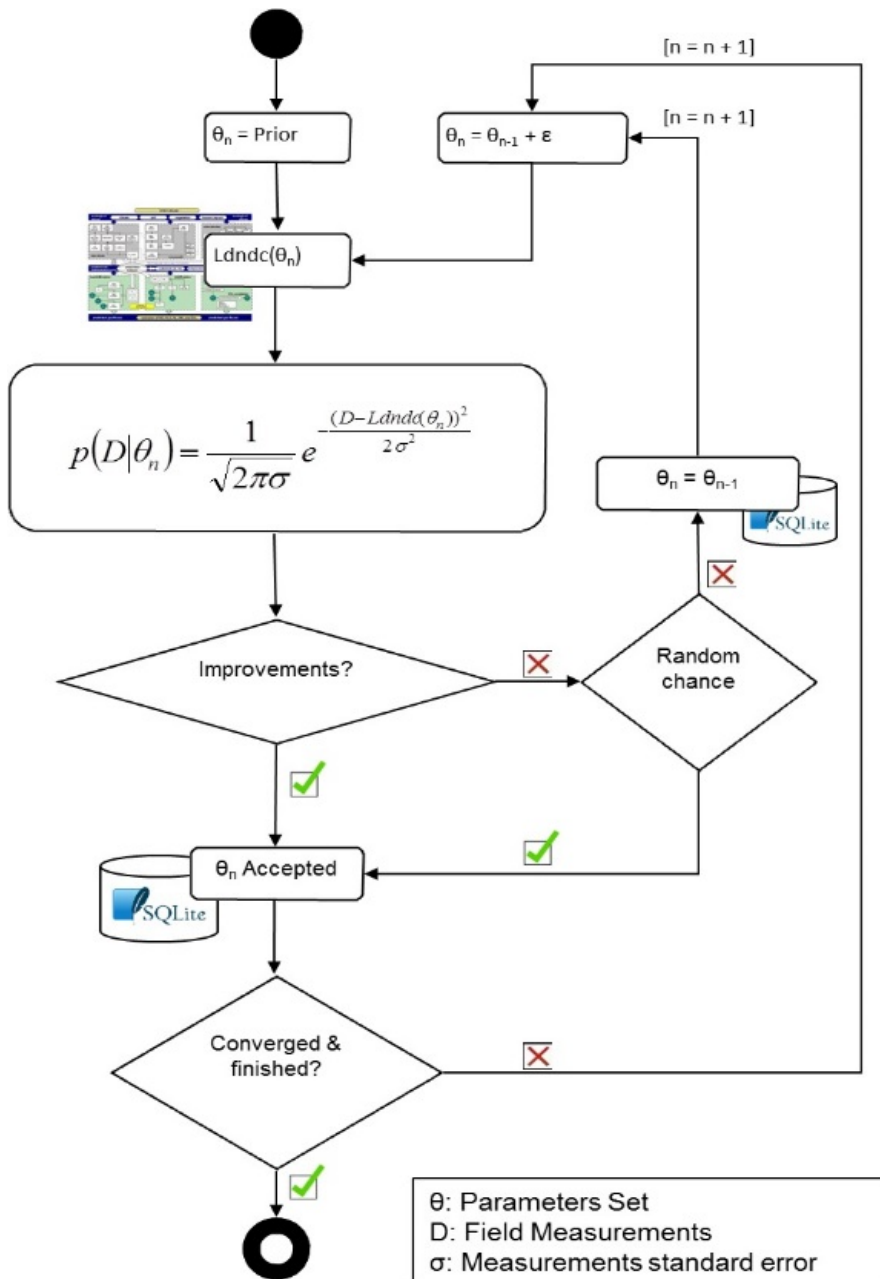
Figure 1.32. Metropolis algorithm for the Bayesian Calibration of the LandscapeDNDC soil biogeochemistry module following the approach of Van Oijen *et al.*, 2005, Rahn *et al.*, 2012.
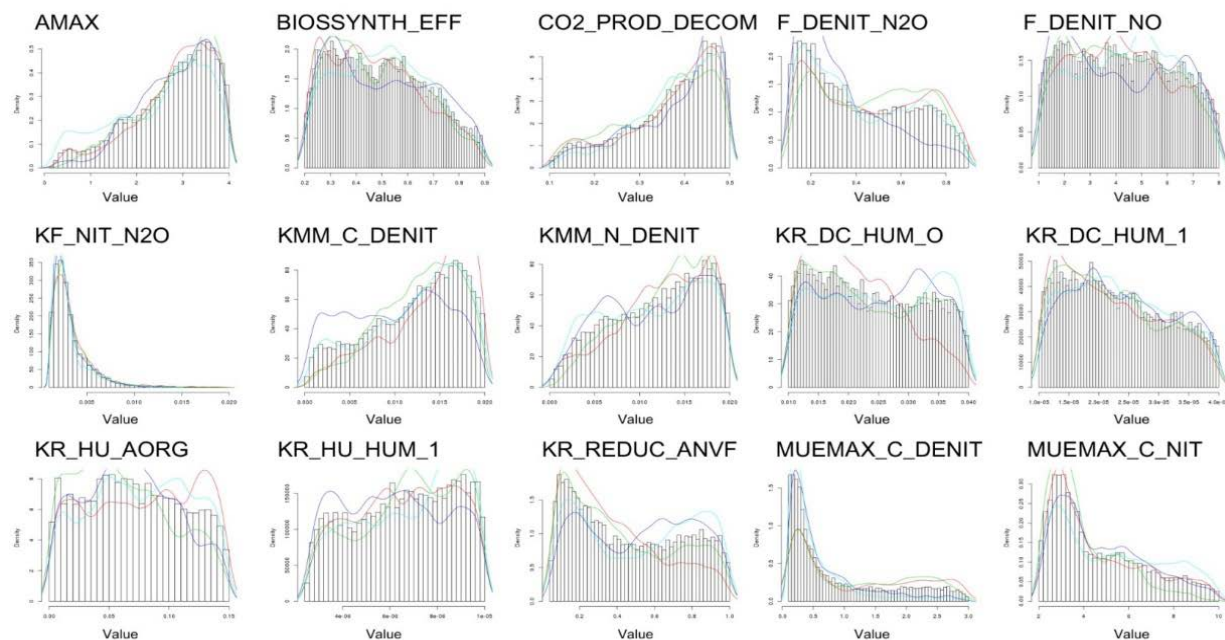
Figure 1.33. Joint parameter distributions resulting from the 4 parallel BC chains (indicated by the 4 coloured lines) after the conversion of the Markov-Chains was reached

Table 1.6: Summary of calibrated parameter values (default, minimum, maximum and optimized parameter value)

Parameter name	default value	minimum	maximum	posterior
CO$_2$_PROD_DECOMP	0.300	0.100	0.500	0.240
F_DENIT_N$_2$O	0.250	0.100	1.000	0.475
MUEMAX_C_DENIT	1.050	0.000	3.000	0.104
KF_NIT_N$_2$O	0.003	0.000	0.020	0.003
KMM_N_DENIT	0.083	0.000	0.020	0.019
AMAX	1.500	0.000	4.000	3.433
KR_HU_AORG	0.015	1.000	0.150	0.004
F_DENIT_NO	4.000	1.000	8.000	5.785
KMM_C_DENIT	0.002	0.000	0.020	0.010
MUEMAX_C_NIT	5.000	2.000	10.000	8.106
KR_HU_HUM_1	0.000	0.000	0.000	0.000
KR_DC_HUM_1	0.000	0.000	0.000	0.000
KR_REDUCTION_ANVF	0.200	0.000	1.000	0.278
BIOSYNTH_EFF	0.565	0.200	0.900	0.447
KR_DC_HUM_0	0.020	0.010	0.040	0.033

ÉCLAIRE Third Periodic Report: November 2015

Table 1.7: Summary of the performance of model simulations for validation of soil NO emissions

Site	number of obsvs.	Measured-mean NO (g N ha^{-1} d^{-1})	Stdev. mean NO (g N ha^{-1} d^{-1})	Simulated mean NO (g N ha^{-1} d^{-1})	r^2	ME	RPMSEn
DE_Hoeglwald_spruce	4382	24.03	3.09	22.5	0.31	0.03	0.99
DE_Hoeglwald_beech	1414	6.8	2.05	7.74	0.23	-0.15	1.07
AT_achenkirchen_spruce	254	0.14	NA	0.1	0.04	-1.50	1.58
UK_glencourse_sitka	358	6.21	1.18	5.67	0.15	0.01	1
UK_glencourse_birch	373	0.46	0.45	1.34	0.01	-1.25	1.5
NL_speulderbos_douglas 2006-2009	729	8.61	0.33	11.59	0.66	0.21	0.89
NL_speulderbos_douglas 2002-2003	341	18.78	1.11	15.02	0.76	0.67	0.58
AT_klausenleopoldsdorf_beech	63	0.17	NA	0.99	0.07	-2.50	2.35
AT_schottenwald_beech	240	4.63	NA	3.38	0.00	-0.73	1.31
HU_matrafuered_oak	4	0.58	0.24	1.59	0.55	-1.18	2.9
HU_matrafuered_spruce	19	0.38	0.32	1.93	0.79	-2.19	4.26
DK_soroe_beech	730	0.65	0.38	1.73	0.02	-3.43	2.1
IT_ispra_oak	154	5.44	3.48	4.6	0.65	0.54	0.68
FR_grignon	412	1.82	1.23	1.54	0.32	0.26	0.86
USA_virginia_maizwinbarley	30	9.44	6.82	5.2	0.02	-0.60	1.24
USA_virginia_soybeanmaiz	26	3.06	1.03	0.77	0.01	-2.25	1.77
FR_paris_wheat	42	6.49	1.53	3.9	0.00	-0.68	1.28
USA_colorado	10	2.54	1.29	1.78	0.28	-0.13	1.01
UA_petrodolinskoe	354	1.17	0.54	1.28	0.19	0.17	0.91
CH_oensingen_qa	361	1.28	1.16	1.78	0.11	-0.02	1.01
HU_bugac_extensive	1291	2.98	NA	1.5	0.05	-0.05	1.02
USA_virginia_grass	23	3.02	NA	2.1	0.02	-0.72	1.28
CH_posieux	103	0.55	NA	0.78	0.02	-1.88	1.69

The evaluation at the daily time scale results in r^2 values ranging from 0.01 to 0.79 while ME values ranged from - 3.42 to 0.67. RMSPE$_n$ values varied from 0.57 to 4.26 (Table 1.7). Measured mean soil NO flux per site was well simulated by LandscapeDNDC (r^2= 0.92, p<0.05, 3) (Figure 1.34). The best performance was seen for forest ecosytem (r^2= 0.95, p<0.05, comparing means of daily NO emission strengths, compare Figure 1.34) rather than for exploited lands r^2= 0.82, p<0.05. Slight model deviations were estimated for sites presenting high data resolution and long term measurements campaigns (i.e. Höglwald-Germany, Speulderbos-Netherlands, Grignon-France, Oensingen-Switzerland) while a higher deviations was seen for sites having scatter measurement points (i.e Matrafuered-Hungary, Virginia-United States, Klausenleopoldsdorf-Austria). Scatter measurements made very difficult to value the performance of the model to represent soil NO fluxes.
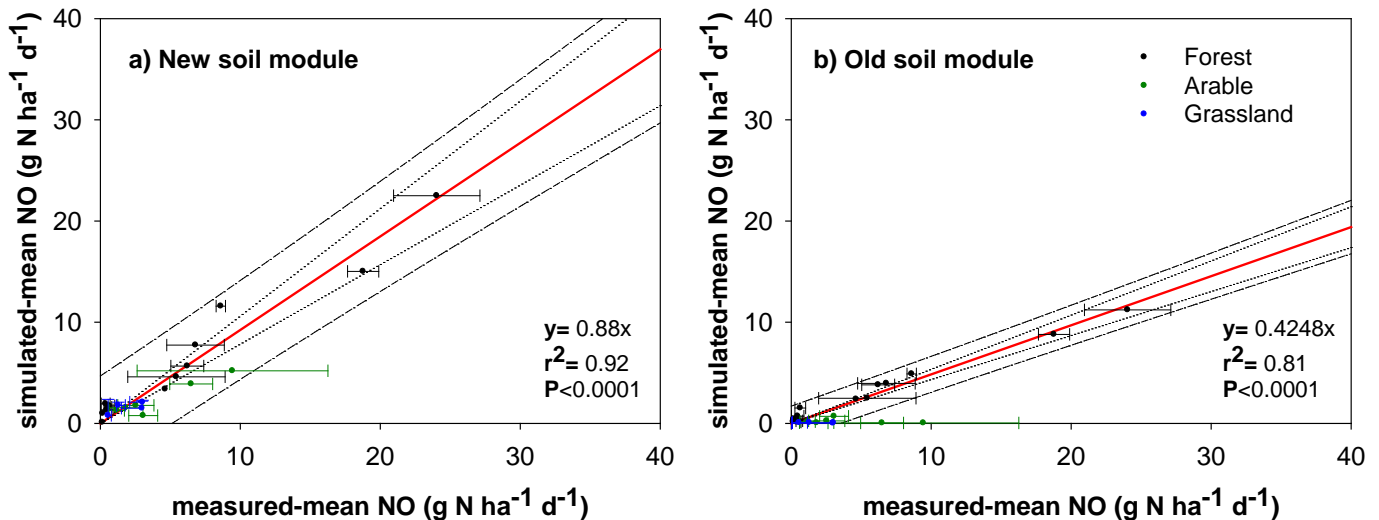
Figure 1.34: Comparison of the new developed versus the default soil biogeochemistry modules on the prediction of daily mean NO emissions. Data shown are means of paired data of daily simulated / observed NO emissions. As for some observations the number of observations is coarse, the data shown does not present yearly averages.

For example, the number of measurement points at the oak forest at Matrafuered-Hungary were 4000 times lower than at the ones from the spruce forest of Höglwald-Germany. We observed that the model performed very well for site having high resolution datasets (Table 1.7, Figs. 1.35A & B) than for the ones having few points. For this reason there is a strong need to support long term field experiment that analyse processes on ecosystem scale (C, N and water cycles). This will guarantee a better representation of processes associated to NO production and will improve future modelling work.

A comparison of the new versus the default soil biogeochemistry module (the default module is based on a generalization of the DNDC soil biogeochemistry process description) to capture soil NO emissions is displayed in Figure 1.34. The inter-comparison indicates that the default module underestimated NO emissions by up 50% for forest ecosystems. For arable and grassland ecosystems, NO emissions were underestimated to a greater extend (see small values at Figure 1.34b).
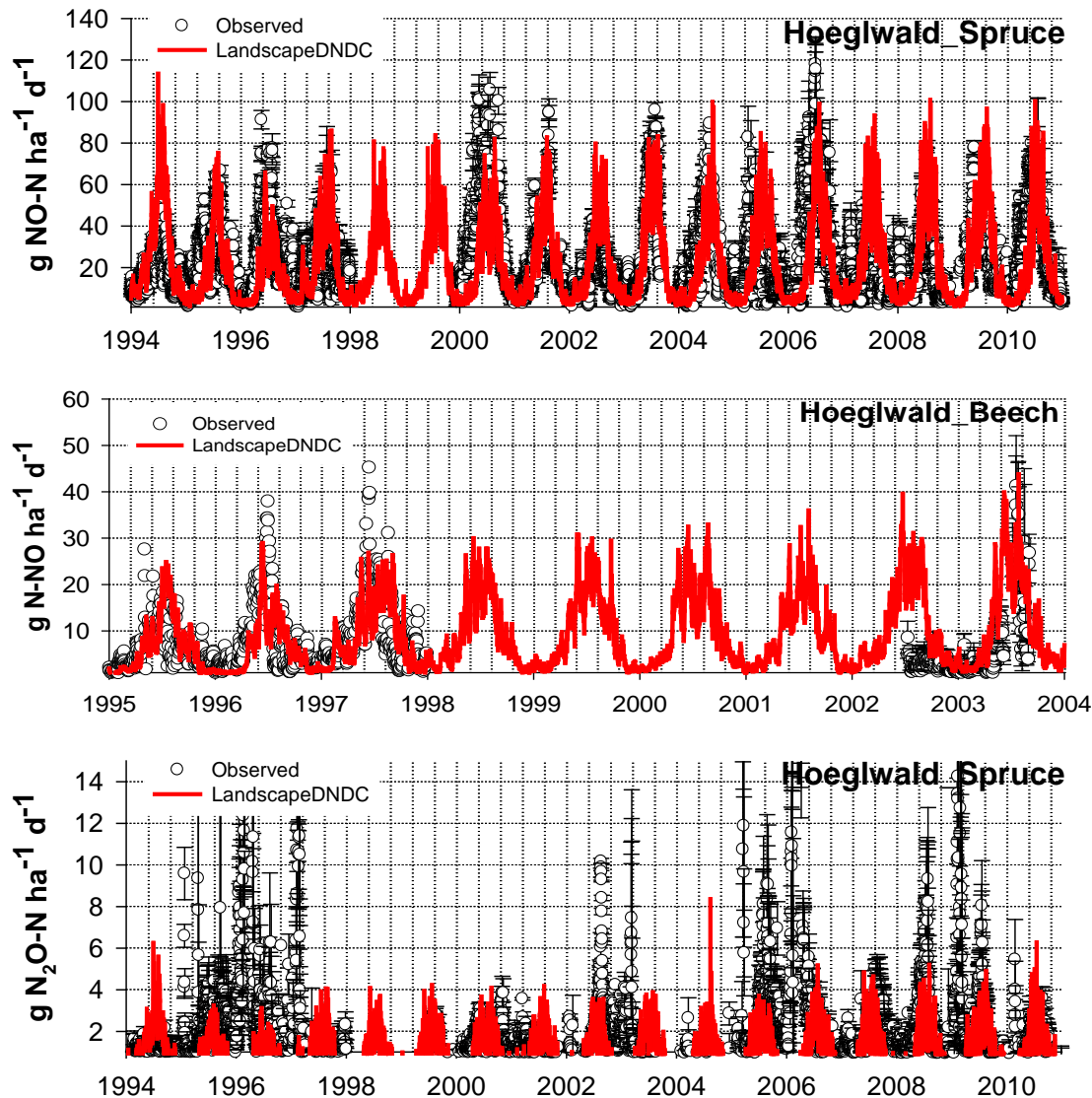
Figure 1.35: (a) Daily NO emissions from a spruce forest (Höglwald, Germany); **(b)** Daily NO emissions from a beech forest (Höglwald, Germany); **(c)** N_2O emissions from a spruce forest (Höglwald, Germany)

In general, the model successfully predicted the inter-annual variations of the simultaneous emission patterns for biogenic NO and N_2O emissions which was the main task of our work. Outstandingly, the parameterization work improved the capability of the model to predict NO and N_2O emissions from managed ecosystems. For forest ecosystem, Figures 1.35a and 1.35c show the simulated daily NO and N_2O emissions of a spruce forest in Germany and the model is capable to predict both trace species simultaneously very well when comparing to the high resolution observations. Model deviation for NO and N_2O was determined during winter seasons at the spruce forest in

Germany. This might corresponds to missing processes in the model such as e.g. the impact of freeze thaw events (de Bruijn and Butterbach-Bahl, 2010). During the winter, the model simulates soil temperature neglecting the influence of solar radiation and is therefore not able to distinguish between sunny and cloudy conditions.

High correlation between measurements and ecosystem properties such as soil pH values were determined. Figure 1.36a illustrates the correlation of soil NO emissions and the average soil pH value (organic layer and mineral soil) across different forest ecosystems across Europe. The high NO emissions for low pH values result mainly from chemo-denitrification. The atmospheric N deposition provides substrate for the microbial nitrogen cycle in the soil (see Figure 1.36b) and via mineral nitrogen availability and it triggers microbial and chemical nitrogen transformation processes in the soil. Figure 1.36b illustrates the correlation between the N deposition and the NO emission which is therefore only indirect via the substrate availability respectively the N limitation of the system.
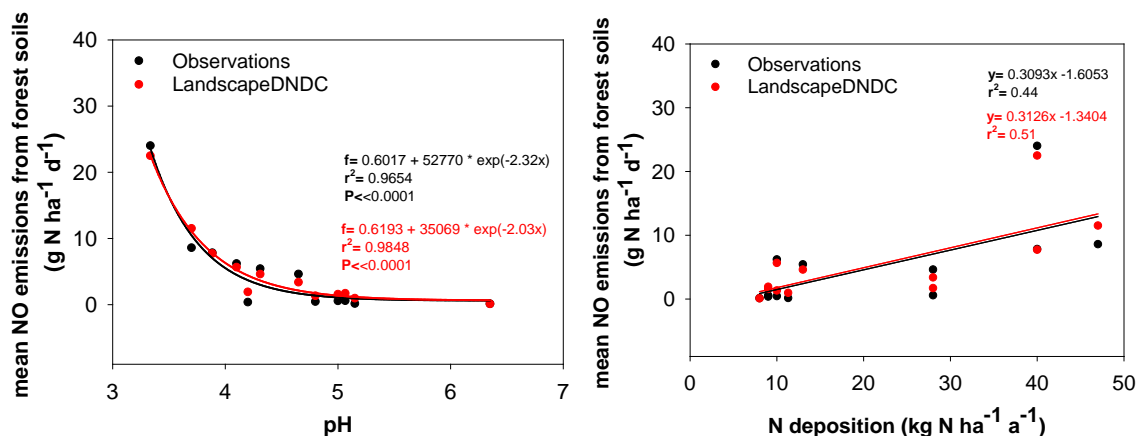
Figure 1.36: (a) Correlation of mean NO emission and soil pH value; **(b)** Correlation of mean NO emissions and N deposition rates

For forest ecosystem, the validation study found the main source for soil NO emissions was the chemo-denitrification process and it was driven by low soil pH values of the topsoil. Figure 1.37 shows the partition of the NO produced during microbial and chemical processes. Nitrogen availability plays also role but the pH value dictate the magnitude of the NO fluxes. For example the amount of N deposition at the spruce and beech forest of Höglwald is the same (40 kg N ha^{-1} a^{-1}, Figure 1.35a and b) however the pH is much lower at the spruce stand. This indicates that vegetation cover type drives chemistry in soil affecting pH and thus soil biogenic emissions.
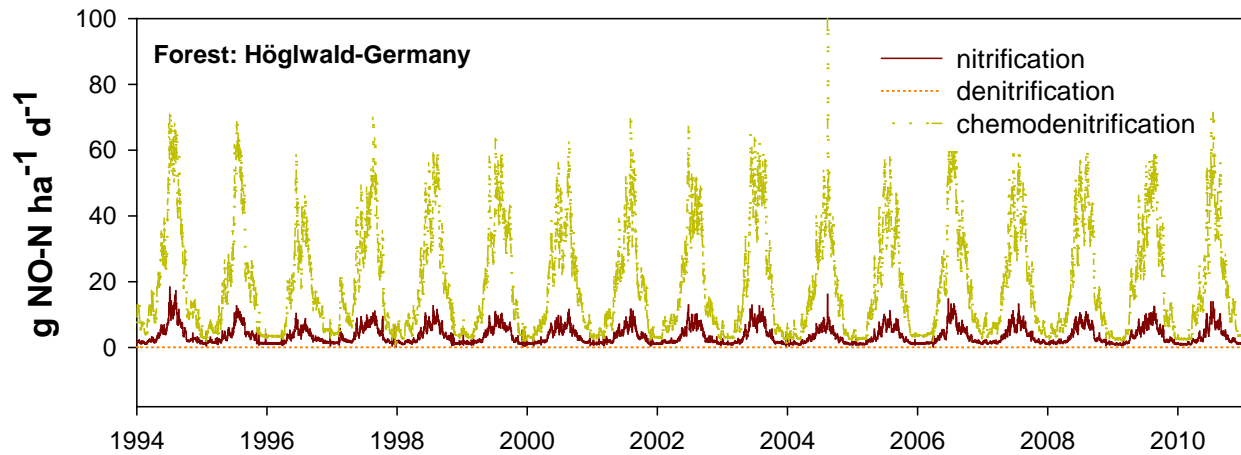
Figure 1.37. Sources of soil NO production from a spruce forest (Höglwald, Germany)

When focusing on arable systems, the abrupt availability of ammonium and nitrate throughout fertilization is governing the budget of soil NO and N_2O emissions, which can be demonstrated in Figure 1.38. LandscapeDNDC is capable of predicting the diurnal pattern of soil NO and N_2O emissions with good agreement compared to the observations. The model captures the emission peaks well within the uncertainty of the observations.

Performing an uncertainty quantification from the results of the BC by sampling parameters sets out of the joint parameter distribution and evaluating the model predictions for all sampled parameter sets (up to hundreds of site simulations) will result in uncertainty ranges of predicted NO and N_2O emissions when statistically analysing (see example Figures 1.39 and 1.40). The uncertainty ranges for the predicted NO and N_2O emission strengths for all validation sites will be evaluated (publication in preparation)

Managed grassland ecosystems (i.e. intensive vs. extensive) are dominated by anthropogenic management practices determining the emission patterns of soil NO emissions. The model is capable to simulate the NO and N_2O emission pulses following N fertilization (mineral and organic N) well within the uncertainty of the observations (Figure 1.43): This was also true for sites under extensive management practices. Discrepancies in low agreement of NO emissions with observations can result from uncertainties in the reported agricultural management and the resulting substrate availability in the soil. Parameter calibrations resulted in a well-balanced nitrogen cycle capable to resolve most of the NO emission pulses while maintaining the background emission patterns as well.

NO emissions from cultivated lands were mainly produced during nitrification and denitrification. The effect of chemodenitrification was null since pH values exceed 6.0 for arable and grassland ecosystems.
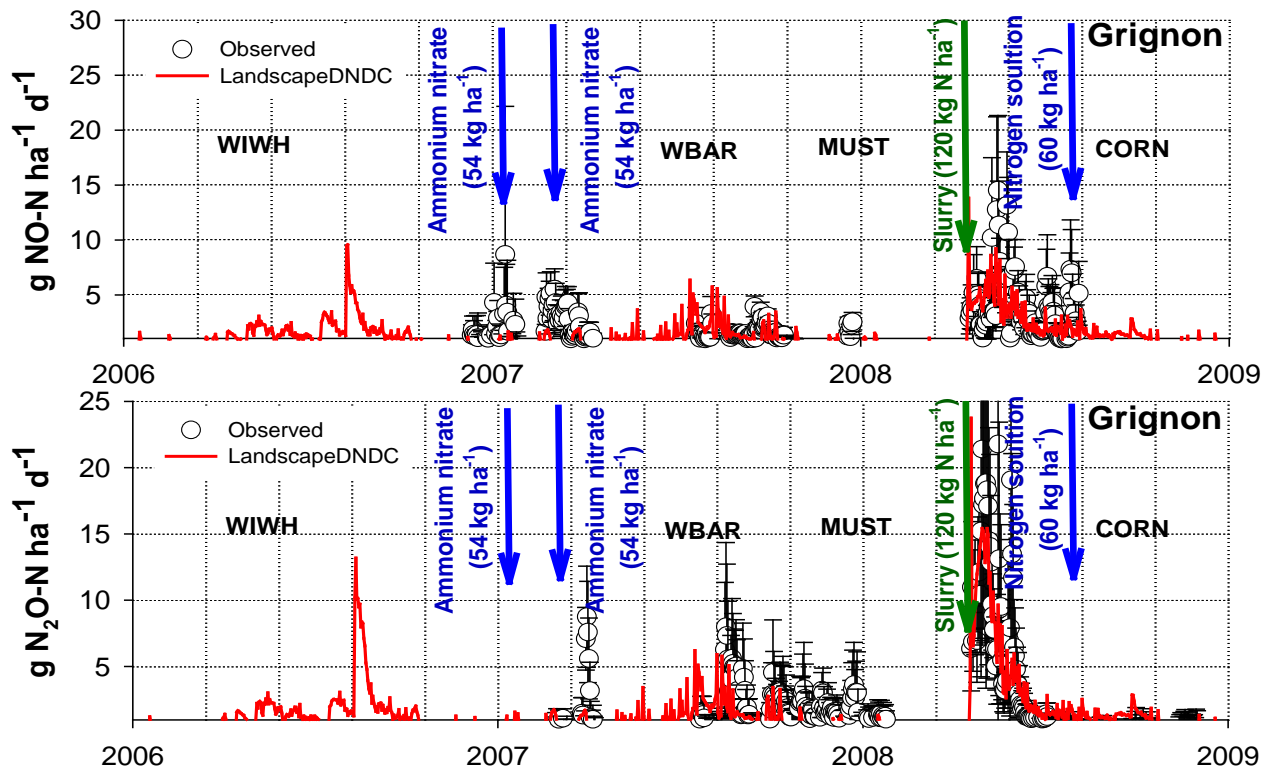
Figure 1.38. (a) Daily NO emissions from arable soils at a research site close to Paris (Grignon, France); **(b)** Daily N_2O emissions from arable soils (Grignon, France)
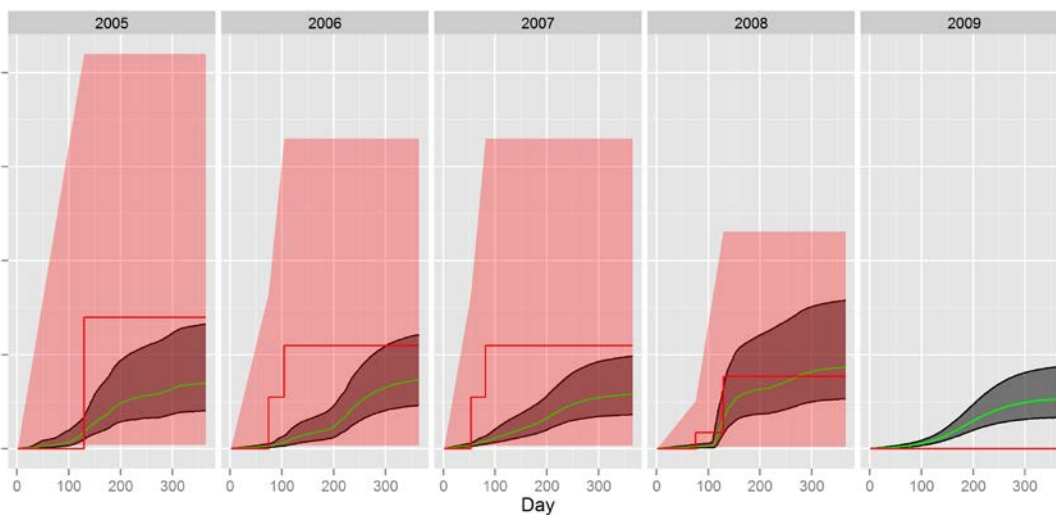
Figure 1.39: Uncertainty range in simulated soil N_2O emissions [kg $N-N_2O$ / ha] for the Grignon-France site as resulting from the BC. Green line: median, black lines: 25 and 75 percentile, grey area: estimated uncertainty range, red line: N_2O emission estimated via

IPCC direct N$_2$O EF (1.0 %), red area: IPCC uncertainty range for IPCC N$_2$O emission estimate. (For 2009, no N Fertilizer data was available)
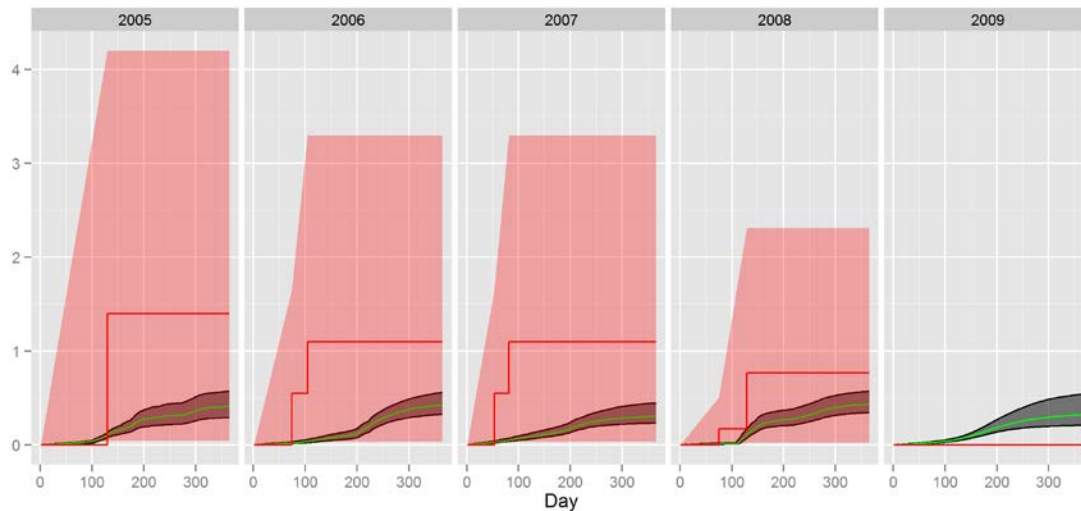
Figure 1.40: Uncertainty range in simulated soil NO emissions [kg N-NO / ha] for the Grignon-France site as resulting from the BC. Green line: median, black lines: 25 and 75 percentile, grey area: estimated uncertainty range, red line: NO emission estimated via IPCC direct NO EF (1.0 %), red area: IPCC uncertainty range for IPCC NO emission estimate. (For 2009, no N Fertilizer data was available)
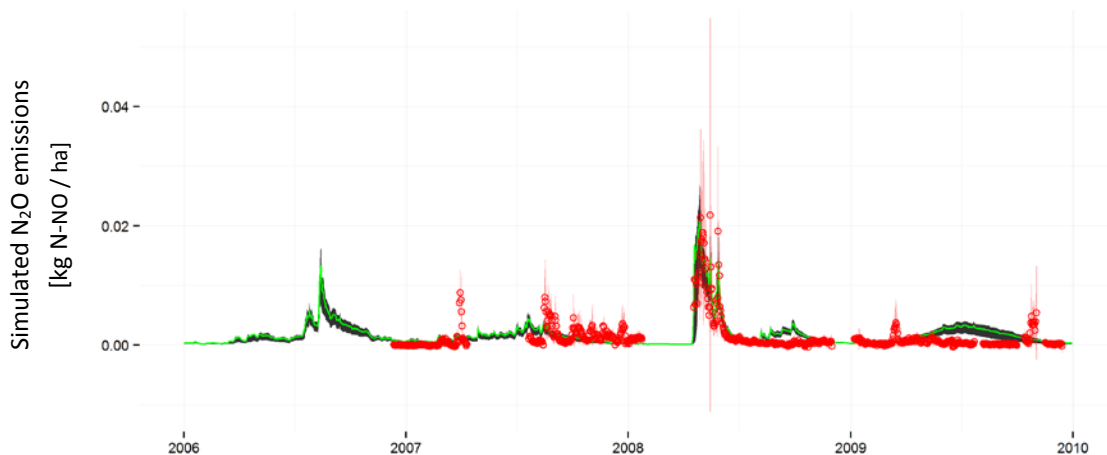
Figure 1.41: Simulated N$_2$O emissions [kg N-N$_2$O / ha] including the uncertainty bands resulting from the BC. Green line: median, black lines: 25 and 75 percentile, grey area: estimated uncertainty range, red circles: field measurements and measurement errors
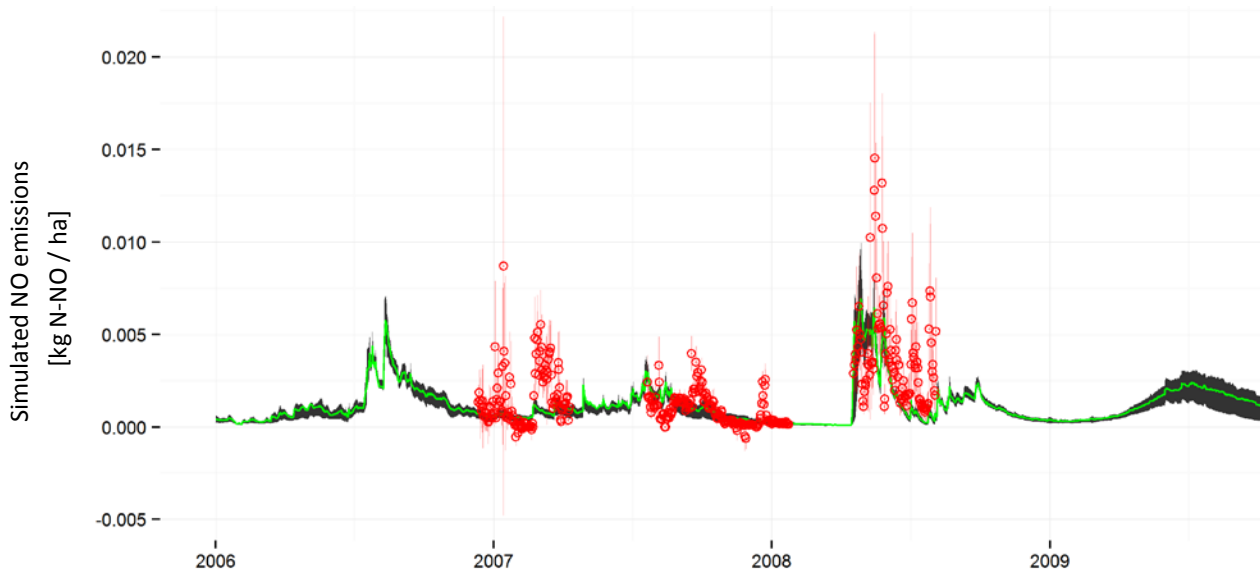
Figure 1.42: Simulated NO emissions [kg N-N$_2$O / ha] including the uncertainty bands resulting from the BC. Green line: median, black lines: 25 and 75 percentile, grey area: estimated uncertainty range, red circles: field measurements and measurement errors

ÉCLAIRE Third Periodic Report: November 2015
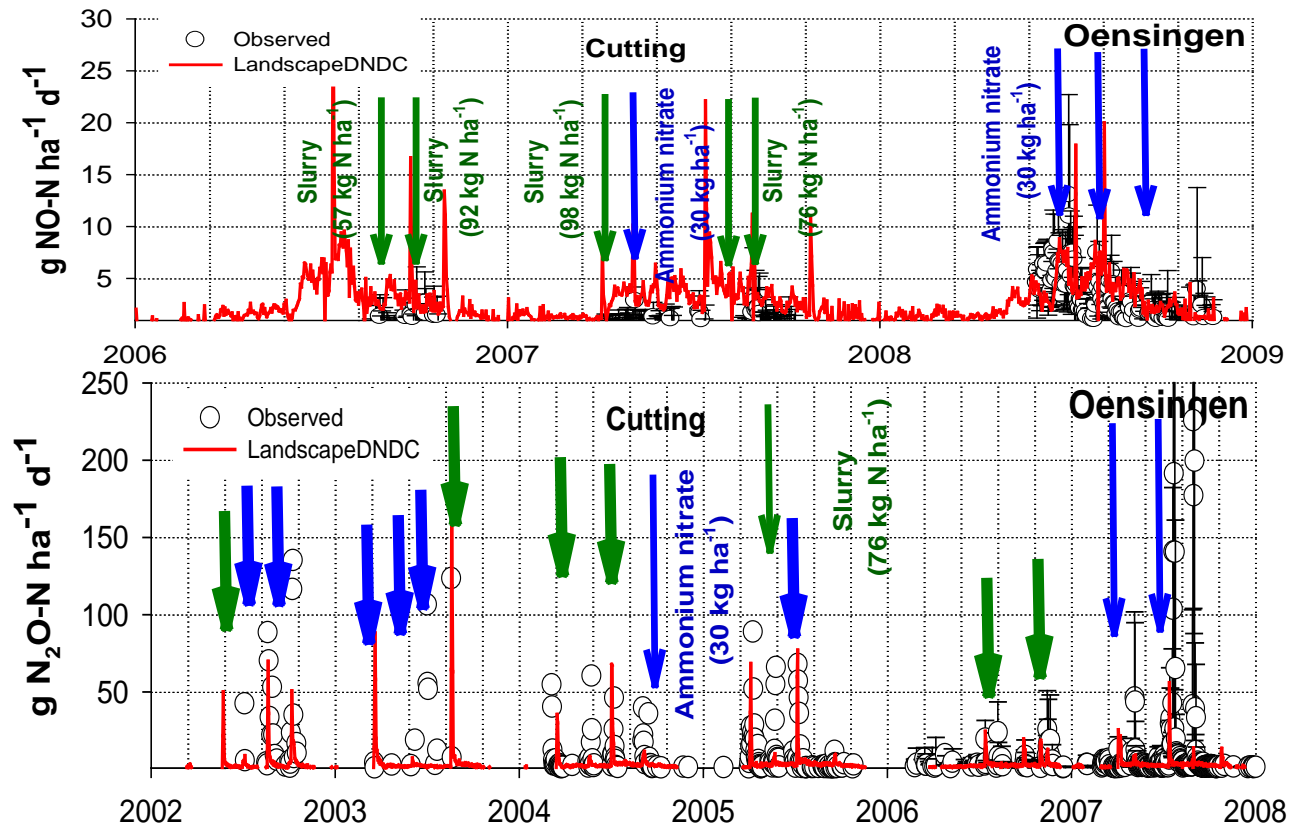
Figure 1.43: (top) Daily NO emissions form managed grassland ecosystems (Oensingen Switzerland); **(bottom)** daily N_2O emissions form managed grassland ecosystems (Oensingen Switzerland).

Regional scale simulations

LandscapeDNDC has been developed in recent years in order to be deployed on the site as well as regional scale and to take advantage of parallelism when running the simulations of high performance computing systems. The model framework is ready to be used on the regional scale for assessments of soil NO and N_2O emissions.

LandscapeDNDC is used with Éclaire in WP 6 for the assessment of soil NO and N_2O emissions from agricultural systems across Europe. This work is still in progress (due to a delay caused by the quality assurance of the regional input data of agricultural management at the EU scale).

The objective of this study is to determine the contribution of the three major landuse types arable land versus grassland versus forests contributing to the soil biogenic NO

emissions for the state of Saxony, Germany. The study was performed for the years 2000, 2005 and 2010 and averaged to minimize the impact of local climate conditions. The impact of ecosystem characteristics with respect to NO were also investigated (mainly: pH, N availability and management practices).

The setup of the regional study is summarized in Table 1.8. The study reviled evidence that forests are stronger sources for soil based NO emissions than arable soils (see Table 1.9 and Figure 1.45) .
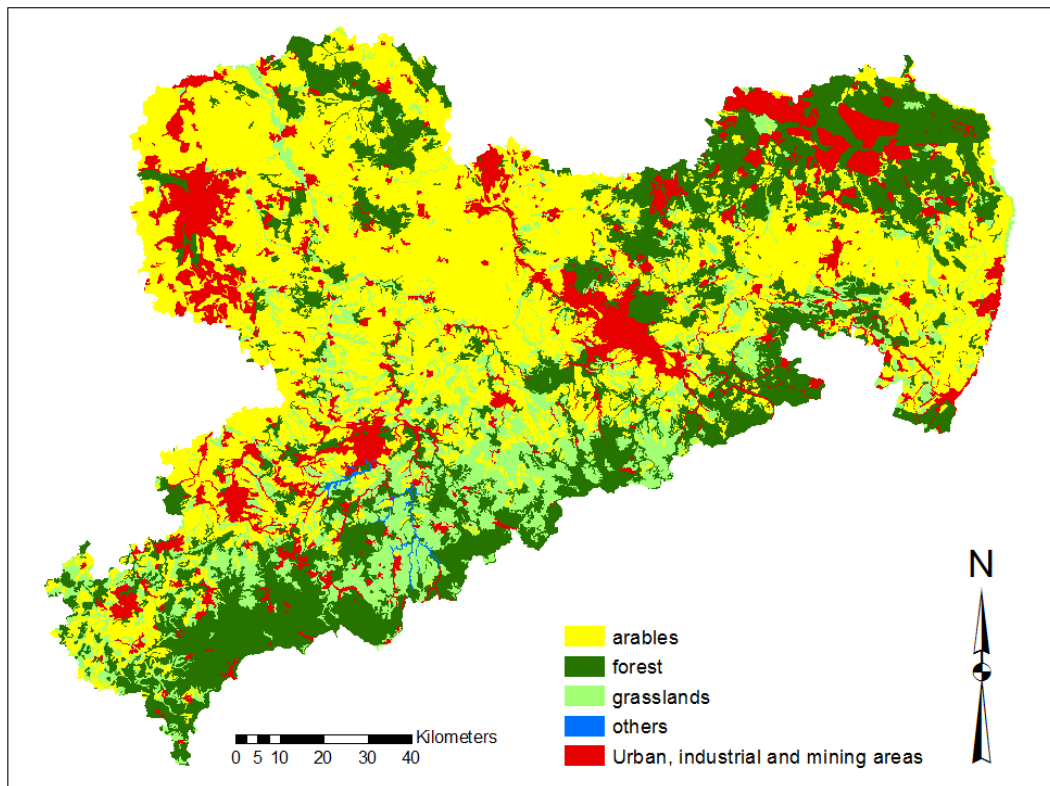
Figure 1.44: Land use information based on the German soil survey map BUEK 200 (resolution 1:200000) of the Environmental, Agricultural and Geological Service of the State of Saxony.
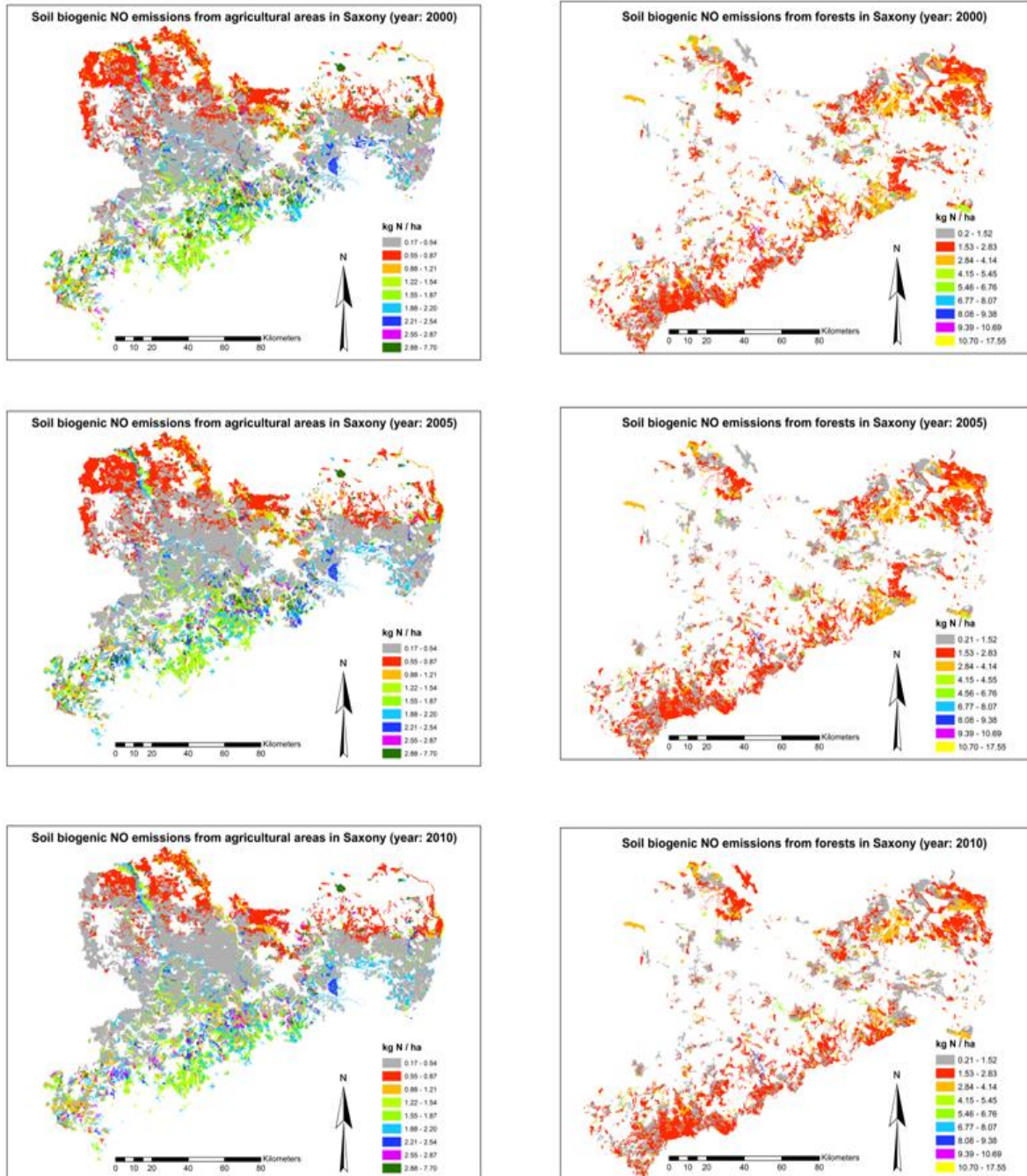
Figure 1.45: LandscapeDNDC model simulations of NO fluxes from different terrestrial ecosystems during 2000, 2005 and 2010.

ÉCLAIRE Third Periodic Report: November 2015

Table 1.8: Summary of number of polygons and area considered for model simulations which has been derived from the German soil survey map BUEK 200 (resolution 1:200000). Source: Environmental, Agricultural and Geological Service of the State of Saxony.

Land use	Total polygons	Polygons to be evaluated	Neglected polygons	Total area (ha)	Area simulated (has)	Area neglected (%)
Arables	4163	4040	123	808671	785570	2.86
Grassland	1676	1483	193	268689	237638	11.56
Forest	3019	2539	480	528392	471410	10.78
Total	8858	8062	796	1605754	1494619	6.92

Table 1.9: Total NO_x emissions simulated with LandscapeDNDC per land use in Saxony

Land use	NO emissions (Gg)			
	area (ha)	2000	2005	2010
Arable	808671	0.99	0.97	0.87
Grasslands	268689	1.25	1.26	1.15
Forest	528392	2.55	2.27	2.15
Total	1605754	4.78	4.50	4.17

Task 3.4 Improvement of the European BVOC modelling framework

Nothing to report.

Progress towards the milestones and deliverables

D3.2 and **D3.3** were delivered in the reporting period.

M12 and **M13** were reached / delivered in the reporting period.

This milestone 12 and the Deliverable 3.2 had been delayed because of the delayed development of the ESX model which was supposed to be used for such comparison. A different strategy was therefore developed in the last year of the project to revise parameterisation of the MNS-2010 model and develop meta-models out of existing CERES-EGC and Volt'air models.

Use of resources and deviations from DoW

A total of 0.6 person months were used in this period.

References

Ammann, C., Spirig, C., Leifeld, J., Neftel, A., 2009. Assessment of the nitrogen and carbon budget of two managed temperate grassland fields. Agriculture, Ecosystems & Environment 133, 150-162.

Barton, L., McLay, C.D.A., Schipper, L.A., Smith, C.T., 1999. Annual denitrification rates in agricultural and forest soils: a review. Soil Research 37, 1073-1094.

Blagodatsky, S., Grote, R., Kiese, R., Werner, C., Butterbach-Bahl, K., 2011. Modelling of microbial carbon and nitrogen turnover in soil with special emphasis on N-trace gases emission. Plant Soil 346, 297-330.

Blagodatsky, S.A., Richter, O., 1998. Microbial growth in soil and nitrogen turnover: a theoretical model considering the activity state of microorganisms. Soil Biology and Biochemistry 30, 1743-1755.

Bouwman, A.F., Stehfest, E., Vankessel, C., 2010. Nitrous oxide emissions from the nitrogen cycle in arable agriculture: estimation and mitigation. estimation and mitigation. Nitrous oxide and climate change. Earthscan, London, 240.

Braker, G., Conrad, R., 2011. Chapter 2 - Diversity, Structure, and Size of N2O-Producing Microbial Communities in Soils—What Matters for Their Functioning? In: Allen I. Laskin, S.S., Geoffrey, M.G. (Eds.), Advances in Applied Microbiology. Academic Press, pp. 33-70.

Butterbach-Bahl, K., Baggs, E.M., Dannenmann, M., Kiese, R., Zechmeister-Boltenstern, S., 2013. Nitrous oxide emissions from soils: how well do we understand the processes and their controls? Philosophical Transactions of the Royal Society B: Biological Sciences 368.

Butterbach-Bahl, K., Kahl, M., Mykhayliv, L., Werner, C., Kiese, R., Li, C., 2009. A European-wide inventory of soil NO emissions using the biogeochemical models DNDC/Forest-DNDC. Atmospheric Environment 43, 1392-1402.

Butterbach-Bahl, K., Stange, F., Papen, H., Li, C.S., 2001. Regional inventory of nitric oxide and nitrous oxide emissions for forest soils of southeast Germany using the biogeochemical model PnET-N-DNDC. Journal of Geophysical Research-Atmospheres 106, 34155-34166.

Chirinda, N., Kracher, D., Laegdsmand, M., Porter, J.R., Olesen, J.E., Petersen, B.M., Doltra, J., Kiese, R., Butterbach-Bahl, K., 2011. Simulating soil N2O emissions and heterotrophic CO_2 respiration in arable systems using FASSET and MoBiLE-DNDC. Plant Soil 343, 139-160.

Corbeels, M., McMurtrie, R.E., Pepper, D.A., O'Connell, A.M., 2005. A process-based model of nitrogen cycling in forest plantations: Part I. Structure, calibration and analysis of the decomposition model. Ecological Modelling 187, 426-448.

de Bruijn, A.G., Butterbach-Bahl, K., 2010. Linking carbon and nitrogen mineralization with microbial responses to substrate availability — the DECONIT model. Plant Soil 328, 271-290.

de Bruijn, A.M.G., Butterbach-Bahl, K., Blagodatsky, S., Grote, R., 2009. Model evaluation of different mechanisms driving freeze–thaw N2O emissions. Agriculture, Ecosystems & Environment 133, 196-207.

Engeland, K., Renard, B., Steinsland, I., Kolberg, S., 2010. Evaluation of statistical models for forecast errors from the HBV model. Journal of Hydrology 384, 142-155.

Gelman, A., Rubin, D.B., 1992. Interference from iterative simulation using multiple sequences. Statitical Science 7, 55.

Haas, E., Klatt, S., Fröhlich, A., Kraft, P., Werner, C., Kiese, R., Grote, R., Breuer, L., Butterbach-Bahl, K., 2013. LandscapeDNDC: a process model for simulation of biosphere–atmosphere–hydrosphere exchange processes at site and regional scale. Landscape Ecology 28, 615-636.

Johansson, C., 1984. Field measurements of emission of nitric oxide from fertilized and unfertilized forest soils in Sweden. J Atmos Chem 1, 429-442.

Johansson, C., Granat, L., 1984. Emission of nitric oxide from arable land. Tellus B 36B, 25-37.

Kesik, M., Ambus, P., Baritz, R., Bruggemann, N.B., Butterbach-Bahl, K., Damm, M., Duyzer, J., Horvath, L., Kiese, R., Kitzler, B., Leip, A., Li, C., Pihlatie, M., Pilegaard, K., Seufert, G., Simpson, D., Skiba, U., Smiatek, G., Vesala, T., Zechmeister-Boltenstern, S., 2005. Inventories of N2O and NO emissions from European forest soils. Biogeosciences 2, 353-375.

Kiese, R., Heinzeller, C., Werner, C., Wochele, S., Grote, R., Butterbach-Bahl, K., 2011. Quantification of nitrate leaching from German forest ecosystems by use of a process oriented biogeochemical model. Environmental Pollution 159, 3204-3214.

Kiese, R., Li, C.S., Hilbert, D.W., Papen, H., Butterbach-Bahl, K., 2005. Regional application of PnET-N-DNDC for estimating the N2O source strength of tropical rainforests in the Wet Tropics of Australia. Global Change Biology 11, 128-144.

Kraus, D., Weller, S., Klatt, S., Haas, E., Wassmann, R., Kiese, R., Butterbach-Bahl, K., 2014. A new LandscapeDNDC biogeochemical module to predict CH_4 and N2O emissions from lowland rice and upland cropping systems. Plant Soil, 1-25.

Laville, P., Hénault, C., Gabrielle, B., Serça, D., 2005. Measurement and Modelling of NO Fluxes on Maize and Wheat Crops During their Growing Seasons: Effect of Crop Management. Nutr Cycl Agroecosyst 72, 159-171.

Li, C., Frolking, S., Crocker, G.J., Grace, P.R., Klír, J., Körchens, M., Poulton, P.R., 1997. Simulating trends in soil organic carbon in long-term experiments using the DNDC model. Geoderma 81, 45-60.

Li, C.S., Aber, J., Stange, F., Butterbach-Bahl, K., Papen, H., 2000. A process-oriented model of N2O and NO emissions from forest soils: 1. Model development. Journal of Geophysical Research-Atmospheres 105, 4369-4384.

Loubet, B., Laville, P., Lehuger, S., Larmanou, E., Fléchard, C., Mascher, N., Genermont, S., Roche, R., Ferrara, R., Stella, P., Personne, E., Durand, B., Decuq, C., Flura, D., Masson, S., Fanucci, O., Rampon, J.-N., Siemens, J., Kindler, R., Gabrielle, B., Schrumpf, M., Cellier, P., 2011. Carbon, nitrogen and Greenhouse gases budgets over a four years crop rotation in northern France. Plant Soil 343, 109-137.

Metropolis, N., Rosenbluth, A.W., Rosenbluth, M.N., Teller, A.H., Teller, E., 1953. Equation of State Calculations by Fast Computing Machines. The Journal of Chemical Physics 21, 1087-1092.

Rahn, K.H., Werner, C., Kiese, R., Haas, E., Butterbach-Bahl, K., 2012. Parameter-induced uncertainty quantification of soil N2O, NO and CO_2 emission from Höglwald spruce forest (Germany) using the LandscapeDNDC model. Biogeosciences 9, 3983-3998.

Ritter, A., Muñoz-Carpena, R., 2013. Performance evaluation of hydrological models: Statistical significance for reducing subjectivity in goodness-of-fit assessments. Journal of Hydrology 480, 33-45.

Slemr, F., Seiler, W., 1984. Field measurements of NO and NO2 emissions from fertilized and unfertilized soils. J Atmos Chem 2, 1-24.

Slemr, F., Seiler, W., 1991. Field study of environmental variables controlling the NO emissions from soil and the NO compensation point. Journal of Geophysical Research: Atmospheres 96, 13017-13031.

Stange, F., Butterbach-Bahl, K., Papen, H., Zechmeister-Boltenstern, S., Li, C.S., Aber, J., 2000. A process-oriented model of N2O and NO emissions from forest soils 2. Sensitivity analysis and validation. Journal of Geophysical Research-Atmospheres 105, 4385-4398.

Van Oijen, M., Rougier, J., Smith, R., 2005. Bayesian calibration of process-based forest models: bridging the gap between models and data. Tree Physiology 25, 915-927.
Venterea, R.T., Rolston, D.E.E., Cardon, Z.G., 2005. Effects of Soil Moisture, Physical, and Chemical Characteristics on Abiotic Nitric Oxide Production. Nutr Cycl Agroecosyst 72, 27-40.

Werner, C., Butterbach-Bahl, K., Haas, E., Hickler, T., Kiese, R., 2007. A global inventory of N2O emissions from tropical rainforest soils using a detailed biogeochemical model. Global Biogeochemical Cycles 21, GB3010.

Yienger, J.J., Levy, H., 1995. Empirical model of global soil-biogenic NOχ emissions. Journal of Geophysical Research: Atmospheres 100, 11447-11464.

Work package 4: Surface exchange modelling

Lead contractor: 13(INRA)
Contributors: 1(NERC), 6(met.no), 12(SEI-Y, UoY), 16(UGOT), 18(FMI), 27(DHMZ), 29 (UBO), 36(WU)

Work package objectives

The general aims of this work package were:
- To improve the description and modelling of surface/ atmosphere exchange processes for atmospheric pollutants under variable climatic conditions (*Tasks 4.1, 4.2 & 4.3*).
- To develop parameterisations for incorporation into European-scale chemistry and transport models (CTM) in Component 2 and for use in the derivation of dose-response relationships in Component 3 (*Tasks 4.1 & 4.2*).
- To investigate the effect of chemical- and gas-aerosol transformations that occur near and within plant canopies in relation to emission, deposition and bi-directional exchange for each of the pollutants considered (*Task 4.3*).
- To use improved exchange models to estimate atmospheric N inputs and O_3 deposition for the ecosystems being investigated at the effect study sites in Component 3 (*Task 4.4*).

Progress and Results

Task 4.1: Surface exchange routines for inorganic reactive nitrogen (N_r) compounds

Objectives:

The general objective of Task 4.1 was to improve the surface exchange parameterisations for the main atmospheric reactive nitrogen (N_r) pollutants and to provide algorithms suitable for inclusion in chemical transport models (CTM):

- improvement of dry deposition/emission routines for NH_3, HNO_3, NO_2, NO_3^- and NH_4^+ (including effect of NH_4NO_3 volatilisation near warm surfaces).
- emphasis on the response of the parameterisations to environmental change (meteorology & atmospheric composition).
- integrating analysis of the reactive nitrogen fluxes from the ÉCLAIRE flux network (WP1).
- parameterisations suitable for translation into European atmospheric transport models, including the EMEP model.

The general strategy adopted within WP4 to improve parameterisations for Nr exchange within CTM applications consisted in the development of a new multi-layer, multi-pollutant surface/atmosphere modelling framework, ESX (ÉCLAIRE Ecosystem Surface eXchange).

We considered that, in order to treat questions related to the impact of climate change and of changing atmospheric composition on dry deposition and bi-directional exchange, a re-parameterisation of existing big-leaf models, based on empirical canopy resistances, would not be sufficient, because the controlling mechanisms are not represented adequately. Instead, the new ESX model (see Deliverable 4.4, and also Section 2.3 in the present report) should treat within- and above-canopy turbulence, diffusion and chemistry explicitly and dynamically, including gas and aerosol phases, as well as the aqueous and particle phases for leaf/canopy surface pollutant pools. (Note that ESX addresses surface exchange not only for Nr but also O_3 and VOC).

Most of the activities that happened under Task 4.1 therefore aimed to provide parameters or component sub-models for the modular-oriented, community-minded ESX model, that will eventually supersede the current big-leaf approach in the EMEP model. However, the concepts and models developed here should also prove suitable for other surface exchange schemes or CTMs.

Results

The main results achieved in Task 4.1 can be summarized under three headings: i) a concept for a generalized NH_3 exchange scheme for CTMs, partly based on ecosystem meta-modelling; ii) modelling of non-stomatal N_r exchange through an explicit representation of chemical interactions between trace gases, aerosol and leaf surface wetness; and iii) a parameterization of near-surface NH_4NO_3 aerosol volatilisation (see ÉCLAIRE Deliverable 4.1 for details).

Concept for a generalized NH_3 exchange scheme for CTMs

For a better representation of ecosystem/atmosphere NH_3 exchange in CTMs, both peak emissions related to fertilizer application and background exchange must be made dependent on the reduced nitrogen (NH_4^+) status of soil and vegetation and on weather and other environmental drivers. In all cases, the Γ concept is central to an improved modelling of fluxes (Flechard et al., 2013). Γ is the ratio of NH_4^+ to H^+ ions in the different substrates of the ecosystem (in leaf apoplast, soil solution, leaf surface water films, leaf litter) and it controls the NH_3 emission (or uptake) potential as a function of temperature only. Γ-based modelling approaches are therefore needed to predict the impact of climate change on NH_3 emissions and deposition (Sutton et al., 2013). Γ values are needed as inputs for the bi-directional NH_3 module of ESX.

The challenge is then to provide temporally varying Γ values for all land uses across the modelling domain, in order to reflect pulse-like effects of crop/grass fertilisation,

differences in vegetation types and in atmospheric N deposition, season and phenology. We propose an approach to provide Γ values (tables or mathematical functions) for stomata (Γ_s), for ground/soil (Γ_g, including fertilizer effects), and for litter (Γ_{litter}), based on both review-based empirical parameterizations (Massad et al., 2010) and on meta-modelling approaches for simplifying process-based (but CPU-intensive) ecosystem or NH_3 volatilization models (Fig. 1.46).
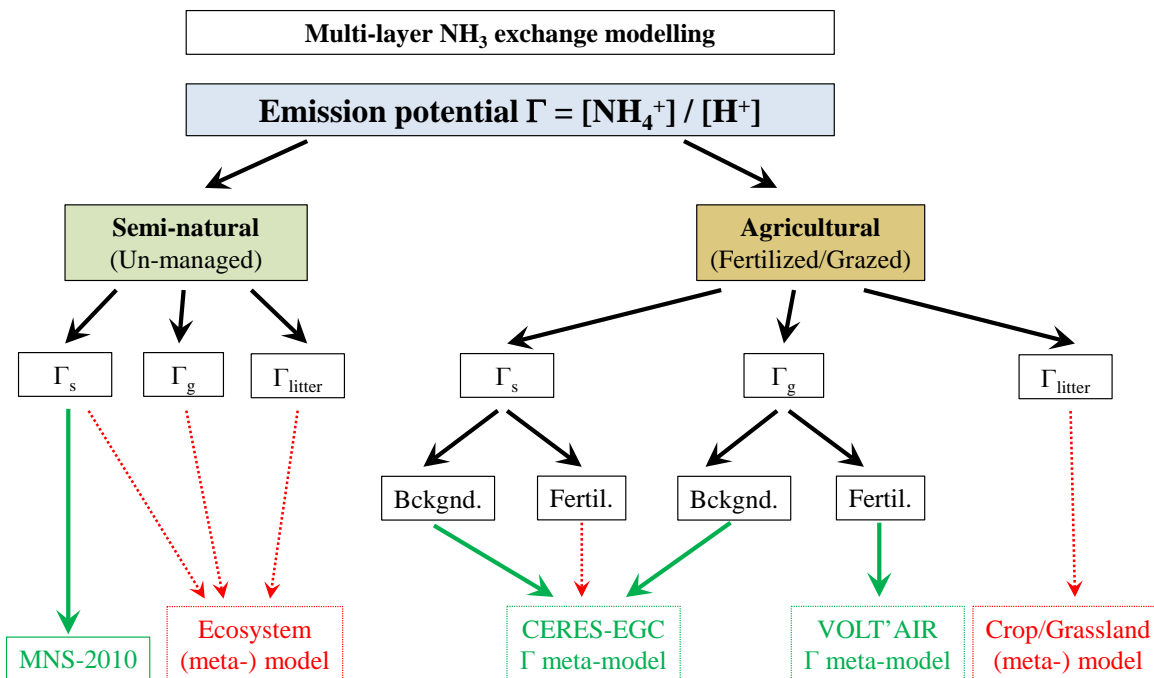
Figure 1.46: Summary of the approach proposed for deriving Europe-wide fields of ecosystem Γ values (NH_3 emission potentials in stomata/apoplast Γ_s, ground/soil including fertiliser Γ_g, and in litter Γ_{litter}), required as inputs to bi-directional exchange models. MNS-2010 refers to the parameterization scheme by Massad et al. (2010). Green solid arrows denote solutions explored within ÉCLAIRE WP3-4; red dotted arrows indicate potential solutions to investigate in future.

Meta-modelling methods to derive simplified functions describing Γ values were applied to the CERES-EGC crop model (for background Γ_g and for plant Γ_s; see Deliverables 3.2 & 4.1) and to the VOLT'AIR NH_3 volatilization model (Fig. 1.47) (see also Deliverable 4.1). The results are available for use with ESX/EMEP.
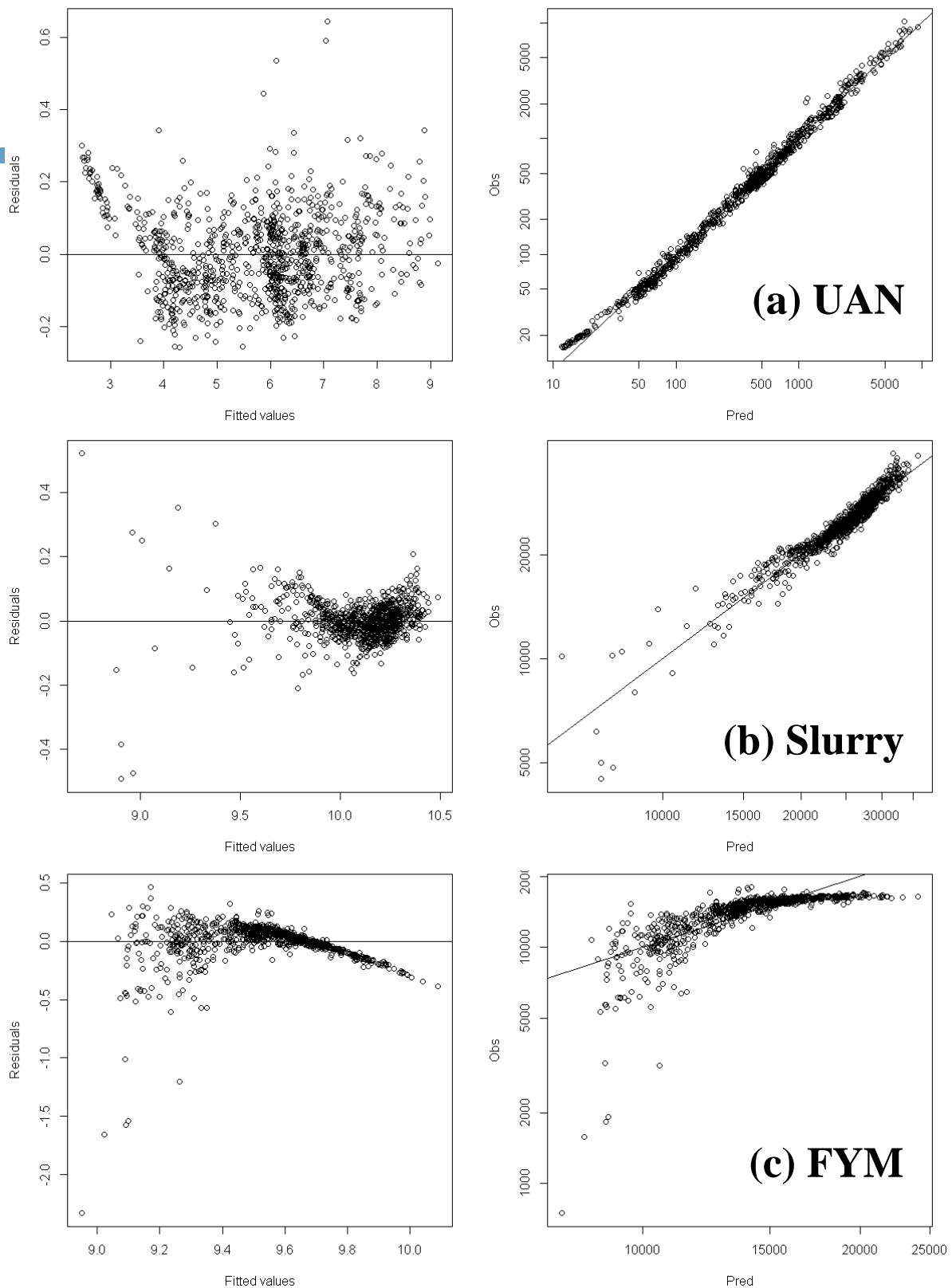
Figure 1.47. Performance of the meta-modelling approach used to derive a simplified model of soil NH$_3$ emission potential (Γ_g) after fertiliser spreading, obtained from multiple runs of the VOLT'AIR volatilization model, for Urea Ammonium Nitrate, slurry and FarmYard Manure. The performance of the meta-model ("Pred") is here assessed versus the full VOLT'AIR model version ("Obs"), not versus measurements.

Chemical modelling of (non-stomatal) gas-aerosol-water interactions

Parameterisations for non-stomatal Nr trace gas exchange are generally empirical and thus inadequate for exploring changes in deposition rates in response to changes in pollution and climate. A more mechanistically explicit treatment of the chemistry of water droplets or thin water films on vegetation surfaces, based on first principles (Henry's law, pH-dependent dissociation rates, condensed phase reaction rates, ion transfer through leaf cuticles, etc), is needed for studying scenarios of change.

The DEWS (Dynamic pollutant Exchange with Water films on vegetation Surfaces) model was adapted from the surface chemistry and exchange model by Flechard et al. (1999) with some substantial modifications to make it eventually compatible with ESX. Although a full operational coupling of DEWS to ESX has not been achieved within the time frame of ÉCLAIRE, significant steps have been achieved in the harmonization of the Fortran codes. Some basic science issues have yet to be addressed, such as the physical basis for the treatment of the transfer resistance (R_d) at the air/water interface, and water-phase transport and kinetics.

While DEWS addresses the chemical composition of visible (macroscopic) leaf wetness and the chemical reactions within, DEWS calculations cannot proceed once surface water has evaporated beyond a certain ionic strength. We sought to address such conditions by invoking two aerosol chemistry models (PD-FiTE and AIOMFAC) in the context of the leaf surface. After consultation with the School of Earth, Atmospheric and Environmental Sciences of the University of Manchester (G. Mc Figgans and D. Topping), the AIOMFAC model (Zuend et al., 2008) was deemed to be more appropriate. We investigated ways to couple AIOMFAC with DEWS, with AIOMFAC taking over from DEWS in dry conditions the calculations of leaf surface water storage, activity coefficients and NH_3, HNO_3 and HCl vapour pressures (Fig. 1.48).

ÉCLAIRE Third Periodic Report: November 2015
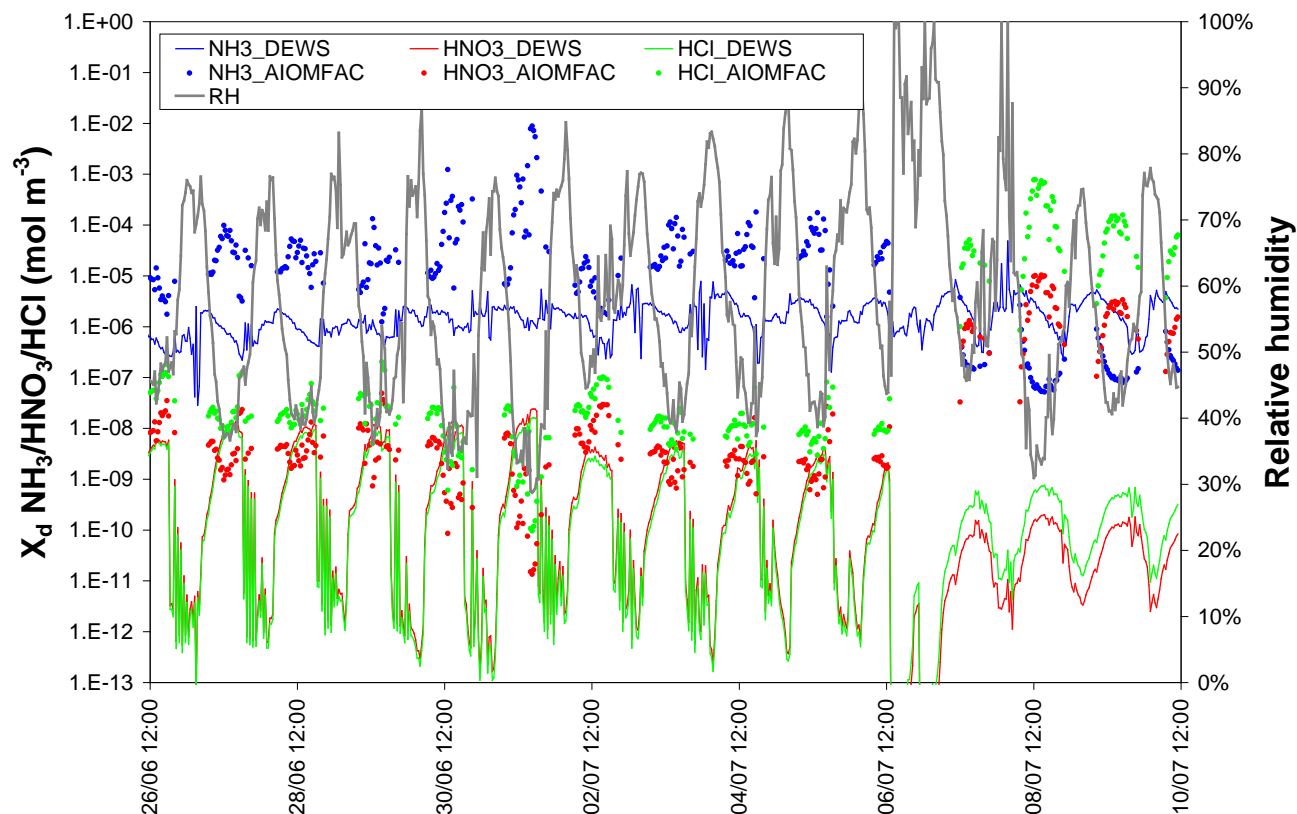
Figure 1.48: Time series of the equilibrium gaseous NH_3, HNO_3 and HCl concentrations (X_d) above leaf surface solutions, as predicted by the DEWS and AIOMFAC thermodynamic modules, during the ÉCLAIRE Bosco Fontana experiment.

Near-surface aerosol NH_4NO_3 evaporation

Recent measurements have shown evidence that fine nitrate and fine ammonium often show effective dry deposition rates in excess of 10 and up to 200 mm s^{-1}, which has been attributed to the effect of volatile ammonium nitrate (NH_4NO_3) evaporating during the deposition process. This process is driven by the increased temperature near and within plant canopies, coupled to the reduced concentrations of NH_3 and HNO_3 in this region, both of which promote evaporation.

An empirical parameterisation has been developed within ÉCLAIRE to account for the enhancement of dry deposition velocity as a function of the relevant drivers, as a kind of subgrid parameterisation of the process. The parameterisation of the dry deposition velocity (V_d) for NH_4NO_3 is a function of friction velocity (u_*), leaf area index (LAI) and atmospheric stability (as characterised by the Obukhov length, L) (Fig. 1.49). Whilst u_* is

expected to be the predominant controller of V_d, $1/L$ was found to be the best descriptor of the residual dependence. It can be shown that this stability parameter is proportional to the product of the temperature gradient (that drives evaporation during the deposition process) and the turbulence transport time scale (which provides time for the evaporation to occur).
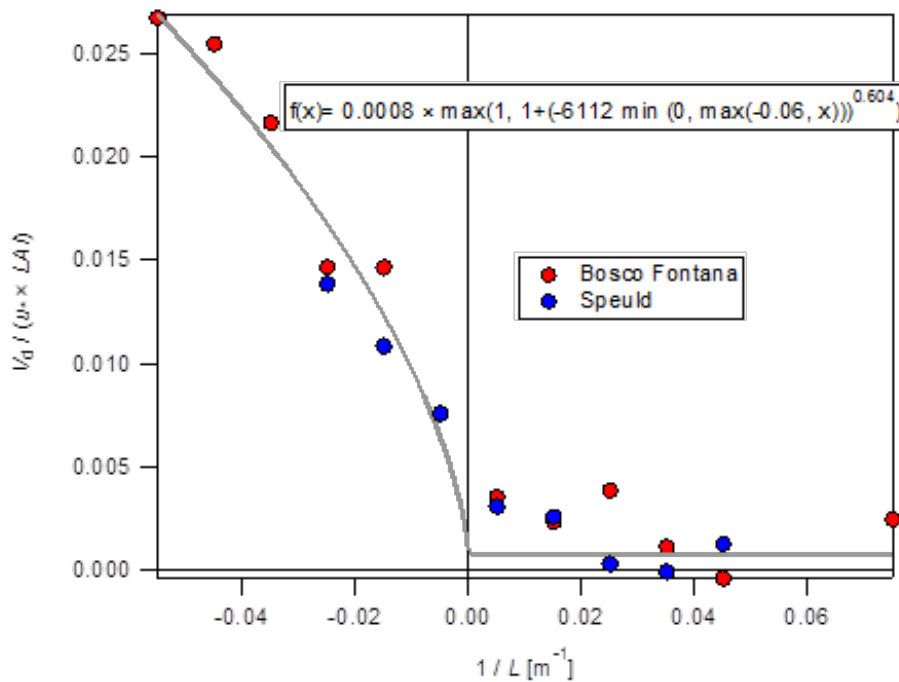
Figure 1.49: Parameterisation of the deposition velocity of fine aerosol nitrate from measurement data. The dependence of $V_d/(u_* \times LAI)$ on $1/L$ in unstable conditions reflects the on-going evaporation near and within plant canopies under conditions of strong vertical temperature gradient.

Task 4.2: Ozone deposition parameterisations

Objectives:

- improvement of the formulation and parameterisation of an existing O_3 deposition model (DO3SE)
- more accurate descriptions of the mechanisms controlling stomatal and non-stomatal deposition of O_3
- parameterizations of the effects of meteorology, canopy wetness, phenology, atmospheric CO_2 concentrations, and BVOC emissions
- feedback effect of O_3 on stomatal function through the inclusion of a photosynthesis-driven carbon based growth model

Results:

Three existing surface/atmosphere exchange models for O_3 (DO3SE, SURFATM and MUSICA) were further developed, and tested versus new ÉCLAIRE datasets as well as other data from previous projects, to better represent the mechanisms controlling ozone deposition and to improve responses to climate and environmental conditions.

Each model was examined with a different focus: DO3SE on stomatal exchange and link with photosynthesis; SURFATM on ground surface deposition, and MUSICA on O_3 deposition to wet leaf cuticles. New parameterisations have thus emerged, including i) a new stomatal uptake module (DO3SE_C) including a photosynthesis-based stomatal conductance; (ii) O_3 deposition to bare soil as a function of surface relative humidity; and (iii) a wet cuticular deposition module based on O_3 reaction rates in water films. The photosynthesis-based stomatal conductance module has been incorporated into the ESX modelling framework, while the ground layer and leaf wetness parameterisations could also potentially be used by ESX.

DO3SE_C module

This new module, that has been developed for use within the DO3SE modelling scheme, enables the estimation of both total ozone deposition and stomatal ozone uptake assuming a coupling between stomatal conductance (g_{sto}) and net photosynthesis (A_{net}). The photosynthesis-based stomatal conductance has substituted the previously used multiplicative g_{sto} module from Jarvis (1976).

This enabled stomatal ozone uptake to be closely related to three processes that are considered primarily responsible for limiting A_{net}: (i) Rubisco activity (Ac), (ii) the regeneration of ribulose-1,5-bisphosphate (RuBP) which is limited by the rate of electron transport (Aj), and (iii) an inadequate rate of transport of photosynthetic products (most commonly triose phosphate utilization). The rate of A_{net}, calculated according to

99

biochemical processes from updated formulations by Farquhar et al. (1980), determines the demand for CO_2 which in turn is considered to feedback onto the CO_2 supply, which is determined by g_{sto}. Theory suggests that g_{sto} will vary to ensure that an optimum supply of CO_2 is provided, which at the same time limits H_2O vapour loss from the plant.

The coupling between A_{net} and g_{sto} is achieved using updated methods first developed by Ball et al. (1987). The instantaneous effect of ozone on this A_{net}-g_{sto} relationship was introduced in the new model to account for the fact that ozone damages the plants maximum carboxylation rate ($V_{c,max}$) (Fig. 1.50). The new module allows for recovery of $V_{c,max}$, which is particularly important when applying the model to real world conditions, where ozone is episodic (rather than the more continuous elevated ozone exposures applied in experimental fumigation studies).

Change in V_{cmax} with slope of k=2 and Fst_2
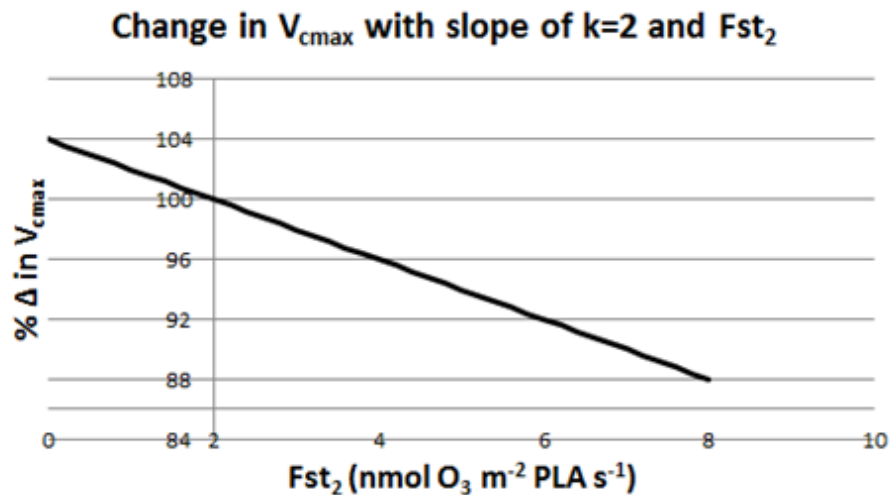
Figure 1.50: The relationship between instantaneous ozone flux above a threshold 'y' (F_{sty}) and the % change in V_{cmax}.

The DO3SE_C model has been parameterised for European land cover types, consistent with those used by the EMEP model. This has required the identification from the literature of 5 parameter values for 9 landcover types made up of 11 different species (see ÉCLAIRE Deliverable 4.3).

Finally, the DO3SE_C model has been incorporated into the ESX model providing the canopy stomatal component of pollutant exchange.

Ozone deposition to bare soil

A new parameterisation of soil resistance for O_3 as a function of surface relative humidity was derived from experimental O_3 flux data over bare soil at the ÉCLAIRE Grignon cropland site (see ÉCLAIRE Deliverable 4.2). The formulation includes a minimal soil resistance and an empirical exponential term. The data show that R_{soil} was largest at high relative humidity and lowest in drier conditions (Fig. 1.51), hinting at the role of O_3 diffusion into the soil. The formulation derived over the Grignon silty loam soil has yet to be generalized to other soil types, since soil properties such as porosity, organic matter content, acidity, are likely to impact the parameters of the R_{soil} relationship to RH.

Period A
$y = 24{,}498e^{0,0234x}$
$R^2 = 0{,}6496$

Period B
$y = 9{,}6873e^{0,0336x}$
$R^2 = 0{,}4071$

Period C
$y = 18{,}755e^{0,0242x}$
$R^2 = 0{,}5727$
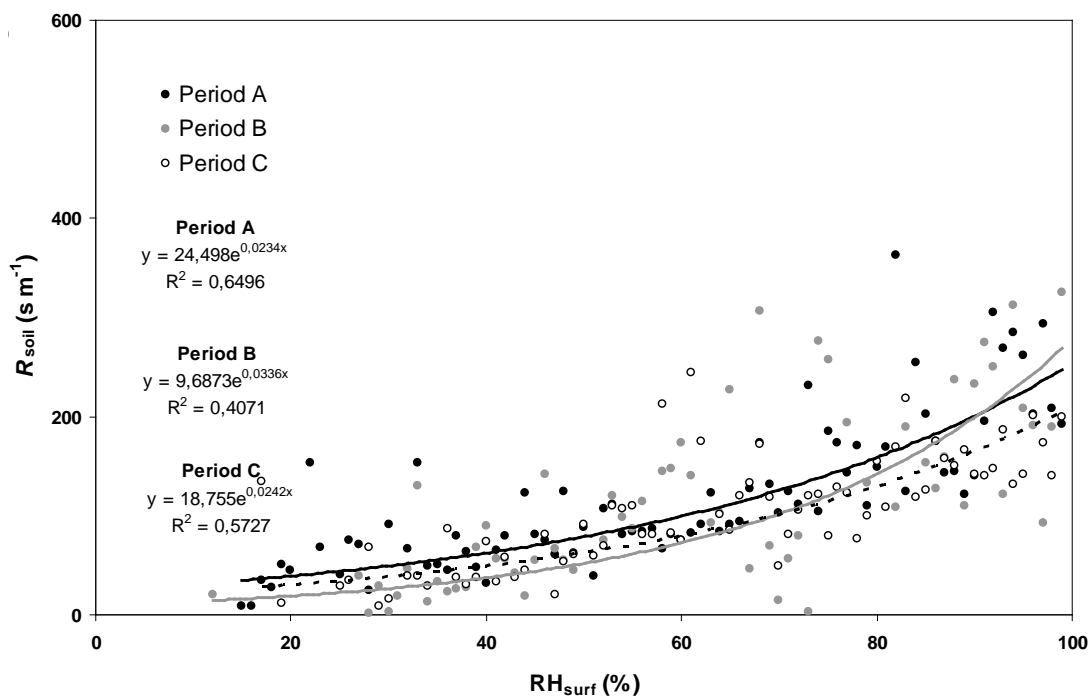
Figure 1.51: Ozone soil resistance (R_{soil}) as a function of surface relative humidity (RH_{surf}), derived from flux measurements over bare soil at Grignon.

Ozone deposition to wet plant cuticles

A parameterisation for O_3 uptake by wet plant surfaces was implemented in the MUSICA model (see ÉCLAIRE Deliverable 4.2). The non-stomatal leaf conductance for ozone, for the case of a wet cuticle, was modelled based on physical and chemical principles. The scheme accounts for ozone solubility in water, its subsequent diffusion into the water film and its adsorption (and subsequent destruction) on the cuticle itself. Ozone destruction during diffusion through the water film was modelled following a similar approach to Tuzet

et al.(2011) for the diffusion of ozone in the apoplast, with the wet cuticle O_3 conductance being derived by solving a first-order reaction-diffusion equation in the liquid film.

The response of the wet cuticle O_3 conductance to the water film thickness depends on the value used for the cuticle adsorption velocity (at the bottom of the water film) and the value of the O_3 reaction rate in the water film (Fig. 1.52). Testing this ozone deposition scheme as part of the MusiCA multi-layer, multi-leaf, soil-vegetation-atmosphere transfer model (Ogee et al., 2003), versus O_3 flux datasets over wheat at the ÉCLAIRE Grignon cropland site, revealed that much larger O_3 reaction rates were needed in the model to match observations during wheat senescence, than during over green leaves earlier in the season. This increase in O_3 deposition was well reproduced by adjusting the reaction rate of ozone in the water film to values corresponding to the reaction rate with ascorbate in the plant cells.

This led to the hypothesis that during senescence, and especially when the leaves are wet, apoplastic anti-oxidants leak out to the leaf surface where they can react with ozone. A question also arises as to whether relatively fresh plant residues at the soil surface would also enhance ozone deposition and how this will interact with soil water. Controlled studies measuring ozone deposition to a range of senescing plants and soil organic matter composition were conducted to verify this hypothesis. Leaves were infused to reproduce wetness obtained in field conditions. Ozone reaction to these infusions (Fig. 1.53) revealed larger reaction rates in senescent leaves than fresh leaves and also differences between species. Equivalent ascorbate concentrations in these infusions varied from 50 to 5000 µM and were larger in senescent than in green leaves, confirming a possible increase of ozone deposition to plant residues in the field (e.g. during leaf fall and decomposition in forests, or after herbicide application in agricultural fields).
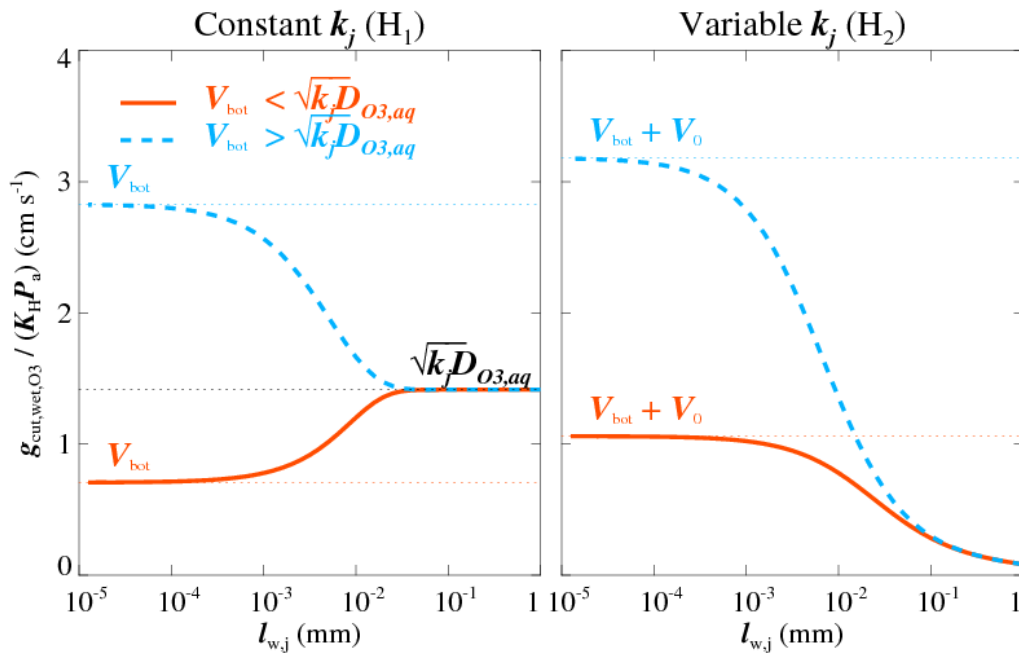
Figure 1.52. Normalised ozone water film conductance as a function of water film thickness (lw,j) for a constant reaction rate kj (H1; left) and variable reaction rate (H2, right). $D_{O3,aq}$ is the molecular diffusion constant of ozone in water, K_H is the Henry constant for ozone (Pa^{-1}), and Pa is the air pressure (Pa), and V_0 is a parameter proportional to the quantity of reactive compound at the surface.
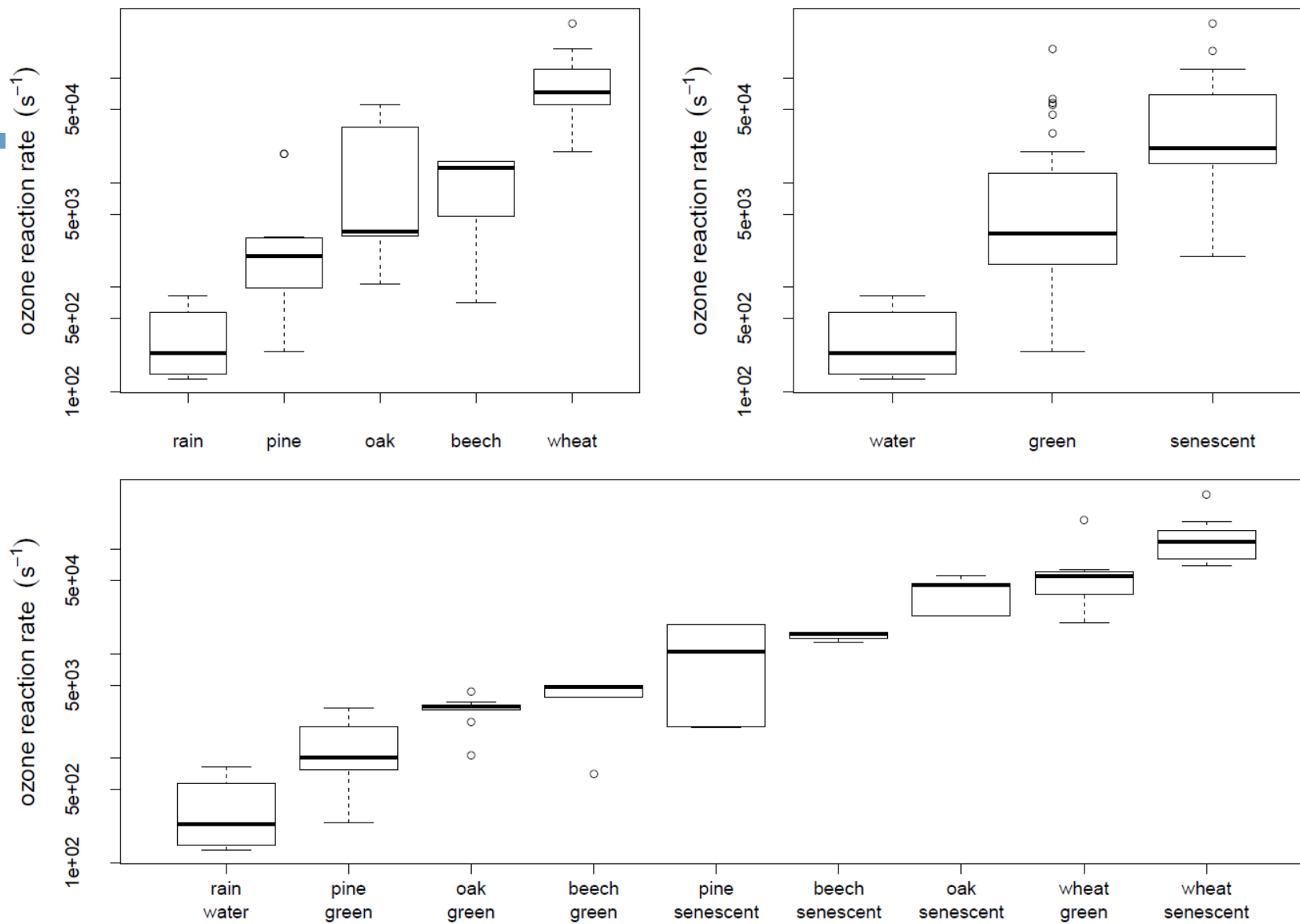
Figure 1.53: Chemical reaction rates (k) of leaf infusions and rain water classified by (a) species, (b) senescent state or (c) both.

Task 4.3: In-canopy chemical processing

Objectives:

- Evaluation and improvement of a computationally efficient coupled multi-layer exchange and chemistry model for site- to global-scale simulations of in-canopy interactions and net exchange fluxes
- Extension of an existing scheme for the NO-NO_2-O_3-VOCs system and the dependence on in-canopy turbulence, to treat the phase partitioning of the NH_3-HNO_3-NH_4NO_3 system
- Assessment and fine-tuning of the model framework against data from the ÉCLAIRE intensive campaigns (WP1) and other suitable datasets and compared against the single-layer approaches
- multi-layer model investigations of the vertical distribution of O_3 concentration and sinks within the canopy, resulting from gradients in irradiance, stomatal conductance and surface wetness

Results

Modelling activities in WP4 focusing on the simulation of in-canopy chemical processing and exchange involved two modelling systems (see ÉCLAIRE Deliverable 4.4 for details):

- *ex-nihilo* development of a new canopy representation in the EMEP modelling system, the ÉCLAIRE Ecosystem Surface eXchange (ESX)
- further development and application of the Multi-Layer Canopy Chemical Exchange Model (MLC-CHEM) system.

A new model of multi-layer canopy column chemistry and exchange: ESX

A new 1-D surface exchange model, called ESX, has been developed within ÉCLAIRE. The structure of the ESX code specifically aims at an integration into the modelling system of EMEP MSC-W, in which it will serve as an advanced dry deposition module that will replace the present big-leaf module of the EMEP CTM. For site-specific analysis, ESX can already be run in a stand-alone mode, with input data and boundary conditions either being set in configuration files or obtained from the EMEP CTM data or directly from in-situ measurements. The ESX code is written in Fortran 90.

ESX makes it possible to resolve the vertical distribution of the key variables that characterize atmosphere–vegetation interactions, i.e. concentration (mol m^{-3}), source/sink exchange rate (mol m^{-3} s^{-1}), source/sink flux density per leaf area (mol m^{-2} s^{-1} PLA), separating the emission and deposition fluxes, and turbulent mixing and chemical reaction rates (mol m^{-3} s^{-1}). Also, a novel feature of ESX is that it makes it possible to minimize the number of the actual model layers that are needed to adequately resolve

the vertical variability especially within and just above vegetation, thus reducing the overall computational cost.

The basic formulation chosen for ESX is the 1-dimensional conservation equation, which relates the change of concentration over time to vertical flux divergence and to source and sink (S) terms (see ÉCLAIRE Deliverable 4.4 for details). S terms include, in addition to chemical kinetics, generic first (D) and zeroth (E) order deposition and emission terms. Within ESX these terms are formulated so as to account for bi-directional exchange occuring at the surfaces of vegetation.

The deposition/emission fluxes in the different exchange pathways are formulated using the common approach of electrical analogy (Fig. 1.54). There are three potential exchange targets within the vegetation canopy: the mesophyll, external leaf surfaces and non-leaf vegetation surfaces. The ESX structure allows for bi-directional exchange for all of these, and similarly for the soil exchange, by defining a 'compensation point' or a non-zero equilibrium concentration at each interface. The leaf exchange, both stomatal and non-stomatal, is defined separately for the adaxial and abaxial leaf surfaces (j = 1,2).
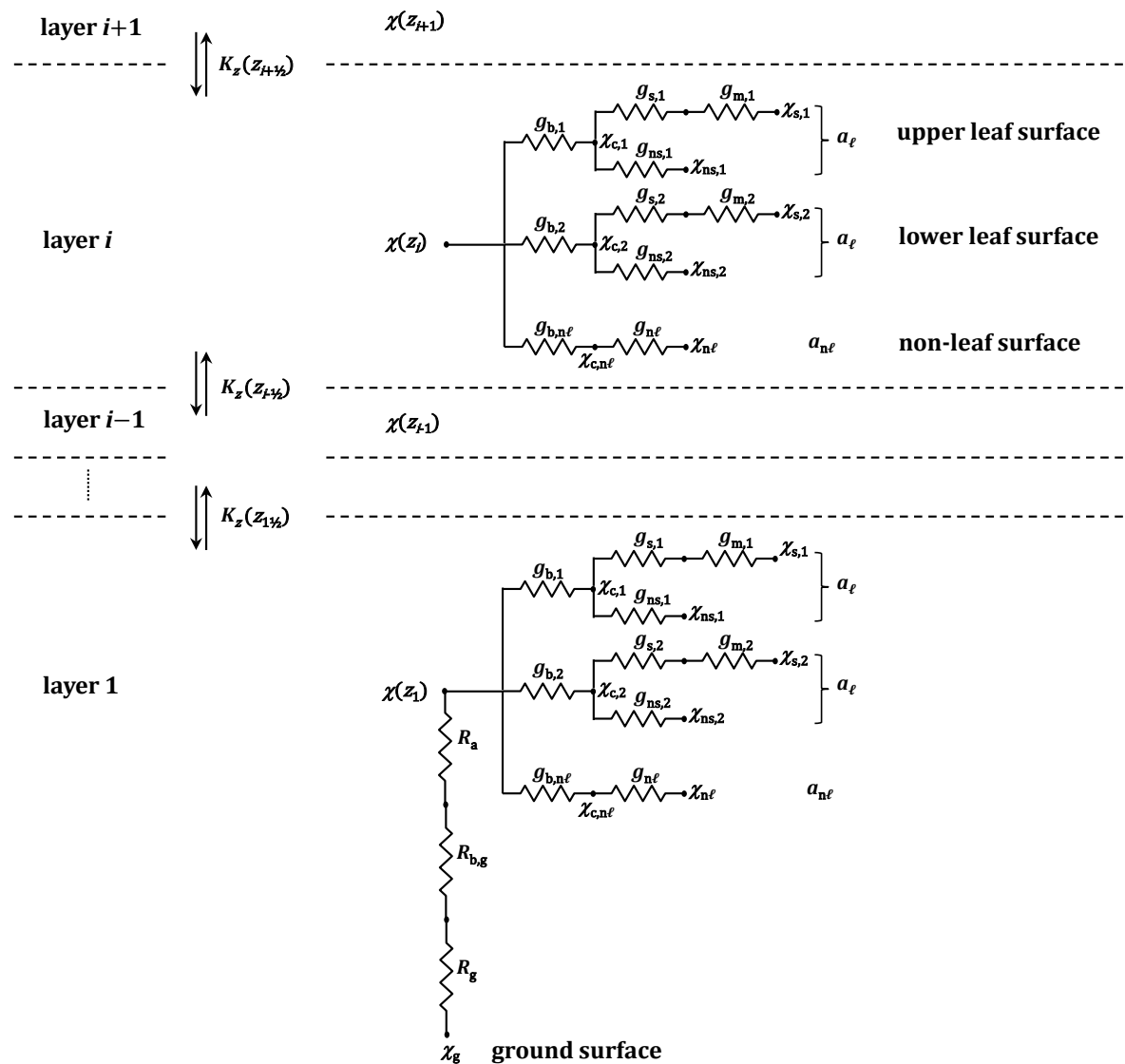
Figure 1.54: Sketch of the main exchange pathways of the ESX model. Within each layer, bi-directional exchange is calculated separately for upper and lower leaf surfaces ($j = 1, 2$), as well as for non-leaf vegetation and ground surfaces if present. The vertical mixing due to turbulence is calculated with eddy diffusivities defined at layer boundaries, $K_z(z_{i+1/2})$.

Modelling of vertical mixing is based on first order turbulent closure. As a default, the eddy diffusivity (K_z) profile within and just above the canopy is calculated in ESX using a slightly modified approach of Leuning (2000). The vertical profiles of the Lagrangian time scale of turbulence (τ_L) and of the standard deviation of vertical wind velocity (σ_w) depend on vegetation height and friction velocity. Since stability corrections are included in the calculation of K_z, we assume the Monin–Obukhov similarity theory of the inertial sublayer is also valid within the roughness sublayer. At the top of the surface layer, this profile is matched to the K_z used within the EMEP MSC-W model (Simpson et al., 2012).

For air column chemistry, as with the standard EMEP CTM (Simpson et al., 2012), a variety of chemical schemes are available for ESX, and new schemes can be readily generated with a chemical pre-processor (GenChem), which is part of the EMEP modelling system. Chemical kinetics are separated from the overall problem of the conservation equation using an operator splitting technique, and solved following the procedures of the EMEP CTM (Simpson et al., 2012). The remaining problem encompassing vertical mixing and surface exchange processes is solved numerically with a mass-conserving finite volume method and semi-implicit Crank-Nicolson time differencing.

Although ESX has not yet been integrated into the EMEP model, it has been tested extensively, in particular for O_3 exchange. In forests, both the canopy and soil act as O_3 sink surfaces, the former being strongly variable due to environmental control of stomatal exchange. ESX simulations show that, while the overall concentration profile is expectedly affected by deposition, the canopy-induced local gradients are modest. In contrast, there is large flux divergence within the canopy layer, and (close-to-)constant-flux layers are formed both above the canopy and within the trunk space (Fig. 1.55).
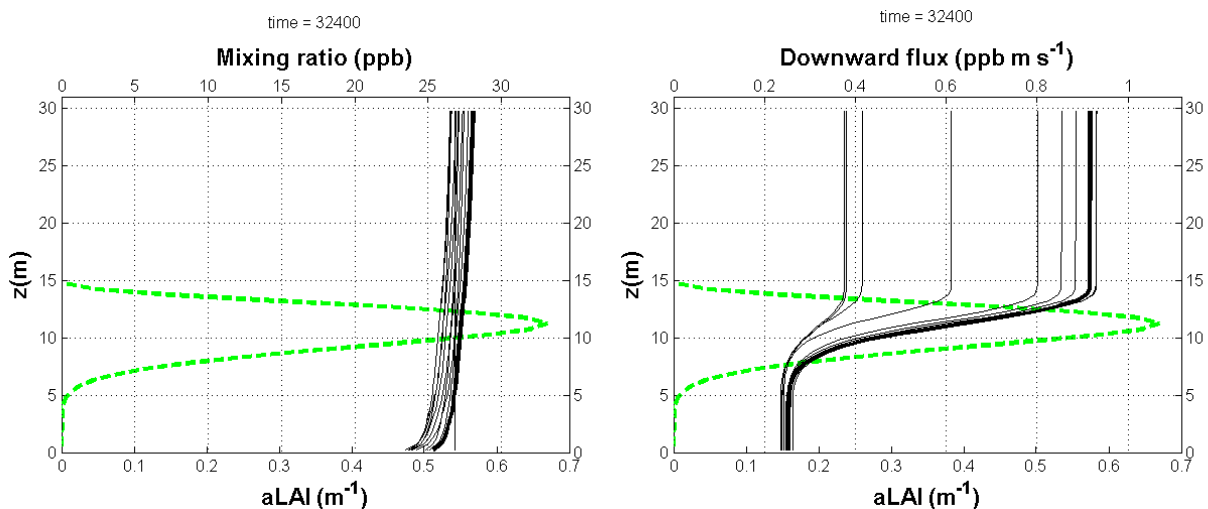
Figure 1.55: Examples of modelled ozone concentration and flux profiles in the atmospheric surface layer (thick black line = midday; thin lines show the profiles of

previous hours). The dashed green line shows the leaf area distribution (aLAI) of a Scots pine forest.

The sensitivity of ESX results to the number of vertical layers (n) used in simulations has been examined in detail. In stand-alone applications of ESX (e.g. to aid in the interpretation of measured field data) n can be set arbitrarily to any value, but for applications as part of CTMs (e.g. EMEP) n needs to minimized for computational cost. Many ESX calculations were thus made, in which the exchange parametrisations, meteorological conditions and vegetation distribution were identical in each run, but vegetation height, h_v, and model layer depth, Δz, varied. The error due to compromised resolution showed that even in a rather extreme case of $\Delta z = h_v$ (all vegetation incorporated into a single model layer), the error was consistently less than 10% for stomatal conductance, and less than 5% for the stomatal sink rate. Overall, these and other simulation results indicated that the new sub-grid integration developed for ESX makes it possible to implement a detailed multi-layer model in a CTM in a cost-effective manner.

Figure 1.56 shows the importance of modelling the vertical profiles of pollutants for a 12h period over a forest with high BVOC and soil-NO emissions. These ESX calculations used EMEP model 'advected' concentrations of O_3 and other long-lived pollutants as boundary conditions at 45 m height, but ESX then calculates changes in these longer-lived compounds, and in addition adds BVOC.

These calculations show for example a strong effect of the (admittedly high) soil-NO emissions on the near-ground NO concentrations - much higher values than seen at upper elevations. HNO_3 on the other hand is changing at high elevation due to changes in the advected concentrations. Within the canopy though, a mixture of processes is seen - deposition losses at most time-intervals but increases near the ground due to conversion of soil-NO through NO_2 chemistry.

The concentrations of the BVOC limonene vary rather straightforwardly, influenced by emissions, turbulent dispersion and, of course, chemistry, with concentrations dropping to near zero above 100 m. This height limitation is clearly reflected in the NO_3 profile - where limonene (and other BVOC) are present, nigh time NO_3 concentrations drop to zero due to rapid reaction with these BVOC. Above the BVOC 'layer', NO_3 concentrations rise rapidly to high values. (The very high NO_3 concentrations shown here are rather untypical, but reflect our high biogenic emission testing). NO_3 concentrations in daytime are near zero simply due to its rapid photolysis.
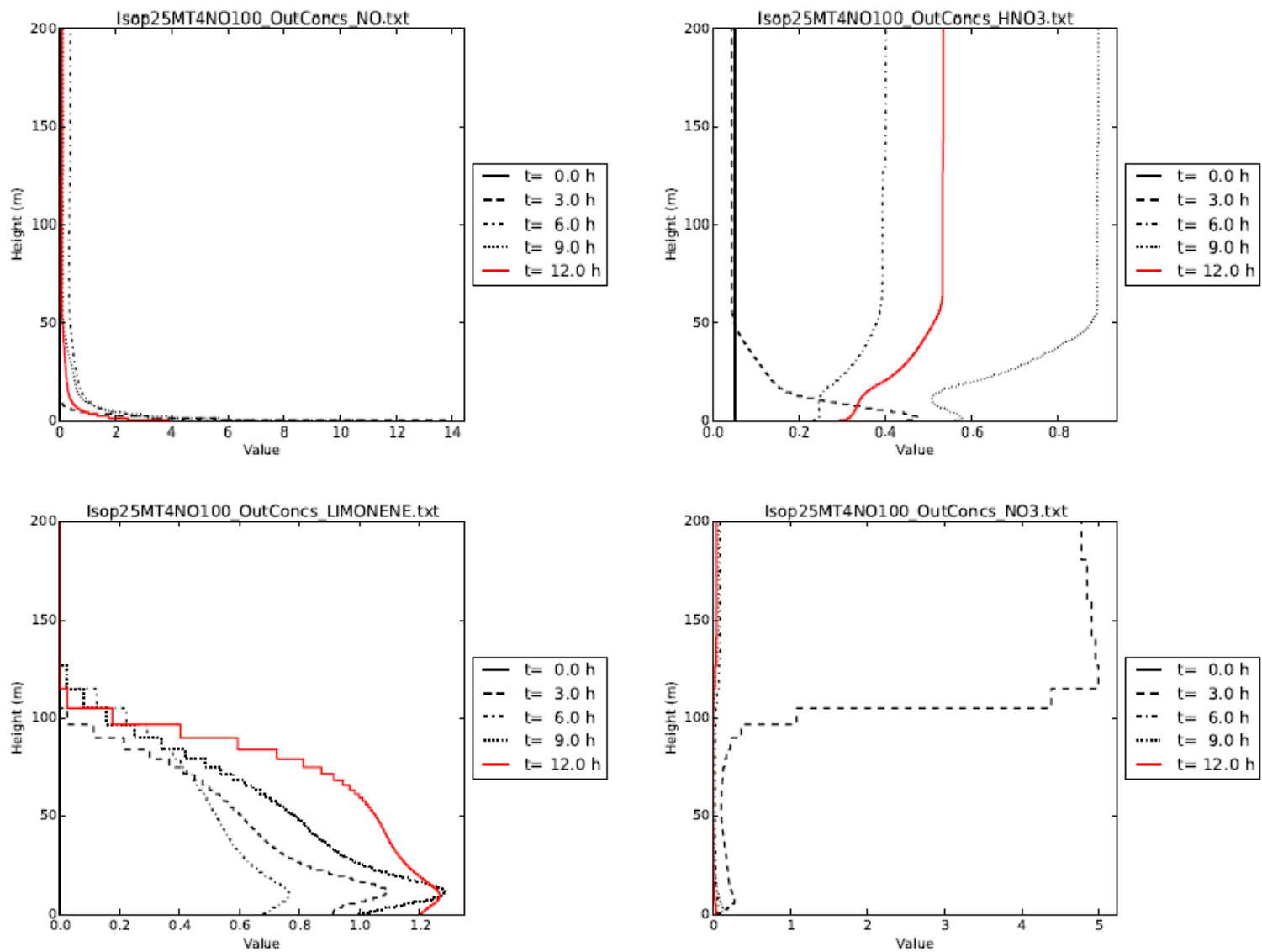
Figure 1.56: Examples of chemical variability from the ESX model: changes from midnight (t=0h) to mid-day (t=12h), for a generic deciduous forest with high BVOC and soil-NO emissions. Results are given for NO (top-left), HNO$_3$ (top-right), limonene (bottom-left) and NO$_3$ radical (bottom-right). All concentrations are in ppb.

ÉCLAIRE Third Periodic Report: November 2015

Comparisons of ESX against ÉCLAIRE O_3 flux measurement data have been carried out for the Hyytiälä scots pine forest in Finland in July 2011. The meteorological input and chemical boundary conditions were obtained from the EMEP MSC-W modelling system. ESX was run over the one-month period by changing input on an hourly basis assuming that a steady state is established at the end of each hour. The results are shown in Fig. 1.57, in which ESX runs in different configurations are compared with measurements.

Significant improvements in model results were obtained over the default configuration, first by introducing a 'shrub' understorey layer, a step forward from the standard big-leaf EMEP/DO3SE model, then by enhancing the limiting effect of water vapour pressure deficit (VPD). The mid-afternoon decline in V_d is still not entirely reproduced by the model; this may be related to other factors affecting stomatal conductance (e.g. soil moisture, not considered here due to lack of data), but also factors related to non-stomatal uptake.
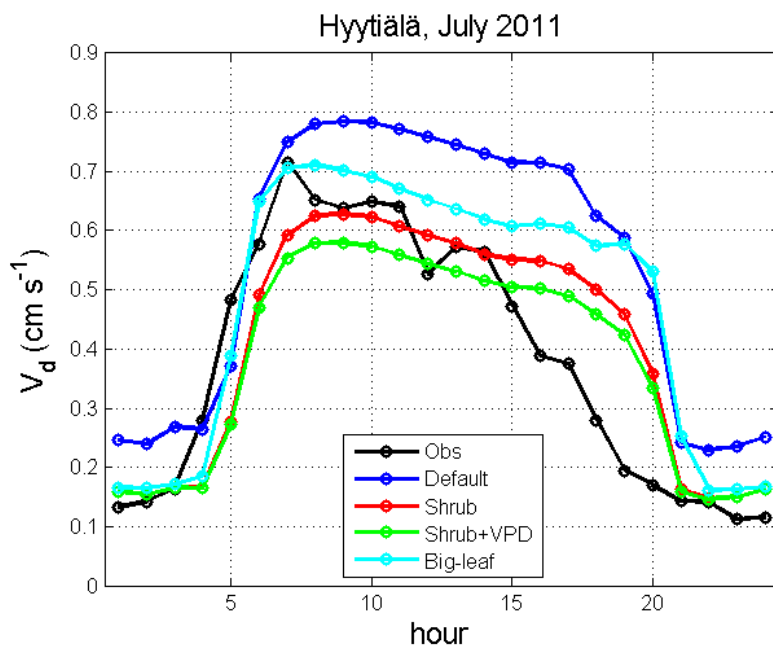
Figure 1.57. Comparison of the modelled and measured (Obs) ozone deposition velocities at Hyytiälä, Finland (mean diurnal cycles in July 2011). 'Default' = ESX with parameter values derived from the EMEP/DO3SE big-leaf model; 'Shrub' = ESX with explicit shrub layer; 'Shrub+VPD' = ESX with explicit shrub layer and more sensitive VPD response; 'Big-leaf' = old EMEP/DO3SE model.

New developments in MLC-CHEM

MLC-CHEM was initially developed and applied in its implementation in a 1-D as well as a global chemistry-climate modelling system (Ganzeveld et al., 2002a and 2002b). It is

now also available as a stand-alone modelling system to facilitate the analysis of field observations of atmosphere-biosphere exchange processes.

In its initial implementation, the model considered only two canopy layers (crown and understorey layer), but has now been extended with a Crank-Nicolson solver to allow, like ESX, a flexible number of canopy layers. This makes it possible to analyse to further assess how resolution affects the simulation of atmosphere-biosphere fluxes, where application of MLC-CHEM in CTMs would preferably require a minimum number of layers for CPU-considerations. Ganzeveld et al. (2002a) showed that two layers suffice to realistically simulate O_3, NO_x and isoprene canopy top fluxes for tropical forest, but it might be different for other ecosystems and other compounds (e.g., NH_3-HNO_3-NH_4NO_3).

New developments also include the coupling of MLC-CHEM, within a 1-D chemistry-climate model system, to the LPJGUESS Dynamical Global Vegetation Model (DGVM), to study the potential relevance of feedbacks involved in the O_3 deposition impact on ecosystem functioning. LPJGUESS has been extended with a first representation of the O_3 deposition impact on NPP and which affects the biogenic emissions of Volatile Organic Compounds (BVOCs) (Arneth et al., 2007), which in turn affect the O_3 production in the boundary layer (BL) and, consequently, O_3 deposition. Long-term offline simulations, as well as seasonal online simulations, suggest that, in pollution-biosphere-boundary layer interactions and feedback mechanisms, there is an important role of changes in the hydrological cycle.

MLC-CHEM has also been further developed and applied within ÉCLAIRE in support of the design of new field campaigns. Figure 1.58 shows an application of MLC-CHEM in a detailed analysis of in-canopy NO_x concentrations as a function of different assumptions on leaf-scale NO_x exchange. Comparison of the observed and simulated in-canopy diurnal cycle in NO_x concentrations for a deciduous forest site revealed that the best agreement between simulated and observed temporal variability was achieved considering the potential role of a leaf-scale NO_2 compensation point.

Task 4.4: Estimating deposition at the ÉCLAIRE effect study sites by combining measured concentrations with a bi-directional exchange model

Original objectives:

- Monthly measurements of atmospheric concentrations of the inorganic reactive nitrogen compounds NH_3, HNO_3, NO_2, NH_4^+ and NO_3^-, using low-cost denuder and filter samplers, and of bulk(wet) deposition, at field-scale experiments effects study sites of WP10.
- Modelling of reactive nitrogen and O_3 dry deposition at these sites using improved inferential models from Tasks 4.1-4.2.

This task was changed at an early stage of the project (see M18 ÉCLAIRE-WP4 Periodic Activity Report), allowing the chemical analytical resources to be re-allocated to extend

the passive measurements during the Po Valley campaign (Task 1.3), which provided a two-month intensive study across 20 sites in the Po Valley, exposing and analysing about 200 samples. As a result Deliverable 4.5 and Milestones 14, 20 and 21 were changed.
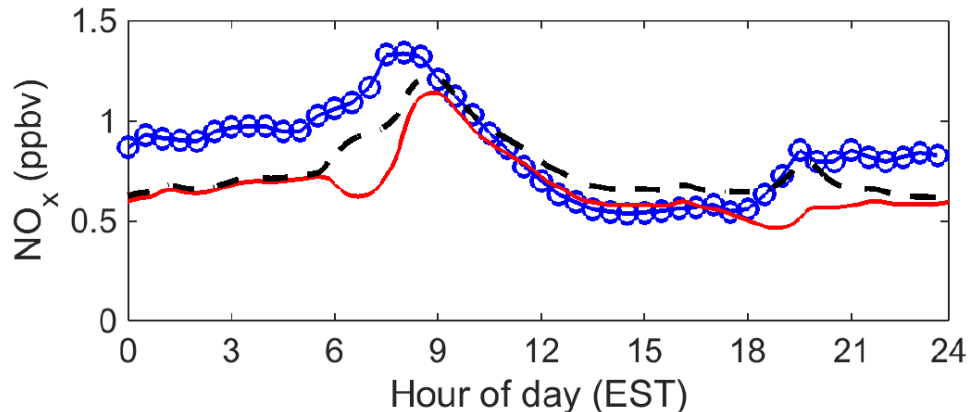
Figure 1.58. Comparison of the observed (blue circles/line) and simulated (MLC-CHEM; default simulation: red line; with NO_2 compensation point: black dashed line) diurnal cycles in NO_x mixing ratios at 15m inside a deciduous forest. The nocturnal underestimation is also due to a misrepresentation of soil NO emissions and in-canopy turbulent transport.

Progress towards the milestones and deliverables

D4.1) Improved pollution- and climate-sensitive exchange parameterisations: Improved pollution- and climate-sensitive exchange parameterisations for the main inorganic Nr compounds, suitable for inclusion in CTMs [*month 36*]

- The deliverable was submitted 23/10/2015.

D4.2) Ozone dry deposition parameterisations: Ozone dry deposition parameterisations, improved with respect to changes in climate and environmental conditions, suitable for inclusion in CTMs [*month 36*]

- The deliverable was submitted 03/11/2014.

D4.3) A coupled pollutant deposition and carbon based growth model: A coupled pollutant deposition and carbon based growth model (DOSE_C), based on the existing DO3SE model for O3 deposition [*month 36*]

- The deliverable was submitted 03/11/2014.

D4.4) Chemical processing model of NO-NO_2-O_3-VOCs and NH_3-HNO_3-NH_4NO_3: A vertically-resolved, multi-layer in-canopy chemical processing model of NO-NO_2-O_3-VOCs and NH_3-HNO_3-NH_4NO_3 exchange [***month 36***]

- The deliverable was submitted 23/10/2015.

D4.5) Current and future estimates of N_r and O_3 deposition: Inferential model current and future estimates of N_r and O_3 deposition at effects study sites of Component 2 [***month 42***]

- **Deliverable 4.5 was changed** as a result of Task 4.4 being changed, see above and M18 ÉCLAIRE-WP4 Periodic Activity Report.

MS14) Measurement network established for monthly N_r concentrations at the ÉCLAIRE effect study sites [***month 12***]

- **MS14 was changed** as a result of Task 4.4 being changed, see above and M18 ÉCLAIRE-WP4 Periodic Activity Report.

MS15) Literature review on the effects of O_3 and N_r deposition on stomatal functioning and on the influence of surface wetness on total O_3 deposition: [***month 12***]

- The literature review has been performed. ~ 40 papers published from the early 1990's up to the present day were collected, these described the role that N_r & O_3 in combination play in altering gas exchange and subsequent C assimilation. These have been used to inform the methods used to incorporate the influence of N deposition on stomatal conductance into DO3SE/A_n-g_{sto} through the effect on leaf/canopy photosynthesis. The influence of surface wetness has been extensively studied using field flux measurements and the MUSICA model.

MS16) New ÉCLAIRE experimental datasets [***month 18***]

- The new DO3SE A_n-g_{sto} model has been compared to observations made on Birch from the Bangor solardome experiment, and the canopy multi-layer – multi-component DO3SE model has also been applied to an existing grassland dataset from the UK.
- The multi-layer MUSICA surface/atmosphere exchange model and the 2-layer SURFATM model have been extensively compared versus O_3 and NH_3 flux measurements at the Grignon ÉCLAIRE field site, as well as other forest field sites in France.

MS17) Improved representation of the influence of environmental drivers on stomatal conductance and the partitioning between stomatal and non-stomatal deposition of O3 and their incorporation in EMEP model [***month 24***]

- The issue of stomatal versus non-stomatal conductance is one of the first priorities of the ESX described above. The new DO3SE A_n-g_{sto} model has been

incorporated/integrated with the ESX model to improve the canopy stomatal deposition term, and the inclusion of the new non-stomatal parametrisations (soil, leaf cuticles, wetness), will allow further investigations of the stomatal/non-stomatal partitioning.

MS18) Incorporation of results from flux monitoring data generated within ÉCLAIRE into modelling framework [*month 24*]

- The O_3 and NO_x surface exchange flux data from Hyytiälä were analysed in parallel to the developments of the ESX model (see D4.4).
- Ammonia flux data in background conditions from Posieux, Bosco Fontana, Grignon and Speulderbos were processed using the Massad-Nemitz-Sutton 2010 bi-directional scheme (see also D3.2).
- Ammonia flux measurements from Bosco Fontana were used to evaluate the DEWS leaf surface wetness chemical model (see D4.1).
- Ammonia emission fluxes following manure spreading at Grignon and Posieux were processed using the VOLT'AIR emission model and Γ_g meta-model (see D4.1).

MS19) Calibration of model parameterisation completed [*month 30*]

- The VOLT'AIR Γ_g meta-model, derived from multiple runs of VOLT'AIR (see Deliverable 3.1), was parameterized for three types of nitrogen fertilizer, and validated against field measurements for cattle slurry (see D4.1).
- The Massad-Nemitz-Sutton (MNS-2010) bi-directional scheme for NH3 exchange was re-parameterised on the basis of ÉCLAIRE and other datasets (see also D3.2)

MS20) Estimates of N_r and O_3 fluxes at the effects study sites inferred from monitored concentrations [*month 30*]

- **MS20 was changed** as a result of Task 4.4 being changed, see above and M18 ÉCLAIRE-WP4 Periodic Activity Report.

MS21) Comparison of inferential model estimates with EMEP model results [*month 33*]

- **MS21 was changed** as a result of Task 4.4 being changed, see above and M18 ÉCLAIRE-WP4 Periodic Activity Report.

MS22) Provision of site based estimates of NH3/NO and VOC exchange for ÉCLAIRE core sites, for present and future environmental conditions [*month 44*]

- Achieved

Use of resources and deviations from DoW

A total of 21 person months were spent on this workpackage in this period.

Deviations from DoW:

Both deliverables D4.1 and D4.4 were delayed until the final month of the project. The delay occurred because there was a change of strategy to tackle the objectives of the work package, which were basically to improve parameterisations for pollutant exchange in *existing models*, while we instead chose to address these objectives by *creating a new multi-layer surface exchange model* (ESX). The basic idea was to reduce empiricism and increase the representation of mechanisms from first physical and chemical principles. Creating a new model takes much more time than to re-parameterize/re-calibrate and existing one, and there were inevitable set-backs and coding issues to deal with.

Shift in Resources:

A shift in budget resources was made between Partners 13 (INRA) and 29 (UBO), with €66,096.27 in EC contribution being re-allocated from INRA to UBO in April 2013. This was used by UBO to hire a post-doctoral researcher (Dr Shyam Pariyar) from July 2013 to June 2014 (full-time), and from July to December 2014 (part-time), to work on the development of the DEWS model and the coupling to canopy surface aerosol models PD-FITE and AIOMFAC, in collaboration with School of Earth, Atmospheric and Environmental Sciences, The University of Manchester.

Publications relevant to WP4

Bertolini T., Flechard, C.R., Fattore, F., Nicolini, G., Stefani, P., Stefano, M., Valentini, R., Vaglio, L.G., Castaldi, S. (2015). Dry and bulk atmospheric nitrogen deposition to a West-African humid forest exposed to terrestrial and oceanic sources. Agricultural and Forest Meteorology (in press).

Burkhardt J., Hunsche M. (2013): 'Breath figures' on leaf surfaces – formation and effects of microscopic leaf wetness. Frontiers in Plant Science, 4; doi: 10.3389/fpls.2013.00422. http://www.frontiersin.org/Journal/10.3389/fpls.2013.00422/full

Burkhardt, J., Pariyar, S. (2015) How does the VPD response of isohydric and anisohydric plants depend on leaf surface particles? Plant Biology http://dx.doi.org/10.1111/plb.12402 Cieslik, S., Tuovinen, J.-P., Baumgarten, M., Matyssek, R., Brito, P. and Wieser, G., 2013. Gaseous exchange between forests and the atmosphere. Developments in Environmental Science 13, 19-36.

Ferrara R.M., Loubet B., Decuq C., Palumbo A.D., Di Tommasi P., Magliulo V., Masson S., Personne E., Cellier P., Rana G., 2014. Ammonia volatilisation following urea fertilisation in an irrigated sorghum crop in Italy. Agricultural and Forest Meteorology, 195-196, 179-191.

Flechard, C.R., Massad, R.-S., Loubet, B., Personne, E., Simpson, D., Bash, J.O., Cooter, E.J., Nemitz, E. and Sutton, M.A. 2013. Advances in understanding, models and parameterisations of biosphere-atmosphere ammonia exchange, Biogeosciences 10, 5183–5225.

Loubet B., Cellier P., Fléchard C., Zurfluh O., Irvine M., Lamaud E., Stella P., Roche R., Durand B., Flura D., Masson S., Laville P., Garrigou D., Personne E., Chelle M., Castell J.-F., 2013. Investigating discrepancies in heat, CO_2 fluxes and O_3 deposition velocity over maize as measured by the eddy-covariance and the aerodynamic gradient methods. Agricultural and Forest Meteorology, 169, 35-50.

Personne, E., Tardy, F., Génermont, S., Decuq, C., Gueudet, J.-C., Mascher, N., Durand, B., Masson, S., Lauransot, M., Fléchard, C., Burkhardt, J. and Loubet, B., 2015. Investigating sources and sinks for ammonia exchanges between the atmosphere and a wheat canopy following slurry application with trailing hose. Agric. For. Meteorol., 207: 11-23.

Potier E. 2014. Étude des mécanismes du dépôt d'ozone sur la végétation: mise en évidence d'un puits chimique sur les feuilles mouillées en période de sénescence. *PhD*, University Pierre et Marie-Curie, Univ. Paris 6, 132p.

Potier E., Jérôme Ogée Julien Jouanguy ; Eric Lamaud; Patrick Stella; Erwan Personne; Brigitte Durand; Nicolas Mascher and Benjamin Loubet, 2014. Multilayer modelling of ozone fluxes on winter wheat reveals large deposition on wet senescing leaves. Agricultural and Forest Meteorol. (submitted).

Simpson, D. and Tuovinen, J.-P., 2014. ÉCLAIRE Ecosystem Surface Exchange model (ESX). In: Transboundary particulate matter, photo-oxidants, acidifying and eutrophying components. EMEP Status Report 1/2014, Norwegian Meteorological Institute, pp. 147-154.

Stella P., Personne E., Lamaud E., Loubet B., Trebs I., Cellier P., 2013. Assessment of the total, stomatal, cuticular, and soil 2 year ozone budgets of an agricultural field with winter wheat and maize crops. Journal of Geophysical Research - Biogeosciences, 118, 3, 1120–1132.

Sutton, M.A.; Reis, S.; Riddick, S.N.; Dragosits, U.; Nemitz, E.; Theobald, M.R.; Tang, Y.S.; Braban, C.F.; Vieno, M.; Dore, A.J.; Mitchell, R.F.; Wanless, S.; Daunt, F.; Fowler, D.; Blackall, T.D.; Milford, C.; Flechard, C.R.; Loubet, B.; Massad, R.; Cellier, P.; Personne, E.; Coheur, P.F.; Clarisse, L.; Van Damme, M.; Ngadi, Y.; Clerbaux, C.; Skjoth, C.A.; Geels, C.; Hertel, O.; Wichink Kruit, R.J.; Pinder, R.W.; Bash, J.O.; Walker, J.T.; Simpson, D.; Horvath, L.; Misselbrook, T.H.; Bleeker, A.; Dentener, F.; de Vries, W. 2013.

Towards a climate-dependent paradigm of ammonia emission and deposition. Philosophical transactions of the Royal Society of London. Series B, Biological sciences 368 (1621) 10.1098/rstb.2013.0166.

References cited

Arneth et al.,, Process based estimates of terrestrial ecosystem isoprene emissions: Incorporating the effects of a direct CO_2-isoprene interaction, Atmos. Chem. Phys., 7, 31–53, 2007, http://www.atmos-chem-phys.net/7/31/2007/.

Ball, J.T., Woodrow, I.E. Berry, J. A. (1987). A model predicting stomatal conductance and its contribution to the control of photosynthesis under different environmental conditions. In J. Biggens (Ed.), Progress in photosynthesis research, Vol IV. Dordrecht: Martinus Nijhoff.

Farquhar, G.D., von Caemmerer, S., Berry, J. A. (1980). A biochemical model of photosynthetic CO_2 assimilation in leaves of C3 species. Planta, 149, 78–90.
Flechard, C. R., Fowler, D., Sutton, M. A., and Cape, J. N.: A dynamic chemical model of bi-directional ammonia exchange between semi-natural vegetation and the atmosphere, Q. J. Roy. Meteor. Soc., 125, 2611–2641, 1999.

Flechard, C.R., Massad, R.-S., Loubet, B., Personne, E., Simpson, D., Bash, J.O., Cooter, E.J., Nemitz, E., Sutton, M.A., 2013. Advances in understanding, models and parameterisations of biosphere-atmosphere ammonia exchange. Biogeosciences Discussions 10, 5385–5497. doi:10.5194/bgd-10-5385-2013

Ganzeveld, L., Lelieveld, J., Dentener, F.J., Krol, M.C., Roelofs, G.-J., Atmosphere-biosphere trace gas exchanges simulated with a single-column model, J. Geophys. Res. 107, 10.1029/2001JD000684, 2002a.

Ganzeveld, L., Lelieveld, J., Dentener, F.J., Krol, M.C., Bouwman, A.F., and Roelofs, G.-J., The influence of soil-biogenic NO_x emissions on the global distribution of reactive trace gases: the role of canopy processes, J. Geophys. Res., 107, doi: 10.1029/2001JD001289, 2002b.

Jarvis, P. G.: The interpretation of the variations in leaf water potential and stomatal conductance found in canopies in the field, Philos. T. R. Soc. Lond., B273, 593–610, 1976.

Leuning, R.: Estimation of scalar source/sink distributions in plant canopies using Lagrangian dispersion analysis: Corrections for atmospheric stability and comparison with a multilayer canopy model, Bound.-Lay. Meteor., 96, 293–314, 2000.

Massad, R.-S., Nemitz, E., and Sutton, M. A.: Review and parameterisation of bi-directional ammonia exchange between vegetation and the atmosphere, Atmos. Chem. Phys., 10, 10359–10386, doi:10.5194/acp-10-10359-2010, 2010.

Ogee, J., Y. Brunet, D. Loustau, P. Berbigier & S. Delzon. 2003. MuSICA, a CO_2, water and energy multilayer, multileaf pine forest model: evaluation from hourly to yearly time scales and sensitivity analysis. Global Change Biology, 9, 697-717.

Simpson, D., Benedictow, A., Berge, H., Bergström, R., Emberson, L. D., Fagerli, H., Flechard, C. R., Hayman, G. D., Gauss, M., Jonson, J. E., Jenkin, M. E., Nyíri, A., Richter, C., Semeena, V. S., Tsyro, S., Tuovinen, J.-P., Valdebenito, Á., and Wind, P.: The EMEP MSC-W chemical transport model – technical description, Atmos. Chem. Phys., 12, 7825–7865, 2012.

Sutton, M. A, Reis, S., Riddick, S. N., Dragosits, U., Nemitz, E., Theobald, M. R., Tang, Y. S., Braban, C. F., Vieno, M., Dore, A. J., Mitchell, R. F., Wanless, S., Daunt, F., Fowler, D., Blackall, T. D., Milford, C., Flechard, C. R., Loubet, B., Massad, R. S., Cellier, P., Personne, E., Coheur, P. F., Clarisse, L., Van Damme, M., Ngadi, Y., Clerbaux, C., Skjøth, C. A., Geels, C., Hertel, O., Wichink Kruit, R. J., Pinder, R. W., Bash, J. O., Walker, J. T., Simpson, D., Horvath, L., Misselbrook, T. H., Bleeker, A., Dentener, F., and de Vries, W.: Towards a climatedependent paradigm of ammonia emission and deposition, Philos. T. R. Soc. B, 368, 20130166, http://dx.doi.org/10.1098/rstb.2013.0166, 2013.

Tuzet, A. Perrier, B. Loubet & P. Cellier. 2011. Modelling ozone deposition fluxes: The relative roles of deposition and detoxification processes. Agricultural and Forest Meteorology, 151, 480-492.

Zuend, A., Marcolli, C., Luo, B. P., and Peter, T.: A thermodynamic model of mixed organic-inorganic aerosols to predict activity coefficients, Atmos. Chem. Phys., 8, 4559-4593, doi:10.5194/acp-8-4559-2008, 2008.

ÉCLAIRE Third Periodic Report: November 2015

2.1.2 Component 2 – Emissions & exchange at local, European to global scales

Lead contractor: KIT, METN0

Component objectives & Specific Objectives of relevance to this component

Component 2 (C2) addresses the currently still poor understanding of both spatial and temporal variation in emissions, transport and transformation of precursor substances of relevance for air pollution and climate. Biogenic and anthropogenic emissions contribute in complex emission patterns and atmospheric reactions and transport to pollution locally, regionally and across large-distances. The impact of climate change on emissions and chemical interactions is a large uncertainty in projections of the climate change-pollution interplay. Component 2 aims to (1) provide past to future simulations of European to global-scale level pollution-climate change interactions, accounting for local and long-distant pollution source contribution; (2) assess how biogenic pollutants and precursors from natural, semi-natural and agricultural ecosystems vary in space and time; (3) apply the analyses of climate change-pollution interplay to combine novel knowledge into pollution metrics across Europe; (4) investigate climate-pollution interplay at high spatial resolution to take into consideration effects of landscape heterogeneity.

Progress and Results

WP5-WP8 are presented by WP below, but we give here some key findings from C2 as a whole, with focus on the findings of the last reporting period:

The largest effects of a changing climate are likely to be on increasing biogenic/agricultural emissions rather than on changing atmospheric lifetimes and the spatial patterns of O_3 levels and N deposition. Nevertheless, the spatial patterns remain extremely important given the combination of scales involved, from hemispheric scale (O_3 background), though regional scale (O_3 and N deposition) to local scale (N deposition and NH_3 exposure)

Modelling work carried out by ÉCLAIRE and other projects allows us to address these interactions (e.g. Langner et al., 2012, Engardt & Langner, 2013, Simpson et al., 2014). Impacts of air pollution on European ecosystems occur over a range of spatial scales from the global scale (O_3 background), though regional scale (O_3 and N deposition) to local scale (N deposition and PM2.5, NH_3 exposure). In a changing climate, the spatial patterns of impacts are likely to change as a result of changing emissions, land use and atmospheric processes.

The vast majority (90-95%) of impacts due to N deposition to European ecosystems are the result of European emissions. At a national level N deposition has contributions from

both national emissions as well as emissions from neighbouring countries (EMEP annual reports, Vieno et al., 2014; Geels et al., 2012).

By contrast, impacts of O_3 in Europe are the result of precursor emissions both from within Europe and worldwide. Summertime ozone concentrations in Europe are strongly influenced by European precursor emissions whereas non-European precursor emissions, of which methane is key, dominate the rest of the year (Wild et al., 2012, Langner et al., 2012, WP5, WP7 results).

A warmer climate will most likely increase European NH_3 emissions (Skjøth and Geels, 2013, Sutton et al., 2013). This would increase the relative contribution of NH_3 to N deposition and thus increase near-source impacts relative to those at longer ranges (Engardt & Langner, 2013, Simpson et al., 2014). A warmer climate may also increase the evaporation of ammonium aerosol, leading to an increase in NH_3 concentrations and may also affect the atmospheric lifetime of ammonia due to changes in compensation points.

A warmer climate would also have a range of other effects, such as changes in meteorological variables (water vapour, precipitation, drought, e.g. Engardt and Langner, 2013, Emberson et al., 2013), but also changes in soil NO and BVOC emissions due to changes in temperature and land-cover.   The impact of climate on isoprene and other BVOC (increasing, decreasing?) and thus on O_3 and aerosol formation is however unclear (WP5,WP6). While there is a tendency for these emissions to increase under warmer conditions, under a future climate parallel increases in CO_2 concentrations may offset this effect for isoprene emissions.

WP 5 Past and future changes of atmospheric pollutants transported into Europe

WP 5 had three objectives, namely:

1. To assess our current understanding of ozone and other air pollution trends, based on knowledge acquired within the UNECE TF HTAP, work for IPCC-AR5 and other projects, with a focus on the inflow regions of Europe;

2. To evaluate the transport of atmospheric pollutants (ozone and precursors, aerosols) into Europe, evaluate the relative contributions of long-range-transported and European pollution on atmospheric composition and deposition to the ecosystems in Europe and in other regions, and provide a range of chemical boundary conditions to regional models within ÉCLAIRE (WP7), taking into account changes in global anthropogenic and natural emissions under current and future climate change conditions;

3. To examine the relative contributions and impacts on air pollution of future biogenic

and soil and fire emissions produced in WP15 of ozone and aerosol precursors on European pollutants levels and their export to the hemispheric and large scale atmosphere.

During the last reporting period, the following tasks were addressed:

Task 5.2, Predicting future pollutant trends.

Selected scenarios of future emissions provided by IPCC AR5 RCPs were used to evaluate the possible global, hemispheric and European evolution of ozone and other air pollutants for 2030, 2050 and 2100. To this end CNRS made major upgrades to their model and performed extensive simulations of a variety of RCP scenarios. JRC performed TM5 FASST analysis of emission scenarios, and –through the CLRTAP Task Force Hemispheric Transport of Air Pollution (TF HTAP) organized and analysed future air pollution scenarios.

Key findings from task 5.2 can be summarised as:

- A detailed description of ammonium sulfate-nitrate and coarse-aerosol nitrate formation was included in the LMDz-INCA model. Good agreement of surface aerosol concentrations and aerosol optical depth was found for Europe and North America. Nitrogen and sulfur deposition were in reasonable agreement in Europe and North America, but systemically underestimated in Eastern Asia.
- Model calculations suggest under the RCP scenarios SO_4 burden is strongly declining, while nitrate and ammonium aerosol burdens are more constant. Agricultural emission of NH_3 may therefore maintain higher levels of cooling than assumed in previous studies. The fraction of ammonium in nitrogen deposition is increasing from about 60-80 % in China. These results are driven by increasing agricultural ammonia emissions in the RCP emission scenario, subject to high uncertainty.
- Comparison of the summer ozone distributions between 2050 and 2010 using the ECLIPSE5.0 emission scenario indicates ozone decreases by up to 7 ppbv in Northern America and by 4-5 ppb in Europe. In China, SE Asia, and India, ozone increases by up to 7 ppb due to increased anthropogenic emissions in these regions. **Climate and land use change by 2050 may augment isoprene emission and lead to ozone increases in large portions of the Northern Hemisphere up to 4,5 ppb, potentially off-setting the ozone reductions by anthropogenic emissions in Europe and North America. However, when including the effect of increasing CO_2 on reducing the isoprene emissions,**

the effect on ozone is much less, with two current parameterizations strongly disagreeing.

- Controlling methane and air pollution emissions in Asia is going to be of critical importance for ozone air quality in Europe. In the absence of controls, further increases in CH_4 emissions are expected to lead to a continued increase in the background concentration of tropospheric O_3 in the northern hemisphere.

Task 5.3, Quantifying the importance of long-range transport for ecosystem impacts.

The task was performed in close collaboration with ÉCLAIRE WP6 and aimed to analyze the evolution of key environmental variables impacting ecosystems (ozone levels, PM levels, N and S deposition) under the various emission and climate scenarios and isolate the role played by long-range transport of pollution, climate change and changing variability, biogenic/emissions, lightning emissions, and anthropogenic emissions in Europe and other regions.

Select key findings from 5.3 were:

- In Europe, comparison of biogenic VOC emissions calculated with the widely used MEGAN emission model and the vegetation model ORCHIDEE, showed 19% higher isoprene emissions, 21% higher methanol and 21% lower monoterpene emissions by the latter. Assumptions on leaf-temperature for shaded and sunlit leaves versus air temperature play an important role in explaining these differences. Assumptions on leaf-area-index (LAI) also are a major uncertainty, with a complex impact on emission variability.
- Globally, comparing the 2040s and the 1990s, Orchidee calculations indicate 25% increase in isoprene, 27% in monoterpenes and 28% in methanol emissions. However, isoprene emission potential may decrease caused by higher levels of CO_2, resulting in complete off-setting of isoprene emissions.
- LPJ-GUESS calculations of BVOC emission in Europe indicate a decline of isoprene and monoterpene emissions by about a factor of 3 comparing the landcover in 2000s to the potential natural vegetation. Simulations are highly sensitive to biases in climate models- leading to ca. 65 % and 20 % lower emissions for isoprene and monoterpene emissions compared to using bias-corrected emissions.
- LPJ-GUESS calculations of BVOC global emissions the RCP4.5 GHG scenario, indicate isoprene emissions increase 41% and monoterpenes 25% in the future compared to current conditions. However, taking the CO_2 Inhibition effect into account, emissions decrease slightly with -2% and -13% respectively for isoprene and monoterpenes. Climate change favours isoprene emitting vegetation.

- LPJ-GUESS calculations of wildfire emissions indicate a complex range of interactions between vegetation, climate change and increasing CO_2, and fire suppression. Comparing 1970-2000 and 2070-2100, overall tropical emissions decline between 15 and 35 % (mostly due human influence), while extratropical emissions increase by 20 % and 45 %. Globally emissions change within a -10 % range.
- While nitrogen input to ecosystems affects yields and can lead to pollution of water sheds in heavily fertilised regions, effects of N deposition on natural ecosystems regarding the historical carbon sink strength are minor. Whether or not nitrogen limitation of plant growth will notably affect future ecosystem carbon storage is under debate, and current modelling studies show conflicting results. Arguably, climate effects of N_2O emissions are of more concern than N-interactions with the C sink; this will be investigated further in the coming years with updated versions of LPJ-GUESS.

Task 5.4, Provision of future European pollutant boundary conditions evaluated the transport of atmospheric pollutants (ozone and precursors, aerosols) into Europe.

The task provided a best estimate and uncertainty range of present and future O_3, O_3 precursors and aerosol as boundary conditions to regional models, for further impact assessment on ecosystems. Simulations with the global LMDz-INCA model were constrained by ÉCLAIRE/ECLIPSE emission inventories for the period 2010, 2030 and 2050; and ensemble modelling work in the Task Force Hemispheric Transport and EMEP on the evaluation of future emission scenarios. Scenario analysis has focused on the evaluation of the widely used IPCC AR5 RCP scenarios for TH HTAP and ÉCLAIRE/ECLIPSE emission inventories for boundary condition files. Deliverable 5.4 has provided the description of the NetCDF files prepared with the LMDz-INCA global model for use by the regional models for the present-day, 2030 and 2030 conditions and for the ÉCLAIRE/ECLIPSE emission scenarios (available via www.eccad.fr), corresponding to both the Current Legislation and Maximum Feasible Reduction conditions.

WP 6 Emissions on regional, European, to global scale

WP6 aimed to provide emission patterns for simulation model experiments on European and global scale, focussing on terrestrial biogenic and pyrogenic emissions from ecosystems with various intensity of land use, and will provide improved temporal resolution of non-agricultural anthropogenic emissions. Specifically, the objectives of this WP were:
- quantify how trace gas emissions from natural, semi-natural and agricultural ecosystems vary in response to interactions of weather and climate, atmospheric CO_2 burden and N deposition, vegetation and soil carbon and nitrogen dynamics, and land use/land cover change;

- provide improved temporal dis-aggregation of non-ecosystem, anthropogenic European pollutant emission patterns for selected source sectors.

WP 6 finished already in month 30 of the project (see Gantt chart p 168 of Part B in the DoW), with all deliverables completed in time. However, there has been work continued along the ÉCLAIRE-objectives, following on from the project's achievements, which is briefly reported below.

Task 6.2, Improved emissions from (semi)natural ecosystems

The BVOC emission module from partner LSCE (Orchidee model) was further developed in the last reporting period. Specifically, work included
- adding new compounds (such as: α-pinene, β-pinene, limonene, myrcene, sabinene, camphene 3-carene, t-β-ocimene and bulk sesquiterpenes)
- re-examining the BVOC Emission Factors (EFs) considering state of the art emission schemes and the most recent field measurements
- adding a light dependency for almost all emitted species as already carried out for isoprene
- improving the multi-layer radiation scheme including the CO_2 inhibition effect for isoprene emissions

The model was applied to the global and European scale. A present-day simulation (from 1990 to 2000) and a future one (from 2040 to 2050) were performed, using climate forcing from a regional climate down-scaling product, based on ECHAM5 A1B-r3 simulation (Kjellstrom et al., Tellus A, 63(1), 24-40 2011). The vegetation distribution was based on the RCP 8.5 Land-Use scenarios and was kept constant using the year 2000. Example results of emissions can be seen in Figure 2.1, identifying a general increase of BVOC emissions for the whole Europe, in particular in June, July and August. With respect to the present-day scenario, the future increase reaches 20% for isoprene, while for other compounds, such as monoterpenes and acetone and for methanol, it reaches 16% - 17%.

Task 6.3, Improved emissions from agricultural sources

Regarding agricultural emissions, additional work has since then been done in order to implement the new and improved dynamical NH_3 emission model in some of the Chemistry-Transport models used in ÉCLAIRE – e.g. the Danish Eulerian Hemispheric Model (DEHM) operated at AU and the WRF-Chem used at WORC. This has led to new results in relation to studying ammonia emissions and the effect of climate and the impact on the environment. The new version of the WRF-Chem model including the dynamic emission model has been used to study a full year of hourly observations from Harwell, UK in comparison to the model simulations. The study does for the first time include a fully consistent description of both chemistry and dynamics in relation to ammonia and

the effect of meteorology on the emissions. The first results indicate that vertical dynamics and the development of the planetary boundary layer (PBL) play an important role in relation to ammonia concentrations at the surface – during day and night (see Figure 2.2). The study suggests that the effect of weather on the emissions of ammonia is currently underestimated in existing ammonia emission models (Werner et al., 2015).

The comparison with observed hourly NH_3 concentrations at Harwell and at the Danish site Risø, show that the modelled diurnal variation in the atmospheric NH_3 concentration in both the DEHM and WRF-Chem are wrong. We are therefore now trying to improve the description of the diurnal variation in the dynamic emission model.
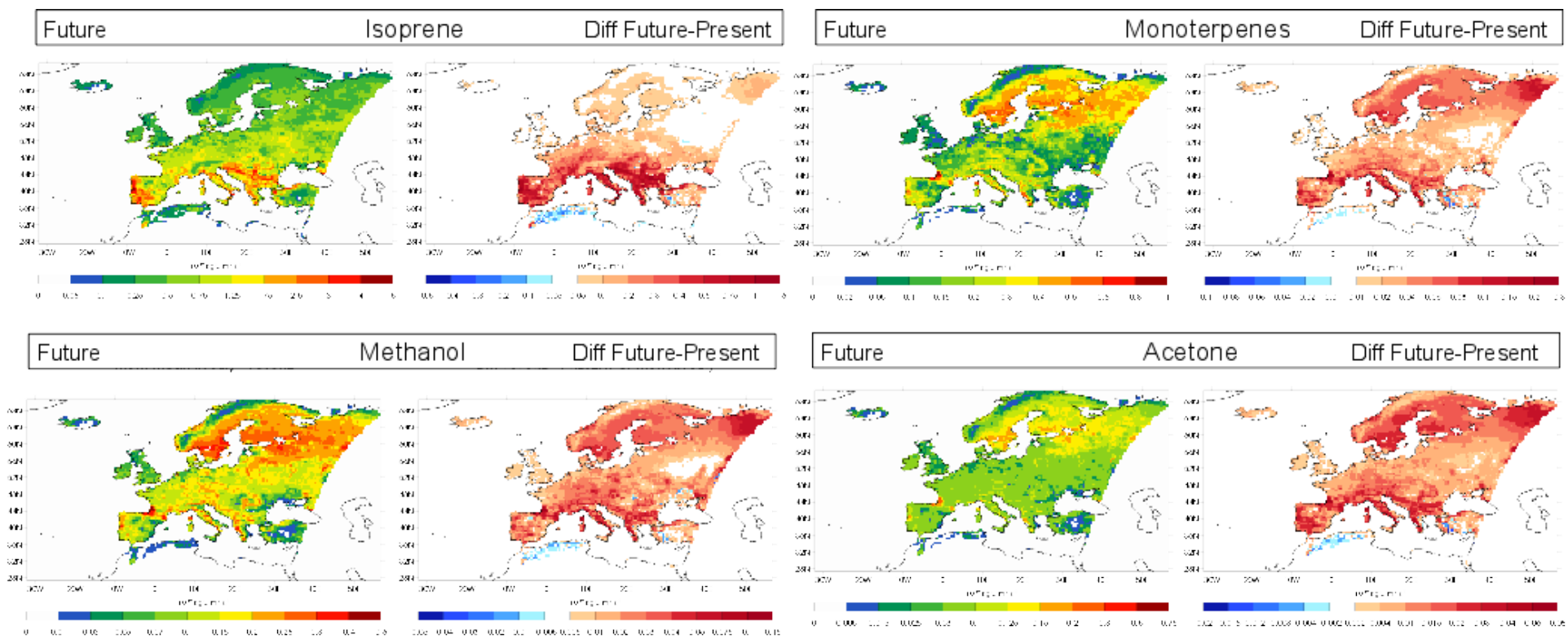
Figure 2.1: European emissions in July for isoprene, monoterpenes, methanol and acetone. For each compound, first panel represents the annual average for the future scenario and second one the difference between the annual average of the future and the present scenarios. Emissions are given in 1010 kgC/m2/s.
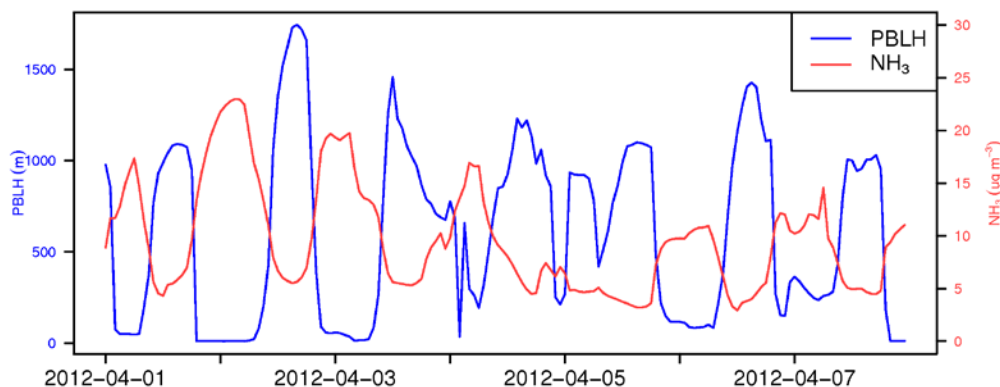
Figure 2.2: The PBL height and surface NH_3 concentration as simulated by WRF-Chem for a few days in April, 2012.

The dynamic global vegetation model LPJ-GUESS was updated with a coupled carbon-nitrogen cycle in the crop module of the code. This allows to assess impacts of N fertiliser on a range of ecosystem processes, and ecosystem services derived from these such as yields, carbon storage of nitrogen leaching. Recently simulation experiments were performed to study how different crop management options such as no-tillage, complete residue removal or irrigation would affect the calculated values for these three services in comparison with a standard simulation set-up. Trade-off analyses of these indicated that –regionally and globally- no-tillage would have relatively small effects on soil C pool size, in accordance with recent (controversially debated) literature. Since the model development is still in progress interpretation of these results, and those related to leaching and yields is relatively premature.

WP 7 Modelling European air pollution and deposition

The objectives of WP7 is to provide maps of O_3-damage metrics and N-deposition over Europe, for current and future scenarios, as inputs to the ecological response and effects packages (C3 and C4) and to integrated assessment modelling (C5). Activities range from global to local scale. The main aims were:

1. To map current air pollution metrics (APMs, mainly ozone damage indicators, POD & AOTx, and N-deposition) using a small ensemble of CTMs, in order to provide a best-estimate and uncertainty range on vegetation effects metrics.

2. To implement on the European scale new modules for stomatal uptake, in-canopy-chemistry, and emissions and sub-grid effects into the EMEP chemical transport model, able to take account of changes in CO_2, N deposition, BVOC emissions and climate over coming decades.

3. To estimate changes in APMs to specific ecosystems up to year 2030 and 2050, accounting for climate-changed induced changes in meteorology, vegetation, and biosphere-atmosphere exchange processes.

Task 7.1 Implementation of advanced exchange models into European CTMs.

Development work has continued with the ÉCLAIRE Ecosystem Surface Exchange (ESX) model, which combines chemistry from the EMEP code with in-canopy emission, dispersion and deposition processes in a 1-D model. During this reporting period the ESX model code and theoretical basis has been substantially improved, and a photosynthesis-based algorithm implemented. The ESX model was set up as an offline model, driven by a combination of EMEP and observed data, and was used to investigate the effects of foliar BVOC and soil NO and NH_3 emissions on near-surface concentrations and deposition velocities.

The photosynthesis module from DO3SE has also been implemented in the EMEP model, and used to study concentrations and depositions in 2010 and 2050 (See Deliverable D7.2). Figure 2.3 gives an example showing calculations of the health metric SOMO35 in both years, with both the standard and new photosynthetic procedures to calculate stomatal conductance.
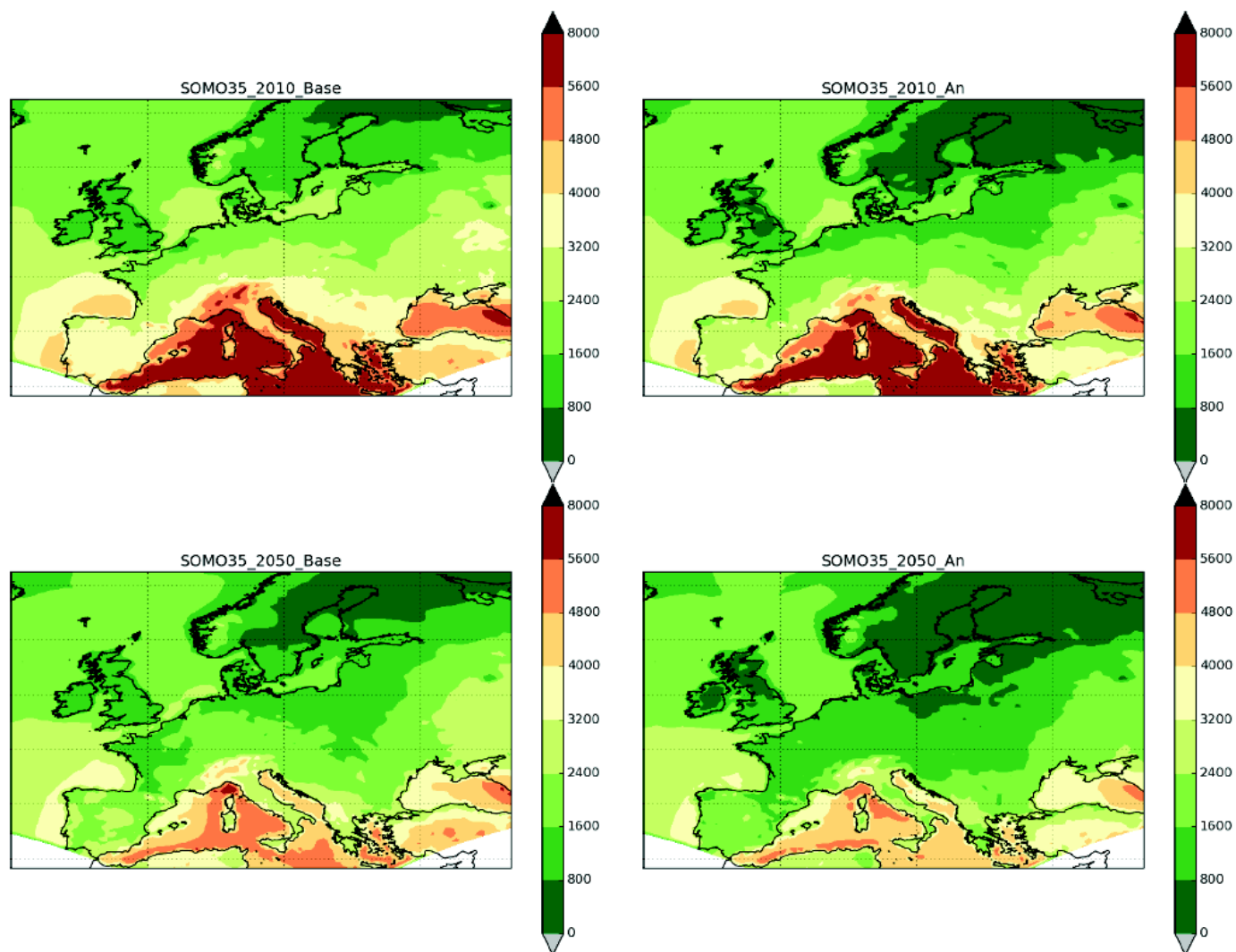
Figure 2.3: EMEP MSC-W calculations of SOMO35 for 2010 (top) and 2050 (bottom). Left column gives results with standard EMEP g_{sto}, right column with photosynthesis-based A_n-g_{sto} (labelled An). Units: ppb.day

Task 7.2: Scenario calculation of climate effects for assessment of air pollution transport and deposition

The EMEP chemical transport model (CTM) was modified in order to take account of physical/chemical changes expected in the future, so that it is better able to predict air pollution metrics. The main modifications are:

- a) CO_2 inhibition of isoprene emissions
- b) CO_2 inhibition of stomatal conductance
- c) Increased NH_3 emissions in a warmer climate
- d) Inclusion of ammonium-nitrate evaporation effect
- e) Addition of stress-induced BVOC to the model
- f) Improved growing season estimates, sensitive to temperature change
- g) Technical improvements to allow different types of climate mode input

The new calculations with the 'climate-enhanced' EMEP model re-inforce the message of earlier ÉCLAIRE reports that emission changes are in general the key driver of future APMs. Although the use of for example a new photosynthesis module, or of CO_2 inhibition of isoprene emissions, modifies most air pollution metrics to a certain extent, the changes are small compared to that of simple emission changes. The most significant exception to this statement concerns metrics which are very sensitive to particular thresholds. For example Figure 2.4 shows calculations of phyto-toxic ozone dose (POD3), with threshold value 3 nmoles/m2/s (see Mills et al. 2011 for explanation), made with the EMEP model. The standard 2050 calculation has somewhat lower POD3 values than the base 2010 case. Accounting for possibly lower BVOC emissions due to CO_2 inhibition alters POD3 only a little. Accounting for the impact of CO_2 inhibition on stomatal conductance (using methods from Klingberg et al., 2011) results in significantly lower POD3 values. These calculations illustrate the uncertainty associated with some metrics, even while others (e.g. SOMO35, Figure 2.3) are rather robust.
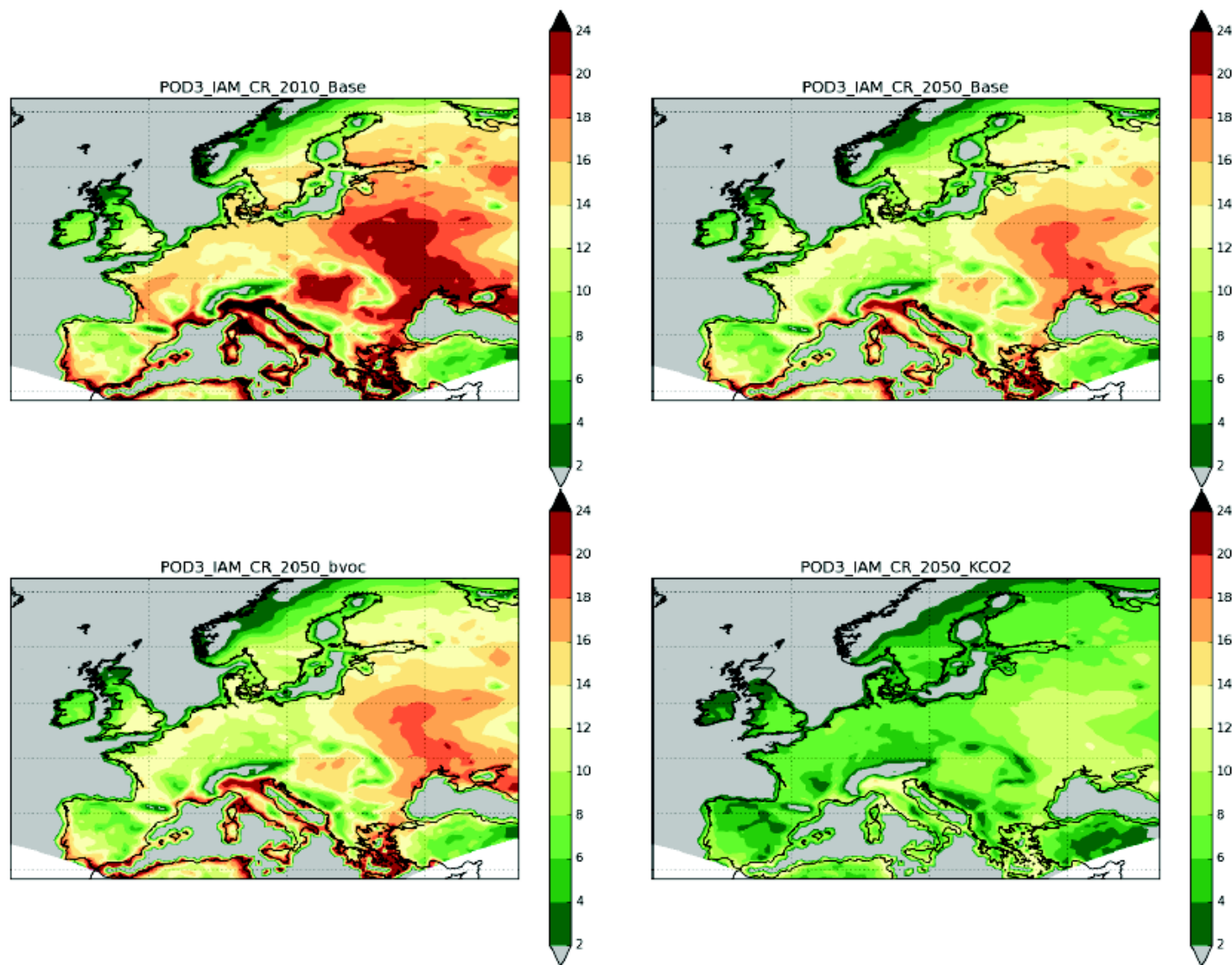
Figure 2.4: EMEP calculations of POD3 for (IAM) crops, for 2010 (top-left) and for three 2050 scenarios: 2050-Base (top right), 2050 with CO_2-inhibition on isoprene emissions (bottom left), and 2050 with CO_2-inhibition on stomatal conductance (Klingerg method). Units: mmole/m^2

Task 7.3: Assessing the importance of biogenic emissions and in-canopy chemistry on pollutant deposition at the European scale

The 1-D ESX was improved and used in a series of tests with one-way nesting to the EMEP model, in order to investigate the impact of biogenic emissions and in-canopy reactions and deposition on ozone and deposition fluxes. Figure 2.5 presents an example of a 1-month calculation for a site in Germany, and deliverable D7.3 presents results for a range of other sites across Europe.
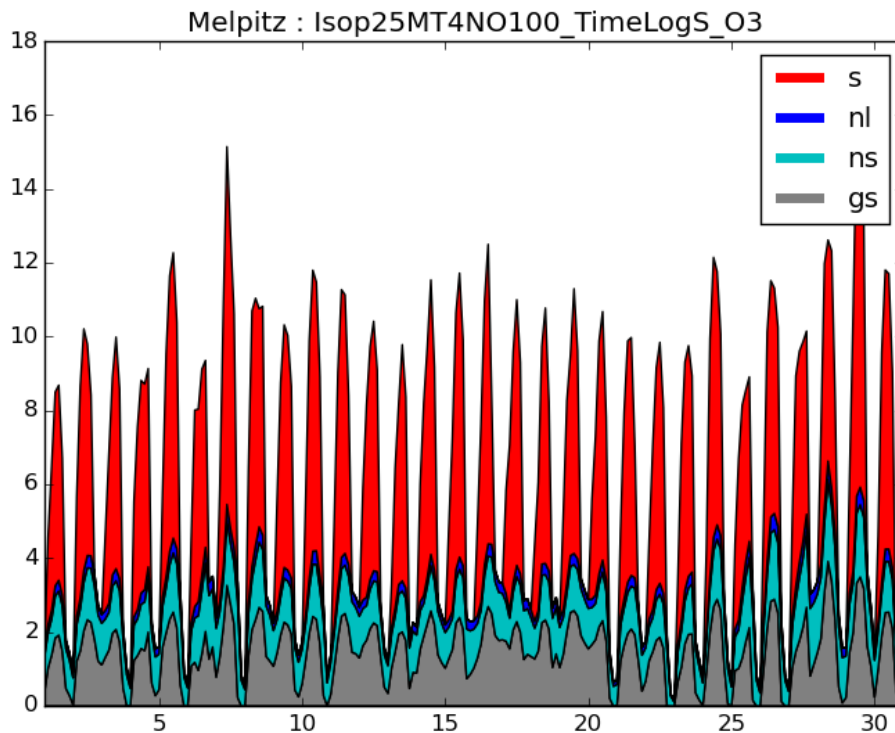
Figure 2.5: Deposition sinks of O_3 within a generic forest canopy located in Germany. Calculations with ESX model, driven by EMEP MSC-W boundary conditions for July 2012. Sink terms are: stomatal (s), non-leaf (nl), non-stomatal leaf (ns) and ground surface (gs). See Deliverable 7.3 for more details and examples where biogenic emissions are varied.

Task 7.4: Calculation of European fields and source-receptor matrices for deposition and pollution metrics/thresholds under future climate change.

Calculations of ozone and N-deposition for the year 2050 has been carried out with the EMEP using a range of climate effects (Figures. 2.3 & 2.4 have presented two examples, many more can be found in Deliverable D7.4). As noted above, the EMEP model has been enhanced so that it can take account of a number of changes which are expected in a future climate. Source-receptor (SR) calculations were then calculated for different climate experiments, considering the impacts of increased CO_2 on BVOC emissions and stomatal uptake, and of possibly increased NH_3 emissions. Deliverable D7.5 reports on how calculated SR results change when these climate enhancements are taken into account, and also compare with changes due to simple emission scenarios.

The main conclusion from these runs is that in most cases the impacts of climate change itself (e.g. CO_2 inhibition of isoprene emissions or stomatal conductance) do not change the basic SR estimates very much, and that the main driver of changes is rather the difference in emissions between the 2010 and 2050 cases. The main exception was for phyto-toxic ozone dose to crops (POD3-IAM-CR, cf Figure 2.4), where the assumptions concerning climate response of stomatal conductance had an appreciable impact on the base-levels of POD3 and on the responses to NO_x emission reduction.

Task 7.5: Ensemble calculation of maps of deposition and pollution metrics and analysis of uncertainty

- Reported in earlier periods (and deliverable D7.1).

WP8 Assessing local and regional variation

The aim of WP8 was to develop a better scientific understanding of the air pollution and climate change relationships at regional/local/landscape-scale and sub-grid approaches for inclusion in large-scale models that enable a good representation of the multitude of processes that play a role on smaller scales (e.g. landscape-scale). By doing this, large-scale concentration and deposition patterns will better represent the local-scale interactions and provide more relevant input, e.g., for European scenario studies that involve one or more of the affected parameters. In particular, the WP 1. synthesized the available knowledge on local interactions in relation to climate and air quality, as well as the way this knowledge is included in local-scale atmosphere-biosphere modelling systems; analysed the sensitivity of the landscape scale effects on changing pollutant fluxes, especially as affected by climate change; 3. included local/landscape-scale effects of climate change and air pollution interactions into large scale/European scale models by means of sub-grid representation of the most important processes.

Task 8.1: Synthesis of existing local-scale transport models with atmosphere-biosphere exchange

The literature study in Task 8.1 has been finalized in this reporting period, later than planned. While the activity (and the resulting literature study) is important for the overall understanding of air pollution / climate interactions the delay did not pose a large problem for the work in the other work packages.

The review focussed on the interaction between air quality and climate change, such as the role it plays in the plant-atmosphere interaction, and the way it is represented in large scale models. An overview was presented of different models that can be used, over different scales, to make predictions of air pollutant concentrations and deposition rates (now or in the future). The overall purpose of the review was to assess to what extent the models are capable of taking into account climate change.

Some important interactions that exist between air quality and climate change were identified as
- Increasing volatilization of ammonia with increasing temperature
- Local cooling effect with increasing aerosol concentrations in the air
- Ozone formed from NO_x/VOC emissions reducing plant productivity, which in turn reduces CO_2 uptake from the atmosphere
- Possibly increasing biogenic VOC emissions with increasing temperature

For accounting of these interactions in simulation experiments a range of models are available, ranging from models describing processes on a plant level to global scale models. Most of the models described in the review are capable of dealing with different atmospheric components, although some are targeted at one particular species (mostly ammonia). Ammonia has been singled-out for special treatment as a result of its high spatial variability, especially close to emission sources. In order to correctly assess the ecological impacts of ammonia (either as the result of elevated concentrations or its contribution to nitrogen deposition), atmospheric processes need to be modelled at a higher resolution than required for the assessment of particulate nitrogen deposition, for example. Most of the work that was presented has been collated from previous activities published in:
- Sutton M.A., Reis S. and S. Baker (eds) Atmospheric Ammonia – Detecting emission changes and environmental impacts (Springer, ISBN 978-1-4020-9120-9), 2009.
- Massad R. and Loubet B. (eds) Review and Integration of Biosphere-Atmosphere Modelling of Reactive Trace Gases and Volatile Aerosols (Springer, ISBN 978-94-017-7284-6), 2015.

Task 8.2: Improved scientific understanding of air quality and climate change relations at the landscape scale

For Task 8.2 the main activities were related to the on-going development of the NitroScape model and the simulations carried out using the EMEP4UK model. Since there was a need (by WP17) for small scale concentration/deposition maps, which were originally to have been produced by NitroScape, a contingency plan consisted of using concentration/deposition maps from existing models and previous projects (as described in previous WP reports). Since this contingency plan was adopted, the focus of the NitroScape development work has been the development and incorporation of new and existing component models (see MS35 report for more details).

Local scale interactions at spatial resolutions of 1×1, 5×5 and 50×50 km^2 were investigated by means of the EMEP4UK model and delivered to WP17. An example map is shown in Figure 2.6. The spatial distribution of the dry deposition of reduced nitrogen is highly dependent on the spatial distribution of ammonia emissions and, therefore, the model resolution. Although different, the total NL budget does not show a large difference between scales. The ammonia deposition velocity is relatively high and eventually most of the available ammonia (i.e. that not used to neutralise SO_4 or NO_3) is dry-deposited within the NL domain. The differences in the NL budgets may be the result of resolving the national borders at the different resolutions.
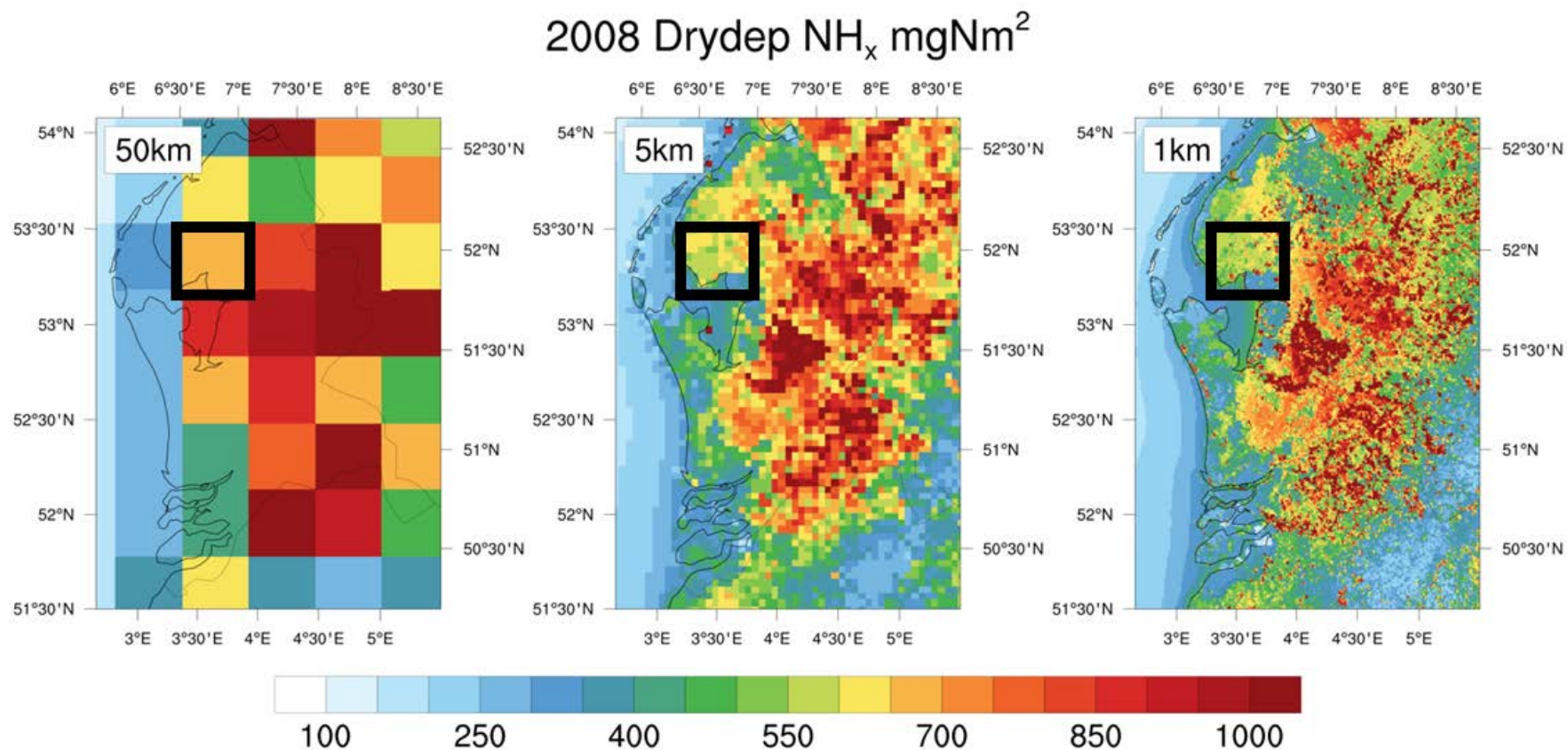
Figure 2.6: EMEP4UK modelled dry deposition for the Dutch domain. The black box shows an arbitrary 50 km × 50 km where the deposition is ~700 mg N m^{-2}. The ranges of deposition in the same 50 km × 50 km grid square are: ~250 – 750 mg N m^{-2} for the 5 km × 5 km resolution and ~250 - >850 mg N m^{-2} for the 1 km × 1km resolution.

Task 8.3: Development of sub-grid parameterisation/corrections for European scale CTMs

The task aimed to develop a parameterisation (module) that can simulate the sub-grid spatial distributions of mean annual concentrations and deposition rates of air pollutants (specifically ammonia, nitrogen dioxide and nitrogen deposition) within the grid cell of a chemical transport model (e.g. the EMEP MSC-W model) using high spatial resolution emission and land cover data. This included a simple parameterisation of short-range dispersion to estimate the spatial distribution (at a resolution of 1×1 km^2) of the concentrations of ammonia (NH_3) and nitrogen dioxide (NO_2) within the 50×50 km^2 (approx.) grid squares of the EMEP model. Pollutant dispersion from emission sources was parameterised using a simple scenario of a single 1×1 km^2 source with a constant emission of 1 tonne km^{-2} yr^{-1} in the centre of a square domain (of dimensions 101×101 km^2). Figure 2.7 shows the overall methodology for producing the sub-grid concentration predictions.

The resulting 'sub-grid distributions' provide an estimate of the spatial variability of the concentrations at a 1 km resolution, which were then used to 'redistribute' the 50×50 km^2 concentration predictions of the EMEP (MSC-W) model. This was done by interpolating the concentration predictions of the EMEP model and the mean concentrations of the sub-grid distribution within each 50×50 km^2 km grid square across the whole domain. The 'sub-grid predictions' were then calculated by multiplying the sub-grid distributions by the interpolated EMEP predictions and then dividing by the interpolated sub-grid distribution The sub-grid model predictions of NO_2 and NH_3 concentrations are shown in Figure 2.8.
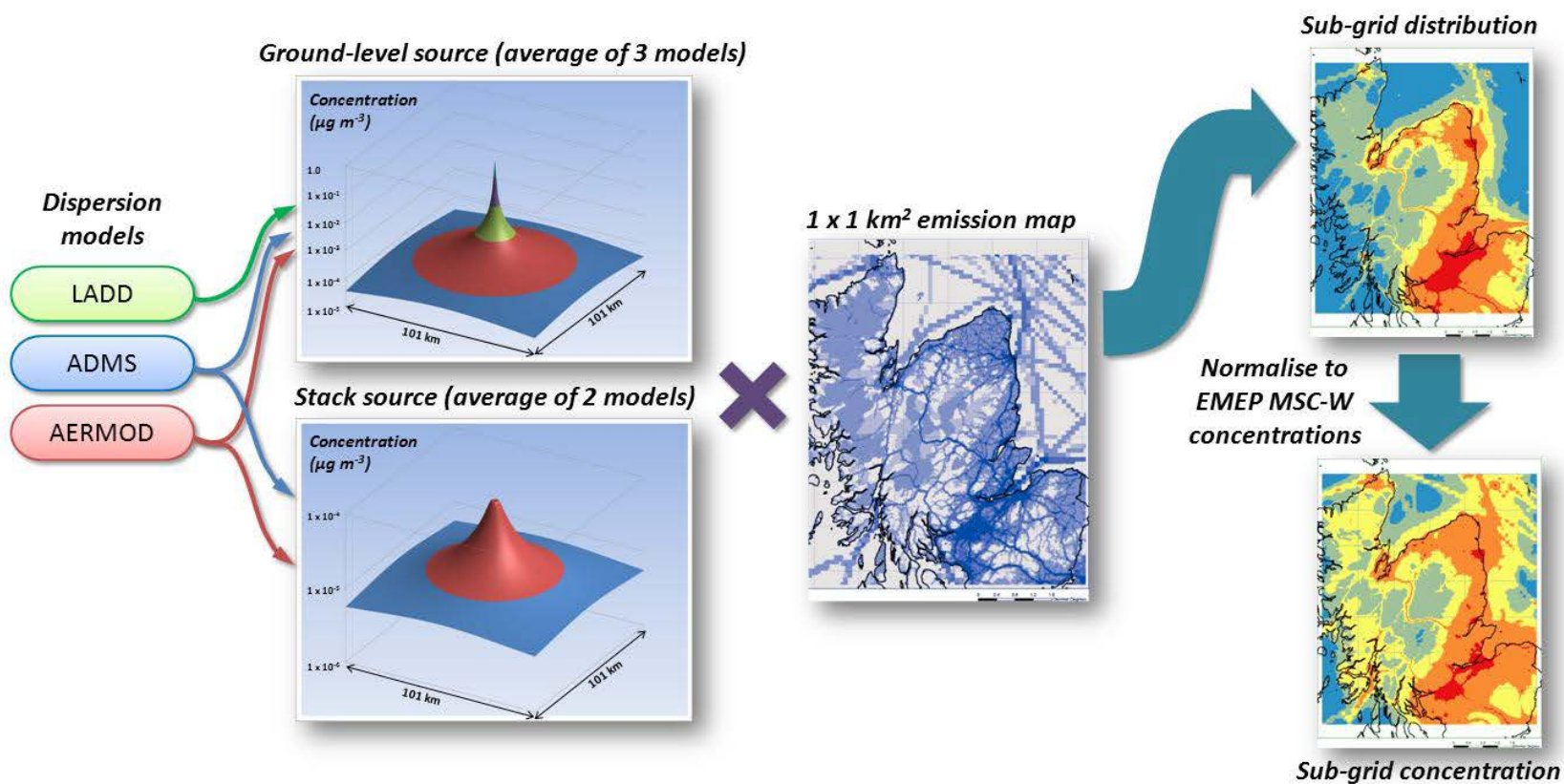
Figure 2.7: Schematic showing the process of producing the sub-grid concentration predictions from short-range dispersion model simulations and high spatial resolution emission data.
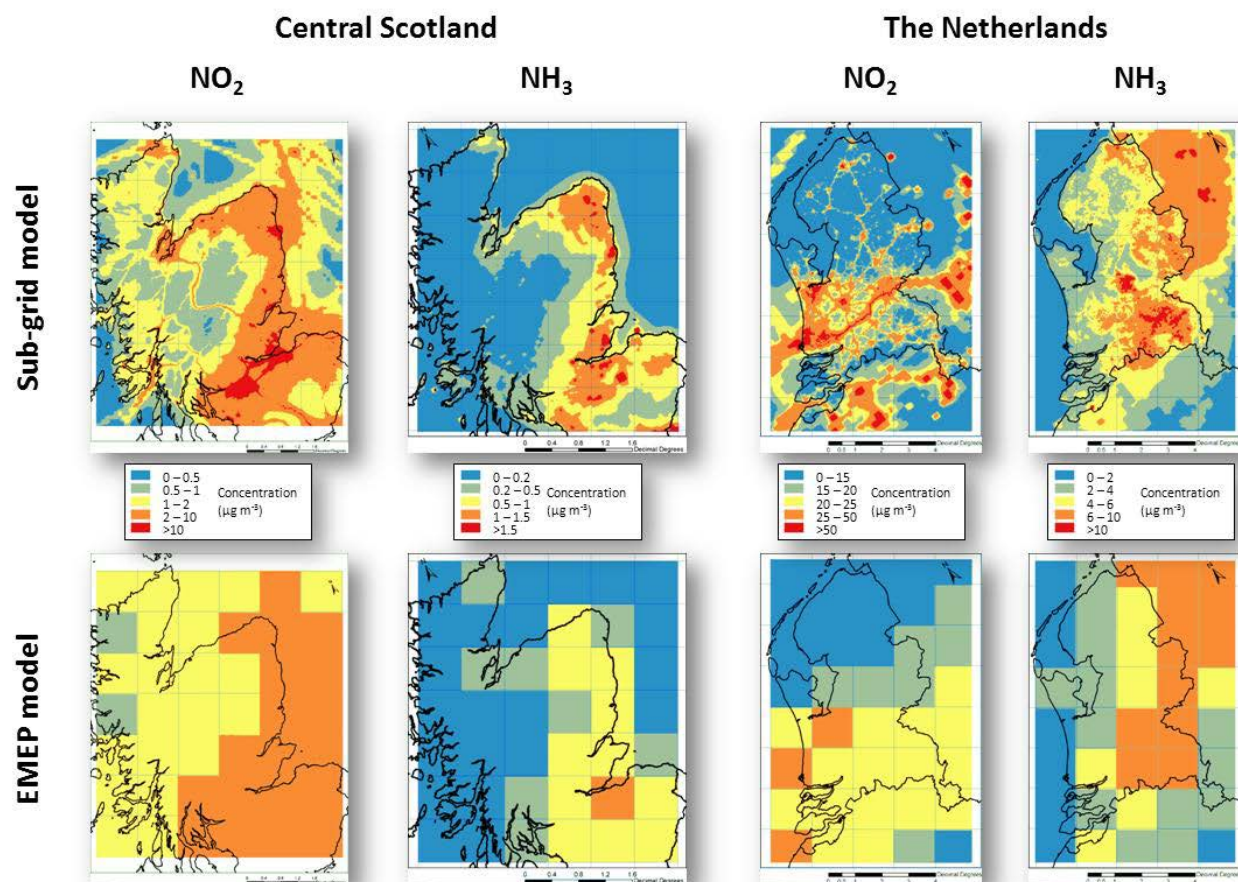
Figure 2.8: Sub-grid model predictions (top row) of mean annual concentrations of NO₂ and NH₃ for the two domains (Central Scotland and The Netherlands). EMEP model predictions at a resolution of 50x50km² are shown for comparison (bottom row).

ÉCLAIRE Third Periodic Report: November 2015

A comparison of the modelled (sub-grid) concentrations with measured values shows that the modelled values compare reasonably with the measured values.

Separate sub-grid parameterisations were also developed for three of the four components of nitrogen deposition (wet oxidised, wet reduced and dry reduced). It was not possible to develop a simple parameterisation for dry deposition of oxidised nitrogen due to the contributions from multiple compounds, each affected by different transport and transformation processes. Dry deposition of reduced nitrogen is mainly the dry deposition of NH_3 and therefore the sub-grid distribution of NH_3 can be used for the sub-grid distribution of the dry deposition of reduced nitrogen. The proxy used to estimate the sub-grid variability of wet deposition was the product of high spatial resolution annual precipitation data and the atmospheric concentrations of nitrate and ammonium (from the EMEP model), for deposition of oxidised and reduced nitrogen, respectively. Sub-grid total nitrogen deposition is calculated as the sum of the total wet deposition and the dry deposition of reduced nitrogen simulated by the sub-grid model plus the EMEP model estimate of dry deposition of oxidised nitrogen. Overall both the EMEP and the sub-grid model underestimate wet deposition of oxidised and reduced nitrogen by an average of 50%. There is very little difference between the predictions of the models for the Netherlands as a result of low spatial variability of the precipitation.

With respect to the development of a sub-grid module, these overall conclusions could be drawn at the end of the project:

- The sub-grid model for nitrogen deposition uses the high resolution NH_3 concentration data to simulate the spatial distribution of dry deposition of reduced nitrogen. The spatial distributions of wet deposition of both reduced and oxidises nitrogen are based on the spatial distributions of high resolution precipitation maps. It has not been possible to develop a sub-grid model for the dry deposition of oxidised nitrogen

- Both sub-models have been applied to two contrasting areas (Central Scotland and the Netherlands) and model performance of both the EMEP model and the sub-grid model has been assessed using monitoring data of atmospheric concentrations and wet deposition for both study areas

- The sub-grid model for atmospheric concentrations represents a substantial improvement on the predictions of the EMEP model reducing both model error and increasing the spatial correlation with the measured concentrations

- The performance of the sub-grid model for wet deposition, however, is similar to that of the EMEP model and provides only a small improvement on the deposition predictions.

Progress towards the milestones and deliverables, use of resources and deviations from DoW

D5.1 Assessment of Current GCMs and CTMS to reproduce recent trends by comparing models and observations

D5.2 Report describing the range of future evolutions of global, hemispheric and European ozone, ozone precursors using a range of anthropogenic and natural emissions

D5.3 Report describing the contribution of Regions and processes on key-environmental variables under future conditions.

D5.4 Boundary conditions for regional conditions

MS23 Evaluation of AR5 and other simulations with climate and other global models

MS24 Future simulations with improved biogenic and soil emissions

D5.1, D5.2, D5.3 and D5.4 have been delivered, with some delays earlier in the project related to a change in computing platforms. Milestones MS23; MS24 have been reached.

MS 33: Inventory of relevant local scale models
   The inventory of different relevant local scale models used in Europe has been completed.

D7.1 Maps of current air pollution metrics (APMs) across Europe, from the EMEP model and five other CTMs

D7.2 Improved EMEP model with climate-change and canopy-chemistry capabilities.

D7.3 Report on effects of in-canopy BVOC and NO emissions on in-canopy O_3 and POD estimates.

D7.4 Report on effects of changes in global climate, chemistry, emissions and landcover changes on APMs.

D7.5 Source-receptor matrices of APMs for current and future conditions.

MS28 Implementation and initial testing of coupled model system.

MS29 Initial ensemble runs for current conditions.

MS30 Incorporation of sub-grid methodology from WP4 into EMEP model (M30)

MS31 Future scenario data-sets ready

MS32 "Final" model-system ready. Commencement of source-receptor calculations.

D7.1, D7.2, D7.3, D7.4 and D7.5 have been delivered, with some delays arising from efforts towards the ESX model development. Milestones MS28, MS29, MS30, MS31 have been reached.

MS 34: Report on local scale models inventory
   This literature study has been completed and submitted as D8.1 (combined with D8.2)

MS 35: update of NitroScape to reflect ÉCLAIRE needs

ÉCLAIRE Third Periodic Report: November 2015

- The achievement of this MS has been seriously delayed and although   major updates to NitroScape have been made they did not come t ogether as a useable final product within the timescale of the project.   Some   contingency   plans   were introduced (e.g. use of alternative high   resolution   model   data   in   WP17)   as   an alternative strategy in order to deliver the needed results for the project..

MS 36: Concentration/Deposition maps
These concentration/deposition maps have been finalised and   delivered   to WP17 for further processing. The work (and resulting maps) are described in D8.2 and D8.3/D17.2.

MS 37: Description of local scale interactions between air quality and climate change (finalised and submitted as D8.1.)
MS 38: Sub-grid module available for implementation in EMEP model
Finalised and submitted as D8.4.

D8.1: Synthesis report on the different local scale models dealing with atmosphere-biosphere exchange

D8.2: Report on local scale interactions between air quality and climate change (Month 30)

D8.3: Concentration and deposition maps (Month 16)

D8.4: Sub-Grid module for inclusion in the EMEP model (Month 30)

Deliverables D8.1, D8.2, D8.3 and D8.4 have been finalized and submitted to the ÉCLAIRE deliverables database.

The main deviation from the ÉCLAIRE Description of Work was related to the NitroScape work in WP8. This work didn't result in a useable product, and since results were needed for WP17, a contingency plan of using concentration/deposition maps from existing models and previous projects. Eventually, this worked out fine and all activities in WP17 could be completed using these alternative datasets.

Publications, posters and other dissemination activities (2014-2015)

Bergström, R.; Hallquist, M.; Simpson, D.; Wildt, J. & Mentel, T. F., Biotic stress: a significant contributor to organic aerosol in Europe? *Atmospheric Chemistry and Physics,* **2014***, 14*, 13643-13660

Begstrröm, R., Cabonaceous Aerosol in Europe, Out of the woods and into the blue? PhD Thesis, Univ. Gothenburg, Sweden, Sept. 2015

Engardt, M., Simpson, D. and Granat, L., Historical and projected (1900 to 2050) deposition of sulphur and nitrogen in Europe, in prep.

Leip, A.; Billen, G.; Garnier, J.; Grizzetti, B.; Lassaletta, L.; Reis, S.; Simpson, D.; Sutton, M. A.; de Vries, W.; Weiss, F. & Westhoek, H. Impacts of European livestock production: nitrogen, sulphur, phosphorus and greenhouse gas emissions, land-use, water eutrophication and biodiversity, Environ. Res. Lett., 2015, 10, 115004

Messina P., Lathière J., Sindelarova K., Vuichard N., Granier C., Ghattas J., Cozic A, Hauglustaine D., "Investigating BVOC emission estimate discrepancies using the ORCHIDEE new emissions scheme and MEGAN model", in prep.

Messina P., Lathière J., Sindelarova K., Hauglustaine D., Vuichard N., Viovy N., Szopa S., Cozic A, Ghattas J., "Biogenic volatile organic compound emissions in ORCHIDEE: future evolution and impact on atmospheric composition", talk at ÉCLAIRE Open Science Conference: Integrating Impacts of Air Pollution and Climate Change on Ecosystems, 1 - 2 October 2014, Budapest, Hungary. 2014.

Messina P., Lathière J., Hauglustaine D., Sindelarova K., Vuichard N., Viovy N., Szopa S., Ghattas J., Cozic A, Zannoni N., Gros V., "Impact of future biogenic volatile organic compound emissions on atmospheric composition", poster at 13th Quadrennial iCACGP Symposium/13th IGAC Science Conference, 22-26 September 2014 Natal, Brazil. 2014.

Sindelarova K., Granier C., Messina P., Lathière J., Guenther A., "Modeling sensitivity of biogenic VOC emissions to environmental factors", poster at The third Chemistry-Climate Model Initiative (CCMI) Workshop, 20-22 May 2014, Lancaster, United Kingdom. 2014.

Messina P., Lathière J., Sindelarova K., Hauglustaine D., Vuichard N., Viovy N., Szopa S., Ghattas J., Cozic A, "Analysing and comparing the inter-annual variability of biogenic volatile organic compound emissions with ORCHIDEE and MEGAN: Impact of leaf area index", poster at Biogenic Hydrocarbons & the Atmosphere - Interactions in a Changing World, Spain, June 29 - July 4 2014, Girona. 2014.

Pleijel, H.; Danielsson, H.; Simpson, D. & Mills, G. Have ozone effects on carbon sequestration been overestimated? A new biomass response function for wheat, *Biogeosciences,* **2014***, 11*, 4521-4528

Schaap, M.; Cuvelier, C.; Hendriks, C.; Bessagnet, B.; Baldasano, J.; Colette, A.; Thunis, P.; Karam, D.; Fagerli, H.; Graff, A.; Kranenburg, R.; Nyiri, A.; Pay, M.; Rouil, L.; Schulz, M.; Simpspn, D.; Stern, R.; Terrenoire, E. & Wind, P. Performance of European chemistry transport models as function of horizontal resolution *Atmospheric Environment ,* **2015***, 112*, 90 - 105

Simpson, D.; Christensen, J.; Engardt, M.; Geels, C.; Nyiri, A.; Soares, J.; Sofiev, M.; Wind, P. & Langner, J., Impacts of climate and emission changes on nitrogen deposition in Europe: a multi-model study, *Atmos. Chem. Physics,* **2014***, 14*, 6995-7017

Simpson, D.; Arneth, A.; Mills, G.; Solberg, S. & Uddling, J. Ozone - the persistent menace; interactions with the N cycle and climate change *Current Op. Environ. Sust.*, **2014,** 9-10, 9-19

Werner, M., Kryza, M., Geels, C., Ellermann, T., and Ambelas Skjøth, C.: Spatial, temporal and vertical distribution of ammonia concentrations over europe – comparing a static and dynamic approach with wrf-chem, Atmos. Chem. Phys. Discuss., 15, 22935-22973, 10.5194/acpd-15-22935-2015, 2015.

Work Package 5: Past and future changes of atmospheric pollutants transported into Europe

Lead contractor: JRC
Contributors: Met.no, CNRS, ULUND

Work package objectives
1. To assess our current understanding of ozone and other air pollution trends, based on knowledge acquired within the UNECE TF HTAP, work for IPCC-AR5 and other projects, with a focus on the inflow regions of Europe.

2. To evaluate the transport of atmospheric pollutants (ozone and precursors, aerosols) into Europe, evaluate the relative contributions of long-range-transported and European pollution on atmospheric composition and deposition to the ecosystems in Europe and in other regions, and provide a range of chemical boundary conditions to regional models within ÉCLAIRE (WP7), taking into account changes in global anthropogenic and natural emissions under current and future climate change conditions.

3. To examine the relative contributions and impacts on air pollution of future biogenic and soil and fire emissions produced in WP15 of ozone and aerosol precursors on European pollutants levels and their export to the hemispheric and large scale atmosphere.

Progress and Results

Task 5.1

Task 5.1 objective: To assess our current understanding of ozone and other air pollution trends, based on knowledge acquired within the UNECE TF HTAP, work for IPCC-AR5 and other projects, with a focus on the inflow regions of Europe.
Task 5.1 was delivered 20/12/2013, and no additional analysis has been made since then.

Key-findings:

• Emission trends of global and regional NO_x are qualitatively in agreement with satellite observations with declines in NO_2 in North America and Europe in the order of 20-30 % for 1996-2011. There is good qualitative knowledge on decreases of precursor gases CO and NMVOC in Europe and the US.

• Deposition trends in Europe are reasonably well understood by global and regional models, transport of reactive nitrogen from outside Europe may contribute by 5-10% to deposition in Europe.

ÉCLAIRE Third Periodic Report: November 2015

• Trend of inflow of ozone at Europe's boundary is only partly understood: attribution of changes typically can explain up to half the observed changes. Possible explanations include important roles of decadal scale variability, and possibly missing information on long-range transport of anthropogenic pollution. Scaling of regional boundary conditions with observations at Mace Head provides an accurate assessment of Europe-wide changes, but may be problematic for future conditions.

Task 5.2

Task 5.2 objective: Selected scenarios of future emissions provided by IPCC AR5 RCPs, and possibly other scenarios, will be used to evaluate the possible global, hemispheric and European evolution of ozone and other air pollutants for 2030, 2050 and 2100. LMDz-INCA- ORCHIDEE will be used to simulate the future impact of biogenic and soil emissions of ozone and aerosol precursors on future levels of pollutants, especially O_3 and reactive N-compounds.

Task 5.2 has been delivered in July 2015. To this end CNRS made major upgrades to their model and performed extensive simulations of a variety of RCP scenarios.
JRC performed TM5 FASST analysis of emission scenarios, and –through the CLRTAP Task Force Hemispheric Transport of Air Pollution (TF HTAP) organized and analysed future air pollution scenarios.

Key findings:

• A detailed description of ammonium sulfate-nitrate and coarse-aerosol nitrate formation was included in LMDz-INCA model. Good agreement of surface aerosol concentrations and aerosol optical depth was found for Europe and North America. Nitrogen and sulfur deposition were in reasonable agreement in Europe and North America, but systemically underestimated in Eastern Asia.
• Model calculations suggest under the RCP scenarios SO_4 burden is strongly declining, while nitrate and ammonium aerosol burdens are more constant. Agricultural emission of NH_3 may therefore maintain higher levels of cooling than assumed in previous studies. The fraction of ammonium in nitrogen deposition is increasing from about 60-80 % in China. These results are driven by increasing agricultural ammonia emissions in the RCP emission scenario, subject to high uncertainty.
• Comparison of the summer ozone distributions between 2050 and 2010 using the ECLIPSE5.0 emission scenario indicates ozone decreases by up to 7 ppbv in Northern America and by 4-5 ppb in Europe. In China, SE Asia, and India, ozone increases by up to 7 ppb due to increased anthropogenic emissions in these regions. Climate and land use change by 2050 may augment isoprene emission and lead to ozone increases in large portions of the Northern Hemisphere up to 4,5 ppb, potentially off-setting the ozone reductions by anthropogenic emissions in Europe and North America. However, when

including the effect of increasing CO_2 on reducing the isoprene emissions, the effect on ozone is much less, with two current parameterizations strongly disagreeing.

• Controlling methane and air pollution emissions in Asia is going to be of critical importance for ozone air quality in Europe.

Task 5.3

Task 5.3 Objectives: to analyze the evolution of key environmental variables impacting ecosystems (ozone levels, PM levels, N and S deposition) under the various emission and climate scenarios and isolate the role played by long-range transport of pollution, climate change and changing variability, biogenic/emissions, lightning emissions, and anthropogenic emissions in Europe and other regions.

Task 5.3 results were delivered in February 2015, activities in the reporting period included simulations and analysis by the CNRS/LSCE group on the global vegetation model ORCHIDEE, and an evaluation of wildfire emissions by the ULUND using the LPJ guess model.

Key findings:

• In Europe, comparison of biogenic VOC emissions calculated with the widely used MEGAN emission model and the vegetation model ORCHIDEE, showed 19% higher isoprene emissions, 21% higher methanol and 21% lower monoterpene emissions by the latter. Assumptions on leaf-temperature for shaded and sunlit leaves versus air temperature play an important role in explaining these differences. Assumptions on leaf-area-index (LAI) also are a major uncertainty, with a complex impact on emission variability.

• Globally, comparing the 2040s and the 1990s, Orchidee calculations indicate 25% increase in isoprene, 27% in monoterpenes and 28% in methanol emissions. However, isoprene emission potential may decrease caused by higher levels of CO_2, resulting in complete off-setting of isoprene emissions.

• LPJ-GUESS calculations of BVOC emission in Europe indicate a decline of isoprene and monoterpene emissions by about a factor of 3 comparing the landcover in 2000s to the potential natural vegetation. Simulations are highly sensitive to biases in climate models- leading to ca. 65 % and 20 % lower emissions for isoprene and monoterpene emissions compared to using bias-corrected emissions.

• LPJ-GUESS calculations of BVOC global emissions the RCP4.5 GHG scenario, indicate isoprene emissions increase 41% and monoterpenes 25% in the future compared to current conditions. However, taking the CO_2 inhibition effect into account, emissions decrease slightly with -2% and -13% respectively for isoprene and monoterpenes. Climate change favors isoprene emitting vegetation.

• LPJ-GUESS calculations of wildfire emissions indicate a complex range of interactions between vegetation, climate change and increasing CO_2, and fire

suppression. Comparing 1970-2000 and 2070-2100, overall tropical emissions decline between 15 and 35 % (mostly due human influence), while extratropical emissions increase by 20 % and 45 %. Globally emissions change within a -10 % range.

• While nitrogen input to ecosystems affects yields and can lead to pollution of water sheds in heavily fertilised regions, effects of N deposition on natural ecosystems regarding the historical carbon sink strength are minor. Whether or not nitrogen limitation of plant growth will notably affect future ecosystem carbon storage is under debate, and current modelling studies show conflicting results. Arguably, climate effects of N_2O emissions are of more concern than N-interactions with the C sink; this will be investigated further in the coming years with updated versions of LPJ-GUESS.

Task 5.4

Task 5.4 Objective: To evaluate the transport of atmospheric pollutants (ozone and precursors, aerosols) into Europe, evaluate the relative contributions of long-range-transported and European pollution on atmospheric composition and deposition to the ecosystems in Europe and in other regions, and provide a range of chemical boundary conditions to regional models within ÉCLAIRE (WP7), taking into account changes in global anthropogenic and natural emissions under current and future climate change conditions.

Task 5.4 results were delivered in January 2014, and since then no updates were made.

Key-findings:

This task provides a best estimate and uncertainty range of present and future O_3, O_3 precursors and aerosol as boundary conditions to regional models, for further impact assessment on ecosystems. We report on two ÉCLAIRE activities: simulations with the global LMDz-INCA model constrained by ÉCLAIRE/ECLIPSE (version number) emission inventories for the period 2010, 2030 and 2050; and ensemble modelling work in the Task Force Hemispheric Transport and EMEP on the evaluation of future emission scenarios. Scenario analysis has focused on the evaluation of the widely used IPCC AR5 RCP scenarios for TH HTAP and ÉCLAIRE/ECLIPSE emission inventories for boundary condition files. Deliverable 5.4 has provideeds the description of the NetCDF files prepared with the LMDz-INCA global model for use by the regional models for the present-day, 2030 and 2030 conditions and for the ÉCLAIRE/ECLIPSE emission scenarios (available via www.eccad.fr), corresponding to both the Current Legislation and Maximum Feasible Reduction conditions.

Progress towards the milestones and deliverables
D5.1 Assessment of Current GCMs and CTMS to reproduce recent trends by comparing models and observations

D5.2 Report describing the range of future evolutions of global, hemispheric and European ozone, ozone precursors using a range of anthropogenic and natural emissions

D5.3 Report describing the contribution of Regions and processes on key-environmental variables under future conditions.

D5.4 Boundary conditions for regional conditions

MS23 Evaluation of AR5 and other simulations with climate and other global models

MS24 Future simulations with improved biogenic and soil emissions

D5.1, D5.2, D5.3 and D5.4 have been delivered. With some delays earlier in the project related to a change in computing platforms. Milestones MS23; MS24 have been reached.

Use of resources and deviations from DoW

Apart from some minor delays as noted above, the work was broadly conducted as planned. A total of 11.6 person months were used in this period.

Work package 6 – Emissions on regional, European, to global scale

Lead contractor: ULUND/KIT
Contributors: NERC, ALTERRA, KIT, CNRS, UEDIN, AU

Work package objectives
The objectives of WP6 are to:
1. quantify how trace gas emissions from natural, semi-natural and agricultural ecosystems vary in response to interactions of weather and climate, atmospheric CO_2 burden and N deposition, vegetation and soil carbon and nitrogen dynamics, and land use/land cover change;
2. provide improved temporal dis-aggregation of non-ecosystem, anthropogenic European pollutant emission patterns for selected source sectors.

Progress and Results

There were no deliverables due in this work package during this reporting period, all deliverables were completed in the last reporting period.

Progress towards the milestones and deliverables

As noted, all deliverables and milestones for this work package have already been achieved.

Use of resources and deviations from DoW
This period focused on utilizing the results generated earlier in the project, however two students were also working on items related to this work package, during this period. This means that the person months used is actually 21, as opposed to the originally budgeted 6 months for this period.

Work package 7 – Modelling European air pollution and deposition

Lead contractor: met.no
Contributors: ULUND, met.no, Juelich, JRC, CNRS, SMHI, WU, TNO

Work package objectives

The objectives of this WP are to provide maps of O_3-damage metrics and N-deposition over Europe, for current and future scenarios, as inputs to the ecological response and effects packages (C3 and C4) and to integrated assessment modelling (C5). Activities range from global to local scale. In brief, the main aims are:

1. To map current air pollution metrics (APMs, mainly ozone damage indicators, POD & AOTx, and N-deposition) using a small ensemble of CTMs, in order to provide a best-estimate and uncertainty range on vegetation effects metrics.

2. To implement on the European scale new modules for stomatal uptake, in-canopy-chemistry, and emissions and sub-grid effects into the EMEP chemical transport model, able to take account of changes in CO_2, N deposition, BVOC emissions and climate over coming decades.

3. To estimate changes in APMs to specific ecosystems up to year 2030 and 2050, accounting for climate-changed induced changes in meteorology, vegetation, and biosphere-atmosphere exchange processes.

Progress and Results

Task 7.1 Implementation of advanced exchange models into European CTMs

In cooperation with WP4, development work has continued with the ÉCLAIRE Ecosytem Surface Exchange (ESX) model, which combines chemistry from the EMEP code with in-canopy emission, dispersion and deposition processes in a 1-D model. During this reporting period the ESX model code and theoretical basis has been substantially improved, and a photosynthesis-based algorithm implemented. The ESX model was set up as an offline model, driven by a combination of EMEP and observed data, and was used to investigate the effects of foliar BVOC and soil NO and NH_3 emissions on near-surface concentrations and deposition velocities.

The photosynthesis module from DO3SE has also been implemented in the EMEP model, and used to study concentrations and depositions in 2010 and 2050 (See Deliverable D7.2). Figure 2.9 gives an example showing calculations of the health metric SOMO35 in both years, with both the standard and new photosynthetic procedures to calculate stomatal conductance.
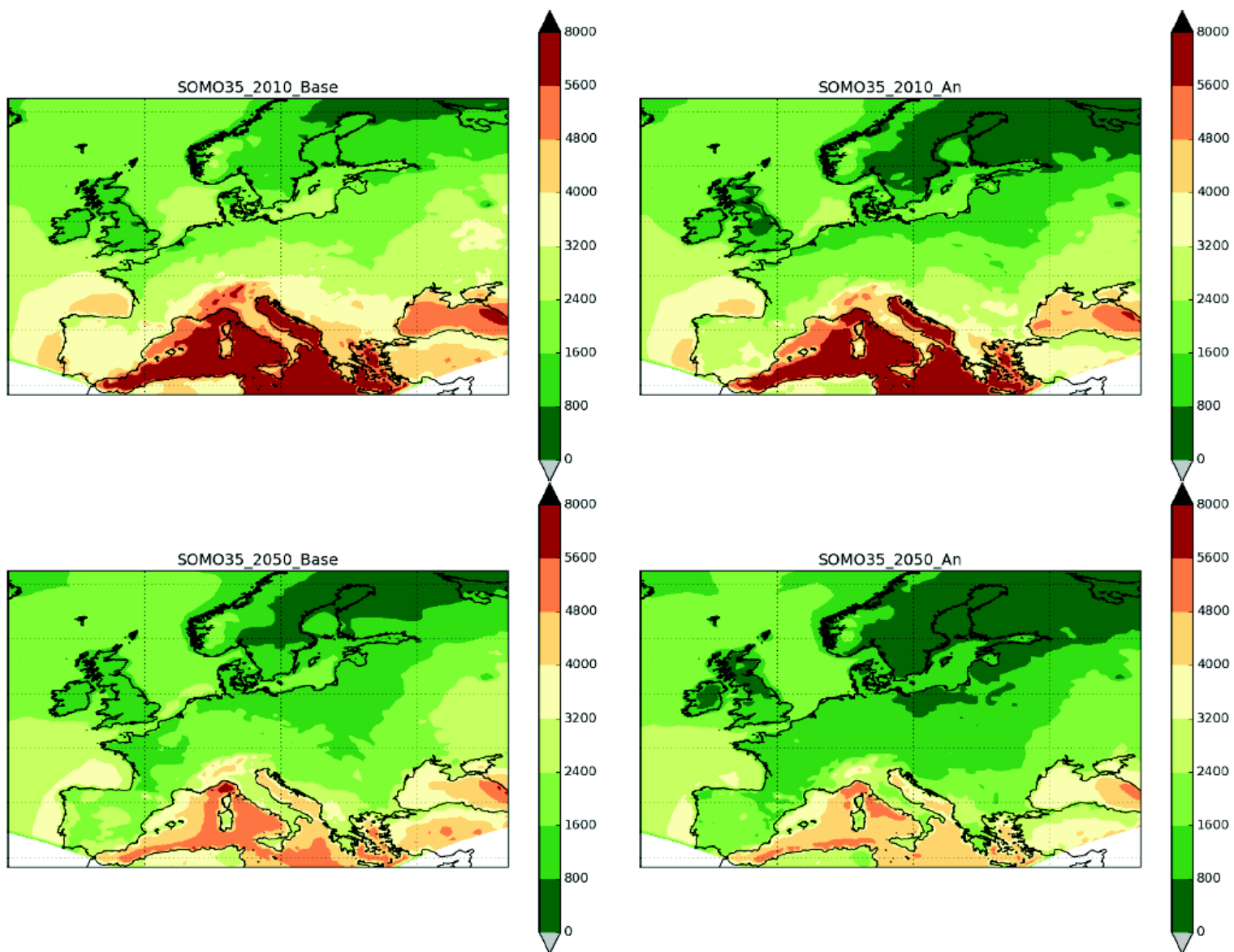
Figure 2.9: EMEP MSC-W calculations of SOMO35 for 2010 (top) and 2050 (bottom). Left column gives results with standard EMEP gsto, right column with photosynthesis-based An-g$_{sto}$ (labelled An). Units: ppb.day.

Task 7.2: Scenario calculation of climate effects for assessment of air pollution transport and deposition

Much of the work towards this task was completed and reportted on in previous reports, and has been published in peer-reviewed journals in the final period. In particular, calculations for 2010 and 2050 from an ensemble of CTMs have been presented in Simpson et al. (2014) (and earlier in Langner et al., 2012). In Simpson et al., an ensemble of four CTMs (EMEP MSC-W, MATCH, DEHM, and SILAM) was used to examine the effects of emissions and climate change on N-deposition fields across Europe up to 2050. The MATCH model was further used to investigate the sensitivity of such results to meteorological driver (Engardt and Langner, 2013).

The main conclusion of the first European climate/chemistry/deposition studies was that with current emission projections the main driver of future N_r deposition or ozone changes would be the specified emission changes by 2050.

Over the period Oct. 2014 to Sep. 2015 remaining activity has focused on model development. In this work, the EMEP chemical transport model (CTM) has been modified in order to take account of physical/chemical changes expected in the future, so that it is better able to predict air pollution metrics. The main modifications are:

a) CO_2 inhibition of isoprene emissions
b) CO_2 inhibition of stomatal conductance
c) Increased NH_3 emissions in a warmer climate
d) Inclusion of ammonium-nitrate evaporation effect
e) Addition of stress-induced BVOC to the model
f) Improved growing season estimates, sensitive to temperature change
g) Technical improvements to allow different types of climate mode input
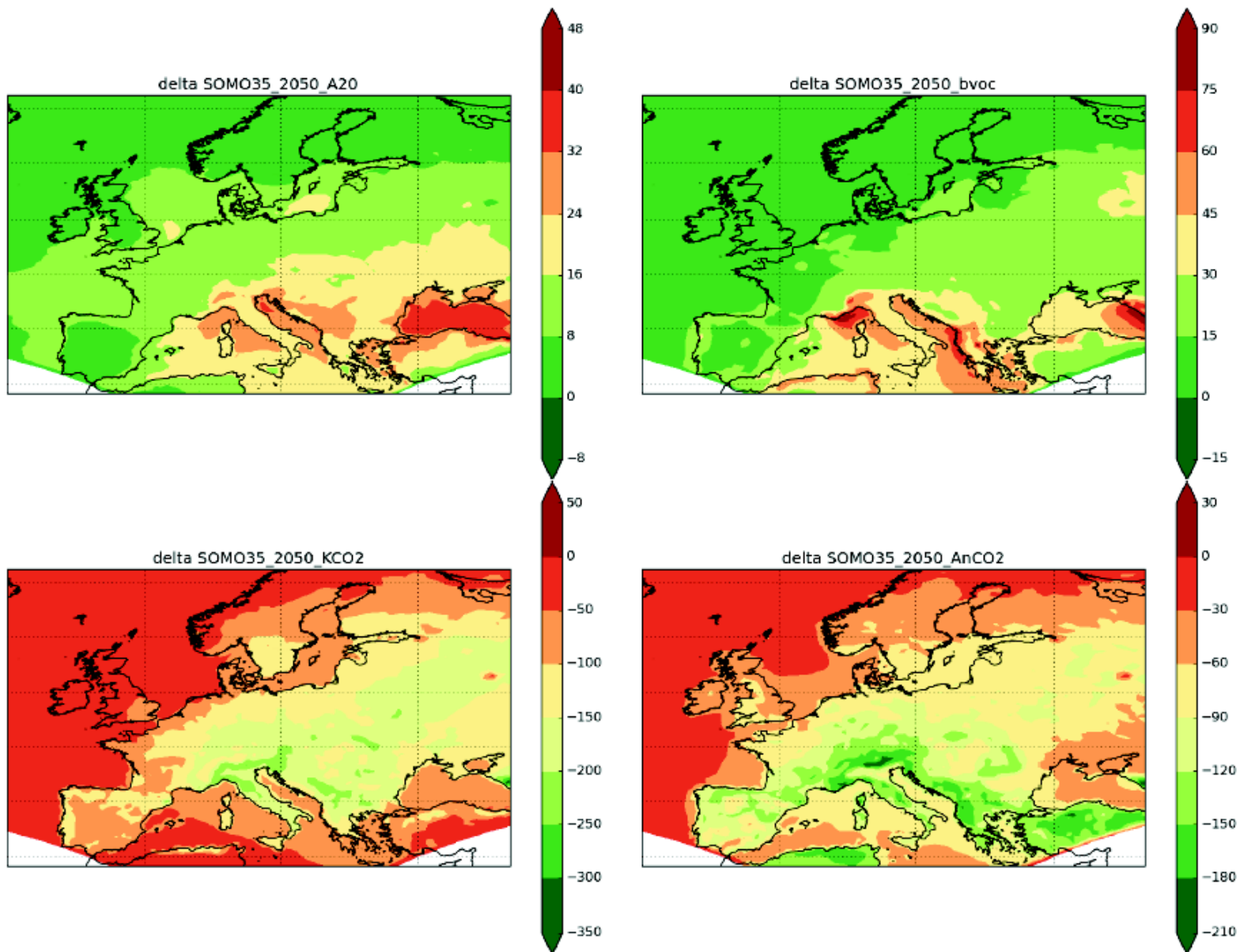
Figure 2.10: Differences between SOMO35 in 2050 between climate-test cases and base-calculation of Figure 2.9 Cases (a-c) should be compared to the standard EMEP run for 2050, and case (d) against the A_n-g_{sto} EMEP run for 2050. Test-cases are (a,top-left) Increased NH_3 emissions, (b, top-right) CO_2 -inhibition on isoprene emissions(top-right), (c, bottom-left) CO_2-inhibition on stomatal conductance, Klingerg method (d, bottom-right) CO_2 -inhibition on stomatal conductance, DO3SE-Photosynthesis method. Note - plots have different colour-scales. Same units as Figure 2.9.

The new calculations with the 'climate-enhanced' EMEP model reinforce the message of earlier ÉCLAIRE reports that emission changes are in general the key driver of future APMs. Although the use of for example a new photosynthesis module, or of CO_2 inhibition of isoprene emissions, modifies most air pollution metrics to a certain extent, the changes are small compared to that of simple emission changes (Figure 2.10). The most significant exception to this statement concerns metrics which are very sensitive to particular thresholds. For example Figure 2.11 shows calculations of phyto-toxic ozone dose (POD3), with threshold value 3 nmoles/m^2/s (see Mills et al. 2011 for explanation), made with the EMEP model. The standard 2050 calculation has somewhat lower POD3 values than the base 2010 case. Accounting for possibly lower BVOC emissions due to CO_2 inhibition alters POD3 only a little. Accounting for the impact of CO_2 inhibition on stomatal conductance (using methods from Klingberg et al., 2011) results in significantly lower POD3 values. These calculations illustrate the uncertainty associated with some metrics, even while others (e.g. SOMO35, Figure 2.11) are rather robust.
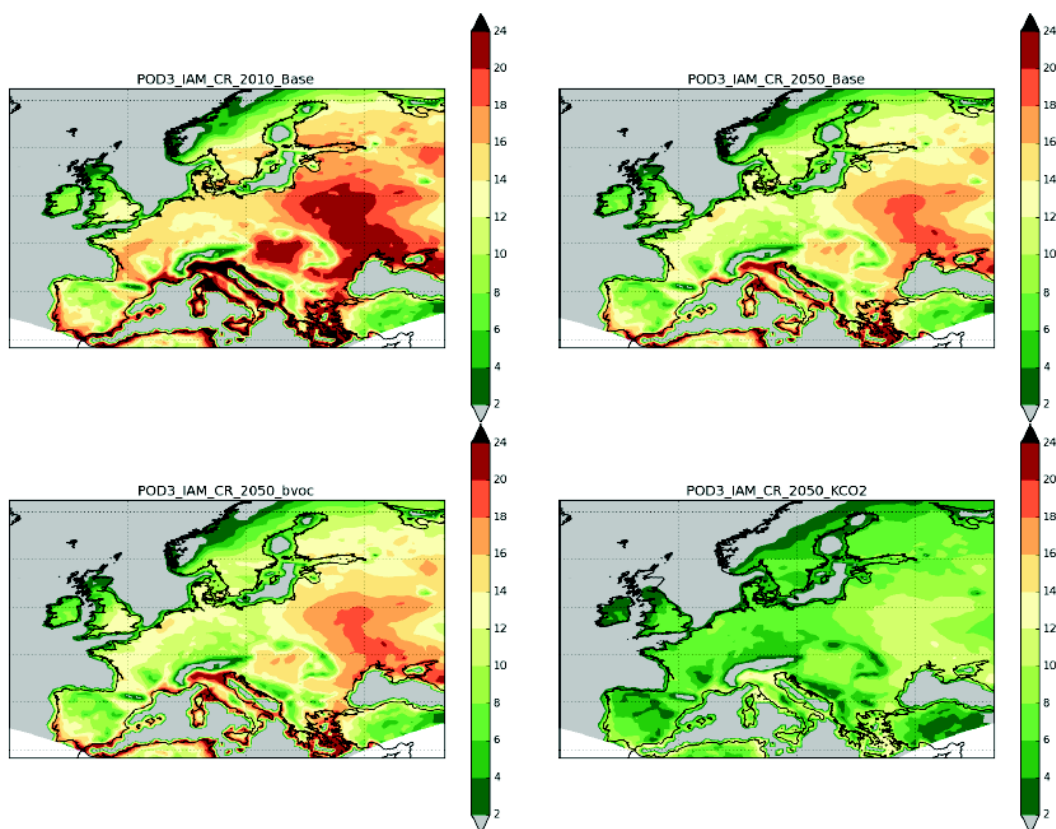
Figure 2.11: EMEP calculations of POD3 for (IAM) crops, for 2010 (top-left) and for three 2050 scenarios: 2050-Base (top right), 2050 with CO_2-inhibition on isoprene emissions (bottom left), and 2050 with CO_2-inhibition on stomatal conductance (Klingberg method). Units: mmole/m2

Task 7.3: Assessing the importance of biogenic emissions and in-canopy chemistry on pollutant deposition at the European scale (met.no (Simpson), WU, JUELICH).

– The development of the ESX 1-D model is progressing well (cf WP4), and in the last period a series of tests with one-way nesting to the EMEP model were conducted, in order to investigate the impact of biogenic emissions and in-canopy reactions and deposition on ozone and deposition fluxes. Figure 2.12 presents an example of a 1-month calculation for a site in Germany, and deliverable D7.3 presents results for a range of other sites across Europe.

– The study by Univ. Gothenburg, Juelich and Met.no to investigate the potential impact on organic aerosol formation from biotic stress-induced emissions (SIE) of

157

organic molecules from forests in Europe has now been published (Bergström et al., 2014). This paper showed that SIE are potentially important for SOA formation and climate impacts but the magnitude of the impact is very uncertain and needs to be constrained by further laboratory, field and modelling studies.
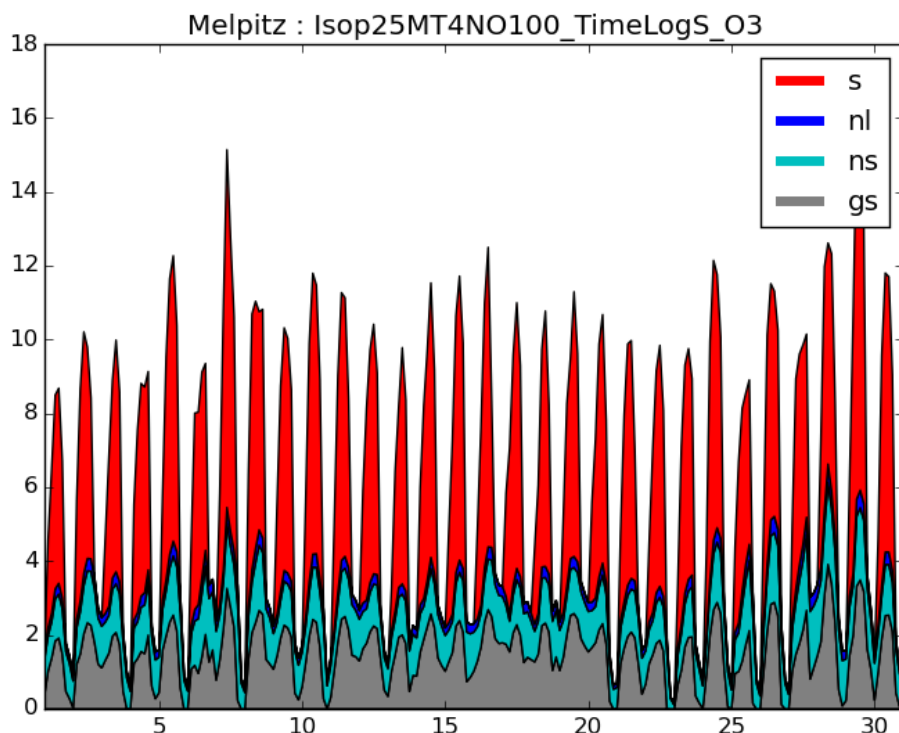
Fig 2.12: Deposition sinks of O_3 within a generic forest canopy located in Germany. Calculations with ESX model, driven by EMEP MSC-W boundary conditions for July 2012. Sink terms are: stomatal (s), non-leaf (nl), non-stomatal leaf (ns) and ground surface (gs). See Deliverable 7.3 for more details and examples where biogenic emissions are varied.

Task 7.4: Calculation of European fields and source-receptor matrices for deposition and pollution metrics/thresholds under future climate change (met.no (Simpson)).

- During the last reporting period calculation of fields of ozone and N-deposition for the year 2050 has been carried out with the EMEP using a range of climate effects (Figure 2.9 has presented one example, Figure 2.12 another, and many more can be found in Deliverable D7.4). As noted above, the EMEP model has been

enhanced so that it can take account of a number of changes which are expected in a future climate. Source-receptor (SR) calculations were then calculated for different climate experiments, considering the impacts of increased CO_2 on BVOC emissions and stomatal uptake, and of possibly increased NH_3 emissions. In Deliverable D7.5 we report in detail on how calculated SR results change when these climate enhancements are taken into account, and also compare with changes due to simple emission scenarios.

- The main conclusion from these runs is that in most cases the impacts of climate change itself (e.g. CO_2 inhibition of isoprene emissions or stomatal conductance) do not change the basic SR estimates very much, and that the main driver of changes is rather the difference in emissions between the 2010 and 2050 cases. The main exception was for phyto-toxic ozone dose to crops (POD3-IAM-CR), where the assumptions concerning climate response of stomatal conductance had an appreciable impact on the base-levels of POD3 and on the responses to NO_x emission reduction.

orig-delta SOMO35_2050_Base_PL_N

(a) base-case

diff in delta SOMO35_2050_A20_PL_N

(b) A20-NH$_3$

diff in delta SOMO35_2050_bvoc_PL_N

(c) CO$_2$-BVOC

diff in delta SOMO35_2050_KCO2_PL_N

(d) CO$_2$-gsto
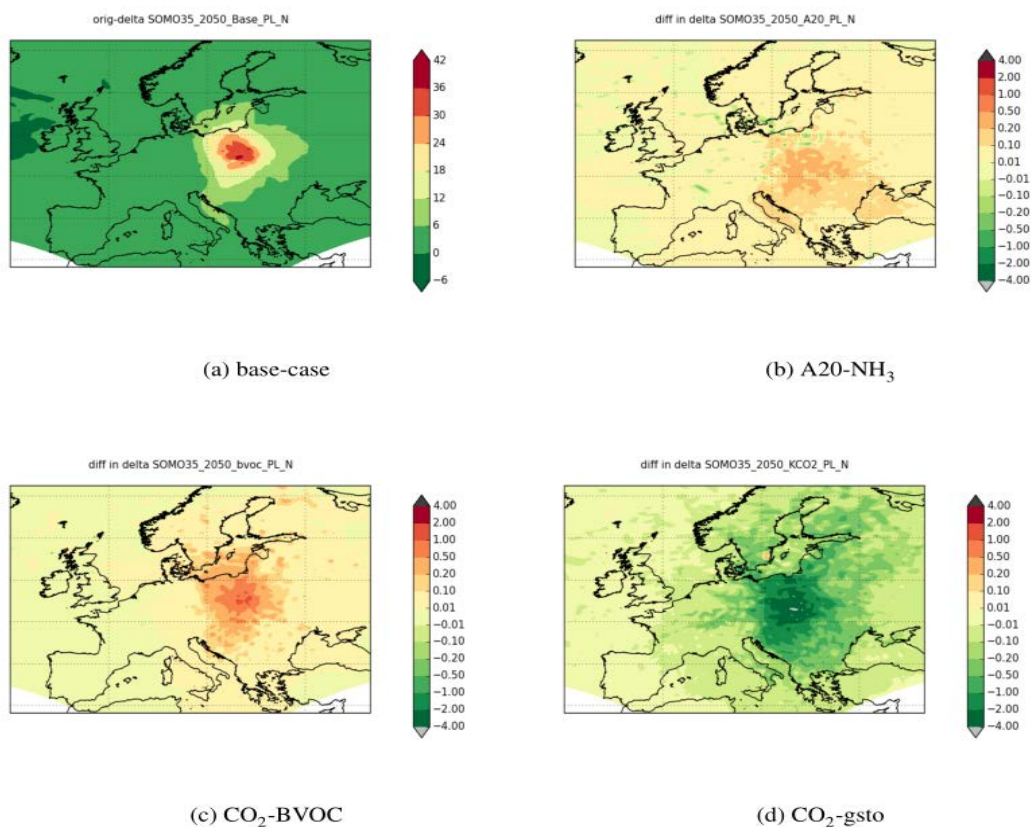
Fig.

Figure 2.13: Source-receptor changes in 2050: the impact of NO$_x$ emissions from Poland on SOMO35. Part (a) gives the base-case Delta-SOMO35 arising from a 15% reduction in Polish NO$_x$ emissions in 2050. Remaining plots show the differences between Delta-SOMO35 for different climate scenarios and the base-case run (see D7.5 for more explanation). Noting the very different colour scale axis for Fig. (a) to Figs (b-c), the main conclusion is that the impact of emission change is much greater than the impact of climate effects.

Task 7.5: Ensemble calculation of maps of deposition and pollution metrics and analysis of uncertainty (ULUND (Arneth), all WP partners).

– Reported in earlier periods (and deliverable D7.1).

– The "ScaleDep. Performance of European chemistry-transport models as function of horizontal spatial resolution", where the EMEP MSC-W, LOTOS-EUROS, CHIMERE, RCGC and CMAQ models have been run at spatial resolutions of 7, 14, 28 and 54 km across Europe has now been published (Schaap et al., 2015).

Progress towards the milestones and deliverables
D7.1 Maps of current air pollution metrics (APMs) across Europe, from the EMEP model and five other CTMs (M18)

- Delivered

D7.2 Improved EMEP model with climate-change and canopy-chemistry capabilities (M40)

Delivered Sept. 2015

D7.3 Report on effects of in-canopy BVOC and NO emissions on in-canopy O_3 and POD estimates (M44)

- Delivered Sept. 2015.

D7.4 Report on effects of changes in global climate, chemistry, emissions and landcover changes on APMs (M48)

ÉCLAIRE Third Periodic Report: November 2015

- Delivered Sept. 2015.

D7.5 Source-receptor matrices of APMs for current and future conditions (M36)

- Delivered Oct. 2015.

MS28 Implementation and initial testing of coupled model system (M24)

- Done, see Deliverable D7.3 (EMEP+ESX).

MS29 Initial ensemble runs for current conditions (M18).

- Achieved.

MS30 Incorporation of sub-grid methodology from WP4 into EMEP model (M30)

- The ESX model has now been used in 1-way nesting mode, driven by EMEP – see Deliverable D7.3.

MS31 Future scenario data-sets ready (M30)

- Delivered to C4.

MS32 "Final" model-system ready. Commencement of source-receptor calculations (M36)

- Done, see Deliverable D7.5

Use of resources and deviations from DoW

In general this WP progressed well, delivering long-period data to C3 and C4 partners, and generating many results concerning climate-effects on future air pollution metrics. Some model improvements (EMEP model) were delayed, awaiting improved algorithms from other parts of the ÉCLAIRE project, but such problems were anticipated and have had no major impact on the rest of the project. A total of 13.3 person months were used in this period, which is as planned.

Publications:

Bergström, R.; Hallquist, M.; Simpson, D.; Wildt, J. & Mentel, T. F., Biotic stress: a significant contributor to organic aerosol in Europe? *Atmospheric Chemistry and Physics,* **2014***, 14*, 13643-13660

Begstrröm, R., Cabonaceous Aerosol in Europe, Out of the woods and into the blue? PhD Thesis, Univ. Gothenburg, Sweden, Sept. **2015**

Engardt, M. & Langner, J., Simulations of future sulphur and nitrogen deposition over Europe using meteorological data from three regional climate projections, *Tellus B,* **2013***, 65*, 20348.

Engardt, M. & Langner, J., Simulations of future sulphur and nitrogen deposition over Europe using meteorological data from three regional climate projections, *Tellus B,* **2013***, 65*, 20348

Klingberg, J.; Engardt, M.; Karlsson, P. E.; Langner, J. & Pleijel, H., Declining ozone exposure of European vegetation under climate change and reduced precursor emissions, *Biogeosciences,* **2014***, 11*, 5269-5283

Leip, A.; Billen, G.; Garnier, J.; Grizzetti, B.; Lassaletta, L.; Reis, S.; Simpson, D.; Sutton, M. A.; de Vries, W.; Weiss, F. & Westhoek, H. Impacts of European livestock production: nitrogen, sulphur, phosphorus and greenhouse gas emissions, land-use, water eutrophication and biodiversity, Environ. Res. Lett., **2015**, 10, 115004

Langner, J.; Engardt, M.; Baklanov, A.; Christensen, J. H.; Gauss, M.; Geels, C.; Hedegaard, G. B.; Nuterman, R.; Simpson, D.; Soares, J.; Sofiev, M.; Wind, P. & Zakey, A. A multi-model study of impacts of climate change on surface ozone in Europe, *Atmos. Chem. Physics,* **2012***, 12*, 10423-10440

Pleijel, H.; Danielsson, H.; Simpson, D. & Mills, G. Have ozone effects on carbon sequestration been overestimated? A new biomass response function for wheat, *Biogeosciences,* **2014***, 11*, 4521-4528

Schaap, M.; Cuvelier, C.; Hendriks, C.; Bessagnet, B.; Baldasano, J.; Colette, A.; Thunis, P.; Karam, D.; Fagerli, H.; Graff, A.; Kranenburg, R.; Nyiri, A.; Pay, M.; Rouil, L.; Schulz, M.; Simpspn, D.; Stern, R.; Terrenoire, E. & Wind, P. Performance of European chemistry transport models as function of horizontal resolution *Atmospheric Environment ,* **2015***, 112*, 90 - 105

Simpson, D.; Christensen, J.; Engardt, M.; Geels, C.; Nyiri, A.; Soares, J.; Sofiev, M.; Wind, P. & Langner, J., Impacts of climate and emission changes on nitrogen deposition in Europe: a multi-model study, *Atmos. Chem. Physics,* **2014***, 14*, 6995-7017

Simpson, D.; Arneth, A.; Mills, G.; Solberg, S. & Uddling, J. Ozone - the persistent menace; interactions with the N cycle and climate change *Current Op. Environ. Sust.*, **2014,** 9-10, 9-19

Sutton, M. A.; Reis, S.; Riddick, S. N.; Dragosits, U.; Nemitz, E.; Theobald, M. R.; Tang, Y. S.; Braban, C. F.; Vieno, M.; Dore, A. J.; Mitchell, R. F.; Wanless, S.; Daunt, F.; Fowler, D.; Blackall, T. D.; Milford, C.; Flechard, C. R.; Loubet, B.; Massad, R.; Cellier, P.; Personne, E.; Coheur, P. F.; Clarisse, L.; Van Damme, M.; Ngadi, Y.; Clerbaux, C.; Skjøth, C. A.; Geels, C.; Hertel, O.; Wichink Kruit, R. J.; Pinder, R. W.; Bash, J. O.; Walker, J. T.; Simpson, D.; Horváth, L.; Misselbrook, T. H.; Bleeker, A.; Dentener, F. & de Vries, W. Towards a climate-dependent paradigm of ammonia emission and deposition *Phil. Trans. R. Soc. B: Biol. Sci.*, **2013**, 368, 20130166

Tuovinen, J.-P.; Hakola, H.; Karlsson, P. E. & Simpson, In Air Pollution Risks to Northern European Forests in a Changing Climate . Climate Change, Air Pollution and Global Challenges Understanding and Perspectives from Forest Research, (D. Matyssek, et al, Eds.), Elsevier, Oxford, UK, **2013**, 13, 77 - 99

Work package 8 – Assessing local and regional variation

Lead contractor: ECN
Contributors: NERC, met.no, KIT, INRA, UPM, AU, ULB

Work package objectives

The aim of WP8 is to develop a better scientific understanding of the air pollution and climate change relationships at regional/local/landscape-scale and sub-grid approaches for inclusion in large-scale models that enable a good representation of the multitude of processes that play a role on smaller scales (e.g. landscape-scale). By doing this, large-scale concentration and deposition patterns will better represent the local-scale interactions and provide more relevant input, e.g., for European scenario studies that involve one or more of the affected parameters. The objectives are:

1. To synthesize the available knowledge on local interactions in relation to climate and air quality, as well as the way this knowledge is included in local-scale atmosphere-biosphere modelling systems;

2. To analyse the sensitivity of the landscape scale effects on changing pollutant fluxes, especially as affected by climate change;

3. To include local/landscape-scale effects of climate change and air pollution interactions into large scale/European scale models by means of sub-grid representation of the most important processes.

Progress and Results

Task 8.1 Synthesis of existing local-scale transport models with atmosphere-biosphere exchange

The literature study in Task 8.1 has been finalized in this reporting period, although later than planned. However, while the activity (and the resulting literature study) is important for the overall understanding of air pollution / climate interactions in the various models, the delay hasn't posed a large problem for the work in the other work packages.

As already mentioned, the review focussed on the interaction between Air Quality and Climate Change, one of the objectives of the Integrated Project ÉCLAIRE. Various aspects of this interaction have been studied in the project, such as the role it plays in the plant-atmosphere interaction, and the way it is represented in large scale models. The review describes a few aspects that play (although perhaps in a more indirect way) a role in this interaction, and the way atmospheric transport and deposition models are able to deal with it.

As part of the review an overview was presented of different models that can be used, over different scales, to make predictions of air pollutant concentrations and deposition rates (now or in the future). The overall purpose of the review is to assess to what extent the models are capable of taking into account climate change.

Some interactions that exist between air quality and climate change are:
- Increasing volatilization of ammonia with increasing temperature
- Local cooling effect with increasing aerosol concentrations in the air
- Ozone formed from NO_x/VOC emissions reducing plant productivity, which in turn reduces CO_2 uptake from the atmosphere
- Increasing biogenic VOC emissions with increasing temperature

However, to what extent is the knowledge about these interactions incorporated into the models that are currently used for describing Air Quality and/or predicting the current or future situation with respect to concentrations and depositions? The Task 8.1 inventory summarizes the different models that exist and gives an overview of the different ways in which these models take into account these interactions.

There are different models available, ranging from models describing processes on a plant level to global scale models. For the purpose of the overview, the main focus is on larger scale models: ranging from landscape scale to regional/global scale. Most of the models described in the review are capable of dealing with different atmospheric components, although some are targeted at one particular species (mostly ammonia). Ammonia has been singled-out for special treatment as a result of its high spatial variability, especially close to emission sources. In order to correctly assess the ecological impacts of ammonia (either as the result of elevated concentrations or its contribution to nitrogen deposition), atmospheric processes need to be modelled at a higher resolution than required for the assessment of particulate nitrogen deposition, for example.

Most of the work that was presented has been collated from previous activities published in:

- Sutton M.A., Reis S. and Baker S. (eds) Atmospheric Ammonia – Detecting emission changes and environmental impacts (Springer, ISBN 978-1-4020-9120-9), 2009.
- Massad R .and Loubet B. Review and Integration of Biosphere-Atmosphere Modelling of Reactive Trace Gases and Volatile Aerosols (Springer, ISBN 978-94-017-7284-6), 2015.

With respect to the air quality / climate interaction it became clear from the model inventory that a full interaction is not available in the models described here. For the most part interactions are included for modelling the effect of a changing climate (with respect to meteorological conditions) on the modelled concentration/deposition.

Task 8.2 Improved scientific understanding of air quality and climate change relations at the landscape scale

For Task 8.2 the main activities are related to the on-going development of the NitroScape model and the simulations carried out using the EMEP4UK model. From the beginning of the project, it was clear that there were large challenges with respect to the development of NitroScape. After an initial delay due to personnel issues, the activity was started but first real results for the ÉCLAIRE test areas (Scotland and Netherlands) were not foreseen until the first half of 2013. Since there was a need (by WP17) for small scale concentration/deposition maps, which were originally to have been produced by NitroScape, a contingency plan was needed for this particular task. This contingency plan consisted of using concentration/deposition maps from existing models and previous projects (as described in previous WP reports). Since this contingency plan was adopted, the focus of the NitroScape development work has been the development and incorporation of new and existing component models such as the FARM-EF farm model, a 2D version of the CERES-EGC agro-ecosystem model and the FIDES-3D-Surfatm atmospheric model, as well as many code improvements and bug-fixes (see MS35 report for more details).

The other part of Task 8.2, local scale interactions at spatial resolutions of 1×1, 5×5 and 50×50 km^2 was done by means of the EMEP4UK model. Work package 17 uses the concentration and deposition maps produced by the model to evaluate critical load exceedances at the different spatial resolutions for domains covering most of Scotland and the whole of the Netherlands (see Figure 2.14).
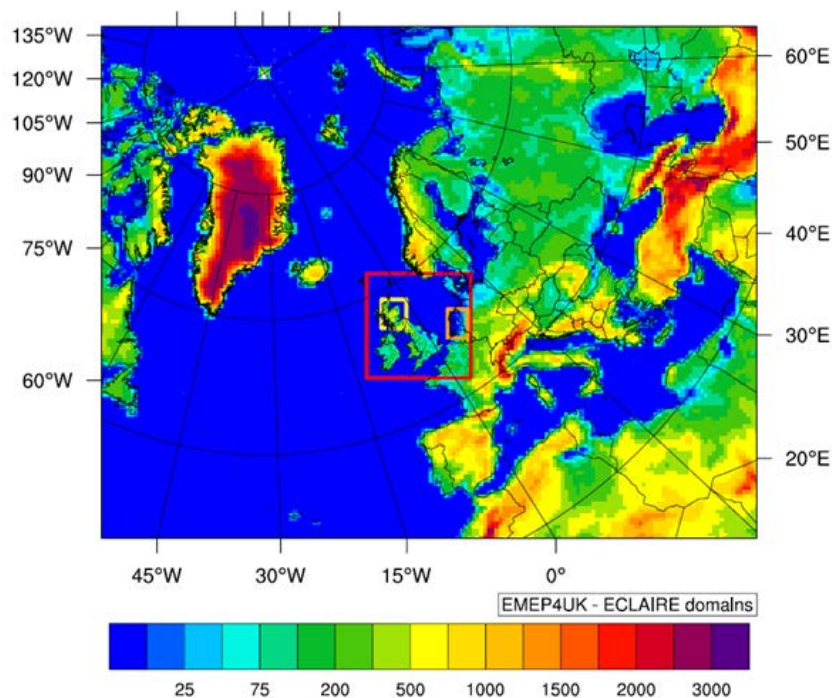
Figure 2.14: EMEP4UK model domains as used for the ÉCLAIRE project. The largest domain has a horizontal resolution of 50 × 50 km^2, a nested 5 × 5 km^2 domain covering the British Isles, part of France, The Netherlands, Belgium (Red box), and two nested domains at 1 × 1 km^2 horizontal resolution covering most of Scotland (Yellow box) and the whole of the Netherlands (Orange box) for detailed analyses.

The calculations for the various domains show that increasing the spatial resolution leads to a decrease in the annual deposition of reduced nitrogen (NH$_x$).

With the Netherlands as an example, for a resolution of 50 × 50 km^2, the deposition of NH$_x$ is 800 mg N m^{-2} (overall budget for the Netherlands = ~28 Gg N), for 5 × 5 km^2 it is 550-1000 mg N m^{-2} (NL budget ~ 25 Gg N), while for 1 × 1 km^2 it is 250- >1000 mg N m^{-2} (NL budget ~ 24 Gg N) (see Figures 2.15 and 2.16). The spatial distribution of the dry deposition of reduced nitrogen is highly dependent on the spatial distribution of ammonia emissions and, therefore, the model resolution. Although different, the total NL budget does not show a large difference between scales. The ammonia deposition velocity is relatively high and eventually most of the available ammonia (i.e. that not used to neutralise SO$_4$ or NO$_3$) is dry-deposited within the NL domain. The differences in the NL budgets may be the result of resolving the national borders at the different resolutions.

168
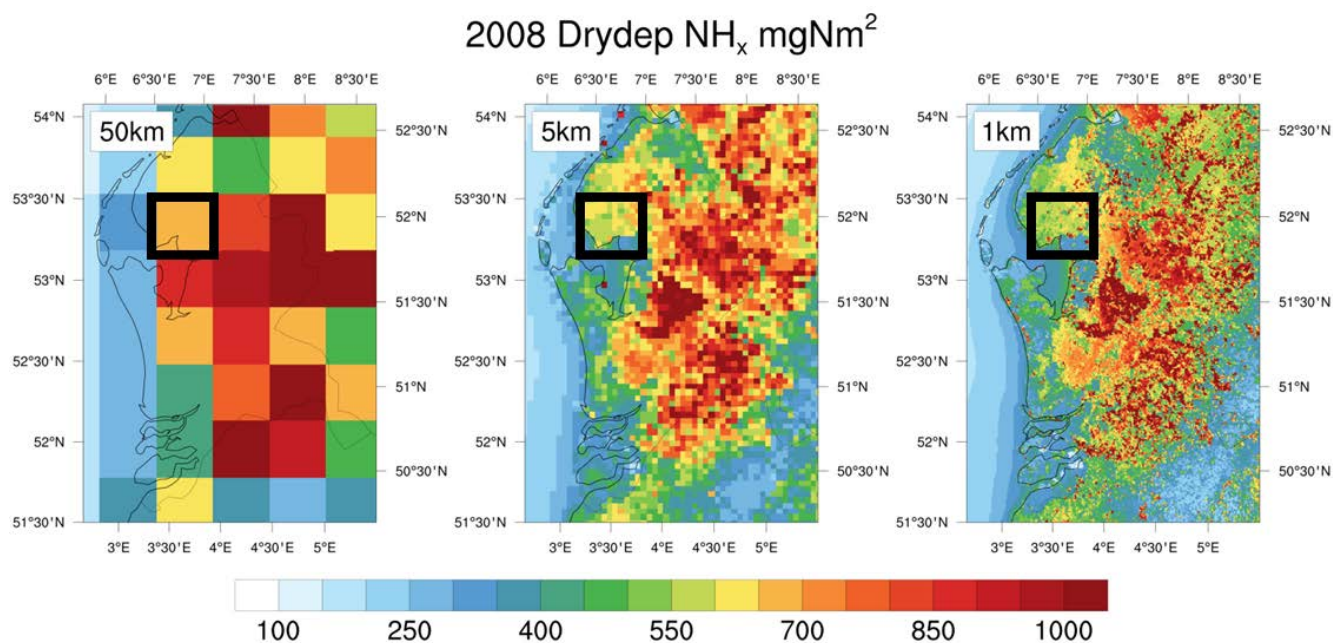
Figure 2.15: EMEP4UK modelled dry deposition for the Dutch domain. The black box shows an arbitrary 50 km × 50 km where the deposition is ~700 mg N m^{-2}. The ranges of deposition in the same 50 km × 50 km grid square are: ~250 – 750 mg N m^{-2} for the 5 km × 5 km resolution and ~250 - >850 mg N m^{-2} for the 1 km × 1km resolution.

2008 Drydep NH$_x$ mgNm^2
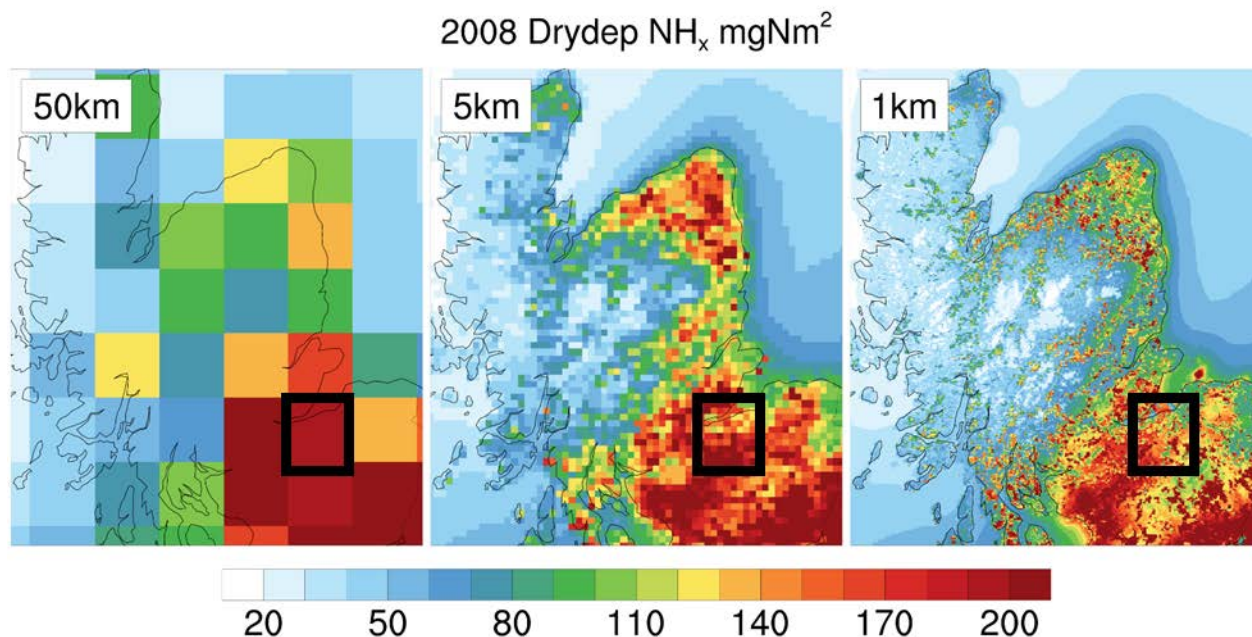
Figure 2.16: EMEP4UK modelled dry deposition for the Scottish domain. The black box shows an arbitrary 50 km × 50 km where the deposition is ~170 mg N m^{-2}year^{-1}. The ranges of deposition in the same 50 km × 50 km grid square are: ~110 – >200 mg N m^{-2}year^{-1} for the 5 km × 5 km resolution and ~50 - >200 mgN m^{-2}year^{-1} for the 1 km × 1km resolution.

Task 8.3 Development of sub-grid parameterisations

The objectives of this task is the development of a parameterisation (module) that can simulate the sub-grid spatial distributions of mean annual concentrations and deposition rates of air pollutants (specifically ammonia, nitrogen dioxide and nitrogen deposition) within the grid cell of a chemical transport model (e.g. the EMEP MSC-W model) using high spatial resolution emission and land cover data.

A sub-grid model was developed that combines high-spatial-resolution emission data and a simple parameterisation of short-range dispersion to estimate the spatial distribution (at a resolution of 1 × 1 km^2) of the concentrations of ammonia (NH$_3$) and nitrogen dioxide (NO$_2$) within the 50 × 50 km^2 (approx.) grid squares of the EMEP model. Pollutant dispersion from emission sources was parameterised using a simple scenario of a single 1 × 1 km^2 source with a constant emission of 1 tonne km^{-2} yr^{-1} in the centre of a square

domain (of dimensions 101 × 101 km^2). Figure 2.17 shows the overall methodology for producing the sub-grid concentration predictions.
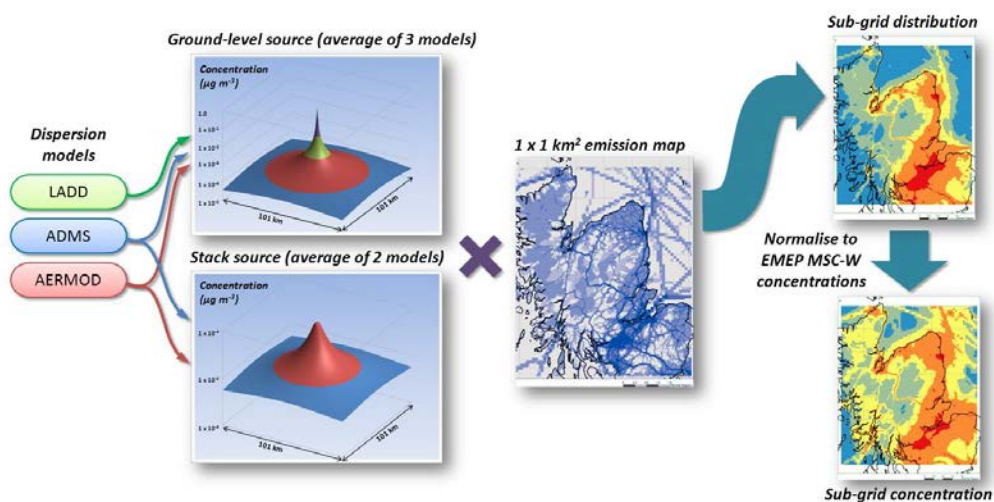
Figure 2.17: Schematic showing the process of producing the sub-grid concentration predictions from short-range dispersion model simulations and high spatial resolution emission data.

The resulting 'sub-grid distributions' (Figure 2.18) provide an estimate of the spatial variability of the concentrations at a 1 km resolution, which were then used to 'redistribute' the 50 × 50 km^2 concentration predictions of the EMEP (MSC-W) model. This was done by interpolating the concentration predictions of the EMEP model and the mean concentrations of the sub-grid distribution within each 50 × 50 km^2 km grid square across the whole domain. The 'sub-grid predictions' were then calculated by multiplying the sub-grid distributions by the interpolated EMEP predictions and then dividing by the interpolated sub-grid distribution (Figure 2.18). The sub-grid model predictions of NO$_2$ and NH$_3$ concentrations are shown in Figure 2.19.
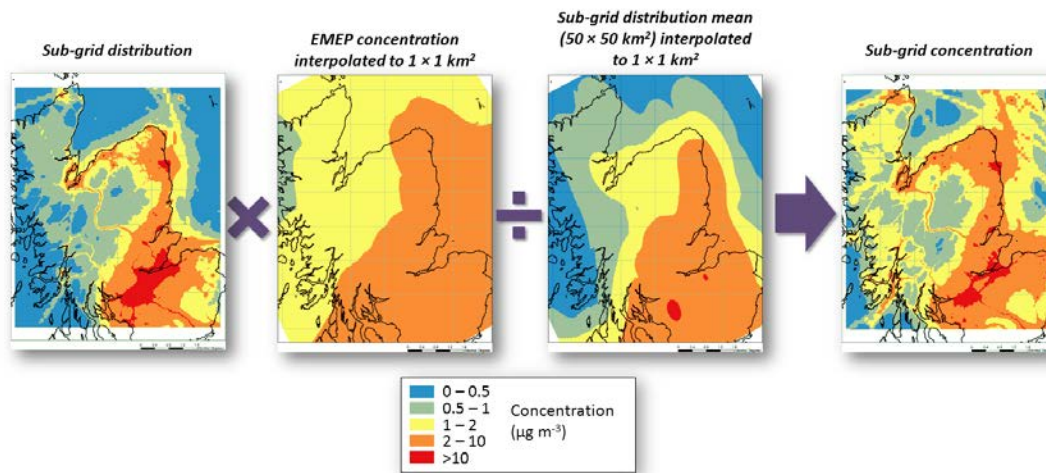
Figure 2.13: The process of converting the sub-grid distributions to sub-grid concentrations for an example dataset (NO_2 in Central Scotland).
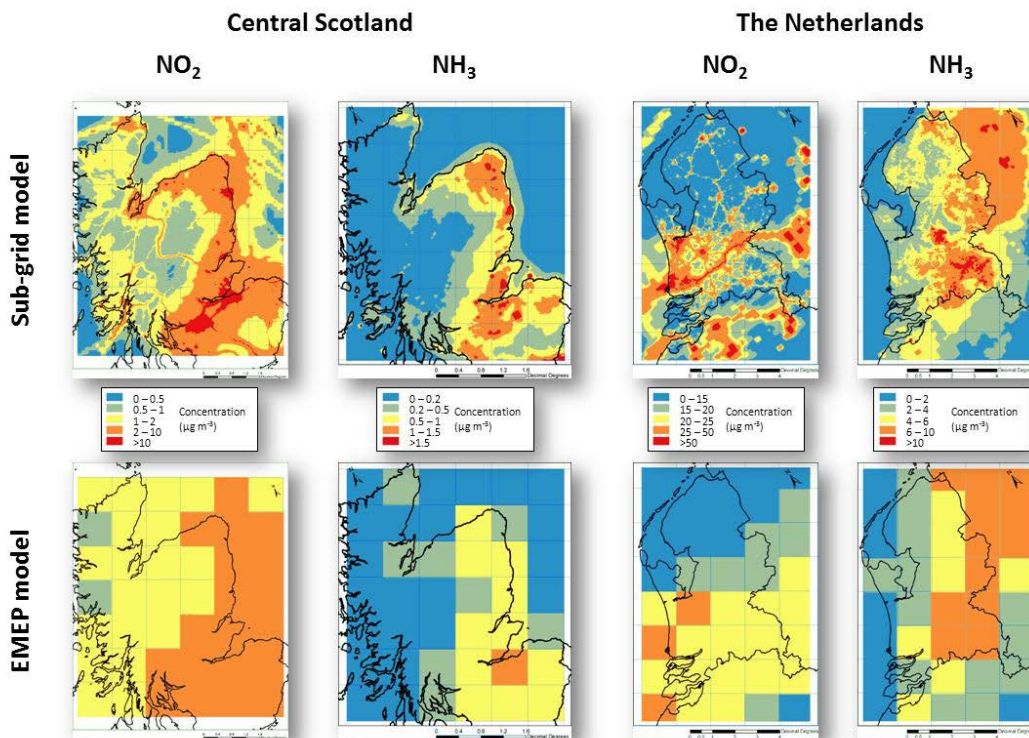
Figure 2.19: Sub-grid model predictions (top row) of mean annual concentrations of NO_2 and NH_3 for the two domains (Central Scotland and The Netherlands). EMEP model predictions at a resolution of 50x50km are shown for comparison (bottom row).

ÉCLAIRE Third Periodic Report: November 2015

A comparison of the modelled (sub-grid) concentrations with measured values shows that the modelled values compare reasonably with the measured values (see Figure 2.20).
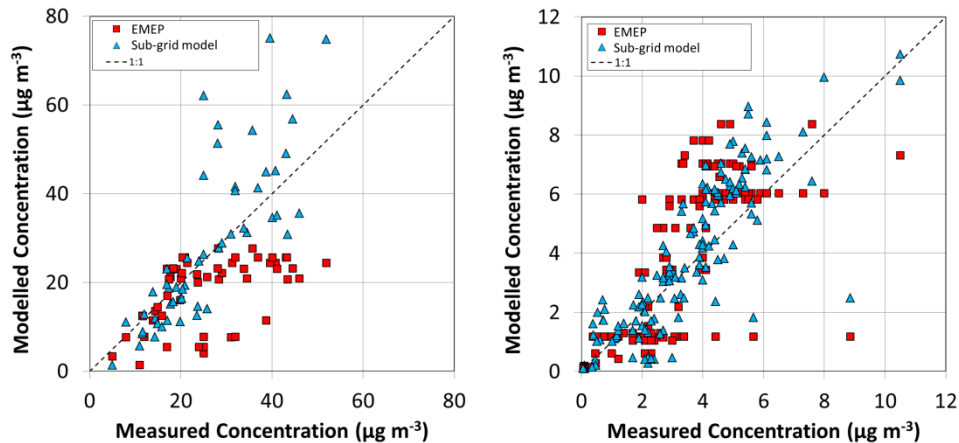
Figure 2.20: Modelled concentrations plotted against measured values for all sites for NO$_2$ (left) and NH$_3$ (right) for all sites in both domains.

Separate sub-grid parameterisations were also developed for three of the four components of nitrogen deposition (wet oxidised, wet reduced and dry reduced). It was not possible to develop a simple parameterisation for dry deposition of oxidised nitrogen due to the contributions from multiple compounds, each affected by different transport and transformation processes. Dry deposition of reduced nitrogen is mainly the dry deposition of NH$_3$ and therefore the sub-grid distribution of NH$_3$ can be used for the sub-grid distribution of the dry deposition of reduced nitrogen. The spatial distribution of wet deposition of nitrogen is influenced both by the atmospheric concentrations of nitrogenous compounds and precipitation rates. The proxy used to estimate the sub-grid variability of wet deposition was the product of high spatial resolution annual precipitation data and the atmospheric concentrations of nitrate and ammonium (from the EMEP model), for deposition of oxidised and reduced nitrogen, respectively. Sub-grid total nitrogen deposition is calculated as the sum of the total wet deposition and the dry deposition of reduced nitrogen simulated by the sub-grid model plus the EMEP model estimate of dry deposition of oxidised nitrogen. For oxidised and reduced nitrogen the comparison with measured deposition is shown in Figure 2.21. Overall both the EMEP and the sub-grid model underestimate wet deposition of oxidised and reduced nitrogen by an average of

50%. There is very little difference between the predictions of the models for the Netherlands as a result of low spatial variability of the precipitation.
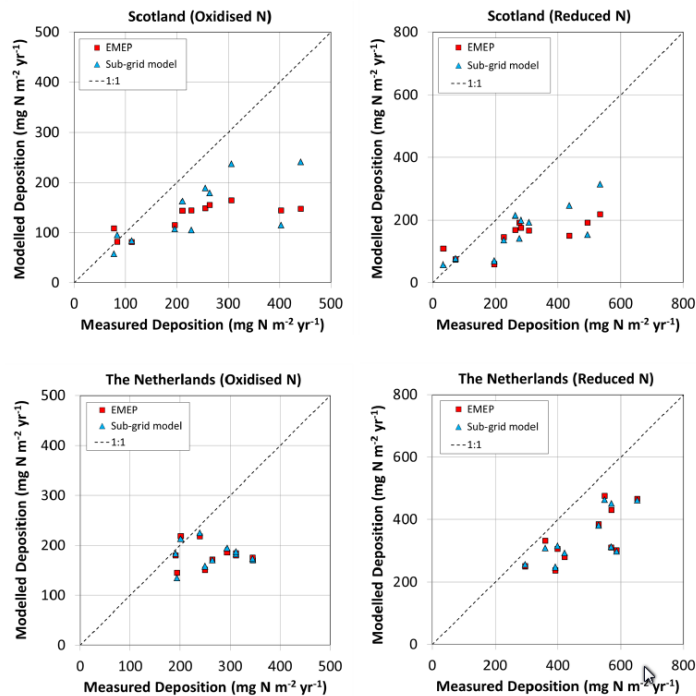
Figure 2.21: Modelled wet deposition of oxidised (left column) and reduced (right column) nitrogen plotted against measured values for the Scotland (top row) and Dutch (bottom row) domains.

With respect to the development of a sub-grid module, these overall conclusions could be drawn at the end of the project:

- The sub-grid model for nitrogen deposition uses the high resolution NH_3 concentration data to simulate the spatial distribution of dry deposition of reduced nitrogen. The spatial distributions of wet deposition of both reduced and oxidises nitrogen are based on the spatial distributions of high resolution precipitation maps. It has not been possible to develop a sub-grid model for the dry deposition of oxidised nitrogen

- Both sub-models have been applied to two contrasting areas (Central Scotland and the Netherlands) and model performance of both the EMEP model and the sub-grid model has been assessed using monitoring data of atmospheric concentrations and wet deposition for both study areas

ÉCLAIRE Third Periodic Report: November 2015

- The sub-grid model for atmospheric concentrations represents a substantial improvement on the predictions of the EMEP model reducing both model error and increasing the spatial correlation with the measured concentrations

- The performance of the sub-grid model for wet deposition, however, is similar to that of the EMEP model and provides only a small improvement on the deposition predictions.

Progress towards the milestones and deliverables

MS 33: Inventory of relevant local scale models
The inventory of different relevant local scale models used in Europe has been completed.

MS 34: Report on local scale models inventory
This literature study has been completed and submitted as D8.1 (combined with D8.2)

MS 35: update of NitroScape to reflect ÉCLAIRE needs
The achievement of this MS was been delayed and although major updates to NitroScape were made they did not come together as a useable final product within the timescale of the project. Contingency plans were therefore introduced (e.g. use of alternative high resolution model data in WP17) to allow the project to deliver the necessary results..

MS 36: Concentration/Deposition maps
These concentration/deposition maps have been finalised and delivered to WP17 for further processing. The work (and resulting maps) are described in D8.2 and D8.3/D17.2.

MS 37: Description of local scale interactions between air quality and climate change
This work has been finalised and submitted as D8.1.

MS 38: Sub-grid module available for implementation in EMEP model
This work has been finalised and submitted as D8.4.

D8.1: Synthesis report on the different local scale models dealing with atmosphere-biosphere exchange
This work was finalized and submitted to the ÉCLAIRE deliverables database.

D8.2: Report on local scale interactions between air quality and climate change (Month 30)
This work was finalized and submitted to the ÉCLAIRE deliverables database.

D8.3: Concentration and deposition maps (Month 16)

ÉCLAIRE Third Periodic Report: November 2015

This work was finalized and submitted to the ÉCLAIRE deliverables database.

D8.4: Sub-Grid module for inclusion in the EMEP model (Month 30)
This work was finalized and submitted to the ÉCLAIRE

Use of resources and deviations from DoW

The main deviation from the ÉCLAIRE Description of Work is related to the NitroScape work. This work didn't result in a useable product, and since results were needed for WP17, a contingency plan of using concentration/deposition maps from existing models and previous projects was deployed. Eventually, this worked out fine and all activities in WP17 could be completed using these alternative datasets. A total of 6.5 person months were spent in this period.

ÉCLAIRE Third Periodic Report: November 2015

2.1.3 Component 3 – Ecological Response Processes and Thresholds

Lead contractor: NERC

Component objectives & Specific Objectives of relevance to this component

Specific objectives for ÉCLAIRE relevant to Component 3:

S4.To integrate the results of meta-analyses of existing datasets with the results of targeted experiments for contrasting European climates and ecosystems, thereby assessing the climate-dependence of thresholds for land ecosystem responses to air pollution, including the roles of ozone, N-deposition and interactions with VOCs, nitrogen form (wet/dry deposition) and aerosol [WPs 9, 10, 11,12].

S5. To develop novel thresholds and dose-response relationships for air pollutants (especially for O_3 and N) under climate change, integrated into process-based models verified by experimental studies at site scales and mapped at the European scale, quantifying the effect of climate change scenarios [WPs 12,13,14, 15,16].

S8. To apply the novel metrics to quantify multi-stress response of vegetation and soils, including effects on carbon storage and biodiversity to improve the overall risk assessments of pollution-climate effects on ecosystems at the European scale as the basis for development of mitigation options [WPs 12, 13, 14, 15,16, 20].

Overall, Component 3 objectives are to deliver:

1. Assessments of the effects of combined air pollution and climate change scenarios on ecosystem C/GHG balance, soil quality and vegetation change at the experimental sites, based on integrated models.
2. A new database and results of meta-analysis on air pollution impacts on land ecosystems including soils.
3. Ecosystem response data on plant responses and ecosystem C balance to experimental changes in air pollution and interacting drivers, including climate and land use differences.
4. Parameterization of the fraction of O_3 that is taken up by leaves due to detoxification by constitutive BVOC, under associated environmental constraints and during leaf development.
5. Assessment of the relative effects of wet/dry and NO_y/NH_x deposition and the role of aerosol deposition in exacerbating drought stress.
6. Novel thresholds for key dose-response relationships for application in regional scale modelling and mapping relevant for ecosystem service assessment.

The results described below, specifically contribute to answering the following ÉCLAIRE Key questions:

Q1: What are the expected impacts on ecosystems due to changing ozone and N-deposition under a range of climate change scenarios, taking into consideration the associated changes in atmospheric CO_2, aerosol and acidification?

Q2: Which of these effects off-set and which aggravate each other, and how do the mitigation and adaptation measures recommended under climate change relate to those currently being recommended to meet air pollution effects targets?

Progress and Results

Component 3 has improved our understanding of the effects of air pollutants, alone and in combination on terrestrial ecosystem functioning and services, and how these effects will be modified in a changing climate. The component comprised five inter-connected work packages covering data mining and data re-use (WP9), experimental studies of effects and novel pollutant interactions (WPs10, 11) and modelling to determine novel thresholds (WP12) and ecosystem-scale impacts (WP13). In this final reporting period, all data and modelling were brought together to provide the required outputs for C3. Thus, results are discussed here under science themes rather than WPs drawing attention to the main findings from Component 3. All data mining, experiments and modelling focussed on responses to realistic ozone (O_3) concentrations, N deposition rates or aerosol concentrations, reflecting current or predicted future concentrations/depositions in the coming decades.

Ozone pollution reduces carbon assimilation in many species

A data mining exercise was undertaken using a common methodology and template to extract data from the scientific literature on the effects of O_3 on photosynthesis parameters in crops, grassland, heath and wetland species (WP9). Using a combination of meta-analysis and mixed-effects modelling in R, responses were calculated as the percentage decrease in each parameter per ppb of O_3 (Table 3.1). All effects of O_3 were negative, with photosynthesis and stomatal conductance reduced by 0.33 to 0.4 percent per ppb of O_3. An example of effects of daylight O_3 mean concentration on the net photosynthetic rate of cereals and non-cereal crops is given in Figure 3.1a. These and other relationships were used in leaf- and plant-scale modelling in WP12 and ecosystem-scale modelling in WP13.

Several experiments in WP10 included measurements of effects of O_3 (with or without added N) on photosynthesis and biomass accumulation. In general, effects of O_3 became more pronounced as the growing season progressed, in part reflecting the earlier senescence or die-back of leaves in elevated O_3. For example, elevated O_3 (seasonal mean of 68 ppb) progressively reduced components of photosynthesis such as the maximum carboxylation velocity ($V_{c\ max}$) in the tree species silver birch by 6% in June, 25% in July and 39% in September relative to the control treatment (Figure 3.2). Negative O_3 effects on photosynthesis were mirrored in negative effects on biomass accumulation as indicated by data mining (Figure 3.1b) and ÉCLAIRE experiments on species such as silver birch, hornbeam, annual pasture species (Figure 3.3), leafy vegetable crops, and barley.

Under WP12, a novel method for modelling effects of O_3 on net annual increment of trees has been developed that uses response functions from experiments with young trees to estimate effects on trees at any stage in their life time. Previous response functions were for effects on relative biomass of young trees (Büker et al., 2015). This new method allows effects on carbon sequestration to be estimated spatially for several tree species making use of national reporting of tree net annual increment to the UN Framework Convention on Climate Change, and includes response functions for minimum, average and maximum effects (Table 3.2). The response functions are based on the stomatal uptake of O_3 taking into account the varying effects of climate, soil moisture, seasonal changes and O_3 on the opening and closing of the leaf stomatal pores.

Table 3.1: Meta-analysis of effects of O_3 on photosynthetic parameters of crops, heath, grassland and wetland species. The effect size is percentage change per ppb of O_3. 9999 iterations were run to calculate the 95% bootstrap confidence interval. The "*" next to the effect size indicates at least a 95% confidence that it is not 0.

Process	Effect size	Bootstrap CI
Biomass	-0.48*	-0.69 to -0.35
A_{sat}	-0.33*	-0.47 to -0.18
J_{max}	-0.15	-0.36 to 0.19
Net photosynthetic rate	-0.36*	-0.51 to -0.22
V_{cmax}	-0.24*	-0.38 to -0.08
Stomatal conductance	-0.40*	-0.53 to -0.28

Note: A_{sat} is the photosynthetic rate at saturating light levels; J_{max} is the maximum rate of electron transport (an indication of the efficiency of the light capturing efficiency of photosynthesis); V_{cmax} is the maximum carboxylation velocity (an indication of the efficiency of the C fixation of photosynthesis).

Table 3.2: Statistical details (regression equation and R^2) of the Net Annual Increment (NAI) dose-response relationships for a variety of European forest tree species. Response functions for the 'standard', 'minimum' and 'maximum' growth curves are shown.

Receptor	PODy	Default	R2	Min	R2	Max	R2
Norway spruce and Scots pine	1	y = -0.0057x + 1.0015	0.72	y = -0.0053x + 1.0014	0.71	y = -0.0065x + 1.0019	0.72
Norway spruce	1	y = -0.0054x + 1.0002	0.56	y = -0.0051x + 1.0003	0.55	y = -0.0062x + 1.0000	0.56
Birch & Beech	1	y = -0.0093x + 0.9461	0.59	y = -0.0090x + 0.9464	0.58	y = -0.0101x + 0.9449	0.59
Oak	1	y = -0.0057x + 1.0167	0.75	y = -0.0052x + 1.0142	0.75	y = -0.0066x + 1.0212	0.75
Aleppo pine	1	y = -0.005x +0.9998	0.64	y = -0.0046x + 0.9989	0.64	y = -0.0058x + 1.0013	0.65
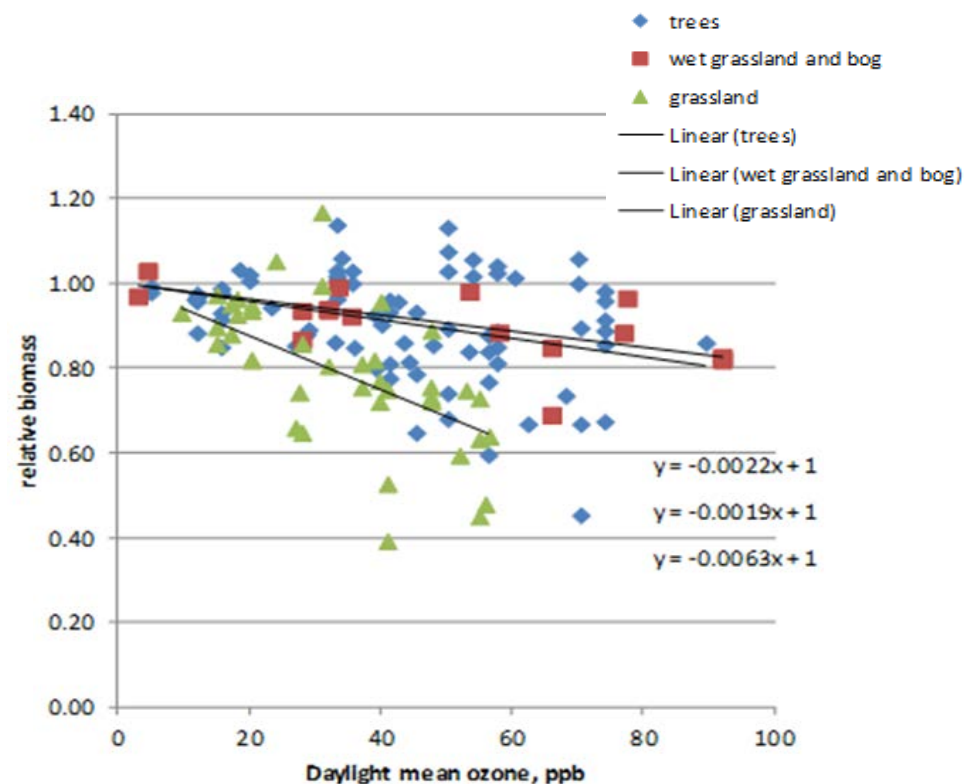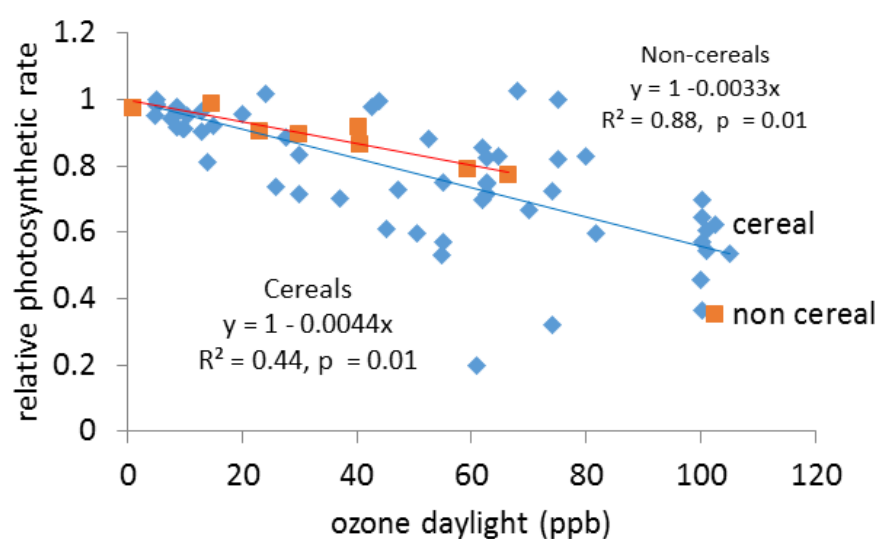
Figure 3.1: Results of data mining for effects of O₃ on (left) the photosynthetic rate of crops and (right) trees, grassland and wetland vegetation.

ÉCLAIRE Third Periodic Report: November 2015

Vcmax by O$_3$ and N treatment, Bangor, Birch
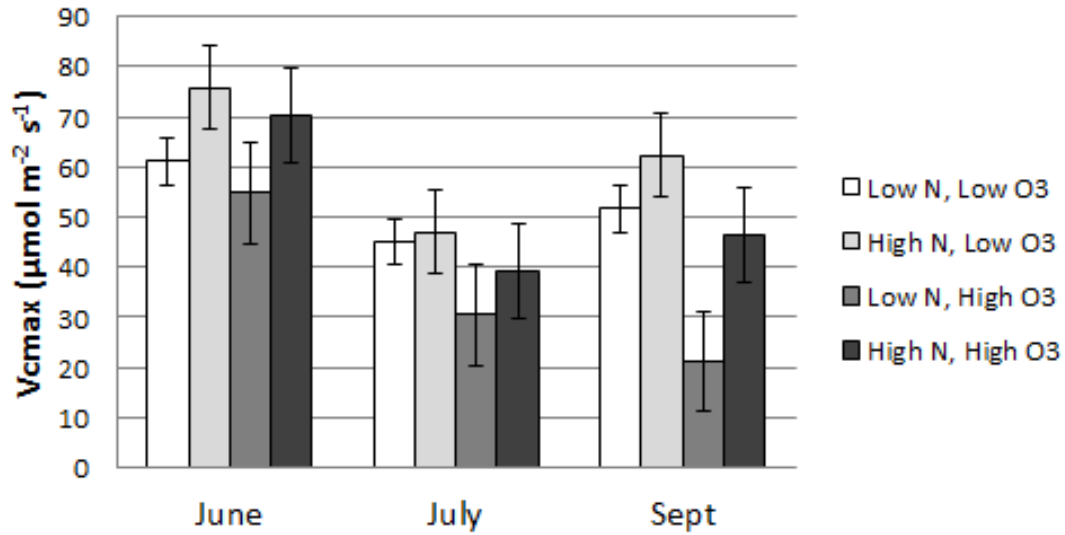
Figure 3.2: Relative variation in the photosynthesis parameter, V$_{cmax}$, by N and O$_3$ treatment over the course of the summer for a deciduous tree species, silver. Low and high N treatments were 10 and 70 kg/ha/yr respectively whilst low and high O$_3$ treatments were 35 and 70 ppb (24 hour mean). Data are means +/- standard error.
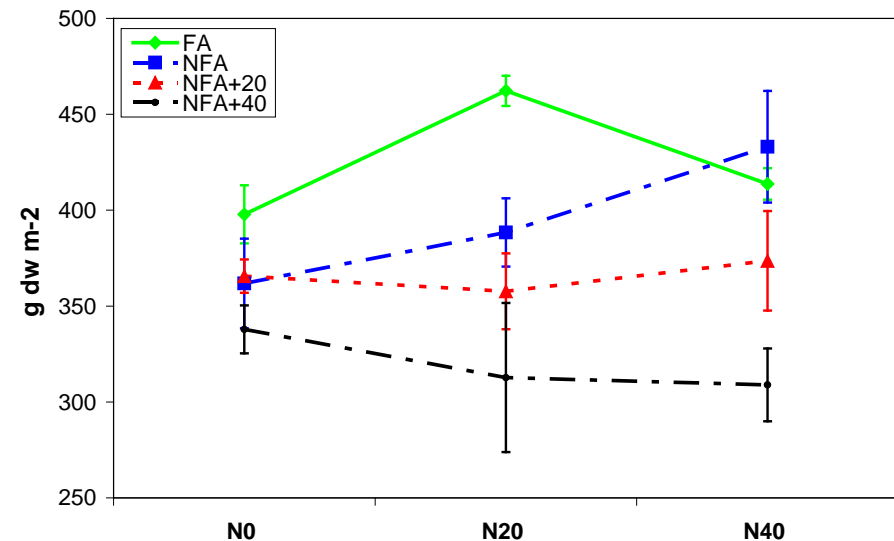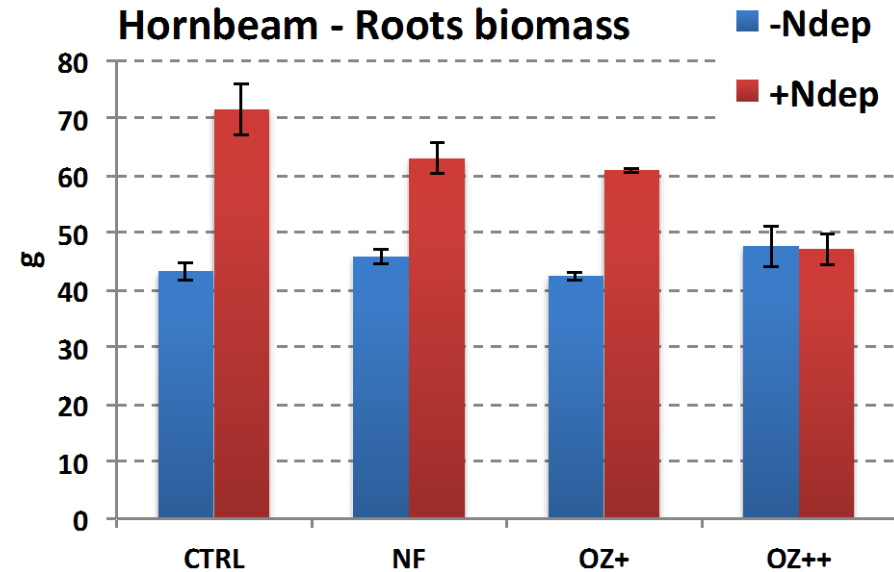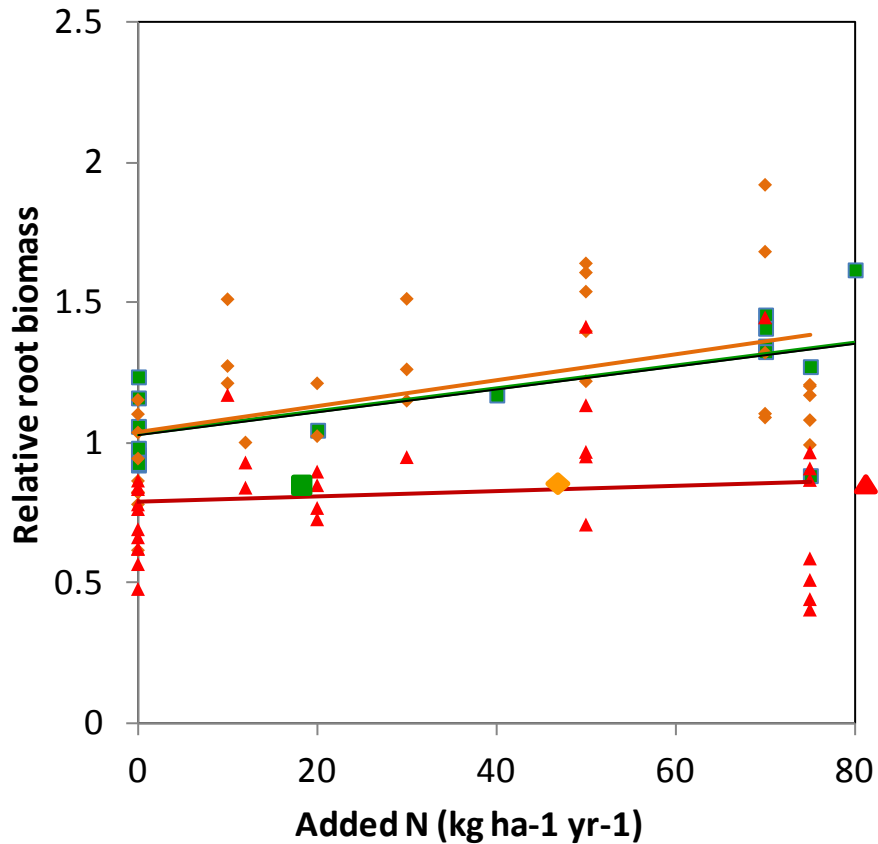
Figure 3.3: Effects of combinations of O_3 and N on (left) root biomass, combined minded data with ÉCLAIRE experimental data. Key: < 35 ppb O_3, 40 – 55 ppb O_3; 60 – 95 ppb O_3; (top right) hornbeam root biomass (Charcoal-filtered air (CTRL), Non-filtered (NF), elevated O_3 (OZ+ and OZ++) and (bottom right) above ground biomass of Mediterranean annual pastures (CF, NF, NF+20 ppb O_3 and NF + 40 ppb of O_3), with no added N (N0), 20kg ha^{-1} y^{-1} added N (N20) and 40kg ha^{-1} y^{-1} added N (N40).

Ozone alters nutrient absorption, utilisation and efficiency

New analysis of published data from exposure experiments conducted on wheat has revealed that O_3 reduces the efficiency of fertilizer inputs (WP9). The fraction of N, P and K added to wheat as a fertilizer that ends up in the grains is negatively affected by O_3 (Figure 3.4a). This means that plants are less able to utilize added nutrients under O_3 exposure which could potentially mean more nutrient losses to water supplies and also has important implications combined effects of O_3 and N pollutants at the ecosystem scale (see section 2.4). Other experiments showed that O_3 reduces the ability of legumes such as clover, a common constituent species of pasture to fix nitrogen (Hewitt et al., 2014, 2015). As well as impacting on the nutrient efficiency and fixation, O_3 also reduces the re-absorption of nutrients from the leaves into the over-wintering parts of plants at the end of the growing season. This effect was detected in data mining and was also found in ÉCLAIRE exposure experiments with silver birch. When all data were combined, there was a clear negative effect of O_3 on nutrient resorption (Figure 3.4b). As a consequence, more N is available in leaf litter for microbial decomposition in the soil, triggering changes in biogeochemical cycling (see also later in this report).
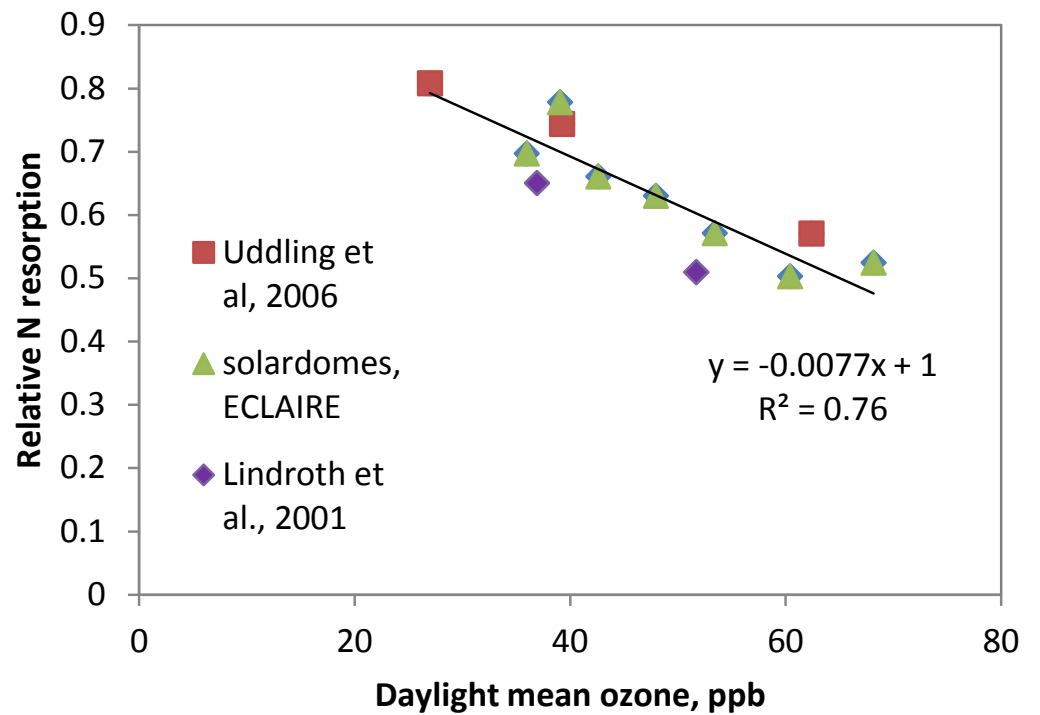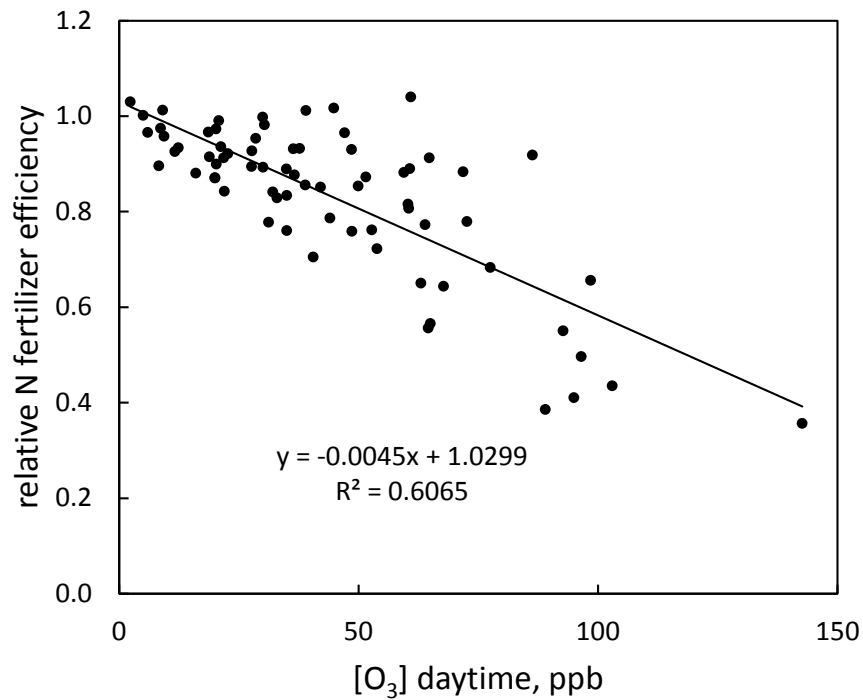
Figure 3.4: Effects of O₃ on (a) relative N fertilizer efficiency in wheat and (b) the resorption of leaf N in trees before litterfall; species are silver birch (solardomes, Uddling et al., 2006) and paper birch (Lindroth et al., 2001) (WP9 activity).

Ozone reduces the growth enhancing effects of nitrogen, and this is driven by effects on photosynthesis

New interaction experiments conducted in WP10 provided insight into the combined effects of O_3 and N on leaf processes and biomass production. Factorial experiments were conducted with two Mediterranean tree species, annual Mediterranean grassland species and silver birch involving 2 to 4 N treatments and 4 to 7 O_3 treatments. Since O_3 reduces growth and nitrogen increases growth, many have suggested that their effects could cancel each other out. When results from experiments in WP10 were combined with mined data from WP9, there was a clear indication that at higher O_3 concentrations in the range 60 – 95 ppb, the stimulating effect of increasing N on root biomass was completely lost (Figure 3.3a). This effect was evident in individual ÉCLAIRE experiments, for example in hornbeam (Figure 3.3b), and was also seen in the above ground biomass of annual Mediterranean pastures (Figure 3.3c; Calvete-Sogo et al., 2014) and total biomass of silver birch (Figure 3.5a).

At the leaf level, added N increased photosynthesis but this effect was less pronounced at higher O_3 (e.g. Figure 3.2); N partially alleviated the negative effects of O_3 on photosynthesis. The dynamics of combined effects of O_3 and N on photosynthesis during the growing season were included in the further development of the photosynthesis-based DO_3SE model of O_3 uptake and C assimilation (WP12). The new model, DO_3SE-C, was able to reproduce the response of biomass to the combined effects of O_3 and N deposition in ÉCLAIRE experiments (Figure 3.5a, b). In both experiments and modelling, the largest tree biomass occurred under situations with low O_3 and high N whilst the lowest biomass occurred under high O_3 and low N. In relative terms, the effect of increasing O_3 under high N is greater than the effects on biomass under low N.
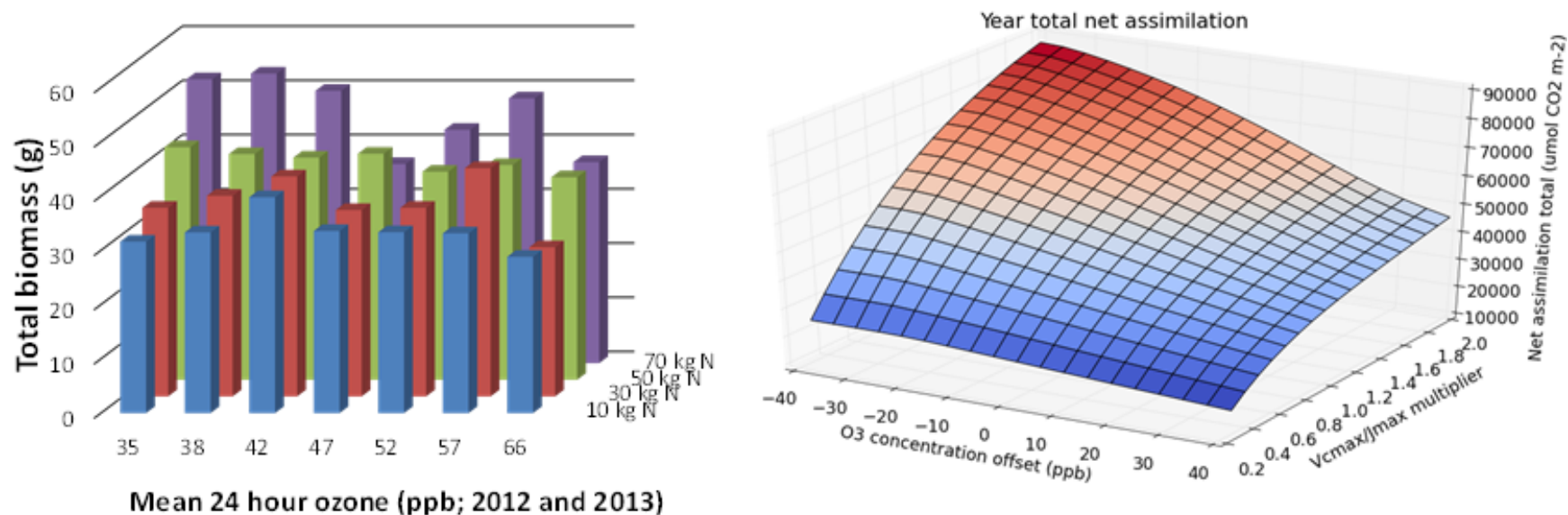
Figure 3.5: Silver birch experimental data (a) from ÉCLAIRE showing total biomass in relation to increasing O_3 concentration (x axis) and increasing N deposition (z axis) compared to silver birch model simulations (b) showing net assimilation (equivalent to biomass) in relation to an increasing O_3 concentration (x axis) and increasing V_{cmax} (proxy for leaf N and N deposition) (z axis).

Combined effects of ozone and N at the ecosystem scale are not additive

The dynamics of the impacts of O_3 and N on ecosystems were studied in several ways in the ÉCLAIRE project, including experimental investigations on grassland ecosystem processes, multi-factorial analysis of long-term forest ecosystems and modelling of temporal changes in greenhouse gas emissions and soil chemistry.

ÉCLAIRE provided funding in WP11 for additional measurements and data analysis for the final phase of a seven-year free air exposure of *Geo-Montani-Nardetum* subalpine grassland at 2000 m.a.s.l. in Switzerland to three O_3 concentrations and five nitrogen deposition rates in a cross-factorial design (Bassin et al., 2013). This high altitude site has a low background N deposition of ca. 4 kg N ha^{-1} y^{-1} and relatively high growing season mean O_3 concentration of 45 – 47 ppb. Under these high O_3 /low N and climatically challenging conditions, added N caused large changes in the community composition, with sedges becoming particularly dominant, whilst added O_3 at 1.2 and 1.6 x ambient had no effect on functional group composition and few effects on productivity; there were no significant O_3 x N interactions (Bassin et al., 2013 and references therein). The lack of sensitivity to O_3 was attributed to enhanced levels of anti-oxidants for tolerance of UV radiation at high altitude, continual exposure to high background rather than peak O_3 and enhanced natural resilience in this long-lived, slow-growing community.

A separate field-scale exposure experiment was conducted in the UK in WP11 in which coastal grassland swards from 7 sites with similar precipitation, soil pH and vegetation type but varying in their historical N deposition from 5.4 kg ha^{-1} yr^{-1} to 26 kg ha^{-1} yr^{-1} were exposed to ambient (mean 28 ppb), medium (mean 36 ppb) and high (mean 48 ppb) O_3 in the Free Air O_3 Exposure facility at NERC-Bangor. Long-term N deposition decreased total species richness whilst many species showed increased leaf injury and/or accelerated leaf senescence with increasing O_3 treatment (data not presented). In addition, the dissolved organic carbon (DOC) content of the water samples increased with increasing N and decreased with increasing O_3, probably corresponding to mesocosm productivity.

Fifteen years (1995 to 2010) of growth and deposition data from the LRTAP Convention's ICP Forests Europe-wide tree monitoring programme was analysed in WP9. It was found that relative forest increment increased up to a threshold of ca. 30 kg ha^{-1} y^{-1} of N, and levelled off at higher N levels. In general, deciduous forests were growing in areas with higher POD1 and N deposition values (17-21 kg N ha^{-1} yr^{-1}, 34-36 mmol POD1 m^{-2}), where POD1 is the accumulated phytotoxic O_3 dose over a threshold flux of 1 nmol m^{-2}, than coniferous forests (11-15 kg N ha^{-1} yr^{-1}, 23 mmol POD1 m^{-2}). For coniferous forests, POD1 and N deposition were strongly positively non-linearly related, making it difficult to disentangle the direct impact of N deposition and POD on growth. Thus, the negative impact of POD1 on forest growth was masked by the positive effect of N deposition and temperature on forest growth. However, at N saturated plots (high foliar N concentrations) POD1 showed a clear negative correlation to forest increment with a 2% decrease of

forest increment per 1 mmol m^{-2} POD1.

To gain further understanding of the combined effects of O$_3$ and N on ecosystems and predict long-term changes over the coming decades, the MADOC model of N and acidity effects on vegetation growth, soil organic matter turnover, acid-base dynamics, and organic matter mobility (Rowe et al., 2014) was expanded in WP13 to include O$_3$ and O$_3$ - N interactions. Following an extensive review of the literature on O$_3$ effects and O$_3$ - N interactions (WP9), strong and consistent evidence was found for two key ecosystem-scale effects: a reduction in Net Primary Productivity (NPP) and early leaf senescence, resulting in reduced resorption of N and a greater concentration of N in leaf litter. These effects were incorporated into the MADOC model using NPP reduction functions derived from the scientific literature in WP9 for wet grassland and bog, other grassland and woodland (Figure 3.2b). Site-specific date were collected from long-term measurement and/or manipulation sites as part of WP9 and used within MADOC for explorations of ecosystem sensitivity to combined air pollution and climate change drivers. Scenarios applied (from 2020) were increases in mean annual temperature of 2 and 4 °C, and increases and/or decreases in N and O$_3$ pollution by +/- 20%. Simulations showed broadly opposing responses to O$_3$ and N pollution at the ecosystem scale. In general, additional N deposition increases the amount of available N within the ecosystem, which in turn stimulates productivity in N-limited semi-natural ecosystems, as shown in Figure 3.6. These modelled increases in NPP have a cascading effect on other ecosystem properties and functions, for example leading to an increase in soil C (implying an increase in CO$_2$ sequestration) and increasing leaching of nitrate and DOC to surface waters. Although the magnitude of these effects are predicted to vary between ecosystems (compare left and right panels of Figure 3.6) the general direction of change is predicted to be consistent.
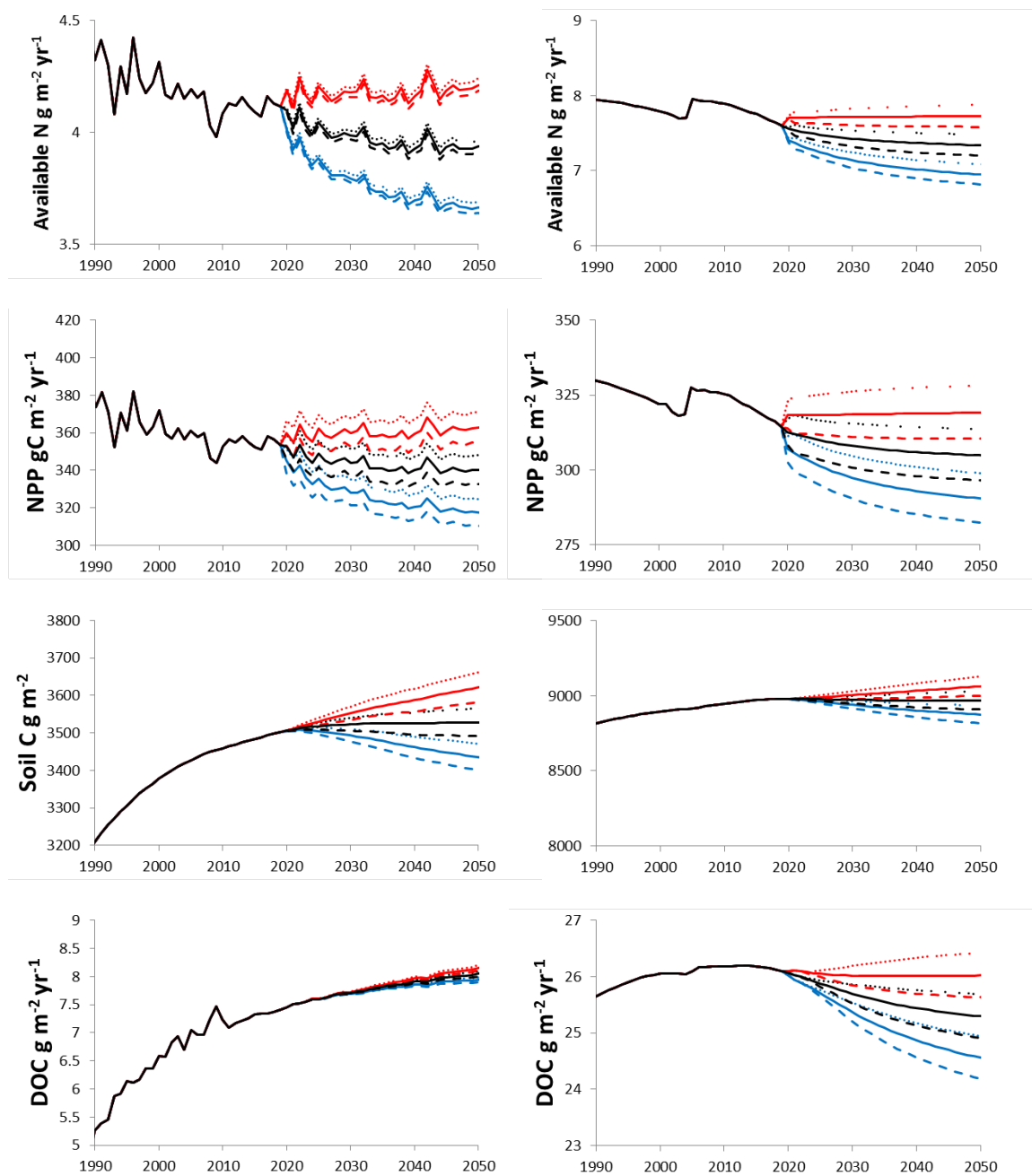
Figure 3.6: MADOC scenario assessment for the effects of changing future N and O₃ on simulations of soil available N, net primary production, soil carbon and leachate dissolved organic carbon for the Gårdsjön forest experimental site (left) and Whim Bog experiment (right). Red, black and blue lines represent high, business as usual and low N deposition scenarios; short-dashed, solid and long-dashed lines represent high, business as usual and low O₃ scenarios.

Aerosols damage stomatal functioning and reduce plant resistance to drought

Experiments were conducted in WP11 to determine the effects of hygroscopic particles on leaves from aerosol and trace gas deposition on stomatal control of water loss from leaves. It was found that ambient concentrations of aerosols depositing on leaves can reduce water use efficiency of plants (Figure 3.7). The particles provide a wick mechanism that increases stomatal conductance of water under conditions of low soil moisture availability – this effect is particularly deleterious for those species that are less able to respond to drying soils by closing stomata when soil moisture is limited. Plant species that have a morphology that is most efficient at capturing particles and/or long-lived leaves/needles are at greatest risk from this effect.

Monitoring of gas and aerosol concentrations in the experimental treatments (ambient and filtered air) in Bonn using resources from C1 (WP5) have provided the basis to establish a first dose response graph using minimum stomatal conductance as a first indicator.
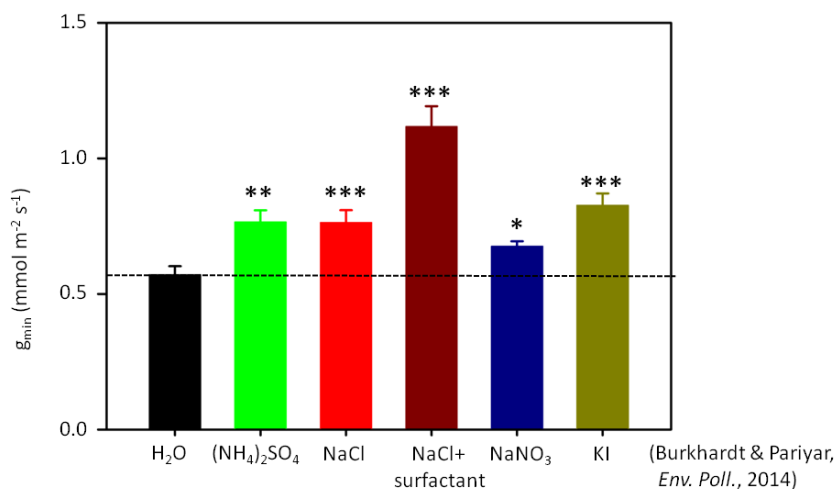
Figure 3.7: Effects of aerosols on the minimum stomatal conductance of leaves

Climate change will modify responses of vegetation and ecosystems to pollutants

A key objective of ÉCLAIRE has been to gain further insight into the combined effects of pollutants in a changing climate. In C3, this was addressed via data mining, experiments and modelling, including through the examples provided above. Additional climate change – interaction experiments were conducted for the crop barley under controlled climatic conditions and for dry heathland under field conditions (WP10). These

ÉCLAIRE Third Periodic Report: November 2015

experiments showed, for example, that for over 100 genotypes of barley, elevated temperature decreased, elevated CO_2 increased, and O_3 caused a small decrease in grain weight (Ingvordsen et al., 2015). Long term ecosystem experiments with dry heathland have demonstrated that drought, progressive nitrogen dilution and non-linear effects between climate change factors can reduce the CO_2 driven photosynthetic stimulation, and when O_3 was added to the system negative effects on photosynthesis were greater when plants were acclimated to long term elevated CO_2 and drought (data not presented). In a different study the effects of climate on inter-annual variability of annual Mediterranean pastures was analysed in WP10 in relation to O_3 sensitivity. In dry years, there was a very high proportion of less O_3 sensitive grass species whilst in moist years, O_3-sensitive herbs, particularly legumes dominated. Ozone fluxes were also lower in the dry than wetter years; if drier years become more prevalent as predicted under climate change, reduced O_3 effects will be offset by reductions in biomass and nutritive quality.

A combination of meta-analysis of published data and measurements of biogenic volatile organic compounds (BVOCs) within and above forest canopies and under experimental O_3 and N combinations was undertaken in order to gain further insight into the many factors that influence their emissions from plants. These are important in a changing climate because, depending on their chemical composition and presence/absence of other O_3 precursors they can lead to either the removal or enhanced formation of O_3. It was found, for example, that isoprenoid emissions increase with increasing temperature, and decrease with increasing CO_2 and soil water stress (Figure 3.8). By contrast, while monoterpene emissions responded less to temperature than isoprene, there was no significant evidence of a trade-off through increased CO_2 concentration. Effects of O_3 and N, single and in combination, were inconsistent in the scientific literature and new ÉCLAIRE measurements were made to provide further insight. In silver birch exposed to O_3 (Figure 3.5), O_3 exposure increased BVOC emissions whilst N treatment decreased emissions of some BVOCs such as α-pinene and β-pinene but increased emissions of others (data not presented). It was concluded that O_3 and N pollution have the potential to affect global BVOC via direct effects on plant emission rates and changes in leaf area.

Field measurements in a Mediterranean Holm oak forest showed that O_3 fluxes are highest during the central hours of warm days. This is due to both stomatal uptake of O_3 into the leaves and non-stomatal deposition of O_3 to leaf surfaces and via chemical reactions with monoterpenes and isoprenes released from the leaves of Holm oak during these climatic conditions. Low temperatures lead to almost negligible BVOC fluxes during the winter reducing non-stomatal sinks for O_3. In addition, during the day NO_2 formed and was deposited to the Holm oak canopy whilst at night O_3 was completely scavenged below the canopy by NO.

éclaire
Effects of climate change on air pollution impacts
and response strategies for European ecosystems
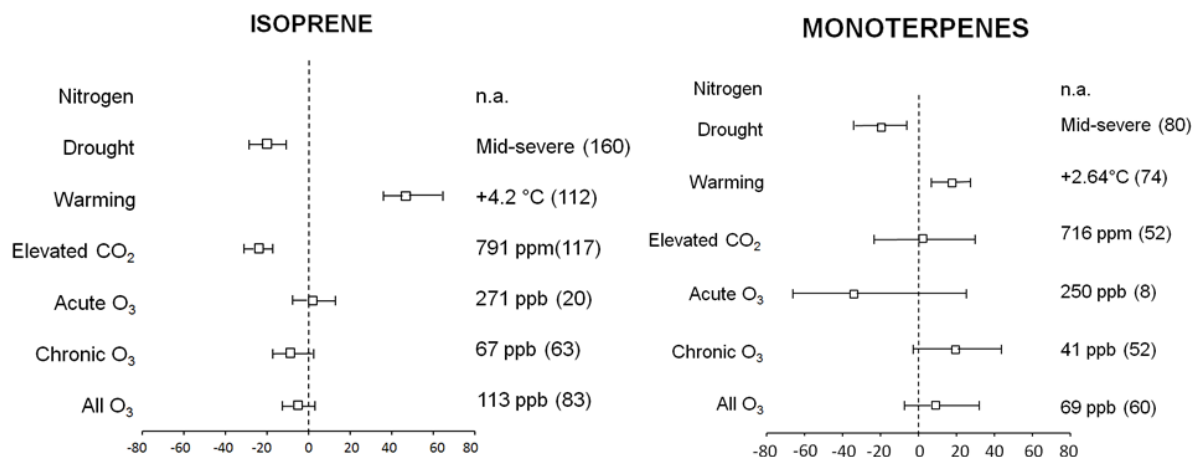
Figure 3.8: Percent change in isoprene and total monoterpenes emission under the effect of different climate change drivers. Symbols are bracketed by 95% bootstrapped confidence intervals. Mean level of stress and number of observations (in parenthesis) are also given.

Progress towards the milestones and deliverables, use of resources and deviations from DoW

Highlights and major achievements during the reporting period

- Integrated scientific approach across component, including outputs from datamining (literature-based, ecosystem-scale data, WP9) and experiments (WPs 10 and 11) being used by modellers in WPs12 and 13.
- A commonality of responses to the combined effects of ozone and nitrogen has been found in C3:
    - The critical importance of combined effects on leaf photosynthesis was identified. Incorporation of such effects into models resulted in a good match to experimental results allowing a range of O_3 and N interactions to be modelled from the leaf to whole plant scale.
    - Combined effects on vegetation are dynamic, with ozone induced increases in senescence becoming dominant later in the season
    - Importance of ozone as a modifier of nutrient (including N) use efficiency and resorption back into the plants as leaves senesce has important implication or the N cycle
    - At higher O_3 concentrations, the stimulating effect of increasing N on root (and whole plant) biomass was completely lost. This effect was evident in individual ÉCLAIRE experiments, for example in hornbeam, annual Mediterranean pastures, and silver birch.

- New information has emerged on BVOCs in forests, including effects of ozone, nitrogen and climate change on isoprene and monoterpene releases and potential effects on ozone deposition.
- Ecosystem-scale modelling has been used to predict future effects of ozone and N on net primary productivity, soil carbon stocks and mineral N leaching. In general, additional N deposition increases the amount of available N within the ecosystem, which in turn stimulates productivity in N-limited semi-natural ecosystems. These modelled increases in NPP have a cascading effect on other ecosystem properties and functions, for example leading to an increase in soil C (implying an increase in CO_2 sequestration) and increasing leaching of nitrate and DOC to surface waters.

Progress towards deliverables (milestones achieved are presented in the WP reports)

All milestones and deliverables for C3 have been achieved (for further detail please see WP reports).

References cited above

Bassin, S., Volk, M., Fuhrer, J., 2013. Species Composition of Subalpine Grassland is Sensitive to Nitrogen Deposition, but Not to Ozone, After Seven Years of Treatment. Ecosystems 16, 1105-1117.

Büker, P., Feng, Z., Uddling, J., Briolat, A., Alonso, R., Braun, S., Elvira, S., Gerosa, G., Karlsson, P.E., Le Thiec, D., Marzuoli, R., Mills, G., Oksanen, E., Wieser, G., Wilkinson, M., Emberson, L. D. New flux based dose-response relationships for ozone for European forest tree species. *Environmental Pollution*, in press

Calvete-Sogo, H., Elvira, S., Sanz, J., Gonzalez-Fernandez, I., García-Gomez, H., Sanchez-Martín, L., Alonso, R., Bermejo-Bermejo, V., 2014. Current ozone levels threaten gross primary production and yield of Mediterranean annual pastures and nitrogen modulates the response. Atmos. Environ. http://dx.doi.org/ 10.1016/j.atmosenv.2014.05.073

Hewitt, D.K.L, Mills, G., Hayes, F, Norris, D., Coyle, M., Wilkinson, S. & Davies, W. N-fixation in Legumes – an assessment of the potential threat posed by ozone pollution. *Environmental Pollution*, in press. doi:10.1016/j.envpol.2015.09.016

Hewitt, D.K.L.; Mills, G.; Hayes, F.; Wilkinson, S.; Davies, W. 2014. Highlighting the threat from current and near-future ozone pollution to clover in pasture. *Environmental Pollution*, 189. 111-117

Ingvordsen CH, Backes G, Lyngkjær MF, Peltonen-Sainio P, Jensen JD, Jalli M, Jahoor A, Rasmussen M, Mikkelsen TN, Stockmarr A, Jørgensen RB. Significant decrease in

ÉCLAIRE Third Periodic Report: November 2015

yield under future climate conditions: Stability and production of 138 spring barley accessions. Eur J Agron 2015; 63:105-113

Lindroth, R.L., B.J. Kopper, W.F.J. Parsons, J.G. Bockheim, D.F. Karnosky, G.R. Hendrey, K.S. Pregitzer, J.G. Isebrands and J. Sober. 2001. Consequences of elevated carbon dioxide and ozone for foliar chemical composition and dynamics in trembling aspen (*Populus tremuloides*) and paper birch (*Betula papyrifera*). Environ. Pollut. 115:395–404

Rowe, E.C.; Tipping, E.; Posch, M.; Oulehle, Filip; Cooper, D.M.; Jones, T.G.; Burden, A.; Hall, J.; Evans, C.D. 2014. Predicting nitrogen and acidity effects on long-term dynamics of dissolved organic matter. Environmental Pollution, 184. 271-282.

Uddling **J**, Karlsson PE, Glorvigen A, Selldén G (2006) Ozone impairs autumnal resorption of nitrogen from birch (*Betula pendula*) leaves, causing an increase in whole-tree nitrogen loss through litter fall. *Tree Physiology* 26: 113-120

Work package 9   Synthesis and meta-analysis of measurements of plant and soil responses

Lead contractor: NERC (BAN)
Contributors: NERC (EDI), SIY-Y, IVL, UGOT, ALTERRA, WSL, DTU

Work package objectives

1. To conduct a pan-European data mining exercise compiling data from previous survey, field-scale manipulation and controlled exposure experiments on air pollution impacts on ecosystem function and services, including interactions with other drivers such as climate change

2. To conduct a meta-analysis on the compiled data to provide a priority analysis for the modelers of the most important effects and associated processes

3. To analyse the data to develop a database of response-relationships for key ecosystem processes, functions and services to air pollutants (singly, and where available, in combination) including the influence of climate change, for use in activities WP12 and WP13.

4. To identify key knowledge gaps that can be filled by experimentation in WP10 and WP11.

Progress and Results

All of the tasks and associated deliverables for this work package were completed in the previous period as noted in the second periodic report.

Progress towards the milestones and deliverables

As above, all deliverables were already completed at the time of reporting.

Use of resources and deviations from DoW

The outcomes of previous work periods were used as input to other work packages during this period, The total person months for this work package, for the project as a whole, was as planned at 47 man months.

Work package 10 – Field Studies on Exchange Processes

Lead contractor: CIEMAT have taken over from DTU
Contributors: UNICATT, FDA-ART, NERC (BAN), DTU, CIEMAT

Work package objectives

1. To conduct relevant field-scale and controlled-exposure experiments on impacts of air pollution components on plant and ecosystem processes including interactions with climate change.
2. To use these experiments to quantify impacts of air pollution, in particular ozone and nitrogen components on key ecosystem processes, greenhouse gas exchange and ecosystem carbon balances
3. To provide inputs for developments and parameterization for modeling (WP13).

Progress and Results

Task 10.1 – Forest site experiments

NERC (BAN) has developed an experiment in solardomes for analysing the interactive effects of ozone and nitrogen on birch (*Betula pendula*). The assay involved 7 ozone treatments (with mean ozone concentrations between 35 and 66 ppb) and 4 nitrogen treatments (10, 30, 50 and 70 kg/ha/yr) and took place in 2012 and 2013. Physiological measurements were made during the course of the experiment and trees were destructively harvested to give biomass measurements after the end of the second growing season. Data analysis has continued subsequently. In addition, data from the experiment has contributed to derivation of response functions to ozone for growth and leaf-N resorption which were subsequently used in ecosystem-scale modelling with the MADOC model (WP13). Leaf-level physiological data from this experiment was used to parameterise and test the new photosynthesis-based DO$_3$SE model (WP12).

Main results are:

- **Analysis of biomass measurements at the end of the second growing season showed that nitrogen stimulated growth of the birch trees, but at high ozone concentrations the stimulating effect of N on biomass was much reduced** (Figure 3.9).

- **At higher ozone concentrations less of the leaf N was transported back into the** tree before the leaves fell than at lower ozone concentrations; this caused a higher N content of the litter, which has potential effects on litter cycling. (Figure 3.10).

ÉCLAIRE Third Periodic Report: November 2015
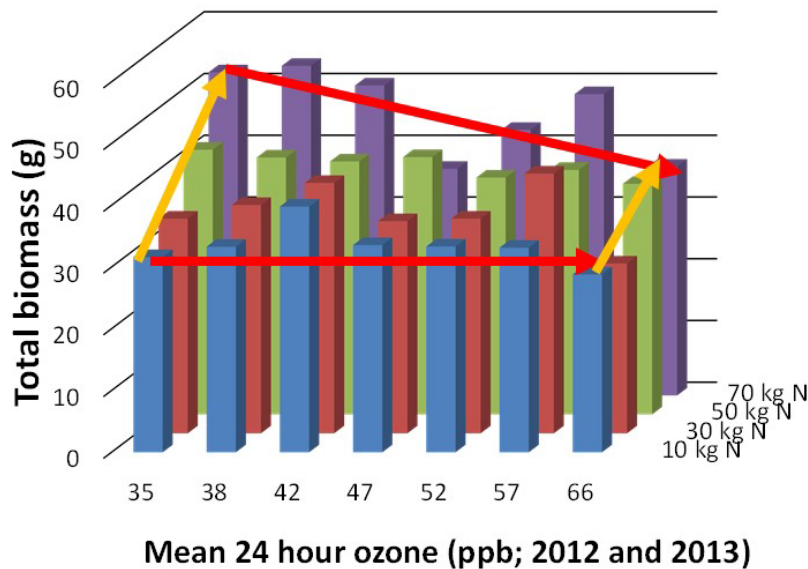
Figure 3.9: Effect of ozone and nitrogen on biomass of birch after 2 growing seasons.
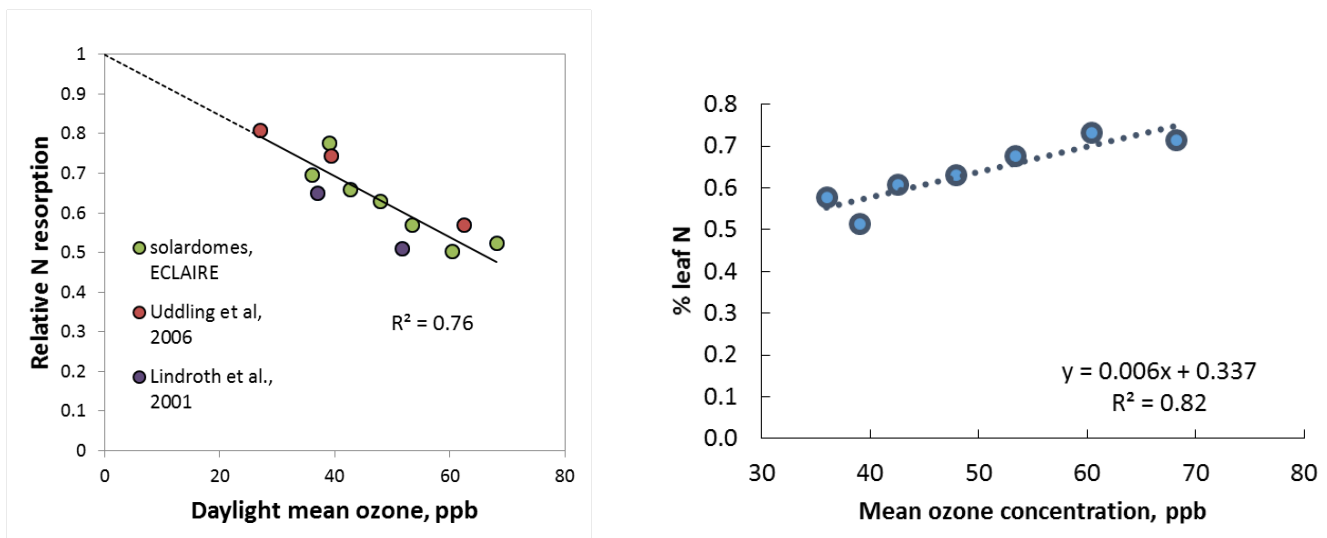
Figure 3.10: Impact of ozone exposure on the leaf nitrogen concentration of silver birch leaves at leaf-fall (a), and relative N resorption from senescing leaves in response to ozone, based on the combined dataset from this experiment and ÉCLAIRE data mining (b).

- **Maximum stomatal conductance (and therefore capacity for ozone uptake) was increased with increasing N** (Figure 3.11) and the increase was approximately 15% when N treatment was increased from 10 to 70 kg/ha/yr. This increase in maximum stomatal conductance was found in both years. Measurements of stomatal conductance made throughout the growing seasons were used to parameterize a stomatal flux model, allowing results to be compared to stomatal ozone uptake in addition to ozone concentration parameters.
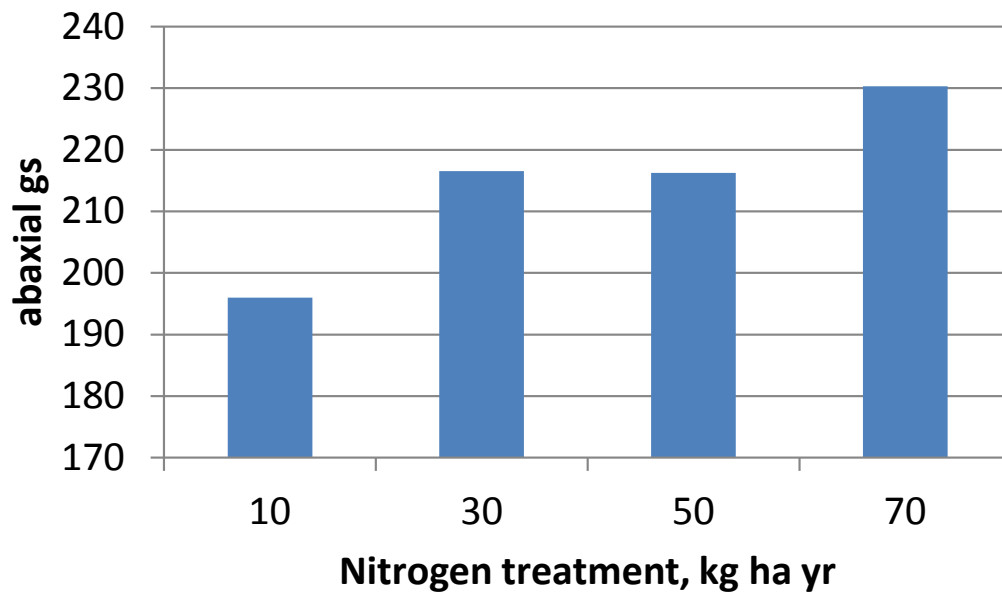
Figure 3.11: Stomatal conductance (abaxial) in response to nitrogen treatment.

- **Early in the season high N supply stimulated photosynthetic capacity of birch leaves with both low and high ozone treatments; in contrast, high ozone reduced photosynthetic capacity** although this was only statistically significant at low N supply. There was no statistically significant interaction between the ozone and N treatments on photosynthetic capacity (Figure 3.12).
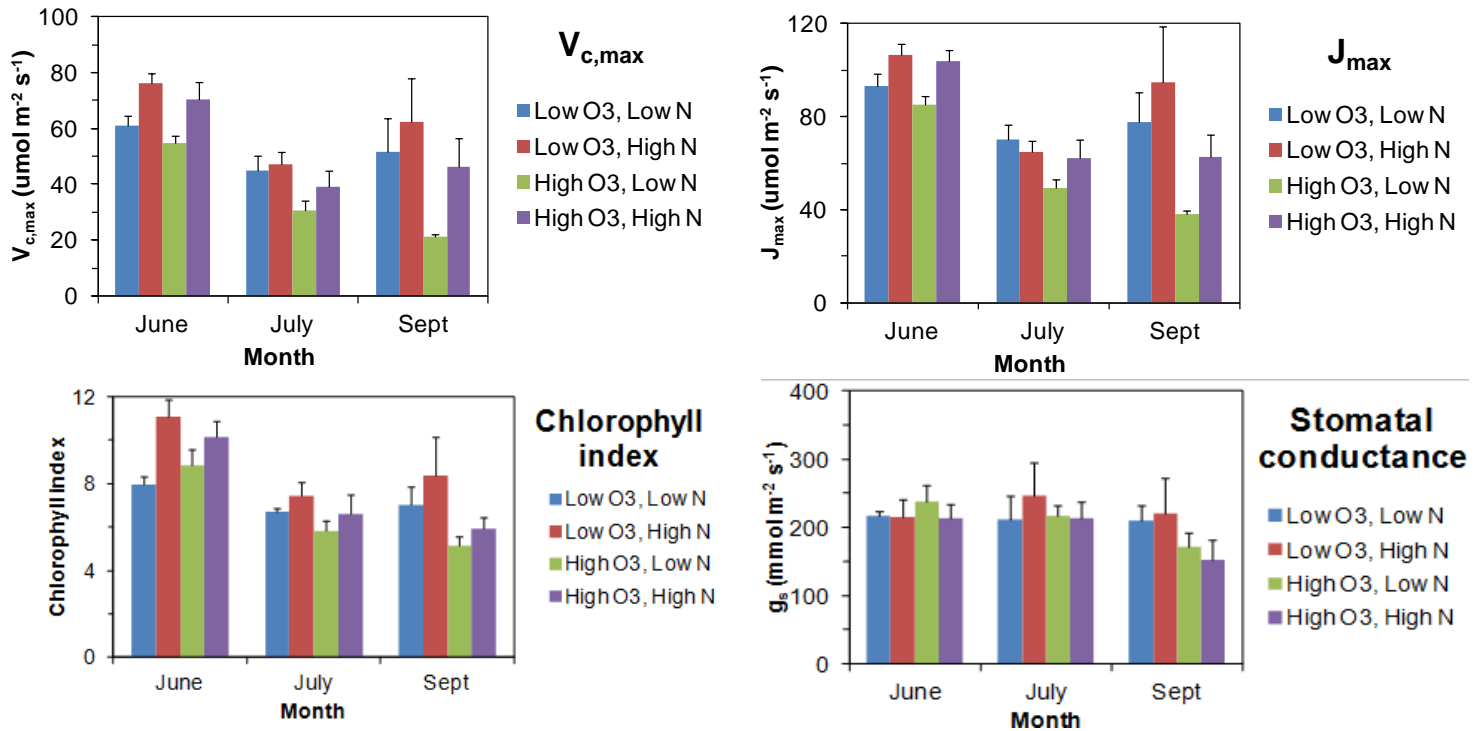
Figure 3.12: Response to ozone and nitrogen on V_{cmax} (top left), J_{max} (top right), chlorophyll index (bottom left) and stomatal conductance (bottom right) of *Betula pendula.*

- **The negative effect of ozone on photosynthetic capacity increased over time, but the interaction with time was statistically significant for J_{max}** (maximum rate of photosynthetic electron transport) and not for V_{cmax} (maximum carboxylation rate allowed by Rubisco).

- The response of chlorophyll index to the ozone and nitrogen treatments was similar to that of V_{cmax}. **There was a linear relationship between A_{sat} and chlorophyll index, indicating that the non-destructive measurement of chlorophyll index can give a good estimation of A_{sat}** (Figure 3.13).
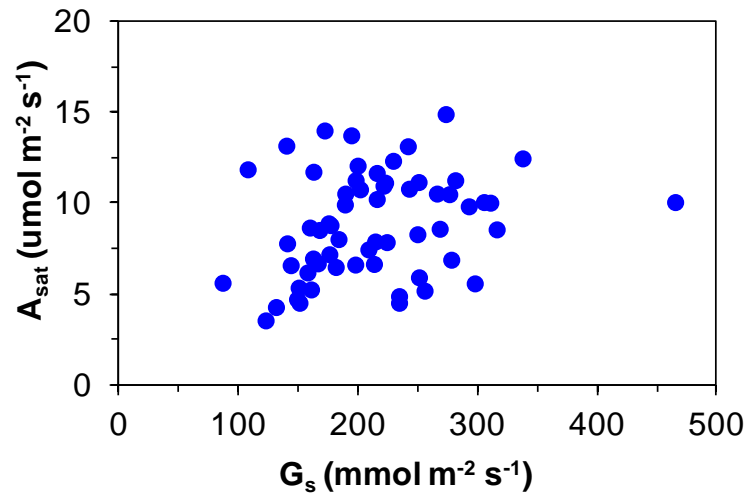
Figure 3.13: Relationship between light-saturated rate of photosynthesis (A_{sat}) and chlorophyll index (left) and stomatal conductance (right).

- **Ozone exposure induced a linear decline in A_{sat}** ($p<0.01$) from data measured at the end of August at an N supply of 10 and 70 kg ha^{-1} y^{-1}) (Figure 3.14). At the end of August, A_{sat} was also measured in additional ozone treatments. **Enhanced N supplied stimulated A_{sat} (P = 0.01) but there was no interaction between ozone exposure and N supply**. A similar response was observed for the chlorophyll index. There was no relationship between A_{sat} and stomatal conductance, suggesting that impacts of treatment on A_{sat} were mainly driven by impacts on photosynthetic capacity of the chloroplasts rather than changes in stomatal conductance.
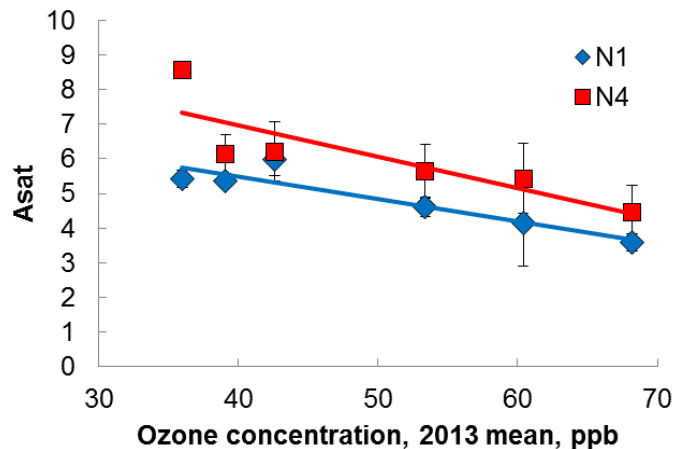
Figure 3.14: Mean light-saturated rate of photosynthesis (A_{sat}) in the last week of August in response to ozone, at low and high nitrogen concentrations.

201

UNICATT performed a two-year Open-Top Chambers experiment on young trees of oak (*Quercus robur*) and European hornbeam (*Carpinus betulus*). The experiment was conducted at the OTCs facility of Curno (Northern Italy), from April 2012 to September 2013. Plants were subjected to 4 different levels of ozone (CF=-50%, NF=-5%, NF+=+35% and NF++=+70% of ambient ozone) and two different levels of nitrogen wet deposition (-N=control and +N=+70Kg/ha year-1). The experiment was aimed at the following main objectives: i) to assess the effect of high levels of O_3 on oak and hornbeam considering their responses at physiological and biomass level, ii) to investigate whether these responses can be significantly altered by increased nitrogen wet deposition.

Main results regarding oak are:

- **Oak plants confirmed to be moderately sensitive to O_3 in particular roots dry biomass** that was significantly reduced on average by 10% after two years of treatments (Figure. 3.15). This might affect the tolerance of the tree to water deficit stress.

ÉCLAIRE Third Periodic Report: November 2015
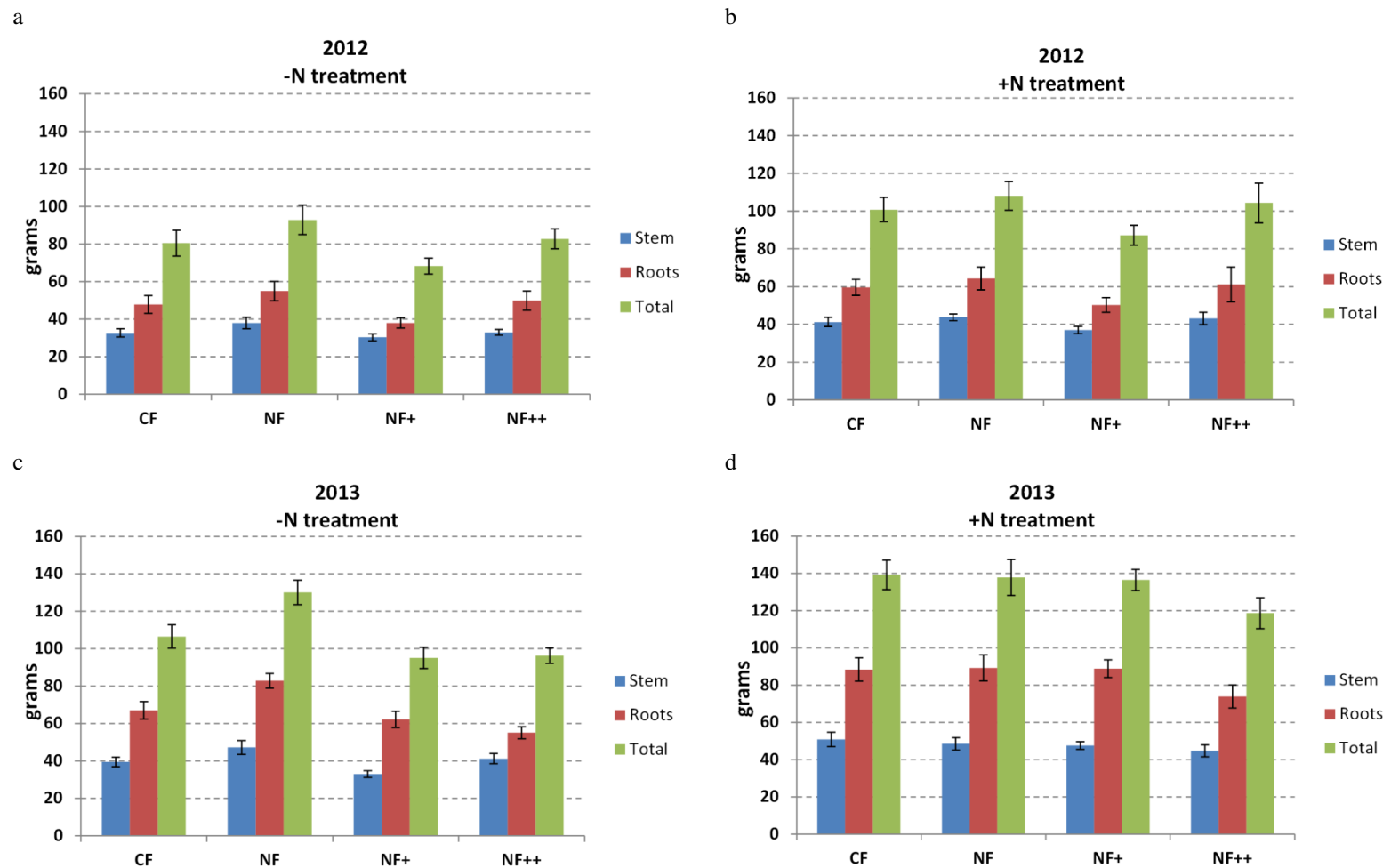
Figure 3.15: Mean dry weight (stem (blue bars), roots (red bars) and total (green bars) of oak at the end of the two growing seasons of the experiment (2012 and 2013) in the four O₃ treatments (CF, NF, NF+ and NF++) and two nitrogen treatment (-N and +N). Bars represent standard error.

éclaire
Effects of climate change on air pollution impacts
and response strategies for European ecosystems

- **Ozone exposure reduced the number of leaves per plant** by 17 unit every 10 ppb of O_3 increase after the second year of treatment (Figure 3.16), but this effect disappeared in nitrogen treated plants.
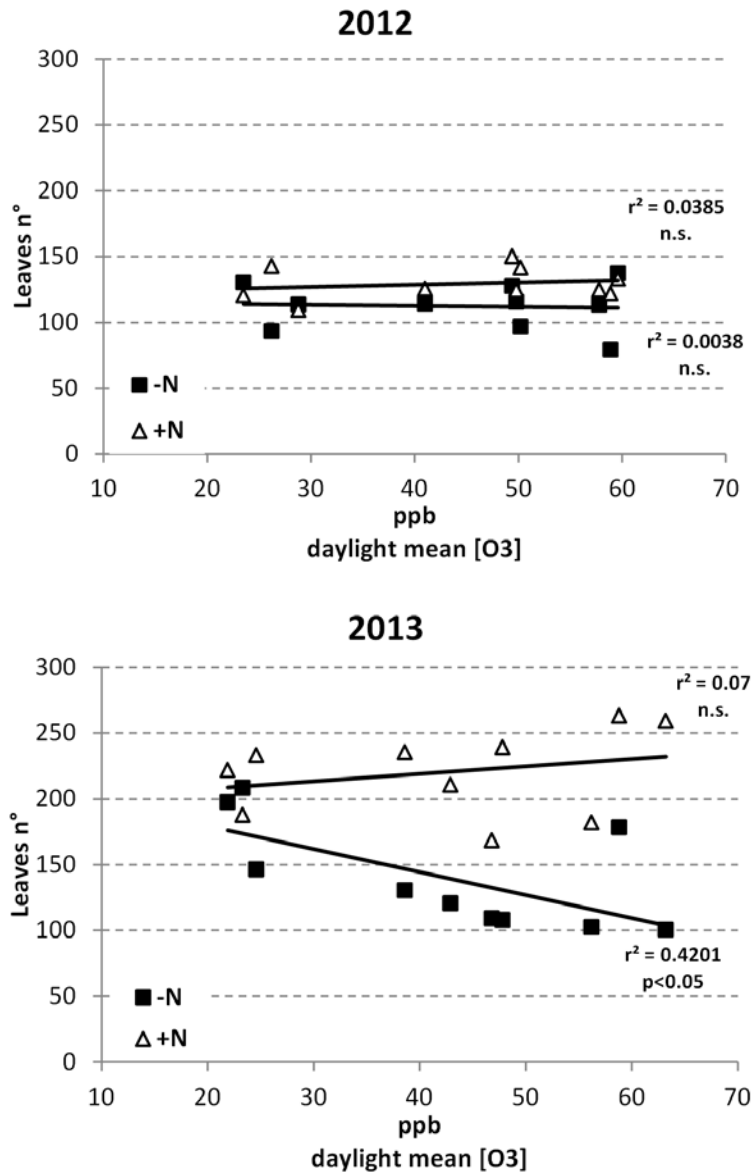
Figure 3.16: Regression analysis between the mean number of leaves of oak at the end of the growing seasons (2012 and 2013) and the seasonal mean O_3 concentration for the daylight 12hours (8 AM – 8 PM) registered in the OTCs. +N= increased nitrogen – N=control.

- **Increased nitrogen deposition enhanced plant growth, both roots and stems, and was partially contrasted by the O₃ impact**, but no significant effect of the interaction between the two factors was found (Table 3.3.).

Table 3.3 Statistical significance of the differences in biomass due to O_3, nitrogen and their interaction (ozone x nitrogen) in oak.

OAK	Ozone	Nitrogen	Ozone x Nitrogen
2012	*p* value	*p* value	*p* value
Stem biomass	0.1042 n.s.	*0.0004* ***	0.6742 n.s.
Roots biomass	0.3587 n.s.	*0.0365* *	0.9959 n.s.
Total biomass	0.2580 n.s.	*0.0060* **	0.9735 n.s.
2013	*p* value	*p value*	*p* value
Stem biomass	0.3338 n.s.	*0.0119* *	0.2734 n.s.
Roots biomass	**0.0330** *	*0.0019* **	0.4539 n.s.
Total biomass	*0.0516 q.s.*	*0.0015* **	0.2921 n.s.

*q.s. p≤0.06 (quasi-significant)   * p≤0.05   ** p≤0.01   *** p≤0.001*

![éclaire logo]
Effects of climate change on air pollution impacts
and response strategies for European ecosystems

- **Ozone caused a decline of both stomatal conductance (g_s) and the Rubisco maximum carboxylation rate (V_{cmax})**. However **some physiological adaptation to the stress was observed after during the second year O_3 exposure**. Then an uncoupling between leaf-level physiological response and plant-level biomass response was found (Figure 3.17).
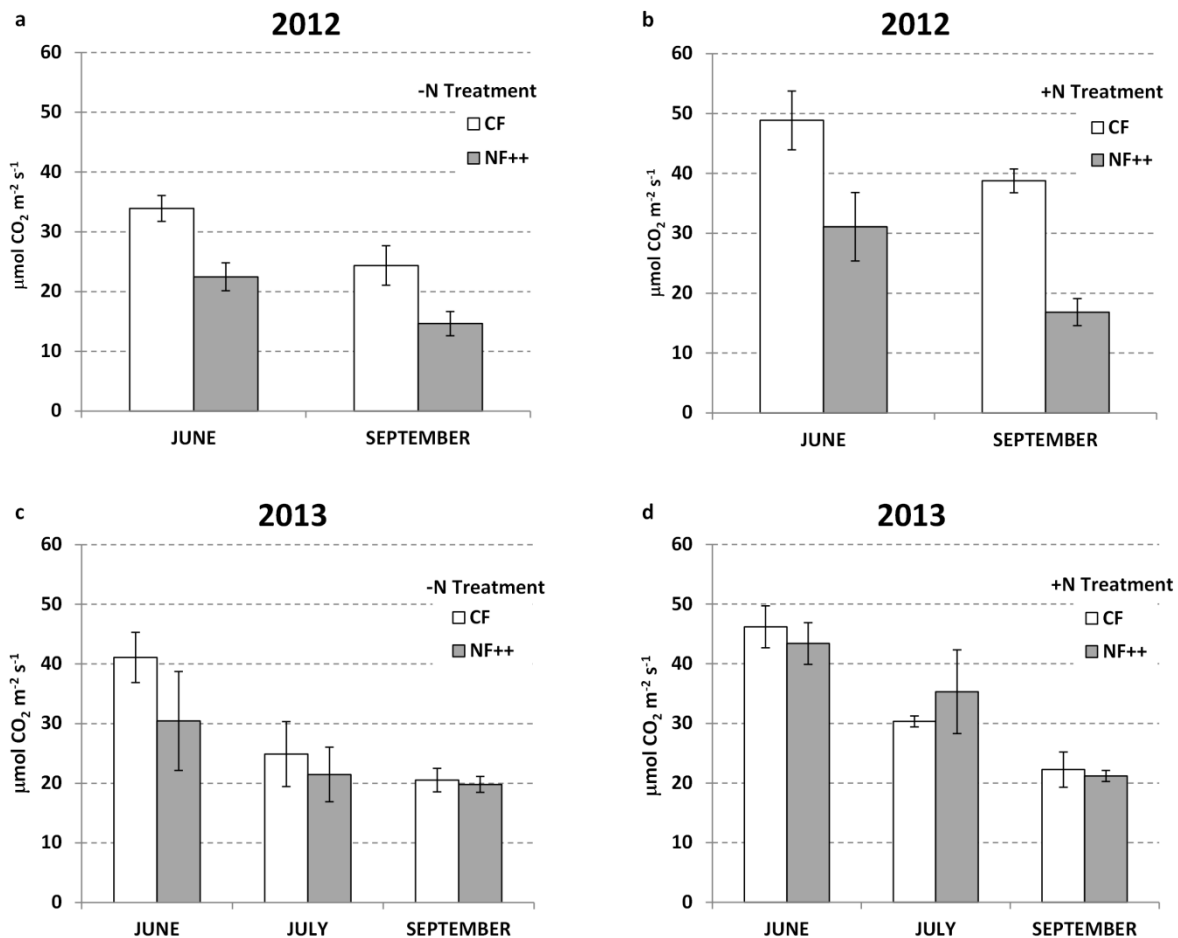
Figure 3.17 Mean maximum carboxylation rate of RuBisCO (V_{cmax}) of oak in the two growing seasons of the experiment. Results are separated between plants without increased N deposition (a, c) and plant with increased nitrogen deposition (b, d). Bars represent standard error. CF=Charcoal-Filtered OTCs, NF++=ozone enriched OTCs.

206

Main results regarding hornbeam:

- **Hornbeam biomass parameters showed no significant reduction due to ozone after two years of exposure** (Figure 3.18).

- **Nitrogen affected positively both biomass and physiological parameters, although the growth stimulation was unbalanced towards the stems.**

- **After two years of treatment nitrogen caused an increase of susceptibility to ozone in hornbeam plants grown in the most enriched ozone treatment (NF++) and this effect was mainly driven by the stem biomass decrease of plants** (Figure 3.18). This interaction effect between ozone and nitrogen was statistically significant for the stem biomass (Table 3.4, $p=0.0175$) and very close to be significant for the total biomass of plants (Table 3.4, $p=0.0576$).
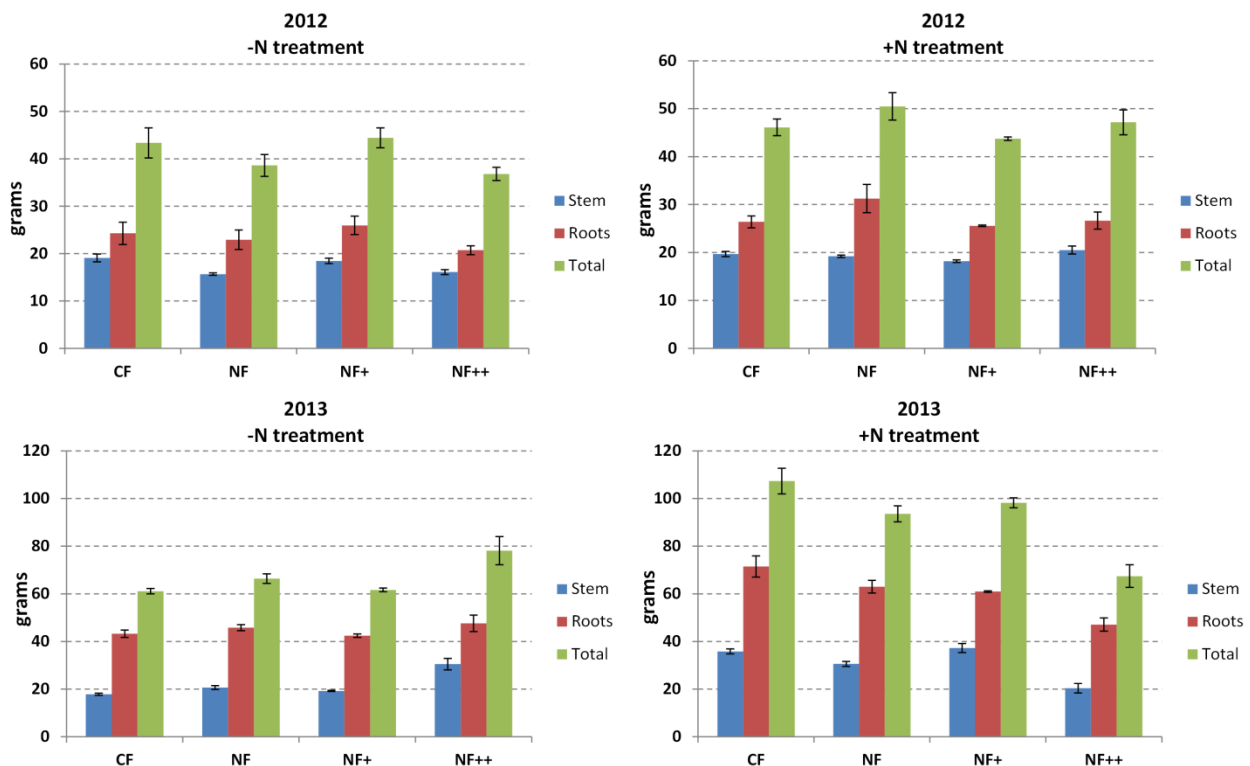
Figure 3.18 Mean dry weight (stem, roots and total) of hornbeam at the end of the two growing seasons of the experiment (2012 and 2013) in the four O_3 treatments (CF, NF, NF+ and NF++) and two nitrogen treatment (-N and +N). Bars represent standard error.

éclaire
Effects of climate change on air pollution impacts
and response strategies for European ecosystems

Table 3.4: Statistical significance of the differences in biomass due to O_3, nitrogen and their interaction (Ozone x Nitrogen) in hornbeam

HORNBEAM	Ozone	Nitrogen	Ozone x Nitrogen
2012	*p* value	*p* value	*p* value
Stem biomass	0.6385 n.s.	**0.0013 ****	**0.0134 ***
Roots biomass	0.7670 n.s.	*0.0535 q.s.*	0.3639 n.s.
Total biomass	0.9010 n.s.	**0.0147 ***	0.1466 n.s.
2013	*p* value	*p* value	*p* value
Stem biomass	0.6801 n.s.	**0.0099 ****	**0.0175 ***
Roots biomass	0.2871 n.s.	**0.0019 ****	0.1433 n.s.
Total biomass	0.4464 n.s.	**0.0046 ****	*0.0576 q.s.*

q.s. p≤0.06 (quasi-significant)   * p≤0.05   ** p≤0.01   *** p≤0.001

- **Ozone exposure produced a slight but not significant negative effect on stomatal conductance and V_{cmax} at the beginning of the second growing season, but this effect became negligible at the end of the experiment** (Figure 3.19).

-

As a general conclusion, data analysis highlighted that **the effects detected at leaf-level, like single-point physiological measurements performed during the growing season, resulted often uncoupled with plant-level responses such as growth and biomass parameters**, which provide a time integrated measurement of the effects at individual level. Moreover, due to the relatively short duration of the experiment, no consideration can be made on the long-term effects of nitrogen soil saturation on plants.
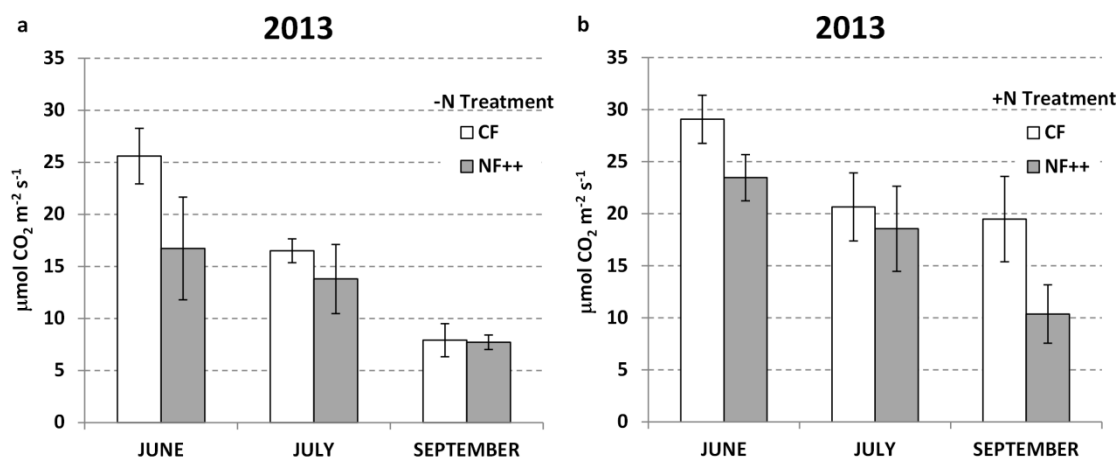
Figure 3.19 – Mean maximum carboxylation rate of RuBisCO (V_{cmax}) of hornbeam in 2013. Results are separated between plants without increased N deposition (a) and plant with increased nitrogen deposition (b). Bars represent standard error. CF=Charcoal-Filtered OTCs, NF++=ozone enriched OTCs.

Between October 2014 and September 2015, data collected during the experiment were statistically analyzed. Measurements performed on biomass and physiology as well as all the ancillary measurements of the experiment (meteorology conditions and ozone monitoring) were organized in two databases and uploaded to the ÉCLAIRE site.

The main results of the experiment have been communicated at the ÉCLAIRE General Assembly of Edinburgh and presented at the ICP Vegetation meeting of Rome in 2015.

Publications:

- Gerosa G., Fusaro L., Monga R., Finco A., Fares S., Manes F., Marzuoli R. 2015. A flux-based assessment of above and below ground biomass of Holm oak (*Quercus ilex* L.) seedlings after one season of exposure to high ozone concentrations. Atmospheric Environment, 113, 41–49. doi:10.1016/j.atmosenv.2015.04.066
- Monga R., Marzuoli R., Alonso R., Bermejo V., Gonzalez-Fernandez I., Faoro F., Gerosa G., 2015. Varietal screening of ozone sensitivity in Mediterranean durum wheat (Triticum durum, Desf.). Atmospheric Environment 110, 18-26. DOI: 10.1016/j.atmosenv.2015.03.04.
- Gerosa G., Finco A., Chiesa M., Marzuoli R. 2014. Plants in the city and their gaseous exchanges with the atmosphere. A possible way to estimate the air pollutant removal by plants and the related biological cost. Agrochimica, 58 (3), 269-289. doi:10.12871/0021857201434.
- Marzuoli R., Monga R., Finco A., Gerosa G. 2015. Biomass and physiological responses of Quercus robur (L.) young trees during two years of treatments with ozone and nitrogen wet deposition (submitted).
- Gerosa G., Finco A., Marzuoli R. 2016. Effects of ozone exposure and increased nitrogen deposition on biomass and physiology of *Carpinus betulus* (L.) young trees (in preparation)

Task 10.2 Agricultural experiments

DTU developed a barley experiment conducted in phytotron. In the study a set of 108 spring barley (*H. vulgare* L.) accessions were cultivated under predicted future levels of temperature and CO_2 as single-factors and their combination (IPCC, AR5, ~ RCP 8.5). Results are currently under publication (submitted to *Journal of Experimental Botany*).

The major results are:

- **Climate change is predicted to decrease future grain yields and influence grain protein concentration**.

- **The found 8% increase in grain protein concentration under the combined treatment of elevated temperature and [CO₂] could not be depicted from the single factor treatments (Table 3.5).**

- **The grain protein harvested only increased under elevated CO₂ and was lowered 23% in the future climate scenario of elevated temperature and CO₂.** In a future scenario with projected lowered grain yield, harvesting as much protein as possible seems desirable

- **Variation in the response of the 108 accessions was identified. This variation should be further exploited to increase the grain protein harvested under future climate change conditions**, in order not only to increase yield but to improve or maintain the quality of the yield.

Table 3.5: Overall averaged parameters for the 108 barley accessions cultivated under future elevated levels of atmospheric carbon dioxide concentration (e[CO₂]), elevated temperature (eTmp) and under the combined treatment (eTmp & e[CO₂]) as well as under ambient (amb). * specifies significant difference from the ambient treatment determined by t-test.

	amb	eTmp & e[CO$_2$]	e[CO$_2$]	eTmp
Grain protein concentration (%)	13.97±1.82	15.06±1.97***	13.33±1.91*	18.03±2.18***
% different from ambient		*7.86*	*-4.85*	*29.11*
Grain yield per plant (g)	6.85±1.29	4.92±1.18***	8.02±1.94***	3.08±1.13***
% different from ambient		*-28.12*	*17.10*	*-54.98*
Grain protein harvested per plant (g)	0.95±0.20	0.74±0.19***	1.07±0.31**	0.55±0.20***
% different from ambient		*-22.53*	*12.46*	*-42.26*

Publications:

- Ingvordsen CH, Backes G, Lyngkjær MF, Peltonen-Sainio P, Jensen JD, Jalli M, Jahoor A, Rasmussen M, Mikkelsen TN, Stockmarr A, Jørgensen RB. 2015. Significant decrease in yield under future climate conditions: Stability and production of 138 spring barley accessions. European Journal of Agronomy 63, 105-113.

- Ingvordsen, C.H., Gislum, R., Jørgensen, J.R., Mikkelsen, T.N., Stockmarr, A., Jørgensen, R.B. Grain protein under future climate conditions. A lesson from 108 4 spring barley accessions (*H. vulgare* L.) (Submitted to Journal of Experimental Botany).

- Albert K.R., Mikkelsen T.N., Ro-Poulsen H., Beier C. Long term acclimation to elevated CO_2 and drought increases the ozone toxicity in plants. (In preparation).

CIEMAT has performed a two-year study analysing ozone effects on the main Mediterranean leafy crops (spinach, lettuce, chard and endive) and the modulation of the response by nitrogen fertilization.

First experiment was developed in two OTC field sites located in two Mediterranean climates: continental (Toledo) and oceanic (Valencia), between February-May 2013. The experiment was an ozone-sensitivity screening of 14 cultivars from 4 species of leafy crops. Four ozone treatments were considered. Different parameters were measured for analysing the physiological mechanisms of the effect: Gas exchange parameters, response curves A/Ci and A/PAR, Growth, leaf C/N rate and leaf damage. A second experiment to analyse the nitrogen modulation of the ozone response considering chard and spinach, the most ozone sensitive species, was set up between May-July 2014. The experiment was developed in the Madrid OTC site in field conditions (grown according to the commercial practices in the area). Two nitrogen (background and 100 kg N ha^{-1}) levels were added to the 4 ozone treatments following and split-plot design. Gas exchange, response curves (A/Ci and A/PAR), growth parameters, C/N leaf rate and leaf damage were measured. Samples are still under lab analysis and statistical analyses are on progress.

Main results were:

- **The raking of ozone sensitivity of the leafy crops based on visible injury, yield and gas exchange parameters was (starting from the most ozone sensitivity): Spinach>Chard>Endive>Lettuce. This ranking is consistent regarding cultivars and climatic conditions.**

- **For Chard and Spinach, the most ozone-sensitive species, the ozone exposure reduced the photosynthetic activity and the stomatal conductance of all the cultivars; although the intensity of the effect was greater in the coastal site** (Figure 3.20). Coastal site presented similar O_3 levels than the continental site but lower VPD that would favour higher stomatal conductance and higher ozone fluxes inside the plant. However stomatal conductance was lower at the coastal site.
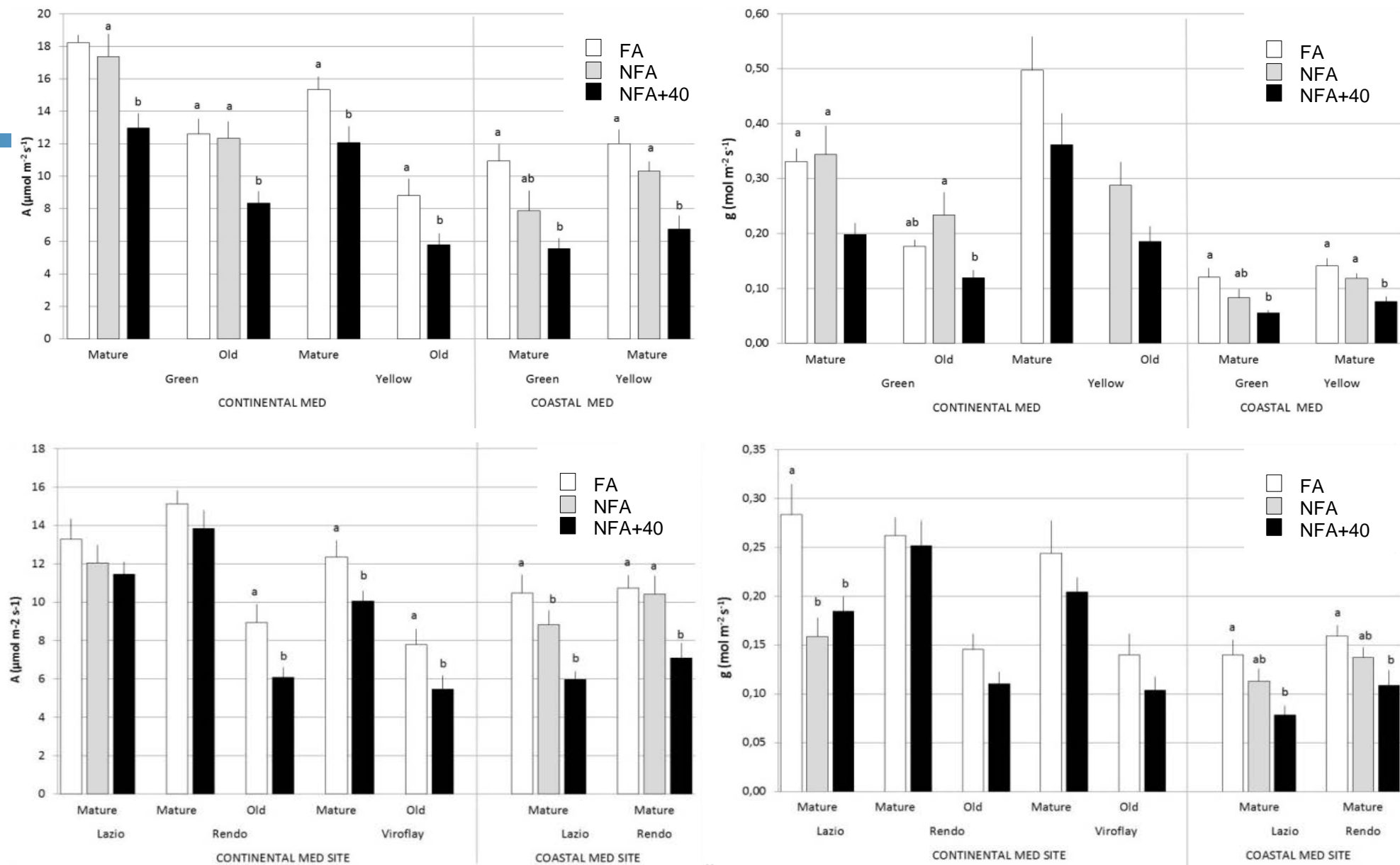
Figure 3.20: Photosynthetic activity (A µmol CO_2 m^{-2} s^{-1}) and stomatal conductance (g mol H_2O m^{-2} s^{-1}) measured in continental and coastal Mediterranean sites for different cultivars, leaf ages (mature, old) and ozone exposures: a) green and yellow chard cultivars b) Lazio, Rendo and Viroflay Spinach cultivars. FA= charcoal filtered air; NFA= non filtered air; NFA+=non filtered air + 20 nl l^{-1} of O_3; NFA++=non filtered air + 40 nl l^{-1} of O_3. (Mean± se).

- **Exposure to ozone reduce the efficiency of the Rubisco carboxylation in the most O$_3$-sensitive leafy crops causing a reduction in the carbon fixation (Figure 3.21)**
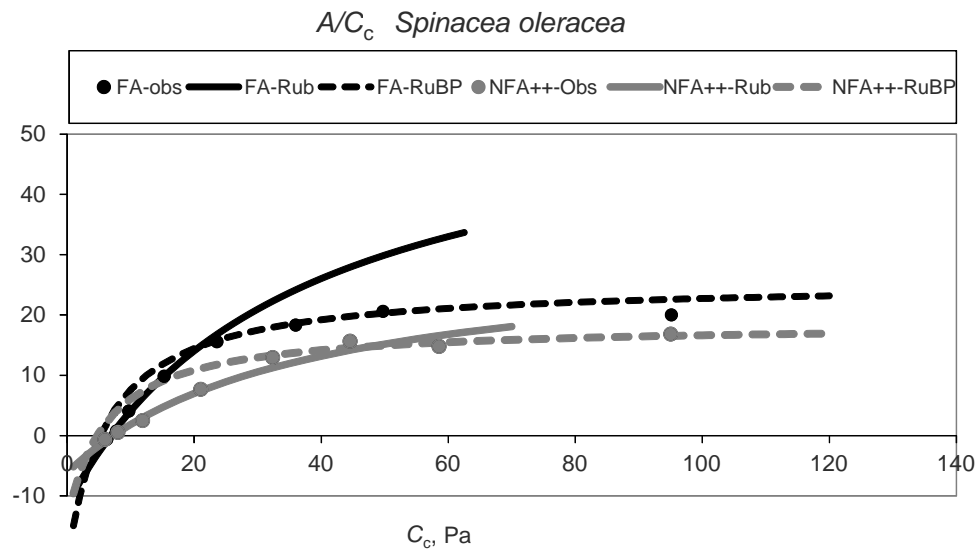
Figure 3.21 A/C$_c$ rate for *Spinacea oleracea* cv. Viroflay. FA= charcoal filtered air; NFA++=non filtered air + 40 nl l^{-1} of O$_3$. (Mean± se).

- **New critical levels for leafy crops based on O$_3$ concentration (AOT40) and O$_3$ doses (PODs) have been settled based on the experimental data sets** acquired during the experiments. Figure 3.22 represents the AOT40 function. Concentration-based critical level for leafy crops was established provisionally at 5400 ppbh for a 5% of yield reduction.
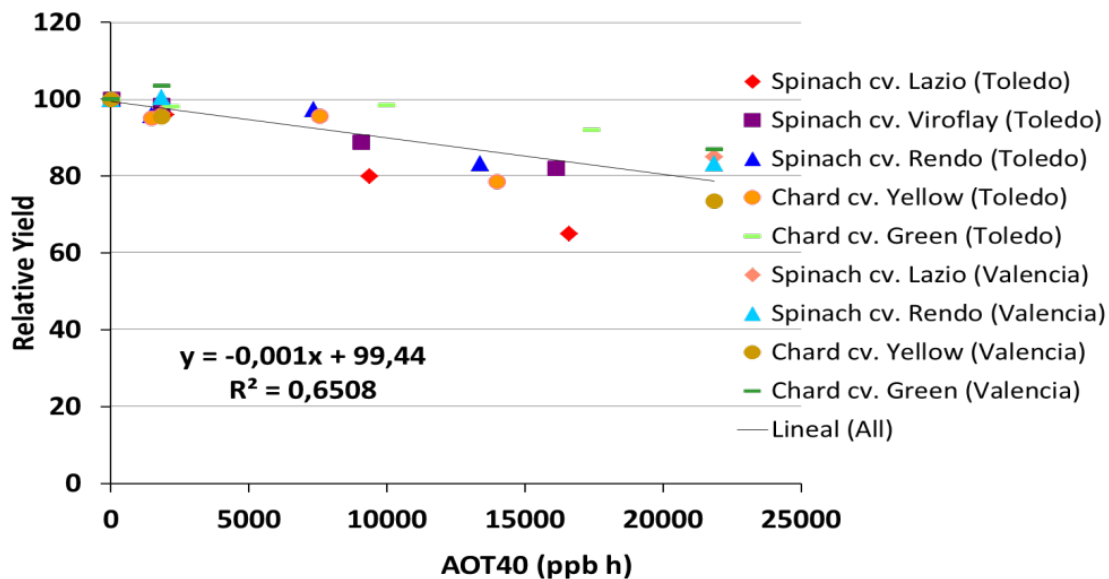
Figure 3.22 New exposure- response function for leafy crops based on chard (*Beta vulgaris*) and spinach (*Spinacea oleracea*), the most ozone sensitive leafy crops. Function is based on 2013 OTC-experiments developed under two Mediterranean conditions: continental (Toledo) and oceanic (Madrid) and six cultivars. Critical levels can be derived from the function.

Experiments has been partially financed by the Spanish government NEREA project (*AGL2012-37815-C05-03*) *"New approaches to efficient use of nitrogen for sustainable agriculture - Potential use of the nitrogen fertilization for mitigating the ozone effects on crops"*: This project allowed the association between CIEMAT and CEAM (Valencia) for developing the leafy crops experiments in two different climates and sites (Madrid and Toledo) and improving the ÉCLAIRE initial experiment.

Publications:

- Ozone effects on physiology and marketable biomass of leafy crops: spinach (*Spinacea oleracea*) and chard (*Beta vulgaris*). González-Fernández, I., Elvira, S., Calatayud,V., Calvo, E., Aparicio, P., Sánchez-Sánchez, M., Alonso, R., Bermejo-Bermejo, V. (In preparation, almost ready to be submitted)
- Monga, R., Marzuoli, R., Alonso, R., Bermejo, V., Gonzalez-Fernandez, I., Faoro, F., Gerosa G. (2015). Varietal screening of ozone sensitivity in Mediterranean durum wheat (*Triticum durum*, Desf.). Atmospheric Environment 110 (2015) 18-26

NERC (BAN) developed a crop experiment in solardomes. Wheat seeds of varieties 'Mulika' and 'Skyfall' (nabim group 1, suitable for breadmaking) were planted in a loam-based compost mix (John Innes 3) in large containers (25 litre) in Spring 2015 and exposed to ozone in the solardomes at CEH Bangor (Figure 3.23), with exposure beginning on 15th May, when plants had reached advanced tillering growth stage. Ammonium nitrate was applied as a soil dressing at anthesis and 2 weeks after anthesis (total N addition of 80 kg/ha). Plants were kept well-watered for the duration of the experiment until the plants were ready for harvest in August. The ozone treatments used were selected to represent scenarios of potential ozone pollution from local (giving episodic peaks) or hemispheric (giving increased background) dominated sources and were low background, medium background, high background, very high background, low peaks, medium peaks, high peaks and very high peaks, with 4 replicate containers of each wheat variety in each ozone treatment.

Figure 3.23: Wheat plants exposed to ozone in solardomes (Bangor, UK).

Measurements made include stomatal conductance (Delta-T AP4 porometer) chlorophyll content of flag leaves (ADC CCM200plus), light saturated photosynthesis (CIRAS II), analysis of soil pore water (at anthesis and shortly after harvest) for pH, conductivity, carbon and nitrogen content, analysis of soil samples for carbon and nitrogen content, and harvest measurements including number of ears, grain number per ear, 1000 grain weight, straw weight and harvest index. Grain samples are currently being analysed for carbon and nitrogen content.

Main results are:

- **A_{sat} (light saturated photosynthesis) was similar in all treatments around flowering** (23rd June) **but was substantially reduced by ozone in late season** (14th July) (Figure 3.24); based on the measurement campaigns on the variety Skyfall during the growing season.

- **There was a much larger effect of peak than background ozone and this was apparent even at the 'medium' ozone treatments** (Figure 3.24).
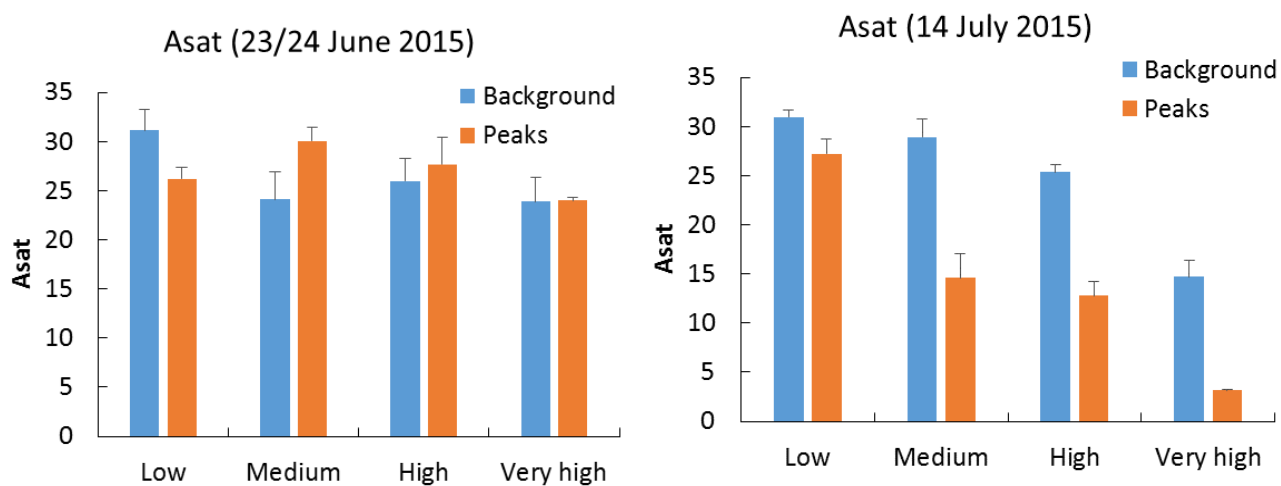
Figure 3.24: Effect of increasing background and peak ozone treatments on Asat of wheat (variety 'Skyfall).

- **Changes in chlorophyll content explained the ozone effects on A_{sat}** (Figure 3.25). **With increasing ozone treatment the flag leaves senesced earlier, and decreased chlorophyll content with increasing ozone treatments started to occur at around anthesis**.

- **Larger effect of ozone with the 'peaks' treatments on the chlorophyll content was found compared with the ozone treatments; but a more prolonged ozone exposure was needed to found this response** (by 14th July) (Figure 3.25).
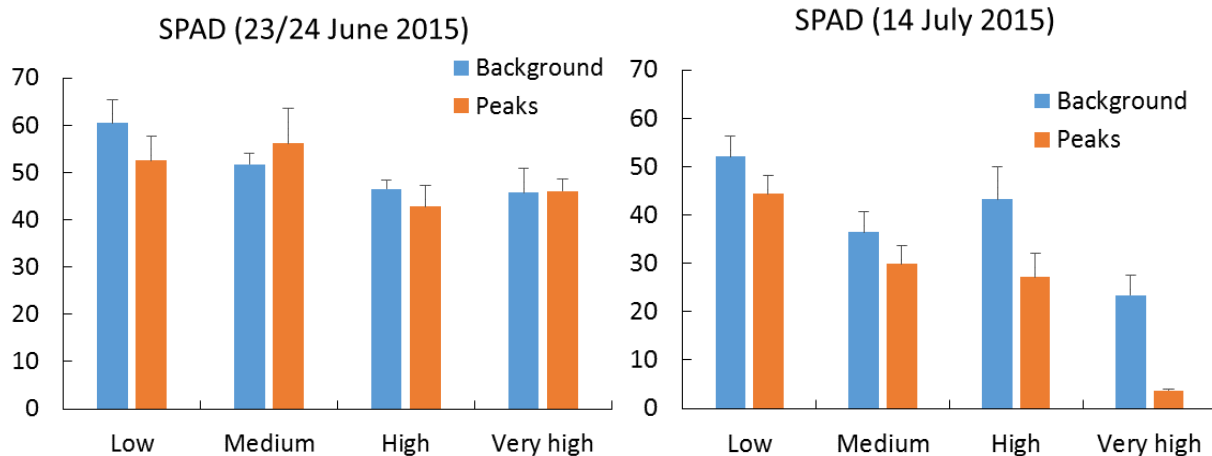
Figure 3.25: Effect of increasing background and peak ozone treatments on chlorophyll content of wheat Skyfall cultivar (SPAD units).

- **Yield of both Mulika and Skyfall cultivars was decreased with increasing ozone treatment, and the reduction was much larger with the 'peaks' treatment rather than 'background'** (Figure 3.26).
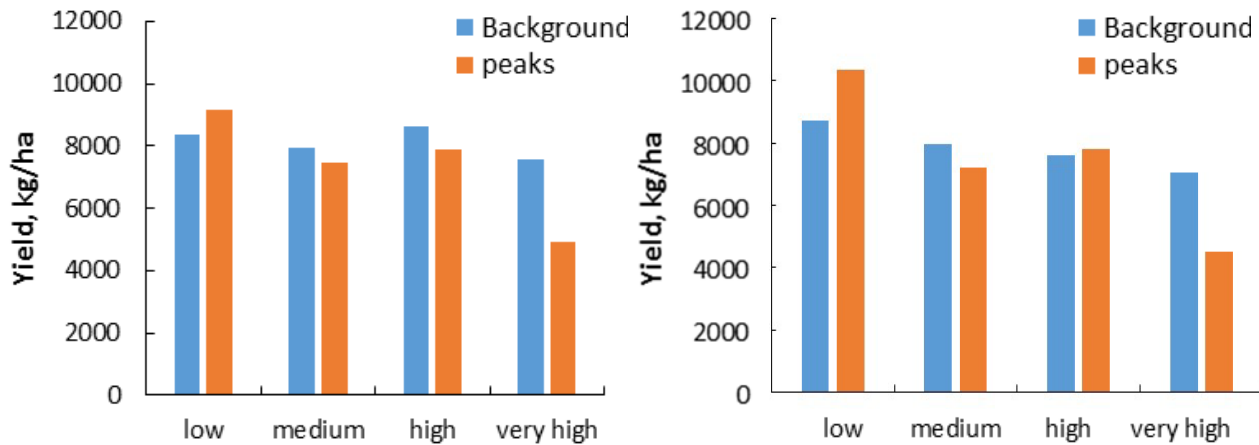
Figure 3.26: Effect of increasing background and peak ozone treatments on the yield of wheat varieties Skyfall (left), and b) Mulika (right).

- **The reduction in yield was largely due to a smaller grain size, with the number of ears per plant and number of grains per ear showing no response**.

- **For both Skyfall and Mulika cultivars, the 1000 grain weight was reduced with increasing ozone, and with a larger reduction in the 'peaks' treatment** (Figure 3.27). With increasing background ozone, only the 'very high' treatment caused reductions in 1000 grain weight, whereas a reduction occurred with 'medium', 'high' and 'very high' peaks treatments.

ÉCLAIRE Third Periodic Report: November 2015
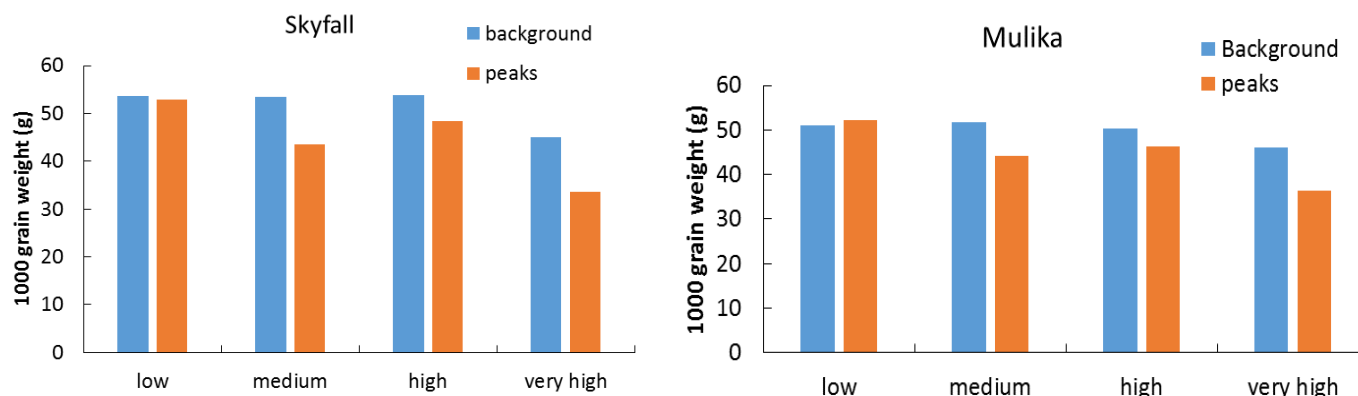
Figure 3.27: Effect of increasing background and peak ozone treatments on the 1000 grain weight of wheat varieties a) Skyfall and b) Mulika.

Analysis of carbon and nitrogen content of grains, soil pore water and soil is ongoing. databases have been uploaded to the ÉCLAIRE site.

Task 10.3 Shrubland site experiments.

UNICATT was formerly committed to perform a 1-year Open-Top Chambers experiment on macchia species investigating the effects of high levels of ozone and nitrogen deposition. However, according to what was suggested during the Component 3 Kick-off Meeting (10th-11st January 2012, Dragor, Denmark) and in agreement with Component Lead Contractor, UNICATT focussed on broadleaves species with a 2-years long experiment on *Quercus robur* and *Carpinus betulus*. Thus UNICATT decided to extend the duration of Task 10.1 experiment from one year to two years.

During the reporting period no new shrubs experiments have been done.

Task 10.4 – Grassland site experiments

FDEA-ART has been delivering data for modelling and new analysis generated from a long-term (7 years) free air fumigation ozone x nitrogen experiment on subalpine grassland. For this purpose, 180 monoliths of a *Geo-Montani-Nardetum* grassland were exposed for seven years at 2000 m a.s.l. to elevated ozone concentrations (ambient, 1.35 x ambient concentration, 1.73 x ambient concentration) and increased nitrogen deposition (background, +5,+10, +25, +50 kg N ha-1 yr-1) in a cross-factorial design. The experiment was finished successfully and first results are available. On average, POD0 and POD1 were increased by a factor of 1.33 and 1.37 and 1.83 and 1.91, respectively, compared to the ozone control treatment. Both maximum (2006) and minimum (2009) POD values occurred in the two warmest and driest years, respectively. In high ozone treatments, POD reached values found to be detrimental to plant growth elsewhere.

- **Substantial increases in aboveground biomass were recorded in response to N** addition (Figure 3.28), mainly as a result of an extraordinary success of sedges, which triplicated their relative abundance up to 30%. **In contrast**, **the ozone treatment did not affect biomass production** (Figure 3.29) **or functional group composition but it accelerated leaf senescence and slightly reduced both ecosystem respiration and gross primary productivity.**

- Surprisingly only a few **ozone x nitrogen interactive effects were observed, predominantly on leaf senescence**.
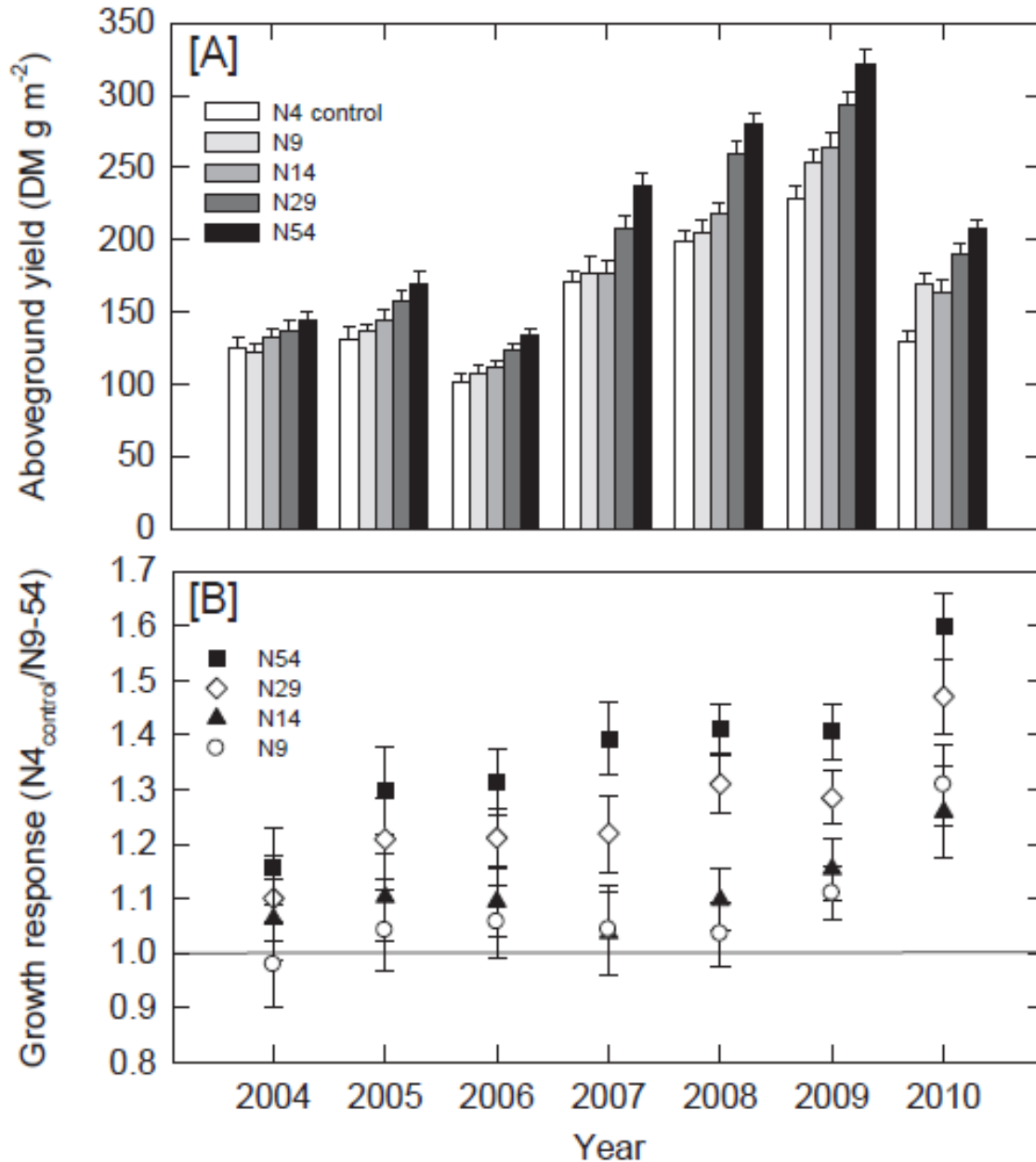
Figure 3.28: a) Annual aboveground yield (dry matter, DM) of harvested phytomass in Alp Flix subalpine grassland (>2 cm height), grouped by N-deposition treatment (means ± 1 SE). N4 control = no extra N deposition, N9 = +5 kg-, N14 = +10 kg-, N29 = +25 kg- and N54 = +50 kg ha^{-1} a^{-1} extra N deposition. b) Relative aboveground growth response as the ratio of yield N4control/yield N54 treatment.
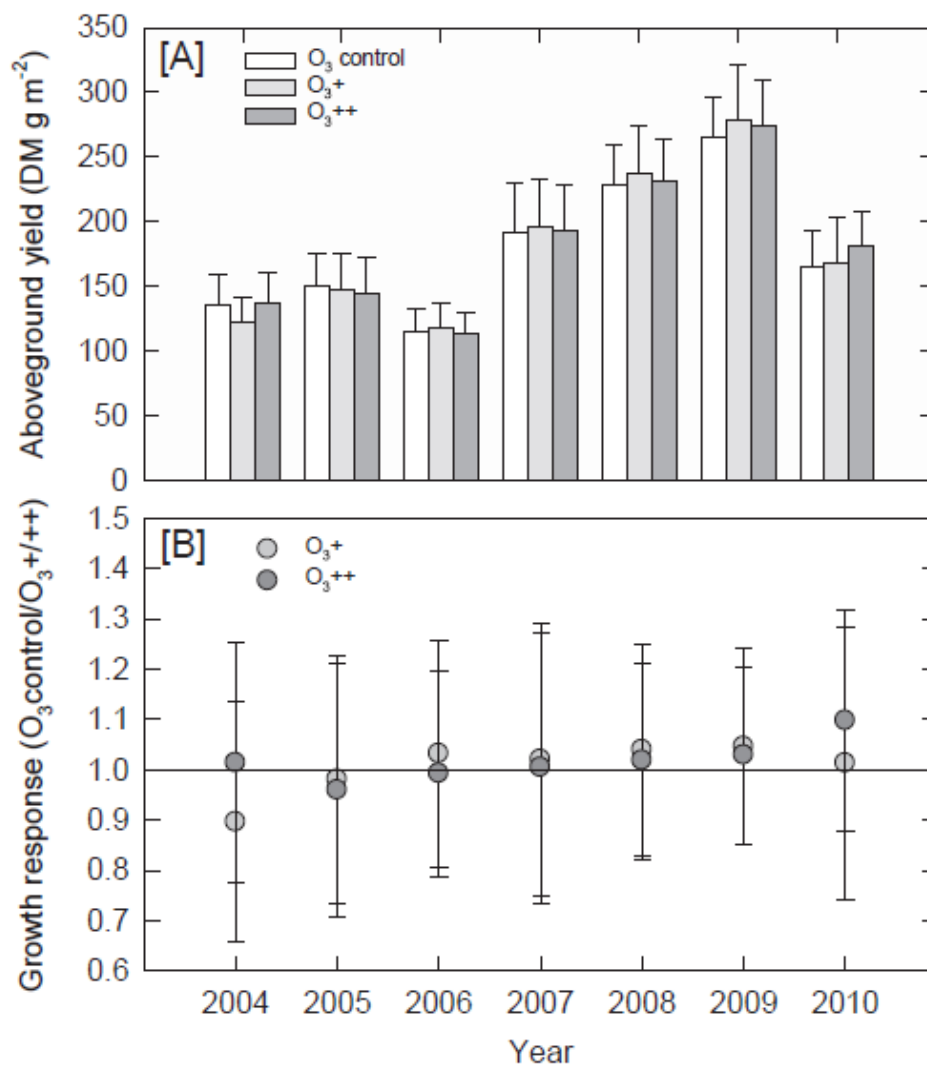
Figure 3.29: a) Annual aboveground yield (dry matter, DM) of harvested phytomass in Alp Flix subalpine grassland (>2 cm height), grouped by O_3 exposure treatment (means ± 1 SE). O_3 control = no O_3 added, O_3+ = ambient conc. x 1.4, O_3++ = ambient conc. x 1.7 b) Relative aboveground growth response as the ratio of yield O_3 control/yield $O_3+/++$ treatment.

Complete dataset has been delivered to the ÉCLAIRE database. Supplemental information for modellers was provided as requested.

ÉCLAIRE Third Periodic Report: November 2015

Publications:

- Bassin, S., Käch, D., Valsangiacomo, A., Mayer, J., Oberholzer, H. R., Volk, M., & Fuhrer, J. (2015). Elevated ozone and nitrogen deposition affect nitrogen pools of subalpine grassland. *Environmental Pollution*, *201*, 67-74.
- Volk, M.; Enderle, J.; Bassin S. Subalpine grassland carbon balance gains more under low compared to high atmospheric N deposition in a seven year field experiment (in preparation).
- Bassin, S; Blanke, V.; Volk, M.; Fuhrer, J. Strong effects of elevated ozone and nitrogen deposition on growth of juvenile subalpine plants and their colonization by arbuscular mycorrhizal fungi (AMF) (In preparation).
- Volk, M., Wolff, V., Bassin, S., Ammann, C., Fuhrer, J. (2014). High tolerance of subalpine grassland to long-term ozone exposure is independent of N input and climatic drivers Environmental Pollution 189: 161-168

DTU developed a field experiment that has been conducted during the 2013/14 season at the Climate Brandbjerg site. Results are under publication (manuscript in preparation).

The most important results are:

- **Photosynthesis mitigates global warming via consumption of increased atmospheric carbon dioxide and drives plant productivity, but climate change and air pollution jeopardize this response.**

- **Long term ecosystem experiments have demonstrated that drought, progressive nitrogen dilution and non-linear effects between climate change factors can reduce the CO_2 driven photosynthetic stimulation.**

- **Ozone is phytotoxic for photosynthesis, but elevated CO_2 and drought can reduce stomatal conductance and thereby minimize ozone flux into leaves. However, the combined influence of episodic ozone, drought and elevated CO_2 on photosynthesis at realistic natural conditions is unknown**.

- **Ozone become more toxic to photosynthesis processes when plants are acclimated to long term elevated CO_2 and drought (Figure 3.30)**.

- **Ozone also persistently reduces photosynthesis in long term multi-factor treatments of elevated CO_2, warming and drought and the combined**

responses were influenced by non-linear interactions between all treatments.

- **As elevated levels of atmospheric CO₂, warming, and drought occur in concert with increasing episodic ozone concentrations then such non-linear interactions will have an increasingly influence in the future. Hence, at future climatic conditions ozone concentration is highly decisive for the rate of plant carbon uptake.**
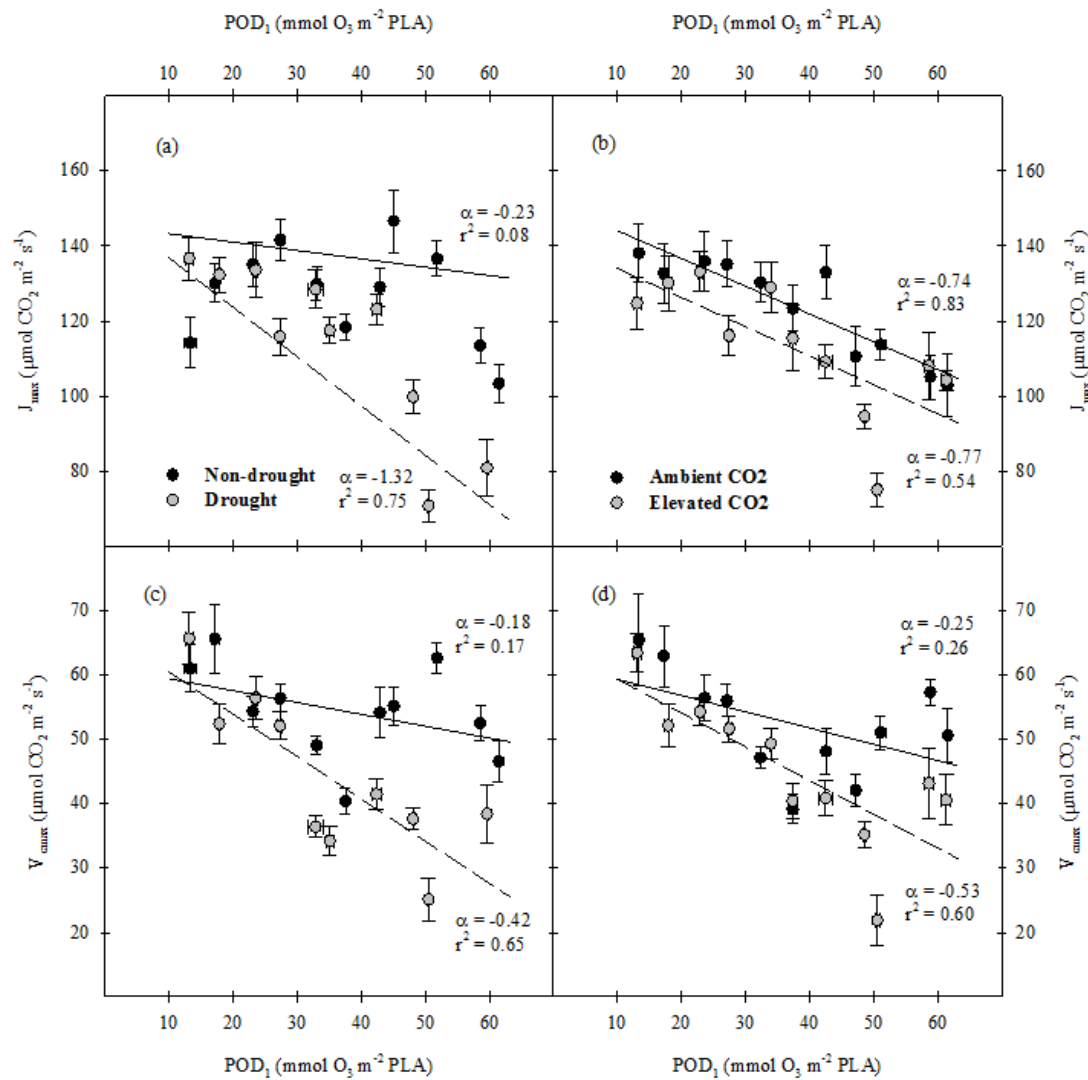
Figure 3.30: Accumulated phytotoxic ozone dose (POD1) versus photosynthetic capacity measures after long term acclimation to drought (left) and elevated CO_2 (right). In (a) and (b) maximal RuBP regeneration rate (J_{max}) and in (c) and (d) maximal carboxylation rate of Rubisco (V_{cmax}). Each point was averaged per POD1 class (5 mmol m⁻² PLA intervals, n=5-35 observations per point; total number of observations = 230).

CIEMAT developed a two growing season experiment under field conditions to assay the effects of the increased levels of ozone and nitrogen deposition on a Mediterranean annual pasture community. Last report presented the results about the effects at canopy scale (Calvete–Sogo et al., 2014). For the reporting period of this report, new findings at species level have been found:

ABOVEGROUND EFFECTS:

- **The response of the component species to ozone and nitrogen is heterogeneous.** Three different patterns were found: 1- clovers group: very sensitive to ozone but not responsive to N; 2- grasses and forbs group: very responsive to N and relatively sensitive to O_3 and, 3- legume non clover: responsive to O_3 but positively and not responsive to N (Figure 3.31).

- **The heterogeneous response to N and O_3 changed the competitive relationships among species, and thus altering the biodiversity of the pasture (structure and composition).**
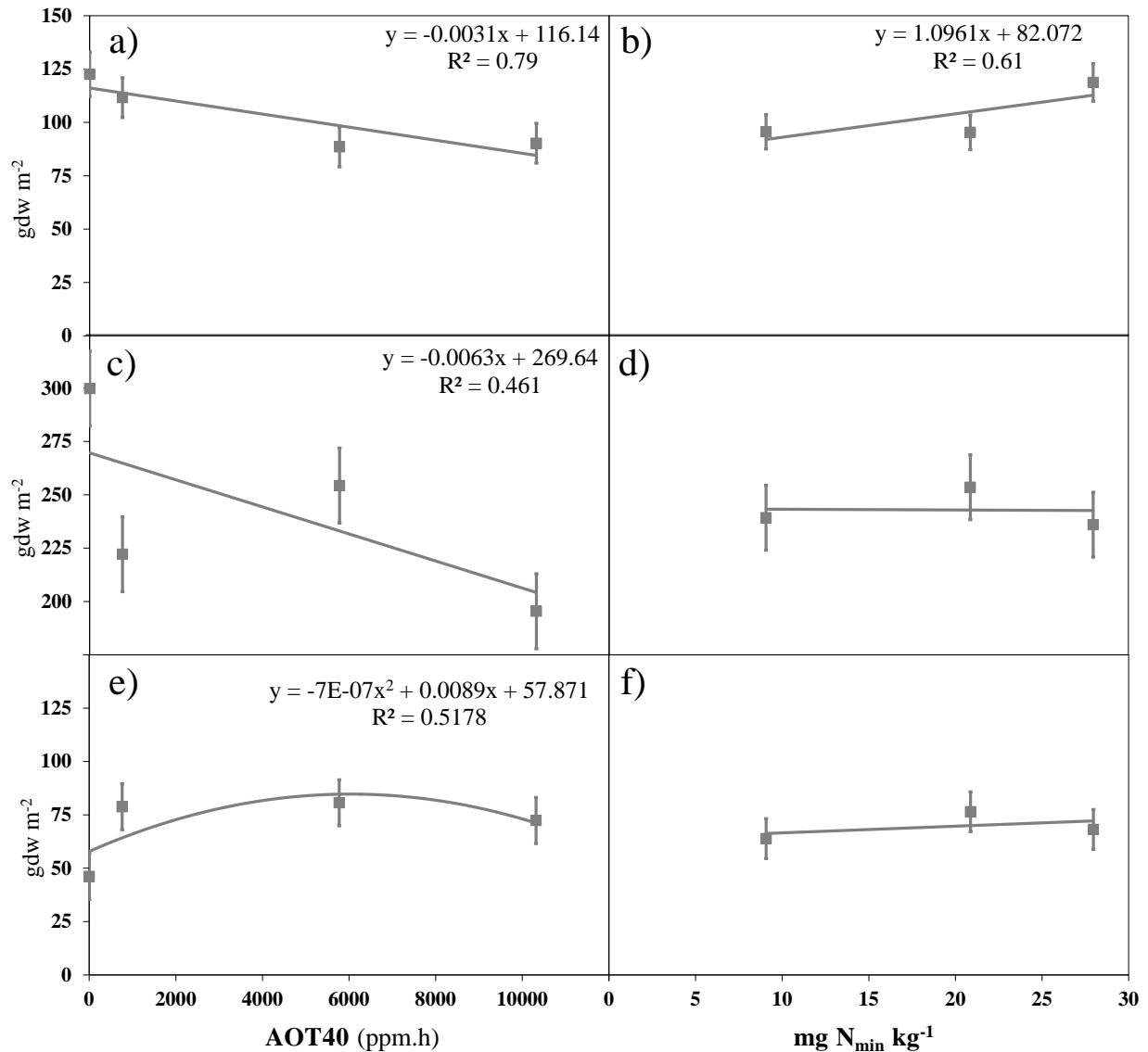
Figure 3.31: Total aerial biomass for the three groups of species identified according to their pollutants response patterns: a) O_3-response of the non-legume sps (*B. maxima* + *C. echinatus* + *S. gallica*), b) N-response of the non-legume sps, c) O_3-response of the clover-legumes (*T. cherleri* + *T. striatum*), d) N-response of the clover-legumes, e) O_3-response of the non-clover legumes (*O. compressus*), f) N-response of the non-clover legumes. AOT40 (cumulative exposure to O_3 atmospheric concentrations over 40 nl l^{-1}) corresponding to the different O_3 treatments (FA, NFA, NFA+, NFA++) (means across N treatments ± se); Total soil N mineral content (N_{min}) corresponding to the different N treatments (N-low, N-medium, N-high) (means across O_3 treatments ± se). From Calvete-Sogo et al., 2015 (under revision in Oecologia).

- **Nitrogen inputs can counterbalance the ozone induced increment of the senescence for *Briza maxima* and the non-legume group, but only when the levels of the pollutant are not very high (Figure 3.32).**
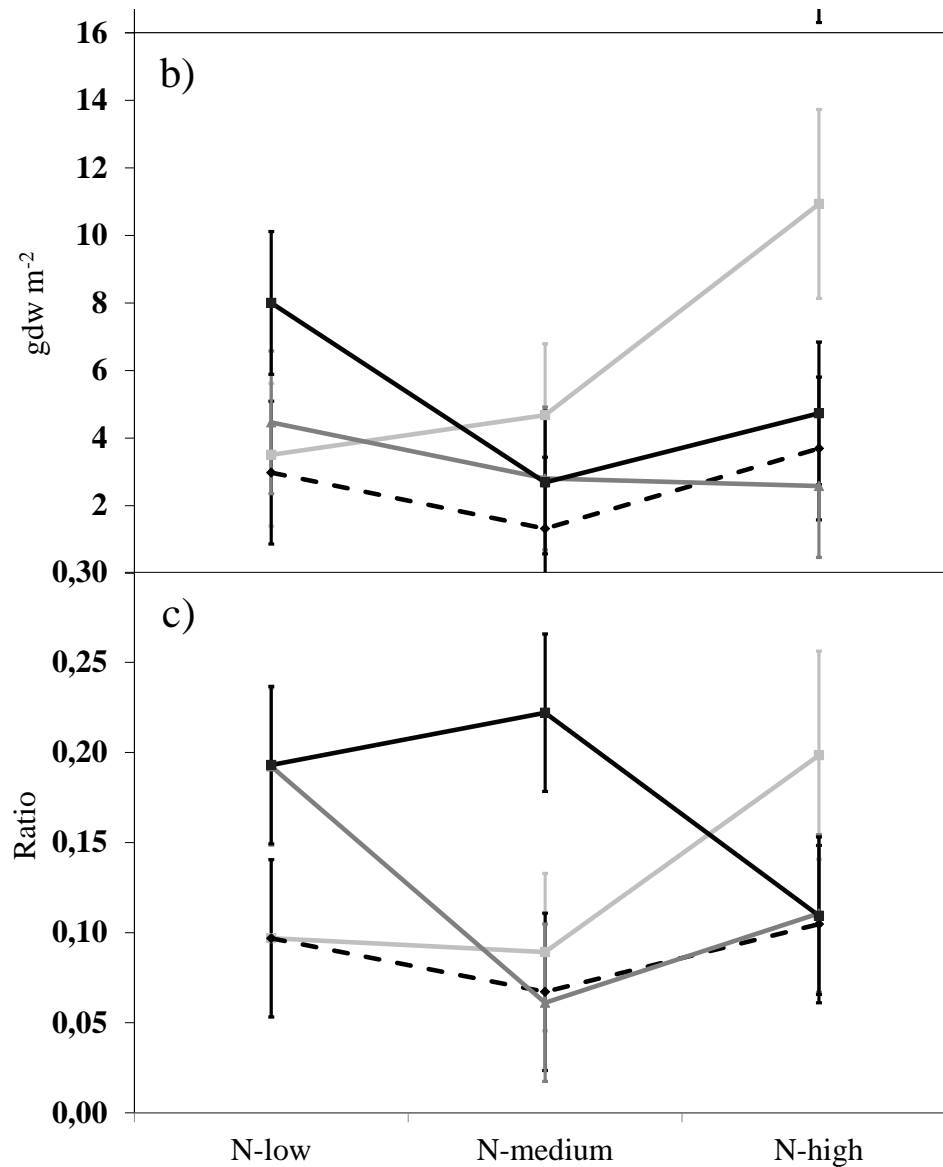
Figure 3.32: Ozone x N significant interactive effects (mean ± se): b) Senescent biomass of *Briza. maxima*, c) Senescent/green rate of B. maxima. N-low = soil N background; N-medium= +20 Kg N ha^{-1}; N-high= + 40 Kg N ha^{-1}.

BELOWGROUND EFFECTS:

- **Ozone increased N$_2$O soil emissions and slightly reduced NO emissions; Nitrogen increased NO soil emissions.**
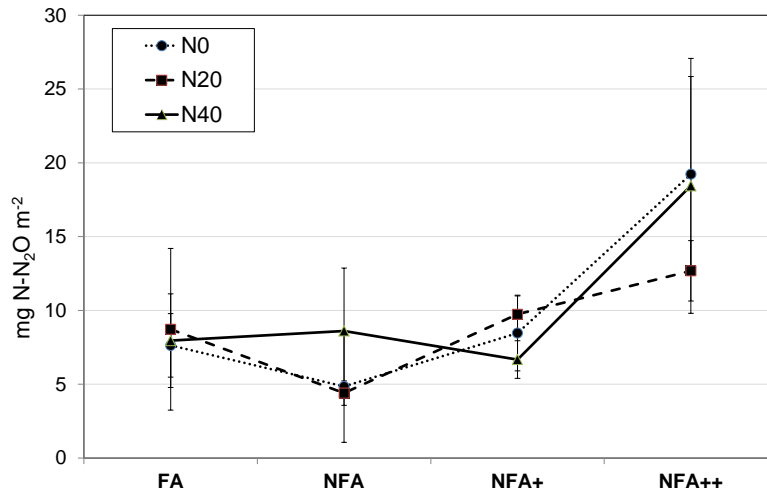
Figure 3.33: Cumulative emissions of N$_2$O under the different O$_3$ and N treatments. (mean±se). FA= charcoal filtered air, NFA= non filtered air, NFA+= non filtered air supplemented with 20 nl l^{-1} of O$_3$, NFA++= non filtered air supplemented with 40 nl l^{-1} of O$_3$. N0= soil N background, N20=20 Kg N ha^{-1}; N40=40 Kg N ha^{-1}.

Possible mechanisms for the observed increment of the N$_2$O emissions O$_3$-mediated (Figure 3.33):

- **The increment of the soil N$_2$O emissions might be related with the competition between plant and soil microorganisms for the soil N.** Two emissions peaks were observed when the physiological activity of the pasture per surface was low: at the beginning of the pasture growth when plants are small, and at the end of the cycle when most aerial biomass is senescent (Figure 3.34).

- **Moreover ozone reduced NEE and plant biomass, leaving more soil N available for soil biological activity and thus favoring soil N$_2$O emissions.**
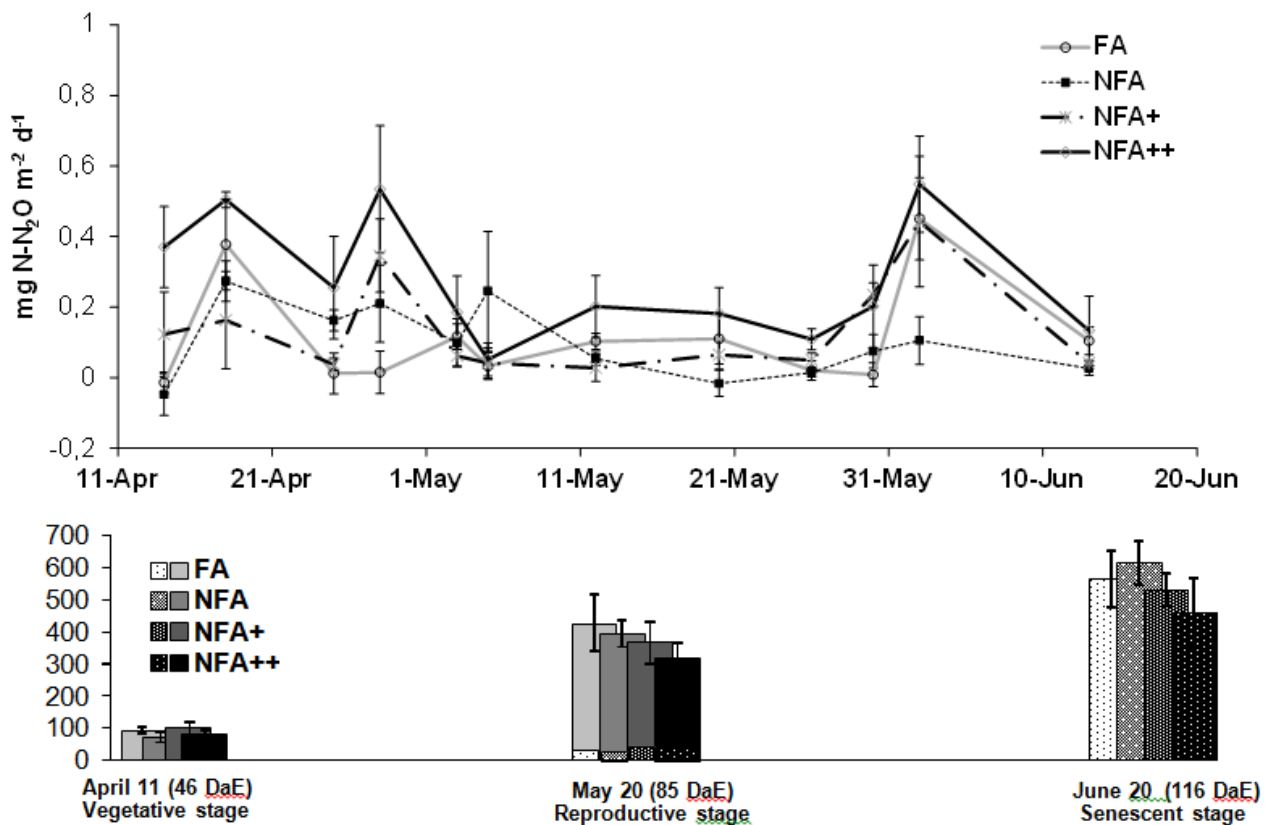
Figure 3.34: a) Daily soil emissions of N_2O under the different O_3 treatments for the growing cycle of the pastures (mean values across N treatments) (mean±se). b) Aerial biomass of the pasture trough the growing cycle; solid colors mean green biomass, dotted colors means senescent biomass. FA= charcoal filtered air, NFA= non filtered air, NFA+= non filtered air supplemented with 20 nl l^{-1} of O_3, NFA++= non filtered air supplemented with 40 nl l^{-1} of O_3.

Belowground effects on GRASSES:

- **Ozone reduces root-N content of the grass (***Briza maxima***) but not the clover (***Trfolium striatum***) and N counterbalances this effect** (Figure 3.35).

- **The O_3-reduced N content on the roots of the grasses might be an important mechanism favoring N_2O emissions, through the more N availability in the soil; due to the mayor proportion of the grass fraction on the soil root biomass compared with the legumes (root grass fraction doubled the root legume fraction).**

- **Interestingly, grass species relatively tolerant to ozone based on the effects on aerial biomass (i.e. *Briza maxima*) could be much more O$_3$-sensitive regarding roots processes, and these belowground effects might have mayor repercussion at ecosystem scale processes like N$_2$O emissions, tolerance to water-stress, etc.**
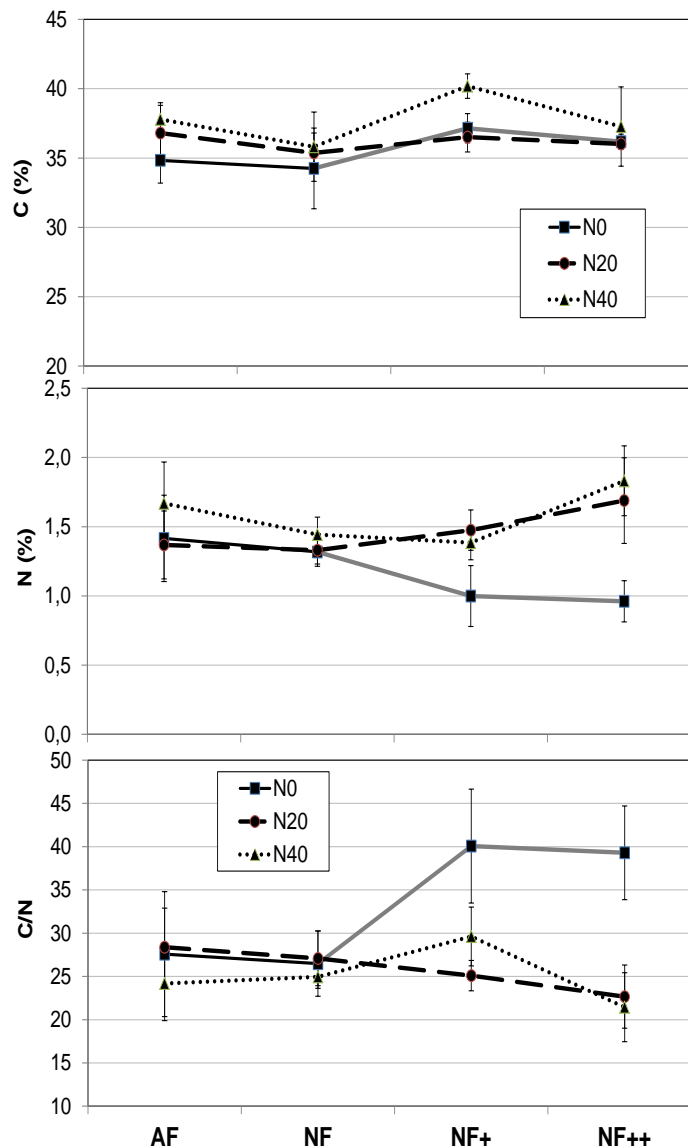
Figure 3.35 Significant interactive effects between N and O$_3$ for the root C (a), N (b) content (a) and the root C/N rate (c) for <u>Briza maxima</u>. FA= charcoal filtered air; NFA= non filtered air; NFA+=non filtered air + 20 nl l-1 of O$_3$; NFA++=non filtered air + 40 nl l-1 of O$_3$; N0=N background levels; N20= supplemented with 20 kg N ha-1; N40= supplemented with 40 kg N ha^{-1}. (mean ± es).

Belowground effects on CLOVERS:

- **Ozone reduces the root biomass of the clover but the response is N-modulated: medium levels of N can counterbalance this effect but, on the contrary, higher N levels shift the response increasing the loss** (Figure 3.36).

- **Ozone-induced reduction on root clover biomass might favor soil-N available for soil biological activity and N_2O emissions.**
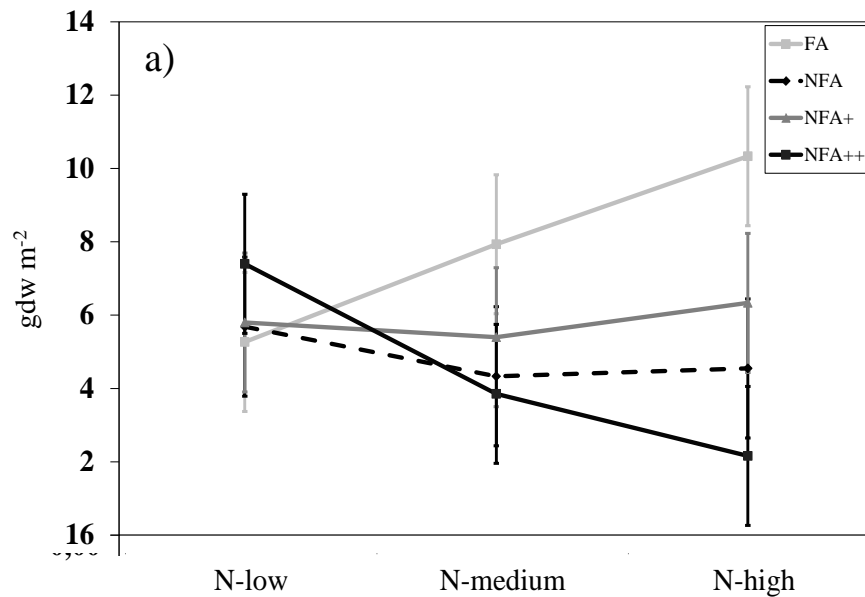
Figure 3.36. Root biomass of Trifolium striatum. FA= charcoal filtered air; NFA= non filtered air; NFA+=non filtered air + 20 nl l-1 of O_3; NFA++=non filtered air + 40 nl l-1 of O_3; N0=N background levels; N20= supplemented with 20 kg N ha-1; N40= supplemented with 40 kg N ha^{-1}. (mean ± es).

Complete dataset of these experiments has been delivered to the ÉCLAIRE database. Supplemental information for modellers was provided as requested.

Publications:

- García-Gómez, H., Garrido, J.L., Vivanco, M.G., Lassaletta, L., Rábago, I., Àvila, A., Tsyro, S., Sánchez, G., González Ortiz, A., González-Fernández, I., Alonso, R., 2014. Nitrogen deposition in Spain: modeled patterns and threatened habitats within the Natura 2000 network. Sci. Total Environ. 485-486, 450–60. doi:10.1016/j.scitotenv.2014.03.112

- García-Gomez, H., Aguillaume, L., Izquieta-Rojano, S., Valiño, F., Àvila, A., Elustondo, D., Santamaría, JM., Alastuey, A., Calvete-Sogo, H., González-Fernández, I., Alonso A. Atmospheric pollutants in peri-urban forests of Quercus ilex: evidence of pollution abatement and threats for vegetation (Accepted in Environmental Science and Pollution Research, Ref.: ESPR-D-15-03914R1)

- Calvete-Sogo, H., González-Fernández, I., Sanz, J., Elvira, S., Alonso, R., García-Gómez, H., Ibáñez-Ruiz, MA., Bermejo-Bermejo, V. Heterogeneous responses of component species to ozone and nitrogen deposition shift the structure of Mediterranean annual pastures (Submitted to Oecologia).

- Elvira, S, González-Fernández, I., Calvete-Sogo, H., Sanz, J., Alonso, R., Bermejo-Bermejo, V. Ozone levels in the Spanish central range are over the thresholds for plant protection: analysis at 2258, 1840 and 995 m (submitted to Atmospheric Environment).

- Sanz, J., Elvira, S, González-Fernández, I., Calvete-Sogo, H., Alonso, R., Bermejo-Bermejo, V Gonzalez. Revision of ozone exposure experiments of annual Mediterranean pastures for setting ozone critical levels (ready to be submitted).

- Sanchez-Martin, L., Garcia-Torres, L., Bermejo-Bermejo, V., Calvete-Sogo H., Alonso, R., Vallejo, A. Impact of ozone and nitrogen deposition on greenhouse gases and nitric oxide emissions in Mediterranean annual pastures (ready to be submitted).

- Elvira, S, González-Fernández, I., Calvete-Sogo, H., Alonso, R., Sanz, J., Bermejo-Bermejo, V. Gas exchange of Mediterranean annual species are affected by the increasing levels of ozone and nitrogen deposition (In preparation).

Progress towards the milestones and deliverables

All milestones and deliverables have been completed, for further details please see individual work package reports.

Use of resources and deviations from DoW

The total person months spent in this period, was 22.1.

UNICATT activities included in the 10.3 task has been modified according to the discussion and decisions from the Component 3 Kick-off Meeting (10th-11st January 2012, Dragor, Denmark) and in agreement with the Component Lead: a two-year experiment in two broadleaves tree species has been settled rather than a one-year experiment on one broadleaf tree and one Mediterranean evergreen species (*cfr* 2.2 Task 1.3 – Shrubland site experiments).

DTU For the reporting period less man-months were expended compared with budgeted. This is due to an over-use in the previous period caused by technical problems in the field (field work was probably under estimated in the budget).

Work package 11 – Investigation of novel ecosystem – air pollution – climate interactions

Lead contractor: Francesco Loreto (CNR)
Contributors: NERC, BOKU, UBO

Work package objectives
The aim of this WP is to conduct studies on three novel concepts in order to establish new empirical relationships for vegetation-air pollution interactions needed to establish novel thresholds (WP12) and ecological modelling (WP13). The specific objectives are:

1. To quantify how climate change, including increasing background ozone concentration will enhance greenhouse gas and NO release and exacerbate the threat to vegetation caused by dry or wet N deposition, including the distinction between oxidized (NO_y) and reduced (NH_x) nitrogen forms.

2. To assess if BVOC emissions from vegetation will increase the potential for O_3 and NO_x uptake by plants, and detoxification of reactive oxygen species, leading to improved antioxidant properties and reduced emission of other stress-induced, reactive BVOC (e.g., LOX compounds).

3. To demonstrate if hygroscopic particles accumulating on leaves from aerosol and trace gas deposition may attract water and lead to enhanced transpiration and reduced drought tolerance.

Progress and Results

Task 11.1

Specific objective: Peat bog experiment on N-climate-O_3 interactions (NERC(EDI) (Sheppard), BFW, NERC(BAN)). To quantify how climate change, including increasing background ozone concentration will enhance greenhouse gas and NO release and exacerbate the threat to vegetation caused by dry or wet N deposition, including the distinction between oxidized (NO_y) and reduced (NH_x) nitrogen forms.

Activities:

(1) Addition of ozone exposure to the Whim bog site
As anticipated in the last report, a new ozone fumigation facility has been installed at Whim, immediately adjoining the dry NH_3 deposition transect (Figure 3.37). New board-walking has been installed to facilitate access to the $100m^2$ O_3 x NH_3 fumigation area (Figure 3.38). The new fumigation area has been designed to provide a 10 x $10m^2$ grid

delivering "low O_3-low NH_3", "low O_3-high NH_3", "high O_3-low NH_3" and "high O_3-high NH_3" deposition treatments.

The ozone fumigation system at Whim is based on those deployed previously at Keenly Fell. The control system uses wind speed and direction parameters to activate the fumigation system to selectively fumigate a selected experimental plot. Two ozone analysers measure ambient and plot ozone concentrations and provide feedback data to the ozone fumigation system to adjust the fumigation concentrations to a set value.
The O_3 fumigation was tested successfully prior to deployment during March 2015. Prior to installation at Whim the ozone generator and oxygen supply unit developed faults. These were sent away to be serviced and a spare ozone generator was purchased to use with a second oxygen unit. The system was eventually installed at Whim at the beginning of May 2015. Background measurements at the site were scheduled until the end of May, so testing of the ozone plume at Whim was held back until these were completed.

In spite of successful prior testing, initial test measurements in June at Whim indicated that the ozone concentration was declining to ambient concentrations at the leading edge of the experimental plot. This meant that most of the plot was not receiving adequate ozone treatment. The height of the fumigation system was adjusted to improve ozone mixing and transport to the experimental plot, but this did not improve the situation sufficiently. The fumigation system has been moved closer to the plot, although this may be affecting the adequate mixing of the ozone plume. This arrangement is currently being tested (pending favourable wind direction – the NH_3 fumigation system is switched on only when the wind direction and wind speed are appropriate ie. > 2.5 m s^{-1} and within the 180-215° sector covering the transect). During this testing both the spare ozone generator and oxygen supply units developed faults and have been replaced with the serviced second set while undergoing repair/exchange.

The current position is that the fumigation units are not capable of supplying sufficient ozone to the plot under the site conditions found at Whim, and quotes for larger units capable of generating greater amounts of ozone have been obtained.

Alpha samplers for ammonia concentration have been deployed in each of the 100 1m^2 quadrats (Figures 3.39; 3.40) during 3 months. The results showed that although the level of the NH_3-concentration is different (this depends on how long the fumigation system has been switched on) the distribution pattern is the same each month. Monthly NH_3 measurements are ongoing on a less intensive scale (23 instead of ~ 90 sampling points) alongside measurements on the dry deposition transect.
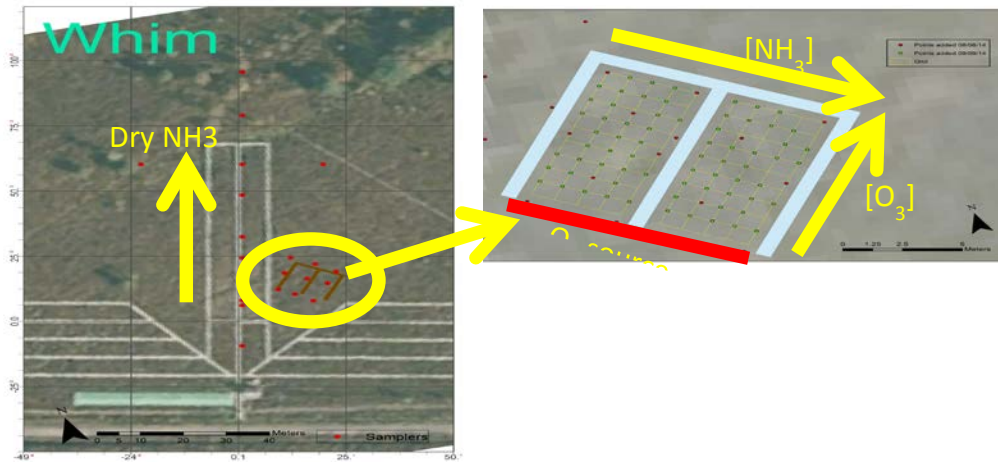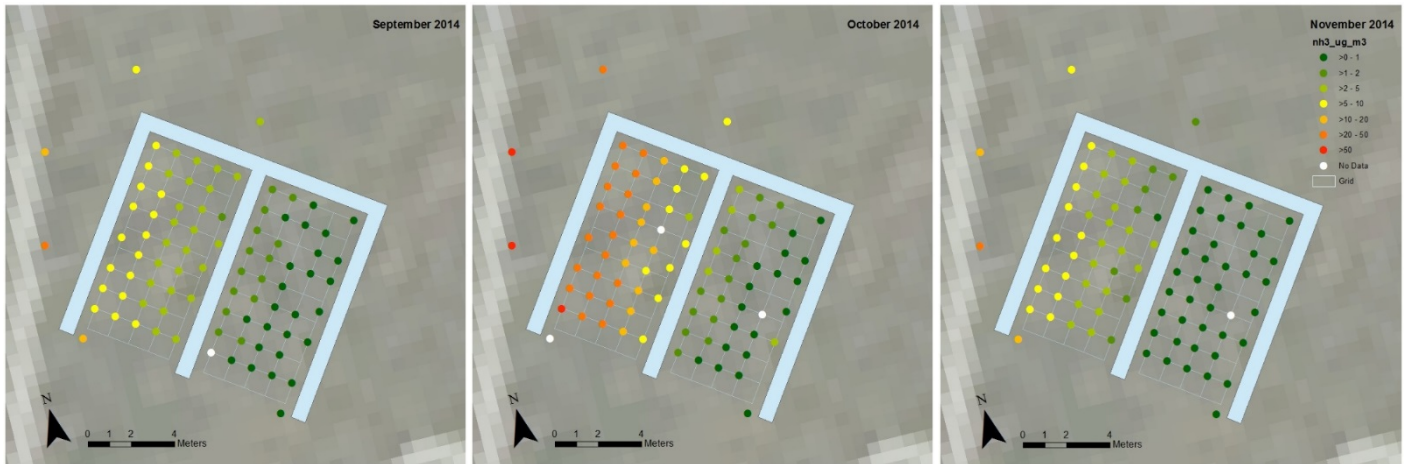
Figure 3.37: New O_3 fumigation experiment at Whim.

Figure 3.38: New board-walk to access the O_3 fumigation area.

Figure 3.39: Alpha samplers installed for characterising distribution of ammonia concentration across the O_3 fumigation grid.
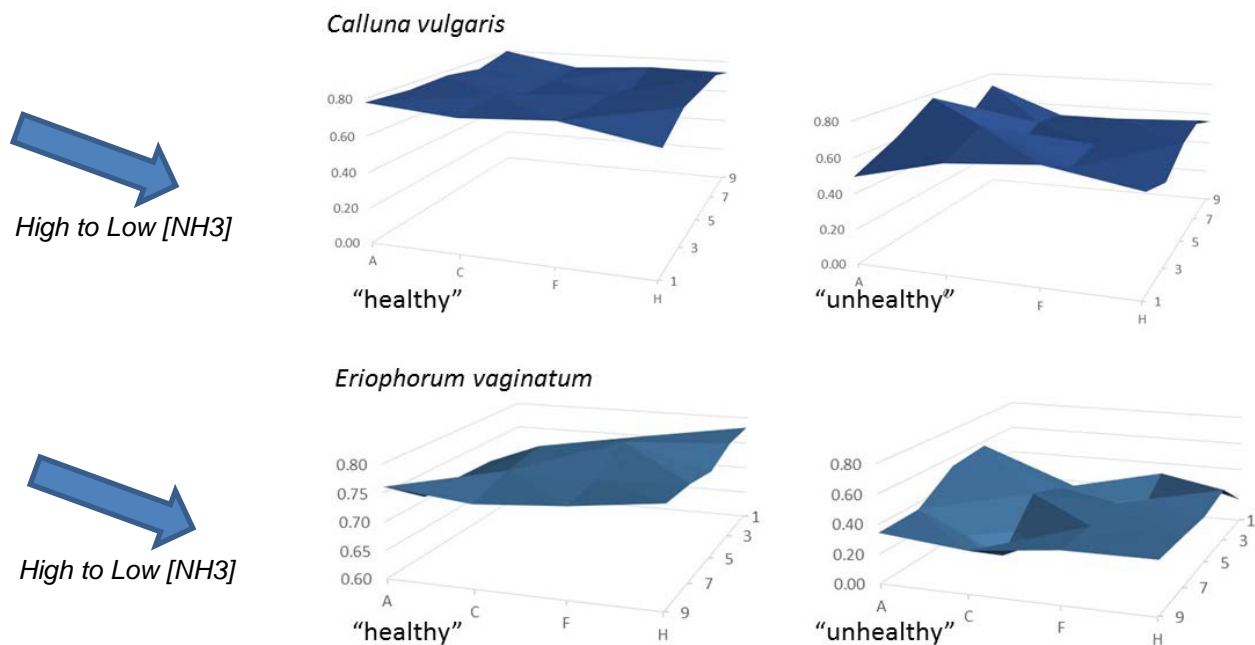
September 2014	October 2014	November 2014

Figure 3.40: Distribution of NH4 concentration across the experimental grid.

Pre-treatment measurements

(i) Fv/Fm for Calluna vulgaris & Eriophorum vaginatum

Following initial measurements in late summer 2014 (described in the previous report), further pre-treatment measurements of Fv/Fm were made on *Calluna vulgaris* and *Eriophorum vaginatum* in May 2015 (as indicated, for example in Figure 3.41).

There is a tendency for Fv/Fm in *E.vaginatum* to be lower at the edge which receives high NH_3 deposition. As expected, Fv/Fm for the "unhealthy" shoots of both species were more variable than in the healthy shoots.

Figure 3.41   Distribution of Fv/Fm measurements across the experimental grid

238

![éclaire logo]
Effects of climate change on air pollution impacts
and response strategies for European ecosystems

Analysis of variability for Fv/Fm

The datasets of the Fv/Fm measurements for the two populations ("healthy" and "unhealthy") shoots of *Calluna* vulgaris were analysed for variability and optimum sample size for detecting an O_3 x NH_3 treatment effect. Figure 3.42 shows the distribution of Fv/Fm values for the two populations. There was no effect of NH_3 dry deposition on Fv/Fm values.
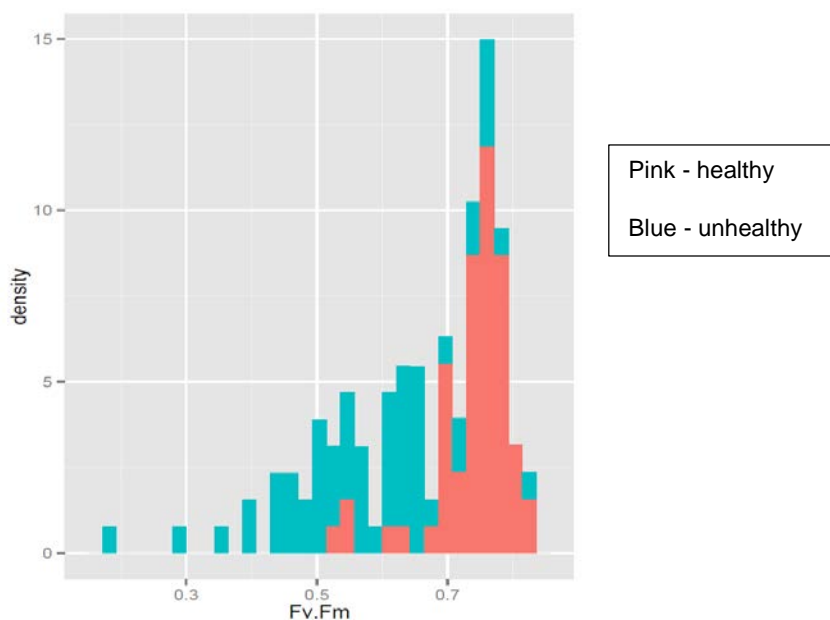
Figure 3.42: Distribution of Fv/Fm values for healthy and unhealthy populations of *Calluna vulgaris* across the experiment grid.

(ii) Fv/Fm and N content for Cladonia portentosa

(Results currently being processed).

Extensive measurements of Fv/Fm were made on the lichen *Cladonia portentosa* transplanted into cages in quadrats within the O_3 x NH_3 fumigation experimental grid, and also along the NH_3 dry deposition transect. In addition, the nitrogen content of the Cladonia thalli were measured for the day they were transplanted ("pre-treatment"), and again at the end of the series of measurements (77 days of NH_3 fumigation treatment).

(iii) Photosynthesis rate (A) and stomatal conductance (Gs)

Following initial measurements in late summer 2014 (presented in the previous report), further pre-treatment measurements of A and G_s in shoots of *Calluna vulgaris* were made in June and twice in July 2015, and in July 2015 for *Eriophorum vaginatum* (this species was not green enough for measurements until July (due to low temperatures during spring

and early summer). Measurements were repeated in August and September 2015, using two ADC LCPro leaf gas exchange cuvette systems.
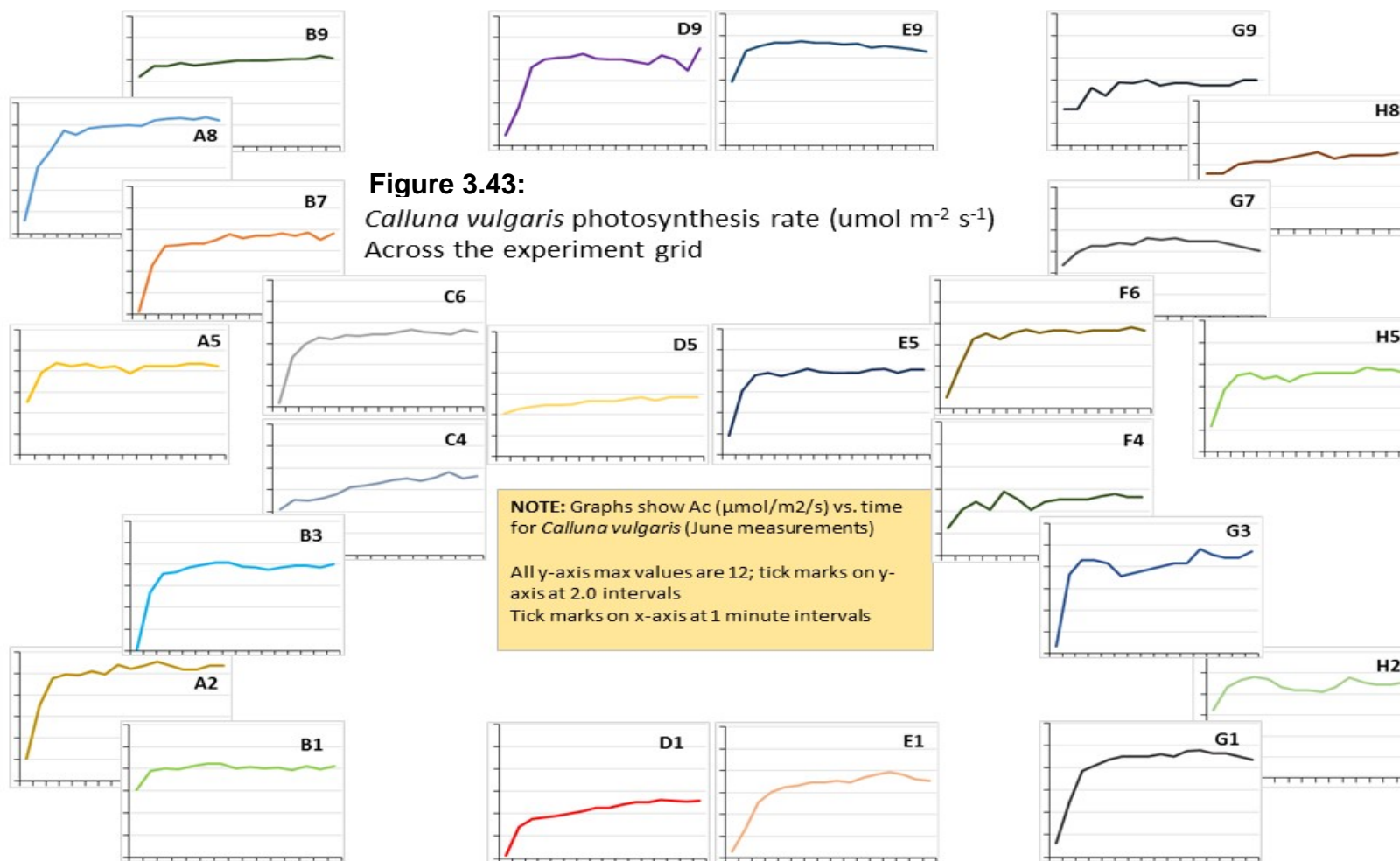
(a) Calluna vulgaris
Figure 3.43 provides an example of the time course of photosynthesis rate and stomatal conductance over 15 minutes for each of the measured shoots across the experimental grid, before the ozone fumigation commenced (June 2015 measurements). There appears to be no effect of dry NH_3 deposition on photosynthesis rates. "Steady state" stomatal conductance varies between 0.25 and 0.75 mol m^{-2} s^{-1}, and lower values were measured furthest from the dry ammonia source, though the data need to be analysed to determine if this is significant or not.

Figure 3.45 shows a 3-D bar chart plot of the photosynthesis and stomatal conductance data for the experiment grid. The difference in variability and the distribution of measurement values across the grid indicate an NH_3 deposition treatment effect, but statistical analyses are needed to confirm this possibility.

(b) *Eriophorum vaginatum*
The difference in variability and the distribution of both photosynthesis rate and stomatal conductance measurement values across the grid indicate an NH_3 deposition treatment effect, with lower values nearer the source, but statistical analyses are needed to confirm this possibility (data not presented).

ÉCLAIRE Third Periodic Report: November 2015

Figure 3.43:

Calluna vulgaris photosynthesis rate (umol m^{-2} s^{-1}) Across the experiment grid

NOTE: Graphs show Ac (µmol/m2/s) vs. time for *Calluna vulgaris* (June measurements)

All y-axis max values are 12; tick marks on y-axis at 2.0 intervals
Tick marks on x-axis at 1 minute intervals
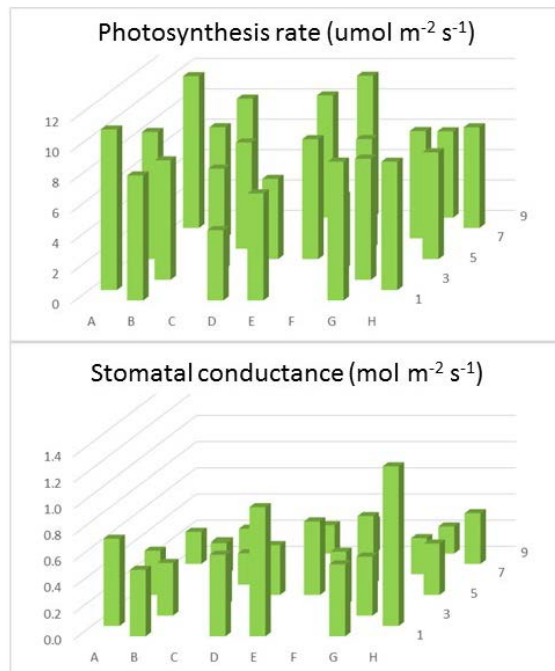
Figure 3.49: Mean photosynthesis rate and stomatal conductance in Calluna vulgaris at 20°C & 500 µmol m^{-2} s^{-1} PAR across the experimental grid for Whim Bog, 15/06/2015.

(iv) Vegetation study

In the ozone deposition experimental grid, the % cover for each species has been estimated in each quadrat. This provides data at a single time point (pre-treatment). The assessment will be repeated during August/September 2015. Data have yet to be quality assured, and mapped. Figure 3.50 shows two grid squares typical of vegetation near to, and far from, the NH$_3$ fumigation source.

For the NH$_3$ dry deposition transect, vegetation plots (three replicates at different distances from the fumigation line) of 40x40 cm were established and marked in 2002 when the experiment started. These plots are divided in 16 10x10 cm squares. At each square the % cover for each species has been estimated. This method has been used from the beginning of the experiment and the plant survey has been done with 2-3 years intervals.

Figure 3.50A: Grid square A3 near to the NH$_3$ fumigation source – typically more *E. vaginatum* and less *C. vulgaris.*

Figure 3.50B: Grid square H5 far from the NH$_3$ fumigation source – typically less *E. vaginatum* and more *C. vulgaris.*

(v) Dipwell samples have been taken from across the experiment grid, and are frozen awaiting analysis for major ions and total N.

(vi) Litter trays have been deployed in June 2015, but pre-treatment measurements are not yet made.

(vii) Ecosystem N$_2$O and CH$_4$ exchange were measured in static chambers ~ 30 cm diam which are installed at the edges and in the centre column of the ozone fumigation experimental grid. This data is still being analysed.

ÉCLAIRE Third Periodic Report: November 2015

Conclusions to date for Whim research

The O_3 x NH_3 fumigation transect is marked out, and the O_3 fumigation system is in the final stage of testing.

A suite of pre-O_3 treatment measurements have been made across the grid. Results so far show that there appears to be an NH_3 treatment effect on stomatal conductance for *Calluna vulgaris* and *Eriophorum vaginatum*, and on photosynthesis rate for *E. vaginatum.* These provide a baseline for future assessment of O_3-N interactions. Due to the challenges with the O_3 release system at this site, the measurements will continue through 2016 and 2017 as part of the longer term programme of the organization. In order to adjust the project for these issues, we established an additional N-O_3 experiment based on cores collected from different N deposition sites, as described below. The result of the original delay, will, in the long term, therefore deliver more outcomes than originally planned within the project.

(2) Exposure of coastal grassland cores of differing historical N deposition to ozone under open field conditions.
Investigation of whether prior N deposition history affects the sensitivity of coastal grassland vegetation to subsequent ozone pollution.

Coastal grassland cores (30 cm diameter, 25 cm deep) were taken from sites in the UK in spring 2014. Sites were selected based on similarity of precipitation, soil pH and vegetation type. Nine cores were taken from 7 sites across the UK, plus additional cores from a long term nitrogen addition experiment on Anglesey, along a nitrogen gradient ranging from 5.4 kg ha^{-1}yr^{-1} to 26 kg ha^{-1}yr^{-1}. Cores were exposed to ozone in the Free Air Ozone Exposure facility at CEH-Bangor which comprises nine 4 m diameter rings supplying ozone at a height of 30 cm. Three ozone treatments were used, with mean ozone concentrations during the experiment of 28, 36 and 48 ppb in 2014. Ozone concentrations were lower in 2015, particularly in the autumn, as prolonged exceptionally calm conditions meant that the windspeed was below the threshold required for ozone delivery.

Above-ground vegetation was non-destructively assessed prior to the start of ozone exposure to determine whether historic nitrogen deposition had influenced the cores. There was a significant effect of nitrogen deposition on total species richness ($p<0.001$), with species richness decreasing with increasing N deposition (Figure 3.51). There was also a change in species composition, with a large decrease in forb cover and small increase in grass cover with increasing nitrogen deposition, resulting in a large change in the grass:forb ratio. This shows that a clear gradient of N deposition effects has been established through the selection of sites across a historic N deposition gradient, which have provided the foundation to address interactions with O_3 exposure.
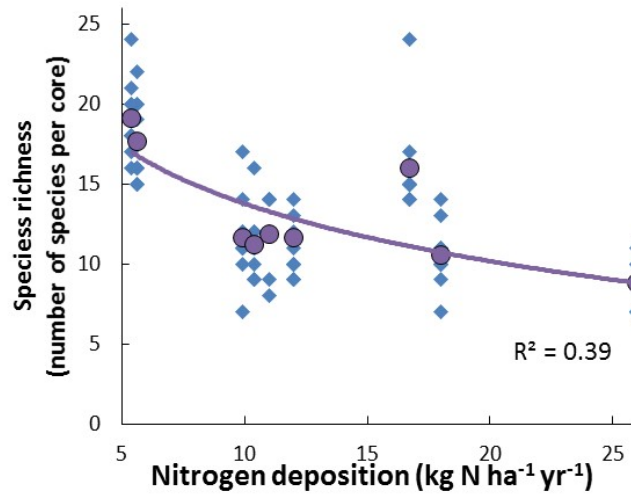
Figure 3.51: Species richness of coastal grassland cores in relation to the N deposition of the site of origin. Diamonds are the values for individual cores, and circles are the mean value per site.

Many species showed increased leaf injury and/or accelerated leaf senescence with increasing ozone treatment, and the total proportion of senesced leaves compared to healthy leaves per core was increased with increasing ozone exposure in both years. The most sensitive species (in terms of injury/senescence) included grasses, sedges and forbs and included *Ruta araveolens, Avenula pubescens, Leontodon spp, Carex arenaria*, *Carex flacca, Hypericum perforatum, Achillea millefolium* and *Galium verum.* It was not possible to determine whether N deposition affected the sensitivity to ozone of the different species, as the species most sensitive to ozone were not found in cores from a sufficient range of N deposition history.

Soil pore water samples were collected from all cores fortnightly between August and November 2014. Overall DOC content of the water samples increased with increasing N and decreased with increasing ozone (Figure 3.52), probably corresponding to mesocosm productivity. Analysis of enzyme activity from soil samples collected at the end of ozone exposure during the 2014 growing season showed increased activity of N-acetyl-beta-D-glucosaminidase with increasing ozone exposure (Figure 3.53). This enzyme converts complex molecules into amino-sugars and is important for C and N cycling in soils. The increase with increasing ozone concentration may be due to increased litter degradation due to accelerated senescence in response to ozone. However, no differences in the activity of B-D-glucosidase, which degrades carbohydrates, particularly cellulose, was found.
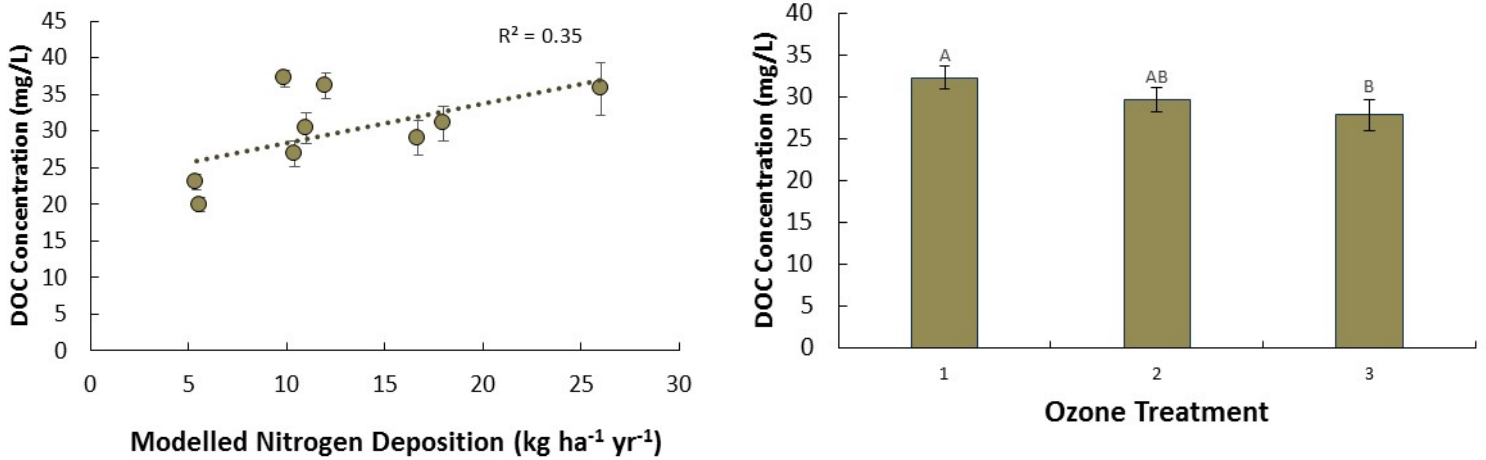
Figure 3.52: DOC content of soil pore water samples in relation to a) nitrogen deposition and b) ozone exposure.
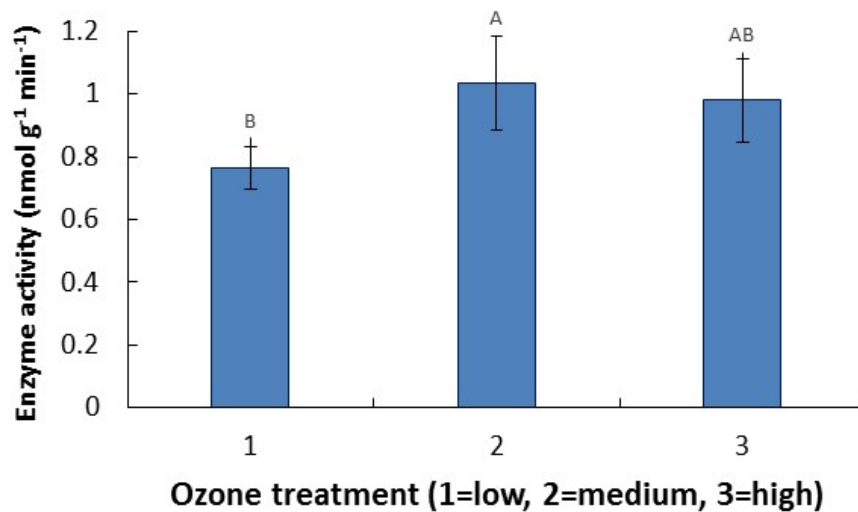
Figure 3.53: Activity of N-acetyl-beta-D-glucosaminidase in soil samples of cores exposed to ozone.

All cores were cut back to 4cm height in spring 2015. Harvested plant material was separated into grasses, sedges and forbs. The historic N deposition to the cores still had the largest influence on vegetation, particularly for the grasses. There was a very large increase in grass dry weight with increasing N deposition (Figure 3.54). The influence of ozone was much more minor and not consistent between cores of different sites. This will have been affected by whether or not the cores contained species that were sensitive to ozone, or were dominated by insensitive species. However, for some sites there were

large decreases in the amount of harvested material with increasing ozone exposure. The cores will overwinter outside at the CEH-Bangor site, and above-ground plant material will be harvested again in Spring 2016.
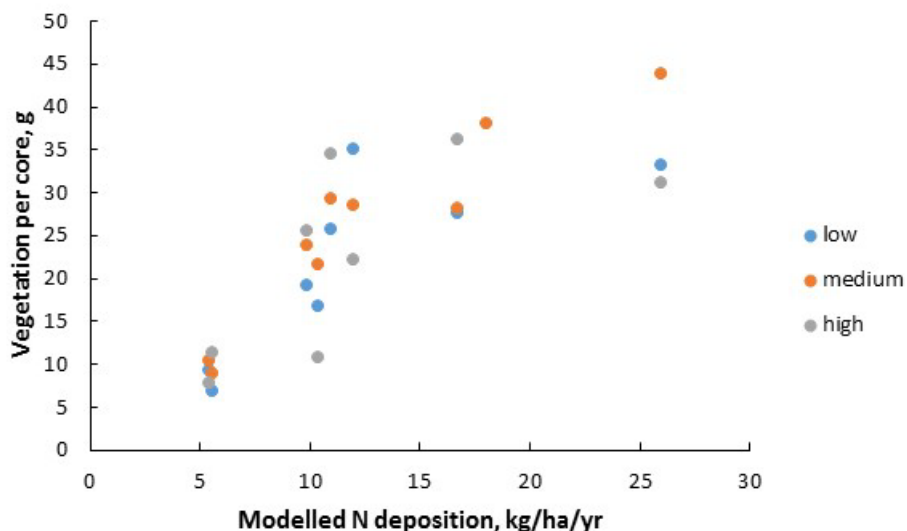
Figure 3.54: Vegetation dry weight per core with ozone treatment and historic N deposition.

Ozone and nitrogen pollution can both affect coastal grasslands, however, since nitrogen deposition alters the species composition of the grasslands, the mechanism of interaction between ozone and nitrogen is difficult to identify. Effects of the pollutants on the coastal grassland community extend beyond immediate effects on the vegetation to processes affecting ecosystem function, including chemistry of soil pore water and activities of soil enzymes.

(3) Ongoing measurements at Whim

Soil water chemistry is monitored once per month in treatment plots and measurements are ongoing. Measured parameters are: DOC, DON, Ca, Mg, Na, K, Cl, NO_3-N, NH_4-N and SO_4^2. Data gathered for the duration of the ÉCLAIRE will continue to be uploaded in ÉCLAIRE database.

Soil pH is measured approx monthly.

Meteorology data (air temperature, PPFD, RH, windspeed, precipitation) and *Soil meteorology data (Soil water content and soil temperature)* are recorded every 15 mins.

Task 11.2

Specific objective: Physiological controls of climate change and pollutant exposure on exchange of BVOCs, NO and O_3 (CNR). To assess if BVOC emissions from vegetation will increase the potential for O_3 and NO_x uptake by plants, and detoxification of reactive oxygen species, leading to improved antioxidant properties and reduced emission of other stress-induced, reactive BVOC (e.g., LOX compounds).

Activities:

Effects of climate change drivers on isoprenoids emission from plants

A survey of all peer-reviewed literature published between 1980 and 2014 was made on the basis of the keywords of "isoprene" or "monoterpene". Articles and measurements were included in this meta-analysis on the basis of the criteria below. (1) the treatments were elevated CO_2, ozone, nitrogen, drought or warming; (2) the variables were isoprene, total monoterpenes, Camphene, Carene, Cymene (or isopropiltoluene), Limonene, Myrcene, Ocimene, Phellandrene, α- and β-Pinene, Sabinene, Terpinene, Terpinolene, Thujene, Tricyclene (or cyclene); (3) the experimental control was ambient air for CO_2 and warming experiments, charcoal-filtered air (CF) or non-filtered air (NF) or ambient air for O_3 treatments, and well-watered or natural growth conditions for drought experiments; (4) the treatment duration was more than 7 days excluding O_3 treatment where acute high O_3 concentrations for several hours were included, e.g. temperature-response curves were not included; (5) the concentration of elevated CO_2 was < 800 ppm but > 500 ppm. After excluding articles based on these criteria, around 90 articles were used for the meta-analysis. Data from the figures were digitized using data extraction software (GRAFULA 3 v.2.10, Wesik SoftHaus, St. Petersburg, Russia). If photosynthesis rate (Pn) and stomatal conductance (gs) were measured simultaneously with the isoprenoids, they were also recorded Parameter values were considered independent if they were obtained from different cultivars/clones, O_3 or CO_2 concentrations, temperatures or water deficient degrees, additional treatments, or if the measurements were made on different hours or dates in the same experiment. The meta-analysis was conducted using a meta-analytical software package (MetaWin2.1.3.4, Sinauer Associates, Inc. Sunderland, MA, USA) (Rosenberg *et al.,* 2000). To estimate the treatment effect, the natural log of the response

ratio (r = variable in treatment / variable in control) was used as the metric for analysis (Hedges *et al.,* 1999; Rosenberg *et al.,* 2000) and reported as the percentage change from control as (r-1)×100% (Curtis & Wang, 1998;Feng et al., 2008; Feng & Kobayashi, 2009). Confidence limits around the effect size were calculated using a bootstrap method (Rosenberg *et al.,* 2000). Levels of each category were included in this analysis if there were at least 10 observations, or three independent articles. To build the relationship between isoprene or MT and Pn or gs, only data recorded at the same time were used.

In addition, the effects of ozone and nitrogen on BVOC emission from a tree species were investigated. Emission of BVOC from plant leaves in response to ozone (O_3) and nitrogen (N) exposure is poorly understood. For the first time, BVOC emissions were explored in a forest tree species (silver birch, *Betula pendula*) exposed for two years to realistic levels of O_3 (36, 49 and 70 ppb as daylight average) and N (10, 30 and 70 kg ha^{-1} yr^{-1}, applied weekly to the soil as ammonium nitrate) at the CEH Bangor solardome facility.

Bi-directional flux of BVOC and ozone

Mediterranean forest ecosystems are exposed to high loads of anthropogenic pollutants and are among the most threatened ecosystems on Earth by climate changes. In order to fully explore plant-atmosphere interactions under environmental stress, bi-directional exchanges of Volatile Organic Compounds (VOCs), nitrogen oxides (NO_x), CO_2, water, and ozone were investigated in a Mediterranean Holm oak forest in Castelporziano presidential estate, a peri-urban forest near the coast of Tyrrhenian sea, 20 km from Rome downtown, Italy. Two intensive field campaigns were carried out to explore seasonal dynamics of fluxes under different climate conditions and physiological activity of plants. Ozone effects on GPP (Gross Primary Productivity), measured at canopy level at the eddy-covariance site of Castelporziano, were investigated by applying sophisticated statistical approaches (wavelet coherence, random forest, G causality, multiple linear and non-linear models) and comparing the results with previous data-bases in Mediterranean ecosystems (*Pinus ponderosa* and *Citrus sinensis*). VOCs were measured using a proton transfer reaction - mass spectrometer (PTR-MS). These included biogenic products as isoprenoids (isoprene, monoterpenes), oxygenated BVOC (OVOC – methanol, acetaldehyde acetone) and VOC of anthropogenic origin (AVOC – acetonitrile, benzene, hexenal, toluene, xylenes). Our measurements comprise high frequency (10 Hz) sampling of VOC concentrations along a 5-level gradient from soil-level to above the canopy. We used eddy covariance technique to calculate half-hour fluxes of all the above mentioned gases, while gradient measurements were used to estimate within-canopy source and sink distribution by applying an Inverse Lagrangian Transport Model.

Highlights:
1. Isoprenoids emission increases with increasing temperature, and decreases with increasing CO_2 and soil water stress (Figure 3.55). Effects of ozone and nitrogen, single and in combination, are still unclear. The meta-analysis also highlighted that the number of experiments on BVOC emission as a response to a climate change driver (nitrogen deposition, drought, warming, elevated CO_2, acute and chronic ozone exposure) is still insufficient. In particular, more experiment under realistic conditions are recommended.
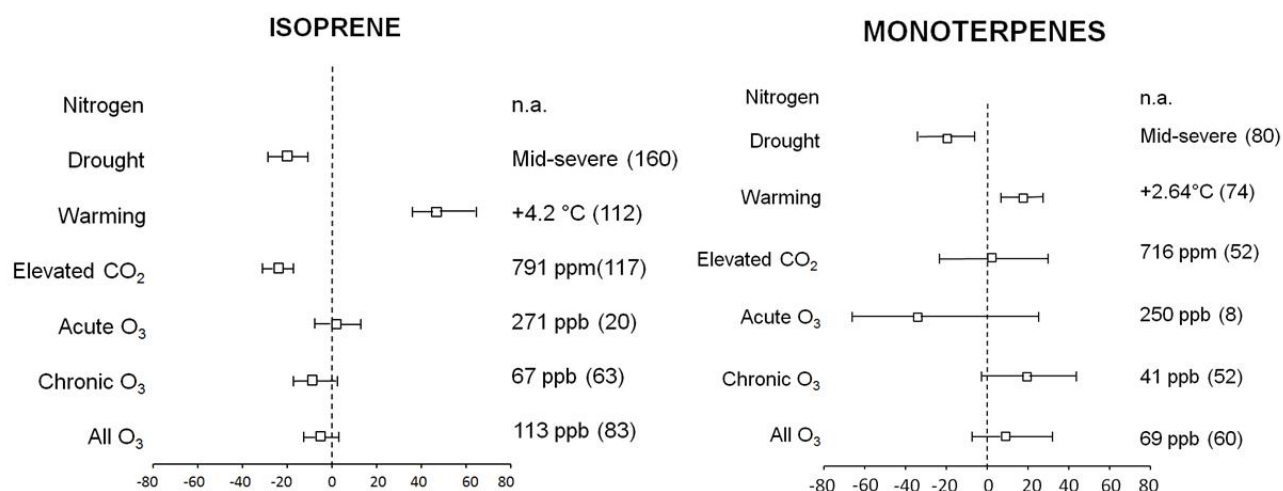

Figure 3.55: Percent change in isoprene and total monoterpenes emission under the effect of different climate change drivers. Symbols are bracketed by 95% bootstrapped confidence intervals. Mean level of stress and number of observations (in parenthesis) are also given.

This is why a specific experiment was carried out on the interactive impacts of O_3 and N on BVOC emission from birch seedlings. The main BVOCs emitted were: α-pinene, β-pinene, limonene, ocimene, (E)-4,8-dimethyl-1,3,7-nonatriene (DMNT) and hexanal. Ozone exposure increased BVOC emission and reduced total leaf area (Figure 3.56). The effect on emission was stronger when a short-term O_3 metric (concentrations at the time of sampling) rather than a long-term one (AOT40) was used. The effect on leaf area was not able to compensate for the stimulation of emission, so that responses to O_3 at leaf-unit and entire-plant level were similar. Nitrogen fertilization increased total leaf area, decreased α-pinene and β-pinene emission, and increased ocimene, hexanal and DMNT emission. The increase of leaf area changed the significance of the emission response to N for most compounds. Nitrogen fertilization mitigated the effects of O_3 exposure on total leaf area, while the combined effects of O_3 and N on BVOC emission were additive and not synergistic. In conclusion, O_3 and N pollution have the potential to affect global BVOC via direct effects on plant emission rates and changes in leaf area.
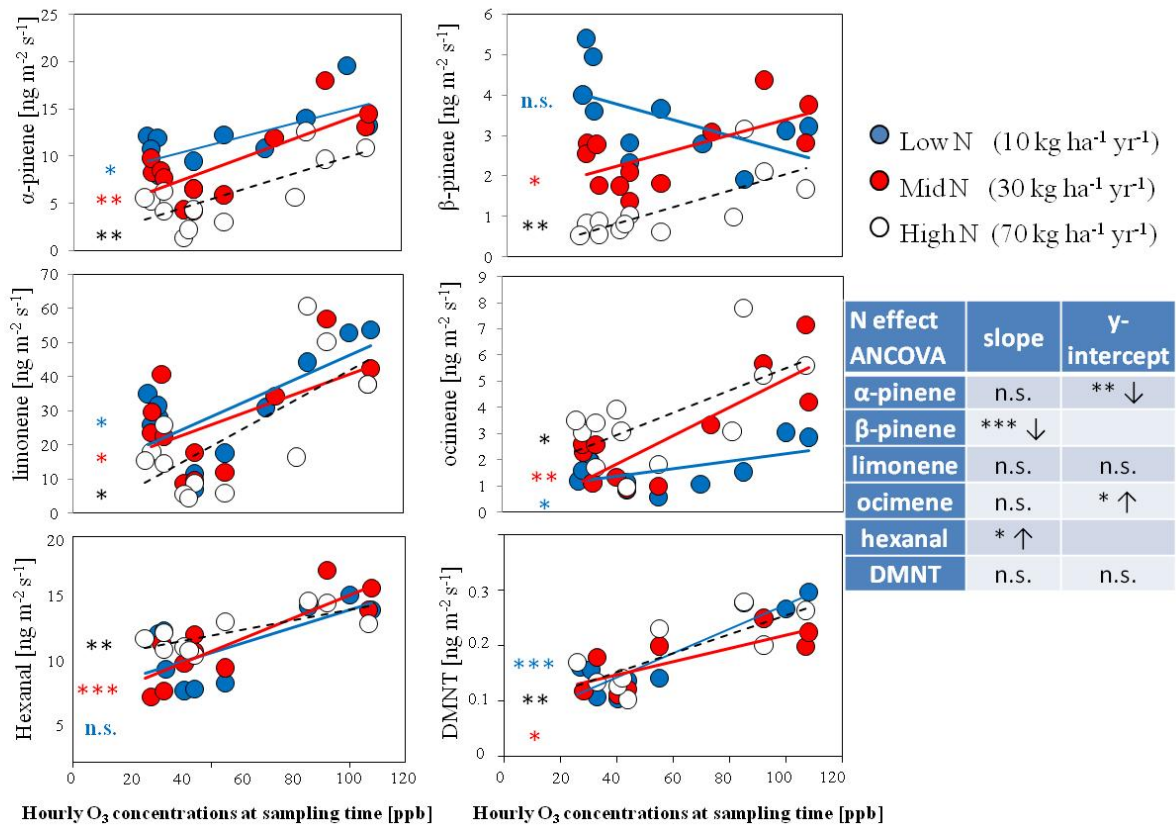
Figure 3.56: the combined effects of ozone and N on BVOC emissions from silver birch.

2. Ozone fluxes are higher during warm days, when non-stomatal sinks (e.g. gas-phase chemistry due to high monoterpene and isoprene fluxes during the warm days of September) are also higher (Figure 3.57. Fluxes peak during the day because primary emitted BVOC depend on light and temperature. Low temperatures lead to almost negligible BVOC fluxes during winter (not shown). Summer fluxes were largely represented by BVOC (mainly monoterpenes) and were recorded in the central hours of the day in response to high light and temperature (green marks the measurements and blue marks data modelled by an inverse lagrangian model). In the same periods, high amount of ozone was sequestrated by plants through stomatal uptake and through non-stomatal deposition. We hypothesize that chemical reactions between BVOC and ozone may have played a role in ozone scavenging. An interesting role of NO_x was observed between day (NO_2 formation ad deposition to the canopy) and night (complete ozone scavenging below the canopy by NO).
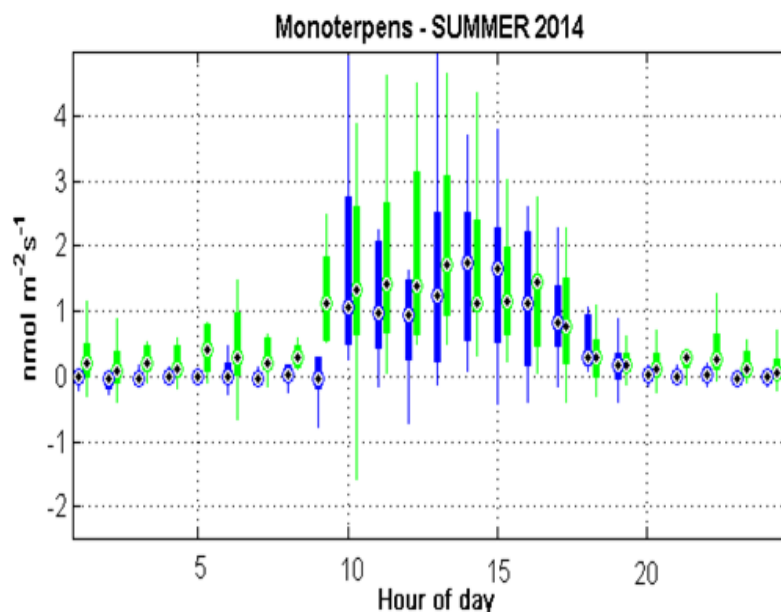
Figure 3.57: Monoterpene emissions from a Holm oak forest (summer 2014).

Task 11.3

Specific objective: Effects of aerosol deposition on stomatal functions. To demonstrate if hygroscopic particles accumulating on leaves from aerosol and trace gas deposition may attract water and lead to enhanced transpiration and reduced drought tolerance.

Activities:

The results of experiments were presented in previous annual reports To support the prior measurements a full year of measurements were made at the experimental site (Central Bonn) to compare aerosol concentrations in ambient air and under the filtered air treatment. Resources re-deployed from the restricting of Task 4.4 allowed these measurements to be made using DELTA denuders. The measurements showed that the filters substantially reduced PM concentrations of the major inorganic fractions, providing a clear basis to process the experimental data and thereby establish a first dose-response relationship between total hygroscopic aerosol loading and the value of minimum stomatal conductance under different levels of drought conditions. Other activities concentrated on preparation and submission of papers, several oral and poster presentations at scientific conferences. Ongoing and future work will focus on further

252

developing dose-response relationships and in providing parametrizations for incorporation in dynamic global vegetation models (DGVMs).

Progress towards the milestones and deliverables

All milestones and deliverables were delivered.

Use of resources and deviations from DoW

A total of 14.7 person months were used in this period. Little deviations did not affect the main results.

ÉCLAIRE Third Periodic Report: November 2015

Work package 12 – Development and Assessment of Novel Thresholds

Lead contractor: SEI UoY
Contributors: NERC, DTU, RIVM, UGOT, IVL

Work package objectives

The general aims of this work package are:

1. To define pollutant-response relationships relevant for ecosystem service evaluation

2. To define intermediate plant processes that relate pollutant deposition and uptake to plant responses

3. To apply the DO$_3$SE model to simulate deposition and uptake for key ÉCLAIRE experimental effect studies

4. To develop and apply other necessary conceptual and quantitative modelling frameworks as a basis for investigating dose response relationships (especially relevant for the novel interactions addressed under WP11)

5. To analyse these data to develop new dose-response relationships and novel thresholds

Progress and Results

Task 12.1 Definition of pollutant response parameters relevant for ecosystem service valuation

This task informed the development of 'ecosystem service' relevant responses that can be used in the integrated risk assessment and policy analysis in C5, ensuring consistency with the responses that can be modelled using the methods developed in C3.

Progress and Results

A report which describes 'The development of 'ecosystem service' relevant responses has been delivered **(D12.1).** This report has been shared with our C5 collaborators.

Task 12.2 Definition of intermediate plant processes determining response to pollutant deposition

This task identified the key plant processes determining response to pollutant deposition and uptake and the eventual 'ecosystem relevant' response. The intention being that an

existing pollutant deposition and impact model (DO$_3$SE) be modified to allow these intermediate processes to be modelled and thereby used in the assessment of pollutant impact of plant physiology and biomass. This model construct was designed to make use of data collected in C3 in the data-mining activity of WP9 and the experimental data collection activities of WP10 and 11.

Progress and Results
The DO$_3$SE model (now termed DO$_3$SE_C or the A$_n$-g$_{sto}$ DO$_3$SE) has been developed and now includes:- i. a coupled A$_n$-g$_{sto}$ algorithm to estimate ozone uptake as a function of CO_2 concentration and prevailing environmental conditions; ii. parameterisation of a key An parameter – maximum carboxylation capacity (V$_{cmax}$) that determines light saturated An and is dependent upon rubisco activity within the leaf. This varies with species types, leaf N content and leaf position in the canopy with parametrisation being defined to account for these different types and conditions; iii. incorporation of the O$_3$ effect on V$_{cmax}$ through the development of an O$_3$-V$_{cmax}$ sub module that allows damage and repair to V$_{cmax}$ dependent upon the instantaneous stomatal flux of O$_3$. Since V$_{cmax}$ is also related to leaf N content (which is related to N availability and hence N deposition) this model framework provides the opportunity to investigate the combined effects of N deposition and O$_3$ pollution on A$_n$ related plant physiology. This is scaled up to effects on biomass since A$_n$ determines growing season C accumulation (i.e. NPP).

The description of the DO$_3$SE_C or the A$_n$-g$_{sto}$ DO$_3$SE model has been delivered (**D12.2**). This report has been shared with C1 and the new DO$_3$SE model is now embedded within the EMEP model and ESX.

*Task 12.3 Apply DO$_3$SE model to analyse ÉCLAIRE experimental data*

This activity collated and transformed the ÉCLAIRE experimental data into a format that could be used by the DO$_3$SE model. This work focussed on two forest tree experimental datasets. A birch dataset collected in Bangor, UK and an oak dataset collected in Curno, Italy. This approach was taken since a key knowledge gap had been identified for forest trees, namely that the existing dose-response relationships and thresholds for this receptor type were not useful for estimating *damage* caused by N and O$_3$ pollution impacts.

Progress and Results
DO$_3$SE model runs for both Bangor and Curno datasets have been performed. These have allowed the further development and calibration of the DO$_3$SE model, and in particular the Vcmax-O$_3$ damage sub module. A key issue in this model development had been developing a method that could account for the effect of both phenology and O$_3$ damage on V$_{cmax}$ over the course of the growing season; this was overcome by defining a phenology-dependant V$_{cmax}$ seasonal profile, upon which the O$_3$-Vcmax effect is super-imposed. The model has been calibrated to the measured seasonal V$_{cmax}$ values and has

been evaluated against other leaf physiological variables (namely A_n and g_{sto}) for both experimental datasets.

Importantly, the DO₃SE model is able to simulate C assimilation and hence biomass (or NPP). This provides the opportunity to assess the combined effect of O_3 and variable leaf N (used as a proxy for variable N deposition) on biomass. Figure 3.58 compares such interactions as described by the experimental data (in this case from Birch grown in Bangor) with the equivalent model simulation

(a)   (b)
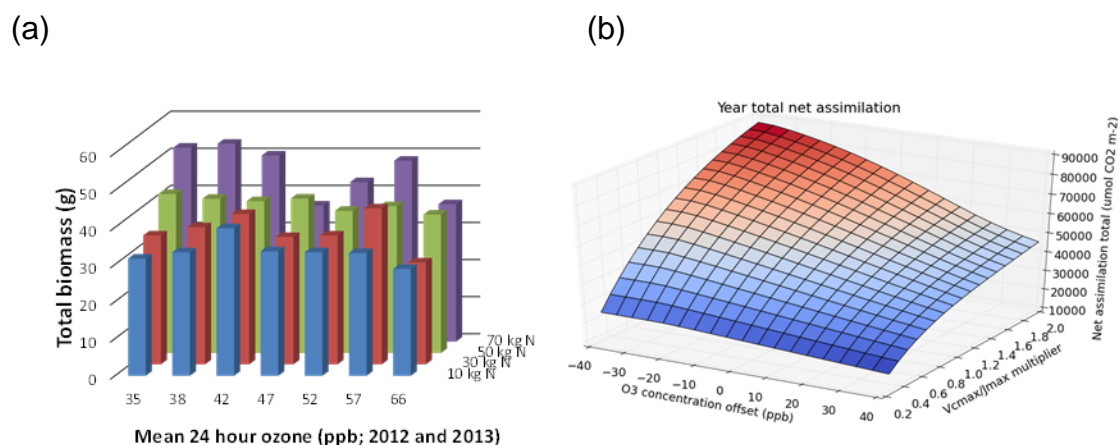
Figure 3.58. Birch experimental data **(a)** from Bangor showing total biomass in relation to increasing [O3] (x axis) and increasing N deposition (z axis) compared to Birch model simulations **(b)** showing net assimilation (equivalent to biomass) in relation to an increasing [O3] (x axis) and a increasing V_{cmax} (proxy for leaf N and N deposition) (z axis).

Fig 3.58 clearly shows that model is able to reproduce the profile of the response surface of biomass to the combined effects of [O₃] and N deposition. The largest biomass occurs under situations with low [O₃] and high N, conversely, lowest biomass occurs under high [O₃] and low N. However, in relative terms, increasing [O₃] under higher N conditions results in a larger reduction in absolute biomass than under low [O₃] conditions.

The description of the application of the DO₃SE model to analyse ÉCLAIRE experimental data has been delivered (**D13.3**). This report has been shared with component leaders to inform of the status in the application and evaluation of the DO₃SE model with experimental data (C3) as well as the capabilities of the DO₃SE model with reference to developing novel thresholds (C5).

Task 12.4 Development of new dose-response relationships and novel thresholds.

This task has defined novel dose-response relationships (DRRs) and where appropriate, novel thresholds. The focus here has been on forest tree species since this was identified as the receptor for which damage estimates had not previously been possible.

Progress and Results
This work has taken three different approaches: i. an approach that focusses on the response parameter (net annual increment) to allow estimates of O_3 damage to forest trees to be made on an annual basis; ii. an approach that has modified existing [O_3] DRRs to account for variable N deposition for risk assessment and finally; iii. an approach that investigates the relationship between O_3 and N deposition to that could be used to inform emission reduction targets.
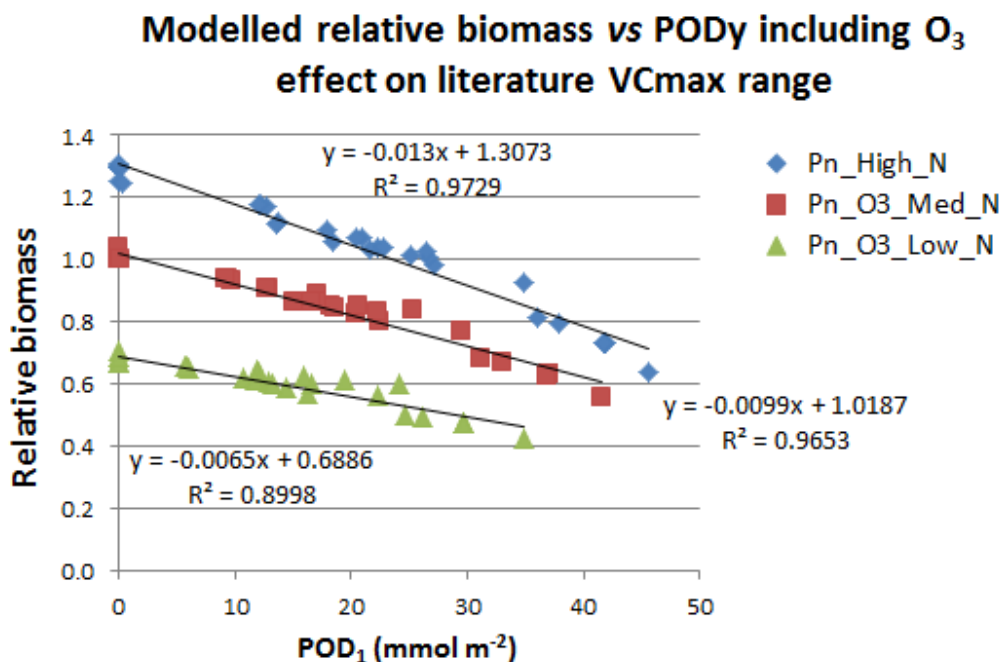
Net annual increment - A new method has been developed to estimate loss in C stocks due to [O_3] exposures for forests growing across Europe. This uses a new forest response parameter (% change in net annual increment) which has been defined from re-analysis of existing data describing O_3 losses on total tree biomass (these dataset are those used within the UNECE Mapping Manual (LRTAP Convention, 2010). An example of the resulting NAI DRRs (and the original total biomass DDR for comparison) is shown in Figure 3.59.
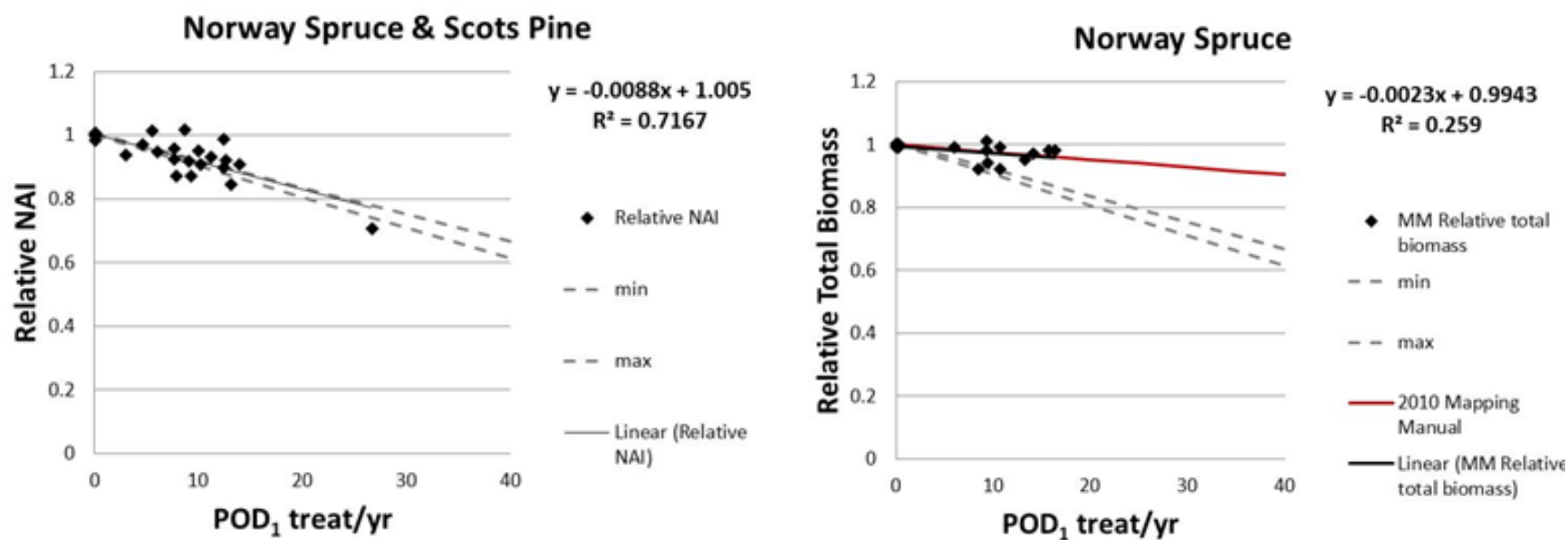
Figure 3.59: NAI and total biomass DRRs for Norway spruce derived from re-analysis of existing ozone fumigation experimental data. Details of the datasets can be found via the UNECE Mapping Manual (LRTAP Convention, 2010).

ÉCLAIRE Third Periodic Report: November 2015

Application of these new NAI flux DRRs should incorporate information on felling rates to allow an assessment of the [O_3] influence on C stocks within the context of annual felling rates and hence timber harvests. These DRRs will allow an assessment of the damage that O3 causes to forests on an annual time-step and therefore will enable estimates of the annual C stock that is lost due to O_3 pollution.

Modifying existing O3 DRRs for variable N deposition - The A_n-g_{sto} DO$_3$SE model has also been used to develop novel DRRs for [O_3] for different N deposition conditions. Again, this work has used the existing UNECE Mapping Manual (LRTAP Convention, 2010) DRR datasets and assumes that these data represent conditions under medium N deposition conditions (using the A_n-g_{sto} model to estimate the POD1 values). The A_n-g_{sto} model has then be re-run assuming high and low N conditions (by changing the V_{cmax} parameterisation in the A_n-g_{sto} model to provide estimates of how N will influence POD$_1$ – this has used V_{cmax} values published in the literature assuming the range in V_{cmax} within species is determined by N availability). These changes in V_{cmax} will also change the A_n (and hence C assimilation). The model simulation of this altered simulation of C assimilation is then used to weight the actual biomass data. The resulting DRRs for low, medium and high N are shown in Figure 3.60.

Modelled relative biomass *vs* PODy including O$_3$ effect on literature VCmax range

$y = -0.013x + 1.3073$
$R^2 = 0.9729$

$y = -0.0099x + 1.0187$
$R^2 = 0.9653$

$y = -0.0065x + 0.6886$
$R^2 = 0.8998$

- Pn_High_N
- Pn_O3_Med_N
- Pn_O3_Low_N

Relative biomass

POD$_1$ (mmol m^{-2})

Figure 3.60: 3 DRRs estimated using the A_n-g_{sto} model to estimate relative biomass for high and low N treatments (in comparison to actual DRR data assumed equivalent to the medium N treatment) and POD$_1$ values estimated by the A_n-g_{sto} model that accounts for O$_3$ and N influence on V_{cmax}.

ÉCLAIRE Third Periodic Report: November 2015

Relationship between O₃ and N deposition for emission reduction targets – The work performed using the An-gsto model has shown rather complex interactions between O₃ and N deposition (the latter using the proxy of Vcmax). A key question is how this information can be used at the European scale to inform emission reduction scenarios. To this end we have used the model to develop isoline graphs that show annual net C assimilation (i.e. NPP) in relation to different levels of N deposition (using Vcmax as a proxy) and [O3] (Figure 3.61).
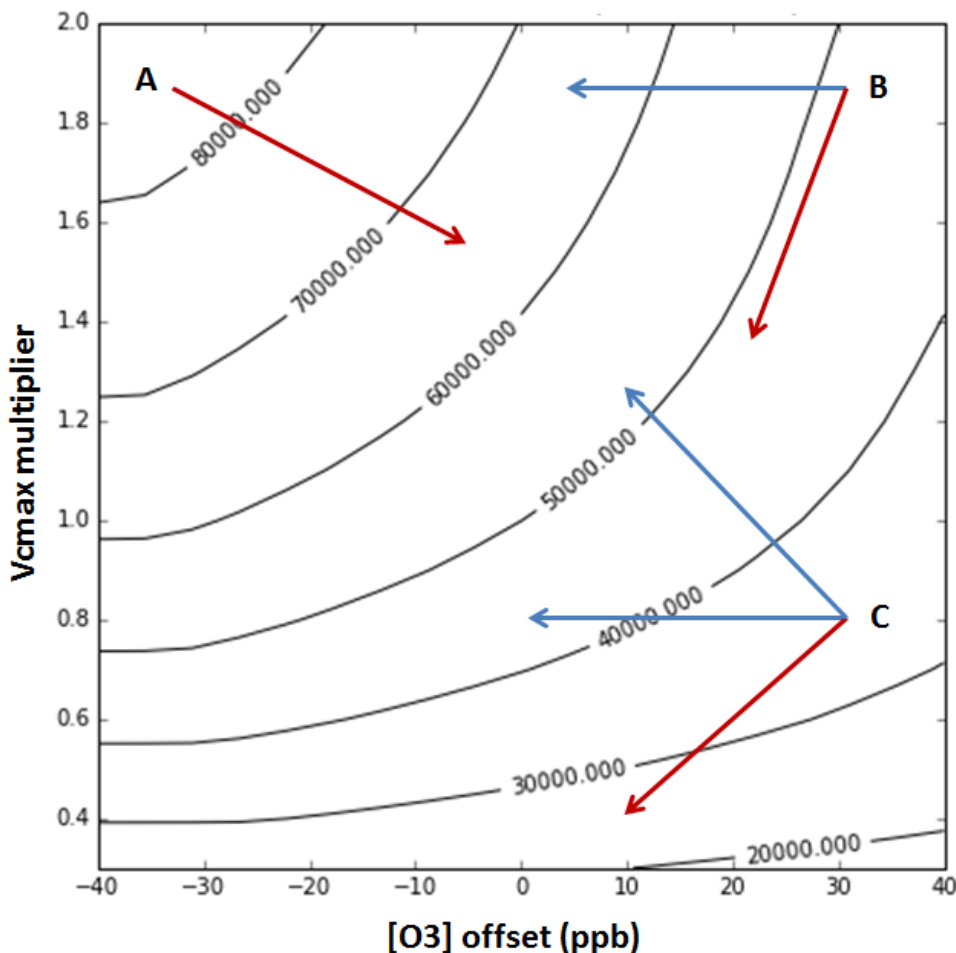
Fig 3.61: Isolines of net annual C assimilation (i.e. NPP) against variable [O₃] (x axis) and variable V$_{cmax}$ (indicating the effect of changing N deposition). The points A, B and C indicate points of the graph and how a reduction in either [O₃] or N deposition would alter NPP (and hence biomass) – see text for further details.

The points (A, B and C) on Fig. 3.61 provide an indication of the effect of scenarios of [O_3] or N deposition changes. Point A represents a high N deposition and low [O_3], were N deposition to be reduced whilst [O_3] is increased a reduction in biomass would be likely to occur. Point B represents a high N deposition and high [O_3] situation, here a decrease in only [O_3] would likely see an increase biomass, whilst a decrease in both [O_3] and N may see little change in biomass. Finally point C represents a high [O_3] and low N deposition situation. A decrease in [O_3] will see a similar or increasing biomass so long as N deposition is not decreased at the same time.

This type of approach could help inform the consequences of emission reduction strategies across Europe **but only when considering productive ecosystems** (for semi-natural ecosystems where biodiversity is the response parameter increases in N are likely to lead to decreases in biodiversity). As such, this approach should be used with care, and perhaps only to inform on likely changes in productivity under a range of emission scenarios.

Progress towards the milestones and deliverables

D12.1 Summary report describing key response parameters derived from empirical studies and suitable for use in the first phase of the ecosystem valuation work (Month 12)
Report completed in month 12 and shared with C5

D12.2 Documentation of the DO3SE_C (A_n-g_{sto}) model
Report describing documentation completed and shared with C1

D12.3 Delivery of novel thresholds for key dose-response relationships. This report summarised the work describing new dose-response relationships for net annual increment for forest trees and made suggestions of methods to develop novel thresholds based on the DO$_3$SE modelling work. The report was shared with C5 and key aspects of the work presented at the Edinburgh meeting to gain feedback for use in finalising the development of novel thresholds.
Report completed 15/12/2014 and shared with C5 and at ÉCLAIRE annual general meeting in Sept 2015.

D12.4 Final Report describing new dose-response relationships and novel thresholds (Month 40). This deliverable has been completed after making some re-analysis of DO3SE model runs incorporating feedback from C5 and the ÉCLAIRE annual general meeting in Edinburgh (Sept 2015).
Report completed 30/09/2015.

Use of resources and deviations from DoW

A total of 7.7 person months were expended in this period. The use of the A_n-g_{sto} DO3SE model to analyse the ÉCLAIRE experimental data collected in WPs 10 and 11 ran behind schedule due to delays in uploading and quality checking the empirical data to the ÉCLAIRE data portal; this work is now finished but did cause a delay in the analysis and development of novel thresholds using the DO3SE model. This work is now completed.

Work package 13 Modelling of carbon stocks, greenhouse gas and vegetation change

Lead contractor: NERC
Contributors: ALTERRA, SEI-Y/UoY, RIVM

Work package objectives

1. To develop a model describing the combined effects of O_3, other atmospheric pollutants and climate on plant CO_2 uptake, net ecosystem exchange (NEE) and C sequestration in soil and vegetation, suitable for linking to existing plant-soil biogeochemistry models.
2. To develop existing dynamic vegetation models to better simulate the impacts of different air pollutants on plant growth and competition, and feedbacks on ecosystem carbon cycling.
3. To incorporate CH_4 and N_2O, as well as dissolved C and N losses, into biogeochemistry models for relevant ecosystems.
4. To integrate models in order to simulate the combined response of soils and vegetation to N, S and O_3-exposure, diffuse radiation and climate change, suitable for application at a range of scales and for addressing a range of ecosystem impacts such as changes in C sequestration, vegetation diversity.
5. To undertake parallel testing of models with different process descriptions and levels of complexity against detailed data from experiments
6. To use the final tested models for prediction of future ecosystem responses to air pollution and climate change at a site level, and to deliver models for regional scale application in C4.

Progress and Results

Task 13.1. Model development and linking

MADOC

Following an extensive review of the literature on ozone effects and ozone-nitrogen interactions (see ÉCLAIRE WP9 reports), strong and consistent evidence was found for two effects: 1) a reduction in Net Primary Productivity (NPP); and 2) early leaf senescence, resulting in reduced resorption of N and therefore a greater concentration of N in leaf litter. These effects were incorporated into the model using functions derived from empirical data in response to ozone, expressed as growing-season daylight-mean ozone concentration. Separate NPP reduction functions were fitted to biomass reduction data from: wet grassland and bog; other grassland; and woodland. A single response function was fitted describing the

effects of O_3 on N resorption at senescence for all vegetation types. These model developments are described in detail in Deliverable 13.3.

DO₃SE

The ozone (O_3) deposition model DO₃SE was improved by substituting the multiplicative with a photosynthesis (A_n) based stomatal conductance (g_{sto}) algorithm, which allows stomatal conductance to be estimated as a function of CO_2 concentration (as utilised by the photosynthesis) as well as other prevailing environmental conditions such as N deposition (through varying levels of leaf N), relative humidity, irradiance, leaf temperature and soil moisture deficit. This enables DO₃SE to model instantaneous O_3 damage taking into account the combined effects of atmospheric O_3 and N pollution on A_n, and hence biomass. This work is described in Deliverable 13.3.

Task 13.2 Model testing

MADOC

The MADOC model was tested against data from a range of experimental and monitoring sites. The acid-base component of the model was tested against long-term soil solution monitoring data from the ICP Forest Level II and UK Environmental Change Network datasets, and shown to provide a good fit to observations from sites spanning a range of vegetation types (conifer and broadleaf woodland, grassland, heathland and bog) and deposition levels (see Deliverable 13.3 for further details). The carbon and nitrogen cycling components of the model was assessed against data from experimental sites including the Whim Bog N addition experiment, and the Gårdsjön long-term catchment-scale deposition manipulation experiment in Sweden (e.g. Figure 3.62).
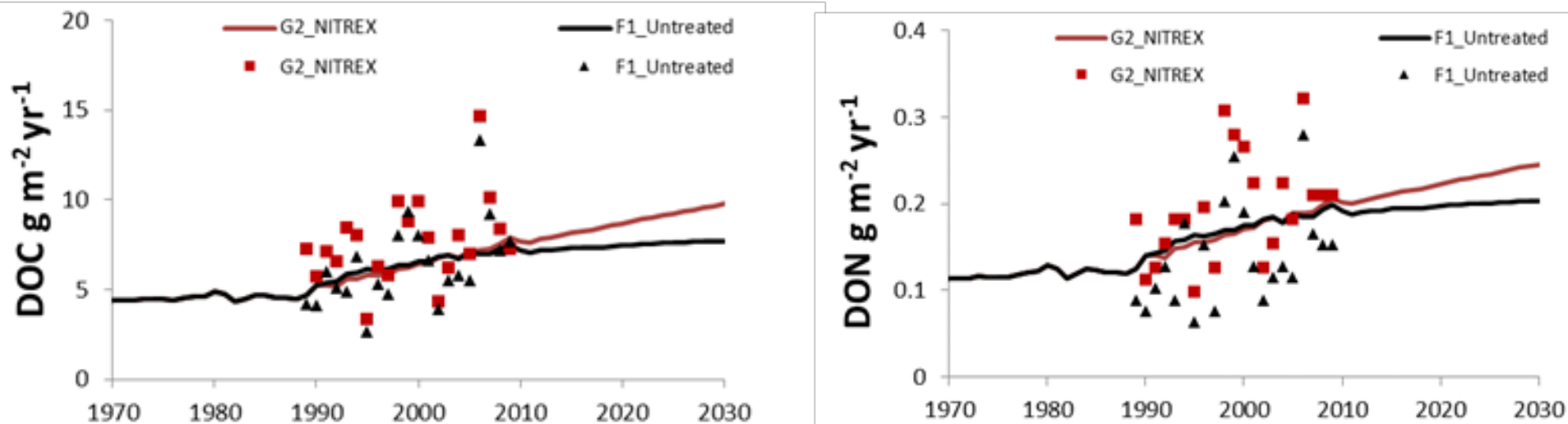
Figure 3.62: Modelled versus observed concenntrations of dissolved organic carbon (DOC) and dissolved organic nitrogen (DON) in leachate at the Gårdsjön clean rain (G2 roof), nitrogen addition (G2 Nitrex) and ambient reference (F1) catchments.

ÉCLAIRE Third Periodic Report: November 2015

The only field experiment in Europe at which ecosystem responses to both N and O_3 exposure have been evaluated is at Alp Flix, an Alpine grassland in Switzerland. MADOC was tested against a range of observations from this site including net primary product (NPP), shown in Figure 3.63. Although test data are scarce, model performance was considered to reflect the separate effects of ozone and N, and the model was used to explore interactions between the two pollutants.
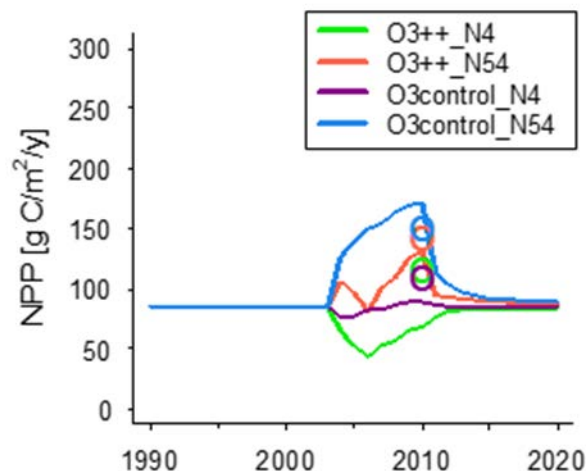

Figure 3.63: Modelled and observed Net Primary Productivity (NPP) at the Alp Flix experimental site, for different combinations of high (N54) and ambient (N4) nitrogen deposition and high (O_3++) and ambient (O_3control) ozone exposure.

DO$_3$SE

The new modules developed within DO$_3$SE representing the key physiological variables leaf temperature, g_{sto} and photosynthesis were tested and evaluated through the application of DO$_3$SE to the ÉCLAIRE Bangor dataset for birch (derived from field experiments carried out under WP 10), which offered the full set of required input and evaluation parameters. The model was found to be capable of simulating realistic ranges of these key physiological variables. The capability of this version of DO$_3$SE to predict NPP has also been demonstrated. Results of model testing are shown in Figures 3.64-3.65, and described in more detail in Deliverable 13.3.
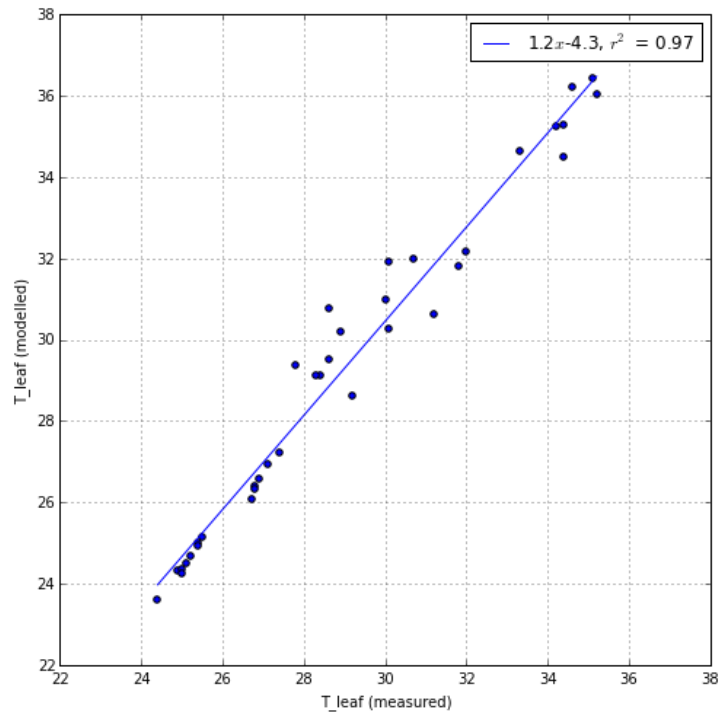
Figure 3.64: Comparison of observed ("measured") and simulated ("modelled") T_{leaf} (based on observed T_{air}) for the Bangor birch dataset at low O_3 concentration and low N deposition.

ÉCLAIRE Third Periodic Report: November 2015
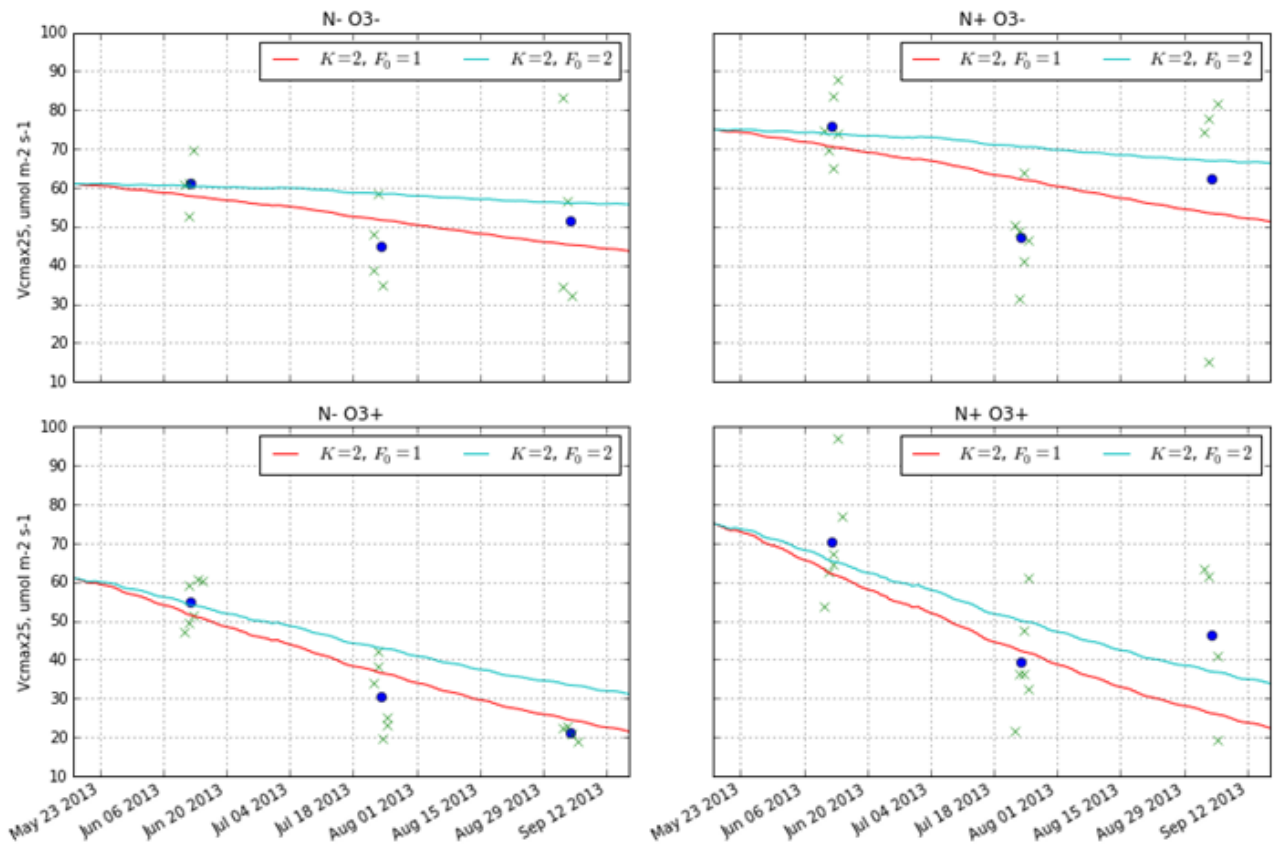
Figure 3.65: The DO$_3$SE A_n-g_{sto} *model* simulation of V_{cmax} over the course of the growing season compared to observations for Birch grown in the Bangor solardomes. Simulations show for high and low conditions of both O$_3$ and leaf N.

Task 13.3 Model application

MADOC

The MADOC model was used to explore ecosystem sensitivity to combined air pollution and climate change drivers. Scenarios applied (from 2020) were increases in mean annual temperature of +2 °C and +4 °C, and increases and/or decreases in N and O$_3$ pollution by +/- 20%. Simulations showed broadly opposing responses to O$_3$ and N pollution at the ecosystem scale. In general, additional N deposition increases the amount of available N within the ecosystem, which in turn stimulates productivity in N-limited semi-natural ecosystems, as shown in Figure 3.66. These modelled increases in NPP have a cascading effect on other ecosystem properties and functions, for example leading to an increase in soil C (implying an increase in CO$_2$ sequestration) and increasing leaching of nitrate and DOC to surface waters. Although the magnitude of these effects are predicted to vary between ecosystems (compare

left and right panels of Figure 3.66) the general direction of change is predicted to be consistent.

The effects of elevated O_3 are broadly opposed to those of N, with vegetation damage by O_3 having a negative effect on productivity. These effects were well-illustrated by the model: for example, a 20% increase in N at the Gårdsjön forest site for ten years increased NPP by 5%, whereas a 20% increase in O_3 decreased NPP by 2%. Figure 3.67 shows the interactive effects of N and O_3 for the Grizedale broadleaf monitoring site across a wider range of pollution levels. In general, for any given percentage change, the model suggests that the effects of N will exceed those of O_3, although actual future ecological changes will depend on both the direction and relative magnitude of N and O_3 changes; for example a reduction in N deposition combined with an increase in O_3 levels will have a reinforcing (negative) effect on productivity. It is also important to note that, whilst a positive change in NPP is associated with a positive change in several ecosystem services (agricultural and forest production, and carbon sequestration) it is often inversely correlated with biodiversity, for example because species typical of infertile environments tend to be more scarce. Therefore it is difficult to characterise the impacts of either pollutant as 'good' or 'bad', because this depends strongly on the relative weight assigned to different outcomes (e.g. biodiversity versus forest productivity) in different locations. For O_3, although negative effects on productivity could be considered beneficial for biodiversity, and ozone could be seen as mitigating the damage to biodiversity caused by N, this mitigation is likely to be partial. Sensitive plant and animal species may be affected directly by ozone as well as by N, and an environment chronically polluted by both of these atmospheric pollutants is likely to be impoverished.

Effects of climate change (increase in mean annual temperate) were similar to the effects of N pollution, with direct impacts on NPP, and also through increased N mineralisation and availability. As with the other pollutants, broad effects simulated via impacts on NPP are unlikely to represent all likely changes, since many species will be unable to adapt to the changed climate at a particular site. Despite these limitations and subtleties, the modelling approach taken proved useful in illustrating the major effects of air pollution and climate change on ecosystems.
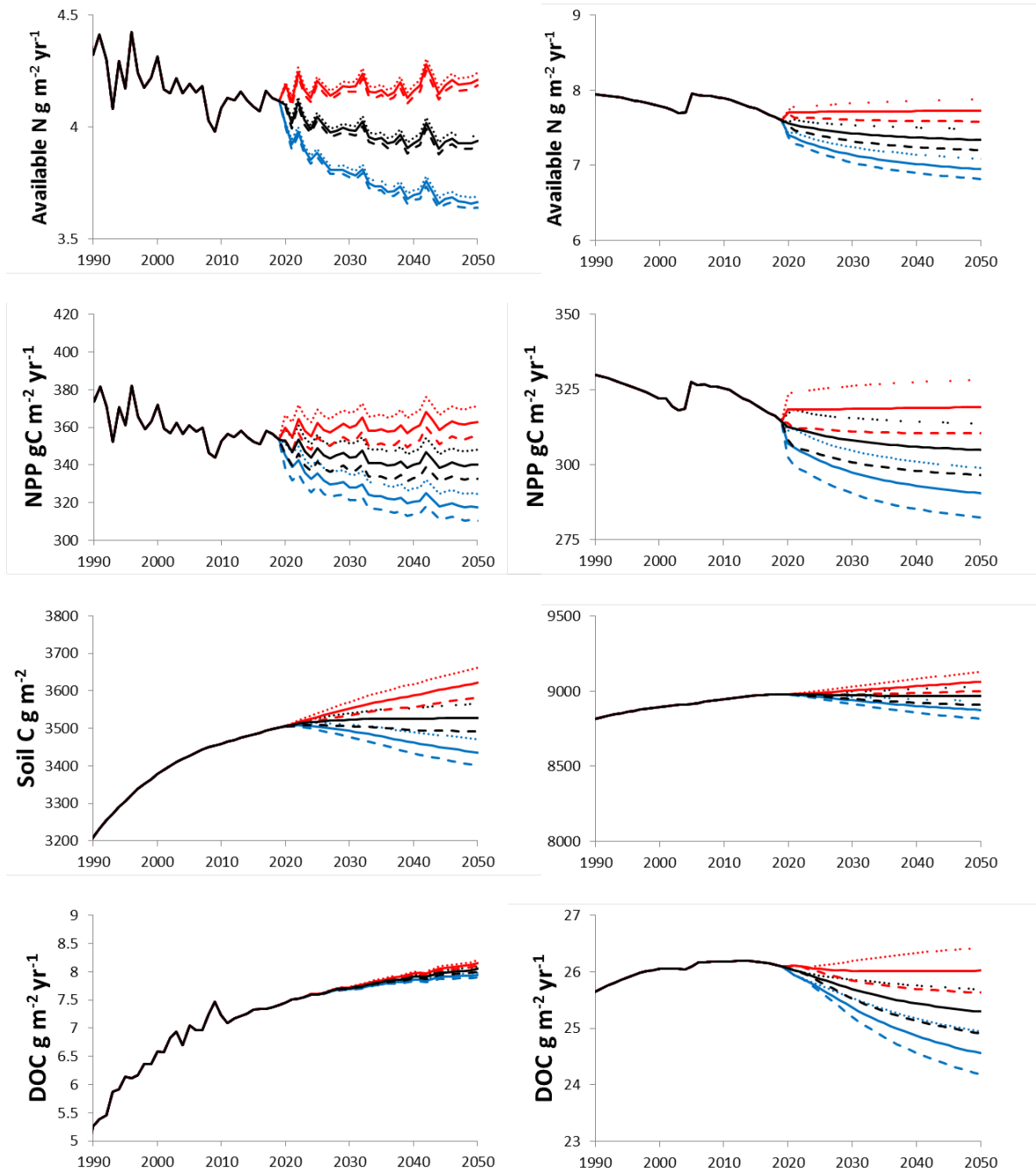
Figure 3.66: MADOC scenario assessment for the effects of changing future N and O3 on simulations of soil available N, net primary production, soil carbon and leachate dissolved organic carbon for the Gårdsjön forest experimental site (left) and Whim Bog experiment (right). Red, black and blue lines represent high, business as usual and low N deposition scenarios; short-dashed, solid and long-dashed lines represent high, business as usual and low O3 scenarios.

270
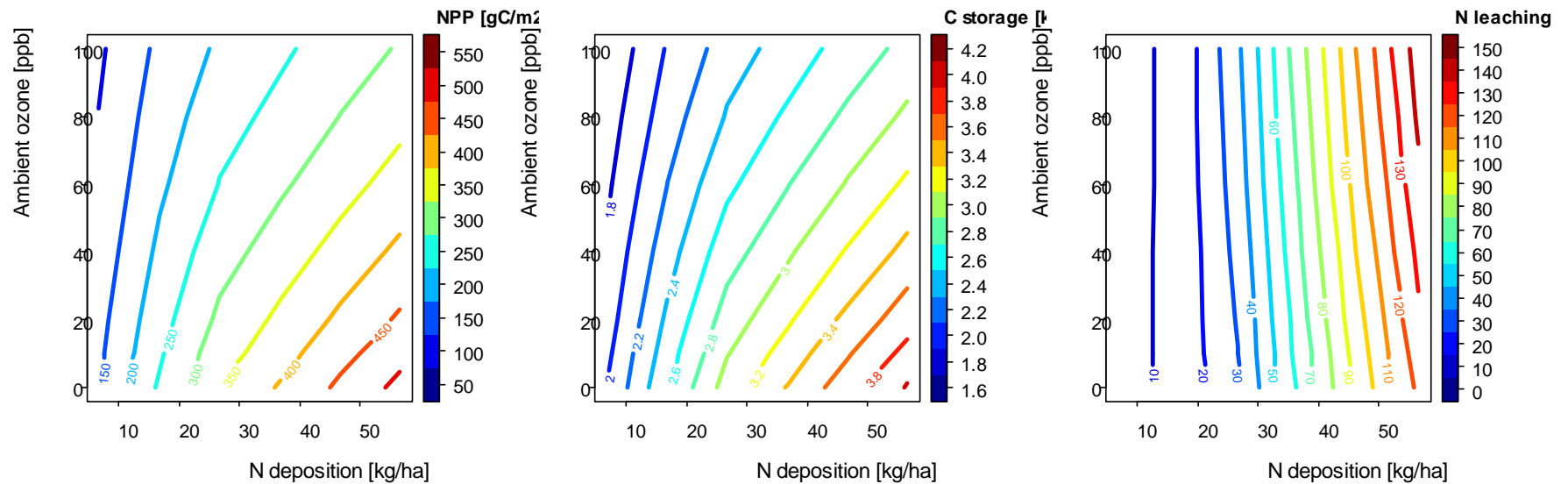
Figure 3.67: Sensitivity of the MADOC model to ozone and nitrogen at the Grizedale long-term monitoring site: effects on a) net primary productivity; b) soil carbon stock after 30 years; c) mineral nitrogen leaching.

DO$_3$SE

The DO$_3$SE model was applied to the Bangor birch experimental plots, and used to predict end-of-season relative NPP over a range of O$_3$ exposure levels, combined with high and low N treatments. The simulations suggest that higher leaf N may provide some protection against the toxic effects of O$_3$, thereby alleviating a small proportion of the negative effect of O$_3$ on productivity (Figure 3.68).
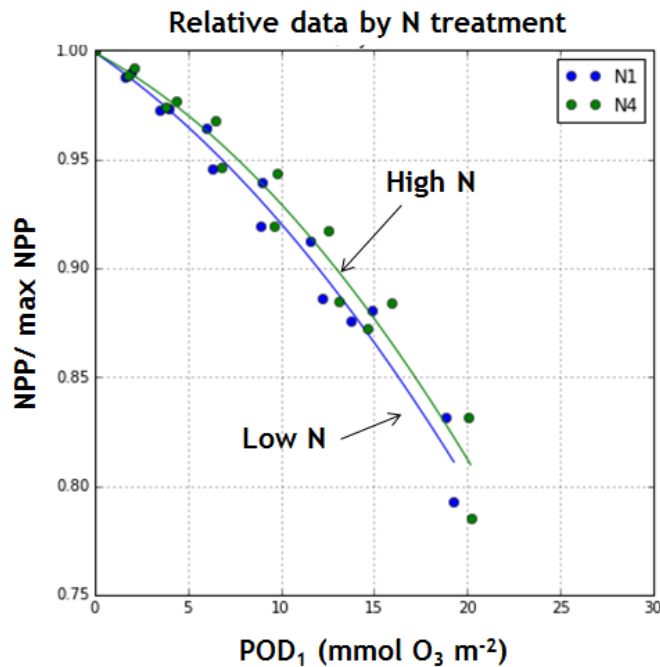
Figure 3.68: A$_n$-g$_{sto}$ DO$_3$SE model simulations of end of season relative NPP against POD$_1$ for the low and high N treatments applied to Birch trees fumigated with ozone in the Bangor solardomes.

3. Progress towards the milestones and deliverables

MS59   Update of experimental datasets, completed testing of site-based and regional-scale models   Due Month 24   Completed Month 42

MS60   Completion of scenario assessments of ecosystem responses to air pollution and climate change   Due Month 36   Completed Month 45

D13.3   Report on performance of site-based and regional-scale models Due Month 24   Submitted Month 43

D13.4   Assessment of the effects of combined air pollution and climate change scenarios   Due Month 36   Submitted Month 47

Use of resources and deviations from DoW
A total of 17.3 person months were spent on activities in this work packages, during the third period.

Work on WP13 was delayed by difficulties in identifying and sourcing suitable model parameterisation and test data, and in obtaining data for individual sites that were not held on the NEU database. The final parameterisation of ozone response functions in MADOC was held back until the data mining and experimental work in WPs 9 and 10 had been completed, in order to ensure that model simulations were fully consistent with the empirical relationships derived within the project. Given the limited number of field data providing robust measurements of ecosystem response to ozone, and to combined ozone and nitrogen in particular, model testing was focused primarily on these sites, rather than on a larger number of less data-rich sites that would not have provided an effective test of model performance, or suitably constrained model calibrations with which to undertake scenario assessments. Testing and scenario assessment work described in D13.3 and D13.4 respectively therefore focused on the core set of well characterised sites.

As noted in the previous activity report, resources originally assigned to ULUND and KIT for LPJ-GUESS and DNDC-MOBILE modelling in WP13 were utilised elsewhere in the project under C2 and C4. In addition, Dynamic Global Vegetation Models (DGVMs) applied in C4 were tested against European-scale flux measurements rather than site data; results of this work are described in C4 reporting.

ÉCLAIRE Third Periodic Report: November 2015

2.2.4 Component 4   Ecological impacts at regional and European scales

Lead contractor: Alterra

Component objectives & Specific Objectives of relevance to this component

The objectives of component 4 are to:
1. Develop improved process-based parameterizations in dynamic global vegetation models (DGVMs) and soil vegetation models (DSVMs) to assess the combined interacting impacts of air quality, climate change and nutrient availability on plant productivity, carbon sequestration and plant species diversity and their uncertainties (WPs 14, 15 and 17).
2. Develop novel thresholds and dose-response relationships for air pollutants (especially for O3 and N) under climate change, integrated into process-based models verified by experimental studies at site scales and mapped at the European scale, quantifying the effect of climate change scenarios (WPs 14, 15 and 16)
3. Apply the novel metrics to quantify multi-stress response of vegetation and soils, including effects on carbon storage and biodiversity to improve the overall risk assessments of pollution-climate effects on ecosystems at the European scale as the basis for development of mitigation options (WPs 14, 15 and 16).

The essence of the specific objectives of the work packages 14-17 are to assess for terrestrial ecosystems the:
1. effects of combined air pollution and climate change scenarios on productivity and ecosystem carbon/greenhouse gas (GHG): WP14.
2. changes in soil quality and plant species diversity under different air pollution and climate scenarios for forests and semi-natural systems: WP15.
3. critical thresholds for nitrogen deposition and ozone uptake and their exceedances, based on impacts on plant species diversity and productivity, respectively: WP16.
4. uncertainty in critical N thresholds and their exceedances based on model simulations at several grid resolutions from 5 x 5 km^2 and 1 x 1 km^2 (regional scale) down to 50 x 50 m^2 (landscape scale): WP17.

The essence of the progress and results for each of these WPs is reported below while details are presented in the separate work package reports,

Progress and Results

WP 14 Air pollution-climate impacts on European carbon stocks and greenhouse gas emissions

The activities of WP14 are divided in two main tasks, i.e.:
1. Task 14.1: Model development: Further develop dynamic global vegetation models (DGVMs) and dynamic soil vegetation models (DSVMs) by including interacting effects of nitrogen, ozone and climate on modelled ecosystem productivity
2. Task 14.2: Model application: Apply the updated models by (i) linking the DGVMs and DSVMs to large scale European databases on meteorology, deposition, air quality, soils and vegetation and (ii) assessing the effects of combined air pollution and climate change scenarios on productivity and ecosystem C/GHG balance for forests, semi-natural and agricultural systems.

Task 14.1: This task included the "improvement of process descriptions in four dynamic global vegetation models (DGVMs), i.e. CLM, OCN, JULES and LPJ-Guess, to include impacts of climate change, CO_2 fertilization, N deposition and ozone exposure on C and N cycling, as described in the previous progress report. Ultimately, the models CLM and O-CN include all drivers, but Jules lacks a fully coupled N cycle, while LPJ-Guess lacks coupling to ozone exposure. During the reporting period, the empirical soil-based model called EUgrow-VSD+, has been finalized, which includes the interactive impact of all above-mentioned drivers

Task 14.2: An "ensemble model application and inter-comparison of the long-term impacts of various scenarios of climate change, air quality change (exposure to O3 and CO_2 and deposition of nitrogen) on net primary production evapotranspiration and water use efficiency of forests and semi-natural systems, has been carried out, using CLM, O-CN, Jules and LPJ-Guess. All models show the positive effect of N deposition and the negative effect of O_3 on NPP but the joint effect of N and O_3 together is different subtle. CLM results indicate that N does not increase NPP if there is O_3, while O_3 reduces NPP whether there is N or not. OCN results indicate that the effect of O_3 is the same whether there is N deposition or not, and that the effect of N is similar whether there is O_3 or not. The effects of N and O_3 on evapotranspiration are largely the same as for NPP. N increases and O_3 decreases evapotranspiration. In CLM, N and O_3 together reduce evapotranspiration much as O_3 alone does, but in OCN the effect of O_3 seems stronger than the effect of N. Examples of model results are described in more detail under WP14.

Results of the empirical model EUgrow-VSD+, show that ongoing tree C sequestration is much larger (above 1000 kgC ha^{-1} yr^{-1}) than soil C sequestration (between -20-20 kgC ha^{-1} yr^{-1}). The model predicts that the fertilizing CO_2 effect is higher at elevated N, than at low N. Similarly, the model predicts that the fertilizing effect of elevated N availability is higher at elevated CO_2 than at low CO_2. In general, O_3 impacts appear to be independent

275

of the other drivers. Climate impacts in relation to other driver are highly site specific and results are not trivial to explain at a European wide scale. In the past the most important driver for growth change has been N deposition and in the future it is expected to be the combination of climate and CO_2, in combination with the reduction in ozone impacts due to a predicted decrease in phytotoxic ozone dose (POD), which largely compensates for the reduced fertilizing effect of N due to reduced N deposition. Again, examples of model results are described in more detail under WP14.

WP 15 Air pollution-climate impacts on biodiversity and soil quality

The activities of WP15 are also divided in two tasks, i.e.:
- Task 15.1: Model development: Further develop a plant species diversity model PROPS (formerly called EUMOVE) that links plant species occurrence in Europe to atmospheric deposition and climate.
- Task 15.2: Model application: Apply the updated models by (i) coupling VSD+ to PROPS and link the coupled model to large scale European databases on meteorology, deposition, air quality, soils and vegetation and (ii) forecast future changes in soil quality and plant species diversity under different air pollution and climate scenarios for forests and semi-natural systems.

Task 15.1: The PROPS model, already presented in the previous progress report, has been further developed to derive occurrence probability functions for vascular plants as a function of abiotic conditions (pH, soil C/N ratio, N deposition, yearly precipitation and yearly average temperature. Soil pH and soil C/N ratio have been estimated for about 800000 relevés, based on relationships between plant species and pH and C/N ratio from a data set consisting of several thousands of relevés with observed plant species and measured abiotic conditions. Response curves were thus derived for about 4000 European plant species

Task 15.2: A final application to Europe of the combined VSD+PROPS model was conducted for the period 2010-2050 evaluating effects of the ÉCLAIRE scenario with changes in climate and N deposition on the so-called habitat suitability index (HSI). Results show a strong influence of climate and a lower impact of N deposition change on the computed change (period 2050-2010) in HSI. This preliminary result suggest that climate change results in a stronger loss of diversity than N deposition.

WP 16 Air pollution-climate impacts on biodiversity and soil quality

The activities of WP16 are divided in three tasks, i.e.:
- Task 16.1: Assessment of effect indicators for critical load mapping
- Task 16.2. Mapping model based critical N loads for plant protection and their exceedances

- Task 16.3. Mapping critical thresholds for ozone uptake and their exceedances

Task 16.1: Documentation on indicators for geo-chemical and biological endpoints has been described before but were not published in two chapters of a book (edited by W. de Vries, J.-P. Hettelingh and M. Posch; C4 component leader, WP 19 leader and WP16 leader, resp.) in 2015.

Task 16.2: In the previous reporting period, the dynamic soil-vegetation model VSD+ has been extended with a functionality that – based on selected targets in terms of pH, [N] and N availability – that can identify appropriate depositions (critical loads). In this period, a routine has been developed such that for any given scenario, the exceedance of biodiversity CLs in view of N and S deposition can be routinely computed. The 'average accumulated exceedance' (AAE), essentially an area-weighted exceedance of the individual CLs of the newly derived biodiversity critical loads has been calculated for the years 2010 and 2050.

Task 16.3: Maps of critical phytotoxic ozone dose (POD) thresholds were derived in the previous reporting period, based on relationships between and relative total biomass data of various tree species. By using new dose response functions on the impact of POD on net annual increment (NAI), NAI reductions have been calculated in response to POD changes for the various tree species. Results indicate that current reductions in NAI of birch vary from about 10-15% in Northern Europe to more than 30% in Central Europe, while estimated future reductions in 2050 are on average about 5% less. Note, however, that this is an estimate for birch which is the most sensitive species, while impacts on other tree species are substantially lower

WP 17 Local variation in threshold exceedance

The activities of WP17 in the reporting period are divided in three tasks, i.e.:
- Task 17.1: Data collection for regional and landscape scale assessments
- Task 17.2. Model application to assess of critical nitrogen thresholds and their exceedances at 5 x 5 km and 1 x 1 km for Scotland and the Netherlands and at 1 x 1 km and 50 x 50 m for two landscapes
- Task 17.3. Uncertainty assessment

Task 17.1: This task has been completed in previous reporting period.

Task 17.2 Critical loads for acidification and eutrophication were calculated using a steady-state solution of the VSD+ model (Bonten et al., 2015) applied to two national-scale domains (The Netherlands and Scotland) and two landscape domains (Noordelijke Friese Wouden (NFW) in the Netherlands and Burnsmuir in Scotland) using the soil and vegetation database compiled in Task 17.1. Land-cover specific nitrogen deposition data were estimated using the EMEP4UK chemical transport model applied at three spatial

resolutions: 1×1 km^2, 5×5 km^2 and 50×50 km^2 and used to calculate the average accumulated exceedance (AAE) for each EMEP 50 x 50 km^2 grid square for each deposition dataset.

For both the Netherlands and Scotland, the general pattern and range of exceedances slightly increased going from 1×1 km^2 to 50×50 km^2 in line with the calculated slightly increasing N deposition in this direction (on average from 21.8 - 22.4 kg N ha^{-1} yr^{-1} in the Netherlands and from 5.1 to 5.4 kg N ha^{-1} yr^{-1} in Scotland).

Task 17.3 A statistical analysis of the AAE calculations shows that for the Netherlands, the AAE estimates calculated with the 50×50 km^2 EMEP4UK deposition dataset are, on average, higher than those calculated using the 1×1 km^2 EMEP4UK deposition dataset, while it is lower for Scotland, showing that there is no consistent change at higher spatial resolution. For both the Dutch and Scottish landscape, average exceedances increased with a decreasing spatial resolution of nitrogen deposition data as a result of an increasing nitrogen deposition to the landscape habitats, highlighting the importance of using high spatial resolution modelling for assessing critical load exceedances in "hot-spot" areas.

Progress towards the milestones and deliverables, use of resources and deviations from DoW

All the relevant milestones and deliverables have been met although there were some delays, especially in WP14. As mentioned in the previous progress report, this was mainly because several modelling teams involved in WP14 have been facing unexpected problems with human resources due to maternity/paternity leave (MPI, MetOffice) or early termination of temporary contracts (JRC and KIT). For this reason several scientists that were involved in the development and application of DGVMs models were no longer available for the analysis of model results (temporary or permanently). Despite these problems, the work has still been completed, although with some delay. In WP 17, there was also some delay as soil and vegetation data were delayed but also here all milestones and deliverables have been met.

Information on the use of resources is given in the various WPs

Work package 14 – Air pollution-climate impacts on European carbon stocks and greenhouse gas emissions

Lead contractor: JRC
Contributors: NERC, ALTERRA, IIASA, JRC, KIT,RIVM, MPG, IPBPSS

Work package objectives
The objectives of WP14 are to:
1. Further develop dynamic global vegetation models (DGVMs) and dynamic soil vegetation models (DSVMs) by including interacting effects of nitrogen, ozone and climate on modelled ecosystem productivity
2. Link the DGVMs and DSVMs to large scale European databases on meteorology, deposition, air quality, soils and vegetation.
3. Assess the effects of combined air pollution and climate change scenarios on productivity and ecosystem C/GHG balance for forests, semi-natural and agricultural systems.

Progress and Results

Task 14.1 Model improvement and linking to databases

This task included the "improvement of process descriptions in four dynamic global vegetation models (DGVMs), i.e. CLM, OCN, JULES and LPJ-Guess, as described in the previous progress report. The final situation is that CLM and OCN have been upgraded to predict the combined impacts of climate change, CO_2 fertilization, N deposition and ozone exposure on C and N cycling, the JULES model includes impacts of climate change, CO_2 fertilization, and ozone exposure but not a fully coupled N cycle (fixed N relationships)while LPJ-Guess includes impacts of climate change, CO_2 fertilization and N deposition, but no coupling yet to ozone exposure. It also includes the development of an empirical soil-based model called EUgrow-VSD+, focusing on forest carbon sequestration

Task 14.2: Model application

This task includes an "ensemble model application and intercomparison of the long-term impacts of various scenarios of climate change, air quality change (exposure to O_3 and CO_2 and deposition of nitrogen) on net primary production/carbon sink strength and water cycling of forests and semi-natural systems, using CLM, O-CN, Jules and LPJ-Guess, further denoted as LPJ. A protocol for model application has been has been described in the previous progress report, including a model validation with observational datasets and a preliminary intercomparison of the four DGVMs. Here, we report the final results of the model intercomparison for 4 scenarios, and the results of the empirical EUgrow-VSD+ model for 16 scenarios. Results of the DGVMs were limited to Net primary productivity

(NPP), Evapotranspiration (ET) and Water use efficiency (WUE) here defined as the gross primary productivity divided by the total evapotranspiration. The impacts of ozone were simulated by CLM, OCN and Jules, of N by CLM, OCN and LPJ-Guess and of N and O3 by CLM and OCN.

The results of EUgrow-VSD+ were limited to carbon sequestration in trees and soils. The various scenarios used are given in Table 4.1.

Table 4.1: Scenarios used to study the impact of each driver. The four scenarios in bold are those used by the DGVMs, including transient climate and CO_2 concentration and fixed or transient O_3 exposure and N deposition, whereas the empirical model evaluated all scenarios

| Scenario	Climate	CO_2	N deposition	Ozone
All drivers constant				
1 S0000[1]	1901	1901	1901	1901
Three drivers constant (one driver variable)				
2 S1000	1901-2050	1901	1901	1901
3 S0100	1901	1901-2050	1901	1901
4 S0010	1901	1901	1901-2050	1901
5 S0001	1901	1901	1901	1901-2050
Two drivers constant (two drivers variable)				
6 S1100	**1901-2050**	**1901-2050**	**1901**	**1901**
7 S1010	1901-2050	1901	1901-2050	1901
8 S1001	1901-2050	1901	1901	1901-2050
9 S0110	1901	1901-2050	1901-2050	1901
10 S0101	1901	1901-2050	1901	1901-2050
11 S0011	1901	1901	1901-2050	1901-2050
One driver constant (three drivers variable)				
12 S1110	**1901-2050**	**1901-2050**	**1901-2050**	**1901**
13 S1101	**1901-2050**	**1901-2050**	**1901**	**1901-2050**
14 S1011	1901-2050	1901	1901-2050	1901-2050
15 S0111	1901	1901-2050	1901-2050	1901-2050
All drivers variable				
16 S1111[1]	**1901-2050**	**1901-2050**	**1901-2050**	**1901-2050**

[1] Neglect in all other scenarios implies that the driver stayed at the 1901 level for the whole 1900–2050 period. For the period 1900-2005, historical data are used and for 2005-2050 predicted data.

Intercomparison of the effects of scenarios on net primary productivity, evapotranspiration and water use efficiency

Figure 4.1 shows effects of each of the atmospheric drivers (identified as the differences between scenarios within each model as described above) for European annual average NPP. All models show the positive effect of N deposition on NPP (black lines, differences between scenarios S1 and S10 are always positive) and the negative effect of O_3 on vegetation (red lines, differences between scenarios S2 and S10 are always negative). The joint effect of N and O_3 together is more subtle. CLM and OCN both show this influence to be closer to zero. However, whilst OCN shows this is consistently varying around the zero line, CLM shows a more systematic negative deviation during the first three quarters of the time period, followed by a more positive deviation over the last quarter of the period.

The effect of N given O_3 is represented by the blue lines in figure 4.1 (only present for CLM and OCN models). This is close to zero for much of the time for CLM, which would suggest that when O_3 is accounted for (or, 'allowed' to influence the simulated vegetation), N deposition doesn't have a very large positive. The sum effect, given O_3 whether with or without N, is reduced vegetation NPP. To the contrary, OCN's response for N given O_3 is much more positive, suggesting that regardless of whether O_3 is present and reducing vegetation NPP, the addition of N will serve to increase that NPP.

A similar effect is seen with these models' simulated effect of O_3 given N (the green lines in figure 4.1). CLM shows a very negative effect of O_3 (in combination with N). What this suggests is that, where there is just the influence of N, the response would be largely positive (as seen for just N), but the presence of O_3 dominates, and inhibits this otherwise positive response. It is not that the influence of O_3 given N is stronger than the influence of just O_3, but rather that O_3 and N do not influence the model individually and independently. N does not increase NPP if there is O_3, and O_3 reduces NPP whether there is N or not. The interaction appears to be asymmetric. OCN, on the other hand, shows a negative effect for O_3 given N, much the same as the effect of O_3 individually. What this suggests is that the influence of O_3 is reducing the positive influence of N, much as the influence of O_3 by itself reduces the NPP of OCN simulations without N. The effects of N and O_3 in OCN appear to counteract each other. The effect of O_3 appears to be the same whether there is N deposition or not, as the effect of N appears similar whether there is O_3 or not. There is no obvious interaction between N and O_3.
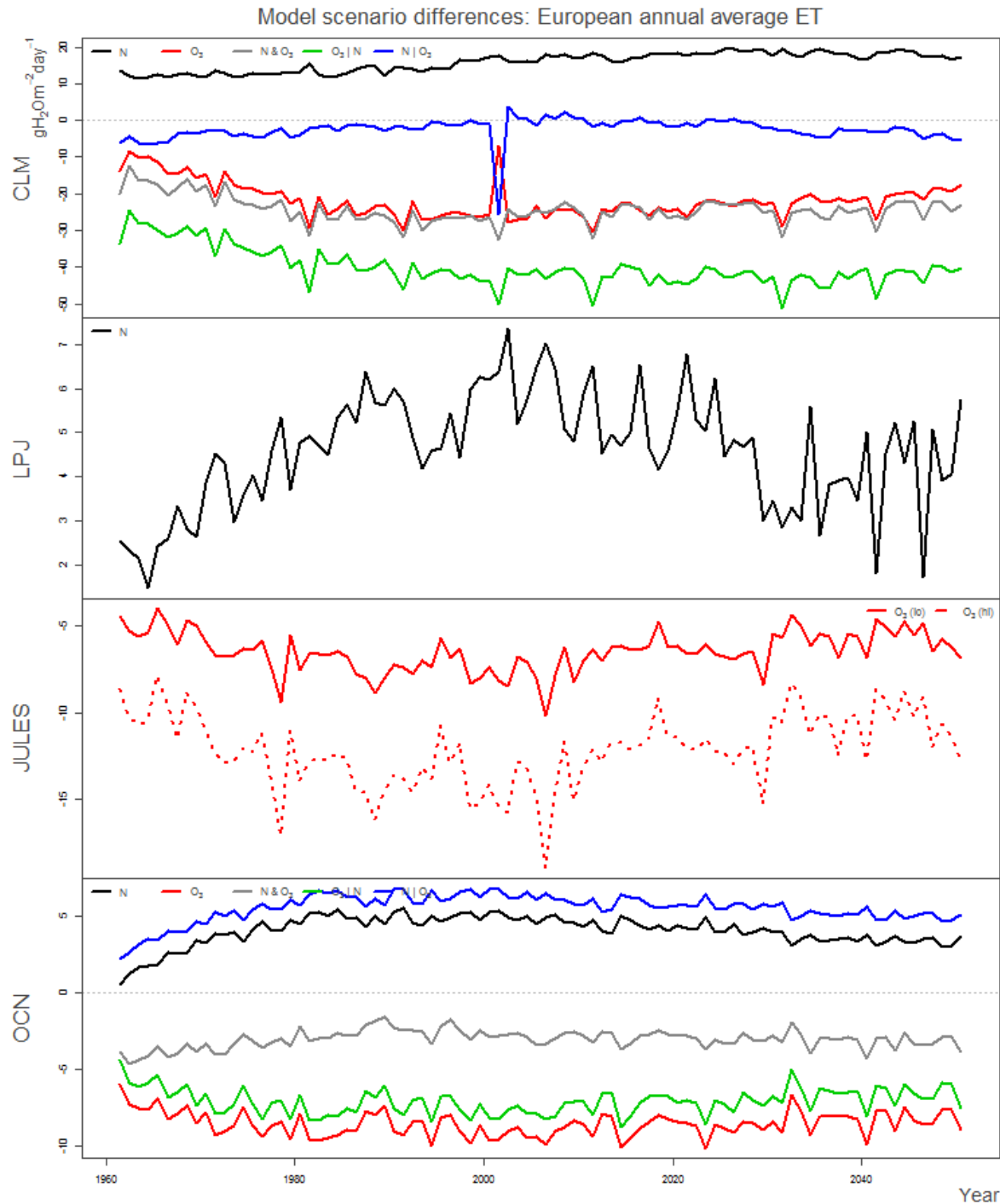
ÉCLAIRE Third Periodic Report: November 2015
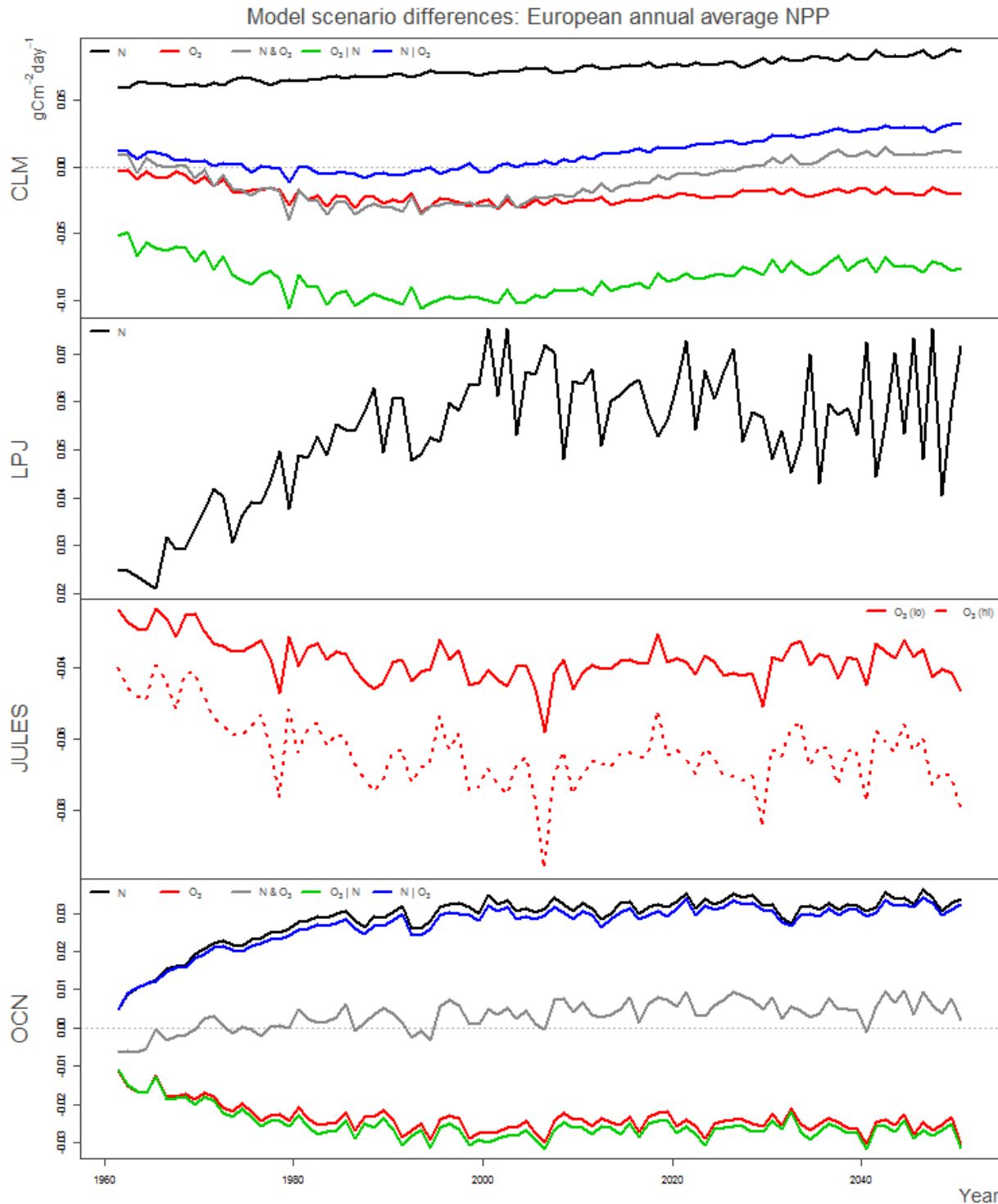
Figure 4.1: Effects of individual and combined atmospheric drivers on European annual average NPP by model. The effects of the different drivers is calculated as: N = S1-S10; O3=S2-S10; N&O3=S0-S10; O3|N=S0-S1; N|O3=S0-S2.
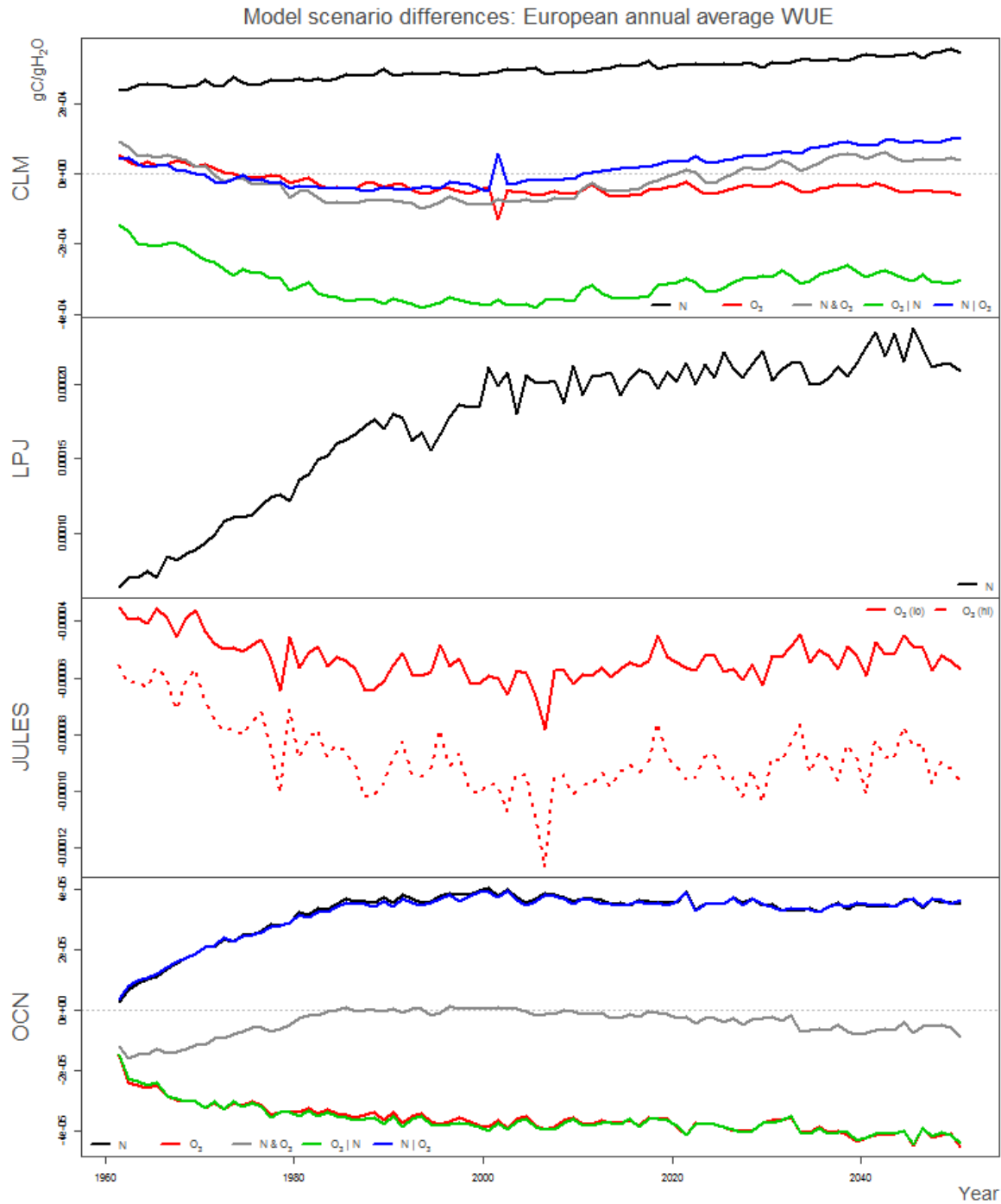
Figure 4.2 shows the effects of individual and combined atmospheric drivers on evapotranspiration. For CLM, effects are largely similar to those identified for NPP. N increases and O_3 decreases evapotranspiration. N and O_3 together reduce evapotranspiration much as O_3 alone does. The effect of N given O_3 is close to zero for the entire 90 years (there is almost no difference between scenario S0 with transient N and O_3, and scenario S2 with fixed N and transient O3). The effect of O_3 given N is again a larger decrease, because the model would otherwise simulate a much larger evapotranspiration with the added N.

The effects of these drivers on evapotranspiration in the other 3 models are largely the same as for NPP. N deposition increases evapotranspiration in LPJ and OCN. O_3 reduces evapotranspiration in JULES and OCN. The effects of N given O_3 and O_3 given N are again somewhat symmetrical in OCN, except this time the effect of O_3 seems stronger than the effect of N.

In terms of the individual and combined effects of atmospheric drivers on water use efficiency in these models, there is a clear pattern in CLM (Figure 4.3). The effect of N deposition is increasing water use efficiency, and the effect of O_3 given this N increase is to inhibit and reduce water use efficiency (as for NPP and evapotranspiration). OCN again shows symmetric and counteracting effects of N given O_3 and O3 given N. These effects are again much smaller than for the other models.

Figure 4.2:. Effects of individual and combined atmospheric drivers on European annual average evapotranspiration, by model. The effects of the different drivers is calculated as: N = S1-S10; O3=S2-S10; N&O3=S0-S10; O3|N=S0-S1; N|O3=S0-S2.

ÉCLAIRE Third Periodic Report: November 2015

Figure 4.3: Effects of individual and combined atmospheric drivers on European annual average water use efficiency, by model. The effects of the different drivers is calculated as: N = S1-S10; O3=S2-S10; N&O3=S0-S10; O3|N=S0-S1; N|O3 = S0-S2.
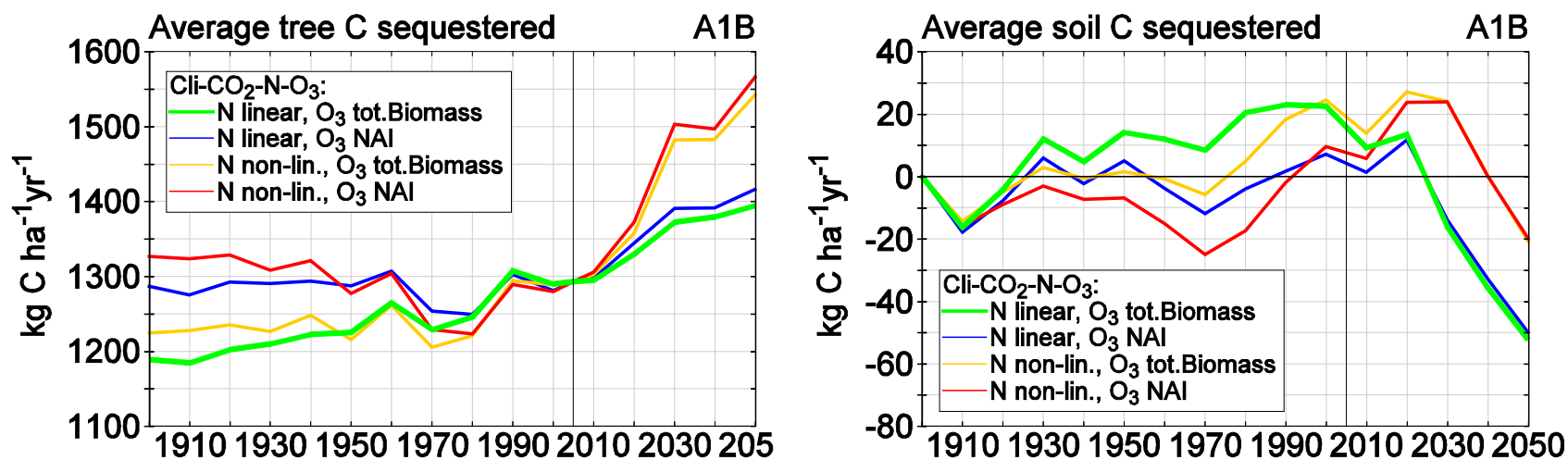
Calculated temporal changes in the European average carbon sequestration in trees and in soil in response to changes in climate, CO_2 concentration, N deposition and O_3 exposure are shown in Figure 4.4. Both the calculate tree and soil carbon sequestration is averaged over 10 year periods. Results show a rather strong impact of the use of the empirically based growth responses to N deposition (linear or non-linear) and an even larger impact of the two empirical O_3 exposure functions, considering either total biomass or net annual increment.

The calculated carbon sequestration in tree increases almost continually over time in the period 1900-2005 when using the linear N deposition response and the O_3 exposure function for total biomass and the same holds for the coming period up to 2050. Instead a non-linear N deposition function does not significantly affect tree growth up to 1970, while it starts to increase from that period onwards (in response to the increased N deposition), and even more after 2005, which is mainly due to climate and CO_2 change, since N deposition decreases in that period. Apparently, the decrease in N deposition has a much smaller (reducing) effect on forest growth, as compared to the linear N deposition function. When using the O_3 exposure function for net annual increment, the calculated tree carbon sequestration stays either nearly constant in the last 100 years or even decreases in time, depending on the N response function used. Unlike N, the impact of O_3 response is much smaller in future predictions. This is most likely mainly due to the estimated smaller change in POD as compared to N (especially NO_x) deposition in the future (see Figure 14.4).

The soil C pool changes reflect on average the changes in tree C pools as this affects the C input by litterfall. However, unlike tree C sequestration, the changes can be negative since soil respiration can be higher than litter C input. The decrease in the period after 2005 to negative values in 2050 for all scenarios is most likely due to climate change, on average increasing soil respiration by an increased temperature. Compared to tree C sequestration, the changes in soil C pools are on average very limited and (between -20-20 $kgC\ ha^{-1}\ yr^{-1}$) being nearly negligible compared to the ongoing tree C sequestration above 1000 $kgC\ ha^{-1}\ yr^{-1}$.

The impacts of individual drivers on tree carbon sequestration assuming the linear nitrogen deposition function and an ozone exposure function based on total biomass is given in Figure 4.5.

Figure 4.4: Temporal development of European average carbon sequestration in trees (left) and in soil (B) in response to changes in climate, CO_2 concentration, N deposition and O_3 exposure for two growth responses to N deposition (linear and non-linear) and O_3 exposure (total biomass and net annual increment, NAI), using the reference model while excluding the impact of nutrient limitation.
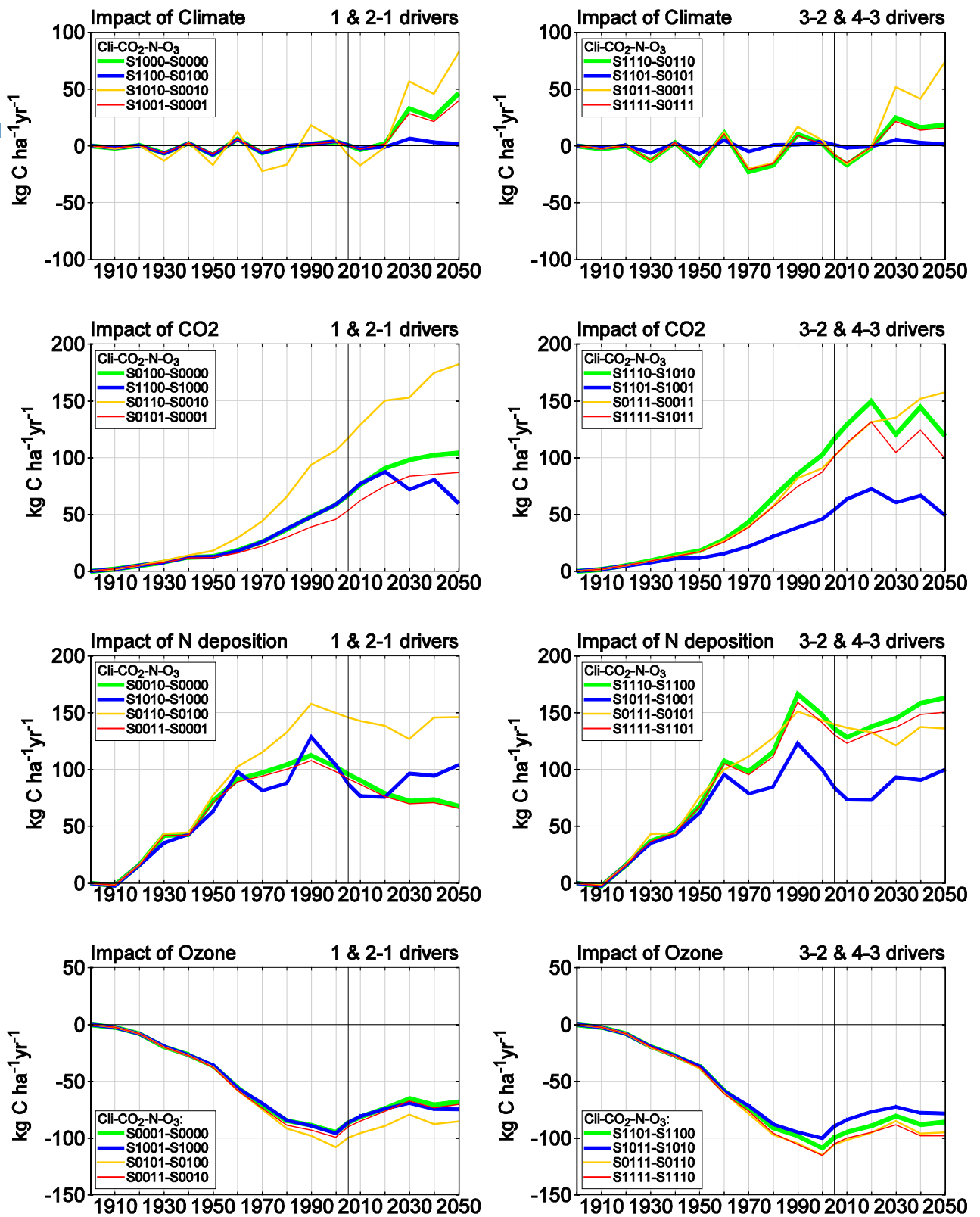
Figure 4.5: Influence of the single drivers computed, using the linear N model and the total biomass O_3 response model.

In general, effects of adding or removing a driver are expected to be highest for the situation where the other drivers enhance growth, because impacts of drivers are included in EUgrow as a fraction of the growth rate. In summary, the model predicts that the fertilizing CO_2 effect is higher at elevated N, (which is the case in the N on scenario) than at low N (which is the case in the N off scenario, implying the use of 1900 N deposition data). Similarly, the model predicts that the fertilizing effect of elevated N availability (N deposition plus N fixation) is higher at elevated CO_2 than at low CO_2. In general, results are quite comparable for ozone since O_3 impacts are assumed to act independently. Climate impacts in relation to other driver are highly site specific and results are thus not trivial to explain at a European wide scale.

Spatial patterns for the time averaged tree and soil carbon sequestration for the period 1900-1950, 1950- 2000 and 2000- 2050 are given in Figure 4.6, for the reference model, including interactions between drivers. Results show that the 50 year average carbon sequestration increases going from 1900-1950 < 1950-2000 < 2000-2050 in central Europe, but not in Northern and southern Europe (Fig 4.6, RH image). In these regions, the growth rate stays rather constant. Apparently, water availability limitations mainly offset the effects of CO_2 and temperature increase in Southern Europe, whereas limitations due to nitrogen availability and ozone exposure seem to offset those effects in Northern Europe.
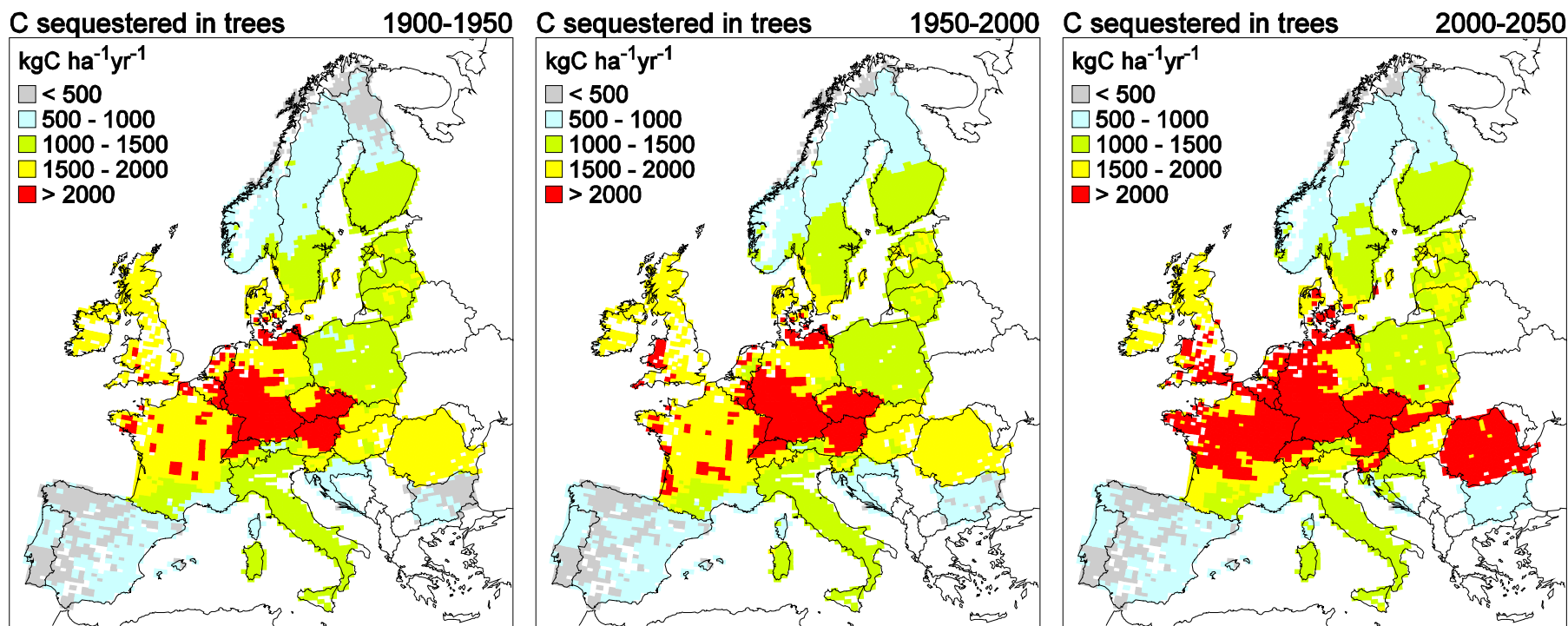
Figure 4.6: Spatial variation in calculated tree C sequestration over Europe in the period 1900-1950, 1950-2000 and 2000-2050, using the reference model with a linear N response model and a total biomass response to POD.

ÉCLAIRE Third Periodic Report: November 2015

Progress towards the milestones and deliverables

During the reporting period (months 37-48), no further milestones were planned, but as much as four deliverables were planned (D14.5-D14.8). All those deliverables were written the reporting period and information is summarized in this progress report, especially related to D14.7 and D14.8. An overview of all deliverables for WP14 is shown below, with those related to the last reporting period in bold.

D14.1 Synthesis of applicable data on impacts of ozone on photosynthesis, stomatal conductance and plant function   Due Month 6 Delivered Month 11

D14.3 Validated and evaluated version of models (DGVMs and DSVMs) using databases on plant productivity   Due Month 24   Delivered Month 36

D14.4 Model runs (DGVMs and DSVMS) using the ÉCLAIRE scenarios of future emissions and climate change   Due Month 30   Delivered Month 36

D14.5 Ensemble dataset of model runs to assess the impact of combined air pollution and climate change scenarios on ecosystem C/GHG balance   Due Month 36   Delivered Month 38

D14.6 Comparison of regional-scale models with validation data of test sites   Due Month 40   Delivered Month 42

D14.7 Report on ensemble application of DGVMs and intercomparison of model results   Due Month 42   Delivered Month 48

D14.8 Report on the impacts of historic and future changes (period 1900-2100) in climate, air quality Due Month 44   Delivered Month 48

Use of resources and deviations from DoW

38.6 person months were spent on WP14.

References

Bonten, L.T.C., G.J. Reinds and M. Posch, 2015. A simple model to calculate effects of atmospheric deposition on soil acidification, eutrophication and C-sequestration. Environmental Software & Modelling (submitted)

Cescatti A., Hooker J., Marcado L., Zaehle, Arnet A., de Vries W. et al. Joined effect of nitrogen and ozone depositions on the primary productivity, evapotranspiration and water use efficiency of European ecosystems (in prep).

ÉCLAIRE Third Periodic Report: November 2015

De Vries, W., M. Posch, D. Simpson, G. J. Reinds and L.T.C. Bonten, 2015. Modelling long term impacts of changes in climate, nitrogen deposition and ozone exposure on carbon sequestration of European forest ecosystems. Environmental Pollution (in prep).

Kramer, K. R.J. Bijlsma, L.T.C. Bonten, G.J. Reinds, W. de Winter and W. de Vries, 2015. Sensitivity analyses of the interactions between climate change, nitrogen deposition and atmospheric ozone on plant growth. Ecological Modelling (in prep).

Work package 15   Air pollution-climate impacts on biodiversity and soil quality

Lead contractor: Alterra
Contributors: NERC, RIVM-CCE

Work package objectives

The objectives for WP15 are to:
- Further develop a plant species diversity model PROPS (formerly called EUMOVE) that links plant species occurrence in Europe to atmospheric deposition and climate.
- Couple updated dynamic soil vegetation models (DSVM) to PROPS and link the coupled model to large scale European databases on meteorology, deposition, air quality, soils and vegetation.
- Forecast future changes in soil quality and plant species diversity under different air pollution and climate scenarios for forests and semi-natural systems.

Progress and Results

Task 15.1: Model linkage and linking to databases

According to the proposal description, this task includes the:
- Development of the plant species model PROPS.
- Linkage of the PROPS model with the EUgrow-VSD+ model and the MADOC model (previously referred to mistakenly as the JULES-MADOC model).
- Linkage of the EUgrow-VSD+-PROPS model to European databases on meteorology, deposition, air quality, soils and vegetation to predict the combined biodiversity and soil quality impacts of air pollution and climate change (in combination with task WP14).

The linkage of the PROPS model with the EUgrow-VSD+ model and the MADOC model linkage and of the VSD+-PROPS model with European-wide data bases has been described in the previous progress report. Below, we describe the finalization of the PROPS model development.

Finalization of the development of the plant species model PROPS
The PROPS model, already presented in the previous progress report, has been further developed to derive occurrence probability functions for vascular plants as a function of abiotic conditions (pH, soil C/N ratio, N deposition, yearly precipitation and yearly average temperature. The nitrate concentration previously used, has been abandoned: the observations were too few and concentrated in a few countries with

ÉCLAIRE Third Periodic Report: November 2015

high N deposition only) Using an existing database (Bioscore; Van Hinsberg et al.), with about 800000 relevés (Figure 4.7), soil pH and soil C/N ratio have been estimated for the sites based on relationships between plant species and pH and C/N ratio from a data set consisting of several thousands of relevés with observed plant species and measured abiotic conditions (Table 4.2).
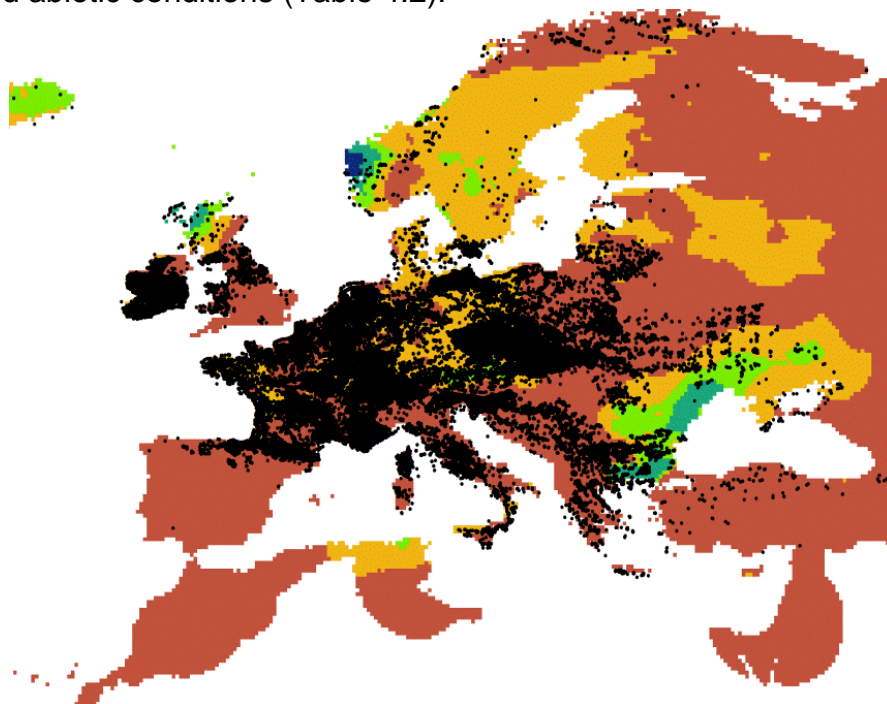
Figure 4.7: Bioscore plots (black dots) used to derive response functions for vascular plants

Table 4.2: Number of sites with species composition and measured soil parameters.

Dataset	pH	C/N	Ntot	pH+C/N	pH+Ntot
Netherlands	6781	2421	2943	2355	2815
Austria	630	630	630	630	630
Ireland	411	430	430	411	411
Denmark	760	503	141	503	32
United Kingdom	586	240	240	240	240
ICP-Forest	529	518	528	518	528
Other	189	102	112	102	112
Total	**9886**	**4844**	**5024**	**4759**	**4768**

This first dataset with measured soil parameters was split up in a calibration part (90% of the dataset) and a validation part (10% of the dataset, each 10th relevé). For each species in the calibration part of the dataset we fitted both one-dimensional and five-dimensional probability curves, in response to pH, C/N ratio, N deposition, yearly average temperature and yearly precipitations. The response curves, that could be regarded as an alternative for species indicator values (e.g. Ellenberg et al., 1991) were used to calculate soil parameters for the BioScore dataset.

Results of the validation indicate that reasonable estimates of pH and C/N ratio can be obtained with the transfer functions, although at part of the sites a substantial deviation between the measured and estimated (optimal) values occurs (Figure 4.8).
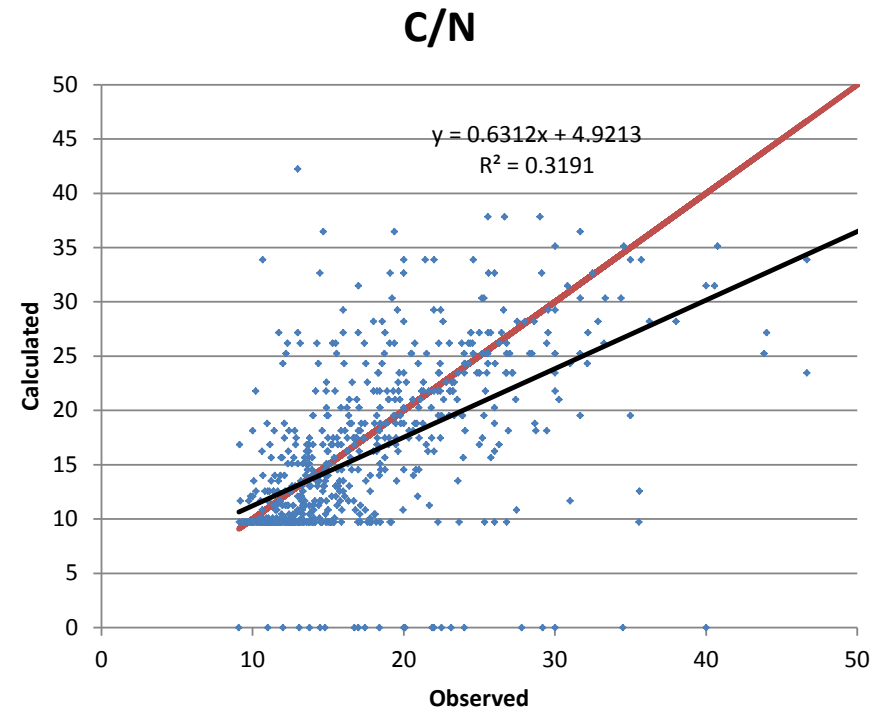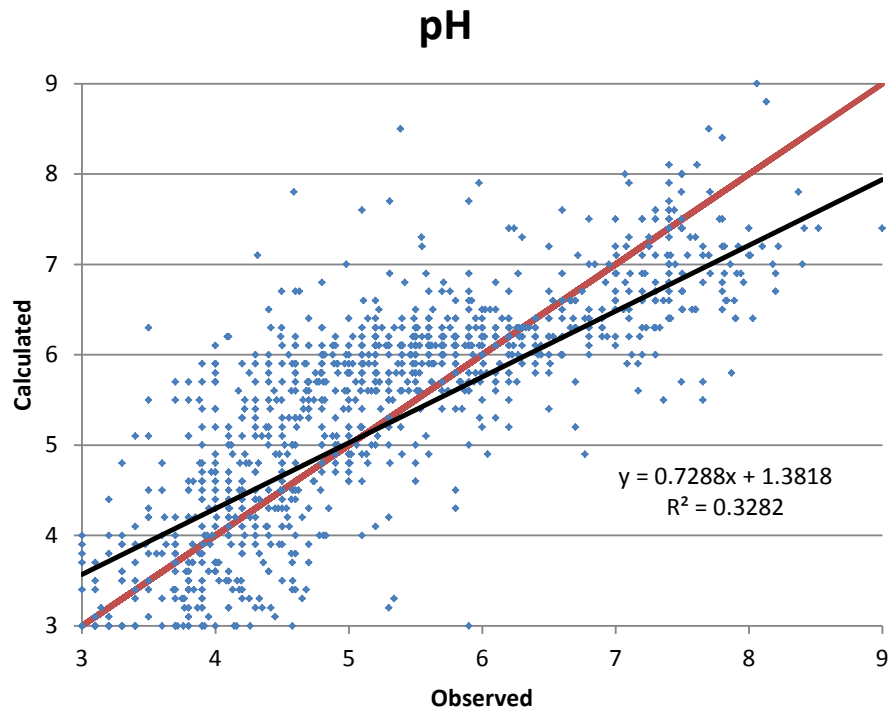
Figure 4.8: Validation of calculated pH and C/N; red line indicates the 1:1 line, the black line the regression between estimated and observed values.

Response curves were derived for about 4000 European plant species using the above mentioned advanced statistical procedures. An example response with a good fit to observed data is provided in Figure 4.9 for *Calluna vulgaris* and *Erica tetralix*. Not all species responses for the about 4000 species were so good, as exemplified in Figure 4.10, illustrating the uncertainty in model approach.
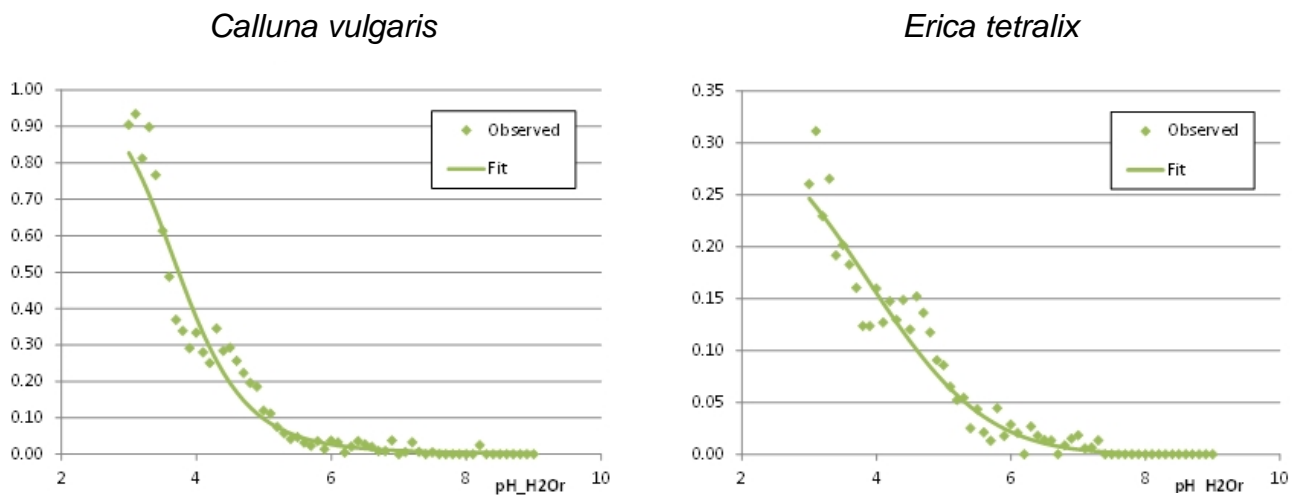
Figure 4.9: Observed and fitted response of two species to soil pH.
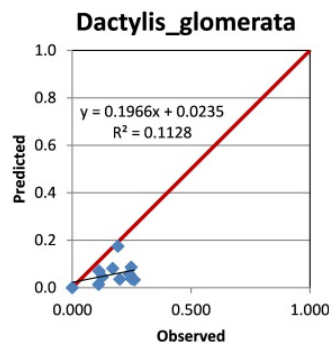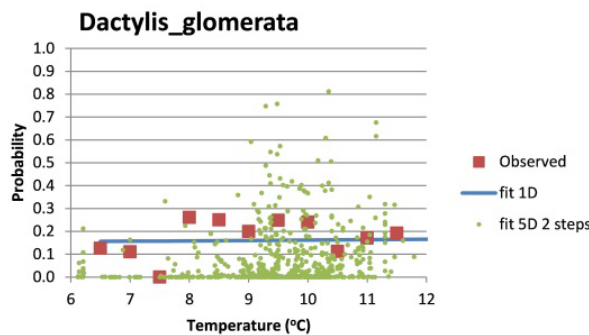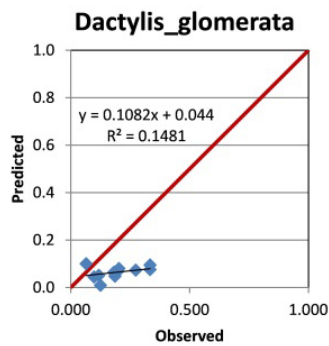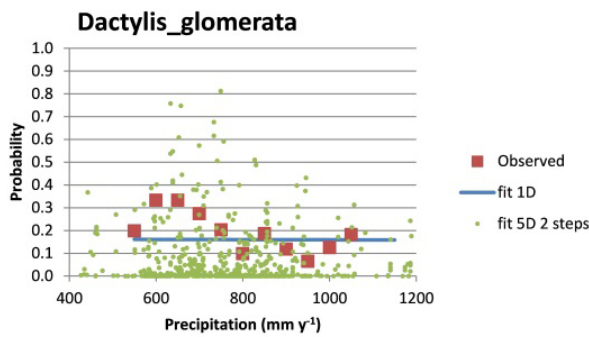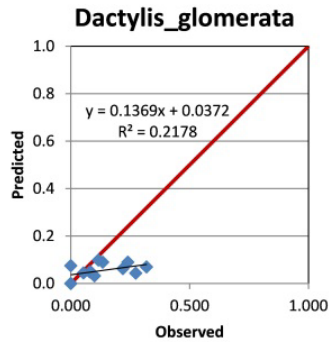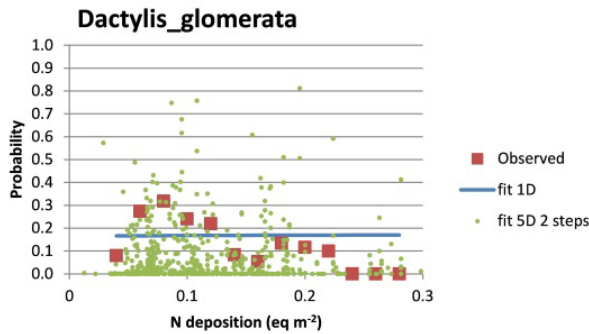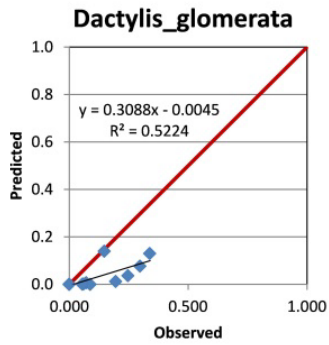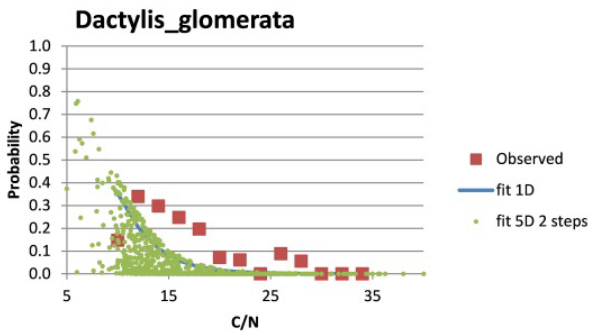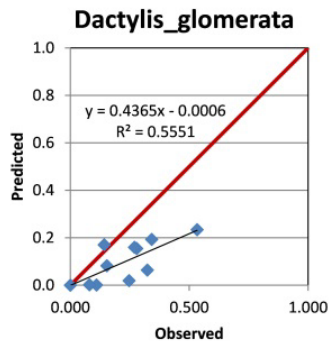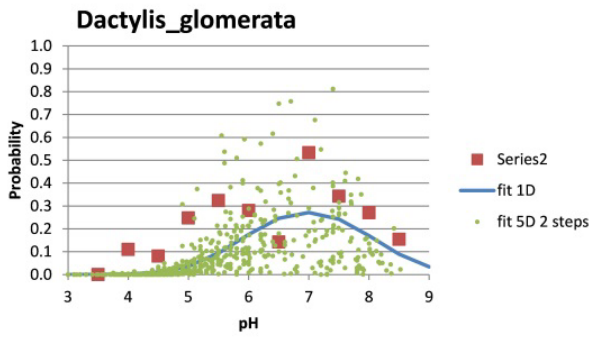
Figure 4.10: Response curves of selected species and the fit betwen observed and predicted occurrence probability.

298

Figure 4.11 shows isolines of such probabilities for the species *Calluna vulgaris* in the C:N-pH plane and the N_{dep}-pH plane (with the 3 other parameters constant).
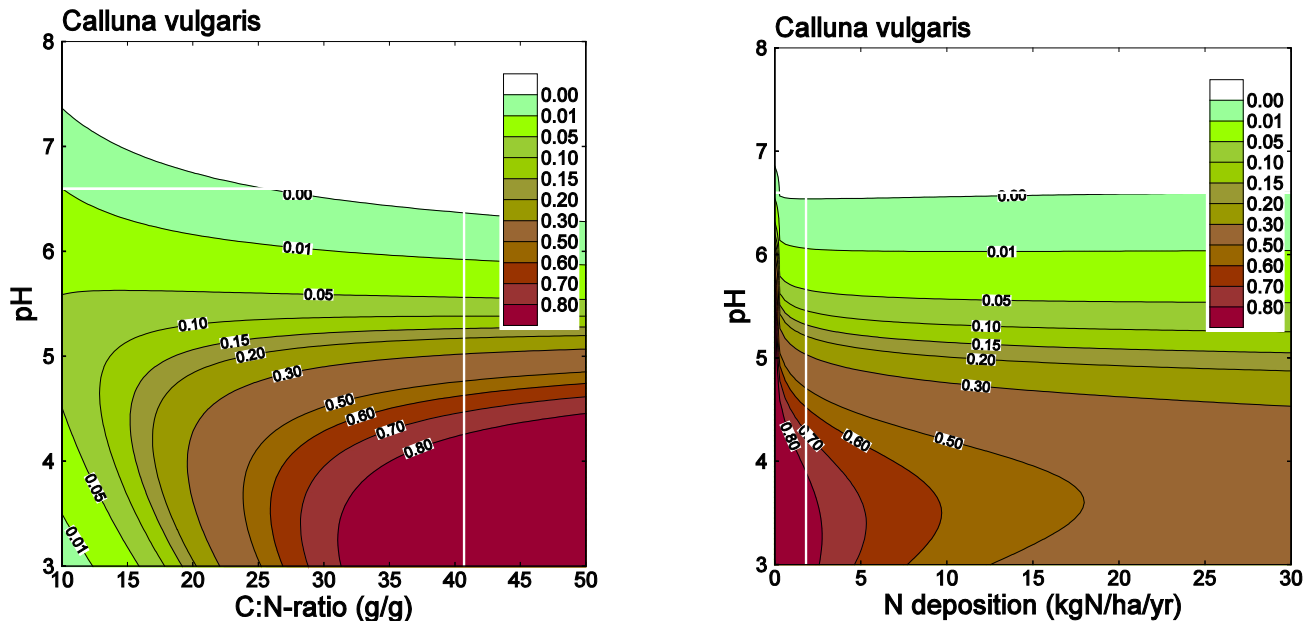
Figure 4.11: Left: Normalised isolines of the occurrence probabilities as function of soil C:N and soil solution pH for species *Calluna vulgaris*. Right: Isolines in the N_{dep}-pH plane for the same species. Both for fixed precipitation and temperature (and N_{dep} resp C:N).

Task 15.2: Model application

According to the proposal description, this task includes the:
- Parameterization of VSD+ and MADOC by including the novel use of a collated European dataset of radiocarbon (14C) data to constrain estimates of soil carbon turnover rates by vegetation and soil type.
- Assessment of long term impacts of climate change and deposition of nutrients on plant species diversity and soil quality, using PROPS linked with the soil model VSD+.

The parameterization of VSD+ and MADOC by including the novel use of a collated European dataset of radiocarbon has been described in the previous progress report. Here we report the application of the VSD+-PROPS model to predict combined biodiversity and soil quality impacts in response to air pollution and climate change.

Long term impacts of climate change and nitrogen deposition on plant species diversity and soil quality

For a European assessment using VSD+-PROPS, a set of plant species was assigned to each habitat type based on species lists defined in the Bioscore project: these lists provide typical (desired) species for about 30, mostly vulnerable, habitats. The PROPS model was applied to assess changes in the occurrence probability of all distinguishes plant species in response to the ÉCLAIRE scenario on changes in atmospheric nitrogen (and sulphur) deposition and climate (precipitation and temperature) and the resulting calculated changes in pH and soil C/N ratio (calculated with VSD+). These results in turn were aggregated to a Habitat Suitability Index that summarizes plant occurrence probabilities into one diversity measure.

Results showed that the ÉCLAIRE scenario leads to a substantial reduction in N deposition in 2050. Only in areas with intensive husbandry (Netherlands, parts of Germany, Brittany and the Po valley), relatively high N depositions can still be found in 2050.Since also S deposition is reduced, acidified soil recover from acidification, leading to an increase in pH in areas that were previously acidified because of acid deposition (mainly central and western Europe and southern Scandinavia). The change in soil C/N ratio is much less pronounced as the carbon pool in soils is normally huge compared to the (change in) N inputs, so changes are only gradual. In Europe, both an increase in C/N ratio can occur (in areas were N deposition is strongly reduced) as well as a decrease in areas with ongoing elevated N deposition. Applying the PROPS model for Europe reveals that sensitive systems can react significantly on increased N richness (Figure 15.6). In dry heath, for example, the Habitat Suitability Index (HSI) decreases with an increased N richness, here expressed as a decrease in C/N ratio and the HSI increases with lower N richness.

ÉCLAIRE Third Periodic Report: November 2015
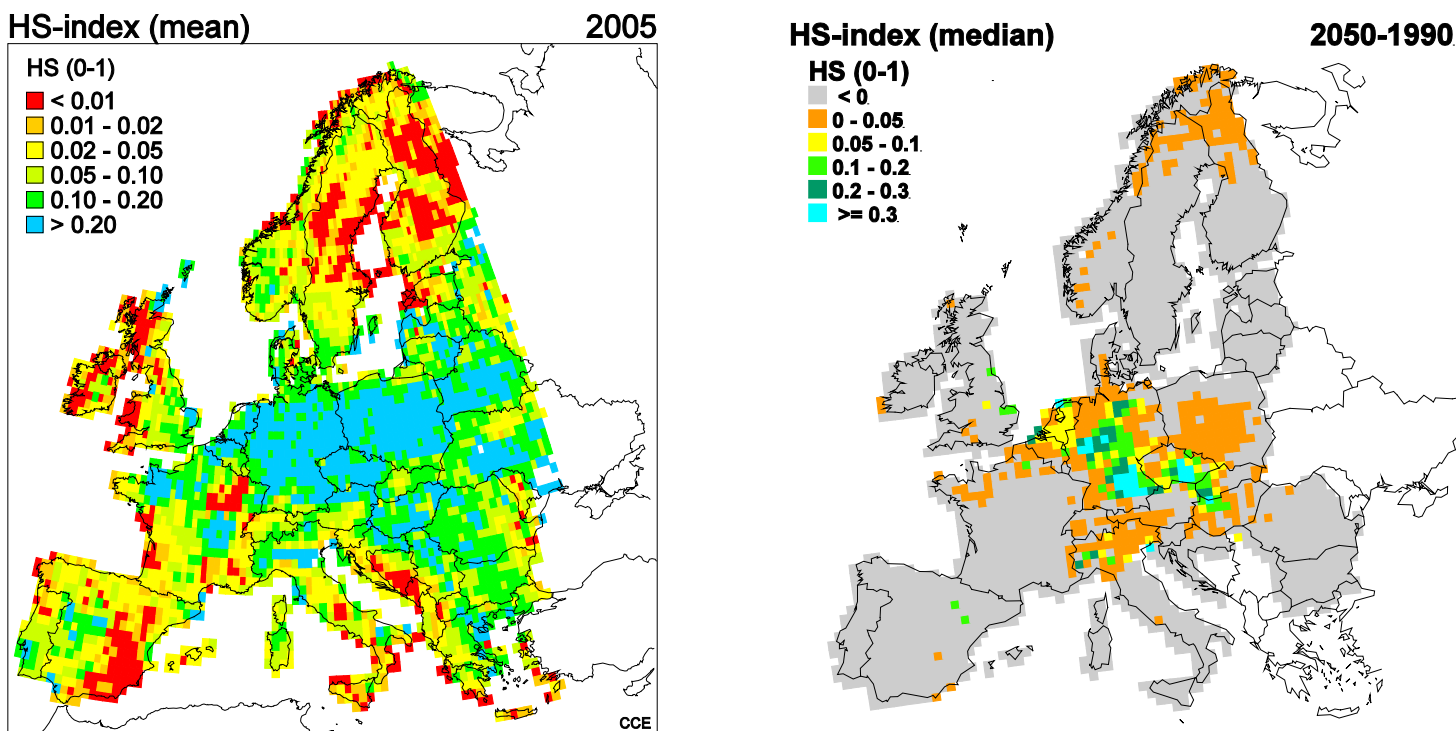
Figure 4.12: The spatial distribution of the habitat suitability index of EUNIS classes in EMEP grid cells in 2005 (Left) and right the calculated increase in HSI between 1990 and 2050; median per grid cell in response to the ÉCLAIRE scenario (right).

Progress towards the milestones and deliverables

During the reporting period (months 37-48), no further milestones were planned and only one deliverable (15.4). The planned deliverable 15.4 was written during the reporting period and information is summarized in this progress report. An overview of all deliverables for WP15 is shown below, with those related to the last reporting period in bold.

D15.1 The model PROPS Due Month 24   Delivered Month 27

D15.2 Collated dataset of European soil 14C data used to define soil turnover times as a function of soil/vegetation type for VSD+ and MADOC model parameterisation Due Month 24   Delivered Month   27

D15.3 The VSD+-PROPS model linked to European databases   Due   Month   30 Delivered Month 32

D15.4 Assessments of the effects of combined air pollution and climate change scenarios on plant species diversity and soil quality   Due   Month   42   Delivered Month 44

Use of resources and deviations from DoW

There have been no serious delays for this work package. A total of 1.9 person months have been used in this work package.

References
De Vries, W., M. Posch, G.J. Reinds, L.T.C Bonten, J.P. Mol-Dijkstra, G.W.W. Wamelink and J-P. Hettelingh, 2015. Integrated assessment of impacts of atmospheric deposition and climate change on forest ecosystem services in Europe. In W. de Vries, J-P. Hettelingh & M. Posch (eds) Critical Loads and Dynamic Risk Assessments: Nitrogen, Acidity and Metals in Terrestrial and Aquatic Ecosystems, Environmental Pollution Volume   25,   Springer   ISSN   1566-0745:   589-612. http://www.springer.com/gp/book/9789401795074.

Hettelingh, J-P., C. Stevens, M. Posch, R. Bobbink and W. de Vries, 2015. Assessing the impacts of nitrogen deposition on plant species richness in Europe. In W. de Vries, J-P. Hettelingh & M. Posch (eds) Critical Loads and Dynamic Risk Assessments: Nitrogen, Acidity and Metals in Terrestrial and Aquatic Ecosystems, Environmental Pollution Volume 25, Springer ISSN 1566-0745: 573-586. http://www.springer.com/gp/book/9789401795074.

Priputina, Irina Elena Zubkova, Vladimir Shanin, Vadim Smirnov, Alexander KOMAROV (2014) Evidence of plant biodiversity changes as a result of nitrogen deposition in permanent pine forest plots in central Russia. Ecoscience. Vol. 21 no 3-4. Pages 286-300. DOI: 10.2980/21-(3-4)-3681.

Rowe, E.C., G.W.W. Wamelink, S.M. Smart, A. Butler, P. A. Henrys, H.F. van Dobben, G.J Reinds, C.D. Evans, J. Kros and W. de Vries, 2015. Field survey based models for exploring nitrogen and acidity effects on plant species diversity and assessing long-term critical loads. In W. de Vries, J.-P. Hettelingh & M. Posch (eds) Critical Loads and Dynamic Risk Assessments: Nitrogen, Acidity and Metals in Terrestrial and Aquatic Ecosystems: 297-326. http://www.springer.com/gp/book/9789401795074

Van Dobben, H.F., A. van Hinsberg, D. Bal, J.P. Mol-Dijkstra, H.J.J. Wieggers, J. Kros and W. de Vries, 2015. Derivation of critical loads for nitrogen for habitat types and their exceedances in The Netherlands. In W. de Vries, J-P. Hettelingh & M. Posch (eds) Critical Loads and Dynamic Risk Assessments: Nitrogen, Acidity and Metals in Terrestrial and Aquatic Ecosystems, Environmental Pollution Volume 25, Springer ISSN 1566-0745: 547-572. http://www.springer.com/gp/book/9789401795074

Under submission
Reinds, G.J., J.P. Mol-Dijkstra, G.W.W. Wamelink, M. Posch, L.T.C. Bonten and W. de Vries, 2015. Combined effects of nitrogen deposition, ozone exposure and climate change on plant species diversity in Europe (in prep).

Wamelink, G.W.W, J.P Mol, R. Jochem, P. Goedhart, G.J. Reinds and W. de Vries, 2015. PROPS: an empirical model to assess the probability of plant species occurrence as a function of environmental factors (in prep).

ÉCLAIRE Third Periodic Report: November 2015

Work package 16   European maps of novel thresholds & exceedances

Lead contractor: RIVM
Contributors: Alterra, IIASA, MetNo, ONU, IPBPS

Work package objectives

The objectives for WP 16 are to map model-based:
- climate-dependent critical nitrogen thresholds, based on criteria for impacts on plant species diversity and accounting for differences in NO_x and NH_y, and their exceedances.
- critical thresholds for ozone uptake, based on criteria for impacts on productivity, and their exceedances

Progress and Results

Task 16.1: Assessment of effect indicators for critical load mapping

This is described in the previous progress report. The documentation on indicators for geo-chemical and biological endpoints has now been published in two chapters of a book (edited by W. de Vries, J.-P. Hettelingh and M. Posch; C4 component leader, WP 19 leader and WP16 leader, respectively).

Task 16.2. Mapping model based critical N loads for plant protection and their exceedances

According to the proposal description, this task includes the
- Improvement of databases on soils and vegetation with a specific emphasis on Russia (IPBPS) and the Ukraine (ONU).
- Mapping of critical thresholds for oxidized versus reduced nitrogen, based on identified thresholds and experimental data,
- Application of the combined steady-state version of the soil-vegetation model VSD+, with the multi-plant species model PROPS to assess climate dependent critical N loads.
- Mapping of exceedances of critical nitrogen loads by comparing present nitrogen loads with updated critical nitrogen loads.
- Evaluation of the use of the newly acquired critical thresholds by the GAINS model. The progress and results for the first three bullet points has been carried out and described in previous progress reports, while initial work on the fourth bullet point was also described in the previous progress report. Here we describe a finalization of what

has been done on mapping of exceedances of critical N loads and their use in the GAINS model.

Assessing climate dependent critical N and S loads for plant species diversity
Every (European) habitat is characterised by a number of 'typical' species. From the plant species response curves (see example in Figure 4.11 in discussion of WP15) one can derive critical (better: optimal) loads of N- and S-deposition, once a threshold value of the HS-index is agreed upon. Using the parameters of those species and the abiotic site characteristics, one can compute the HS indices for the respective habitat for a range of N and S deposition, in this way determining for which pair (N_{dep},S_{dep}) the HS index is optimal. Taking this HS_{opt} as starting point, a simple procedure has been developed to derive a critical load function (CLF) in the N_{dep}-S_{dep} plane, which is graphically illustrated in Figure 16.1.
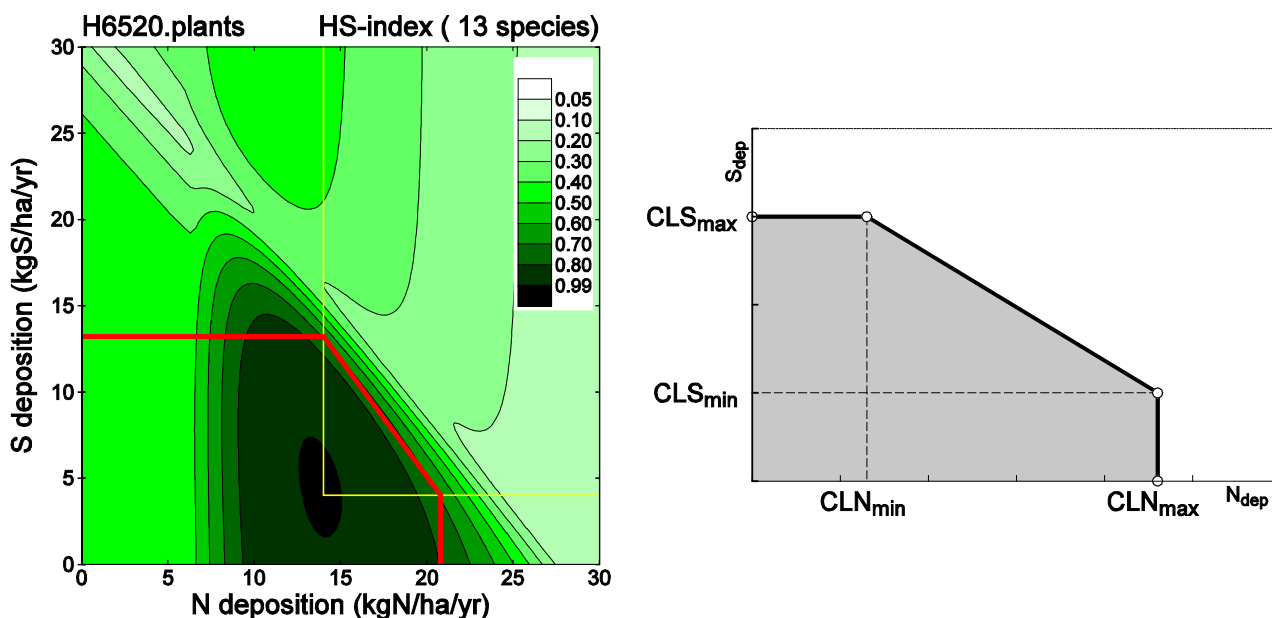
Figure 4.13: Left: N-S critical load function (CLF; red line) derived from the chosen HS-index limit value. Right: General shape of N-S CLF defined by the 4 quantities CLN_{min}, CLS_{max}, CLN_{max} and CLS_{min}.

The above methodology has been applied to a newly created European data base, obtained from combining the existing 'European background data base' with a European habitat map from the BioScore project. Figure 4.14 shows maps of percentiles of a critical load quantity (CLN_{max}) within the grid cells covering Europe, derived from about 1,300,000 habitat sites (see Slootweg et al. (2015) for further details).

ÉCLAIRE Third Periodic Report: November 2015

Exceedances of critical loads of N and S

For any given N and S deposition scenario, the exceedance of those biodiversity CLs can now be routinely computed. Exceedance for a collection of habitats in a grid cell is expressed as the 'average accumulated exceedance' (AAE), essentially an area-weighted exceedance of the individual CLs – a measure routinely used in European assessments since more than 15 years. In Figure 4.15 exceedances (AAEs) of the newly derived biodiversity critical load are shown for the years 2010 and 2050.Results show large exceedances in the Netherlands and the Po area, which still stay in 2050, even after the predicted N deposition reduction.
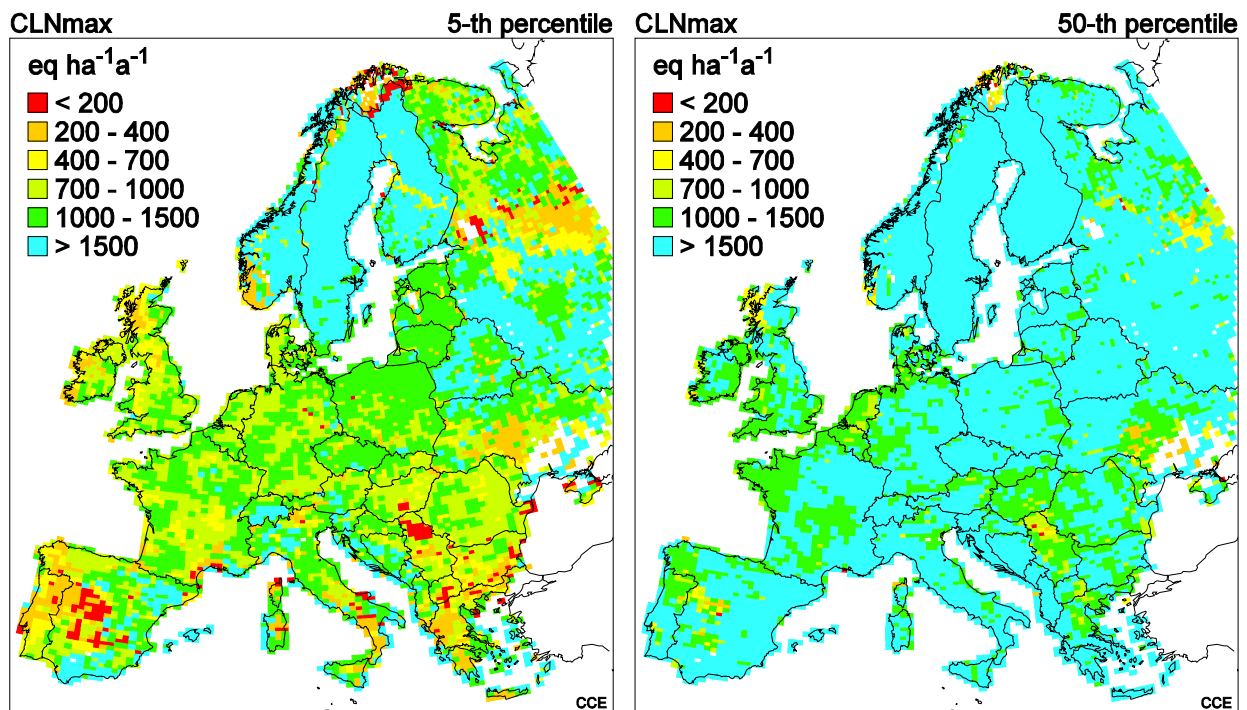
Figure 4.14: 5-th and 50-th percentile of critical loads of CLN$_{max}$ in every grid cell, derived from the HS-index computed with the PROPS model and steady-state soil model.

ÉCLAIRE Third Periodic Report: November 2015
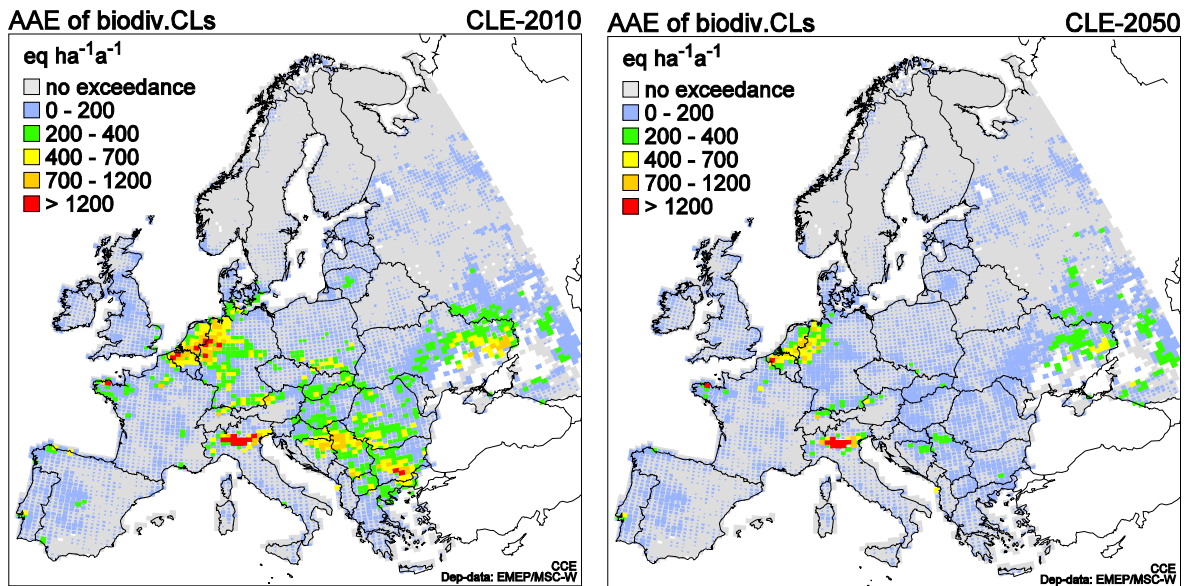
Figure 4.15: Exceedance of N-S CLs for biodiversity under 2010 (left) and 2050 (right) N and S deposition.

The biodiversity CL data provided by Component 4 have been successfully incorporated into the GAINS model and used in first assessments of cost-optimal emission reduction scenarios – see Figure 4.16 which shows an illustration of results of such an optimisation, presented in a recent meeting of Components C5 and C4.
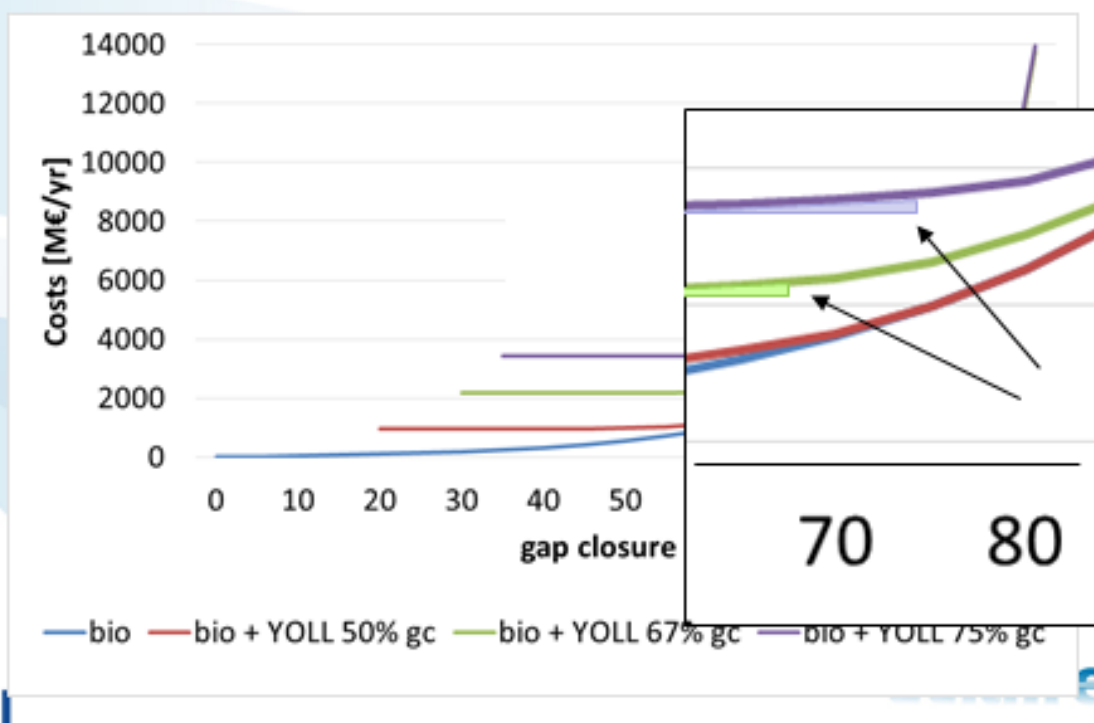
Figure 4.16: European (marginal) costs to achieve given percentage emission reductions between the 'Current Legislation' scenario and Maximum Feasible Reductions (MFR) using biodiversity CLs ('bio') in combination with human health related targets ('YOLL') (output from the GAINS model).

Notwithstanding further desirable improvements, it was concluded in a joint meeting of Component 5 and 4 (29-30 June 2015) that the biodiversity CL information provided by Component 4 can be used in integrated assessments with the GAINS model).

Task 16.3. Mapping critical thresholds for ozone uptake and their exceedances

According to the proposal description, this task includes the

- Mapping of critical ozone uptake thresholds, based on a spatial explicit assessment of tree species and crop types with different ozone critical limits.
- Mapping present ozone uptake for specific tree species and crop types and related exceedances of critical ozone uptake thresholds for those vegetation categories by applying the updated photosynthesis-based DO3SE approach coupled to the EMEP model.

In the previous progress report, progress and results were described, including maps of critical ozone uptake thresholds, that were derived on the basis of relationships between phytotoxic ozone dose (POD) and relative yield data of forests, distinguishing Norway spruce, Scots pine, Other conifers, Beech/Birch, Oak and Other broadleaves.

Whereas earlier the phytotoxic ozone doses were related to yield (total biomass) reductions (see Deliverable D16.2), these are now related to net annual increment (NAI). E.g., NAI (in %) for beech/birch is linearly related to POD_1 (in mmol/m^2) by NAI = 100–1.01·POD_1. Assuming an acceptable NAI reduction of 5% leads to a critical POD_1 threshold of 5/1.01 ≈ 5 mmol/m^2 for beech/birch.

Using data from a database on the coverage of 20 tree species (groups) on a 0.01°×0.01° grid (about 0.5 km×1km) covering Europe, the exceedance of this POD threshold for birch is shown in Figure 4.17 for the years 2000 and 2050 (the latter under the common ÉCLAIRE scenario RCA3-ECHAM5_A1B-r3) on the rotated Lon-Lat grid (grid size: 0.44°×0.44°) used for all European modelling within ÉCLAIRE.
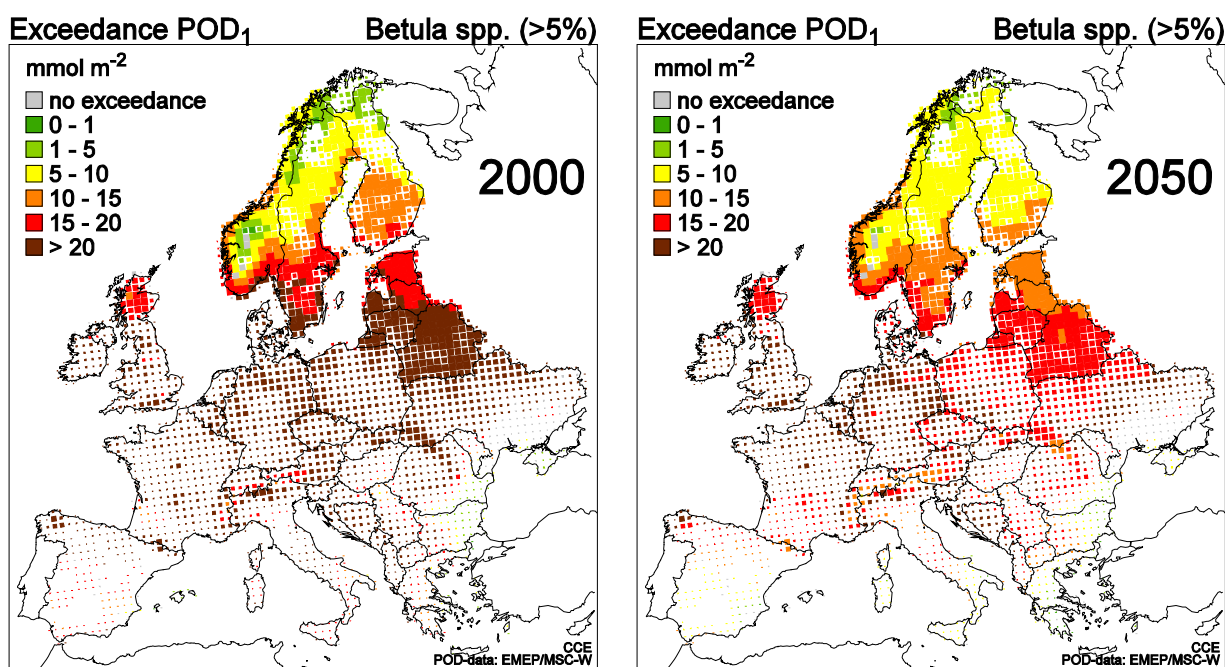
Figure 4.17: Exceedance of the POD_1 critical threshold (averting a NAI reduction of > 5%) for birch (*betula* spp.) in the year 2000 (left) and 2050 (right) under the RCA3-ECHAM5_A1B-r3 scenario (Note: the size of the coloured grid cells reflects the coverage of birch within the resp. grid cell).

ÉCLAIRE Third Periodic Report: November 2015

Using the linear relationship between POD_1 and NAI, Figure 4.18 shows the corresponding NAI reductions for birch in the years 2000 and 2050. Results indicate that current reductions in NAI of birch vary from about 10-15% in Northern Europe to more than 30% in Central Europe, while estimated future reductions in 2050 are on average about 5% less. Note, however, that this is an estimate for birch which is the most sensitive species, while impacts on other tree species are substantially lower.
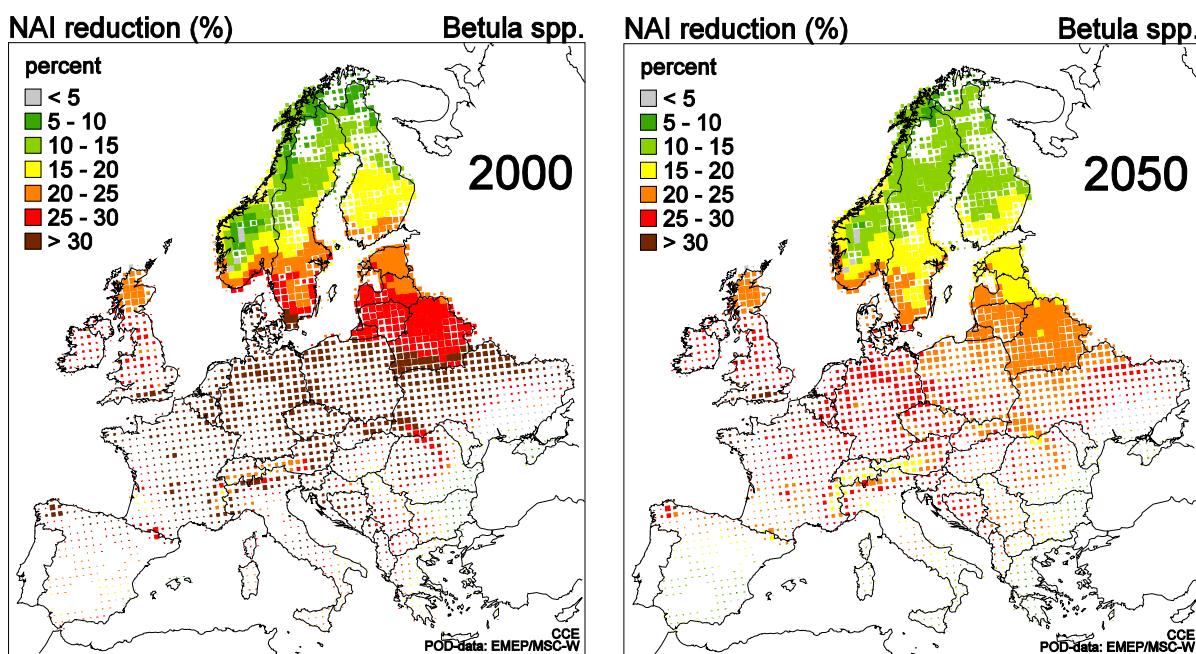
Figure 4.18: NAI reductions for birch (*Betula* spp.) in the year 2000 (left) and 2050 (right) under the RCA3-ECHAM5_A1B-r3 scenario (Note: size of coloured grid cells reflects coverage of the species).

Analogous relationships have been compiled for other tree species (groups) and crops. Note, that current thresholds are independent of geographical location and local (soil) parameters.

Progress towards the milestones and deliverables

During the reporting period (months 37-48), one milestone (MS70) was planned and one deliverable (D 16.4). The planned deliverable 16.4 was written during the reporting period and information is summarized in this progress report.

Milestones

MS70 Analysis of exceedances of critical thresholds for N-compounds (concentrations and depositions) and ozone uptake and their interlinkages   Due   Month   44   Delivered Month 46

Deliverables

An overview of all deliverables for WP16 is shown below, with those related to the last reporting period in bold

D16.1 Indicators for geo-chemical and biological endpoints. Due: month 12; delivered month: 12

D16.2 A map of critical ozone uptake thresholds at European scale. Due: month   24; delivered month: 26

D16.3 Map of critical N loads based on an inverse VSD+PROPS approach at European scale. Due month: 34; delivered month: 37

D16.4 Map of critical N load and critical ozone uptake exceedances using EMEP model results.   Due month: 40; delivered month: 44

D16.5 Feedback from the GAINS model on the applicability of the newly acquired critical thresholds in scenario analysis".   Due month: 36; delivered month: 44

Use of resources and deviations from DoW

During this reporting period no significant delays were encountered. A total of 8.8 person months were used.

References

De Vries, W., M. Posch, H.U. Sverdup, T. Larssen, H.A. de Wit, R. Bobbink and J.-P. Hettelingh, 2015. Geochemical indicators for use in the computation of critical loads and dynamic risk assessments. In: W. de Vries, J.-P. Hettelingh & M. Posch (eds) Critical Loads and Dynamic Risk Assessments: Nitrogen, Acidity and Metals in Terrestrial and Aquatic Ecosystems, Environmental Pollution Volume 25, Springer ISSN 1566-0745: 15-58. http://www.springer.com/gp/book/9789401795074

Van Dobben, H.F., M. Posch, G.W.W. Wamelink, J-P. Hettelingh and W. de Vries, 2015. Plant species diversity indicators for use in the computation of critical loads and dynamic risk assessments. In: W. de Vries, J-P. Hettelingh & M. Posch (eds) Critical Loads and Dynamic Risk Assessments: Nitrogen, Acidity and Metals in Terrestrial and Aquatic Ecosystems, Environmental Pollution Volume 25, Springer ISSN 1566-0745: 59-81. http://www.springer.com/gp/book/9789401795074

Posch, M., W. de Vries and H.U. Sverdrup, 2015. Mass balance models to derive critical loads of nitrogen and acidity for terrestrial and aquatic ecosystems. In: W. de Vries, J.-P. Hettelingh & M. Posch (eds) Critical Loads and Dynamic Risk Assessments: Nitrogen, Acidity and Metals in Terrestrial and Aquatic Ecosystems, Environmental Pollution Volume 25, Springer ISSN 1566-0745: 171-205. http://www.springer.com/gp/book/9789401795074

Reinds, G.J., M. Posch, J. Aherne and M. Forsius, 2015. Assessment of critical loads of sulphur and nitrogen and their exceedances for terrestrial ecosystems in the Northern Hemisphere. In: W. de Vries, J-P. Hettelingh & M. Posch (eds) Critical Loads and Dynamic Risk Assessments: Nitrogen, Acidity and Metals in Terrestrial and Aquatic Ecosystems. Series: Environmental Pollution, Vol. 25, 662pp. Springer, Dordrecht, Netherlands: 403-417. http://www.springer.com/gp/book/9789401795074

Slootweg, J., Posch, M., Hettelingh, J.-P. (eds), 2015. Modelling and mapping the impacts of atmospheric deposition of nitrogen and sulphur: CCE Status Report 2015. Coordination Centre for Effects, RIVM, Bilthoven, Netherlands, *in press*

Under submission
Posch, M., G.J. Reinds, J.P. Mol-Dijkstra, G.W.W. Wamelink and W. de Vries, 2015: Critical nitrogen loads and their exceedances at European scale based on protection of plant species diversity.

.

Work package 17   Local variation in threshold exceedance

Lead contractor: UPM
Contributors: NERC, ALTERRA

Work package objectives

Mapping nitrogen thresholds and their exceedance at a European scale with low resolution models hides a substantial amount of sub-grid variation, which may have significant policy consequences. The aims for this WP are:

1. To establish common databases containing atmospheric concentrations of reactive nitrogen compounds and nitrogen deposition data at the regional and landscape scales (from WP8)

2. To establish common databases containing current soil and vegetation data at the regional and landscape scales

3. To assess critical N thresholds and their exceedances at several grid resolutions from 5 x 5 km^2 and 1 x 1 km^2 (coarse and fine regional scales) down to 50 x 50 m^2 (landscape scale) and evaluate the uncertainty in these

Progress and Results

Task 17.1: Data collection for regional and landscape scale assessments.
This task has been completed in previous reporting period.

Task 17.2: Model application
Critical loads for acidification and eutrophication were calculated using a steady-state solution of the VSD+ model (Bonten et al., 2015) applied to two national-scale domains (The Netherlands and Scotland) and two landscape domains (Noordelijke Friese Wouden (NFW) in the Netherlands and Burnsmuir in Scotland) using the soil and vegetation database compiled in Task 17.1. For habitats in the Scottish domain for which no model input data were available, UK empirical critical loads for nitrogen were used (Hall et al., 2015). Figure 4.19 shows the spatial distribution of 5th percentile critical loads in the Dutch and Scottish domains and Figure 4.20 shows the critical loads for the two landscapes.

ÉCLAIRE Third Periodic Report: November 2015

eq ha^{-1} yr^{-1}

- 300
- 300 - 400
- 400 - 600
- 600 - 1000
- > 1000
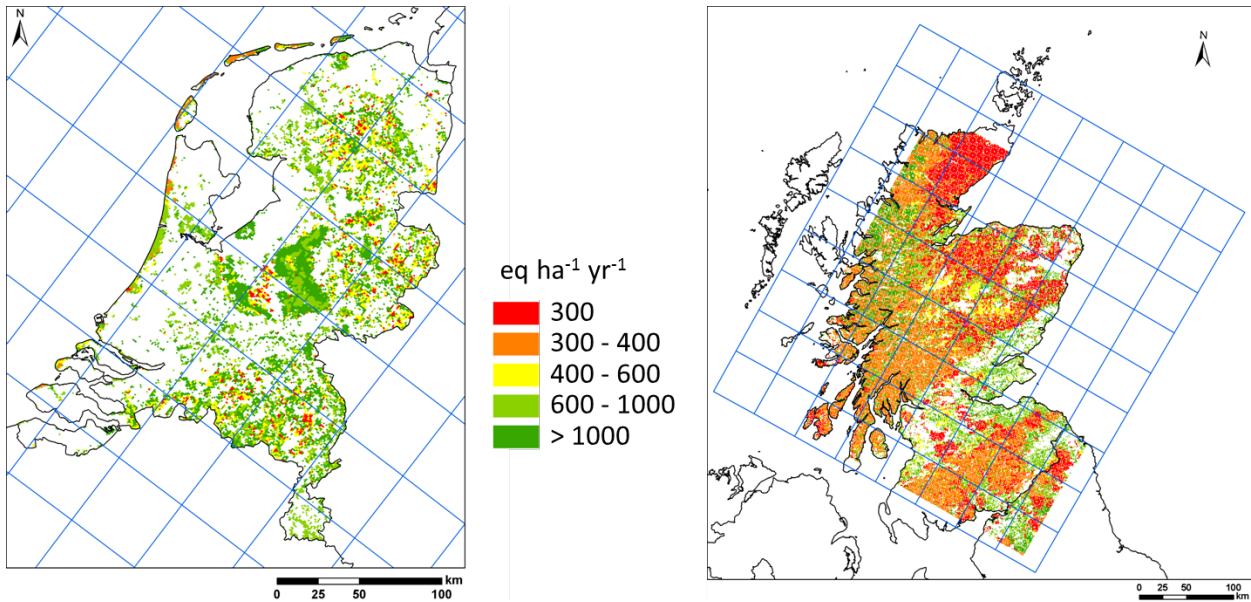
Figure 4.19: 5th percentile critical loads for the 1 km grid cells in the Dutch and Scottish domains. The blue grid shows the EMEP 50 x 50 km^2 grid squares.

ÉCLAIRE Third Periodic Report: November 2015
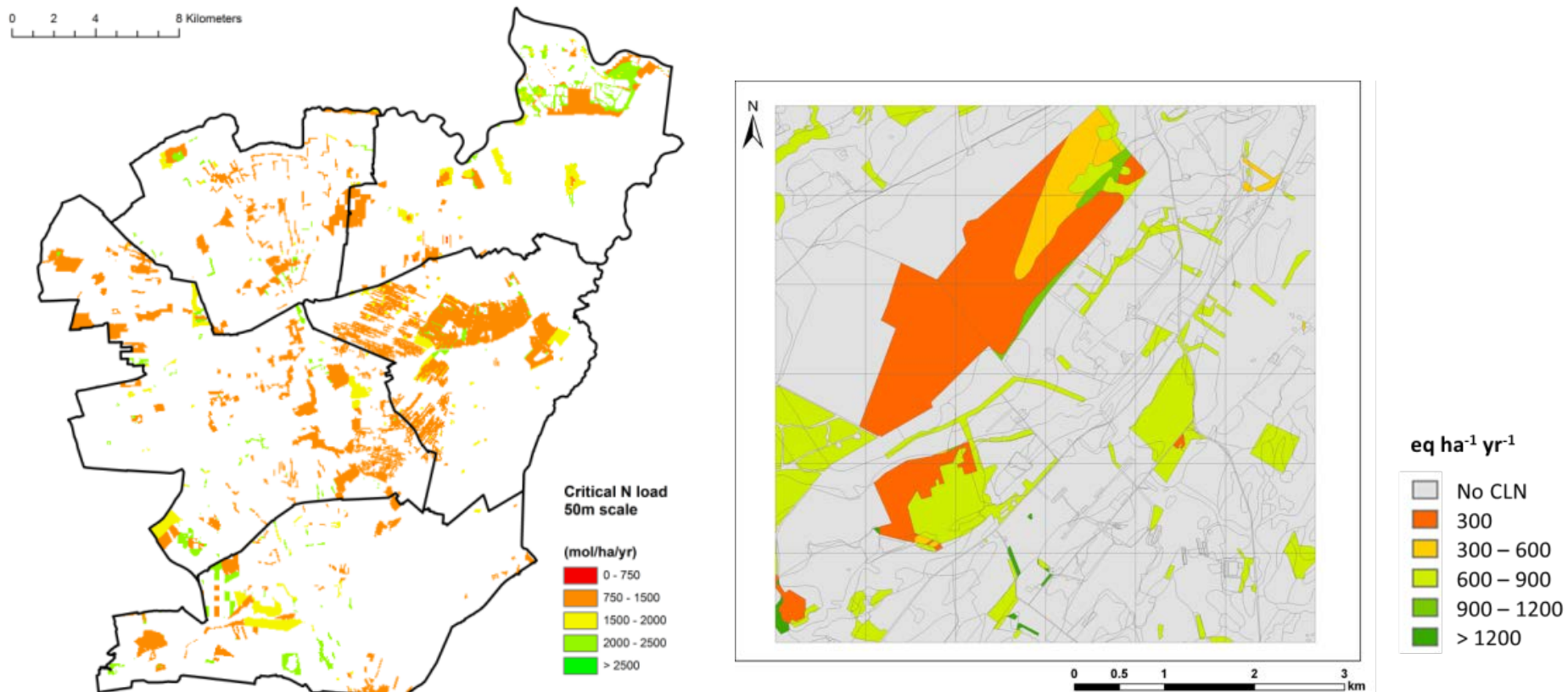
Figure 4.20: Critical loads for (left) the NFW domain at a spatial resolution of 50×50 m^2 and (right) the Burnsmuir landscape at a spatial resolution of 25×25 m^2.

Land-cover specific nitrogen deposition data were estimated using the EMEP4UK chemical transport model applied at three spatial resolutions: 1×1 km², 5×5 km² and 50×50 km² (see Deliverables D8.3 and D17.2) and used to calculate the average accumulated exceedance (AAE) for each EMEP 50×50 km² grid square for each deposition dataset. Two additional deposition datasets at spatial resolutions of 5×5 km² and 50×50 km² were produced by aggregating the 1×1 km² deposition data in order to look at the effect of changing the resolution of the deposition data whilst keeping the total deposition to the domain constant. Results of this action are shown in Deliverable 17.3.

Figure 4.21 shows the AAEs for the 50×50 km² grid squares that make up the Netherlands calculated using the three different spatial resolutions of nitrogen deposition data, while Figure 4.22 shows similar maps for the Scottish domain. Although there are small differences between the individual AAE values for a particular 50×50 km2 grid square, the general pattern and range of exceedances slightly increases going from 1×1 km² to 50×50 km² in line with the calculated slightly increasing N deposition in this direction are similar for all deposition datasets for both domains.(on average from 21.8 - 22.4 kg N ha^{-1} yr^{-1} in the Netherlands and from 5.1 to 5.4 kg N ha^{-1} yr^{-1} in Scotland).
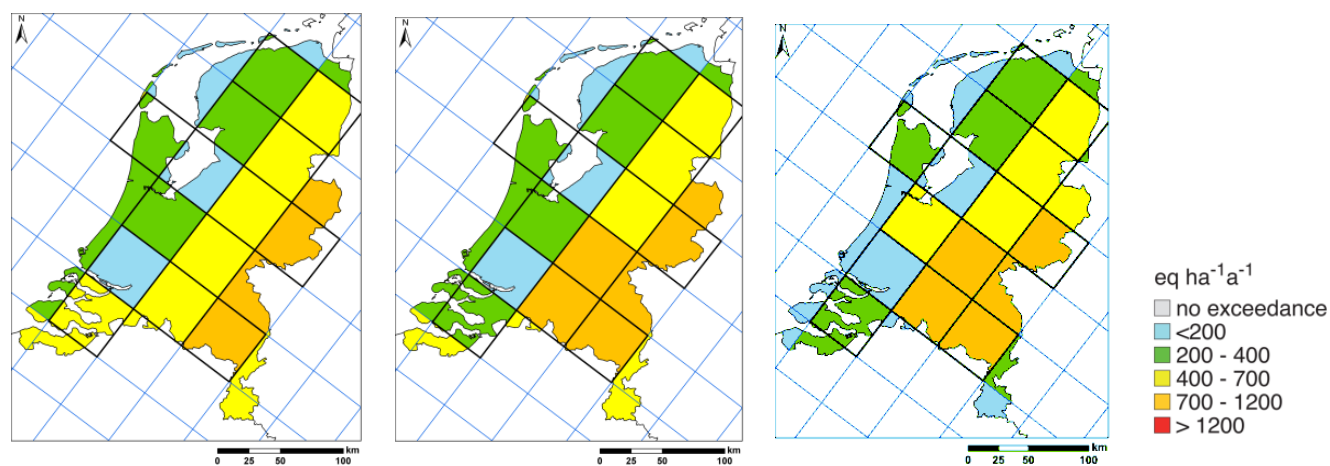
Figure 4.21: Average accumulated exceedances for 50×50 km² grid squares in the Netherlands calculated using nitrogen deposition data at the three model spatial resolutions (left: 1×1 km²; centre: 5×5 km² and right: 50×50 km²).
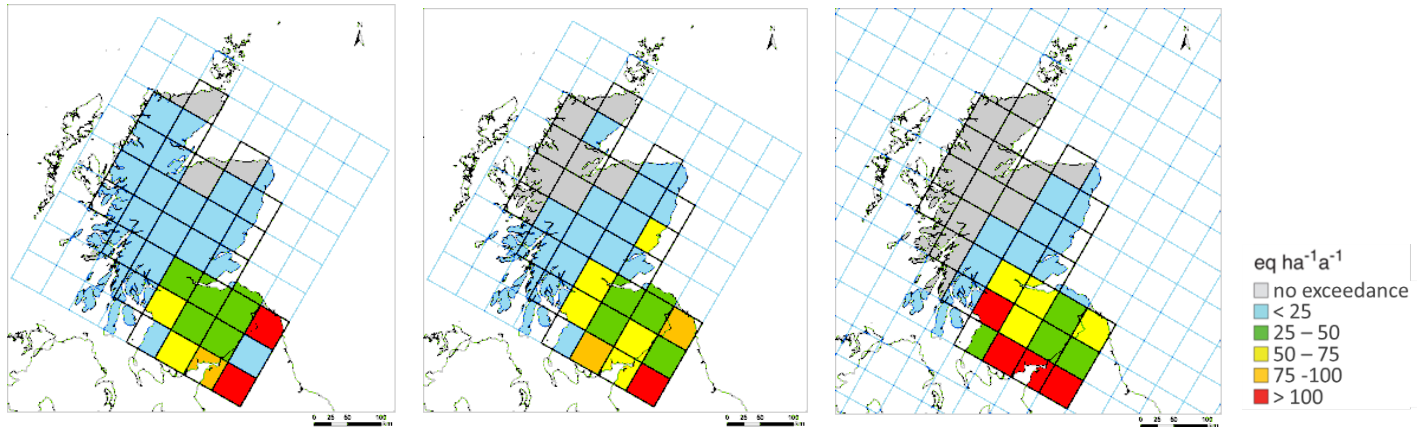
Figure 4.22: Average accumulated exceedances for 50 × 50 km^2 grid squares in Scotland calculated using nitrogen deposition data at the three model spatial resolutions (left: 1 × 1 km^2; centre: 5 × 5 km^2 and right: 50 × 50 km^2). Note: different exceedance range to the Dutch maps.

Figure 4.23 shows the AAE maps for the NFW landscape at three different spatial resolutions and Figure 4.24 shows them for the Scottish landscape at two different spatial resolutions.
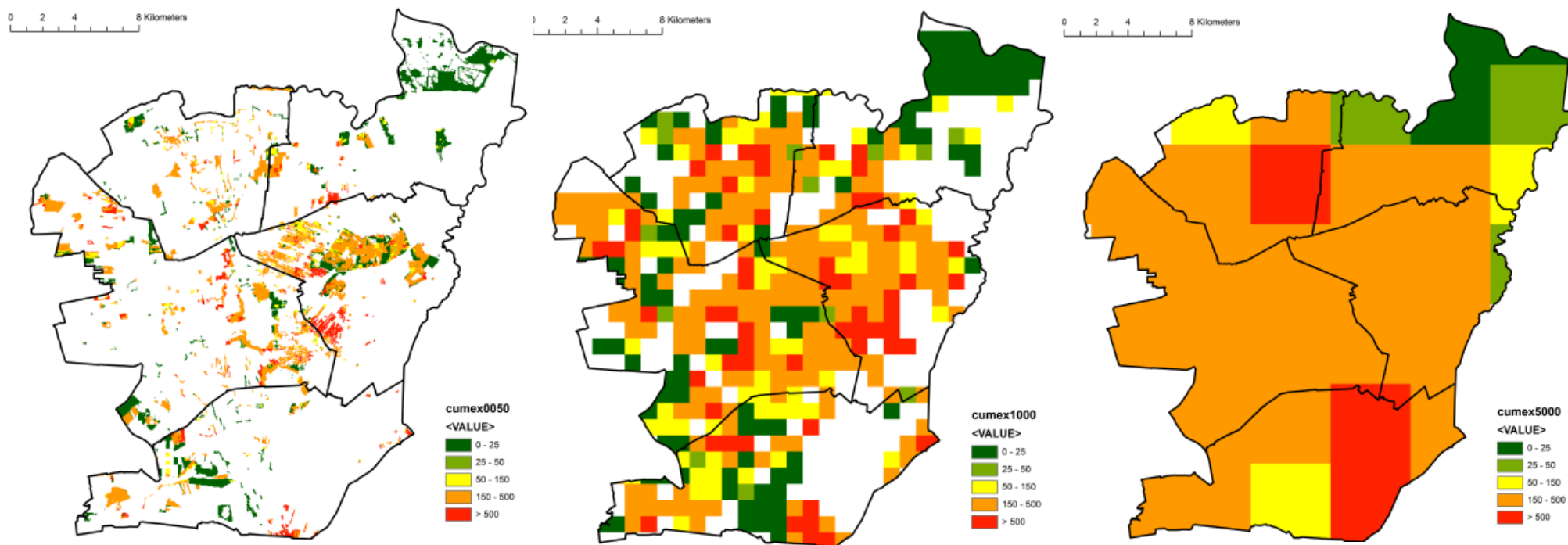
Figure 4.23: Average accumulated exceedances for the NFW landscape at a resolution of 50 x 50 m^2, 1 × 1 km^2 and 5 × 5 km^2.

ÉCLAIRE Third Periodic Report: November 2015
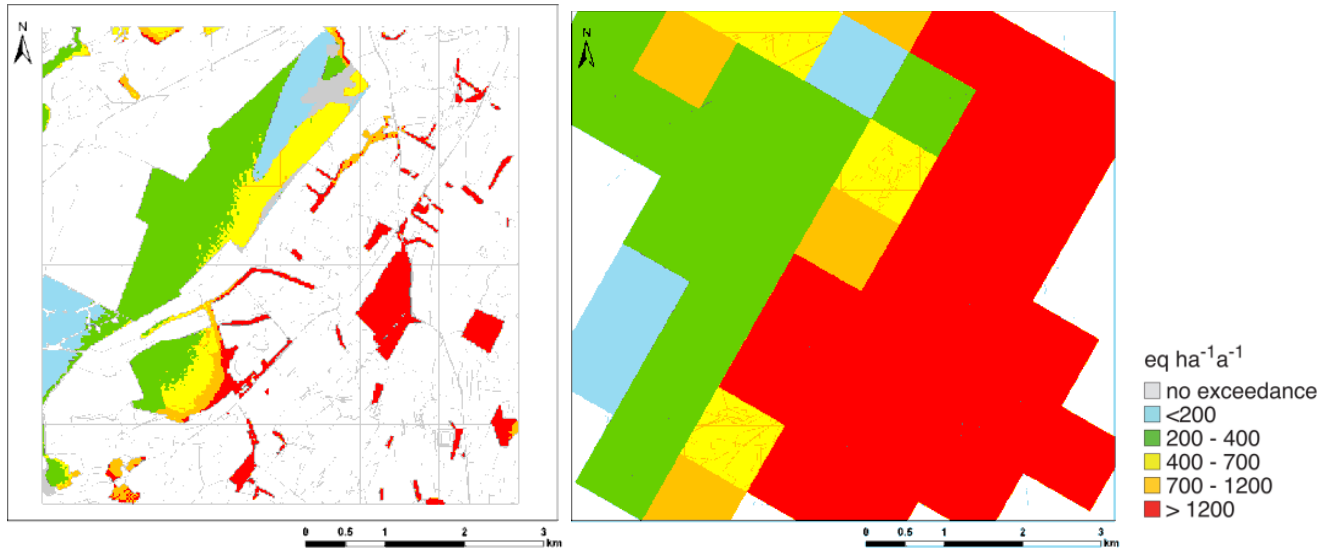
Figure 4.24: Average accumulated exceedances for the Burnsmuir landscape assessed for (left) 25 x 25 m² grid squares and (right) 1 x 1 km² grid squares, using nitrogen deposition data at a spatial resolution of 25 x 25 m².

Task 17.3: Uncertainty assessment

A statistical analysis of the AAE calculations shows that for the Netherlands, the AAE estimates calculated using the 50 × 50 km² EMEP4UK deposition dataset are, on average, approximately 15% higher than those calculated using the 1 × 1 km² EMEP4UK deposition dataset. By contrast, the AAE estimates calculated using the 50 × 50 km² deposition dataset aggregated from the 1 × 1 km² data are, on average, 7% higher (Figure 4.25). For Scotland, the use of the 50 × 50 km² EMEP4UK deposition dataset leads to an estimated exceedance in 62% of the grid squares compared with 91% when the 1 × 1 km² EMEP4UK dataset is used (Figure 4.26). When the 50 × 50 km² deposition dataset aggregated from the 1 × 1 km² data is used, the proportion of exceeded squares increases to 74%. Comparing only those squares where exceedance is estimated at both resolutions, the AAE estimates calculated using the 50 × 50 km² EMEP4UK deposition dataset are, on average, 20% higher than those calculated using the 1 × 1 km² EMEP4UK deposition dataset. By contrast, the AAE estimates calculated using the 50 × 50 km² deposition dataset aggregated from the 1 × 1 km² data are, on average, 8% lower.

319
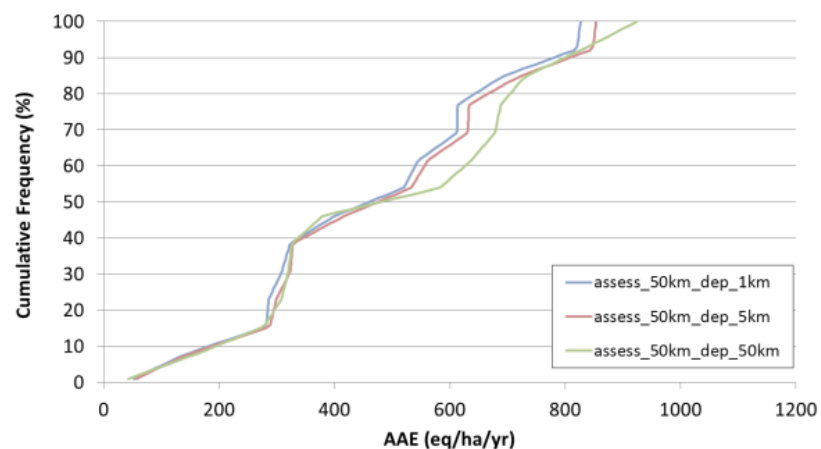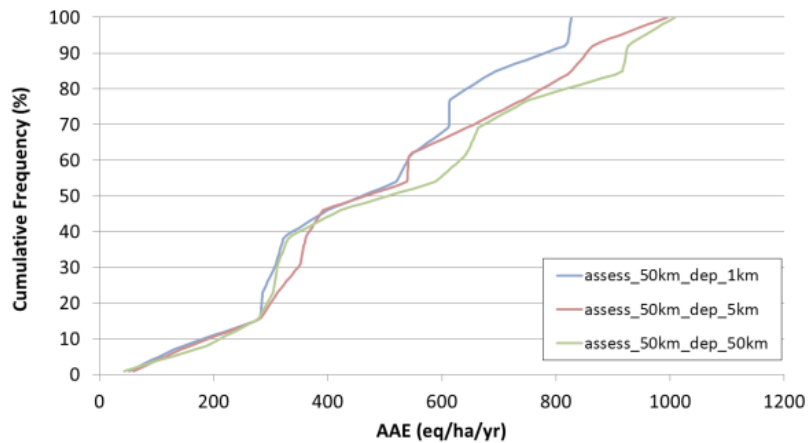
Figure 4.25: Cumulative frequency distributions for the Netherlands of the exceedances calculated using (left) EMEP4UK nitrogen deposition data at the three spatial resolutions and (right) deposition data aggregated from the 1 x 1 km² EMEP4UK deposition dataset.
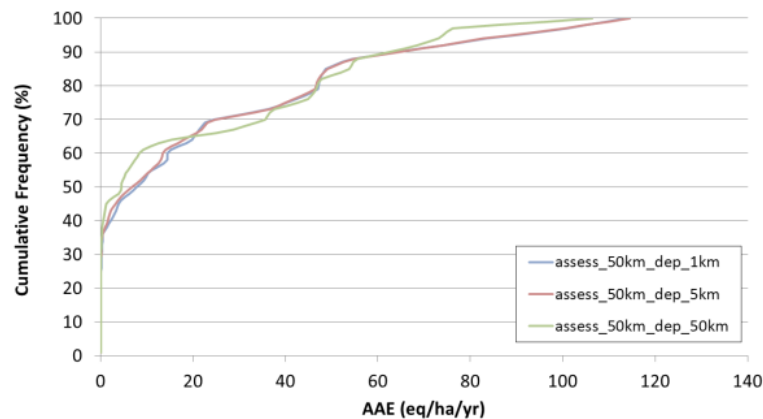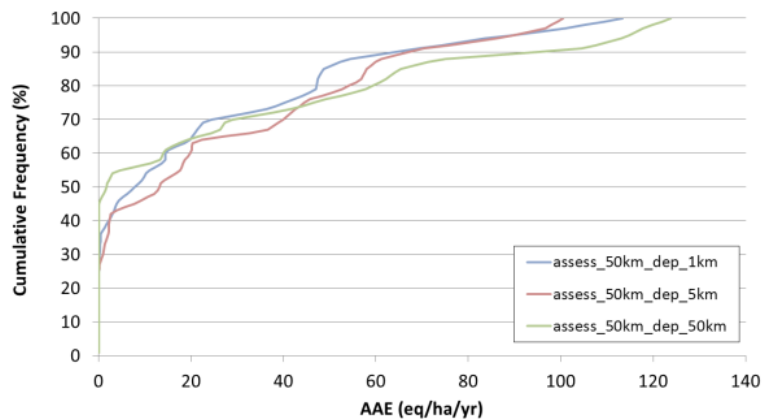
Figure 4.26: Cumulative frequency distributions for Scotland of the exceedances calculated using (left) EMEP4UK nitrogen deposition data at the three spatial resolutions and (right) deposition data aggregated from the 1 x 1 km² EMEP4UK deposition dataset.

For the Dutch landscape, average exceedances also increased with a decreasing spatial resolution of nitrogen deposition data, again as a result of an increasing nitrogen deposition to the landscape habitats (Figure 4.27).
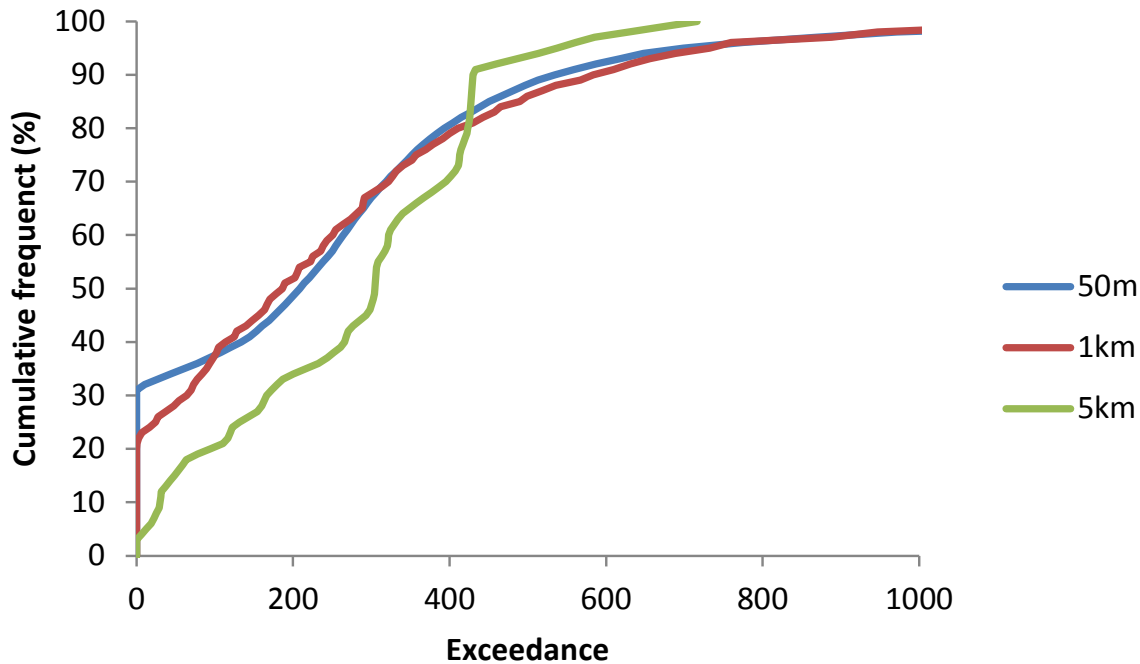
Figure 4.27: Cumulative frequency distribution of the AAE based on total N deposition at a resolution of 50 x 50 m^2, 1 × 1 km^2 and 5 × 5 km^2 for the NFW.

For the Scottish landscape, mean exceedances calculated using the 1 × 1 km^2 EMEP4UK deposition data were at least an order of magnitude smaller than those calculated using 25 × 25 m^2 deposition data from a local-scale atmospheric dispersion model, highlighting the importance of using high spatial resolution modelling for assessing critical load exceedances in "hot-spot" areas (figure 4.28).
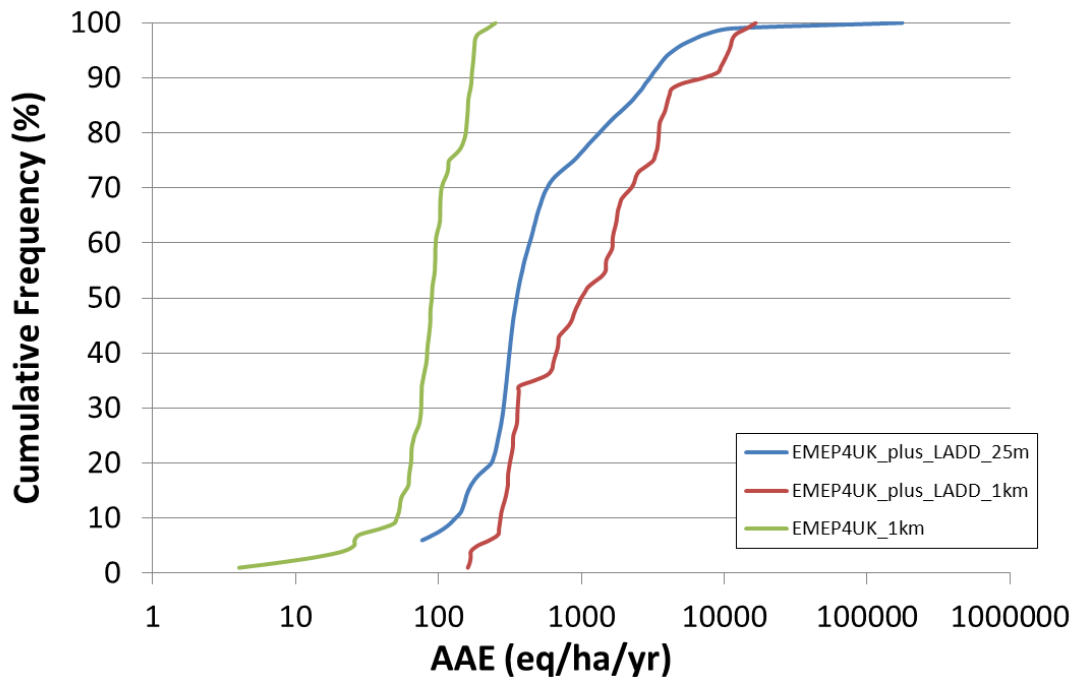
Figure 4.28: Cumulative frequency distribution of the AAE for the Burnsmuir landscape using nitrogen deposition data at a spatial resolution of 25 x 25 m^2 and assessed for (blue) 25 x 25 m^2 grid squares, (red), 1 x 1 km^2 grid squares and (green) using the EMEP4UK 1 x 1 km^2 deposition and assessed for 1 x 1 km^2 grid squares. Note: logarithmic scale for AAE.

Progress towards the milestones and deliverables

During the reporting period two milestones have been achieved and one deliverable submitted:

- MS76: Critical threshold and exceedance modelling complete for regional and landscape scales
- MS77: Uncertainty assessment complete and peer-review article submitted
- D17.3: Assessments of uncertainty of critical thresholds for N and their exceedances at the European scale

Use of resources and deviations from DoW
During the reporting period, a total of 5.4 person months have been spent on this work package. At the start of the reporting period this work was delayed by four months as a result of delays in the previous stages of the project. However, time has been made up in the last year of the project reducing these delays and making it possible for it to be

completed within the timeframe of the project. Since these analyses represent an 'end-point' of the work of WP17 in ÉCLAIRE, there are no knock-on effects of this delay.

References

Kros, J., M.M. Bakker, P. Reidsma, A. Kanellopoulos, S. Jamal Alam and W. de Vries, 2015. Impacts of agricultural changes in response to climate and socio economic change on nitrogen deposition in nature reserves. Landscape Ecology 30:871–885.

Note: Three peer-review articles are being prepared as a result of this work but have not been submitted at the time of writing.

Dragosits, U., M.R. Theobald , E. Rowe, M. Vieno, G.J Reinds, J Kros and W. de Vries. Impact of spatial resolution on calculated critical load exceedances at landscape scale

Kros, J. and W. de Vries, 2015. Impact of spatial resolution of input data on nitrogen losses to air and water from a rural landscape. Geoderma (in prep).

Theobald, M.R., U. Dragosits, M. Vieno, E. Rowe, G.J Reinds, J Kros and W. de Vries. Impact of spatial resolution on calculated critical load exceedances at national scale

2.2.5 Component 5 – Integrated risk assessment & policy tools

Lead contractor: IIASA

Component objectives & Specific Objectives of relevance to this component

ÉCLAIRE C5 intends to quantify and valuate ecosystem effects, implement new effect indicators and critical thresholds in the GAINS modelling system. Cost optimization of abatement measures under climate change conditions and Cost-benefit analysis (CBA) will allow relevant policy recommendations

Progress and Results

Work Package 18: Deriving economic impacts and valuation of ecosystem services

Providing input for cost-benefit analysis, WP18 for the first time has quantified ecosystem impacts according to:
- Willingness to pay for biodiversity protection (nitrogen)
- Agricultural crop losses (ozone)
- Forest production losses (ozone)
- Carbon sequestration (forests, ozone)

This allows to provide damage costs due to air pollution on ecosystems, which are about an order of magnitude smaller than health-related costs. Here it is important to note that measures taken to improve health are largely supportive also for ecosystem impacts, thus allowing for measures along a common direction.

Work in WP18 furthermore quantified the impact of climate change on agricultural land use and the resulting damage costs. It turns out that technical measures for air pollution abatement are able to alleviate only about 6% of the damage encountered. Losses in 2050 are expected to increase by about one third, considering also the switch of impacts that will become more relevant in tomato production compared to the current effects on wheat.

Work Package 19: Integrating effects of air pollution under climate change

The novel critical threshold "habitat suitability index" has been used to develop new "critical loads for biodiversity" (CL_{bio}). The method was presented and reviewed to the community of the International Cooperative Programme on Modelling and Mapping critical levels and loads and air pollution effects, risks and trends (ICP M&M), which hosted a dedicated ÉCLAIRE session. Refinements of the method were developed following discussions at the C5 final workshop in June 2015. Habitat-suitability-index based critical

loads have been used for developing the ÉCLAIRE optimization scenario. A sensitivity study allowed to identify impacts of using different parametrisation of the index (which identified a low sensitivity). The impact of climate scenarios (using downscaled results of global circulation models for 2050 and 2100) was tested and indicated considerable increase of the sensitivity of protected ecosystems on air pollution under any climate scenario: for future climate, impacts of air pollutants will become stronger.

Work Package 20: Implications for mitigation and adaptation strategies

Implementation of the ÉCLAIRE optimization scenario allows to assess the interrelation between commitments under discussion for human health protection and proposed measures for ecosystem protection. It turns out that the optimization scenario can provide considerable positive effects to biodiversity at rather low initial costs. Under conditions of climate change, additional action will be needed just to maintain a given target, due to the increased sensitivity of biodiversity impacts under climate change conditions. These "adaptation costs" also depend on the level of previously defined targets, and become significant for more ambitious levels of biodiversity protection. Impacts have been assessed quantitatively for 2050, and the instruments to extend to a "nominal 2100" scenario are all there, except for overly optimistic scenarios developed under IPCC (outside ÉCLAIRE) on NO_x and SO_2 emissions in that period, where improvements are on the way. Nevertheless conclusions are robust, that the most effective way forward is to reduce emissions of NH_3 in Europe to halt the loss of biodiversity, and of CH_4 at the hemispheric scale to reduce ozone damage.

Progress towards the milestones and deliverables, use of resources and deviations from DoW

The whole structure of ÉCLAIRE with experiments and modelling at the beginning, and policy analysis and recommendations towards the end of the project created the (expected) problem that some results came in delayed. As this was anticipated, prior action was taken and sometimes outside information was taken advantage of when ÉCLAIRE results were delayed. Still, this structural problem also resulted in delayed submission of deliverables, which however could be largely compensated toward finalization. At the time of finalizing this document, all Milestones have been achieved, and all Deliverables have been provided. It is expected that the further scientific evaluation as well as the dissemination to policy and other interest groups will be provided beyond the formal completion of ÉCLAIRE as planned. This will in particular include further publication of results and provision of support to the European Commission in relation to revision of the National Emissions Ceilings Directive and the UNECE Convention on Long-range Transboundary Air Pollution.

ÉCLAIRE Third Periodic Report: November 2015

Work package 18 – Deriving economic impacts and valuation of ecosystem services

Lead contractor: EMRC
Contributors: EMRC, RIVM, Aarhus University, NERC (BAN), IVL, SEI, IIASA

Work package objectives

Work Package 18 is designed to derive economic impacts and valuation of changes in ecosystem services through the following objectives:

- To link the concept of ecosystem services with existing mapping of European ecosystems and pollutant impacts.
- To characterise the links between pollutant exposure, impact and value to permit quantification of pollutant damage.
- To assess change in the value of ecosystem services across different scenarios using a marginal approach to the extent possible.
- To prioritise gaps in the existing knowledge base such that further research can be targeted on the parameters likely to have the greatest economic impact.

Progress and Results

Task 18.4 Linking ecosystem services to the assessment

Response functions for forests have been provided by SEI, enabling quantification of impacts to productivity and carbon sequestration. These express impacts on productivity using the POD (Phytotoxic Ozone Dose) approach.

Response functions for a limited range of crops (wheat, tomato, potato) have been supplied by NERC, linked to work by ICP Vegetation. These again use the POD (Phytotoxic Ozone Dose) approach. As assessment for three crops would clearly provide only a partial assessment of crop related impacts, further work has been undertaken led by EMRC to generate response functions for all crops, drawing on a broader range of data on sensitivity supplied by NERC. This extrapolation leads to perhaps significant uncertainty in estimates for some crops. However, these uncertainties will to some extent cancel out, with the effect that the overall level of uncertainty is considered acceptable for inclusion in policy assessment.

For the scenario analysis of Task 18.6, impacts to ecosystems are assessed via changes in the risk of exceedance of critical loads, particularly for nitrogen. These data are supplied by IIASA.

Task 18.5 Identify valuation data

This activity has involved Aarhus University (analysis of future crop distributions and production values under a changing climate), IVL (in relation to forest valuation), NERC (ecosystems and crops valuation) and EMRC (integrating inputs for the final analysis).

The work on crop distribution showed that under a changing climate some economically important crops are likely to grow in importance (e.g. tomatoes) as the area suitable for their cultivation increases, whilst others may decline, either as land becomes less suitable for their growth or they are displaced by more valuable crops. Overall, the economic value of crop losses in response to ozone exposure is anticipated to increase over time as a result of these changes, despite falling ozone levels.

For forests, the effects of any change in productivity within Europe are expected to be small at the continental scale, as utilisation rates (fellings/growth) are significantly lower than 100% in all countries with the exception of Albania. On this basis, falling ozone levels are not likely to lead to an increase in extraction rates, as there seems to be no current market for additional timber. Recognising that this could change, additional scenarios have been generated to illustrate the benefits that would arise for falling ozone if there was increased demand for timber products (e.g. through population growth) or for firewood (for biomass energy schemes). Climate effects are likely to be positive across Europe except for the southern countries, where increased risks have been identified, for example by IPCC. To account for changes in carbon sequestration a range of prices has been adopted, from €9/t CO_2 to €187/t CO_2. This range accounts for different approaches to valuation of climate effects and associated uncertainties.

For ecosystems, it is noted that there is still an inadequate basis for quantification of the effects of marginal changes at a European scale on a willingness to pay basis, reflecting appreciation of biodiversity. There are some exemplar studies, particularly the work of Christie et al, but to provide a robust assessment at the European scale further work is needed to demonstrate differences in valuation across the EU. With this in mind, four approaches have been developed for the analysis to generate a range of possible costs, based on:
- Willingness to pay at a coarse level of detail
- Willingness to pay at a finer level of detail
- Restoration costs
- Revealed preference from earlier regulatory decisions

The results from analysis using these methods indicates potential benefits of air pollution policies in the coming years running to several €billion, depending on scenario and the method used for valuation.

ÉCLAIRE Third Periodic Report: November 2015

Task 18.6 Scenario analysis

The scenario analysis has been performed by EMRC, drawing on the above inputs and pollution data provided from IIASA. The framework for this analysis is designed to fit with the methods in place for assessment of EU policies using the ALPHA-RiskPoll model used regularly in assessment for the European Commission.

The analysis has addressed effects of scenarios for 2000, 2010, 2030 and 2050. For 2030 and 2050 three scenarios have been investigated, addressing emissions under 'current legislation' (CLE), 'maximum feasible reduction' (MFR, applying all technical abatement measures included in the GAINS model) and an intermediate scenario, closing the 'gap' between CLE and MFR by 75% (BIO75). BIO75 is considered more policy relevant than MFR, as it excludes measures that are least cost-efficient for emission reduction, measures for which potential benefits are very likely to be inferior to costs.

The analysis includes not only assessment for ecosystems, crops and forests, but also health impacts. No updates of the methods for health analysis were carried out under ÉCLAIRE, though they were updated to reflect the recommendations of the WHO HRAPIE (Health Response to Air Pollutants in Europe) study, completed in 2013) as part of other related activities. Health impacts, as expected, dominate the analysis. However, it remains important to understand the ecological benefits that are possible in order to fine tune policies appropriately.

The report on this task includes a brief discussion of the overall validity of the methods employed for valuation. For impacts on productive services methods are appropriate. For impacts on biodiversity, however, there is concern that the willingness to pay approach provides only a partial perspective on the value of ecological change. This arises for several reasons – a lack of familiarity of ecosystem services for example, and resource limitations for individuals. It is noted that the resource limitation issue seems likely to be less important for health impacts given that individuals are more in control of their own health than of the environment in which they live.

Task 18.7 Dissemination

Results of the work have been discussed at the annual ÉCLAIRE meetings and additional meetings organised within the project team (for example at IIASA, in June 2015). Plans are in place for a series of papers from the work package addressing damage to crops, forests and ecosystems.

Progress towards the milestones and deliverables

During the reporting period, Milestones 79, 80 and 81 were achieved, and deliverables 18.2, 18.3 and 18.4 completed.

Use of resources and deviations from DoW

The total person months spent on this work package was 10.7.

During the course of the Work Package there was some slippage of time scales, partly resulting from the need to link to other work packages. However, the work has now been completed and objectives met.

Work package 19 – Integrating effects of air pollution under climate change

Lead contractor: RIVM
Contributors: Alterra (C4-WP14, 15 & 16), IIASA (C5-WP20), MET_NO (C2)

Work package objectives
Objectives under WP19 are:
(1) To operationalize new critical thresholds for the GAINS assessment of adverse effects of air pollution abatement scenarios (incl. climate change) on plant species diversity and ecosystem services
(2) To provide operational indicators for the support of policy with the assessment of scenario-specific adverse effects
(3) To analyse the robustness, the magnitude and location of scenario specific adverse effects on a regional scale.

Progress and Results

The objectives of WP19 have been achieved.

The focus in the reporting period was on the development and testing of methods and possible indicators to assess exceedances of "critical loads for biodiversity" (CL_{bio}) in Europe. Under component C4 and C5 novel critical loads for biodiversity have been derived from the Habitat Suitability Index (see D16.4), and implemented in the GAINS system (WP20).

The method was presented and reviewed (**following –WP19/MS85**) to the community of the International Cooperative Programme on Modelling and Mapping critical levels and loads and air pollution effects, risks and trends (ICP M&M), at the 25th CCE workshop hosted by the Croatian Meteorological Institute (Zagreb, 20-23 April 2015, http://www.wge-cce.org/Activities/Workshops/Past_workshops/Croatia_2015).   A common session was held addressing methods developed under C4 and C5 of the ÉCLAIRE project and the progress under the Convention, as contribution to the Component 5 meeting (**following-WP19/MS93**; Laxenburg, 29-30 June 2015; http://user.iiasa.ac.at/~winiwart/ÉCLAIRE_June_2015/).

Exceedances of the critical loads for biodiversity have been assessed for 4 different scenarios in which measures to abate air pollution and, the two last scenarios in particular, to also curb climate change (D20.6) i.e. "Current Legislation in 2010" (CLE2010), "Current Legislation in 2050, "Decarbonisation in 2050" (DECARB), and Maximum Control Effort in 2050" (MCE).

The European critical loads database for biodiversity, developed under C4 and C5 of the ÉCLAIRE project, now completes two already existing GAINS system impact indicators, i.e. the European critical load database of critical loads for eutrophication (CL_{nut}; Hettelingh et al., 2015a) and empirical critical loads (CL_{emp}; Hettelingh et al., 2015b). The European database of CL_{nut} is based on geo-chemical parameters, while CLemp has been compiled based on field measurements of impacts of nitrogen deposition (Bobbink and Hettelingh, 2011; Bobbink et al., 2015).

Results, described in this report, indicate that nitrogen deposition puts important parts of European ecosystems at risk because of the exceedance of critical loads. The area at risk varies depending of which critical load is used.

Finally, CL_{bio}, CL_{nut} and CL_{emp} are used to assess the robustness analysis (Hettelingh et al., 2015a) of ecosystem impacts of GAINS scenarios. It is based on the analysis of the location and magnitudes of exceedances of various critical thresholds, following the principle of "ensemble modelling".

Task 19.1 New critical thresholds

Progress was made in the development of a novel indicator, the "habitat suitability index" (HSI) developed in collaboration with ÉCLAIRE-C4 and the community of the ICP M&M at the CCE workshop under the auspices of the LRTAP Convention, hosted by the Croatian Meteorological Institute (MS85; Zagreb, 20-23 April 2015).

Critical loads for biodiversity (CL_{bio}) have been compiled in Europe for 23 habitats (see D15.4), in about 1.3 million ecosystem data points, covering around 2.4 million km^2 including various classes following the EUropean Nature Information System (EUNIS; Davies and Moss 1999).

This database of new critical thresholds (see objective 1) has led to a "European critical loads for biodiversity" (CL_{bio}) which completes the already existing databases available at the CCE of " European critical loads for acidification and eutrophication" (CL_{nut}) and of "European empirical critical loads (CL_{emp}).

Task 19.2 Dynamic modelling

The PROPS model (C4) has been applied to compute the critical loads for biodiversity (CL_{bio}) on a Europeaan scale. Use is also made of the *background database* on soil chemistry (see also Posch and Reinds, 2005) and EUNIS vegetation for application under ÉCLAIRE in a collaboration between C4 and C5. This background database is consistent over Europe and may be employed in addition to – or instead of – country specific data

submissions. The latter has been reviewed at the 34th session of the Working Group on Effects in 2015.

Task 19.3 Dose response relationships

This task addresses the use in GAINS system scenario analysis of relationships in European natural areas between scenario specific nitrogen dose in combination with climate change. Critical loads for biodiversity have been developed, implemented in the GAINS system and applied to assess effects of emissions and related depositions that are distinguished in 4 different scenarios of measures to abate air pollution and curb climate change (see a detailed description in D20.6) . These scenarios are "Current Legislation in 2010" (CLE2010), "Current Legislation in 2050, "Decarbonisation in 2050" (DECARB), and Maximum Control Effort in 2050" (MCE).

Task 19.4 Robustness analysis of GAINS scenario impacts

The robustness of exceedances is derived in this section in analogy to the way in which uncertainties are addressed in the Fourth Assessment Report of the IPCC, as described in IPCC (2005). In this logic, the robustness of an assessment that ecosystem areas are at risk can range on a scale from "exceptionally unlikely" to "virtually certain".
Robustness analysis of ecosystem impacts of the 4 GAINS scenarios (see task 19.3), is based on the analysis of the location and magnitudes of exceedances of three different critical loads. The European critical loads database for biodiversity, developed under C4 and C5 of the ÉCLAIRE project, now completes two already existing GAINS system impact indicators, i.e. the European critical load database of critical loads for eutrophication (CL_{nut}; Hettelingh *et al.*, 2015a) and empirical critical loads (CL_{emp}; Hettelingh *et al.*, 2015b). The European database of CL_{nut} is based on geo-chemical parameters, while CL_{emp} has been compiled based on field measurements of impacts of nitrogen deposition (Bobbink and Hettelingh, 2011; Bobbink *et al.*, 2015).

The ÉCLAIRE deliverable, i.e. CL_{bio} are used in conjunction with critical load databases already included in the GAINS system, i.e. CL_{nut} and CL_{emp} to assess the robustness analysis (Hettelingh *et al.*, 2015a) of ecosystem impacts of GAINS scenarios.

The method is based on the analysis of the location, coverage and magnitudes of exceedances of various critical thresholds, following the principle of ensemble assessment (Hettelingh *et al.* 2015a) whereby a phenomenon (i.e. exceedances) is more likely when it occurs using different methods (i.e. three types of critical loads). *Robustness analysis would be geared around the question whether nitrogen deposition causes* scenario specific impact indicators to point in the same direction. The availability of three different endpoints (soil chemistry, plant species diversity and habitat Suitability)

leads to three types of critical loads, each of which can be exceeded. This leaves an ecosystem area with the following possibilities of being at risk of atmospheric deposition of nitrogen:

1. None of the critical loads are exceeded
2. One single type of critical load is exceeded
3. Two types of critical loads are exceeded
4. Three types of critical loads are exceeded:
    a. with a likelihood in the interval (0, 0.33] ; i.e the ecosystem is "likely" to be at risk
    b. with a likelihood in the interval (0.33, 0.66]; i.e. the ecosystem is "very likely" to be at risk
    c. with a likelihood > 0.67; the ecosystem is "virtually certain" to be at risk.

We use The likelihood of an exceedance in an EMEP grid cell as said to be likely, very likely or virtually certain if the cube root of the product of the percentages of protected ecosystem areas based on CL_{nut}, CL_{emp} and CL_{bio} are in ranges of 0-33, 33-67 and >67% (Hettelingh *et al.*, 2015a).

It is assumed that none of the three types of critical loads is preferred to any other. This implies that a situation where less than three types of critical loads are exceeded leaves it up to experts to weigh whether or to what extent the area should be considered at risk. In this report, such areas at risk are distinguished geographically by whether none, one or two critical loads are exceeded.

Task 19.5 Workshops

(1) CCE workshop (Zagreb, 20-23 April 2015)

The 25th CCE workshop (Zagreb, 20-23 April 2015) under the Convention on Long-range Transboundary Air Pollution was held (included in MS85). The workshop, which was held back to back with the thirty first Task Force meeting of the ICP-Modelling and Mapping of the LRTAP Convention, was attended by 52 experts from 19 countries. The workshop included:
(a) sessions on the review of the 2012-2014 call for data on "no net loss of biodiversity" and its follow-up, i.e. the development of the HSI indicator (see 2.1),
(b) a session entitled "Novel critical thresholds, status of ÉCLAIRE ("C5 session") other scientific progress and effect-oriented policy support" (MS91)
(c) sessions reporting on impacts of nitrogen and ozone in the field and under laboratory conditions.

ÉCLAIRE Third Periodic Report: November 2015

The objectives of the meetings included:

(a)   To review the response to the call for data on indicators, issued in 2014 by the Coordination Centre for Effects with a deadline in March 2015, following a request of the Working Group on Effects at its thirty third session (17-19 September 2014);

(b)   To hold a training session addressing (National Focal Centre-) specific issues on dynamic soil-vegetation modelling related to the requirements of the call for critical load on biodiversity data;

(c)   To share national results related to field measurements, tools and modelling developed in order to assess the impacts of air pollution on ecosystems and their biodiversity in general and nitrogen and ozon in particular. A session was foreseen addressing ÉCLAIRE methods and results to assess effects of nitrogen and ozon and their interaction (including C4 and C5 interaction)

(2) <u>Alterra-RIVM Seminar "Critical Loads and Dynamic Risk Assessments for nitrogen, acidity and metal inputs and the future of effect-oriented policy support" (Wageningen, 27 May 2015).</u>

In March 2015, a book has been published entitled "Critical Loads and Dynamic Risk Assessments: Nitrogen, Acidity and Metals in Terrestrial and Aquatic Ecosystems" edited by Wim de Vries of Alterra, Jean-Paul Hettelingh and Maximilian Posch of RIVM.

The book provides an overview of the development of critical load research for terrestrial and aquatic ecosystems, and effect oriented applications in support of air pollution abatement policies during the past 25 years. It includes progress made under the ÉCLAIRE project, which funding is acknowledged in the book. The book consists of 26 chapters, divided over five major themes on impacts and risks of nitrogen, acidity and metals:
  1. Assessment of indicators and thresholds for air pollutant impacts
  2. Empirical and process-model based critical loads for characteristic ecosystems
  3. Dynamic modelling approaches for abiotic changes at the site-specific scale
  4. Critical loads and dynamic model applications on a regional scale
  5. Integrated assessment of changes in environmental quality and ecosystem services as affected by air pollution under a changing climate.

At this workshop, the major achievements described in the book were highlighted and the challenges ahead, both in terms of research (ÉCLAIRE and follow up) and in science policy interface, are set forward.

The meeting included a forum discussion on the future of the need for scientific knowledge on environmental effects of European air pollution policies in general and of the Convention on Long-range Transboundary Air Pollution in particular. Forum members and the audience are challenged to review how scientific knowledge on effects can help find a sustainable balance between the economy and the health of people and nature.

Questions that were addressed included whether effect-oriented knowledge help improve synergies and alleviate undesired trade-offs between, e.g., agriculture and nature policies, between local and regional health and environmental issues, between the effects of ozone and nitrogen, or between European Union strategies on air pollution, climate change and biodiversity.

Progress towards the milestones and deliverables

All Milestones and deliverables of WP 19, in the project period October 2011-October 2015, have been finalized at the time of writing this 3rd Activity report..

CCE workshops including their reporting were successfully held in Copenhagen (8-11 April 2013; MS88) and in Rome (7-10 April 2014; MS89). and Zagreb (20-23 April 2015; MS85).

Results and minutes of these meetings were presented at the 32nd (Geneva, 12-13 September 2013; MS83), the 33rd session of the Working Group on Effects (Geneva, 17-19 September 2014; MS84) and the 1st joint session of EMEP and (the 34th session of) the Working Group on Effects (Geneva, 14-18 September 2015) respectively.

MS90 (Modelling Framework in place) was completed in collaboration with C4 and presented at various meetings under the Convention on LRTAP (see above). It included the design and use of a novel threshold (Dose-Response relationship) in the GAINS system. MS92, the first complete set of scenario specific adverse effects has been completed and illustrations were presented in C5 and C4-C5 cross component meetings at the General ÉCLAIRE Assembly (Budapest, 29 September – 2 October 2014). A core set of scenarios for use under ÉCLAIRE in 2015 is being finalized under WP20 for use under C5 and C4.

The modelling system (D19.2) was applied in support of a technical EEA report, submitted in September 2013 to the EEA, which finally appeared as EEA Technical Report 11/2014 (http://www.eea.europa.eu/publications/effects-of-air-pollution-on)

Deliverable D19.3 (Report on the magnitude, location and robustness) was presented in the C5 component meeting of the General ÉCLAIRE Assembly (Budapest, 29 September – 2 October 2014). The final Deliverable D19.3 will be reflected in chapters of the CCE Status Report 2014 (*in prep)*. The CCE Status Report 2014 will be at the basis of D19.4.

Deliverable 19.4, the final deliverable of WP19 (Final Report on the development and scenario application of methods) has been finalized and submitted in July 2015.

Use of resources and deviations from DoW
A total of 4.9 person months were spent on this work package.

Presentations and publications:

2013 presentations by the CCE (including C5)

29th Session of the Task Force on the Modelling and Mapping of Critical Loads and Levels and Air pollution Effects, Risks and Trends under the Convention on Long-range Transboundary Air Pollution (Copenhagen, 8-11 April 2013)

EU Greenweek (Brussels, 4-8 June 2013) entitled "Air quality and ecosystems: Benefits of air pollution control for biodiversity and ecosystem services and use in integrated assessment"

JNCC conference "Nitrogen deposition and the habitat Directive Impacts & Responses: Our shared Experience (Peterborough, UK, 2-4 December 2013), entitled "Regional (Incl. Natura 2000 areas) scenario assessments of nitrogen critical load exceedances and of tentative impacts on species richness".

32nd Session of the Working Group on Effects (Geneva, 12-13 September 2013)

ÉCLAIRE General Assemblee (Zagreb, October 2013)

Task Force on Integrated Assessment Modelling under the Convention on Long-range Transboundary Air Pollution (Zagreb, 2013)

32nd Meeting of the Executive Body under the Convention on Long-range Transboundary Air Pollution, entitled "Guidance document on health and environmental improvements using new knowledge, methods and data"

2013 publications (including C5 in collaboration with C4)

Hettelingh J-P, Posch M, Velders GJM, Ruyssenaars P, Adams M, De Leeuw F, Lükewille A, Maas R, Sliggers J, Slootweg J, 2013. Assessing interim objectives for acidification, eutrophication and ground-level ozone of the EU National Emission Ceilings Directive with 2001 and 2012 knowledge. *Atmospheric Environment* 75: 129-140; DOI: 10.1016/j.atmosenv.2013.03.060

Holmberg M, Vuorenmaa J, Posch M, Forsius M, Lundin L, Kleemola S, Augustaitis A, Beudert B, De Wit HA, Dirnböck T, Evans CD, Frey J, Grandin U, Indriksone I, Krám P, Pompei E, Schulte-Bisping H, Srybny A, Váňa M, 2013. Relationship between critical load exceedances and empirical impact indicators at Integrated Monitoring sites across Europe. *Ecological Indicators* 24: 256-265; DOI: 10.1016/j.ecolind.2012.06.013

Kopáček J, Hejzlar J, Posch M, 2013. Quantifying nitrogen leaching from diffuse agricultural and forest sources in a large heterogeneous catchment. *Biogeochemistry* 115: 149-165; DOI: 10.1007/s10533-013-9825-5

2013 Reports under the Convention on Long-range Transboundary Air Pollution

32nd session of the Working Group on Effects (Geneva, 12-13 September

- ECE/EB.AIR/WG.A/10 – Technical Report of the Coordination Centre for Effects and the Task Force on Moddelling and Mapping
- Informal document No. 4: DRAFT Guidance document VII on heath and environmental improvements using new knowledge, methods and data, Room document.
- ECE/EB.AIR/WG.1/2013/14 – CCE contribution to ICP-V (eds.): Benefits of Air Pollution Control for Biodiversity and Ecosystem Service, and related:
  - o informal document 1, full report.
  - o informal document 7, brochure.
  - o EB 32 version of the document
- ECE/EB.AIR/WG.1/2013/3 – CCE contribution to WGE-extended Bureau (eds.): 2013 joint report on activities of the International Cooperative Programs and the Joint Task Force on the health aspects of Air Pollution

32nd Session of the Executive Body (Geneva, 09-13 December 2013)

ECE/EB.AIR/WG.1/2013/8 , Guidance document VII on heath and environmental improvements using new knowledge, methods and data

2014 presentations

30th Session of the Task Force on the Modelling and Mapping of Critical Loads and Levels and Air pollution Effects, Risks and Trends under the Convention on Long-range Transboundary Air Pollution (Rome, 7-10 April 2014)

33rd Session of the Working Group on Effects (Geneva, 17-19 September 2014)

ÉCLAIRE General Assembly, October 2014.

2014 publications (including C5 in collaboration with C4)

European Environment Agency: Hettelingh J-P, Posch M, 2014. Effects of Air Pollution on European Ecosystems: Past and future exposure of European freshwater and terrestrial habitats to acidifying and eutrophying air pollutants, European Environment Agency, Technical report 11/2014 prepared by the CCE with contributions from the ETC-ACM and the EEA, http://www.eea.europa.eu/publications/effects-of-air-pollution-on

Slootweg J, Posch M, Mathijssen L, Hettelingh J-P (eds.) CCE Status Report 2014, *in prep (Publication expected in December 2014-January 2015)*

2015 presentations

31st Session of the Task Force on the Modelling and Mapping of Critical Loads and Levels and Air pollution Effects, Risks and Trends under the Convention on Long-range Transboundary Air Pollution (Zagreb, 20-23 April 2015)

ÉCLAIRE C5 Summary Workshop, International Institute for Apllied Systems Analysis, 29-30 June 2015, Laxenburg, Austria

Alterra-RIVM Seminar "Critical Loads and Dynamic Risk Assessments for nitrogen, acidity and metal inputs and the future of effect-oriented policy support" (Wageningen, 27 May 2015).

1st joint session of EMEP and the Working Group on Effects (WGE, 34th session) , Convention on Long-range Transboundary Air Pollution, Geneva, 14-18 September 2015

ÉCLAIRE General Assembly, Edinburgh, 1-4 September 2015

2015 publications (including C5 in collaboration with C4)

MULDER, C., BENNETT, E.M., BOHAN, D.A., BONKOWSKI, M., CARPENTER, S.R.,CHALMERS, R., CRAMER, W., DURANCE, I. EISENHAUER, N., HAUGHTON, A.J., HETTELINGH, J.-P., HINES, J., IBANEZ, S., JEPPESEN, E., KRUMINS ADAMS, J., MA, A., MANCINELLI G., MASSOL, F., MCLAUGHLIN, Ó., NAEEM, S., PASCUAL, U., PEÑUELAS, J., PETTORELLI, N., POCOCK, M.J.O., RAFFAELLI, D., RASMUSSEN, J.J., RUSCH, G.M., SCHERBER, C., SETÄLÄ, H., SUTHERLAND, W.J., VACHER, C., VOIGT, W., VONK, J.A.,WOOD, S.A., WOODWARD, G. (2015).10 Years later: Revisiting priorities for science and society a decade after the Millenium Ecosystem Assessment. – *Advances in Ecological Research 53*: (in press).

Mulder, C., Hettelingh, J.-P., Montanarella, L., Pasimeni, M.R., Posch, M., Voigt, W., Zurlini, G., 2015. Chemical footprints of anthropogenic nitrogen deposition on recent soil C:N ratios in Europe. *Biogeosciences* 12: 4113–4119 (doi:10.5194/bg-12-4113-2015)

De Vries W, Hettelingh J-P, Posch M (eds), 2015. *Critical Loads and Dynamic Risk Assessments: Nitrogen, Acidity and Metals in Terrestrial and Aquatic Ecosystems.* Environmental Pollution Series Vol. 25, Springer Science+Business Media, Dordrecht, xxviii+662 pp.; ISBN 978-94-017-9507-4; DOI: 10.1007/978-94-017-9508-1

De Vries W, Hettelingh J-P, Posch M, 2015. The history and current state of critical loads and dynamic modelling assessments. Chapter 1 in: De Vries et al. (eds), *op.cit.*, pp. 1-11; DOI: 10.1007/978-94-017-9508-1_1

De Vries W, Posch M, Sverdrup HU, Larssen T, De Wit HA, Bobbink R, Hettelingh J-P, 2015. Geochemical indicators for use in the computation of critical loads and dynamic risk assessments. Chapter 2 in: De Vries et al. (eds), *op.cit.*, pp. 15-58; DOI: 10.1007/978-94-017-9508-1_2

Van Dobben H, Posch M, Wamelink W, Hettelingh J-P, De Vries W, 2015. Plant species diversity indicators for use in the computation of critical loads and dynamic risk assessments. Chapter 3 in: De Vries et al. (eds), *op.cit.*, pp. 59-81; DOI: 10.1007/978-94-017-9508-1_3

Bobbink R, Tomassen H, Weijters M, van den Berg L, Strengbom J, Braun S, Nordin A, Schütz K

and Hettelingh J-P, 2015, Effects and Empirical Critical Loads of Nitrogen for Europe. Chapter 4 in: De Vries et al. (eds), *op.cit.*, pp. 85-127; DOI: 10.1007/978-94-017-9508-1_4

Hettelingh J-P, Stevens CJ, Posch M, Bobbink R, De Vries W, 2015. Assessing the impacts of nitrogen deposition on plant species richness in Europe. Chapter 23 in: De Vries et al. (eds), *op.cit.*, pp. 573-586; DOI: 10.1007/978-94-017-9508-1_23

De Vries W, Posch M, Reinds GJ, Bonten LTC, Mol-Dijkstra JP, Wamelink GWW, Hettelingh J-P, 2015. Integrated assessment of impacts of atmospheric deposition and climate change on forest ecosystem services in Europe. Chapter 24 in: De Vries et al. (eds), *op.cit.*, pp. 589-612; DOI: 10.1007/978-94-017-9508-1_24

Hettelingh J-P, Posch M, Slootweg J, Reinds GJ, De Vries W, Le Gall A-C, Maas R, 2015. Effects-based integrated assessment modelling for the support of European air pollution abatement policies. Chapter 25 in: De Vries et al. (eds), *op.cit.*, pp. 613-635; DOI: 10.1007/978-94-017-9508-1_25

Hettelingh J-P, De Vries W, Posch M, 2015. Synthesis. Chapter 26 in: De Vries et al. (eds), *op.cit.*, pp. 637-647; DOI: 10.1007/978-94-017-9508-1_26

2015 Reports under the Convention on Long-range Transboundary Air Pollution

CCE 2015, Report by the Coordination Centre for Effects and the Task Force on Modelling and Mapping to the 1st joint session of EMEP-WGE (Geneva, 14-18 September 2015), ECE/EB.AIR/GE.1/2015/17–ECE/EB.AIR/WG.1/2015/10

WGE, 2015. 2015. Joint progress report on policy-relevant scientific findings to the 1st joint session of EMEP-WGE (Geneva, 14-18 September 2015), ECE/EB.AIR/GE.1/2015/3–ECE/EB.AIR/WG.1/2015/3.

Slootweg J, Posch M, Hettelingh J-P, CCE Status Report 2015 (*in press*)

Work package 20 – Implications for mitigation and adaptation strategies

Lead contractor: IIASA
Contributors: NERC, ALTERRA, ECN, RIVM

Work package objectives

WP20 uses the GAINS model and the GAINS system to analyse effects of air pollution on ecosystems and the minimization of such effects under situations of climate change and climate adaptation.

Progress and Results

Task 20.1 Interact with policy makers

Policy links to both UNECE and EU Commission were maintained also in the final project phase. Notably, results of WP20 were prepared for and presented at the CCE/ICPMM meeting in Zagreb, April 2015. ÉCLAIRE results were also communicated in the meeting of the Task Force on Reactive Nitrogen in Lisbon, April 2015, and the Task Force on Integrated Assessment Modelling meeting in Edinburgh, May 2015. All these activities attempt to work out the scientific and the technical feasibility of integrating ecosystem protection into air quality policy. While the feasibility now can be demonstrated, policy implementation has not been successful.

Task 20.2: Extend GAINS into more distant future years

With the GAINS model limited to 2050, parameters of change beyond 2050 have been identified in order to address and discuss an "indicative 2100" scenario. Specifically, the following indicators of future development have been singled out: change in anthropogenic activity, developments in mitigation technology, direct climate effects on emissions, altered ecosystem sensitivity under a different climate regime, and the active choice of humans to embark or not on specific mitigation options. It turned out that among all of these aspects influencing the overall impacts on ecosystems, still the human choice (chosen policy) will decide most strongly on the impacts of air pollution to ecosystems, even in 2100. The analysis, which is also closely linked to the work of the "scenario team" under ÉCLAIRE WP21, also included assessing the quality of externally available data on atmospheric emissions for 2100, notably NO_x and SO_2, which proved to be not adequate to be applied for the purpose of ÉCLAIRE.

Task 20.3 Analyze scenarios with respect to policy options

As the key result of work in the project phase, a new ÉCLAIRE optimization scenario has been developed and discussed in several bilateral meetings and workshops (4th ÉCLAIRE GA, Budapest; final C5 workshop, Laxenburg; 5th ÉCLAIRE GA, Edinburgh). For this scenario, the interrelation between commitments under discussion for human health protection and those for ecosystem protection have been taken advantage of. It turns out that, assuming health protection is implemented politically, at very marginal additional costs considerable increase overall in protection of ecosystems can be achieved. This ÉCLAIRE scenario takes advantage of the newly developed "habitat suitability index" to describe the biodiversity maintained for a given vegetation class (following EUNIS specification).

As an element of analysing sensitivities, the ÉCLAIRE scenario also allows to point out potential climate adaptation requirements. If a given level of ecosystem protection is to be maintained, climate change triggers additional measures to keep these pre-defined standards, as ecosystem sensitivities increase and also as ammonia emissions are expected to rise with climate change. Costs of such adaptation measures depend on the level of protection set, and may add to the originally set abatement costs almost a similar amount.

The ÉCLAIRE scenario has been provided to project partners to perform further analyses with regard to ecosystem response, with the aim to quantify other vegetation impacts than biodiversity at the level of vegetation classes, the metric used for the optimization procedure.

Task 20.4 Cost-benefit analysis and conclusions

Developing an optimized ÉCLAIRE scenario allowed to allocate costs required for emission abatement to maintain a given ecosystem quality, or to protect biodiversity to a given extent. The respective benefits were taken from a legal framework rather than an economic assessment, such that the benefits refer to the "no net loss of biodiversity" target set for protected area. Main conclusions were developed during the final C5 meeting in Laxenburg and the ÉCLAIRE GA in Edinburgh and have been published as ÉCLAIRE deliverable D20.8. One key result refers to the positive impacts human health related measures to air pollution (in terms of tackling PM exposure in ambient air) would provide to ecosystems. This is not the case for ozone impacts to vegetation, which prove much less sensitive to local and regional measures anyway and also require tackling pollutants (NO_x) that need more cost-intensive measures for abatement. Typically these are not covered in cost-effective emission scenarios developed for human health or biodiversity protection.

Progress towards the milestones and deliverables

MS 98 (Results finalized for evaluation and dissemination – component 5 workshop) was the only milestone still open for the final phase. This milestone was adopted with the final C5 meeting in Laxenburg, June 2015.

Deliverable D20.6 has been submitted in November 2014, deliverables D20.7 and D20.8, which includes the results and conclusions derived from the work package, have been finalized by the end of the project in late September 2015 and take advantage of all the discussion points from the final ÉCLAIRE workshop in Edinburgh held earlier that month.

Use of resources and deviations from DoW

WP20 has been successfully concluded, with all milestones achieved and all deliverables provided. Despite of moderate delays throughout the modelling chain in the project, results are largely in line and have been achieved mostly consistent with the original time schedule. Minor adjustments were needed, e.g. concerning lacking quantification of ecosystem damages by air pollution, which in turn renders a quantification of benefits from air pollution-related measures meaningless. In short, WP20 has been completed successfully with the end of the project.

Person-months spent on WP20 are 3.7.

2.2.6 Work Package 21: Standards and data management

Work package objectives

The overall aim of this cross-cutting work package is to ensure effective integration, communication, standardization, and management of data between the different Science Components of ÉCLAIRE. It has the following objectives:

1. To facilitate the selection and harmonisation of scenarios used throughout the project
2. To develop and implement common measurement protocols across all measurement activities within the project
3. To establish, document and implement common modelling protocols to ensure reliable and transparent model results
4. To establish and implement methods for assessing uncertainties in modelling
5. To ensure data quality and implement procedures for quality control
6. To set up a Data management Committee (DMC), consisting of a Data Manager for each of the ÉCLAIRE Science Components (C1 – C5), the ÉCLAIRE web portal manager, the consultancy services of the NERC(EDI) Informatics Liaison Team, the IP secretariat.
7. To produce a Data Policy and a comprehensive, working Data Management Plan.
8. To establish two Data Centres appropriate to (i) ÉCLAIRE Components 1-3, and (ii) ÉCLAIRE Components 4-5.
9. To establish a single data portal, to harmonize and make available spatial data and model output, and to provide easy, secure upload and data access facilities for the field and laboratory measurements.

The above objectives are addressed under four tasks:

- Task 21.1: Harmonization of scenarios (Objective 1)
- Task 21.2: Common measurement protocols (Objective 2)
- Task 21.3: Model protocols and uncertainty (Objectives 3 and 4)
- Task 21.4: Data quality and database management (Objectives 5-9)

Progress under each of these tasks is reported below. A total of 7.4 person months was spent on this work package during the second reporting period.

ÉCLAIRE Third Periodic Report: November 2015

Task 21.1 – Harmonization of scenarios

Lead contractor: IIASA
Contributors: JRC, SMHI, NERC(EDI)

Task objectives

Task 21.1 (harmonization of scenarios) aimed to ensure that the scenarios used in ÉCLAIRE (climate-affected meteorological scenarios, land use scenarios and emission scenarios) were used consistently across the project. A "scenario team" was responsible for making available existing scenario data on each of these terms to ÉCLAIRE participants, and to advertise their own activities within the project partners.

Progress and Results

In the final project year no further need existed to develop or guide on scenarios. Instead, it became important to document what had been done, and to assess – as much as possible – which input information was used in what parts of the project. As some scenario results had to be integrated in the very early project phase, these could not take advantage of later external developments that were found useful for elements starting towards the end of the project. Experiences and problems with applying certain external data have also been reported separately in the specific deliverables of other work packages (see deliverable D20.7 and the difficulties to adequately use SO_2 and NO_x emissions for 2100 from the RCP database). A report (D21.2) was prepared tracing the respective information sources used in order to address the compatibility between the respective model results.

Progress towards the milestones and deliverables

Deliverable D21.2 ("ÉCLAIRE scenario reference") was finalized with the end of the project in September 2015. The content of the deliverable was also used to replace the previous implementation of the scenario guide on the internal ÉCLAIRE web pages (accessible via the "Modelling" tab for logged-in users).

Use of resources and deviations from DoW

No significant deviations from the planned activities need to be reported.

Task 21.2: Common measurement protocols

Lead contractor: FDEA-ART
Contributors: NERC, DTU

Task objectives

- Establishing common protocols for the network measurement activities in components C1 and C3 in close collaboration with the concerned WP leaders (WP1 and WP10)
- Ensuring that measurement protocols are consistent with the data requirements for initializing, driving, and validating the process models in collaboration with modellers - Link with Task 21.4 to ensure the consistency of measurement protocols and data reporting procedures.

Progress and Results

The nature of this task required the work be performed at the start of the project, and the two deliverables associated with it were due months 8 and 9 and were completed during the first reporting period. As detailed in the first periodic report, intense information exchange and discussions between modellers and experimentalists took place in the first 12 project months and the work of the task was successfully completed.

Progress towards the milestones and deliverables

No milestones or deliverables were due in this period.

Use of resources and deviations from DoW
There have been no deviations from the description of work for this task.

Task 21.3: Model protocols and uncertainty

Lead contractor: UEDIN

Task objectives

As mentioned earlier, the task objectives are:
- To establish, document and implement common modelling protocols to ensure reliable and transparent model results
- To establish and implement methods for assessing uncertainties in modelling

As a cross-cutting activity this task was designed to ensure that the modelling community developed and maintained a dialogue on modelling and uncertainty protocols within the project to ensure consistency in the use of data, the reporting of results and the handling of uncertainty.

Progress and Results

The work of the early phase of the project was to enable communication between the modelling communities, resulting in common modelling protocols. This work was to lead to a shared understanding of what uncertainty studies could feasibly be performed within the scope of the project and agreeing between the scientists involved on what would be required to make the models comparable and uncertainty studies possible. The modelling protocols were established, the discussions on needs for uncertainty work were had and the relevant milestones and deliverables met.

The second part to the overall task was then to bring together information on some of the uncertainty studies which had then been performed (according to the earlier discussions on feasibility) during the project. As noted in the previous periodic report, it was found that the studies which would be most relevant to report were not yet concluded, so reporting on their activities was neither timely nor relevant. Instead, a rationale for the report was submitted, which has now been followed in the delivery of the report for this period. The rationale outlined the scope of the report as bringing together summary information for uncertainty/intercomparison studies undertaken as part of the ÉCLAIRE work. The report provides this information and links to the relevant deliverables and scientific findings. Due to the diverse nature of the work undertaken, there was no possibility (or advantage) to directly compare between the work of each of the studies. However overall it should be noted that the studies have proved valuable within the ÉCLAIRE work and in the case of the CTM studies, more intercomparisons were provided than initially anticipated, due to increased collaboration. Both objectives of this task have therefore been fulfilled.

Progress towards the milestones and deliverables

MS103 Final report on uncertainty in model output due to structural elements - due month 48. Completed.

D21.6 Final report on uncertainty in model output due to structural elements – due month 48. Completed.

Use of resources and deviations from DoW

There were no deviations to this Task.

Task 21.4: Data quality and database management

Lead contractor: NERC

Task objectives

1. To set up a Data management Committee (DMC), consisting of a Data Manager for each of the ÉCLAIRE Science Components (C1 – C5), the ÉCLAIRE web portal manager, the consultancy services of the NERC(EDI) Informatics Liaison Team, the IP secretariat.

2. To produce a Data Policy and a comprehensive, working Data Management Plan.

3. To establish two Data Centres appropriate to (i) ÉCLAIRE Components 1-3, and (ii) ÉCLAIRE Components 4-5.

4. To establish a single data portal, to harmonize and make available spatial data and model output, and to provide easy, secure upload and data access facilities for the field and laboratory measurements.

Progress and Results

WP1 Data submissions

WP1.1: Field measurement data

15 months of high temporal resolution flux data (O_3, NO, CO_2, H_2O) + meteorology across a 9-site European flux network (Aug 2012 - Oct 2013)

All sites have submitted data for the requested length of time series. Most have submitted data to January 2014. There are still small datasets to come for a few sites for certain parameters. 1 min meteorology has been delivered for all sites where they had the instrumentation (except Bosco Fontana and Petrodolinskoye).

WP1.4: Bosco Fontana campaign data

Data forms have been added to the database. Data has now been uploaded to the database system

WP1.5: Targeted measurements of NH_3 exchange with Mediterranean vegetation

Measurements have also been taken at a Mediterranean site in Spain. The data concerned did not look entirely as expected, and further quality investigation has been made into this dataset.

WP2: Controlled studies on exchange processes

WP2.1 - data has been delivered (Controlled emission measurements of CO_2, CH_4, N_2O, NO and NH_3 using monoliths and litter from the ÉCLAIRE flux network) - BFW

WP2.4 - data has been delivered for WP2.4 (plant chamber-reaction chamber system (JPAC) in order to separate stress induced emissions, O_3 & NO_x deposition within the eco-system, and photo-chemical ozone formation) – JUELICH

WP2.2 Providing data on NO emissions after rewetting events on soil cores – KIT. Final data is being processed and the time series experiment and statistical data will be archived in the ÉCLAIRE database.

WP2.3 (Assessment of primary and secondary BVOC exchange rates) data captured and submitted

WP 9 - Literature data mining

No more updates since last report.

WP10/WP11 Data submissions

Data have been uploaded for the 4 different ecosystem types:

ÉCLAIRE Third Periodic Report: November 2015

Table 21.1: Data uploaded for different ecosystem types.

Ecosystem	Site 1	Site 2
Forest	Bangor (UK) 2012-2013	Curno (It) 2012-2014
Grassland		Alp Flix (Sui) 2004-2010
Agriculture	Santa Olalla (Es) 2011-2012	Riso Phytotron (Dk) 2009-2011
Shrubland	Brandburg (Dk) 2006-2012	Whim Bog (UK)2012-2013

Additional measurements have associations with WP11 where they have also contributed to the overall measurements in WP10:

- Whim Bog (2013)
- Bonn (2012)

WP 11.1: Peat bog experiment on N-climate-O_3 interactions.

Measurements are ongoing on the O_3 'field release' experiment on the Whim ombrotrophic bog set up in 2014/15. This experiment will continue after the end of ÉCLAIRE using national funding and will continue to use the ÉCLAIRE database.

WP11.3: Effects of aerosol deposition on stomatal function

Datasets for sunflowers, pine and beech experiments have all been submitted to the database.

WP21

ÉCLAIRE data portal (D21.8)

The ÉCLAIRE data portal now has 74 registered users. Further updates and feature requests have been documented for future development and improvements.

Data Centre for Components 4 and 5: Afolu data centre – JRC

Due to a server upgrade at JRC, the AFOLU database is no longer operational. We are working with JRC on the best longterm option for storage of spatial datasets and in the meanwhile an interim web-based alternative is being used effectively to share information necessary between scientists working on the project.

Progress towards the milestones and deliverables
MS100 Common measurement protocols for C1 and C3 agreed and distributed Complete.

MS104 DP and DMP first drafts written and agreed by DMC (**D21.7**) Complete and online

MS106 ÉCLAIRE data portal online with user registration. Online with 74 users http://ÉCLAIREdata.ceh.ac.uk

MS107 Data uploaded and QA checked for months 1-18 Completed

MS108 Data uploaded and QA checked for months 19-36. Completed

MS109 Final data uploaded. Completed

D21.14 Final database report on intermediate content, including QA/QC report. Report completed. QA/QC report - delivered.

2.2.7 Work Package 22: Co-ordination and management

This section summarises the activity within the management WP of the ÉCLAIRE project, however a more detailed 'Management Report' is also provided in Section 2.3 as per Commission's guidelines.

Work package objectives

The objectives of WP 22 are:
1. To establish and operate the ÉCLAIRE project office
2. To provide scientific coordination of the project
3. To provide financial and administrative coordination of the project
4. To facilitate and ensure comprehensive, complete and timely reporting to the EC
5. To facilitate and organise an annual report for policymakers on progress with the 'Objectives, Key Questions and Specific Questions' of the project
6. To organise the General Assembly and other project meetings
7. To support the Executive Steering Committee and the Scientific Advisory Board
8. To oversee the appointment of a Gender Action Committee and its associated activities

Progress and Results

Task 22.1: Scientific project co-ordination and management

A project office was in place for the start of the project, consisting of the project co-ordinator (Professor Mark Sutton), scientific project manager (Dr Clare Howard) and a finance officer (Mrs Agnieszka Becher). The coordination team has continued through the year to provide smooth operation of all the functions listed under the objectives above. Key tasks that have taken substantial time this year included:

  a) Provision of support to the European Commission, European Parliament and the UNECE regarding the dissemination of results of ÉCLAIRE in relation to current policy developments (e.g. NEC Directive revision).
  b) Provision of input to DG Research as requested, to support a study on future research challenges at the "Junction of Health Environment & Bioeconomy" (JHEB).
  c) International dissemination of outcomes from ÉCLAIRE in many audiences, including with the United Nations Environment Programme (UNEP) and in media dissemination.
  d) Preparation and finalization of a Special Report of the European Nitrogen Assessment (ENA) as an ÉCLAIRE dissemination task: "Nitrogen on the Table", with international media engagement of the Key Messages, and a full report launch planned for the European Parliament in January 2016.

e) Preparation and finalization of published volume, "Costs of ammonia abatement and the climate co benefits.",　　Reis S., Howard C.M. and Sutton M.A., ISBN:978-94-017-9721-4, which was published in June 2015.
f) Auditing of ÉCLAIRE under ISO9001 accreditation.
g) Management of the Amendments to the Grant Agreement and changes to Partners′ legal details and budgets, as required.

The 'Annual progress report year 4' (D22.4) has been delivered under the title 'ÉCLAIRE Key Messages for Policy Makers - Year 4' along with the earlier report 'ÉCLAIRE Key Messages for Policy Makers - Year 3' (D22.3).

These reports focus on answering the key messages of ÉCLAIRE and also include a summary of outputs, including press engagement (TV, Radio, National Press, Briefings etc), presentations and other papers (D22.4) and the specific report on dissemination (see section 2.2.9.)

Communication has been developed and maintained between the Executive Steering Group (ESG), the Stakeholder Advisory Board, project PI's and the full ÉCLAIRE community. This includes organising regular teleconferences of the ESG, circulating minutes and providing information through the ÉCLAIRE website and e-mail distribution lists.

Experience from this year has shown that a major fraction of the time was required by the co-ordinator to deliver effective external representation and dissemination of the project. However, this has served to provide an extremely strong visibility of the ÉCLAIRE outputs internationally, including providing access to useful feedback to refine the research agenda.

Task 22.2: Project administration and financial management

During the current period the project office organised the 4th and Final General Assembly in Edinburgh (1st-4th Sep, 2015). This final meeting allowed the project participants to discuss not only the progress on work packages and deliverables, but also start to formulate answers to the key questions posed at the start of the project. This activity was invaluable in starting the process of developing clear messages for policymakers and wider audiences which would be included in the 'ÉCLAIRE Key Messages for Policy Makers – Year 4' and Final Report required by the Commission.

In advance of the final round of reporting, the project office provided information and support to the project partners on the requirements of financial and activity related reporting. Activity reports were collected and collated and the financial reports have been submitted in the Participant Portal. The project office has also been liaising with the component leaders in the development and refinement of items for the final report (S &

T results and key messages/impact).There has been no payment from the EC referring to the second periodic report. The contract has been amended following the inclusion of the Exeter University as a Third Party to partner NERC. There have been several changes in legal signatories in Partner organisations.

During the last 12 months, there have been budget changes between the following partners: NERC and UEDIN. A proportion of the 'unallocated budget' was assigned to partners BOKU, INRA, NERC, Juelich, TNO. This was spent on activities already predicted in the DoW.

Task 22.3 Gender Action Plan activities

As noted in previous reports, in the first year of the project, the gender questionnaire was produced and shared with all project staff. 90% of the staff surveyed indicated that ad-hoc gender activities would be sufficient, rather than gender sessions during the General Assemblies. During the 4th & Final General Assembly two opportunities were provided which explored some of the issues surrounding gender (and other) inequality(ies). These are outlined below.

Assertiveness Training

Following feedback from the first year ÉCLAIRE gender questionnaire (where assertiveness was perceived as a factor that can prevent gender equality), a short assertiveness training was organised during the 4th & Final General Assembly. This training will be reported in more detail under the 'Training' activities section (WP23). The training was used as an opportunity to highlight the potential role of gender in assertiveness, which was explored through a discussion of personality types (which can be present in both males and females) and some extra literature which the trainer complied and printed for attendees. Both males and females were encouraged to attend the training.

Working Group Session: 'Is discrimination an issue? Have we learnt from ÉCLAIRE & what needs to be done?'

The above session was organised during the 4th and Final General Assembly of the ÉCLAIRE project. It provided an opportunity for participants to provide feedback (online and in person, anonymously if they wished) on their experiences during the project, both positive and negative, to see if there were any lessons which could be learnt for future projects/gender actions etc. This was set-up through the use of an online questionnaire - 'ÉCLAIRE Equality Feedback Form' - for participants to fill in (if they wished) and then the

feedback and any issues which had arisen from this could be discussed in the dedicated session during the 4th and Final General Assembly.

The 'ÉCLAIRE Equality Feedback Form', contained the following questions:

Do you think that you have been discriminated against in any way during the lifetime of the ÉCLAIRE project?:

Yes/No (please select)

Further comments:

Have you witnessed discrimination against anyone else involved in the ÉCLAIRE project?:

Yes/No (please select)

Further comments:

Have we learned any lessons from ÉCLAIRE, if not, what do you think we should consider in future projects to tackle discrimination?:

Comments:

Further comments:

The participants felt that it would be useful to gain feedback not just on gender equality but any issue regarding equality, hence the scope of the questions. The form was posted on the ÉCLAIRE website (www.ÉCLAIRE-fp7.eu/node/279) in the non-membership area (to allow the possibility for anonymous comments). The existence of the form was advertised on our full ÉCLAIRE mailing list, with a request for responses in advance of the session at the 4th and Final General Assembly.

The responses received in advance of the session at the 4th and Final General Assembly all stated that they had not felt either discriminated against themselves or witnessed it occurring to others, in relation to the project. It was also noted in more than one response that the project approach of providing space for communication on such issues was a good one. Here are a couple of example responses:

"Thank you for the attention given to the issue of discrimination during this project. I believe that any potential for discrimination have been avoided, or at least tempered, by the precautionary approach of giving participants channels to communicate on the issue."

"I am glad these questions has remained on the table all along the project. I really think that's a good starting point."

The session during the 4th and Final General Assembly was not well attended, so based on the positive responses from the questionnaire, we concluded that we had followed a useful approach in the project regarding gender and other forms of discrimination. The

ÉCLAIRE Third Periodic Report: November 2015

only specific lesson to take forward was that we should continue to raise the issue of gender (and other potential equality issues) in future projects, including multiple opportunities for communication in order that the issues should not be forgotten and arising issues be addressed as required.

Following the session we received one more questionnaire response, where again they note no specific discrimination events, but commented that the gender balance at component, steering and advisory level was still mostly male. Due to the level at which these scientists operate they noted the gender imbalances of the past have likely contributed to this situation, but would like it noted for future consideration. Again they emphasised that the good communication fostered in the ÉCLAIRE project was a good starting point to address these issues in the future.

Progress towards the milestones and deliverables

All deliverables have been completed.

D22.3 - Dissemination report 'ÉCLAIRE Key Messages for Policy Makers – Year 3' [Annual progress report year 3]. This deliverable continued to use the format developed for the year 2 report at the specific request of the Stakeholder Advisory Board.

D22.4 - Dissemination report 'ÉCLAIRE Key Messages for Policy Makers – Year 4' [Annual progress report year 4]. This deliverable continued to use the format developed for the year 2 report at the specific request of the Stakeholder Advisory Board.

D22.7 - Final periodic Gender Action Report

MS116 – 'Second periodic Gender Action Report' was delivered at the start of this period.

MS113 Final periodic project meeting held. The final meeting was held in Edinburgh, 1st-4th September (discussed further in the 'Management' section, 2.2).

Use of resources and deviations from DoW

A total of 12.5 person months was spent on this work package during the third reporting period. There were no deviations from the DoW.

2.2.8 Work package 23 – Training

Lead contractor: UPM
Contributors: NERC, SEI-Y / UoY, BOKU, UEDIN, INRA

Work package objectives

This work package coordinates training activities across the ÉCLAIRE project. Its objectives are:
1. To organise specialised training events for postgraduate students and young scientists with the aim to train participants in advanced measurement techniques and modelling methodologies;
2. To develop a plan for and organise, run and evaluate a summer school for young scientists from within ÉCLAIRE and related projects around the topic of air pollution effects on ecosystems under climate change conditions.

Most of the budget of this Work Package is reserved for travel and subsistence to support young scientist training activities, including attendance from outside the ÉCLAIRE consortium. A reserve budget is also included to be able to respond to developments during the life of the project. The seed activities listed here are conducted in the context of other training instruments (e.g. Marie Curie, COST 0804, European Science Foundation) in order to maximize synergies and overall effectiveness.

Progress and Results

Task 23.1 Co-ordination of ÉCLAIRE training activities

No specific training activities were planned for this period of the project, however an assertiveness training was organised during the 4th and Final General Assembly. The 2 hr training was provided free of charge to those taking part in the 4th and Final General Assembly and was attended by 12 people. The outline of the course is provided below:

An Introduction to Assertiveness
This enjoyable introduction course will help you to develop your own abilities to deal with difficult situations & be assertive and also understand others better.

Workshop contents
• Recognise what assertiveness is and what assertiveness is not.
• Be able to identify and be aware of your own understanding of assertiveness.
• Know the difference between assertive, aggressive, manipulative and passive behaviour.
• Support & encourage you to develop your assertiveness skills.

The course was led by an experienced trainer and was backed up by a course booklet, group and individual practical exercises. The trainer also provided further information on the links between gender, personality type and assertiveness.

Task 23.2 Organisation of Summer Schools and dedicated workshops

The summer school (which was eventually held as a winter school) was held in the previous period and reported in the second periodic report. No further summer school activities were planned for this period.

Progress towards the milestones and deliverables

D23.4 Final periodic report on training activities – completed.

Use of resources and deviations from DoW

A total of 0.4 person months was spent on this workpackage during the third reporting period. There were no deviations from the DoW, only the delivery of an extra training opportunity for ÉCLAIRE project members, as described above.

2.2.9 Work Package 24: Networking and dissemination

Lead contractor: NERC
Contributors: ULUND, ALTERRA, DTU, IIASA

Work package objectives

The objectives of this work package are:
1. To coordinate networking activities with other projects and international bodies
2. To facilitate dissemination activities across the project
3. To develop and maintain a project web portal for project internal and external communication

Progress and Results

Task 24.1: Networking

Activity under this task continued during the third period as it has throughout the project, through links between Executive Steering Group members and other projects and networks. This includes with other projects funded by the Commission such as PEGASOS and the ACCENT+ network and outwith the Commission such as the UNECE Convention on Long Range Transboundary Pollution (LRTAP Convention) including through the co-chair of the task Force on Reactive Nitrogen and members of the International Co-operative Programme (ICP) for Forests and Vegetation (and other groups under the LRTAP Convention). The project co-ordinator is also involved in the 'Foresight Expert Panel on the Junction of Health Environment and Bioeconomy' of the European Commission as well as the recently formed European Union Nitrogen Expert Panel. Further details can be found in the project dissemination report on the Participants Portal, which contains a large number of press (TV and Radio) contributions, in the 'ÉCLAIRE Key Messages for Policy Makers' (Final Report, D22.4) and the ÉCLAIRE final report uploaded onto the participants portal. See also Box 9.1 below, for key highlights.

ÉCLAIRE Third Periodic Report: November 2015

Box 9.1: Example inputs into Policy Processes from the ÉCLAIRE Co-ordinator, Prof. Mark A. Sutton 2013-2015.

UNECE Ammonia Framework Code: Managed Stakeholder comments and replies from the Task Force on Reactive Nitrogen concerning the "Draft Revision of the UNECE Framework Code for Good Agricultural Practice for Reducing Ammonia Emissions" (Informal document n° 3) Executive Body of the CLRTAP (EB-33), Geneva (8-12 Dec 2014). This led to the revised Framework Code, now published by the UNECE.
http://www.unece.org/fileadmin/DAM/env/documents/2014/AIR/EB/ECE_EB_AIR_2014_8_E.pdf
ECE/EB.AIR/2014/8

ÉCLAIRE Key messages presented to UNECE: The 2014 policy report of ÉCLAIRE was presented to the Executive Body of the CLRTAP (EB-33), Geneva (8-12 Dec 2014).
http://www.unece.org/fileadmin/DAM/env/documents/2014/AIR/EB/Informal_Document_4_ÉCLAIRE_Policymakers_report.pdf

ÉCLAIRE Dissemination Product: Special Report on Nitrogen and Food. This report was coordinated by the ÉCLAIRE office together with the UNECE Task Force on Reactive Nitrogen. Westhoek H., Lesschen J.P., Leip A., Rood T., Wagner S., De Marco A., Murphy-Bokern D., Pallière C., Howard C.M., Oenema O. & Sutton M.A. (2015) Nitrogen on the Table: The influence of food choices on nitrogen emissions and the European environment. (European Nitrogen Assessment Special Report on Nitrogen and Food.) Centre for Ecology and Hydrology, Edinburgh, UK. Full report to be launched in January 2016 at the European Parliament. Task Force on Reactive Nitrogen http://www.clrtap-tfrn.org/.

ÉCLAIRE Supports Nitrogen Indicator Development at the OECD: The following report was prepared by the ÉCLAIRE team: Bleeker A., Sutton M., Winiwarter W. and Leip A. (2013) Economy-wide nitrogen balances and indicators: Concept and methodology. Organisation for Economic Cooperation and Development (OECD) (Working Party on Environmental Information), ENV/EPOC/WPEI(2012)4/REV1. Paris. In addition, the ÉCLAIRE coordinator presented results to the OECDs Environmental Policy Committee (EPOC).

Supporting NECD Revision The ÉCLAIRE coordinator and partners have been extremely active in dissemination in support of the National Emissions Ceilings Directive Revision. This has included providing advice to DG Environment and presenting findings to MEPs at the European Parliament, in addition to ongoing engagement through the many groups of the UNECE Convention on Long-range Transboundary Air Pollution (LRTAP).

Task 24.2: Dissemination

The project website http://www.ÉCLAIRE-fp7.eu continues to be a source of information for project participants and the wider community and has 134 users. The final dissemination and communication plan has been completed, to allow the project to maximise dissemination after the project ends. A list of selected dissemination highlights can be found below in Box 9.2.

Box 9.2: Key dissemination highlights from the ÉCLAIRE Co-ordinator,Prof. Mark A. Sutton, 2013-2015.

European Green Week, Brussels, June 2013. Session: "Air Quality and Agriculture" hosted by DG Environment. Invited Keynote lecture: "Why worry about ammonia and what can we do about it?" and panel discussion with industry and NGO representatives (in support of the EU Air Quality policy review).

European Parliament, "Forum on fertilizers and nutrients for growth", Brussels, 28th May 2013. Mark Sutton gave a keynote presentation entitled "Our Nutrient World: The challenge to produce more food and energy with less pollution" and also took part in the panel discussion with MEPs.

BBC World News TV, 22nd July 2014, live interview with Mark Sutton, jointly with Fuchsia Dunlop (writer / journalist on Chinese cuisine) on beef, food choice and the environment, (Interviewer: Ros Atkins).

The Guardian, 21st July 2014. Interview with Damian Carrington, Giving up beef will reduce carbon footprint more than cars, says expert. http://www.theguardian.com/environment/2014/jul/21/giving-up-beef-reduce-carbon-footprint-more-than-cars

BBC News, 21st July 2014. Interview with Matt McGrath: Beef environment costs 10 times that of other livestock.. www.bbc.com/news/science-environment-28409704

BBC Radio 4 Farming Today programme, 25 April 2014. Interview on Nitrogen Pollution, Meat Consumption, Hedgehogs. (Interviewer Charlotte Smith). [Key findings of ENA Special Report on Nitrogen and Food]. http://www.bbc.co.uk/programmes/b0418wy3

The Times, 25th April 2014, article by Ben Webster. Raise taxes on meat to turn us into demitarians, says UN, p 17 (also web edition: "Put tax on meat to cut pollution and improve diet, says UN report": [Key findings of ENA Special Report on Nitrogen and Food]. http://www.thetimes.co.uk/tto/environment/article4072005.ece

Reuters, 25th April 2014, article by Nina Chertsey: EU should halve meat, dairy consumption to cut nitrogen - report. [Press launch of ENA Special Report on Nitrogen and Food] also at: Wn.Com; News.nom.co.; Topix Global Warming; SPI News; Morningstar; Popbuzz; Envinews.EU; Climatiq; and around 400 other news websites. http://www.reuters.com/article/2014/04/25/food-environment-idUSL6N0NH1X120140425

The Guardian, 25th April 2014, article by Adam Vaugham: Halving meat and dairy consumption could slash farming emissions. Adopting a 'demitarian' diet would lead to a 25-40% reduction in nitrogen emissions from agriculture in Europe, report shows. http://www.theguardian.com/environment/2014/apr/25/halve-meat-dairy-consumption-slash-emissions-farming [Key Findings of ENA Special Report on Nitrogen and Food]

BBC Radio 4, Farming Today programme, 11th April 2014. Interview on effects of nitrogen on nature and the options for ammonia mitigation in European policy development. (Interviewer, Kaz Graham).

BBC Radio 4, Frontiers programme, 4th December 2013: 'Nitrogen Fixing'.   Half-hour documentary. 100 years since the first synthetic fertilizers, Prof Andrea Sella looks at efforts to reduce our dependence on the legendary Haber-Bosch process. Interviews with Mark Sutton and others. http://downloads.bbc.co.uk/podcasts/radio4/frontiers/frontiers_20131204-2145a.mp3

BBC World, 11th November 2013. Live TV interview hosted by Jon Sopel with Mark Sutton and Robin McKie (Science Editor, the Guardian). Haber Nitrogen – from war to environmental challenges.

The Observer (Guardian, Sunday edition), 3rd November 2013, p15. Article by McKie, Robin: From fertiliser to Zyklon B: 100 years of the scientific discovery that brought life and death. http://www.theguardian.com/science/2013/nov/03/fritz-haber-fertiliser-ammonia-centenary [Haber centenary and nitrogen impacts on the environment].

CEH News Release, 13th November 2014: "Experts meet in Edinburgh to agree international action on reducing agriculture's contribution to air pollution". http://www.ceh.ac.uk/news/press/ammonia-framework-code-edinburgh-workshop-press-release.asp

BBC Radio Scotland, News Drive, 25th April 2014. Live interview with Mhairi Stuart (anchor), Mark Sutton and Nigel Miller (President of National Farmers Union for Scotland)..

European Commission, Science for Environmental Policy, In-Depth Report: Nitrogen Pollution and the European Environment: Implications for Air Quality Policy. September 2013, 28 pp. http://ec.europa.eu/environment/integration/research/newsalert/pdf/IR6.pdf [EC public write-up of outcomes from NitroEurope and the European Nitrogen Assessment etc].

Lancet Respiratory Medicine, Editorial: Short-lived climate pollutants: a focus for hot air. (31 October 2015) 386, 1707. [Following up our article Brunekreef et al http://dx.doi.org/10.1016/ on National Emissions Ceilings, agriculture and human health].

The Economist, Wizard ideas for cleaning up nitrogen pollution', The Economist (Nov/Dec 2015), p 34. [Article on the theme of Harry Potter and the Nitrogen Cycle. Reflections on ENA etc.]

BBC Radio 4 Farming Today programme (0645, 1 October 2015). Interview on ammonia emission reduction ahead of the vote by MEPs on the proposed National Emissions Ceilings. Interview together with Pekka Pesonen, Secretary General, COPA-COGECA (Interviewer: Charlotte Smith). http://www.bbc.co.uk/programmes/b06d935c

EM (Air & Waste Management Association's Magazine for Environmental Managers), Nitrogen pollution in the EU: Best management strategies, regulations and science needs Winiwarter W., Grizzetti B. and Sutton M.A.   (Special Issue: Reactive Nitrogen and possible management approaches)   Air & Waste Management Association   vol. 65 01/09/2015 p. 18-23 ISSN: 1088-9981

Parliamentary Letter, Sharon A.M. Dijksma, Staatssecretaris van Economische Zaken (Netherlands Minister for Economic Affairs), Kamerbrief over internationale review ammoniak (Parliamentary letter on the International Review on Ammonia) Omgevingsweb 08/09/2015, http://omgevingsweb.nl/nieuws/kamerbrief-over-internationale-review-ammoniak (See: www.rijksoverheid.nl/documenten/kamerstukken/2015/09/08/kamerbrief-over-internationale-review-ammoniak for full letter and review report).

United Nations Economic Commission for Europe, Article, "UNECE joins international effort to reduce nitrogen pollution". [Article on INMS plenary meeting, May 2015, Lisbon] http://www.unece.org/info/media/unece-weekly/news-detail.html?extern=1&inter_lang=en&news=652&profil=default

Science for Environmental Policy. News Alert. European Commission, Agricultural ammonia emissions could be reduced without affecting crop yield. Issue 414. 21 May 2015. [Article based on Sanz-Cobena et al., P.219, Env. Res. Lett. 2014] http://ec.europa.eu/environment/integration/research/newsalert/newsalert.htm

Article, European Commission, Joint Research Centre. Nitrogen – too much of a good thing. 4 May 2015 [Article on the launch of the WWF nitrogen report] https://ec.europa.eu/jrc/en/news/nitrogen-%E2%80%93-too-much-good-thing?search

Acid News, Kajsa Lindqvist. Editorial: Ammonia emissions are cheap to reduce. Acid News 2014, no. 4. [drawing on TFRN ammonia abatement costings for CLRTAP] http://www.airclim.org/acidnews/editorial-ammonia-emissions-are-cheap-reduce

UNEP Yearbook 2014, UNEP (2014) Excess nitrogen in the environment. Chapter 1 in: UNEP Yearbook 2014 emerging issues. pp 6-11. United Nations Environment Programme
http://www.unep.org/yearbook/2014/PDF/chapt1.pdf

CEH News Release, "Experts meet in Edinburgh to agree international action on reducing agriculture's contribution to air pollution" (13 November 2014) http://www.ceh.ac.uk/news/press/ammonia-framework-code-edinburgh-workshop-press-release.asp

Progress towards the milestones and deliverables

D24.4 Final dissemination and communication plan (month 48) Completed

D24.7 Final report to the GA on networking activities (month 48) Completed

Use of resources and deviations from DoW

A total of 2.8 person months was spent on this workpackage during the second reporting period. There are no deviations from the DoW.

2.2   Project management during the period

As mentioned earlier (section 2.2.7), the management of the project is handled by a project office, which consists of a project co-ordinator, scientific project manager and a finance officer. Main events during the last reporting period are; organisation and holding of the fifth and final general assembly (Edinburgh, September 2015).

There have been no major changes within the consortium during the reporting period, apart from the addition of a Third Party for Partner NERC and several changes to legal representatives of project Partners.

The following management meetings have been held in the last reporting period:
- Fifth General Assembly, Edinburgh, Scotland, 1-4th September 2015

As mentioned in previous sections, a project website was created for the start of the project and provides information for project partners and the wider community http://www.ÉCLAIRE-fp7.eu . ÉCLAIRE scientists and other interested parties can become members of the website if they would like more detailed information.

All of the project milestones and deliverables have been now been delivered. Although we experienced some delays during this final year, this did not affect final delivery of the work. Any deviations or significant delays which were encountered in the past year have been listed in the relevant work packages and components. No deviations required any intervention from the management level (e.g. the Executive Steering Group- ESG) of the project. The work from the deliverables and milestones has now been used to answer the 7 key questions posed at the end of the project.

Appendix 1: List of authors and affiliations.

Co-ordinating Lead Authors

FAMILY NAME	FIRST NAME	ORGANISATION	COUNTRY
Sutton	Mark A.	NERC	UK
Howard	Clare M.	NERC/UEDIN	UK
Nemitz	Eiko	NERC	UK
Arneth	Almut	KIT IMK-IFU	Germany
Simpson	David	MET.NO	Norway
Mills	Gina	NERC	UK
de Vries	Wim	ALTERRA	The Netherlands
Winiwarter	Wilfried	IIASA	Austria
Amann	Markus	IIASA	Austria

Lead Authors

FAMILY NAME	FIRST NAME	ORGANISATION	COUNTRY
Alonso	Rocio	CIEMAT	Spain
Ammann	Christof	ART	Switzerland
Bealey	William J.	NERC	UK
Bermejo	Victoria	CIEMAT	Spain
Bleeker	Albert	ECN	The Netherlands
Cescatti	Alessandro	JRC	Belgium
Dentener	Frank	JRC	Belgium
Emberson	Lisa	SEI-Y, UoY	UK
Evans	Chris	NERC	UK
Flechard	Chris	INRA	France
Haas	Edwin	KIT IMK-IFU	Germany
Hettelingh	Jean-Paul	RIVM	The Netherlands
Holland	Mike	EMRC	UK
Mentel	Thomas	JUELICH	Germany
Paoletti	Elena	CNRS	France
Posch	Maximilian	RIVM	The Netherlands
Reinds	Gert Jan	ALTERRA	The Netherlands
Theobald	Mark R.	CIEMAT/UPM	Spain

Contributing Authors

FAMILY NAME	FIRST NAME	ORGANISATION	COUNTRY
Albert	Kristian	DTU	Denmark
Ambelas Skjøth	Carsten	AU	Denmark
Andersen	Helle Vibeke	AU	Denmark
Ashworth	Kirsti	KIT IMK-IFU	Germany
Åström	Stefan	IVL	Sweden

ÉCLAIRE Third Periodic Report: November 2015

FAMILY NAME	FIRST NAME	ORGANISATION	COUNTRY
Azouz	Niramson	INRA	France
Bassin	Seraina	ART	Switzerland
Becher	Agnieszka	NERC	UK
Beier	Claus	DTU	Denmark
Briolat	Alan	SEI-Y, UoY	UK
Broberg	Malin	UGOT	Sweden
Bueker	Patrick	SEI-Y, UoY	UK
Burkhardt	Juergen	UBO	Germany
Butterbach-Bahl	Klaus	KIT IMK-IFU	Germany
Calvete	Héctor	CIEMAT	Spain
Carozzi	Marco	INRA	France
Cellier	Pierre	INRA	France
Centoni	Federico	UEDIN	UK
Chiesa	Maria	UNICATT	Italy
Cieslik	Stanislaw	JRC	Belgium
Clarisse	Lieven	ULB	Belgium
Coheur	Pierre	ULB	Belgium
Coyle	Mhairi	NERC	UK
Decuq	Celine	INRA	France
Di Marco	Chiara	NERC	UK
Diaz-Pines	Eugenio	KIT IMK-IFU	Germany
Djuricic	Vesna	DHMZ	Croatia
Doherty	Ruth	UEDIN	UK
Dragosits	Ulli	NERC	UK
Drouet	Jean-Louis	INRA	France
Dzaja Grgicin	Vedrana	DHMZ	Croatia
Egger	Florian	BOKU	Austria
Elvira	Susana	CIEMAT	Spain
Engardt	Magnuz	SMHI	Sweden
Etzold	Sophia	WSL	Switzerland
Falk	Richard	NERC	UK
Fares	Silvano	CNR	Italy
Fauvel	Yannick	INRA	France
Finco	Angelo	UNICATT	Italy
Flura	Dominique	INRA	France
Fowler	David	NERC	UK
Franz	Martina	MPG	Germany
Frumau	Arnoud	ECN	The Netherlands
Fumagalli	Ivano	JRC	Belgium
Ganzeveld	Laurens	WU	The Netherlands
García Gómez	Héctor	CIEMAT	Spain
Gasche	Rainer	KIT IMK-IFU	Germany

FAMILY NAME	FIRST NAME	ORGANISATION	COUNTRY
Geels	Camilla	AU	Denmark
Genermont	Sophie	INRA	France
Gerosa	Giacomo	UNICATT	Italy
González Fernández	Ignacio	CIEMAT	Spain
González-Aparicio	Iratxe	JRC	Belgium
Gritsch	Christine	BOKU	Austria
Gruening	Carsten	JRC	Belgium
Hagberg	Daniel	ULUND	Sweden
Hakan	Pleijel	UGOT	Sweden
Haller	Helmut	BOKU	Austria
Harmens	Harry	NERC	UK
Hasler	Berit	AU	Denmark
Hauglustaine	Didier	CNRS	France
Hayes	Felicity	NERC	UK
Hendriks	Carlijn	TNO	Norway
Hertel	Ole	AU	Denmark
Heyes	Chris	IIASA	Austria
Hicks	Kevin	SEI-Y, UoY	UK
Höglund-Isaksson	Lena	IIASA	Austria
Horváth	László	FRI/HMS	Hungary
Houborg	Rasmus	JRC	Belgium
Joensuu	Johanna	UHEL	Finland
Jones	Laurence	NERC	UK
Karlsson	Per Erik	IVL	Sweden
Klimont	Zbigniew	IIASA	Austria
Komarov †	Alexander	IPBPSS	Russia
Kramer	Koen	ALTERRA	The Netherlands
Lamaud	Eric	INRA	France
Langford	Ben	NERC	UK
Lathiere	Juliette	CNRS	France
Leaver	David	NERC	UK
Leip	Adrian	JRC	Belgium
Lequy	Emeline	INRA	France
Lindblad	Maria	IVL	Sweden
Loubet	Benjamin	INRA	France
Loretto	Francesco	CNR	Italy
Maas	Rob	RIVM	The Netherlands
Marzuoli	Riccardo	UNICATT	Italy
Massad	Raia Silvia	INRA	France
Maury	Olivier	INRA	France
Medinets	Sergiy	ONU	Ukraine
Mercado	Lina	NERC	UK

ÉCLAIRE Third Periodic Report: November 2015

FAMILY NAME	FIRST NAME	ORGANISATION	COUNTRY
Messina	Palmira	CNRS	France
Migliavacca	Mirco	JRC	Belgium
Mikkelsen	Teis	DTU	Denmark
Molina Herrera	Saúl	KIT IMK-IFU	Germany
Monga	Robert	UNICATT	Italy
Moring	Andrea	NERC/UEDIN	UK
Munzi	Silvana	NERC	UK
Nainggolan	Doan	AU	Denmark
Ngadi	Yasmine	ULB	Belgium
Ogée	Jérôme	INRA	France
Olin	Stefan	ULUND	Sweden
Oliver	Rebecca	NERC	UK
Ots	Riinu	NERC/UEDIN	UK
Owen	Susan	NERC	UK
Pariyar	Shyam	UBO	Germany
Pokorska	Olga	JRC	Belgium
Potier	Elise	INRA	France
Priputina	Irina	IPBPSS	Russia
Rabago	Isaura	CIEMAT	Spain
Rantala	Pekka	UHEL	Finland
Reay	Dave	UEDIN	UK
Reis	Stefan	NERC	UK
Rinne	Janne	UHEL	Finland
Roberts	Elin	NERC	UK
Robinson	Emma	NERC	UK
Rowe	Edwin	NERC	UK
Ruuskanen	Taina	UHEL	Finland
Sanz	Javier	CIEMAT	Spain
Sanz-Cobena	Alberto	UPM	Spain
Sawicka	Katarzyna	NERC	UK
Schaap	Martijn	TNO	Norway
Schallart	Simon	UHEL	Finland
Schöpp	Wolfgang	IIASA	Austria
Sharps	Katarina	NERC	UK
Sheppard	Lucy	NERC	UK
Škevin Sovic	Jadranka	DHMZ	Croatia
Skiba	Ute	NERC	UK
Smith	Ben	ULUND	Sweden
Tiefenbacher	Alexandra	BOKU	Austria
Tomlinson	Sam	NERC	UK
Tuovinen	Juha-Pekka	FMI	Finland
Twigg	Marsailidh	NERC	UK

ÉCLAIRE Third Periodic Report: November 2015

FAMILY NAME	FIRST NAME	ORGANISATION	COUNTRY
Valino	Fernando	CIEMAT	Spain
Vallejo	Antonio	UPM	Spain
Van Damme	Martin	ULB	Belgium
Van Dijk	Netty	NERC	UK
Velikova	Violeta	BAS	Bulgaria
Vellinga	Nico	IIASA	Austria
Vidic	Sonja	DHMZ	Croatia
Vieno	Massimo	NERC	UK
Voylokov	Polina	INRA	France
Vuolo	Maria Raffaella	INRA	France
Weidinger	Tamas	ELTE	Hungary
Wichink Kruit	Roy	TNO	Norway
Wolff	Veronika	ART	Switzerland
Woolley	Roy	NERC	UK
Wu	Cheng	JUELICH	Germany
Zaehle	Sonke	MPG	Germany
Zechmeister - Boltenstern	Sophie	BOKU	Austria
Zuazo	Pablo	KIT IMK-IFU	Germany
Zubkova	Elena	IPBPSS	Russia

† deceased